

**FORMULATION DEVELOPMENT, MANUFACTURE AND EVALUATION OF
HYDRALAZINE HYDROCHLORIDE MICROSPHERES**

by

Shakemore Tinashe Kangausaru

*A Thesis Submitted to Rhodes University in
Fulfilment of the Requirements for the Degree of*

**MASTER OF SCIENCE (PHARMACY)
IN PHARMACEUTICS**

February 2017

Faculty of Pharmacy
RHODES UNIVERSITY
Grahamstown
South Africa

ABSTRACT

Despite improvements in its detection and treatment since the 1970s, hypertension is the most common and important risk factor for cardiovascular diseases. Hypertension is a chronic condition often underdiagnosed and/or inadequately treated in Sub-Saharan Africa. Recent survey results illustrate that the condition continues to contribute significantly to mortality and morbidity in adults and that it is poorly controlled in clinical practice. Hydralazine (HYD) is used either alone or in combination for the management of chronic hypertension, chronic cardiac failure and hypertensive crises.

Due to its short plasma half-life of between 2 to 4 hours, HYD is normally administered two to four times daily, therefore making it a potential candidate for inclusion in sustained release formulations. The formulation of sustained release microsphere dosage forms may be useful to improve patient adherence and to achieve predictable and optimised therapeutic plasma concentrations.

A stability indicating reversed-phase high performance liquid chromatography (RP-HPLC) method for the quantitation of HYD in pharmaceutical dosage forms was developed and optimised using a Central Composite Design (CCD) approach. UV/Vis detection method was selected as HYD contains an ultraviolet light-absorbing chromophore. The method was validated with respect to linearity and range, limits of quantitation (LOQ) and detection (LOD), accuracy, precision, sensitivity, selectivity and specificity as per International Conference on Harmonisation (ICH) guidelines. The method was applied to commercially available HYD tablets. No interfering peaks were observed from excipients used in the commercially available tablets.

Preformulation studies were conducted to ensure the manufacture of high quality, stable sustained release HYD microspheres. The results revealed that there was an interaction between HYD and Carbopol® 971P, therefore Carbopol® polymers were not included during formulation studies. HYD was found to be compatible with Methocel® K100LV, Eudragit® RS PO and Avicel® 101 and HYD formulations were developed and optimised using these excipients.

An oil-in-oil (o/o) solvent evaporation technique was selected for the manufacture of HYD microspheres due to its simplicity and to avoid exposure of HYD to moisture that could have been encountered if a water-in-oil (w/o) manufacturing process was used. The selection of o/o

solvent evaporation technique was also based on the hydrophilicity of HYD and the polymers selected. Different grades of Methocel[®] and Eudragit[®] were selected to evaluate their effect on encapsulation efficiency (EE), *in vitro* release and microparticle shape and morphology. The best combination of these polymers which resulted in the desired EE, *in vitro* release, microparticle shape and size were then selected for formulation optimisation.

A numerical optimisation approach was used to predict a formulation composition that would produce minimal HYD release initially and maximum HYD release after 12 hours of dissolution testing. The release kinetics of HYD from the manufactured microspheres were established by fitting *in vitro* release data to several mathematical models. The *in vitro* release data for the optimised formulations was best described using Higuchi model.

The short-term stability of the optimised formulations was established by undertaking stability studies at 4°C, 25 °C/60 % RH and 40 °C/75 % RH. The results revealed that there was no significant change in appearance and physicochemical properties of the microspheres over a period of one month. However, long-term stability studies would be required to determine the shelf-life of the formulations.

In addition, a gas chromatographic (GC) method was selected for determining residual amounts of acetone and *n*-hexane in the optimised formulations. GC methods were developed and optimised by evaluation of process parameters. System suitability testing was performed with respect to resolution, theoretical number of plates and selectivity. Method validation was performed with respect to linearity, range, inter- and intra-day precision, retention time (R_t) precision, limit of quantitation (LOQ) and detection (LOD). A solvent extraction method was used to analyse residual solvents in the optimised formulations. The drying process was sufficient in evaporating acetone and *n*-hexane from the optimised formulations.

Solvent evaporation technique has been successfully used in the manufacture of HYD microspheres. The microspheres have potential for further development, scale up formulation studies and long-term stability studies.

ACKNOWLEDGEMENTS

This research was made possible with the assistance and guidance from many people. Words cannot express my sincere token of appreciation to everyone who made my journey bearable with both spiritual, mental, physical and social support. Rhodes University I thank you for providing a conducive environment for the successful completion of my higher studies.

My supervisor, Prof R.B. Walker for giving me this opportunity and accepting me into his research group. His vast experience, knowledge, wisdom and understanding in the pharmaceutical field was of great help to the successful completion of this research. I thank him for his guidance, financial and academic support, understanding, assistance and patience while writing this thesis.

My co-supervisor, Dr S.M.M. Khamanga for his financial, academic support and assistance with Statistical Design of Experiments and Response Surface Methodology and for his guidance and encouragement throughout my studies.

It is with great pleasure in expressing my sincere thanks to Dr R Tandlich for the great opportunity to utilise the Gas Chromatography equipment. His dedication, help, guidance and supervision is extremely appreciated.

I thank Mr T. Samkange, Mr L. Purdon, Mr C. Nontyi, Mr T Fleck, Mr O Khitsane, Ms A Zuma, Ms L. Emslie and Mrs T. Kent for their technical and administrative support. I am also thankful to Prof Watkins for allowing me to use the DSC and FT-IR instruments and the staff at electron microscopy unit at Rhodes University. I acknowledge Brian Carlson for proofreading this work.

My friends and colleagues in the Faculty of Pharmacy for their help, understanding and support: Ms Sonya Koekemoer, Mr Archibald Svogie, Dr Sonal Patel, Mr Chiluba Mwila, Mr Potiwa Purazi, Mr Kudzayi Michael Zvidzayi, Mr Cyril Dube, Ms Mellisa Chikukwa, Mr Hari Mani Krishna Veerubhotla, Mr Bwalya Witika, Mr Pascal Ntemi, Ms Anjana Makan, Dr Ashmita Ramanah, Ms Janeeta Ranchhod, Ms Seeprarani Rath, Mr Arthur Manda, Ms Tsitsi and Amanda Mudyahoto, Ms Lola Oridota, Mr Siyabonga Melamane, Ms Kudzai Makoni, Ms Grace Govere and Ms Tanyaradzwa Musakana.

My immediate and extended family members for their encouragement, love and support. Special thanks to Mr and Mrs N Kangauseru, Mr and Mrs L Kangauseru, Mr and Mrs R

Mabhonga, Mr E Muzinda, Mr and Mrs S Mandebvu, Mr L Gore and Mr M Madzingo. My late grandparents Mr and Mrs Wilson Chinho, Mr and Mrs G Kangauseru for having played a major role in my upbringing. The late Miss Shamiso Chinho for her support and love. My special thanks to Theodora for her unending support, love, encouragement and sacrifices.

My parents Mr and Mrs S Kangauseru and Mrs N Chinho for their support, prayers, encouragement and love throughout my entire life. Without them, nothing would have been possible. I am forever thankful and indebted to my parents for the teachings, values and beliefs that they instilled in me as well as for the sacrifices they made to support my education.

This research would not have been possible without financial assistance from Rhodes University thus I sincerely express my gratitude.

I would like to give thanks to Almighty God for giving me strength, protection and for giving me knowledge and understanding. His everlasting grace on all flesh was more than enough for me. The Lord God Almighty demonstrated his love for us, in that while we were sinners, Christ died for us (Romans 5v8).

This thesis is dedicated to:

My beloved parents

STUDY OBJECTIVES

Hypertension accounts for approximately 9.4 million deaths worldwide [1]. It is an important medical and public health challenge [2,3] as it is anticipated to increase to approximately 1.56 billion by 2025 [4–6]. Cardiovascular diseases (CVD) are the leading cause of death in developed and developing countries. HYD is used either alone or in combination for the management of hypertension, chronic cardiac failure and hypertensive crises [7–9]. It is well absorbed from the gastrointestinal tract (GIT) and is metabolised in the gastric mucosa and liver by acetylation, hydroxylation and conjugation with glucuronic acid [8,10]. HYD has a short plasma half-life of between 2 to 4 hours and consequently requires multiple dosing [7,11]. HYD, therefore, is a potential candidate for sustained oral delivery, although the high water solubility of the molecule presents significant formulation challenges. The rationale for developing a sustained release formulation was to provide an approach that may release the molecule at a desired rate.

The objectives of this study were therefore:

- I. To collect and interpret information relating to the physicochemical, pharmacological and biopharmaceutical properties of HYD.
- II. To develop and validate a suitable, selective, specific and stability indicating HPLC method for quantitative analysing of hydralazine hydrochloride.
- III. To conduct preformulation studies to evaluate the compatibility between HYD and excipients.
- IV. To incorporate HYD into polymer based matrix microspheres and conduct preliminary formulation studies to identify a suitable formulation in terms of release and sphericity.
- V. To study the dissolution profiles and release mechanism of HYD from formulated microspheres.
- VI. To investigate the effects of different polymers on HYD release.
- VII. To use RSM approaches in conjunction with CCD to optimise the formulation.
- VIII. To use model-independent and model-dependent approaches to establish the kinetics of HYD release from formulations.
- IX. To carry out short-term stability studies on optimised formulations.
- X. To develop and validate a suitable GC method for quantitation of residual solvent.

TABLE OF CONTENTS

| | |
|--|------|
| ABSTRACT | i |
| ACKNOWLEDGEMENTS | iii |
| STUDY OBJECTIVES | v |
| TABLE OF CONTENTS | vi |
| LIST OF TABLES | xvii |
| LIST OF FIGURES | xix |
| CHAPTER 1 | 1 |
| 1.1 INTRODUCTION | 1 |
| 1.2 PHYSICOCHEMICAL PROPERTIES OF HYD | 2 |
| 1.2.1 Description | 3 |
| 1.2.2 Biopharmaceutics Classification System (BCS) | 3 |
| 1.2.3 Solubility | 3 |
| 1.2.4 Dissociation constant | 4 |
| 1.2.5 Melting point | 4 |
| 1.2.6 Hygroscopicity | 4 |
| 1.2.7 Ultraviolet (UV) absorption spectrum | 4 |
| 1.2.8 Fourier Transform Infrared absorption (FT-IR) spectrum | 5 |
| 1.2.9 Storage | 6 |
| 1.3 SYNTHETIC PATHWAY | 6 |
| 1.3.1 Synthetic route | 6 |
| 1.4 STABILITY | 8 |
| 1.4.1 Stability in aqueous solution | 8 |
| 1.4.2 Stability in solid state | 9 |
| 1.4.3 Stability in solution pH | 9 |
| 1.6 CLINICAL PHARMACOLOGY | 10 |
| 1.6.1 Mechanism of Action | 10 |
| 1.6.2 Indications | 10 |
| 1.6.3 Dosages | 10 |
| 1.6.3.1 Adult dose | 10 |
| 1.6.3.2 Paediatric dose | 11 |
| 1.6.3.3 Overdosage | 11 |
| 1.6.4 Drug interactions | 11 |
| 1.6.5 Contraindications | 12 |

| | |
|---|----|
| 1.6.6 Adverse effects | 13 |
| 1.6.7 Mutagenicity | 13 |
| 1.6.8 Precautions | 14 |
| 1.6.8.1 Pregnancy | 14 |
| 1.6.8.2 Lactation | 14 |
| 1.6.8.3 Porphyria | 14 |
| 1.6.8.4 Geriatric | 14 |
| 1.6.8.5 Renal Impairment | 14 |
| 1.6.8.6 Hepatic Impairment | 15 |
| 1.7 CLINICAL PHARMACOKINETICS | 15 |
| 1.7.1 Absorption | 15 |
| 1.7.2 Bioavailability | 16 |
| 1.7.3 Distribution | 16 |
| 1.7.4 Metabolism | 16 |
| 1.7.5 Excretion | 19 |
| 1.8 CONCLUSIONS | 19 |
| CHAPTER 2 | 20 |
| 2.1 INTRODUCTION | 20 |
| 2.1.1 Overview | 20 |
| 2.2 HIGH PERFORMANCE LIQUID CHROMATOGRAPHY (HPLC) | 21 |
| 2.2.1 Fundamental principles of HPLC | 21 |
| 2.2.2 Reversed-phase HPLC | 22 |
| 2.2.3 Mobile phase selection | 22 |
| 2.2.3.1 Buffer selection | 23 |
| 2.2.4 Column selection | 23 |
| 2.2.5 Methods of detection | 24 |
| 2.2.5.1 Spectrophotometry | 24 |
| 2.2.5.2 Fluorescence | 24 |
| 2.2.5.3 Electrochemical | 25 |
| 2.3 RESPONSE SURFACE METHODOLOGY | 25 |
| 2.3.1 Overview | 25 |
| 2.3.2 Central composite design (CCD) | 26 |
| 2.4 PUBLISHED ANALYTICAL METHODS FOR HYDRALAZINE | 26 |
| 2.5 EXPERIMENTAL | 30 |

| | |
|--|----|
| 2.5.1 Aim..... | 30 |
| 2.5.2 Materials and reagents..... | 30 |
| 2.5.3 Instrumentation..... | 30 |
| 2.5.4 Preparation of buffer solutions and mobile phase..... | 30 |
| 2.5.5 Chromatographic conditions | 31 |
| 2.6 METHOD DEVELOPMENT..... | 31 |
| 2.6.1 Column selection..... | 32 |
| 2.6.2 Column evaluation and specifications..... | 33 |
| 2.6.3 System suitability testing..... | 34 |
| 2.6.3.1 Number of theoretical plates (N)..... | 34 |
| 2.6.3.2 Peak tailing factor (A_s)..... | 35 |
| 2.6.3.3 Resolution factor (R_s)..... | 35 |
| 2.6.3.4 Capacity factor (K') | 36 |
| 2.6.3.5 Selectivity factor (α)..... | 36 |
| 2.6.4 Internal standard selection..... | 37 |
| 2.6.5 HPLC apparatus | 38 |
| 2.6.6 Method of detection..... | 38 |
| 2.7 METHOD OPTIMISATION..... | 39 |
| 2.7.1 Chemicals and reagents..... | 39 |
| 2.7.2 Central composite design | 39 |
| 2.7.3 Model fitting and statistical analysis | 41 |
| 2.7.3.1 Retention time of HYD | 42 |
| 2.7.3.2 HYD peak tailing | 47 |
| 2.7.3.3 Resolution | 49 |
| 2.7.3.4 Effect of injection volume on tailing..... | 50 |
| 2.7.4 Preparation of stock solutions | 51 |
| 2.7.4.1 Preparation of HYD stock solutions..... | 51 |
| 2.6.4.2 Preparation of IS stock solutions..... | 52 |
| 2.7.5 Preparation of mobile phase | 52 |
| 2.7.6 Optimised chromatographic conditions..... | 52 |
| 2.8 METHOD VALIDATION | 54 |
| 2.8.1 Introduction..... | 54 |
| 2.8.2 Limits of quantitation (LOQ) and detection (LOD) | 54 |
| 2.8.3 Linearity and range..... | 55 |

| | |
|---|-----------|
| 2.8.4 Precision..... | 57 |
| 2.8.4.1 Intermediate precision..... | 58 |
| 2.8.4.2 Intra-day precision | 59 |
| 2.8.4.3 Reproducibility..... | 60 |
| 2.8.5 Accuracy | 60 |
| 2.8.6 Specificity | 62 |
| 2.9 CONCLUSIONS | 63 |
| CHAPTER 3..... | 65 |
| 3.1 INTRODUCTION | 65 |
| 3.2 EXPERIMENTAL | 65 |
| 3.2.1 Aim..... | 65 |
| 3.3.2 Materials..... | 65 |
| 3.3 APPLICATION OF THE ANALYTICAL METHOD..... | 66 |
| 3.3.1 Specificity and selectivity..... | 66 |
| 3.3.2 <i>In vitro</i> release..... | 67 |
| 3.4 STABILITY STUDIES | 68 |
| 3.4.1 Stability in solution | 69 |
| 3.4.1.1 Stability of HYD stock solutions..... | 70 |
| 3.4.1.2 Stability of HYD in mobile phase..... | 70 |
| 3.4.2 Temperature studies | 71 |
| 3.4.2.1 Dry heat..... | 71 |
| 3.4.2.2 Effect of temperature on HYD solutions..... | 71 |
| 3.4.3 Forced degradation studies..... | 72 |
| 3.4.3.1 Acid studies..... | 72 |
| 3.4.3.1.1 <i>Hydrochloric acid studies</i> | 72 |
| 3.4.3.1.2 <i>Phosphoric acid studies</i> | 74 |
| 3.4.3.2 Alkaline studies..... | 77 |
| 3.4.3.3 Oxidative studies..... | 78 |
| 3.4.3.4 Neutral hydrolysis..... | 81 |
| 3.4.3.5 Photostability studies | 83 |
| 3.5 CONCLUSIONS | 84 |
| CHAPTER 4..... | 86 |
| 4.1 INTRODUCTION | 86 |
| 4.2 SELECTION OF PHARMACEUTICAL EXCIPIENTS | 86 |

| | |
|--|-----|
| 4.2.1 Introduction..... | 86 |
| 4.2.2 Materials..... | 87 |
| 4.2.2.1 Methacrylic acid copolymers | 87 |
| 4.2.2.2 Hydroxypropyl methylcellulose (HPMC) or hypromellose | 88 |
| 4.2.2.3 Microcrystalline cellulose (MCC)..... | 89 |
| 4.2.2.4 Acrylic acid polymer..... | 89 |
| 4.3 API-EXCIPIENT COMPATIBILITY | 90 |
| 4.3.1 Types of Interaction | 91 |
| 4.3.1.1 Physical interaction..... | 92 |
| 4.3.1.2 Chemical interaction..... | 92 |
| 4.3.1.3 Therapeutic interaction (TI)..... | 93 |
| 4.3.2 Drug excipient compatibility..... | 93 |
| 4.3.2.1 TGA | 94 |
| 4.3.2.2 DSC | 94 |
| 4.3.2.3 FT-IR | 95 |
| 4.3.2.4 XRPD..... | 95 |
| 4.4 METHOD | 96 |
| 4.4.1 SEM | 96 |
| 4.4.2 Melting point determination..... | 96 |
| 4.4.3 NMR..... | 96 |
| 4.4.4 DSC..... | 97 |
| 4.4.4.1 Sample preparation..... | 98 |
| 4.4.5 TGA | 98 |
| 4.4.6 FT-IR..... | 99 |
| 4.4.7 XRPD..... | 99 |
| 4.5 RESULTS AND DISCUSSION..... | 99 |
| 4.5.1 SEM | 99 |
| 4.5.2 Characterization of HYD..... | 101 |
| 4.5.2.1 Melting point..... | 101 |
| 4.5.2.2 DSC..... | 101 |
| 4.5.2.3 TGA | 102 |
| 4.5.2.4 FT-IR | 103 |
| 4.5.2.5 XRPD..... | 104 |
| 4.5.2.6 NMR | 105 |

| | |
|---|------------|
| 4.5.3 Compatibility studies using FT-IR, DSC and TGA..... | 109 |
| 4.5.3.1 DSC, TGA and FT-IR of HYD and Eudragit® RS PO | 109 |
| 4.5.3.1.1 DSC..... | 109 |
| 4.5.3.1.2 TGA..... | 110 |
| 4.5.3.1.3 FT-IR | 111 |
| 4.5.3.2 DSC, TGA and FT-IR of HYD and Methocel® K100LV..... | 113 |
| 4.5.3.2.1 DSC..... | 113 |
| 4.5.3.2.2 TGA..... | 114 |
| 4.5.3.2.3 FT-IR | 115 |
| 4.5.3.3 DSC, TGA and FT-IR of HYD and Avicel® 101..... | 117 |
| 4.5.3.3.1 DSC..... | 118 |
| 4.5.3.3.2 TGA..... | 119 |
| 4.5.3.3.3 FT-IR | 120 |
| 4.5.3.4 DSC, TGA and FT-IR of HYD and Carbopol® 971P | 122 |
| 4.5.3.4.1 DSC..... | 122 |
| 4.5.3.4.2 TGA..... | 123 |
| 4.5.3.4.3 FT-IR | 124 |
| 4.5.3.5 Compatibility studies of a mixture of HYD, Eudragit®, Methocel® and Avicel® | 125 |
| 4.5.3.5.1 DSC..... | 126 |
| 4.5.3.5.2 TGA..... | 126 |
| 4.5.3.5.3 FT-IR | 127 |
| 4.5.3.5.4 XRPD | 128 |
| 4.5.3.5.4 XRPD of a 1:1 mixture of HYD and Carbopol® 971P | 130 |
| 4.6. CONCLUSIONS | 132 |
| CHAPTER 5..... | 135 |
| 5.1 INTRODUCTION..... | 135 |
| 5.1.1 Microspheres | 136 |
| 5.1.1.1 Types of microspheres..... | 137 |
| 5.1.1.1.1 Bioadhesive microspheres..... | 137 |
| 5.1.1.1.2 Magnetic microspheres | 137 |
| 5.1.1.1.3 Floating microspheres | 137 |
| 5.1.1.1.4 Radioactive microspheres | 138 |
| 5.1.1.1.5 Polymeric microspheres..... | 138 |
| 5.1.2 Solvent evaporation..... | 139 |

| | |
|--|-----|
| 5.2 MECHANISMS OF DRUG RELEASE FROM ORAL CONTROLLED RELEASE SYSTEMS..... | 140 |
| 5.2.1 Physical mechanisms..... | 140 |
| 5.2.1.1 Dissolution..... | 140 |
| 5.2.1.2 Diffusion..... | 140 |
| 5.2.1.2.1 Reservoir system..... | 141 |
| 5.2.1.2.2 Matrix system..... | 141 |
| 5.2.1.3 Erosion..... | 142 |
| 5.2.1.4 Osmotic..... | 143 |
| 5.2.1.5 Ion-exchange..... | 144 |
| 5.2.1.6 Swelling..... | 144 |
| 5.2.2 Chemical mechanisms..... | 145 |
| 5.2.2.1 Chemical degradation..... | 145 |
| 5.2.2.2 Enzymatic degradation..... | 145 |
| 5.3 PROPOSED FORMULATION STUDIES..... | 146 |
| 5.3.1 Background..... | 146 |
| 5.3.2 Rationale for microspheres..... | 146 |
| 5.4 MATERIALS..... | 147 |
| 5.4.1 HYD..... | 147 |
| 5.4.2 Methocel® K100LV, K15M and K100M..... | 147 |
| 5.4.3 Eudragit® RS PO and Eudragit® L 100..... | 148 |
| 5.4.4 Avicel® (MCC)..... | 148 |
| 5.5 EXPERIMENTAL..... | 148 |
| 5.5.1 Aim..... | 148 |
| 5.5.1 Choice of method of manufacture..... | 149 |
| 5.5.2 Screening for polymers..... | 149 |
| 5.5.3 Preparation of microspheres..... | 150 |
| 5.6 EVALUATION OF HYD MICROSPHERES..... | 153 |
| 5.6.1 Physical appearance..... | 153 |
| 5.6.2 SEM..... | 153 |
| 5.6.3 Yield..... | 153 |
| 5.6.4 Assay..... | 153 |
| 5.6.5 Encapsulation efficiency (EE)..... | 154 |
| 5.6.6 <i>In vitro</i> release..... | 154 |
| 5.7 RESULTS AND DISCUSSION..... | 156 |

| | |
|---|------------|
| 5.7.1 Physical appearance | 156 |
| 5.7.2 SEM of preliminary formulations..... | 157 |
| 5.7.3 Yield..... | 158 |
| 5.7.4 Assay | 159 |
| 5.7.5 Encapsulation efficiency (EE)..... | 159 |
| 5.7.6 <i>In vitro</i> release..... | 160 |
| 5.7.6.1 Mechanism of HYD release | 161 |
| 5.6.6.2 Formulation F1..... | 162 |
| 5.6.6.3 Formulation F2..... | 163 |
| 5.6.6.4 Formulation F3..... | 164 |
| 5.6.6.5 Formulation F4..... | 165 |
| 5.6.6.6 Formulation F5..... | 166 |
| 5.6.6.7 Formulation F6..... | 167 |
| 5.8 SCREENING FOR APPROPRIATE DILUENT | 170 |
| 5.9 CONCLUSIONS | 172 |
| CHAPTER 6..... | 174 |
| 6.1 INTRODUCTION | 174 |
| 6.2 EXPERIMENTAL | 174 |
| 6.2.1 Aim..... | 174 |
| 6.2.2 Materials..... | 175 |
| 6.2.3 Method | 175 |
| 6.2.4 Experimental design | 175 |
| 6.2.5 Manufacture of HYD microspheres..... | 179 |
| 6.2.6 Evaluation of HYD sustained release | 179 |
| 6.2.7 Stability testing..... | 179 |
| 6.3 MATHEMATICAL MODELLING OF HYD RELEASE | 179 |
| 6.3.1 Overview | 179 |
| 6.3.2 Zero-order model..... | 180 |
| 6.3.3 First-order model..... | 180 |
| 6.3.4 Higuchi model..... | 181 |
| 6.3.5 Hixson-Crowell model | 181 |
| 6.3.6 Korsmeyer-Peppas model..... | 182 |
| 6.3.7 Approaches for selecting the best-fit mathematical model..... | 183 |
| 6.4 RESULTS AND DISCUSSION | 183 |

| | |
|--|------------|
| 6.4.1 Central composite design | 183 |
| 6.4.2 Model fitting..... | 185 |
| 6.4.2 Evaluation of the model for response Y_1 and Y_7 | 185 |
| 6.4.3 Diagnostic plots..... | 189 |
| 6.4.3.1 Diagnostic plots for the model for response Y_1 | 189 |
| 6.4.3.2 Diagnostic plots for the model for response Y_7 | 190 |
| 6.4.4 Response surface plots | 192 |
| 6.4.4.1 Response surface plots for response Y_1 | 192 |
| 6.4.4.2 Response surface plots for response Y_7 | 194 |
| 6.4.5 Mathematical modelling..... | 196 |
| 6.4.6 Formulation optimisation | 200 |
| 6.4.6.1 <i>In vitro</i> release from optimised formulations | 201 |
| 6.4.6.2 EE and assay | 202 |
| 6.4.6.3 Yield..... | 203 |
| 6.4.6.4 Characterisation of optimised formulations | 203 |
| 6.4.6.4.1 SEM | 203 |
| 6.4.6.4.2 FT-IR | 204 |
| 6.4.6.4.3 DSC..... | 205 |
| 6.4.6.4.4 XRPD | 206 |
| 6.4.6.5 Comparison of OPT 1 and OPT 2 <i>in vitro</i> dissolution profiles | 208 |
| 6.4.7 Stability studies | 209 |
| 6.5 CONCLUSIONS | 213 |
| CHAPTER 7..... | 215 |
| 7.1 INTRODUCTION | 215 |
| 7.2 INSTRUMENT OVERVIEW | 216 |
| 7.2.1 Carrier gas | 216 |
| 7.2.2 Injector | 216 |
| 7.2.3 Column (packed or capillary)..... | 216 |
| 7.2.3.1 Packed column | 216 |
| 7.2.3.2 Capillary columns | 217 |
| 7.2.4 Column oven | 217 |
| 7.2.5 Detector..... | 217 |
| 7.2.5.1 Flame ionisation (FID)..... | 218 |
| 7.2.6 Monitor..... | 218 |

| | |
|---|------------|
| 7.3 SOLVENT CLASSIFICATION | 219 |
| 7.3.1 Analytical procedures | 220 |
| 7.4 PUBLISHED GC ANALYTICAL METHODS FOR ACETONE AND HEXANE | 220 |
| 7.5 EXPERIMENTAL | 222 |
| 7.5.1 Aim | 222 |
| 7.5.2 Materials and instrumentation | 222 |
| 7.6 METHOD DEVELOPMENT | 222 |
| 7.6.1 Column selection | 222 |
| 7.6.2 Internal standard selection | 222 |
| 7.6.3 Solvent selection | 223 |
| 7.6.4 System suitability testing | 223 |
| 7.6.4.1 Resolution | 223 |
| 7.6.4.2 Theoretical number of plates (<i>N</i>) | 224 |
| 7.6.4.3 Selectivity factor | 224 |
| 7.6.5 Optimised chromatographic conditions | 225 |
| 7.6.5.1 Optimised chromatographic conditions for Acetone | 225 |
| 7.6.5.2 Optimised chromatographic conditions for <i>n</i> -Hexane | 225 |
| 7.7 METHOD VALIDATION | 230 |
| 7.7.1 Linearity and range | 230 |
| 7.7.2 Precision | 232 |
| 7.7.2.1 Intraday precision | 233 |
| 7.7.2.2 Inter-day precision | 233 |
| 7.7.2.3 Retention time (<i>R_t</i>) precision | 234 |
| 7.7.3 Dead volume | 234 |
| 7.7.4 Detection limit | 235 |
| 7.7.5 Quantitation limit | 235 |
| 7.8 APPLICATION OF GC TO SOLVENT EVAPORATION TECHNIQUES | 235 |
| 7.8.1 Acetone extraction studies | 235 |
| 7.8.2 <i>n</i> -Hexane extraction studies | 235 |
| 7.8.3 Acetone extraction efficiency | 236 |
| 7.8.4 <i>n</i> -Hexane extraction efficiency | 236 |
| 7.8.5 Results and discussion | 236 |
| 7.9 CONCLUSIONS | 237 |
| CHAPTER 8 | 238 |

| | |
|--------------------------|-----|
| REFERENCES | 243 |
| APPENDIX I | 243 |
| APPENDIX II | 275 |

LIST OF TABLES

Chapter 1

| | |
|--|---|
| Table 1.1 Solubility of HYD in different solvents | 3 |
| Table 1.2 FT-IR spectrum band assignments for HYD [37] | 6 |

Chapter 2

| | |
|--|----|
| Table 2.1 Common solvents used in reverse phase HPLC (adapted from [129,130,132,142])..... | 23 |
| Table 2.2 Commonly used buffers ([135,140])..... | 23 |
| Table 2.3 Brief summary of published chromatographic methods for analysis of HYD | 28 |
| Table 2.4 Summarised column selection studies for HYD | 33 |
| Table 2.5 Chromatographic conditions for quality assurance of the column | 33 |
| Table 2.6 Summary of chromatographic system suitability parameters for the proposed method..... | 37 |
| Table 2.7 Evaluation of internal standard retention time and peak tailing | 38 |
| Table 2.8 Translation of the coded levels used in CCD | 40 |
| Table 2.9 Experimental conditions for CCD runs..... | 41 |
| Table 2.10 ANOVA for retention time of HYD | 43 |
| Table 2.11 Statistical analysis for HYD retention time..... | 43 |
| Table 2.12 Summarised data for response y_1 to y_3 | 47 |
| Table 2.13 Optimised RP-HPLC conditions for HYD analysis | 53 |
| Table 2.14 Summarised results obtained for LOQ determination of HYD using HPLC method..... | 55 |
| Table 2.15 Typical summarised calibration curve data for HYD over the concentration range 0.3- 140.0 $\mu\text{g/mL}$ (n=5)..... | 57 |
| Table 2.16 Inter-day precision studies for HYD (0.3-140 $\mu\text{g/mL}$) (n=5)..... | 59 |
| Table 2.17 Intra-day precision studies for HYD (n=5) | 60 |
| Table 2.18 Accuracy results for HYD analysis (n=5)..... | 62 |
| Table 2.19 Summarised method validation parameters | 63 |

Chapter 3

| | |
|--|----|
| Table 3.1 Assay results for commercially available HYD tablets (n=5)..... | 67 |
| Table 3.2 Summary of dissolution test conditions | 68 |
| Table 3.3 Stability studies of HYD in stock solution (n=5)..... | 70 |
| Table 3.4 Stability studies of HYD in the mobile phase | 71 |
| Table 3.5 Summary of the effect of temperature on HYD (n=5) | 72 |
| Table 3.6 Degradation studies of 100 $\mu\text{g/mL}$ HYD in 0.1N HCL at 37 $^{\circ}\text{C}$ | 73 |
| Table 3.7 Degradation studies of 100 $\mu\text{g/mL}$ HYD in 0.1N HCL at 100 $^{\circ}\text{C}$ | 74 |
| Table 3.8 Degradation studies of 100 $\mu\text{g/mL}$ HYD in 0.1M H_3PO_4 at 37 $^{\circ}\text{C}$ | 76 |
| Table 3.9 Degradation studies of 100 $\mu\text{g/mL}$ HYD in 0.1M H_3PO_4 at 100 $^{\circ}\text{C}$ | 76 |
| Table 3.10 Degradation studies of 100 $\mu\text{g/mL}$ HYD in 0.1M NaOH at 100 $^{\circ}\text{C}$ | 78 |
| Table 3.11 Degradation studies of 100 $\mu\text{g/mL}$ HYD in 3%, 15% and 30% v/v H_2O_2 in the dark at 22 $^{\circ}\text{C}$ for 8 hours..... | 80 |
| Table 3.12 Degradation studies of 100 $\mu\text{g/mL}$ HYD in HPLC grade water at 22 and 100 $^{\circ}\text{C}$ for 8 hours..... | 82 |

Chapter 4

| | |
|--|-----|
| Table 4.1 Excipients used in preformulation studies..... | 87 |
| Table 4.2 Techniques used to determine API-excipient and excipient- excipient compatibility [254,256,261,263,269,270,286–292] | 91 |
| Table 4.3 Interpretation of FT-IR spectra for HYD [37]..... | 104 |
| Table 4.4 Proton-NMR for HYD [54]..... | 108 |
| Table 4.5 Carbon- NMR Data for HYD [54] | 109 |
| Table 4.6 Interpretation of FT-IR results for Eudragit [®] RS PO..... | 112 |
| Table 4.7 Interpretation of FT-IR results of a 1:1 binary mixture of HYD and Eudragit [®] RS PO..... | 113 |
| Table 4.8 Interpretation of FT-IR spectra for Methocel [®] K100LV..... | 116 |
| Table 4.9 Interpretation of FT-IR spectra of binary mixture of HYD and Methocel [®] K100LV | 117 |
| Table 4.10 Interpretation of FT-IR spectra for Avicel [®] 101 | 121 |
| Table 4.11 Interpretation of FT-IR results for the binary mixture of HYD and Avicel [®] 101..... | 121 |

| | |
|---|-----|
| Table 4.12 Interpretation of FT-IR spectra for Carbopol® 971P | 125 |
| Table 4.13 Interpretation of FT-IR spectra for the binary mixture of HYD and Carbopol® 971P | 125 |

Chapter 5

| | |
|---|-----|
| Table 5.1 Summarised constant formulation parameters | 150 |
| Table 5.2 Summarised formulation screening studies | 150 |
| Table 5.3 Summary of dissolution test conditions | 156 |
| Table 5.4 Percentage Yield of F1 to F6 | 158 |
| Table 5.5 Assay of F1 to F6 (n=3) | 159 |
| Table 5.6 Encapsulation Efficiency (EE) of F1 to F6 (n=3) | 160 |
| Table 5.7 Diluent screening studies | 171 |

Chapter 6

| | |
|--|-----|
| Table 6.1 Translation of the coded levels used in CCD | 176 |
| Table 6.2 Actual experimental conditions for the CCD | 177 |
| Table 6.3 Interpretation of diffusional release mechanisms from polymeric films(adapted from [476–478]) | 183 |
| Table 6.4 Summary of best fit models and significant factors | 185 |
| Table 6.5 Summary of the model selection criteria for response Y_1 and Y_7 | 186 |
| Table 6.6 ANOVA for the 2FI and Quadratic models for Y_1 and Y_7 respectively | 188 |
| Table 6.7 Summary of mathematical model and release kinetic parameters for selected CCD runs | 199 |
| Table 6.8 Optimised formulations | 201 |
| Table 6.9 Summary of mathematical model parameters for the optimised formulations | 202 |
| Table 6.10 Difference and similarity factors for dissolution profiles obtained from OPT 1 and OPT 2 | 209 |
| Table 6.11 Results of stability testing for the optimised formulations stored in the refrigerator at 4 °C | 212 |
| Table 6.12 Results of stability testing for the optimised formulations stored at 25°C/60% RH | 212 |
| Table 6.13 Results of stability testing for the optimised formulations stored at 40°C/75% RH | 212 |
| Table 6.14 Model independent approach on comparison of the release of OPT 1 and OPT 2 under stability testing conditions | 213 |

Chapter 7

| | |
|--|-----|
| Table 7.1 Classification of residual solvents (adapted from [38]) | 220 |
| Table 7.2 Summarised published GC methods for acetone and hexane | 221 |
| Table 7.3 Summarised compounds tested as potential IS | 223 |
| Table 7.4 Different solvents tried on the ZB-Wax column | 223 |
| Table 7.5 Summarised resolutions values between compounds of interest | 224 |
| Table 7.6 Summary of selectivity factor values | 225 |
| Table 7.7 Optimised chromatographic conditions for acetone and n-hexane | 227 |
| Table 7.8 Typical summarised calibration curve data for acetone over the concentration range 608-12171 ppm (n=3) | 231 |
| Table 7.9 Typical summarised calibration curve data for n-hexane over the concentration range 76-1530 ppm (n=3) | 232 |
| Table 7.10 Intraday precision data for acetone | 233 |
| Table 7.11 Intraday precision data for n-hexane | 233 |
| Table 7.12 Inter-day precision data for acetone | 233 |
| Table 7.13 Inter-day precision data for n-hexane | 234 |
| Table 7.14 Summarised retention times for acetone, n-hexane, ethanol and acetophenone | 234 |
| Table 7.15 Dead volumes for acetone and n-hexane | 235 |
| Table 7.16 Summarised extractions and limits of acetone and n-hexane | 236 |

LIST OF FIGURES

Chapter 1

| | |
|---|----|
| Figure 1.1 Chemical structure of hydralazine hydrochloride, Molecular weight =196.64 g/mole and Molecular formula of $C_8H_8N_4HCl$ | 3 |
| Figure 1.2 Typical UV absorption spectrum of HYD in water at 25 °C | 5 |
| Figure 1.3 Typical FT-IR of HYD generated from 4000 cm^{-1} to 650 cm^{-1} | 6 |
| Figure 1.4 Synthetic pathways of HYD adapted from [37]..... | 8 |
| Figure 1.5 Metabolic pathways of HYD [37] | 18 |

Chapter 2

| | |
|---|----|
| Figure 2.1 Typical UV spectrum of HYD obtained using a PDA detector from 210–400 nm wavelength | 39 |
| Figure 2.2 Normal probability plots of residuals for HYD retention time | 44 |
| Figure 2.3 Plot of residuals versus predicted for HYD retention time | 45 |
| Figure 2.4 Plot of predicted versus actual responses for HYD retention time | 45 |
| Figure 2.5 Box-Cox plot for HYD retention time..... | 46 |
| Figure 2.6 Contour plot depicting the impact of ACN content and buffer molarity on HYD retention time | 46 |
| Figure 2.7 3D response surface plot depicting the impact of ACN content and buffer molarity on HYD retention time | 47 |
| Figure 2.8 Contour plot depicting the impact of ACN content and buffer pH on HYD tailing..... | 48 |
| Figure 2.9 3D plot depicting the impact of ACN content and buffer pH on HYD tailing..... | 49 |
| Figure 2.10 Contour plot depicting the impact of ACN content and buffer pH on the resolution..... | 50 |
| Figure 2.11 3D plot depicting the impact of ACN content and buffer pH on the resolution factor..... | 50 |
| Figure 2.12 Plot of tailing versus injection volume | 51 |
| Figure 2.13 Typical chromatogram depicting the separation of HYD (100 $\mu g/mL$) and PROP (50 $\mu g/mL$) using the optimised separation conditions..... | 53 |
| Figure 2.14 Typical calibration curve for HYD in the concentration range 0.3-140.0 $\mu g/mL$ | 57 |

Chapter 3

| | |
|---|----|
| Figure 3.1 Typical chromatogram obtained from commercially available HYD tablets..... | 67 |
| Figure 3.2 HYD release from Hyperphen® 50 mg tablets | 68 |
| Figure 3.3 A schematic representation of the stability studies [231]..... | 69 |
| Figure 3.4 Typical chromatogram obtained after acidic stress studies of HYD in 0.1N HCL at 37 °C for 8 hours..... | 73 |
| Figure 3.5 Typical chromatogram obtained after acidic stress studies of HYD in 0.1N HCL at 100 °C for 8 hours..... | 74 |
| Figure 3.6 Typical chromatogram obtained after acidic stress studies of HYD in 0.1M H_3PO_4 at 37 °C for 8 hours | 75 |
| Figure 3.7 Typical chromatogram obtained after alkaline stress studies of HYD in 0.1M H_3PO_4 at 100 °C for 8 hours..... | 77 |
| Figure 3.8 Typical chromatogram obtained after alkaline stress studies of HYD in 0.1M NaOH at 100 °C for 8 hours..... | 78 |
| Figure 3.9 Typical chromatogram obtained from oxidative stress studies of HYD in 3% v/v H_2O_2 at 22 °C for 8 hours | 80 |
| Figure 3.10 Typical chromatogram obtained from oxidative stress studies of HYD in 15% v/v H_2O_2 at 22 °C for 8 hours .. | 81 |
| Figure 3.11 Typical chromatogram obtained from oxidative stress studies of HYD in 30% v/v H_2O_2 at 22 °C for 8 hours .. | 81 |
| Figure 3.12 Typical chromatogram obtained from oxidative stress studies of HYD in HPLC grade water at 22 °C for 8 hours | 82 |
| Figure 3.13 Typical chromatogram obtained from oxidative stress studies of HYD in HPLC grade water at 100 °C for 8 hours..... | 83 |
| Figure 3.14 Typical chromatogram of 100 $\mu g/mL$ HYD after exposure to 550 Watts/ m^2 for 24 hours..... | 84 |

Chapter 4

| | |
|--|-----|
| Figure 4.1 Summarises how the DSC for HYD, excipients and 1:1 Drug-excipient mixture sample were prepared..... | 98 |
| Figure 4.2 SEM image of HYD | 100 |
| Figure 4.3 SEM image for Methocel® K100 LV | 100 |
| Figure 4.4 SEM image for Eudragit® RS PO | 100 |
| Figure 4.5 SEM image for Carbopol® 971P..... | 100 |
| Figure 4.6 SEM image for Avicel® 101 | 101 |
| Figure 4.7 Typical DSC thermogram of HYD generated at a heating rate of 10 °C/min..... | 102 |
| Figure 4.8 Typical TGA thermogram of HYD generated at a heating rate of 10 °C/min from 30 to 600 °C..... | 103 |

| | |
|--|-----|
| Figure 4.9 Typical FT-IR spectrum of HYD generated from 4000 cm ⁻¹ to 650 cm ⁻¹ | 103 |
| Figure 4.10 X-ray Diffraction patterns of crystalline HYD | 105 |
| Figure 4.11 600 MHz ¹ H NMR spectrum of HYD in DMSO | 107 |
| Figure 4.12 600 MHz ¹³ C NMR spectrum of HYD in DMSO | 108 |
| Figure 4.13 Typical DSC thermogram of Eudragit® RS PO generated at a heating rate of 10 °C/min | 110 |
| Figure 4.14 Typical DSC thermogram of a 1:1 binary mixture of HYD and Eudragit® RS PO generated at a heating rate of 10 °C/min | 110 |
| Figure 4.15 Typical TGA thermogram of a 1:1 binary mixture of HYD and Eudragit® RS PO generated at a heating rate of 10 °C/min from 30 to 600 °C | 111 |
| Figure 4.16 Typical FT-IR spectrum of Eudragit® RS PO generated from 4000 cm ⁻¹ to 650 cm ⁻¹ | 112 |
| Figure 4.17 Typical FT-IR spectra of HYD and a 1:1 binary mixture of HYD and Eudragit® RS PO generated from 4000 cm ⁻¹ to 650 cm ⁻¹ | 113 |
| Figure 4.18 Typical DSC thermogram of Methocel® K100LV generated at a heating rate of 10 °C/min | 114 |
| Figure 4.19 Typical DSC thermogram of a 1:1 binary mixture of HYD and Methocel® K100 LV generated at a heating rate of 10 °C/min | 114 |
| Figure 4.20 Typical TGA thermogram of a 1:1 binary mixture of HYD and Methocel® K100 LV generated at a heating rate of 10 °C/min from 30 to 600 °C | 115 |
| Figure 4.21 Typical FT-IR spectra of Methocel® K100LV generated from 4000 cm ⁻¹ to 650 cm ⁻¹ | 116 |
| Figure 4.22 Typical FT-IR spectra of HYD and a 1:1 binary mixture of HYD and Methocel® K100LV generated from 4000 cm ⁻¹ to 650 cm ⁻¹ | 117 |
| Figure 4.23 Typical DSC thermogram of Avicel® 101 generated at a heating rate of 10 °C/min | 118 |
| Figure 4.24 Typical DSC thermogram of a 1:1 binary mixture of HYD and Avicel® 101 generated at a heating rate of 10 °C/min | 119 |
| Figure 4.25 Typical TGA thermogram of a 1:1 binary mixture of HYD and Avicel® 101 generated at a heating rate of 10 °C/min from 30 to 600 °C | 120 |
| Figure 4.26 Typical FT-IR spectrum of Avicel® 101 generated from 4000 cm ⁻¹ to 650 cm ⁻¹ | 120 |
| Figure 4.27 Typical FT-IR spectra of HYD and a 1:1 binary mixture of HYD and Avicel® 101 generated from 4000 cm ⁻¹ to 650 cm ⁻¹ | 121 |
| Figure 4.28 Typical DSC thermogram of Carbopol® 971P generated at a heating rate of 10 °C/min | 122 |
| Figure 4.29 Typical DSC thermogram of a 1:1 binary mixture of HYD and Carbopol® 971P generated at a heating rate of 10 °C/min | 123 |
| Figure 4.30 Typical TGA thermogram of a 1:1 binary mixture of HYD and Carbopol® 971P generated at a heating rate of 10 °C/min from 30 to 600 °C | 124 |
| Figure 4.31 Typical FT-IR spectra of Carbopol® 971P generated from 4000 cm ⁻¹ to 650 cm ⁻¹ | 124 |
| Figure 4.32 Typical FT-IR spectra of HYD and a 1:1 binary mixture of HYD and Carbopol® 971P generated from 4000 cm ⁻¹ to 650 cm ⁻¹ | 125 |
| Figure 4.33 Typical DSC thermogram of a 1:1 mixture of HYD, Eudragit® RS PO, Methocel® K100LV and Avicel® 101 generated at a heating rate of 10 °C/min | 126 |
| Figure 4.34 Typical TGA of a 1:1 mixture of HYD and all excipients used in formulation development and optimisation generated at a heating rate of 10 °C/min from 30 to 600 °C | 127 |
| Figure 4.35 Typical FT-IR spectra of HYD and a 1:1 mixture of HYD and all excipients (Eudragit®, Methocel® and Avicel®) used for formulation development and optimisation generated from 4000 cm ⁻¹ to 650 cm ⁻¹ | 128 |
| Figure 4.36 XRPD patterns of a 1:1 binary mixture of HYD, Eudragit®, Methocel® and Avicel® 101 | 129 |
| Figure 4.37 XRPD patterns of crystalline HYD (in black) and a 1:1 binary mixture of HYD, Eudragit®, Methocel® and Avicel® 101 (in red) | 130 |
| Figure 4.38 XRPD patterns of the binary mixture of HYD and Carbopol® 971P | 131 |
| Figure 4.39 XRPD patterns of crystalline HYD (in black) and a 1:1 binary mixture of HYD and Carbopol® 971P (in red) | 132 |

Chapter 5

| | |
|--|-----|
| Figure 5.1 Drug release from microparticles (adapted from [395,396]) | 143 |
| Figure 5.2 Schematic representation of solvent evaporation technique used in the manufacture of microspheres. Adapted from [153] | 152 |
| Figure 5.3 Design of the glass baskets (right) compared to conventional baskets (left) adapted from ([426]) | 155 |
| Figure 5.4 SEM image for F1 | 157 |
| Figure 5.5 SEM image for F2 | 157 |
| Figure 5.6 SEM image for F3 | 158 |
| Figure 5.7 SEM image for F4 | 158 |

| | |
|--|-----|
| Figure 5.8 SEM image for F5 | 158 |
| Figure 5.9 SEM image for F6 | 158 |
| Figure 5.10 Cumulative % HYD released from formulation F1 | 163 |
| Figure 5.11 Cumulative % HYD released from formulation F2 | 164 |
| Figure 5.12 Cumulative % HYD released from formulation F3 | 165 |
| Figure 5.13 Cumulative % HYD released from formulation F4 | 166 |
| Figure 5.14 Cumulative % HYD released from formulation F5 | 167 |
| Figure 5.15 Cumulative % HYD released from formulation F6 | 168 |
| Figure 5.16 Cumulative % HYD released from formulations F1 to F6 | 169 |

Chapter 6

| | |
|--|-----|
| Figure 6.1 Normal plot of residuals for response Y ₁ | 189 |
| Figure 6.2 Plot of residuals vs. predicted for response Y ₁ | 190 |
| Figure 6.3 Box-Cox plot for response Y ₁ | 190 |
| Figure 6.4 Normal plot of residuals for response Y ₇ | 191 |
| Figure 6.5 Plot of residuals vs. predicted for response Y ₇ | 191 |
| Figure 6.6 Box-Cox plot for response Y ₇ | 192 |
| Figure 6.7 Contour plot depicting the effect of Eudragit® RS PO and Methocel® K100LV on EE | 193 |
| Figure 6.8 3D contour plot depicting the effect of Eudragit® RS PO and Methocel® K100LV on EE | 193 |
| Figure 6.9 Contour plot depicting the effect of homogeniser speed and Methocel® K100LV on EE | 194 |
| Figure 6.10 3D plot depicting the effect of homogeniser speed and Methocel® K100LV on EE | 194 |
| Figure 6.11 Contour plot depicting the effect of Eudragit® RS PO and Methocel® K100LV on release at 12 hours..... | 195 |
| Figure 6.12 3D plot depicting the effect of Eudragit® RS PO and Methocel® K100LV on release at 12 hours..... | 195 |
| Figure 6.13 Photographs of sustained release HYD microspheres in capsules at (A) 4 minutes (B) 30 minutes (C) 6 hours and (D) 12 hours | 196 |
| Figure 6.14 Cumulative % HYD released from OPT 1 (n=6)..... | 201 |
| Figure 6.15 Cumulative % HYD released from OPT 2 (n=6)..... | 202 |
| Figure 6.16 SEM image for OPT 1 | 204 |
| Figure 6.17 SEM image for OPT 2 | 204 |
| Figure 6.18 Measured diameters for OPT 1 | 204 |
| Figure 6.19 Measured diameters for OPT 2 | 204 |
| Figure 6.20 Typical FT-IR spectra of HYD and OPT 1 generated from 4000 cm ⁻¹ to 650 cm ⁻¹ | 205 |
| Figure 6.21 Typical FT-IR spectra of HYD and OPT 2 generated from 4000 cm ⁻¹ to 650 cm ⁻¹ | 205 |
| Figure 6.22 DSC thermogram of OPT 1 generated at a heating rate of 10 °C/min | 206 |
| Figure 6.23 DSC thermogram of OPT 2 generated at a heating rate of 10 °C/min | 206 |
| Figure 6.24 XRPD patterns of OPT 1 | 207 |
| Figure 6.25 XRPD patterns of OPT 2 | 207 |
| Figure 6.26 Comparative cumulative % HYD released from OPT 1 and OPT 2 | 209 |
| Figure 6.27 SEM images of optimised formulations after stability studies for 1 month | 211 |

Chapter 7

| | |
|--|-----|
| Figure 7.1 Schematic diagram of components of a typical GC (adapted from [130,310,513])..... | 219 |
| Figure 7.2 Typical chromatogram obtained of 1000 ppm acetone and 8 g/L ethanol in acetophenone solvent | 228 |
| Figure 7.3 Typical chromatogram of 2000 ppm n-hexane in acetophenone solvent | 229 |
| Figure 7.4 Typical calibration curve for acetone in the concentration range 608-12171 ppm | 231 |
| Figure 7.5 Typical calibration curve for n-hexane in the concentration range 76-1530 ppm | 232 |

CHAPTER 1

HYDRALAZINE HYDROCHLORIDE

1.1 INTRODUCTION

Hypertension accounts for approximately 9.4 million deaths worldwide annually and about 45% of deaths are due to heart diseases and 51% due to stroke. Hypertension can also lead to kidney failure, blindness, rupture of blood vessels and cognitive impairment [1,12–17]. It is the leading risk factor for cardiovascular diseases (CVD) [13,18] and in 2010 approximately 31% of the adult population were living with hypertension [19]. The awareness, prevention, detection, treatment and control of hypertension in sub-Saharan Africa are haphazard and suboptimal due to a combination of lack of resources and/or health-care systems, non-existent effective preventive strategies, lack of sustainable drug therapy and barriers to adherence with prescribed medications [13,16,20].

Hypertension is an important medical and public health challenge worldwide [2–4,14,21] as it is anticipated to increase to approximately 1.56 billion by 2025 [4–6]. Adequate and appropriate treatment of hypertension lowers cardiovascular risk, however the biggest challenge for controlling hypertension is adherence to treatment [16,22]. Regardless of the availability of effective and cost-effective treatment, target blood pressure levels are rarely achieved and hypertension and related risk factors such as obesity, hyperlipidaemia and diabetes mellitus remain uncontrolled in many patients [16].

Literature survey shows that hypertension is a risk factor that constitutes approximately 55% of all hospital admissions for non-communicable diseases (NCD) and is a leading risk factor for morbidity, hospitalisation and mortality [3,23]. Reports suggest that NCD are rapidly growing as a cause of mortality in sub-Saharan Africa and hypertension is a driver of this epidemic [24]. Data from Sub-Saharan Africa have highlighted the increasing need to understand the importance of NCD [2,3,25].

In 2006, it was estimated that between 10 and 20 million people in Sub-Saharan Africa presented with hypertension [5,26]. Furthermore, the adequate treatment of hypertension may prevent as many as 250,000 deaths. However, hypertension in Sub-Saharan Africa is under diagnosed or is inadequately treated, with the result that extensive end-organ damage and

premature death occur [26] as it has been observed that it contributes to renal disease and blindness [1].

The Global Burden of Disease (GBD) report in 2010 [17] is a stark reminder of the challenges that hypertension will pose in the future as the disease occurs in economically developed and developing countries and regions [15,17]. Hypertension has a substantial impact on the burden of cardiovascular disease worldwide and a concerted effort is required to address prevention, diagnosis, treatment and control of hypertension otherwise, the pandemic of cardiovascular disease will increase globally [27,28].

Hydralazine (HYD) is a phthalazine-substituted hydrazine antihypertensive compound that reduces blood pressure by acting specifically on arterial smooth muscle to cause vasodilation with a subsequent reduction in total peripheral vascular resistance [7,8,29,30]. The drug is used either alone or in combination for the management of hypertension, chronic cardiac failure and hypertensive crises [7–9,38]. It is well absorbed from the gastrointestinal tract (GIT) and is metabolised in the gastric mucosa and liver by acetylation, hydroxylation and conjugation with glucuronic acid [8,10]. HYD has a short plasma half-life of between 2 to 4 hours and is normally administered two to four times daily [7,11]. Following oral administration, antihypertensive effects are observed within 20 to 30 minutes of dosing [8]. Approximately between 2 and 4% HYD is excreted unchanged renally [7]. The use of controlled release formulations may reduce fluctuations in plasma concentration and reduce the frequency of dosing [31], improving patient convenience and adherence [32–34]. The basic rationale of a controlled release drug delivery system is the optimisation of biopharmaceutical, pharmacokinetic and pharmacodynamic properties of a drug [35]. HYD is commercially available in South Africa as Hyperphen[®] and Sandoz Hydralazine[®] [7]. These formulations are immediate release tablets containing either 10, 25 or 50 mg HYD [7].

HYD is used as 4th line antihypertensive therapy [7] and is used to treat patients that are uncontrolled when treated with 1st, 2nd and 3rd line therapies due to inefficacy or adherence issues. If the latter, patients are unlikely to adhere to the 2-4 times a day hydralazine treatment regimen simply because previous experience with antihypertensive medications has been unsuccessful. Therefore, there is a necessity to develop a delivery technology that permits dosing of hydralazine over longer dosing intervals.

1.2 PHYSICOCHEMICAL PROPERTIES OF HYD

1.2.1 Description

HYD is a phthalazine derivative with a hydrazine moiety at the 1-position of the heterocyclic ring (Figure 1.1) [11,36] and is known chemically as 1-hydrazinophthalazine hydrochloride that occurs as a white or almost white, crystalline powder [37,38]. HYD is used as a vasodilator for the treatment of hypertension [30,38]. Hydralazine hydrochloride contains not less than 98.0% and not more than 101.0% $C_8H_8N_4HCl$, calculated with reference to anhydrous material [38,39]. The chemical structure of HYD is depicted in Figure 1.1 and the CAS registration number is 304-20-1 [37].

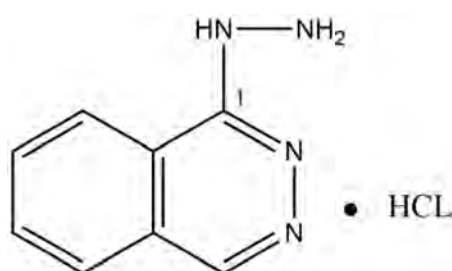


Figure 1.1 Chemical structure of hydralazine hydrochloride, Molecular weight =196.64 g/mole and Molecular formula of $C_8H_8N_4HCl$

1.2.2 Biopharmaceutics Classification System (BCS)

The biopharmaceutical classification system (BCS) is a classification system for drug molecules defined on the basis of their solubility and permeability [40–43]. HYD is highly water soluble and exhibits low gastrointestinal permeability and is a BCS Class III compound [44]. The low permeability of HYD may be attributed to the hydrophilic nature of the compound.

1.2.3 Solubility

HYD is highly water soluble and slightly soluble in 96% v/v ethanol. A 2% w/v solution of HYD in water has a pH of 3.5 to 4.2 [39,45]. The solubility profile of HYD is summarised in Table 1.1.

Table 1.1 Solubility of HYD in different solvents

| SOLVENT | SOLUBILITY | DESCRIPTION | REFERENCE |
|---------------|--|-----------------------|--------------|
| Water | 30.1 mg/mL at 15°C 39.0 mg/mL at 25°C | Very Soluble | [38] [37] |
| Methanol | 6.9 mg/mL | Freely soluble | [37,38] |
| 96% Ethanol | 1.9 mg/mL | Slightly soluble | [37,45] |
| Isopropanol | 0.1 mg/mL | Practically insoluble | [37] |
| Ethyl acetate | <0.1 mg/mL | Practically insoluble | [37] |
| Acetonitrile | <0.1 mg/mL | Practically insoluble | [37] |

1.2.4 Dissociation constant

The pK_a of hydralazine hydrochloride is 7.4 [37,46], which is slightly different to that of HYD. The pK_a of HYD is different in different solvents and in water the pK_a of HYD is 7.1 and is 4.7 in 90% v/v acetone [37].

1.2.5 Melting point

Hydralazine hydrochloride melts with decomposition at 275 °C [38], and between 275 and 280°C, crystalline HYD decomposes to form ammonia, nitrogen and 1,4-dihydro-1,1'-bipthalazine [37,47]. The melting point of HYD was determined using a Stuart SMP30 melting point apparatus (Stone, Staffordshire, UK) by placing three samples of HYD into 100 mm glass capillary tubes to a plateau temperature of 260 °C at a ramping rate of 2.0 °C/min. No changes were observed from the plateau temperature (260 °C) to 272 °C. The melting point was found to be in range from 273 °C to 275 °C and correlates with previously reported melting point for HYD [37].

1.2.6 Hygroscopicity

HYD is slightly hygroscopic when stored under conditions where the relative humidity (RH) is < 100%, in that, when HYD was stored at 50 °C and 100% RH for 30 days the moisture content of the material increased by 3% [48].

1.2.7 Ultraviolet (UV) absorption spectrum

Ultraviolet (UV) spectroscopy is used extensively when establishing degradation rate, equilibrium, acid-base dissociation constants and sample analysis [49]. The UV absorption spectrum of a 100 µg/mL HYD solution in water is depicted in Figure 1.2. The spectrum was generated using a PerkinElmer Lambda 25 UV/VIS Spectrometer (Beaconsfield, England). Solutions of HYD in water, methanol and acetonitrile (ACN) indicate that the molecule exhibits maximum absorption at 211, 240, 260, 303 and 315 nm and are similar to those previously reported [37,38].

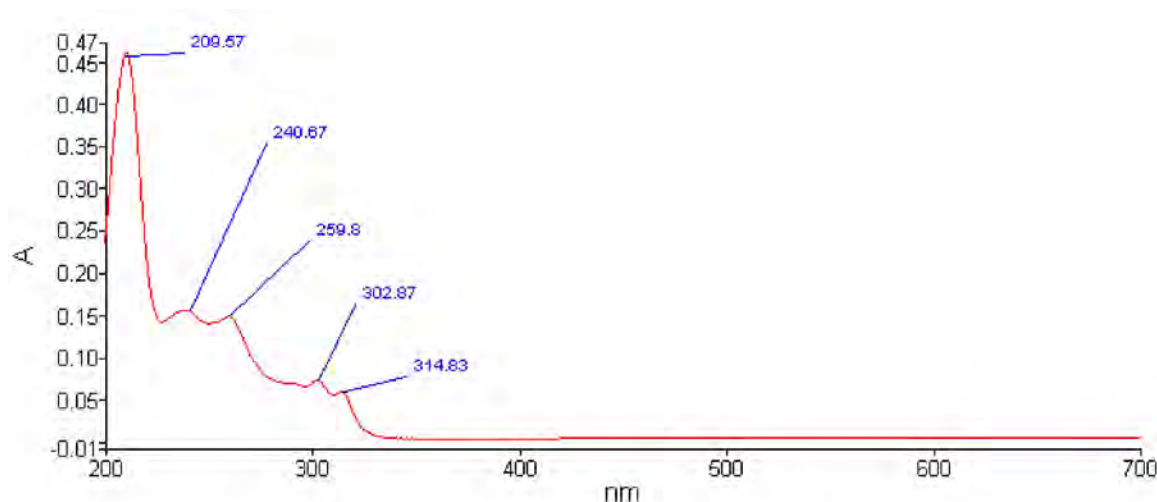


Figure 1.2 Typical UV absorption spectrum of HYD in water at 25 °C

1.2.8 Fourier Transform Infrared absorption (FT-IR) spectrum

Infrared Spectroscopy (IR) is an analytical technique used for identification of compounds and is based on functional group responses to infrared light of different wavelengths and are dependent on the nature and behaviour of specific functional groups [49,50]. A KBr disc method was used to generate the Fourier Transform Infrared absorption (FT-IR) spectrum of crystalline HYD powder in the range 4000–650 cm^{-1} using a Spectrum 100 PerkinElmer® FT-IR Spectrophotometer (Beaconsfield, England).

Resonance at 3429, 3027 and 1668 cm^{-1} were assigned to N-H functional group, aromatic C-H and aromatic C=C stretching respectively. The FT-IR spectrum of HYD is depicted in Figure 1.3 and characteristic absorption bands are summarised in Table 1.2 and are similar to reported data [37].

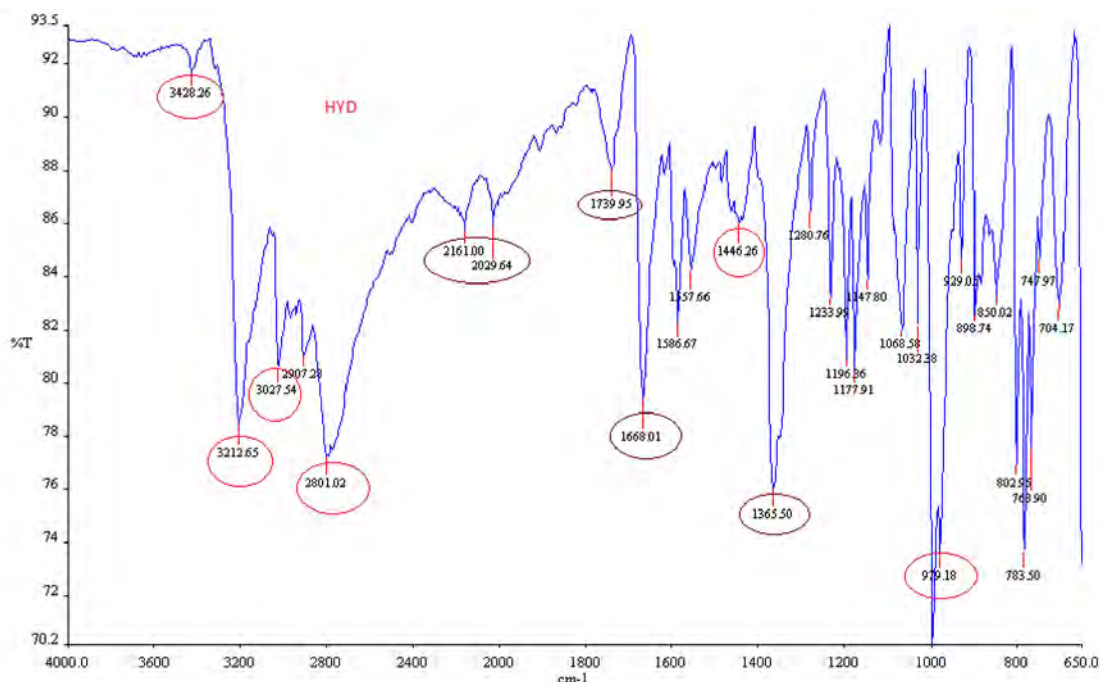


Figure 1.3 Typical FT-IR of HYD generated from 4000 cm^{-1} to 650 cm^{-1}

Table 1.2 FT-IR spectrum band assignments for HYD [37]

| Frequency (cm^{-1}) | Intensity | Assignment |
|--------------------------------|------------------|---|
| 3429 | w | N-H symmetric and asymmetric stretch (secondary amines) |
| 3210 | s, sharp | N-H stretch (primary amine) |
| 3027 | m-s | Ar C-H stretch |
| 1446-1670 | m-s (four bands) | Ring C=C stretch |
| 1668 | s | C=C stretch |
| 650-1500 | - | Fingerprint peaks (region) |

w - weak, s - strong, m - medium

1.2.9 Storage

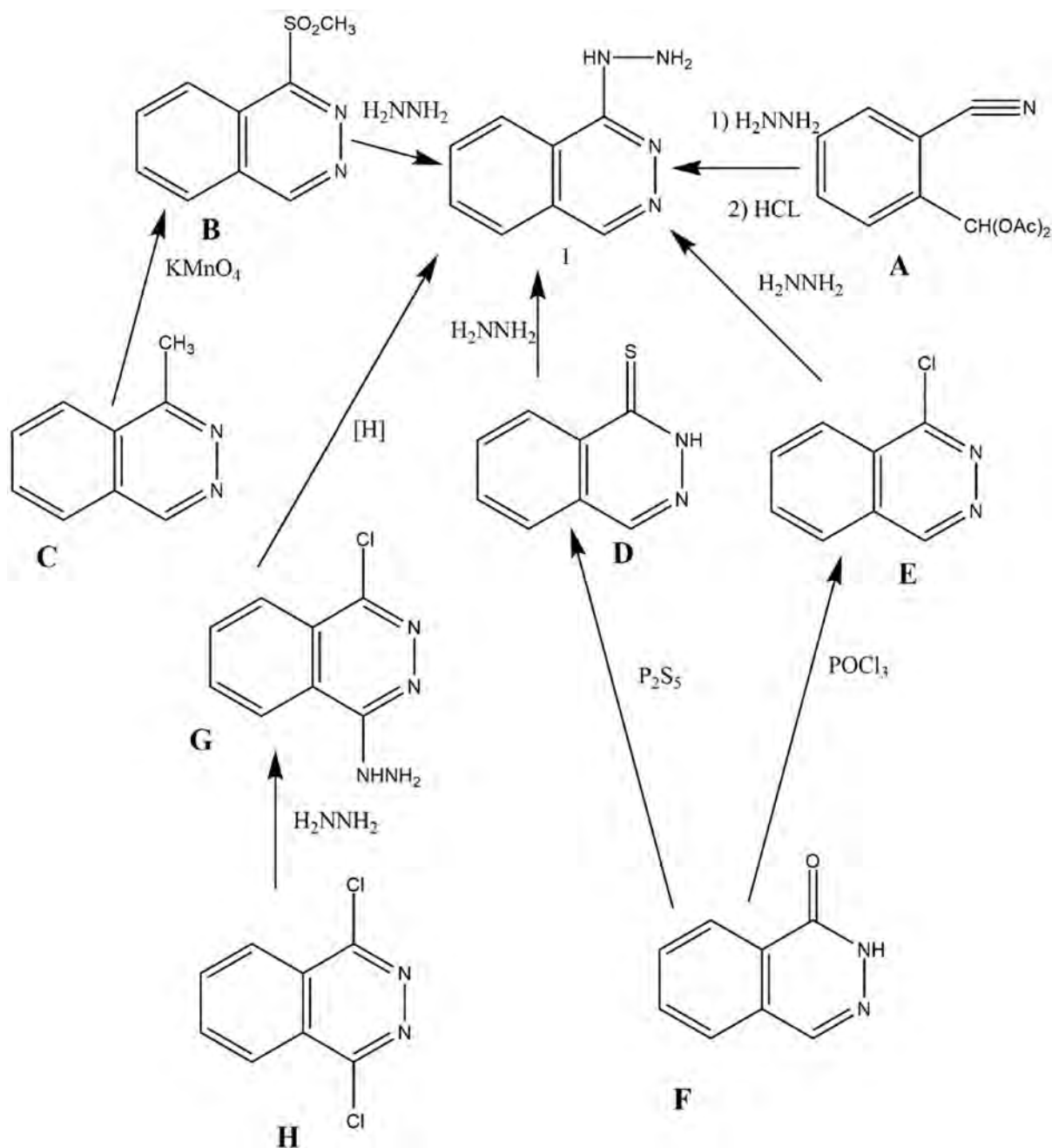
HYD should be stored in airtight containers at a temperature of 25 °C and protected from light and heat [38,39,45]. Tablets and capsules should be stored in light and air proof containers between 15 °C and 40 °C and ampoules should be maintained at the same temperature as tablets and should not be frozen [51].

1.3 SYNTHETIC PATHWAY

1.3.1 Synthetic route

HYD {1} is synthesised using various procedures from 1-cyano-2-benzal acetate {A}, 1-(methylsulfonyl)-phthalazine {B}, phthalazine-1-thione {D}, 1-chlorophthalazine {E} or 1,4-dichlorophthalazine {H} [37]. Schematic representations of the synthetic pathways of HYD and intermediate products are summarised in Figure 1.4. Phthalazone {F} undergoes a reaction with phosphoryl chloride to form 1-chlorophthalazine {E}, in which substitution of the chloride

atom with a hydrazine moiety (H_2NNH_2) to form HYD [52–54]. HYD can also be synthesised from 1,4-dichlorophthalazine **{H}** by substitution of a chlorine atom and addition of hydrogen atom to form HYD and hydrochloric acid. HYD can also be synthesised by reacting phthalazone **{F}** with a sulfurizing agent like phosphorus pentasulfide (P_2S_5) to form phthalazine-1-thione **{D}**. The sulphur atom is then aromatically substituted by hydrazine moiety to form HYD and hydrogen sulphide (H_2S). HYD can be synthesised from 1-methylphthalazine **{C}** using potassium permanganate (KMnO_4) to form 1-(methylsulfonyl)-phthalazine **{B}** which is then reacted with phthalazine to form HYD. The reaction between 1-cyano-2-benzal acetate, hydrazine and hydrochloric acid also yields HYD [37].



1 - Hydralazine, H_2NNH_2 - Hydrazine, 1-cyano-2-benzal acetate {A}, 1-(methylsulfonyl)-phthalazine {B}, 1-methylphthalazine {C}, phthalazine-1-thione {D}, 1-chlorophthalazine {E}, Phthalazone {F}, 4-chlorohydralazine {G}, 1,4-dichlorophthalazine {H}

Figure 1.4 Synthetic pathways of HYD adapted from [37]

1.4 STABILITY

1.4.1 Stability in aqueous solution

Aqueous solutions of HYD are stable for an extended period of time at 25 °C. HYD decomposes to form phthalazine in solutions of $\text{pH} > 7$. The rate of degradation varies with

pH, temperature, presence of oxygen, exposure to light, presence of metallic ions and the vehicle in which HYD is dissolved [55]. In biological fluids, HYD degrades rapidly at 25 °C. The hydrazine moiety present in HYD reacts with aldehyde and ketone functional groups to form hydrazones [55]. HYD forms a complex with metal ions as it is a reducing agent. Studies of the rate of degradation of HYD in sweetened aqueous liquids revealed that glucose, fructose, lactose and maltose reduce the stability of HYD in solution and these studies suggest that HYD degrades by 10% after 3 weeks in mannitol or sorbitol vehicles [45,56]. Therefore, HYD should be used immediately when in these vehicles. Solutions containing starch have been reported to react with HYD to form phthalazine, hydrazone and/or triazolophthalazine derivatives. Starch has been reported to adsorb HYD, leading to retention and delays in dissolution when undertaking dissolution tests, extraction and/or bioavailability effects [57]. The terminal aldehydes in starch have been shown to react with the hydrazine moieties of HYD and form phthalazine, hydrazone and/or triazolophthalazine derivatives [57].

1.4.2 Stability in solid state

HYD exhibits good stability in a crystalline state [37] and direct exposure of HYD samples to 50°C/100% RH for 30 days resulted in a colour change from white or almost white to a rose beige, slightly agglomerated sticky powder [48]. In another study, the water content in the samples following storage at 25 °C at 75 and 93% RH for one year were 0.6 and 0.8%w/w, respectively. The low water uptake of HYD may be attributed to the slow kinetics of hydrate formation in the solid state [58].

1.4.3 Stability in solution pH

The hydrolysis of HYD in aqueous solutions of pH between 1 and 12 at 35, 50 and 70 °C was investigated and hydrolysis due to reaction with the dicationic and the cationic forms of the drug was observed [55]. The degradation of HYD is catalysed by phosphate (HPO_4^-) ions. The rate of hydrolysis under nitrogen follows first-order kinetics at constant pH, temperature and buffer concentration. The pH degradation profile reveals that HYD exhibits maximum stability at or near a pH of 3.5 and decomposes to form phthalazine and other products [55]. The rate of hydrolysis of HYD was found to be pH dependent in addition to temperature and the vehicle used [55].

1.6 CLINICAL PHARMACOLOGY

1.6.1 Mechanism of Action

HYD acts directly on arterial smooth muscle to cause vasodilation that results in the reduction in total peripheral vascular resistance with a subsequent lowering of blood pressure if cardiac output remains constant [29,30,59,60]. To date, the mechanism by which HYD facilitates vasodilation is not yet well understood [61]. Recent investigations suggest that HYD inhibits calcium release in the sarcoplasmic reticulum of smooth muscles by blocking inositol trisphosphate (IP₃) which induces calcium release, thereby reducing calcium turnover within the cell [62]. Vasodilation reduces cardiac afterload and increases cardiac function in patients who present with heart failure [63–65]. HYD does not dilate epicardial coronary arteries or relax venous smooth muscle, thus the effects of the molecule are confined to the cardiovascular system [59].

HYD ensures smooth muscle hyperpolarisation through the opening of potassium channels resulting in hyperpolarisation of vascular smooth muscle (VSM) cells and prolongs the opening of potassium channels that sustains vasodilation within arterioles [59]. HYD stimulates the formation of nitric oxide (NO) in the vascular endothelium leading to cGMP-mediated vasodilation [59]. In addition, HYD may activate guanylate cyclase leading to increased cGMP levels [58,59].

1.6.2 Indications

HYD is used as a fourth-line treatment for hypertension and as a supplementary drug for the treatment of chronic cardiac failure [7] and may also be used to treat congestive heart failure [7,66,67]. In patients with chronic heart failure and low cardiac output, HYD has produced sustained beneficial hemodynamic and clinical effects [68,69]. HYD is as effective as digoxin in improving cardiac function over a short period, however reduction in systemic arterial pressure may potentially be harmful to normotensive patients [67].

1.6.3 Dosages

1.6.3.1 Adult dose

The initial oral adult dose of HYD for the treatment of hypertension is 20-25 mg administered twice daily which may be increased, to between 25 and 100 mg, according to patient response [7]. Although the recommended maximum dose for the treatment of hypertension is 200 mg

daily, doses > 100 mg daily are associated with an increased incidence of lupus erythematosus particularly in women and patients who exhibit slow acetylation metabolic reactions [45].

When treating hypertensive emergencies, HYD is administered in doses of 5 to 10 mg by slow intravenous injection that may be repeated after 20 to 30 minutes, if required. Alternatively, HYD may be administered by continuous intravenous infusion using an initial dose of 200 to 300 µg/minute with subsequent administration of a maintenance dose of 50 to 150 µg/minute [45].

1.6.3.2 Paediatric dose

The safety and efficacy of HYD in paediatric patients have not yet been established in controlled clinical trials [70,71]. The oral dose of HYD for paediatric patients ranges between 0.75 mg/kg/day to 7.5 mg/kg/day administered in 2 or 4 divided doses [7]. The intravenous or intramuscular administration of HYD requires doses of 0.8 to 3.5 mg/kg/day to be delivered every 4 to 6 hours [45,71,72].

1.6.3.3 Overdosage

Overdosing with HYD generally results in severe hypotension, tachycardia, myocardial ischaemia, arrhythmias, shock and coma [45,73]. If overdosing occurs, activated charcoal may be administered if the patient presents within one hour of ingestion. Symptomatic and supportive treatment, including the use of plasma expanders to treat shock and the use of a beta blocker to treat tachycardia if deemed necessary. In addition, the patient should be placed in a supine position to accommodate the impact of hypotension [7,45].

1.6.4 Drug interactions

The synergistic effect experienced when HYD is used with other antihypertensive agents is due to an enhancement of the hypotensive effect and attenuation of superoxide formation when used with nitrates, mono-amine oxidase inhibitors (MAOI) and nonsteroidal anti-inflammatory drugs (NSAIDS) [7,30,74] such as indomethacin that has been reported to decrease the efficacy of HYD [75].

Severe hypotension may result if HYD and diazoxide are used concomitantly, however these interactions may be beneficial in some cases [45].

HYD should not be administered concurrently with alcohol as the hypotensive effects of the molecule are enhanced, as is the case when HYD and phenothiazines are administered concurrently. In addition, HYD raises the blood level of timolol [75].

The concomitant use of HYD and furosemide has been reported to result in a decrease in the half-life of furosemide due to an increase in the plasma clearance of the drug. Plasma concentrations of furosemide are decreased despite an unchanged clearance of endogenous creatinine indicating that the increase in clearance of furosemide is due to an increase in renal blood flow as a consequence of HYD use [76]. Close monitoring of serum electrolyte levels and creatinine clearance should be undertaken when both drugs are used together [77].

It has been established that the hypotensive effects of HYD are reduced by Ma Huang, consequently the concomitant use of Ma Huang is not advised in patients on antihypertensive therapy [78].

The concomitant use of HYD and metoprolol has been established to result in the inhibition of pre-systemic metabolism of metoprolol, resulting in increased metoprolol bioavailability and blood levels. HYD is an inhibitor of the CYP2D6 enzyme which may result in an increase in the plasma concentrations of metoprolol, leading to a decrease in the cardio-selectivity of metoprolol [79]. HYD also increases the oral bioavailability of other beta-blockers such as propranolol and oxprenolol [80,81].

Yohimbine has been found to counteract the hypotensive effects of HYD resulting in inadequate blood pressure control in hypertensive patients and was found to increase blood pressure in hypertensive and normotensive patients [82,83].

The bioavailability of HYD has been reported to be enhanced or decreased in the presence of food and therefore consistent dosing with respect to meals is recommended [7,84].

1.6.5 Contraindications

HYD is contraindicated in patients with aortic stenosis or hypertrophic obstructive cardiomyopathy, tachycardia and systemic lupus erythematosus [7,30,74]. It is also contraindicated in patients who present with severe tachycardia, dissecting aortic aneurysm, heart failure with high cardiac output, cor pulmonale or myocardial insufficiency due to mechanical obstruction such as, aortic or mitral stenosis or constrictive pericarditis [45,85].

1.6.6 Adverse effects

The adverse effects of HYD occur less frequently at low doses and are generally resolved following discontinuation of therapy. The common adverse effects of HYD include tachycardia, anorexia, severe headache, flushing, palpitations, dizziness, oedema and postural hypotension [7,45,59,75]. Infrequently observed adverse effects include angina pectoris, nasal congestion, lupus-like syndrome with fever, arthralgia, myalgia, skin manifestation and the presence of anti-histone antibodies may also occur [7,11,29,30,74,76,86]. Rare adverse effects include blood dyscrasia, lacrimation, rash and paraesthesia [11].

HYD may deplete pyridoxine in the body leading to peripheral neuropathy with numbness and tingling of the extremities [45] that can be alleviated by administration of pyridoxine. Occasionally, hepatotoxicity, haemolytic anaemia, difficulty in urination, glomerulonephritis, constipation, paralytic ileus, depression and anxiety may occur [45]. Antinuclear antibodies may be produced following prolonged use of high doses of HYD and the incidence has been found to be greater in slow acetylating patients with renal impairment, women and patients taking in excess of 100 mg HYD daily. Acute overdosing may result in hypotension, tachycardia, myocardial ischaemia, arrhythmias, shock and coma [45,87].

1.6.7 Mutagenicity

HYD has been reported to induce structural and/or conformational changes to DNA and has a clastogenic effect in the liver that may be the main target site for genotoxicity [88]. It has been reported that a HYD-DNA pyrimidine interaction resulting in a response to HYD and nuclear antigens in which antibodies native to DNA may occur and are a possible explanation for the occurrence of HYD-induced lupus erythematosus [89]. Recent observations have demonstrated that in the presence of metal ions or peroxidase enzyme, HYD undergoes one-electron oxidation to form hydralazyl radical which then further decomposes to form various products or may react with molecular oxygen to generate reactive oxygen-centred radicals [89]. HYD inhibits DNA methyltransferase by inhibiting the transfer of a methyl group to DNA in several tumour suppressors [89]. HYD increased free radical production and site-specific DNA-damage may therefore occur and this may be a possible explanation for HYD-induced lupus, mutation and cancer [88,90–93].

1.6.8 Precautions

Patients with heart failure treated with HYD should be monitored for the occurrence of orthostatic hypotension and tachycardia following initiation of therapy. HYD should be used with caution in patients with cerebrovascular disorders [45].

1.6.8.1 Pregnancy

A meta-analysis of randomised control trials data reported by Magee *et al.* [94], evaluated the use of HYD during pregnancy and revealed that HYD should not be used as first-line treatment [75,86,94]. HYD is in Category C pregnancy compound and should be avoided in the first and second trimesters of pregnancy due to the occurrence of maternal and neonatal lupus-like syndrome [7,29,75,86,95].

1.6.8.2 Lactation

Although small amounts of HYD are excreted in breast milk, the concentration is too low to result in a pharmacologically significant effect in feeding infants and HYD can, therefore, be used during lactation. However, the feeding infant should be closely monitored for the appearance of possible adverse effects [7,75,86].

1.6.8.3 Porphyria

HYD is a porphyrinogenic compound [75,96] and should therefore only be prescribed for compelling reasons, to porphyric patients and precautions should be taken in all patients [7,30,45,75].

1.6.8.4 Geriatric

Geriatric patients may be more sensitive to postural hypotension when dosed with HYD and the compound should be administered with caution in such patients [7,45,85,97,98].

1.6.8.5 Renal Impairment

Patients with renal impairment may be more sensitive to the hypotensive effects of HYD and therefore it should be used with caution in patients with severe renal impairment [7]. The dose of HYD should be reduced or the dosage interval prolonged when treating patients with renal impairment [45].

1.6.8.6 Hepatic Impairment

Since HYD undergoes extensive hepatic metabolism the dose should be reduced or the dosage interval prolonged in patients with hepatic impairment [45,86]. HYD-induced hepatotoxicity may manifest as hypersensitivity-type injury, acute hepatitis, cholestatic jaundice, hepatocellular injury or centrilobular necrosis [59,86,94,99].

1.7 CLINICAL PHARMACOKINETICS

HYD can be administered orally, intramuscularly or intravenously. Following storage in a syringe for up to 12 hours, discolouration of HYD solution has been observed and therefore caution must prevail when administering HYD intravenously [39,45,55]. HYD reacts with metals and therefore should be prepared, using non-metallic sterile filters, and administered as soon as possible, to avoid reaction with the needle [45,100]. Parenterally administered HYD is used for the management of severe hypertension when oral administration is not possible or when the blood pressure must be lowered immediately [8].

Attempts to describe the pharmacokinetics of HYD have been reported to be complicated due to the instability of HYD and circulating metabolites, in plasma and/or alkaline solutions during analysis [45]. Consequently, many techniques reported for the measurement of HYD that are non-selective yield an overestimation of unchanged HYD. Studies using poorly selective analytical approaches have resulted in an apparent bioavailability, for orally administered HYD, of between 38 and 69% in slow acetylators and 22 to 32% in fast acetylators. In contrast, more selective assays have yielded values of between 31 and 35% or 10 and 16% for slow and fast acetylators, respectively. Pharmacokinetic data have suggested that while the hepatic first-pass effect for HYD is dependent on the phenotype for acetylation, systemic clearance is not dependent on acetylation. The duration of the hypotensive effect of HYD has been reported to exceed that predicted from the rate of elimination considerably, possibly due to the accumulation of HYD at the site of action in the arterial walls or due to the presence of pharmacologically active metabolites [45].

1.7.1 Absorption

HYD, when administered orally, is rapidly absorbed from the GIT [11,101] with a bioavailability of approximately 20-35% in slow acetylators and lower in fast acetylators [11,45,59]. Peak plasma concentrations occur after approximately one hour [45] and the

maximum therapeutic effect occurs between 2 and 4 hours following administration and that persists for up to 24 hours [75].

1.7.2 Bioavailability

Bioavailability is a measurement that indicates both the rate of drug absorption and the total amount of drug that reaches the systemic circulation from an administered dosage form [102,103]. It is measured specifically for an active drug substance without consideration of the presence of metabolites [102]. The bioavailability exhibited by a drug is very important in determining whether a therapeutically effective concentration will be achieved at the site(s) of action [103]. The use of selective assay procedures permits quantitation of a mean fractional bioavailability of approximately 0.30 to 0.35 for slow acetylators and 0.10 to 0.16 for rapid acetylators [81,104]. Food may enhance the bioavailability of HYD [81].

1.7.3 Distribution

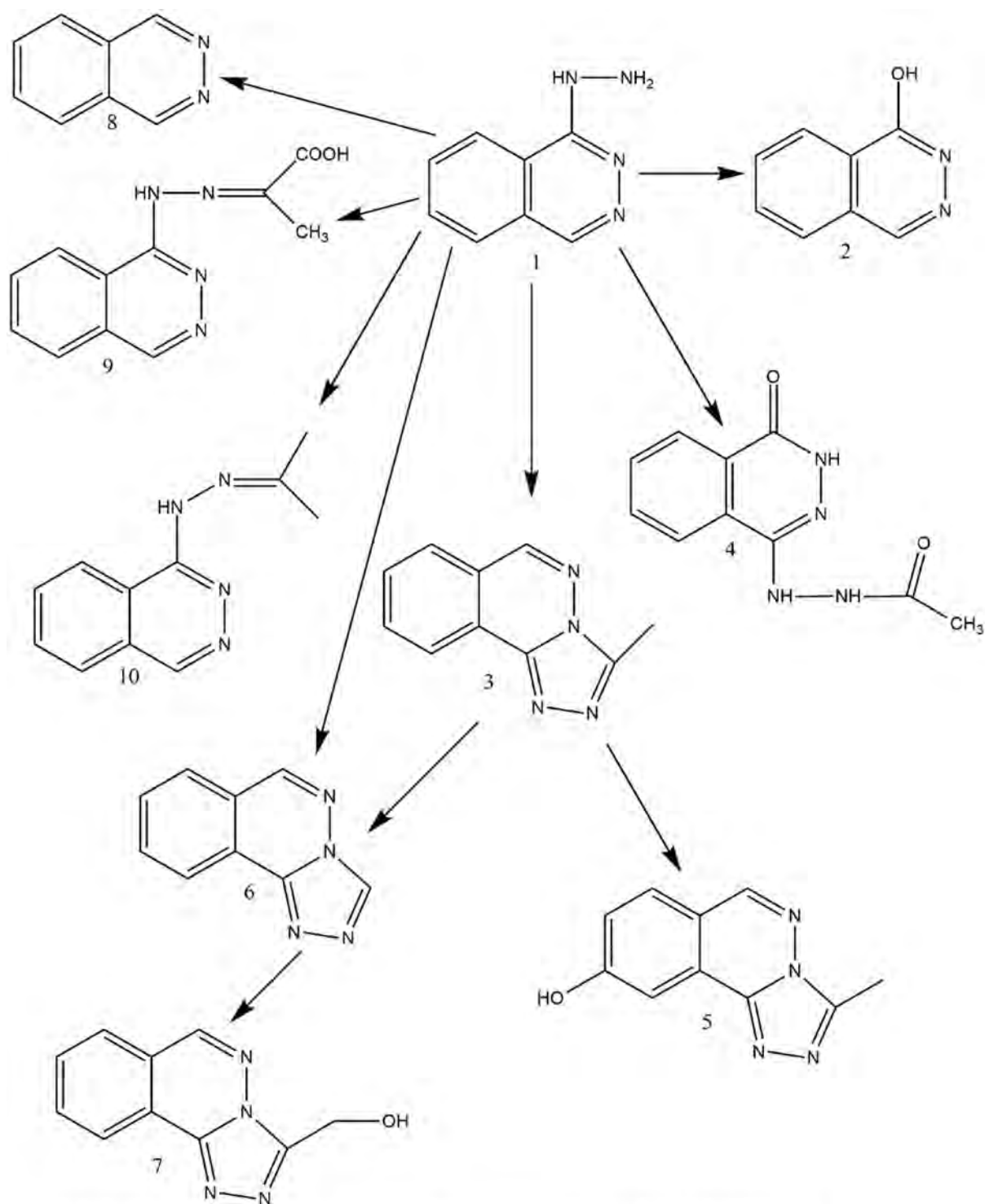
HYD is highly plasma bound [10] to the extent of approximately 87 to 90% [45]. HYD is widely distributed to the liver, kidneys, adrenal glands and lungs. The volume of distribution (Vd) of HYD ranges between 0.5 to 0.9 L/kg and may increase to approximately 7 to 16 L/kg in patients with renal failure [75].

1.7.4 Metabolism

HYD is unstable in plasma, with a half-life of approximately 6 minutes at 37 °C. Studies in healthy volunteers and hypertensive patients indicate that HYD undergoes extensive acetylator phenotype-dependent first-pass metabolism in the liver and GIT mucosa. Systemic metabolism in the liver occurs due to hydroxylation of the ring system and conjugation with glucuronic acid and *N*-acetylation does not appear to be of major importance in systemic clearance of HYD, therefore acetylator status does not appear to affect elimination [11,45]. The metabolism of HYD is not dependent on the rate of acetylation and the half-life does not differ extensively between slow and fast acetylators [37].

The major metabolites of HYD include 3-methyl-1,2,4-triazolo-(3,4a) phthalazine **{3}**, 4-(2-acetylhydrazino) phthalazin-1-one **{4}**, 3-hydroxymethyl-1,2,4-triazolo(3,4a) phthalazine **{5}** and hydralazine pyruvic acid hydrazine **{9}** [37,105]. A schematic of the metabolism of HYD is depicted in Figure 1.5. HYD undergoes oxidative metabolism to form 4-(2-acetylhydrazino)

phtalazin-1-one **{4}** [81]. Acetylation of HYD lead to the formation of 3-methyl-1,2,4-triazolo-(3,4a) phthalazine **{3}** [81]. The acetylation product, 3-methyl-1,2,4-triazolo-(3,4a) phthalazine, can be hydroxylated to form 3-hydroxymethyl-s-triazolo-(3,4a) phthalazine**{5}** [37]. When oxidation precedes acetylation, 4-(2-acetylhydrazino) phtalazin-1-one **{4}** is formed during the metabolism of HYD [81]. A major metabolite recovered from plasma is hydralazine pyruvic acid hydrazine **{9}** that is formed when HYD reacts with pyruvic acid in plasma or blood and the compound has a longer half-life than HYD, however it is not very active [45,59,106]. The rate and extent of metabolism is genetically determined and depends on the acetylator status of individual patients [11,81].



1:Hydralazine, 2: N-(1-phthalazinyl)-hydrozone, 3: 3-methyl-s-triazolo [3,4a] phthalazine
 4: 4-(2-acetylhydrazino)-phthalazinone, 5: 3-hydroxymethyl-s-triazolo[3,4a] phthalazine,
 6: s-triazolo [3,4a] phthalazine, 7: 9-hydroxy-3-methyl-s-triazolo [3,4a] phthalazine, 8:phthalazine, 9: N-(1-phthalazinyl)-hydrozone of pyruvic acid, 10: N-(1-phthalazinyl)-hydrozone of acetone

Figure 1.5 Metabolic pathways of HYD [37]

1.7.5 Excretion

HYD undergoes extensive hepatic metabolism and the metabolites are excreted via the renal route [45,95]. Approximately 65% of the total oral dose is excreted in the urine within 24 hours of dosing. Slow acetylators eliminate 15 to 20% HYD as 4-(2-acetylhydrazino) phthalazin-1-one and 10% as conjugated 3-hydroxymethyl-1, 2, 4-triazolo (3,4a) phthalazine. Fast acetylators eliminate approximately 30% as 4-(2-acetylhydrazino) phthalazin-1-one and 10 to 30% as conjugated (3-hydroxymethyl-1,2,4-triazolo (3,4a) phthalazine in urine. Approximately 10% of a dose is excreted in the faeces [37]. HYD combines with circulating α -keto acids to form hydrazones [59], therefore reducing the excretion of the metabolites of HYD. The elimination half-life of HYD is between 3 and 7 hours [45,73]. The half-life is prolonged in renal impairment and may be as long as 16 hours in patients with a creatinine clearance < 20 mL/minute [45].

1.8 CONCLUSIONS

Adherence has a significant impact on the management and/or treatment of chronic diseases such as hypertension [107]. Adherence is difficult to achieve in asymptomatic hypertensive patients and the growing burden of CVD requires the development and optimisation of novel HYD formulations as an approach to improve the management of patients with hypertension. HYD is a selective vasodilator and is used in the management of hypertension and cardiac failure. Due to its short half-life, HYD is administered two to four times a day [7,45]. The short half-life of HYD and the need for multiple dosing makes the compound a potential candidate for inclusion in controlled release formulations. Furthermore, HYD is unstable in aqueous media and formulation strategies to ensure molecule remains active following administration are necessary. Controlled release formulations may enhance adherence and efficacy since they obviate the need for frequent dosing and reduce plasma level fluctuations [108,109].

Hypertension is universally underdiagnosed and/or inadequately treated in Sub-Saharan Africa [26]. HYD is a relatively cheap API and is widely used in Africa. In South Africa, HYD is supplied as Hyperphen[®] and Sandoz Hydralazine[®] [7]. The manufacture of microspheres may be an approach to address adherence issues currently experienced in South Africa and other Sub-Saharan African countries with the potential to enhance therapeutic outcomes.

CHAPTER 2

DEVELOPMENT AND VALIDATION OF AN RP-HPLC METHOD FOR THE ANALYSIS OF HYDRALAZINE HYDROCHLORIDE

2.1 INTRODUCTION

2.1.1 Overview

Chromatography is a physical technique that is used in the separation of the components of a mixture by a continuous distribution of the components between two phases [110–112]. Chromatography, according to United States Pharmacopeia (USP), can be defined as a procedure by which solutes are separated by a differential migration process in a system consisting of two or more phases, one of which moves continuously in a given direction [110,111]. Separation is achieved due to differences in absorption, partition, solubility, vapour pressure, molecular size or ionic charge density [111]. Liquid chromatography (LC) is a term generally used to describe the separation of components following the differential migration of solutes in a liquid flowing through a column [113,114]. It is now one of the most powerful tools in analytical chemistry due to its ability to separate, identify and quantify compounds that are present in sample mixtures [115] and is continuously being refined and improved [116].

High-performance liquid chromatography (HPLC) is a modern form of LC that uses small particle columns through which the mobile phase is pumped at high pressure [111]. The basic HPLC components are a high-pressure solvent delivery system, a packed column, a sample injector and a detector [117]. The separation of components depends on the extent of interaction between the solute component and the stationary phase [111]. The component that has the lowest affinity for the stationary phase will elute first. HPLC is becoming a preferred method of analysis among various analytical methods for pharmaceuticals as it provides rapid analysis, greater sensitivity, high resolution, easy sample recovery, and precise and reproducible results [111,115]. It is the most accurate analytical method widely used for quantitative, qualitative analysis and determination of drug product stability [115].

The development of selective, sensitive and reliable bioanalytical methods for the quantitative evaluation of drugs and their metabolites in biological matrices is crucial for successful drug development [118]. The objective of these studies was to develop and validate a simple, sensitive, selective, accurate and precise stability-indicating RP-HPLC method for the

quantitation of HYD in dosage forms, to optimise the method using response surface methodology (RSM) and to validate it according to ICH guidelines.

2.2 HIGH PERFORMANCE LIQUID CHROMATOGRAPHY (HPLC)

2.2.1 Fundamental principles of HPLC

Chromatography involves eluting a sample through a stationary phase [119]. Adsorption chromatography is when the stationary phase is solid and the mobile phase is liquid or gas. HPLC is an adsorption type of chromatography [110] and thin layer and paper chromatography are older examples of liquid chromatography (LC), whereas HPLC and Ultra-Performance Liquid Chromatography (UPLC) are modern LC techniques [120,121]. LC is a technique in which the liquid mobile phase facilitates compound separation [122]. Modern LC offers several advantages over older LC methods in terms of convenience, speed and accuracy. Separation is achieved by modifying the mobile phase and changing the stationary phase according to the properties of the analyte of interest [123–125].

HPLC is the most powerful, versatile and widely used elution chromatographic technique [114,126–128]. The technique is used to identify, separate, quantitate and determine species in a variety of organic, inorganic, biological, ionic and polymeric materials [126,129]. Different compounds separate due to solute/stationary-phase interactions. These include liquid-solid adsorption, liquid-liquid partitioning, ion exchange, size exclusion and solute/mobile-phase interactions [130]. HPLC is routinely used for both qualitative and quantitative analyses of environmental, pharmaceutical, nutraceutical, industrial, forensic, clinical and consumer product samples [129,130]. Furthermore, it has been practically used as an analytical tool in cosmetics, industrial chemicals, biotechnology, biomedical, food and biochemical industries [128,129,131].

HPLC is a highly improved form of column chromatography and, instead of allowing the solvent to drip through a column under gravitational force, it is externally forced through the column under high pressures [129]. HPLC methods are diversified according to the type of interactions that occurs between an analyte and a stationary phase and the difference in polarity between the stationary phase and mobile phase. HPLC is divided into two distinct modes, namely normal and reverse phase HPLC [103]. Normal-phase HPLC (NP-HPLC) is mainly used for polar solutes. Non-polar hydrocarbon-soluble solutes are difficult to retain and very polar and water-soluble solutes are difficult to elute sufficiently using normal phase HPLC

[103]. NP-HPLC uses a polar stationary phase and a non-polar mobile phase. Adsorption strengths increase with increased analyte polarity, and the interaction between the polar analyte and the polar stationary phase increases the elution time [132]. NP-HPLC mode of separation is not commonly used for pharmaceutical applications because most of the drug molecules are polar in nature and hence take a longer time to elute [110,133].

2.2.2 Reversed-phase HPLC

Reversed-phase chromatography is when the solute is eluted by a polar mobile phase through a hydrophobic stationary phase [103]. The separation between the stationary phase and the mobile phase is solvophobic [103]. Hydrophobicity of the stationary phase is achieved by bonding a coating onto the silica support and the most common bonded phases are alkyl silanes of C₁₈ (octadecylsilane, ODS), C₈ (octylsilane, OS), and CL (trimethylsilane) [103].

In RP-HPLC, polar compounds have shorter retention times compared to non-polar compounds [103]. The fundamental mechanism involved in RP-HPLC is the adsorption of polar functional groups in the mobile phase onto polar functional groups of the stationary phase [103]. Other factors that affect separation include organic modifier content, flow rate, pH, solvent strength and the type of silica packing [110,134,135].

2.2.3 Mobile phase selection

The HPLC mobile phase is important for transporting compounds through the column and detector [117,136]. The mobile phase, that may either be a single liquid or a mixture of two or more liquids, is pumped at high pressure into a temperature controlled oven, where it first gains entry into an equilibration coil to bring it to the operating temperature [117,137]. The polarity index is the most commonly used tool that has been developed to assist in mobile phase selection [130]. The mobile phases of intermediate polarity can be fashioned by mixing together two or more of the mobile phases [130]. At sufficiently low pH, acidic analytes remain unchanged thereby increasing their retention time (R_t). Conversely, at higher pH neutral basic compounds will be more retained, and ionised acidic compounds will elute faster [110]. The pH of a buffer does not greatly affect the retention of non-ionisable sample components [110,138].

The choice of the buffer is typically governed by the desired pH [110,135,139]. The usual pH range for the reversed-phase on silica-based packing is pH 2 to 8. It is important that the buffer

has a pKa close to the desired pH [110,129,140]. For small molecules, a buffer concentration range of 10 to 50 mM is usually adequate to maintain pH [110,141]. The most commonly used solvents in HPLC are summarised in Table 2.1.

Table 2.1 Common solvents used in reverse phase HPLC (adapted from [129,130,132,142])

| Solvent | Polarity (<i>P'</i>) | UV Cut-off (nm) |
|------------------|------------------------|-----------------|
| Water | 10.2 | 185 |
| ACN | 5.8 | 190 |
| Methanol | 5.1 | 210 |
| Ethyl acetate | 4.4 | 255 |
| Ethanol | 4.3 | 210 |
| <i>n</i> -hexane | 0.1 | 210 |
| Dichloromethane | 3.1 | 205 |
| Diethyl ether | 2.8 | 218 |

2.2.3.1 Buffer selection

Buffers are commonly used in HPLC to maintain a specific pH [135] as ionisation of compounds is affected by pH [112,143,144]. The choice of the buffer is mostly governed by the desired pH and phosphoric acid and its sodium or potassium salts are the most common buffer systems for HPLC [110,129,140]. Table 2.2 shows most commonly used buffers in RP-HPLC and their UV cut-offs.

Table 2.2 Commonly used buffers ([135,140])

| Buffer | pKa | Useful pH range | UV cut-off (nm) |
|----------------------|-----|-----------------|-----------------|
| Phosphoric acid | 2.1 | 1.1-3.1 | <200 |
| Acetic acid | 4.8 | 3.8-5.8 | 210 |
| Trifluoroacetic acid | < 2 | 1.5-2.5 | 210 |
| Formic acid | 3.8 | 2.8-4.8 | 210 |

2.2.4 Column selection

The column type, size and packing affect retention of compounds [145]. Modern HPLC makes use of packing which essentially consists of small and rigid particles with a very narrow particle size distribution [137]. The column is the heart of an HPLC system, thus, choosing the best column requires consideration of stationary phase chemistry, retention capacity, particle size, and column dimensions [115].

The most modern HPLC column packing materials are produced using silica-based matrices as they withstand high pressures generated during HPLC [139]. Silica packing provides high mechanical strength and compatibility with water and most organic solvents but they are not ideal for basic compounds as they contain silanol groups which are acidic in nature. The

interaction between basic compounds and silanol groups results in an increase in R_f and peak tailing [146,147].

2.2.5 Methods of detection

HPLC detectors are designed to analyse some physical or chemical attributes of either the solute or mobile phase in the chromatographic process [148]. The main function of a detector is to monitor the mobile phase coming out of the column, which in turn emits electrical signals that are directly proportional to the characteristics either of the solute or the mobile phase [137]. Numerous detectors have been developed for use in monitoring HPLC separations [130] but the most popular detector is ultraviolet (UV). Many detectors exist which have different valuable performance features [126] but only three types of detectors are summarised in this Chapter.

2.2.5.1 Spectrophotometry

The most common HPLC detectors are based on spectroscopic measurements [130,133]. Spectroscopic detectors range from simple designs to the essentially modified spectrophotometer. When using a UV/Vis detector, the resulting chromatogram is a plot of absorbance as a function of elution time [130]. The limitation of using absorbance is that the mobile phase may strongly absorb at the chosen wavelength [130]. UV-detectors are based on the principle of absorption of UV visible light from the effluent emerging out of the column and passed through a photocell placed in the radiation beam [137]. UV absorption detectors are useful in detecting compounds that absorb light in the UV region [148,149]. In reversed phase chromatography, the solvents usually employed are water, methanol, ACN and tetrahydrofuran (THF), all of which are transparent to UV light over the total wavelength range normally used by UV detectors [149]. All the UV/VIS detectors are based on Beer-Lambert law [126]. UV detectors require the use of a mobile phase with a UV cut-off below the wavelength of the analyte of interest [142]. Spectroscopic detectors are able to measure partial or complete energy absorption or energy emission [117].

2.2.5.2 Fluorescence

Fluorescence detectors (FD) measure the optical emission of light by solute molecules after they have been excited at a higher energy wavelength and can be very sensitive to compounds that have native fluorescence or that can be made to fluoresce through derivatisation [148]. FD

are very specific and selective amongst the other optical detectors and require the use of electrically conductive HPLC mobile phases [126,129]. FD are highly selective because few compounds fluoresce [116,137,149]. The resulting chromatogram is a plot of fluorescence intensity as a function of time [130].

2.2.5.3 Electrochemical

Electrochemical detectors (ECD) are based on electrochemical measurements such as amperometry, voltammetry, conductivity and coulometry [130]. As only a narrow spectrum of compounds undergo electrochemical oxidation, such detectors are quite selective [137,148]. ECD requires three electrodes, which include a working electrode, an auxiliary electrode and a reference electrode [126]. Effluent from the column passes through the working electrode that is maintained at a potential favourable level for oxidising or reducing the compound being analysed. The potential is held constant relative to a downstream reference electrode and the current flowing between the working and auxiliary electrodes is measured [126,130]. The electrical output is an electron flow generated by a reaction that takes place at the surface of the electrodes [149]. ECD is one of the most sensitive and selective HPLC detector available for compounds that can be oxidised or reduced [148].

2.3 RESPONSE SURFACE METHODOLOGY

2.3.1 Overview

Response surface methodology (RSM) is the most popular optimisation method used in recent years [150]. There are so many works based on the application of RSM in pharmaceutical, chemical and biochemical process [150–154]. RSM consists of a group of mathematical and statistical techniques used in the development of an adequate functional relationship between a response of interest, y , and a number of associated control or input variables, x , [155]. The objective of RSM is to optimise response(s), which are influenced by several independent variables. Series of experiments are performed in which changes are made to the input variables in order to identify the reasons for changes in the output response [155].

The application of RSM in the optimisation of analytical procedures is principal because of its advantages to generate a large amount of information from a small number of experiments and the possibility of evaluating the interaction effect between the variables on the response [156]. In order to employ this methodology in experimental optimisation, it is necessary to choose an

experimental design, to fit an adequate mathematical function and to evaluate the quality of the fitted model and its accuracy in relation to the experimental data obtained [156].

The main objective is to optimise the response surface that is influenced by different process parameters. RSM also quantifies the relationships between controllable input parameters and the resultant response surfaces that have been generated [156,157].

2.3.2 Central composite design (CCD)

RSM combined with central composite design (CCD) is an efficient technique for experimentally exploring relationships between investigated factors and system response [158]. CCD enables estimation of the regression parameters to fit a second-degree polynomial regression model to a given response [158].

CCD combines two-level full or fractional factorial designs with additional axial or star points and at least one point at the centre of the experimental region being investigated which allows the determination of both linear and quadratic models [159–161]. The most common optimisation designs are CCD, Box-Behnken, Doehlert, D-optimal and mixture design [160]. CCD is a better alternative to the full factorial three-level design as it employs a smaller number of experiments while providing comparable results [159]. The number of experimental runs for k factors in CCD is $2^k + 2k + \text{centre point replications}$ [160]. CCD optimisation is based on design space, which is the multidimensional combination and interaction of input variables and process parameters which have combinational effects on output variables [160].

Among the various experimental designs, CCD is preferred for prediction of nonlinear responses due to its flexibility in terms of experimental runs [162]. CCD is a symmetrical second-order experimental design most utilised for the development of analytical procedures [156] and therefore it was selected for optimisation studies of the chromatographic conditions.

2.4 PUBLISHED ANALYTICAL METHODS FOR HYDRALAZINE

A number of analytical methods have been developed for the quantitation of HYD in different chromatographic conditions. Prior to the development and validation of an HPLC method, literature review of published HPLC methods was undertaken and summarised in Table 2.3. This information provides a brief overview of the chromatographic methods and provided a basis to undertake preliminary studies for the development of a simple, reliable, economic and

sensitive analytical method with stability-indicating properties. Most reported methods of analysis of HYD were performed on plasma samples and solutions using μ Bondapak columns and spectrophotometric detection methods, using either methanol or ACN as solvents of choice (Table 2.3). Methanol has been reported to increase the viscosity of mobile phase and increase back pressure when mixed with water or buffer [146,147,163], therefore ACN was considered as the preferable solvent for the method development and validation. The mobile phases used are complex and more time consuming during preparation compared to simple buffers like phosphate buffer. A flow rate of 1mL/min was commonly used with a variety of detection wavelengths. Based on the specifications of the column selected for these studies, it is recommended that a phosphate buffer should be used. This may be due to compatibility with the stationary phase in the column selected. The applicability of RSM on HYD was assessed as it has never been used for HPLC method development for HYD.

Table 2.3 Brief summary of published chromatographic methods for analysis of HYD

| Mobile phase | RT (mins) | Sample | Column | Flow rate (mL/min) | Detector | LOD | Internal standard | Ref |
|---|-----------|--------------------------------|--|--------------------|----------|------------|------------------------|-------|
| methanol-2% acetic acid solution (60:40, v/v) | 22 | Solution | PBondapak Phenyl, 10 μ m (Waters) 30 cm x 3.9 mm I.D | 1 | UV 295nm | - | - | [164] |
| methanol: 2% acetic acid solution (60:40, v/v) | 7.4 | Solution | μ Bondapak Phenyl column (30 cm x 3.9 mm I.D., 10 μ m) | 1 | 295 nm | - | 4-methylhydralazine | [165] |
| 66% methanol in 0.055 M citric acid/0.02 M dibasic sodium phosphate (pH 2.5) | <8 | Solution | Supelcosil LC-18-DB (5 μ m) reversed-phase column kept at 28 °C | 1.5 | ECD | - | - | [166] |
| 2.3g of tetraethylammonium perchlorate in 900 mL of distilled water, adding 2 mL acetic acid to the mixture and bringing the final volume to 1litre with methanol. pH of mobile phase was adjusted to 2.7 with acetic acid. | 5.1 | Syrup compound ed from tablets | Supelco Partisil ODS-3 C18 column (250 x 4.6 mm) | 1.4 | UV 254nm | - | Procaine hydrochloride | [167] |
| acetonitrile/5 mM SDS/phosphoric acid (150/850/0.45, v/v/v) | | | 10 μ m ODS stationary phase (Waters μ Bondapak) at room temperature | 2.0 | 220nm | 0.2 ppm | - | [168] |
| MeCN: 1.5mM aqueous phosphoric acid in ratio of 15: 85 | 6.7 | Blood | 10 μ m μ Bondapak phenyl | 2 | 250nm | 1 ng/mL | 4-methylhydralazine | [169] |
| MeCN: 150 mM pH 3.0 sodium acetate buffer 70:30 | 3.5 | Blood | 300 x 3.9 μ Bondapak CN | 2 | UV 365nm | LOQ 1ng/mL | 4-methylhydralazine | [170] |
| MeCN: buffer 80:20, pH 3 (buffer was 0.75% phosphoric acid and 0.5% trimethylamine in water) | 6.4 | Blood | 250 x 4 3 μ m Spherisorb ODS-2 | 0.7 | UV 406nm | 1ng/mL | Methyl red | [171] |
| MeOH: 15mM KH ₂ PO ₄ : glacial acetic acid 0.5:99.4:0.1 | 5 | Tablets | 300 x 3.9 μ Bondapak phenyl | 3 | UV 256nm | - | hydrochlorothiazide | [172] |
| MeOH: buffer 20: 80 (buffer was 7mM sodium heptanesulfonate: 50mM triethylamin adjusted to pH 3.1 wit dilute phosphoric acid 80:20.) | 5 | Tablets | 250 x 4 3 μ m Spherisorb CN | 1 | UV 260nm | - | - | [173] |
| MeCN: 5mM sodium octanosulfonate : phosphoric acid 15:85:0.045 | 10.86 | Tablets | 300 x 3.9 μ Bondapak C18 | 2 | UV 220nm | - | - | [174] |
| MeOH : buffer 15:85 (buffer was 40mM sodium formate and 62 mM formic acid, pH 3.5) | 3.7 | Solution | 150 x 4.6 5 μ m Ultrasphere CN | 1 | UV 258nm | - | phenylephrine | [175] |
| MeCN:0.025% phosphoric acid: buffer 25:10:5 (A) or 60:25:15 (B) (Buffer was | 6.46 (A) | Solution | 250 X 4,6 5 μ m Supelcosil LC-DP (A) or 250 x 4 5 μ m LiChrospher 100 RP-8 (B) | 0.6 | UV 229nm | - | - | [176] |

| | | | | | | | |
|--|----------|----------|--|---|----------|---|-------|
| 9mL concentrated phosphoric acid and 10mL trimethylamine in 900mL water, adjust pH to 3.4 with dilute phosphoric acid, make up to 1L.) | 3.49 (B) | | | | | | |
| acetonitrile-sodium acetate buffer (0.01 A& pH 4) (13:87). | 13 | Solution | μ Bondapak C18 (30 cm x 4 mm I.D.) (Waters). | 1 | UV 240nm | - | [177] |
| Mix 22 volumes of acetonitrile R and 78 volumes of a solution containing 1.44 g/L of sodium lauryl sulphate R and 0.75 g/L of tetrabutylammonium bromide R, then adjust to pH 3.0 with 0.05 M sulfuric acid. | 10-12 | Powder | Size: l = 0.25 m, ϕ = 4.6 mm Stationary phase: nitrile silica gel for chromatography R1 (10 μ m). | 1 | UV 230nm | - | [38] |
| Dissolve 1.44g of sodium dodecyl sulphate and 0.75g of tetrabutylammonium bromide in 770 mL of water, and add 230 mL of acetonitrile. Adjust with 0.1 N sulfuric acid to a pH of 3.0. | 1 | Powder | 4.0-mm x 25-cm; 10- μ m packing L10 | 1 | UV 230nm | - | [39] |

2.5 EXPERIMENTAL

2.5.1 Aim

The main objective of these studies was to develop and validate a simple, e, selective, accurate and precise RP-HPLC method for the quantitation of HYD in pharmaceutical dosage forms.

2.5.2 Materials and reagents

HYD and propranolol (PROP) (internal standard) USP reference standard were purchased from Sigma Aldrich® (St Kouis, MO, USA). Acetonitrile 200 for UV was purchased from Microsep® (Port Elizabeth, South Africa) and 85 % w/v *ortho*-phosphoric acid was procured from Merck® Laboratories (Merck®, Wadeville, South Africa). HPLC grade water was purified using a Milli-RO®-15 A water purification system (Millipore, Bedford, MA, USA) which is made up of a Super-C® carbon cartridge, two Ion-X® ion-exchange cartridges and an Organex-Q® cartridge. The water was filtered through a 0.45 µm Millipak® stack filter prior to use (Millipore, Bedford, MA, USA). NaOH pellets were purchased from Merck Chemicals Ltd (Modderfontein, South Africa). All reagents were at least of analytical grade. Commercial tablets, viz. Hyperphen®-10, Sandoz hydralazine®-25 and Hyperphen®-50 were purchased from Wallace's Pharmacy (Grahamstown, South Africa).

2.5.3 Instrumentation

The modular RP-HPLC system used consisted of a Waters® Alliance Model 2695 separation module equipped with a solvent delivery module, autosampler, online degasser and a Model 2489 UV/Vis Detector (Waters®, Milford, MA, USA). Data acquisition, processing and reporting were achieved using Waters® Empower software (Waters® Milford, MA, USA). The stationary phase was a Nucleosil® 100-10 C₈ column 250 mm x 4 mm i.d x 10 µm (Macherey-Nagel®, Düren, German). A Crison GLP21 pH meter (Crison Instruments, Johannesburg, South Africa) was used in all studies to monitor pH, a Colora® ultra-thermostat water bath (Colora®, Lorch, Germany) was used for stress testing studies to maintain temperature and an Atlas SUNTEST® CPS+ (Lisengericht, Germany) was used for photolytic degradation studies.

2.5.4 Preparation of buffer solutions and mobile phase

During the design of experiment (DoE), different buffer molarities were prepared by pipetting specific volumes of the 85% w/w *ortho*-phosphoric acid into a 1000 mL A-grade volumetric

flask. HPLC grade water was added to the 1000 mL mark and the pH was adjusted to pH=3 with 0.1M NaOH solution using a Crison Model GLP21 pH meter (Crison Instruments, Barcelona, Spain). Different molarity and pH were used to obtain an optimised buffer solution with desired R_t and less tailing and/or fronting. The optimal buffer was found to be a 5mM phosphate buffer adjusted to pH of 3 using a 0.1M NaOH. The buffer prepared was filtered through a Millipore[®] HVLP 0.45 μ m filter membrane (Merck Millipore[®] Ltd, Cork, Ireland) with the aid of an Eyela[®] Aspirator A-2S vacuum pump (Rikakikai[®] Co. Ltd, Tokyo, Japan) and degassed for 20 minutes using a Branson[®] B12 ultrasonic bath (Shelton, CN, USA). The mobile phase was prepared on a daily basis.

The mobile phase consisted of 5mM phosphate buffer solution adjusted to pH=3 (using 0.1M NaOH) and ACN mixed online. The buffer solutions were filtered using a 0.45 μ m membrane filter and degassed under vacuum using an Eyela[®] Aspirator A-2S vacuum pump, whilst ACN was neither filtered nor degassed as it was of HPLC grade.

2.5.5 Chromatographic conditions

The separation of peaks was achieved using a Waters[®] Alliance system with a 2489 UV/Vis Detector set at 240 nm on a Nucleosil[®] 100-10 C₈ 250 mm x 4.0 mm i.d. x 10 μ m stationary phase and mobile phase consisting of a mixture of ACN and 5mM phosphate buffer (pH=3) in a 65:35% v/v ratio. The HPLC system was operated in isocratic mode at a flow rate of 0.8 mL/min and a column temperature of 25.0 ± 0.5 °C.

2.6 METHOD DEVELOPMENT

Analytical method development is the process of creating a procedure to enable a compound of interest to be identified and/or quantified in a matrix. A compound can often be measured by several methods and the choice of the analytical method involves many considerations such as chemical properties of the analyte, concentration levels, sample matrix, the cost of the analysis, the speed of the analysis, quantitative or qualitative measurement, the precision required and necessary equipment [178].

The initial steps include collecting information about the analyte with regard to the physicochemical properties and determining which mode of detection would be suitable for analysis. Sample preparation, which includes centrifugation, filtration, and/or sonication, plays an integral role in method development because this may affect the chromatography and the

recovery of the analytes. Determination of the solution stability in the diluent is also important during early method development. If the solution is not stable, it will become increasingly more challenging to compare subsequent method development analysis. The type of stationary phase is very important mainly with regard to bonded phase stability at the operational mobile phase pH. Different stationary phases can provide differences in selectivity [141].

A good method development strategy should require only as many experimental runs as are necessary to achieve the desired result(s) [131]. The aim of these studies was to develop an RP-HPLC method for analysis of HYD. The most important outcomes for method development are optimal resolution and the asymmetric factor [179].

2.6.1 Column selection

Bonded columns, *viz.* C₁₈, C₈ and Octyl, are the commonly used HPLC columns [133]. Appropriate column and mobile phase selection are critical in HPLC [180] as these can lead to the production of a good chromatographic separation which in turn provides an accurate and reliable analysis [115]. The type of column chosen for a particular separation depends on the compound and the aim of analysis [110]. Choosing the best column for application requires consideration of stationary phase chemistry, retention capacity, particle size and column dimensions [115,180]. Column selection is the first and the most important step in method development that can have significant consequences on the effectiveness of the separation [115,138,181]. The development of a reproducible method is impossible without the availability of a high performance column [115].

Most columns listed in section §2.4 were not available or accessible and the mobile phases were complex, therefore different columns were tested for the analysis of HYD with the main goal of retaining HYD within 10 minutes and an asymmetric factor of < 1.5. After trying many columns, the best column was found to be Nucleosil® 100-10 C₈ (250 mm x 4 mm i.d, 10µm) with a non-complex mobile phase and a R_t within 10 minutes. The results in Table 2.4 show some columns that were tried for the analysis of HYD. The selection was mainly according to R_t and tailing of HYD. The trial and error method was used during these studies.

Table 2.4 Summarised column selection studies for HYD

| Column | Conditions | HYD R_t (min) | HYD Tailing | Comments |
|---|---|--------------------|----------------|---|
| Luna® 5u C18 250 x 4.6 mm | Phosphate buffer (20%) pH=3 and ACN (80%) Flow rate 0.6 mL/min and Temperature 25 °C | 3.7 | 2.5 | Peak broadening and tailing more than 1.2. |
| Spherisorb® S5 ODS2 250 x 4.0 mm | Phosphate buffer (20%) pH=3 and ACN (80%) Flow rate 1 mL/min and Temperature 25 °C | 8.9 | 6.8 | Peak broadening of HYD and tailing greater than 1.2 |
| Spherisorb® 5µ ODS 4.6 x 250 mm | Phosphate buffer (20%) pH=3 and ACN (80%) Flow rate 0.8 mL/min and Temperature 25 °C | 6.0 | 3.6 | Tailing greater than 1.2 and peak broadening observed. |
| Novapak® C18 150 x 3 mm | Phosphate buffer (20%) pH=3 and ACN (80%) Flow rate 0.6 mL/min and Temperature 25 °C | 1.5 | 5.6 | HYD eluted too quickly with tailing greater than 1.2 |
| Synergi® 150 x 3 mm | Phosphate buffer (20%) pH=3 and ACN (80%) Flow rate 1 mL/min and Temperature 25 °C | 1.3 | 1.4 | HYD eluted quickly |
| Nucleosil® 100-10 C ₈ (250 mm x 4mm i.d., 10 µm) | Phosphate buffer (20%) pH=3 and ACN (80%) Flow rate 0.6 mL/min and Temperature 25 °C | 3.1 | 1.4 | Peak asymmetric and tailing close to 1.2. This column was selected for optimisation studies |

2.6.2 Column evaluation and specifications

Quality assurance of the new column was performed before any analyses were undertaken using the column. Column quality was measured with respect to the number of theoretical plates, R_t and column pressure for phenol and naphthalene. The chromatographic conditions for column quality testing are summarised in Table 2.5.

Table 2.5 Chromatographic conditions for quality assurance of the column

| | |
|--------------------------------|---|
| Column | Nucleosil® 100-10 C ₈ (250mm x 4mm i.d.) |
| Mobile phase conditions | Acetonitrile: water (80:20) |
| Column pressure | 30 bars |
| Injection volume | 4.0 µL |
| Detection | 254 nm |
| Temperature | RT (22 °C) |
| Flow rate | 1.00 mL/min |

The R_t for phenol and naphthalene were found to be 2.5 and 3.1 with USP plate counts of 10125 and 10106 respectively. The retention times were found to be the same as indicated in the quality assurance certificate and met the required criteria. The pressure was found to be around 32 to 40 bars which was close to the specified column pressure of 30 bars.

2.6.3 System suitability testing

2.6.3.1 Number of theoretical plates (N)

According to Martin and Synge [182], a chromatographic system consists of discrete layers of theoretical plates [110]. Plate count (N) is a measure of the quality of separation [183] and measures the efficiency of the column. The nature, shape and particle size of the silica support effects separation [115,139]. Smaller particles result in a greater N and an increase in back pressure during chromatography [139,184]. Several methods have been developed to calculate N but all these are based on the general formula shown in Equation 2.1 [136]. N is also referred to as column efficiency and is an indirect measure of peak width for a peak at a specific R_t . Columns with high plate numbers are considered more efficient and have higher column efficiency compared to those with a lower plate count. A column with a high number of theoretical plates will have a narrower peak at a given R_t than a column with a lower N [113].

$$N = \sigma \left(\frac{V_r}{W} \right)^2 \quad \text{Equation 2.1}$$

Where,

N - Number of theoretical plates

V_r - Retention volume

W - Peak width

Due to tailing of the drug, the 5σ method was used to calculate N . The 5σ method used in calculating N is shown in Equation 2.2.

$$N = 25 \left(\frac{V_r}{W_{5\sigma}} \right)^2 \quad \text{Equation 2.2}$$

Where,

N - Number of theoretical plates

V_r - Retention volume

$W_{5\sigma}$ - Peak width at 4.4% of the peak height

In general, N should be > 2000 [111,185,186]. The efficiency of the column was determined by injecting 100 $\mu\text{g/mL}$ HYD and 50 $\mu\text{g/mL}$ PROP using optimised chromatographic conditions shown in §2.6.6, at a flow rate of 0.8 mL/min using an injection volume of 10 μL , and a wavelength of 240 nm at a temperature of 22 $^{\circ}\text{C}$. Uracil was used to obtain the void

volume. The average N for HYD and PROP, using the USP plate count method, were found to be approximately 5289 and 6190 respectively, which are all well above 2000. N was monitored every three months to ensure the quality of the column as it is usually constant for a peak and mainly affected by particle size and packing [187].

2.6.3.2 Peak tailing factor (A_s)

The peak tailing factor (A_s) is also referred to as the peak symmetry factor and is important for peak shape assessment. A chromatographic peak is assumed to have a Gaussian shape under ideal conditions [185], however there is always a deviation from a normal distribution which indicates a non-uniform migration and non-uniform distribution process. Peak tailing should normally be between 1.0-1.5 and values > 2 are unacceptable as they affect the quantitative analysis process as it affects peak integration [188]. The peak asymmetry is computed by utilising Equation 2.3 [185].

$$A_s = \frac{B}{A} \quad \text{Equation 2.3}$$

Where,

A_s - peak asymmetry factor

B - distance from the point at peak midpoint to the trailing edge (measured at 10% of peak height)

A - distance from the leading edge of peak to the midpoint (measured at 10% of peak height)

Equation 2.3 can be used to determine peak shape, peak tailing as well as peak fronting. Peak tailing and fronting affect accuracy and precision. Ideally, tailing should be ≤ 1.5 [186,189]. If the value is 1, then there is no tailing. If the value is > 1 , then it indicates that there is tailing. If the value is < 1 , then it indicates that there is fronting. The asymmetry factor of HYD and PROP were calculated using Equation 2.3 and were found to be approximately 1.3 and 1.1 respectively, which were deemed suitable and acceptable for chromatographic analysis.

2.6.3.3 Resolution factor (R_s)

Resolution is a parameter describing the separation power of the complete chromatographic system relative to the particular components of the mixture [110,119]. R_s is an indication of how two or more peaks are separated on a chromatogram and indicates the degree and quality of separation between components in a mixture [139]. R_s should be ≥ 2 [185,189,190]. Values less than 1.5 indicate poor resolution and are therefore unacceptable. Equation 2.4 was used to

determine the resolution of the internal standard (IS) and the drug of interest [119,136,185]. R_s was calculated using Equation 2.4 and was found to be approximately 5.8 which is above 2 indicating that the HYD and PROP peaks were well resolved.

$$R_s = \frac{V_2 - V_1}{0.5(W_1 + W_2)} \quad \text{Equation 2.4}$$

Where,

R_s - Resolution factor

V_2 - Elution volume of compound 2

V_1 - Elution volume of compound 1

W_2 - Peak width of compound 2 at baseline

W_1 - Peak width of compound 1 at baseline

2.6.3.4 Capacity factor (K')

Capacity factor (K') or retention factor is defined as the ratio of the number of molecules of solute in the stationary phase to the number of molecules of the same in the mobile phase [110,185]. It is a measure of the R_t of the peak of interest relative to the void volume or the R_t of an unretained compound and it ranges from 2-10 [110,185]. However, in HPLC it is usually kept between 1 and 10 [127]. K' was determined using Equation 2.5 and was found to be approximately 2.6 when uracil was used as the unretained compound, and thus the column was deemed appropriate for chromatographic use.

$$K' = \frac{V_1 - V_0}{V_0} \quad \text{Equation 2.5}$$

Where,

K' - Capacity factor

V_0 - Void volume or R_t of an unretained peak

V_1 - Retention volume of the analyte

2.6.3.5 Selectivity factor (α)

Selectivity factor (α) is equivalent to the relative retention of the solute peaks and depends strongly on the chemical properties of the chromatography medium [112,131]. Selectivity can be changed by modifying mobile phase composition [112,131]. It measures peak separation of compounds. Equation 2.6 shows how the selectivity factor can be determined between two compounds. The selectivity factor of HYD and PROP was found to be 1.6, which is > 1 , so the column was deemed appropriate for separation of the compounds.

$$\alpha_{1,2} = \frac{K'_{12}}{K'_{11}} \quad \text{Equation 2.6}$$

Where,

$\alpha_{1,2}$ - Selectivity of compound 1 and compound 2

K'_{12} - Retention factor of compound 2

K'_{11} - Retention factor of compound 1

The system suitability parameters monitored in method development are summarised in Table 2.6. The chromatographic conditions met all the requirements, therefore the method was further optimised and validated.

Table 2.6 Summary of chromatographic system suitability parameters for the proposed method

| Factor | Acceptable range | Value |
|----------|------------------|-----------------------|
| N | > 2000 | HYD-5289 PROP-6190 |
| A_s | < 2 | HYD- 1.3 PROP- 1.1 |
| K' | ≥ 2.0 | 2.6 |
| α | > 1 | 1.6 |
| R_s | ≥ 2.0 | 5.8 |

2.6.4 Internal standard selection

Quantitation using the IS method improves the precision and accuracy of results where volume errors are difficult to predict and control [191]. The IS usually is selected on the basis of its similarity in physicochemical properties to those of the analyte of interest [192]. The internal standard is selected on the basis that it does not interfere with the analyte of interest, and it should be pure, stable and must be monitored at the same wavelength [192,193]. It should not elute at the same time as that of the analyte. The IS method outperforms the external standard method regardless of the analyte, choice of IS, method of introduction of IS and the injection volume [193]. The volume of sample injected may fluctuate during analysis, hence it is necessary to consider using an IS to eliminate such fluctuations in order to reduce errors and improve precision [142,194].

IS selection was performed by evaluating different drugs that could absorb UV at the same wavelength of HYD. The drugs were selected on a trial and error basis. The IS selection criteria were limited to the number of drugs readily available and accessible. Theophylline, caffeine, paracetamol, hydrochlorothiazide (HCTZ), salicylic acid, carbamazepine (CBZ) and PROP were selected and assessed. All the drugs were of USP grade and the results obtained are summarised in Table 2.7. A mobile phase composition of 5mM buffer and ACN (35:65) was

used at a flow rate of 0.8 mL/min using the same wavelength of HYD. PROP and CBZ were potential IS but PROP was the best IS as it had a $R_t < 10$ minutes and a sharp asymmetric peak. PROP was selected based on resolution, R_t , retention factor and peak tailing parameters.

Table 2.7 Evaluation of internal standard retention time and peak tailing

| Internal standard | R_t (mins) | Peak shape and tailing | R_s | Comments |
|---------------------|--------------|--|-------|--|
| Caffeine | > 15 | - | - | Not a good IS because of long run time expected. |
| Paracetamol | 2.9 | - | 0 | Not a good IS because retention time was too close to that of HYD and no resolution was observed. Too close to void as well. |
| Salicylic acid (SA) | 4.3 | Tailing of 3.6 and broad peak observed | 8.0 | Good resolution but peak tailing should be less than 1.2, therefore SA can be a potential standard as long as the peak tailing is reduced. |
| Theophylline | - | - | - | Did not elute after 15 minutes |
| HCTZ | 3.8 | Fronting of the peak (3.3) | 6.4 | Potential IS if fronting is resolved and if tailing is reduced to 1.2. |
| CBZ | 5.6 | Fronting was observed (3.1) | 2.9 | Potential IS if fronting is resolved and if tailing is reduced to less than 1.2. |
| PROP | 8.6 | Sharp peak with less tailing (1.1) | 4.5 | Both retention time and peak shape were found to be ideal, therefore propranolol was found to be the best internal standard. |

2.6.5 HPLC apparatus

The modular RP-HPLC system used consisted of an Alliance Waters E2695 Separations Module and a 2489 UV/Vis Detector (Milford, USA). Data was captured using the Empower[®] monitoring system. The separation was achieved using Nucleosil[®] 100-10 C₈ (250 mm x 4 mm i.d x 10 μ m) stationary phase.

2.6.6 Method of detection

The choice of detector depends on the chemical nature of the analyte, potential interference, detection limit required, availability, accessibility and cost [110,135]. RP-HPLC is most frequently coupled with UV detectors because of their convenience and applicability for most organic samples [148,184,195].

A 100 μ g/mL HYD solution in ACN: Water (50:50% v/v) was prepared and scanned over a wavelength of 210 – 400 nm using a 2998 Photodiode array (PDA) Detector (Milford, USA). As shown in Figure 2.1, HYD maximum absorption occurred at wavelengths of 210, 234, 240, 260 and 315 nm. A solution of a mixture of HYD and PROP was also scanned over the wavelength of 210 – 400 nm using a PDA detector and it was observed that PROP absorbs

more UV at 240 nm compared to other maximum absorption wavelengths of HYD, viz. 210, 234 and 260 nm. As shown in §2.4, most published methods used UV detectors. A wavelength of 240nm was selected for further studies during the HPLC method development and the wavelength was above the UV cut-off wavelengths of water and ACN.

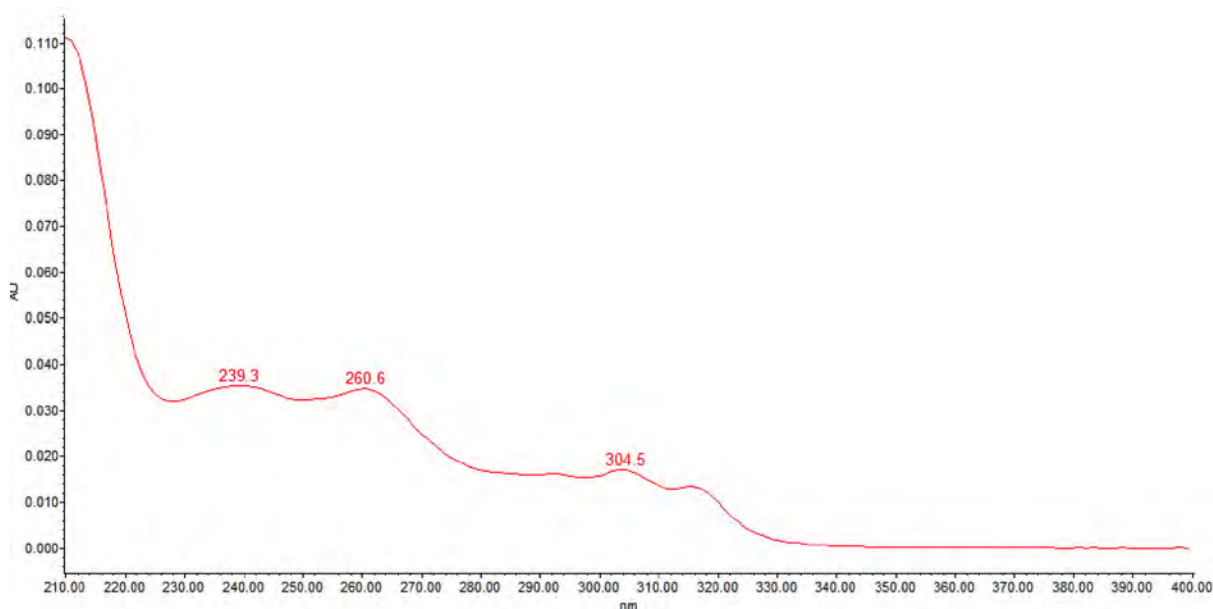


Figure 2.1 Typical UV spectrum of HYD obtained using a PDA detector from 210–400 nm wavelength

2.7 METHOD OPTIMISATION

2.7.1 Chemicals and reagents

All chemicals used in these studies were of analytical reagent grade. HYD was purchased from Sigma Aldrich® (St Louis, USA). HPLC grade far UV ACN and 85% w/v *ortho*-phosphoric acid were purchased from Microsep (Port Elizabeth, South Africa) and Merck® Laboratories (Wadeville, South Africa) respectively. NaOH solution was prepared by dissolving 0.4 g of NaOH pellets (Gauteng, South Africa) in 100 mL of HPLC grade water. 5mM phosphate buffer was prepared by measuring 342 µL using a 1000 µL pipette into a 1000 mL A-grade volumetric flask to which HPLC grade water was added to the mark.

2.7.2 Central composite design

A CCD approach was used to optimise the developed method by varying independent variables and evaluating their effects on R_t , tailing and resolution of HYD and PROP. The independent variables were ACN composition (x_1), buffer molarity (x_2), buffer pH (x_3) and flow rate (x_4). The dependent variables include R_t , tailing and resolution of HYD and PROP. After

establishing the range of values of independent variables, they were coded into factorial, centre and axial points. A randomised full factorial design was used, in which the four factors were evaluated at five levels ($-\alpha$, $+\alpha$, -1, 0 and +1) with six replicates at the centre point as summarised in Table 2.8. Analysis of variance (ANOVA) was used to analyse the data.

Table 2.8 Translation of the coded levels used in CCD

| Independent factors | Level | | | | |
|---------------------|-----------|-----|------|-----|-----------|
| | $-\alpha$ | -1 | 0 | +1 | $+\alpha$ |
| Acetonitrile % | 10.0 | 20 | 40.0 | 60 | 80.0 |
| Buffer molarity mM | 5.0 | 20 | 35.0 | 50 | 65 |
| Buffer Ph | 2.0 | 3.0 | 4.0 | 5.0 | 6.0 |
| Flow rate mL/min | 0.25 | 0.5 | 0.75 | 1 | 1.25 |

Due to experience, the upper and lower limits for the x_1 were 20 and 60% v/v respectively. For x_2 , the upper and lower limits were set at 20 and 50mM respectively. For x_3 , the upper and lower limits were set at 3.0 and 5.0 respectively, which were ± 1 of the centre buffer pH. The x_4 upper and lower limits were 0.5 and 0.75 mL/min respectively. The experimental conditions for CCD were selected after a series of trial and error experiments were performed and are summarised in Table 2.9. The responses monitored were R_t of both HYD and PROP, peak tailing and resolution, which were considered as critical responses. The experiments were performed randomly in order to eliminate any possible experimental bias and the resultant HPLC data were analysed using Design Expert[®] version 8.0.2 software (Stat-Ease Inc., Minneapolis, MN, USA). ANOVA was used to assess the significance of the factors investigated. The influence and any correlation between the independent and responses were best explained using contour, 3D Response Surface plots and quadratic polynomial equations.

Table 2.9 Experimental conditions for CCD runs

| Experimental run | Standard run | Type | ACN (%) | Buffer molarity (mM) | pH | Flow rate (mL/min) |
|------------------|--------------|-----------|---------|----------------------|-------|--------------------|
| | | | x_1 | x_2 | x_3 | x_4 |
| 21 | 1 | Axial | 40 | 35 | 2 | 0.75 |
| 20 | 2 | Axial | 40 | 65 | 4 | 0.75 |
| 22 | 3 | Factorial | 40 | 35 | 6 | 0.75 |
| 29 | 4 | Centre | 40 | 35 | 4 | 0.75 |
| 4 | 5 | Factorial | 60 | 50 | 3 | 0.5 |
| 11 | 6 | Factorial | 20 | 50 | 3 | 1 |
| 7 | 7 | Factorial | 20 | 50 | 5 | 0.5 |
| 23 | 8 | Factorial | 40 | 35 | 4 | 0.25 |
| 18 | 9 | Factorial | 80 | 35 | 4 | 0.75 |
| 24 | 10 | Factorial | 40 | 35 | 4 | 1.25 |
| 8 | 11 | Factorial | 60 | 50 | 5 | 0.5 |
| 27 | 12 | Centre | 40 | 35 | 4 | 0.75 |
| 9 | 13 | Factorial | 20 | 20 | 3 | 1 |
| 19 | 14 | Factorial | 40 | 5 | 4 | 0.75 |
| 28 | 15 | Centre | 40 | 35 | 4 | 0.75 |
| 1 | 16 | Factorial | 20 | 20 | 3 | 0.5 |
| 25 | 17 | Centre | 40 | 35 | 4 | 0.75 |
| 15 | 18 | Axial | 20 | 50 | 5 | 1 |
| 5 | 19 | Axial | 20 | 20 | 5 | 0.5 |
| 17 | 20 | Factorial | 10 | 35 | 4 | 0.75 |
| 2 | 21 | Axial | 60 | 20 | 3 | 0.5 |
| 3 | 22 | Axial | 20 | 50 | 3 | 0.5 |
| 14 | 23 | Axial | 60 | 20 | 5 | 1 |
| 26 | 24 | Centre | 40 | 35 | 4 | 0.75 |
| 10 | 25 | Factorial | 60 | 20 | 3 | 1 |
| 13 | 26 | Axial | 20 | 20 | 5 | 1 |
| 30 | 27 | Centre | 40 | 35 | 4 | 0.75 |
| 6 | 28 | Factorial | 60 | 20 | 5 | 0.5 |
| 12 | 29 | Axial | 60 | 50 | 3 | 1 |
| 16 | 30 | Factorial | 60 | 50 | 5 | 1 |

2.7.3 Model fitting and statistical analysis

Since the relationship between a response and their independent variables can be linear or nonlinear based on the experimental results, it is important to check the best relationship that represents the response and independent variable data. This should be done by checking the fit summary. The fit summary tells the best relationship (linear, two-factor interaction, quadratic, logarithmic, etc.) between the response and its independent variables based on the experimental results [196].

One useful statistical outcome is the adequate precision which measures the ratio of the range of variation in the predicted response to an estimate of the standard error of the predictions [196]. A high value indicates that the variation is large in relation to the underlying uncertainty of the fitted model [196].

Another useful statistical tool is the p -value which is obtained from the ANOVA table of the model and should be observed to be less than 0.05 for the model to be significant [196]. So the

p -value represents the significance of a result, and the smaller the p -value the more significant the factor is [196]. The F -values, which are tests of comparing models and their terms with a residual variance, are calculated for a model and its terms by dividing the respective mean square of the model and its terms with a residual mean square [196]. The statistic to check for model adequacy in the ANOVA table includes lack of fit, R^2 , adjusted R^2 , predicted R^2 and adequate precision. Lack of fit statistic represents how data fit the model. For model adequacy, lack of fit should be insignificant [196].

The results obtained were analysed using ANOVA, Box-Cox, normal plots of residuals and plots analysis with reference to the effect of ACN (x_1), phosphate buffer molarity (x_2), buffer pH (x_3) and flow rate (x_4). The effect of injection volume was analysed after obtaining the optimal chromatographic conditions so as to determine the best injection volume to be used for analysis.

2.7.3.1 Retention time of HYD

Statistical analyses were used to generate second-order quadratic equations that best fitted the experimental data and for the prediction of responses. The model F -value of 21.80 and p -value of < 0.0001 generated for HYD retention time (y_1) indicates that the model was significant. The buffer pH and flow rate were significant on HYD peak tailing with F -values of 57.84 (p -value < 0.0001) and 237.59 (p -value < 0.0001) respectively. The ACN composition and buffer molarity were insignificant for y_1 with F -values of 2.86 and 1.95 and p -values of 0.1113 and 0.1832 respectively. Table 2.10 shows the ANOVA results for R_t of HYD.

Table 2.10 ANOVA for retention time of HYD

| Source | Sum of Squares | Df | Mean Square | F-Value | p-Value Prob > F | Comments |
|------------------------|----------------|----|-------------|------------|---------------------|-----------------|
| Model | 3.33 | 14 | 0.24 | 21.80 | < 0.0001 | Significant |
| x_1 -CAN | 0.031 | 1 | 0.031 | 2.86 | 0.1113 | |
| x_2 -Buffer molarity | 0.021 | 1 | 0.021 | 1.95 | 0.1832 | |
| x_3 -pH | 0.63 | 1 | 0.63 | 57.84 | < 0.0001 | Significant |
| x_4 -Flow rate | 2.60 | 1 | 2.60 | 237.59 | < 0.0001 | Significant |
| x_1x_2 | 2.086E-003 | 1 | 2.086E-003 | 0.19 | 0.6683 | |
| x_1x_3 | 7.046E-005 | 1 | 7.046E-005 | 6.451E-003 | 0.9370 | |
| x_1x_4 | 1.381E-003 | 1 | 1.381E-003 | 0.13 | 0.7271 | |
| x_2x_3 | 1.003E-003 | 1 | 1.003E-003 | 0.092 | 0.7661 | |
| x_2x_4 | 1.096E-003 | 1 | 1.096E-003 | 0.10 | 0.7558 | |
| x_3x_4 | 3.831E-004 | 1 | 3.831E-004 | 0.035 | 0.8540 | |
| x_1^2 | 0.015 | 1 | 0.015 | 1.35 | 0.2634 | |
| x_2^2 | 0.020 | 1 | 0.020 | 1.86 | 0.1924 | |
| x_3^2 | 2.493E-003 | 1 | 2.493E-003 | 0.23 | 0.6397 | |
| x_4^2 | 3.348E-003 | 1 | 3.348E-003 | 0.31 | 0.5880 | |
| Residual | 0.16 | 15 | 0.011 | | | |
| Lack of Fit | 0.10 | 10 | 0.010 | 0.85 | 0.6152 | Not significant |
| Pure Error | 0.061 | 5 | 0.012 | | | |
| Cor Total | 3.50 | 29 | | | | |

The standard deviation should be as small as possible to indicate the precision of the design space. The Predicted R^2 of 0.8051 is in reasonable agreement with the Adjusted R^2 of 0.9094 for y_1 , indicating that the model fits the expectation and that it can be used to navigate the design space in the region presented. R^2 is not a good statistic since its value can be artificially inflated by adding insignificant model terms [196]. Adjusted R^2 is a better statistical measure of the amount of observed variability in the response since its value will only increase if the additional terms are statistically significant [196]. The PRESS value should be as small as possible and a small value of 0.68 indicate that the model is appropriate for the analysis of y_1 . Adequate precision measures the signal to noise ratio and should be > 4 . The adequate precision for y_1 was 17.798 indicating an adequate signal for the design space and therefore this model is adequate to navigate the design space. Table 2.11 shows the statistical analysis results for y_1 of HYD.

Table 2.11 Statistical analysis for HYD retention time

| Parameter | Value |
|--------------------|--------|
| Standard deviation | 0.10 |
| Mean | 1.53 |
| C.V. % | 6.81 |
| PRESS | 0.68 |
| R^2 | 0.9531 |
| Adjusted R^2 | 0.9094 |
| Predicted R^2 | 0.8051 |
| Adequate Precision | 17.798 |

The quadratic equation that was generated following fitting of experimental data represents the quantitative values for coefficients of independent variables. The HPLC independent variables

and quadratic terms with positive coefficients were directly proportional, whereas the negative terms have an inverse relationship to the response. The quadratic equation for y_1 is shown in Equations 2.7.

$$y_1 = 1.54 - 0.036x_1 - 0.030x_2 + 0.16x_3 - 0.33x_4 - 0.011x_1x_2 - 2.099e^{-003}x_1x_3 - 9.292e^{-003}x_1x_4 + 7.916e^{-003}x_2x_3 - 8.275e^{-003}x_2x_4 + 4.893e^{-003}x_3x_4 + 0.023x_1^2 - 0.027x_2^2 - 9.533e^{-003}x_3^2 + 0.011x_4^2 \quad \text{Equation 2.7}$$

The adequacy of the derived models should be investigated before drawing conclusions from ANOVA since no matter how accurate experimental trials may be conducted, experimental errors (or residuals) still occur [196]. The residual from the least squares fit is important in judging model adequacy. A check of normality assumption may be made by constructing a normal probability plot of residuals as shown in Figure 2.2. If the normal probability plot of residuals are approximately along a straight line, then the normal assumption is satisfied. Figure 2.2 satisfies the normal assumption as the values are approximately along the straight line.

The normal probability plot of residuals for y_1 revealed that the data points were distributed along a straight line indicating that the error was equally distributed across each individual point. The normal plot of residuals indicates a linear type of response, which is also shown by a high R^2 value of 0.95 which is close to 1 and denotes a high degree of correlation.

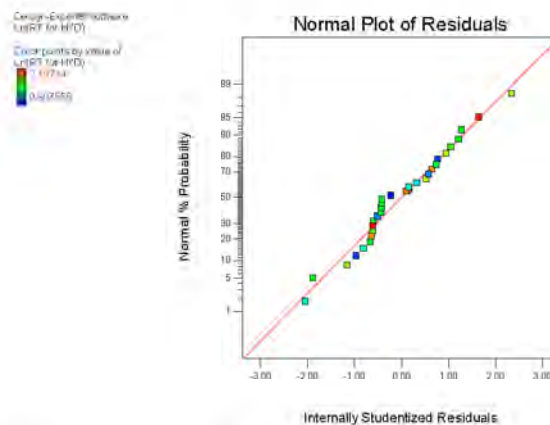


Figure 2.2 Normal probability plots of residuals for HYD retention time

Figure 2.3 shows a plot of residuals versus predicted response. When the residuals are scattered randomly on the display, it suggests that the variance of the original observations is constant throughout the values of the response. However, if the residuals are not randomly scattered,

the model should be transformed. Non-random patterns indicate the inadequacy of such a model which can be resolved by model transformation.

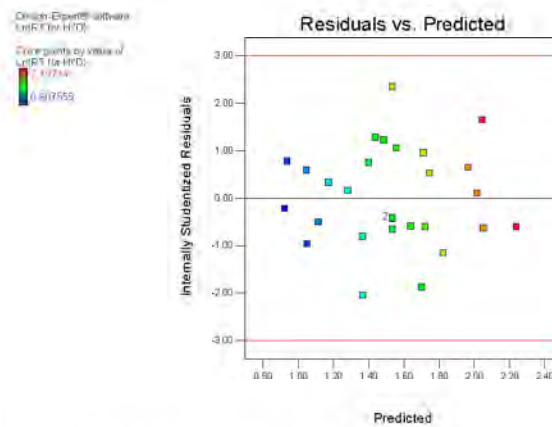


Figure 2.3 Plot of residuals versus predicted for HYD retention time

The plot of predicted versus actual values in Figure 2.4 reveals that all points fall nearly in the same region, confirming that the model can be used to predict response values like retention time for the independent input values, x_1 , x_2 , x_3 and x_4 .

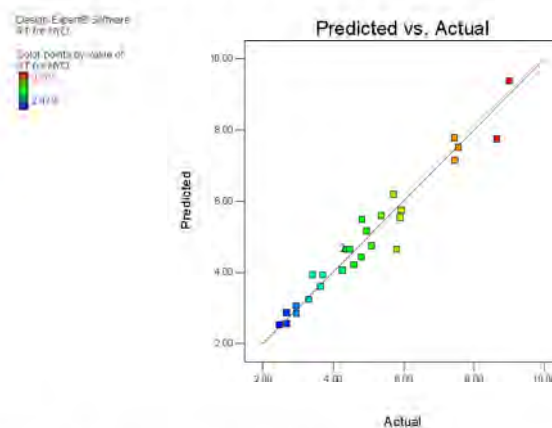


Figure 2.4 Plot of predicted versus actual responses for HYD retention time

Box-Cox plots are statistically valid and meaningful tools that help determine the most appropriate power transformation to apply to response data. This is usually done through the lambda plotting technique [196]. The Box-Cox plot (Figure 2.5) was used to select the most appropriate power law transformation and the lowest point of the plot. It was also used to confirm model adequacy. The red lines represent the 95% confidence interval surrounding the best lambda value. The green line represents the best lambda value, which is -0.82. Natural log transformation was required to enable the current lambda to be within the 95% confidence interval. Model adequacy checking was performed using a Box-Cox plot for power

transformation, a normal probability plot of residuals, a plot of studentized residuals versus predicted values and a plot of predicted versus actual values.

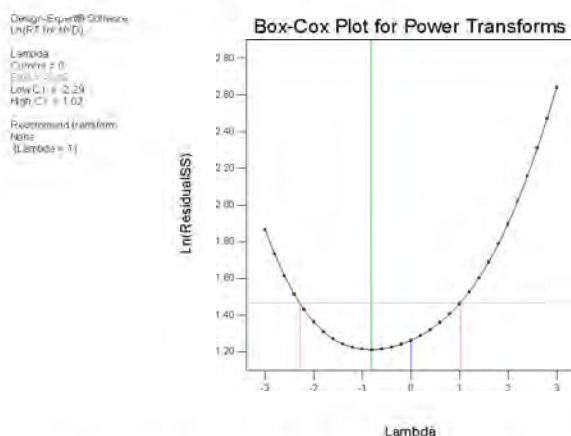


Figure 2.5 Box-Cox plot for HYD retention time

The effect of ACN was investigated with other factors that might affect retention and resolution constant. ACN is frequently the preferred organic modifier as its lower viscosity reduces operational back pressure and tailing [188,197]. It also has lower UV cut-off of 190 nm [138]. Samples containing ionisable compounds are strongly influenced by the pH of the mobile phase [198]. The pK_a of hydralazine hydrochloride is 7.4 [37] and as such, at low pH values, the amine functional groups are ionised to a zwitterion form which has less affinity for the stationary phase and more affinity for the mobile phase. As pH increases, HYD will be unionised, leading to its increased affinity for the stationary phase causing an increase in tailing. The contour and 3D response surface plots evaluating the effect of ACN content and buffer molarity are shown in Figures 2.6 and 2.7 respectively.

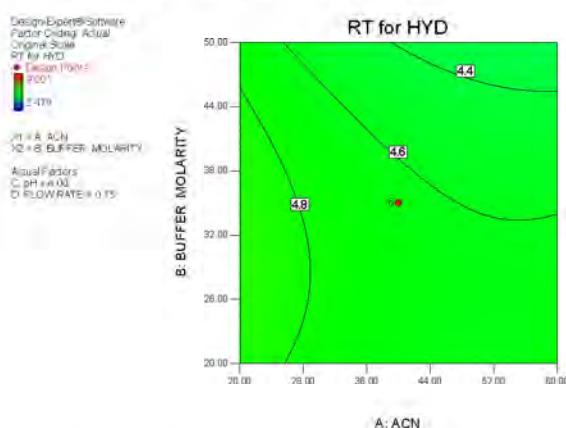


Figure 2.6 Contour plot depicting the impact of ACN content and buffer molarity on HYD retention time

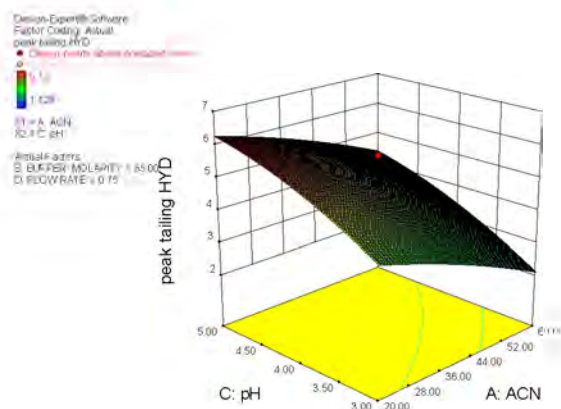


Figure 2.9 3D plot depicting the impact of ACN content and buffer pH on HYD tailing

2.7.3.3 Resolution

The resolution (y_3) between HYD and the IS was also investigated. The results reveal that the model F -value was 3.65 and the p -value was 0.0126 rendering the model significant for the design space. The F -value for x_1 and x_4 were 2.73 and 1.34 respectively, thereby indicating that ACN and flow rate have a significant effect on y_3 for these two compounds. The low F -values of 0.68 and 0.17 reported for x_2 and x_3 suggest that buffer molarity and pH do not have a significant effect on the y_3 . The adequate precision was 6.747 which is > 4 indicating that the model was significant for the design space. The resulting quadratic equation for y_3 is shown in Equation 2.9. Positive values indicate positive effects on response whereas negative values indicate negative effects on response.

$$y_3 = 1.48 - 0.14x_1 - 0.069x_2 - 0.034x_3 + 0.094x_4 + 0.066x_1x_2 - 0.58x_1x_3 + 0.041x_1x_4 - 0.040x_2x_3 - 0.032x_2x_4 - 0.014x_3x_4 - 0.17x_1^2 - 0.053x_2^2 - 0.10x_3^2 - 0.19x_4^2$$

Equation 2.9

The 2D and 3D response surface plots constructed to study the interactions of input variables on y_3 for HYD and PROP depicted in Figure 3.10 and Figure 3.11 reveal that an increase in ACN content up to about 45% resulted in an increase in resolution between the compounds. An increase in ACN content above 45% resulted in a decrease in resolution due to interactions with the surfaces of the stationary phase in competition with analyte molecules for these sites. A slight increase in the buffer pH of the mobile phase resulted in a significant increase in y_3 when ACN composition was less than 45% due to pH affecting the degree of ionisation of compounds. A slight increase in the buffer pH of the mobile phase resulted in a decrease in y_3 when the ACN composition was above 45%, most probably due to the resolution being affected

mainly by ACN composition. PROP has a pKa of 9.45 [199,200]. At pH less than 6, most of the PROP is cationic, so R_f of PROP increases because the basic solutes ionisation degree decreases with an increase in the mobile phase pH. This also accounts for the increase in resolution between HYD and PROP.

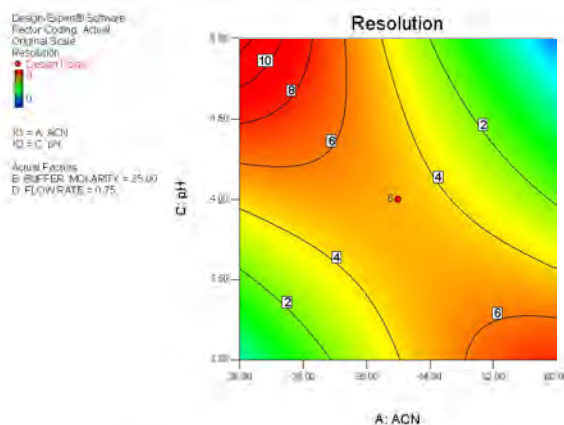


Figure 2.10 Contour plot depicting the impact of ACN content and buffer pH on the resolution

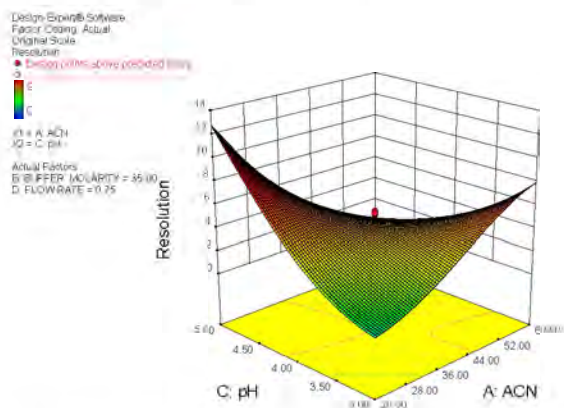


Figure 2.11 3D plot depicting the impact of ACN content and buffer pH on the resolution factor

2.7.3.4 Effect of injection volume on tailing

An increase in the injection volume will increase the amount of an analyte that is loaded onto a column. Therefore to avoid undesirable effects on peak shapes and retention times, it was necessary to investigate the effect of different injection volumes on the separation. Figure 2.12 shows the effect of injection volume on tailing of HYD and PROP. The effect of injection volume on tailing was investigated by changing the injection volume and determining the average tailing and standard deviation (SD). The results indicate that increasing injection volume results in an increase in tailing. The tailing of HYD was not affected greatly when the injection volume was increased from 5 to 10 μ L. The tailing of both HYD and PROP was

increased greatly when the injection volume was increased above 10 μL . This could be due to column overloading or an increase in a number of molecules that can interact with the column. In this study, an injection volume of 10 μL was found to be ideal as it gave an appropriate peak shape.

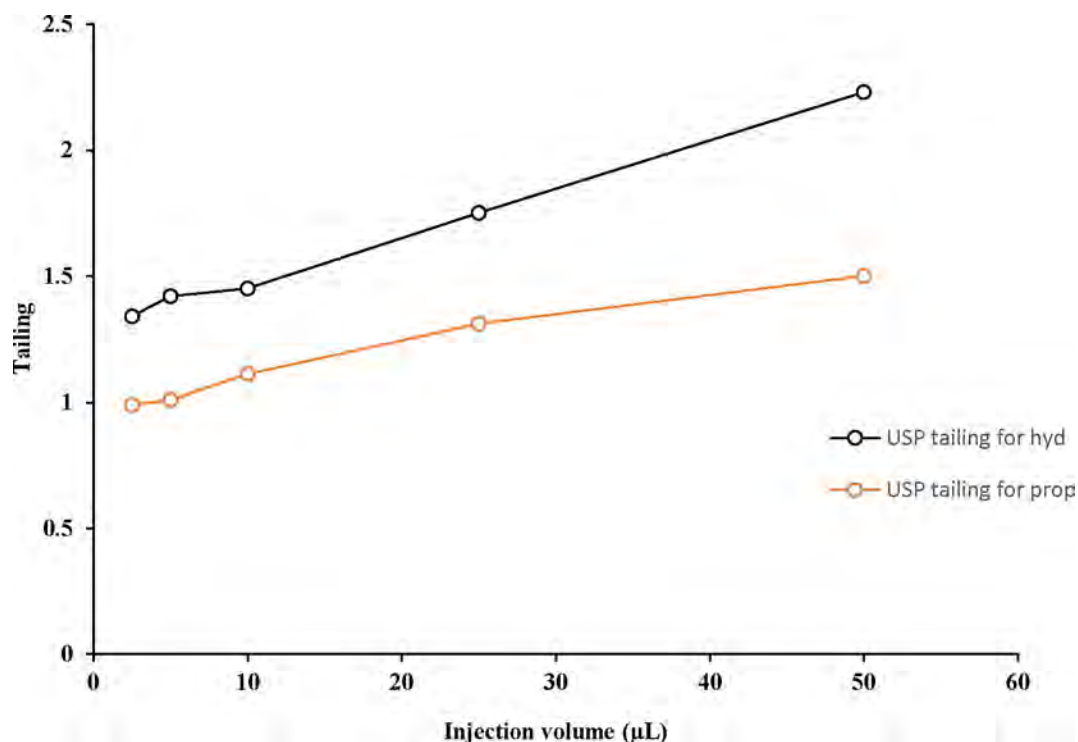


Figure 2.12 Plot of tailing versus injection volume

2.7.4 Preparation of stock solutions

2.7.4.1 Preparation of HYD stock solutions

Sample preparation is a critical step of method development that the analyst must investigate [115,135]. Approximately 200 $\mu\text{g/mL}$ of HYD stock solutions were prepared by accurately weighing 20 mg HYD using a Mettler® Model AG135 top-loading analytical balance (Mettler®, Zurich, Switzerland) and then transferring the powder into a 100 mL A-grade volumetric flask. 50% water and 50% ACN were mixed by measuring 50 mLs of each. This mixture was transferred into the 100 mL volumetric flask containing 20 mg HYD to make a 200 $\mu\text{g/mL}$ HYD solution. The volumetric flask was covered with aluminium foil prior to sonicating because HYD is light sensitive and it was then sonicated for 15 minutes using a Branson® B12 ultrasonic bath (Shelton, CN, USA) to ensure optimal dissolution of the drug. Analytical standards were prepared by using the serial dilution method to produce concentrations of 0.3, 1.2, 2.0, 20.0, 60.0, 100.0 and 140.0 $\mu\text{g/mL}$.

2.6.4.2 Preparation of IS stock solutions

Approximately 50 µg/mL of PROP stock solutions (SS) were prepared by accurately weighing 5 mg PROP using a Mettler® Model AG135 top-loading analytical balance (Mettler®, Zurich, Switzerland) and transferring it into a 100 mL A-grade volumetric flask. 100 mL of 50% water and 50% ACN was added to dissolve PROP. The solution was sonicated for 10 minutes using a Branson® B12 ultrasonic bath (Shelton, CN, USA). 0.5 mL of PROP was added to 1.0 mL of standard solutions of HYD and mixed in an amber coloured vial prior to analysis. Homogenous mixing was achieved using a Vortex-Genie® 2 mixer (New York, USA) on all vials before quantitative analysis.

2.7.5 Preparation of mobile phase

The most popular buffers for silica-based columns in HPLC with UV detection are phosphate and acetate because they cover the entire pH range of 2 – 8 [201]. 5mM buffer solutions were prepared by pipetting 342 µL of 85% v/v *ortho*-phosphoric acid using a 1000 µL pipette into a 1L A-grade volumetric flask and making up to volume with HPLC grade water. The pH of the buffer solution was adjusted to pH 3 using 0.1M NaOH solution. A model GLP 21 Crison pH meter (Crison, Lasec, South Africa) was used to monitor the pH. The buffer solution was degassed under vacuum using an Eyela® Aspirator A-2S vacuum pump (Rikakikai® Co. Ltd, Tokyo, Japan) prior to use. Phosphate buffer was prepared on a daily basis. ACN was of HPLC grade and was used without purification processes being performed. The phosphate buffer and ACN were mixed online.

2.7.6 Optimised chromatographic conditions

After the evaluation of the effect of buffer molarity, ACN concentration, pH and flow rate on retention times, peak shape, peak tailing and resolution of HYD and PROP, the optimal chromatographic conditions were selected and used throughout the HPLC method validation and stability studies. Changes in buffer molarity and ACN content had the greatest influence on the outcomes observed, and therefore optimisation of the two major factors was crucial in obtaining the desired outcomes. Buffer pH was selected on the basis of stability studies performed by Halasi *et al.* [55] that showed that HYD has maximum stability at pH 3.5. This important information was useful for the choice of the acidic buffer pH range. The best outcomes in terms of symmetry, resolution and sharpness were observed when a mobile

phase was used containing ACN and 5mM phosphate buffer adjusted to pH 3 in the ratio of 65:35 respectively mixed online at a flow rate of 0.8 mL/min with the column temperature maintained at 25.0 ± 0.5 °C. The mobile phase had a polarity index of 7.34. This resulted in a R_t of 5.8 minutes for HYD and 8.6 minutes for PROP. Optimisation was based on achieving appropriate R_t (<10 minutes), tailing and appropriate separation between HYD and PROP. Table 2.13 shows the finalised optimised conditions for the analysis of HYD.

Table 2.13 Optimised RP-HPLC conditions for HYD analysis

| | |
|--------------------------|--|
| Detector | Waters® 2489 UV/Vis Detector |
| HPLC system | Waters® Alliance solvent delivery module |
| Recorder | Empower® monitoring system |
| Column | Nucleosil® 100-10 C ₈ (250 mm x 4 mm i.d x 10 µm) |
| Column pressure | 450-600 psi |
| Mobile phase composition | 5mM phosphate buffer adjusted to pH=3: ACN (35:65) ratio and mixed online. |
| Mode | Isocratic |
| Flow rate | 0.8 mL/min |
| Column temperature | 25 °C |
| Injection volume | 10 µL |
| Detection wavelength | 240 nm |
| Internal standard | PROP |
| Run time | 10 minutes |
| R_t | HYD - 5.8 minutes PROP- 8.6 minutes |

The chromatogram below indicates a typical chromatogram observed using the optimised chromatographic conditions. Figure 2.13 depicts a typical chromatogram obtained when approximately 100 µg/mL HYD and 50 µg/mL PROP were injected and chromatographically separated using the optimised chromatographic conditions.

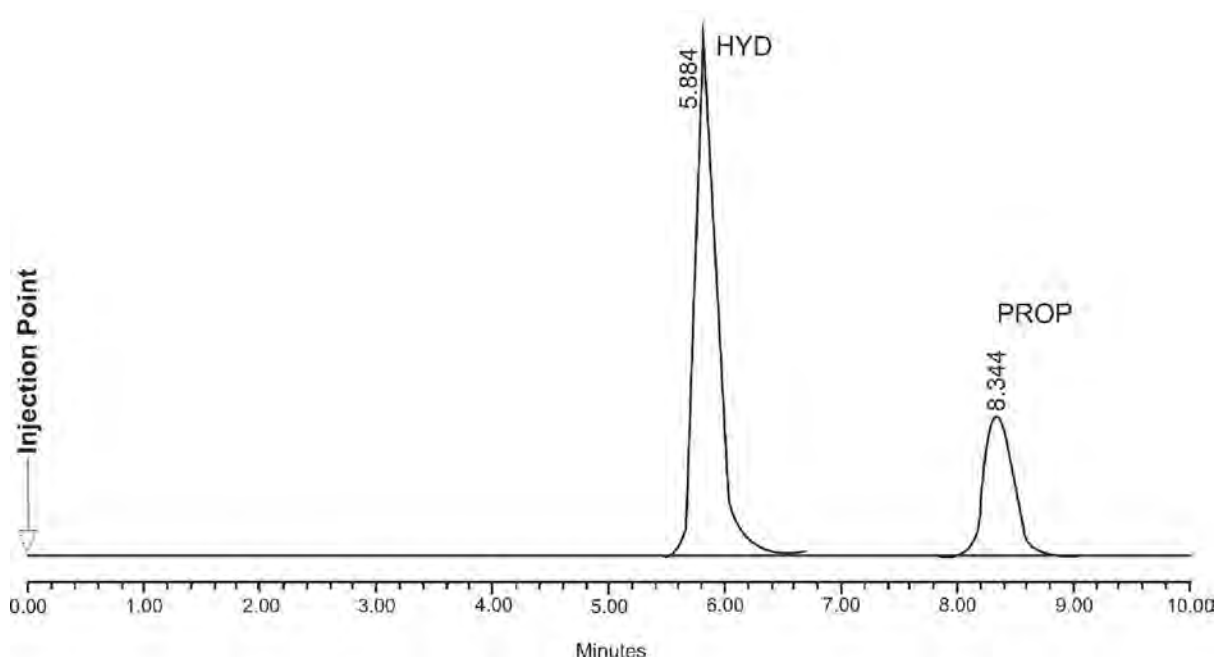


Figure 2.13 Typical chromatogram depicting the separation of HYD (100 µg/mL) and PROP (50 µg/mL) using the optimised separation conditions

2.8 METHOD VALIDATION

2.8.1 Introduction

Analytical method validation is an important regulatory requirement in pharmaceutical analysis [202]. It is the process by which the performance characteristics of the method meet the requirements for the intended analytical application [39,140]. Validation is required for any new or amended method to ensure that it is capable of giving reproducible and reliable results when used by different operators employing the same equipment in the same or different laboratories [115].

Once an analytical method has been developed for its intended use, it must be validated [203]. Analytical method validation demonstrates the scientific reliability of the developed method [204]. The various validation parameters include linearity, accuracy, precision, ruggedness, robustness, limit of detection (LOD), limit of quantitation (LOQ), selectivity and specificity [139,205]. These factors are also validated when any changes are made to an analytical method and when a method is used in different laboratories [205].

The objective of validation of an analytical procedure is to demonstrate that it is suitable for its intended purpose [205]. The purpose of the developed method was mainly to test dosage forms that were to be formulated in the laboratory; therefore, to ensure that the method was applicable for use, marketed HYD tablets were tested using the optimised chromatographic condition (§2.7.6).

2.8.2 Limits of quantitation (LOQ) and detection (LOD)

According to ICH guidelines, the LOD is the lowest amount of analyte in a sample which can be feasibly and reliably detected under stated experimental conditions but not necessarily quantitated as an exact value [115,205]. LOQ is defined as the lowest amount of analyte in a sample which can be quantitatively determined with suitable precision and accuracy [111,205–207]. Visual evaluation, use of the signal-to-noise ratio, calculations based on the standard deviation of the response and the slope of calibration curve are the commonly used method to determine LOQ and LOD [205,208]. LOQ is mainly affected by the detector sensitivity and accuracy of sample preparation [111,209].

The method to calculate the LOQ was practically based on percentage relative standard deviation (%RSD). A series of low concentrations were prepared using aliquots to make

concentrations of 0.1, 0.2, 0.3, 0.5, 0.7, 0.8, 1.0, 1.5, 2.0, 5.0 and 7.0 µg/mL as indicated in Table 2.14. An IS was added to the above concentration to eliminate injection volume variability. These were analysed using an optimised HPLC method and the peak area ratio calculated. The LOQ was determined by estimating the lowest concentration of HYD that resulted in %RSD value less than 5%. The LOQ was found to be 0.3 µg/mL with a %RSD of 2.05 and the LOD was estimated to be a third of the LOQ [102]. Thus LOD was set at approximately 0.1 µg/mL. The results for the determination of LOQ are shown in Table 2.14. Determination of LOQ and LOD was crucial as it gives an indication of the minimum concentration that can be used when constructing a calibration curve.

Table 2.14 Summarised results obtained for LOQ determination of HYD using HPLC method

| Concentration (µg/mL) | Average (HYD/PROP) ± SD | %RSD |
|-----------------------|-------------------------|-------|
| 0.1 | 0.0044 ± 0.0013 | 18.53 |
| 0.2 | 0.0070 ± 0.0006 | 6.49 |
| 0.3 | 0.0128 ± 0.0002 | 3.03 |
| 0.5 | 0.0231 ± 0.0007 | 2.98 |
| 0.7 | 0.0264 ± 0.0004 | 1.72 |
| 0.8 | 0.0471 ± 0.0004 | 0.84 |
| 1.0 | 0.0650 ± 0.0009 | 1.44 |
| 1.5 | 0.1103 ± 0.0014 | 1.29 |
| 2.0 | 0.1459 ± 0.0011 | 0.77 |
| 5.0 | 0.4366 ± 0.0018 | 0.41 |
| 7.0 | 0.5098 ± 0.0012 | 0.23 |

2.8.3 Linearity and range

A method is linear when there is a linear relationship between the analyte response and concentration over a specified range of concentration [113,140]. The linearity of an analytical procedure is its ability to obtain results that are directly proportional to the concentration of the analyte in the sample [110,115,191,210]. It is essential to determine the useful range at which the instrumental response is proportional to the analyte concentration. A graph is plotted with the relative responses on the Y-axis and the corresponding concentrations on the X-axis on a log scale [191]. The range of an analytical procedure is the interval between the upper and lower concentrations of analyte for which it has been demonstrated that the analytical procedure has a suitable level of precision, accuracy and linearity [202]. It is established by confirming that the analytical procedure provides an acceptable degree of linearity, accuracy and precision when applied to samples containing amounts of an analyte within or at the extremes of the specified range of the analytical procedure [111,178,204].

The linearity of a method is a measure of how well a calibration plot of response versus concentration approximates a straight line. Linearity can be assessed by performing single

measurements at several analyte concentrations. The data is then processed using a linear least-squares regression. The resulting plot slope, intercept and correlation coefficient provide the desired information on linearity [185]. A linear relationship should be evaluated across the range of the analytical procedure. It is demonstrated directly on the drug substance by dilution of a standard stock solution of the drug product components, using the proposed procedure [115].

A calibration curve was used to determine the linearity and range for HYD. The concentration range of 0.3 to 140.0 µg/mL was used to obtain the calibration curve and injected in ascending order of concentration, *viz.* 0.3, 1.2, 2.0, 20.0, 60.0, 100.0 and 140.0 µg/mL of HYD. The peak area ratio (PAR) of HYD to PROP was calculated and a calibration curve of the PAR versus concentration was plotted and is shown in Figure 2.14. Least squares linear regression analysis was performed on the data obtained to evaluate the correlation between absorption and concentration. The equation for the best-fit least squares regression line obtained was $y=0.0485x - 0.0273$ with an R^2 of 0.9998. The R^2 should be ≥ 0.999 for linearity to be established [190,202]. The y-intercept of 0.0273 was close to zero, which satisfies the specific criteria for linearity that specifies that the y-intercept should be $< 2\%$ of the response or near zero [211,212]. The linearity results indicate that, within the selected range, the calibration curve follows the Beer-Lambert law. Table 2.15 shows the summarised data obtained for the calibration curve and the %RSD. The %RSD should be $< 2\%$ [202] and all the %RSD obtained were $< 2\%$, therefore, linearity was established in the specified range selected. There is a clear direct correlation between concentration and absorbance.

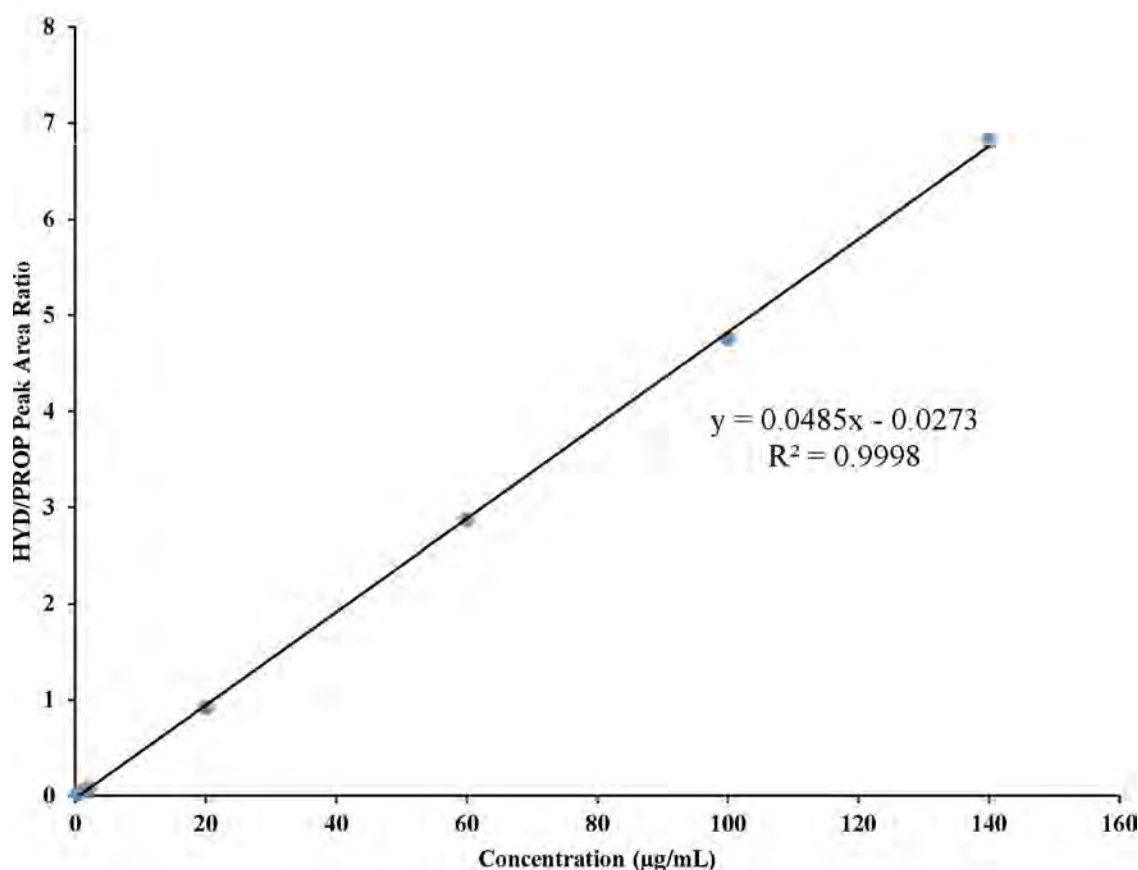


Figure 2.14 Typical calibration curve for HYD in the concentration range 0.3-140.0 µg/mL

Table 2.15 Typical summarised calibration curve data for HYD over the concentration range 0.3- 140.0 µg/mL (n=5)

| Concentration (µg/mL) | Average (HYD/PROP) Area Ratio ± SD | %RSD |
|-----------------------|------------------------------------|------|
| 0.3 | 0.0147 ± 0.0040 | 1.85 |
| 1.2 | 0.0467 ± 0.0007 | 1.47 |
| 2.0 | 0.0732 ± 0.0002 | 0.30 |
| 20.0 | 0.9182 ± 0.0005 | 0.05 |
| 60.0 | 2.8680 ± 0.0003 | 0.01 |
| 100.0 | 4.7581 ± 0.0163 | 0.34 |
| 140.0 | 6.8152 ± 0.0099 | 0.15 |

2.8.4 Precision

Precision is a measure of the extent of reproducibility and repeatability of an analytical method. The precision of a method is the degree of scattering of results, usually recorded as a percentage relative to standard deviation [111,113,140,184,213]. It expresses closeness of agreement between a series of measurements obtained from multiple sampling of the same homogeneous sample under the prescribed conditions [102]. Precision may be considered at three levels, *viz.* repeatability (intra-assay precision), intermediate precision (inter-day precision) and reproducibility (between laboratory precision) [102,115]. Precision measures the closeness of agreement of a series of measurements between the series measurement obtained from multiple

sampling from the same sample under the same condition at the same time [209,214] and reflects the random errors which occur in a method [215].

2.8.4.1 Intermediate precision

Intermediate precision was established to study the effects of random events, i.e. days, on the precision of the analytical procedure [216]. The intermediate precision is generally studied by multiple preparations of samples and standard solutions [111,209]. Intermediate precision can also refer to within laboratory variation due to random events such as differences in experimental periods, analysts and equipment [217].

Intermediate precision studies were performed by running freshly prepared calibration curve samples on 3 consecutive days. Inter-day precision studies were performed by preparing three fresh unknowns and running them three times a day. The PAR of HYD to PROP was determined at each concentration. The standard deviation and %RSD for each sample were calculated to assess precision. The R^2 was assessed and R^2 should be ≥ 0.999 [202]. The R^2 values of three calibration curves were 0.999, 0.9996 and 0.9997 indicating a direct proportion between concentration and absorbance. The y -intercept should be $< 2\%$ of the response or near zero to establish the accuracy and linearity [211,212]. The y -intercepts for the three calibration curves were 0.0077, 0.0326 and 0.0397, that are close to zero indicating that the method shows linearity and accuracy in the selected calibration curve range. Table 2.16 shows the summarised inter-day precision studies.

Table 2.16 Inter-day precision studies for HYD (0.3-140 µg/mL) (n=5)

| Day | Concentration (µg/mL) | Average Peak Area Ratio ± SD | %RSD | Equation | R ² value |
|-----|-----------------------|------------------------------|------|------------------|----------------------|
| 1 | 0.3 | 0.0113 ± 0.0003 | 1.47 | y=0.0466x-0.0077 | 0.9997 |
| | 1.2 | 0.0479 ± 0.0003 | 0.72 | | |
| | 2.0 | 0.0841 ± 0.0002 | 0.29 | | |
| | 20.0 | 0.9715 ± 0.0035 | 0.36 | | |
| | 60.0 | 2.7416 ± 0.0056 | 0.20 | | |
| | 100.0 | 4.5859 ± 0.0058 | 0.13 | | |
| | 140.0 | 6.5711 ± 0.0025 | 0.04 | | |
| 2 | 0.3 | 0.0064 ± 0.0002 | 1.55 | y=0.048x-0.0326 | 0.9996 |
| | 1.2 | 0.0408 ± 0.0001 | 0.20 | | |
| | 2.0 | 0.0807 ± 0.0013 | 1.58 | | |
| | 20.0 | 0.9428 ± 0.0042 | 0.45 | | |
| | 60.0 | 2.7497 ± 0.0033 | 0.12 | | |
| | 100.0 | 4.7259 ± 0.0299 | 0.63 | | |
| | 140.0 | 6.7652 ± 0.0099 | 0.15 | | |
| 3 | 0.3 | 0.0212 ± 0.0005 | 1.43 | y=0.0491x-0.0397 | 0.9990 |
| | 1.2 | 0.0495 ± 0.0003 | 0.69 | | |
| | 2.0 | 0.0779 ± 0.0009 | 1.16 | | |
| | 20.0 | 0.9126 ± 0.0010 | 0.10 | | |
| | 60.0 | 2.8630 ± 0.0011 | 0.04 | | |
| | 100.0 | 4.7196 ± 0.0021 | 0.6 | | |
| | 140.0 | 6.9693 ± 0.0025 | 0.04 | | |

The data clearly show that all %RSD values were < 2% for all concentrations of HYD investigated and therefore the method was deemed precise. The R² value was close to 1 showing that the calibration curve indicated linearity in the range 0.3 to 140.0 µg/mL.

2.8.4.2 Intra-day precision

Repeatability, also referred to as intra-day precision, is a measure of precision of analysis in one laboratory by one operator using one piece of equipment [178,218,219]. ICH recommends a minimum of nine determinations covering the specified range for the procedure or a minimum of six determinations at 100% of the test concentration for evaluation of repeatability which should be reported as standard deviation, relative standard deviation or confidence interval [185]. ICH defines intermediate precision as long-term variability of the measurement process and is determined by comparing the results of a method run within a single laboratory. The objective of intermediate precision validation is to verify that the method will provide the same results in the same laboratory once the development phase is over [133].

Intra-day precision studies were analysed using replicate samples (n=5) at three concentrations of 5.0, 50.0 and 120.0 µg/mL that are indicative of low, medium and high levels within the linear range. The analysis was performed over a short period of time on the same day and the %RSD was used to assess precision. An upper limit of 2% was set for precision in our laboratory. The %RSD results for intra-day precision studies were all within the 2% limit (Table 2.17), indicating that the method is precise.

Table 2.17 Intra-day precision studies for HYD (n=5)

| Time | Theoretical concentration (µg/mL) | Actual concentration (µg/mL) ± SD | %RSD | %Recovery |
|-------|-----------------------------------|-----------------------------------|------|-----------|
| 09H30 | 5 | 5.0380 ± 0.0013 | 0.62 | 100.76 |
| | 50 | 48.3908 ± 0.0011 | 0.05 | 96.78 |
| | 120 | 120.4756 ± 0.0027 | 0.04 | 100.40 |
| 12H30 | 5 | 5.1899 ± 0.0046 | 1.11 | 103.80 |
| | 50 | 48.3954 ± 0.0020 | 0.08 | 96.79 |
| | 120 | 120.3546 ± 0.0019 | 0.03 | 100.30 |
| 17H30 | 5 | 5.0322 ± 0.0009 | 0.43 | 100.64 |
| | 50 | 48.7463 ± 0.0115 | 0.49 | 97.49 |
| | 120 | 118.5217 ± 0.0131 | 0.23 | 98.77 |

The precision data is generally expressed in the form of standard deviation, RSD and confidence intervals. To ensure precision of method for major analytes, RSD should be $\leq 2\%$ [111]. The method showed both inter- and intra-day precision as the %RSD was less than 2%. The developed method can be used at any time of the day and no time-to-time variations or day-to-day variations should occur.

2.8.4.3 Reproducibility

Reproducibility expresses precision of analysis of the same sample by different analysts in different laboratories using operational and environmental conditions that may differ but are still within the specified parameters of the method [178,209]. The objective of reproducibility studies is to verify that the method will provide the same results despite differences in room temperature, humidity, variedly experienced operators, different equipment, variations in material and instrument conditions, columns from different suppliers, different batches of solvents, reagents and other materials with different quality [205,209,220]. Reproducibility studies were not performed as all the analytical experiments were performed by the same analyst, using the same equipment and same laboratory.

2.8.5 Accuracy

Accuracy refers to the exactness or closeness of agreement between a measured quantity value and a true quantity value [102,191,205,207] and is generally expressed as percentage recovery [139]. It has an inverse relation to both random and systematic errors and is evaluated by analysing the test drug at different concentration levels. ICH recommends accuracy evaluation using a minimum of nine determinations over a minimum of three concentration levels covering the range specified [111,215].

Accuracy is determined by spiking and analysing known amounts of the analyte [207] and is calculated as the percentage recovery of the analyte amount [191,207]. Accuracy should be

assessed using a minimum of nine determinations over a minimum of three concentration levels covering the specified range [111] or a minimum of five determinations per concentration with a minimum of three concentrations in the selected range [178]. Accuracy should be reported as percent recovery by the assay of the known added amount of analyte in the sample or as the difference between the means and the accepted true value together with the confidence intervals. The concentration should cover the range of concern. The expected recovery depends on the sample matrix, the sample processing procedure, and the analyte concentration. The reported limits for accuracy for drug substances and drug products are 98.0 - 102.0% and 97.0 – 103.0% respectively [111].

Accuracy was established by analysing HYD standards of known concentration, *viz.* low, medium and high. It was determined by using three known concentrations of pure HYD which were analysed along with the tablet samples. The percent recovery for each concentration was calculated. The %RSD was less than 5%. The accuracy of the method was established by evaluating three different concentrations of HYD in three replicate procedures and the percentage bias was calculated using Equation 2.10.

$$\% \text{ Bias} = \frac{\text{measured value} - \text{expected value}}{\text{expected value}} \times 100 \quad \text{Equation 2.10 ([178])}$$

The unknowns were quantified together with calibration curves on different days. The results obtained showed that the percentage bias was less than 5%, demonstrating that the method was accurate. The mean percent recovery for different days ranged from 97.04 to 103.83%, with the %RSD in the range 0.01% - 1.32% and bias ranging from -3.84 to 2.96%. The results for accuracy studies are summarised in Table 2.18. It is clear that the method is accurate.

Table 2.18 Accuracy results for HYD analysis (n=5)

| DAY | Theoretical concentration (µg/mL) | Actual concentration (µg/mL) ± SD | %RSD | %Recovery | %Bias |
|-----|-----------------------------------|-----------------------------------|------|-----------|-------|
| 1 | 5.0 | 5.0921 ± 0.0077 | 1.32 | 101.84 | 1.84 |
| | 50.0 | 49.921 ± 0.0022 | 0.10 | 99.84 | 0.16 |
| | 120.0 | 122.0010 ± 0.0165 | 0.29 | 101.67 | 1.67 |
| 2 | 5.0 | 5.0082 ± 0.0008 | 0.40 | 100.16 | 0.16 |
| | 50.0 | 48.5940 ± 0.0054 | 0.01 | 97.19 | -2.81 |
| | 120.0 | 119.1397 ± 0.0122 | 0.22 | 99.28 | -0.72 |
| 3 | 5.0 | 5.1918 ± 0.0015 | 0.68 | 103.83 | -3.84 |
| | 50.0 | 49.0716 ± 0.0745 | 1.14 | 98.14 | 1.86 |
| | 120.0 | 117.4807 ± 0.0028 | 0.05 | 97.90 | 2.10 |
| 4 | 5.0 | 4.9814 ± 0.0047 | 1.19 | 99.63 | 0.37 |
| | 50.0 | 47.8838 ± 0.0068 | 0.29 | 97.04 | 2.96 |
| | 120.0 | 119.2134 ± 0.0005 | 0.01 | 99.34 | 0.66 |

2.8.6 Specificity

The specificity of an analytical method is the ability to assess unequivocally the analyte of interest in the presence of excipients, impurities or degradation compounds. The specificity of a test method is determined by comparing test results from an analysis of samples containing impurities, degradation products, or placebo ingredients with those obtained from an analysis of samples without impurities, degradation products, or placebo ingredients. Specificity can best be demonstrated by resolution between the analyte peak and the other closely eluting peak [206]. This parameter is concerned with the extent to which other substances interfere with the identification and quantitation of the analyte(s) of interest [110,115,135,205].

To determine if the method was specific for HYD, commercially available tablets were used. There was no interference between HYD and excipients used in these tablets, therefore the method can be considered selective and specific for the analysis of HYD in pharmaceutical dosage forms. Table 2.19 shows a summary of the analytical method validation parameters evaluated according to ICH guidelines Q2 (R1) [205,216].

Table 2.19 Summarised method validation parameters

| Number | Parameter | Method |
|--------|---------------------|--|
| 1 | LOQ and LOD | The values for LOQ were determined based on the standard deviation of the response. The LOQ was determined by estimating the lowest concentration of HYD that resulted in %RSD value less than 5%. The LOD was estimated to be a third of the LOQ. |
| 2 | Linearity and range | A linear relationship was evaluated across the range of 0.3 to 140.0 µg/mL. A calibration curve was obtained by plotting PAR against the concentration of standard and finding regression coefficient (R^2). |
| 3 | Precision | Precision was reported as standard deviation and relative standard deviation for each type of precision investigated. (Acceptance Criteria: %RSD of low, mid and high should be less than 2%). |
| 4 | Accuracy | Accuracy was assessed using 3 concentration levels covering the specified range. Percentage recovery was calculated by performing recovery studies in triplicates of three concentration levels, viz. 5 (low), 50 (medium) and 120 (high) by adding a known amount of standard solution of HYD. These samples were then analysed and the results obtained were compared with expected results. |
| 5 | Specificity | Specificity was determined using commercially available HYD tablets. No interfering peaks were obtained on the chromatograms obtained. |

2.9 CONCLUSIONS

A RP-HPLC method with UV detection at 240nm has been developed, optimised and validated for *in vitro* quantitation of HYD in pharmaceutical dosage forms according to internationally accepted and established ICH guidelines [205]. The UV detection of 240nm was above the UV cut-off of the mobile phase so as to avoid interference of this phase with the analyte of interest.

Method development was first based on trial and error basis where different columns were tried on HYD. Using CCD, method optimisation was achieved by manipulating mobile phase composition, buffer molarity, buffer pH and flow rate, and monitoring dependent variables, viz. the R_t of HYD and IS, tailing and resolution. Thirty experimental runs were performed to evaluate the effects of four critical analytical independent variables. The ACN content was varied between 20 and 60% v/v, buffer molarity between 20 and 50 mM, buffer pH between 3 and 5 and flow rate between 0.5 and 1 mL/min. Statistical analysis was used to evaluate the impact and significance of input variables to output variables. The significance of the model was analysed using F -values and p -values. The experimental data revealed that ACN content, buffer molarity and pH had the most significant effects on the R_t and resolution of HYD and PROP. The effects of the input variables on the chromatographic responses were explained using 2D contour and 3D response surface plots. The normal probability plot revealed that the residual and predicted points fell approximately in a straight line, indicating that the experimental error for these studies was evenly distributed and suggesting that the model can be used to navigate the design space. The analytical method was validated in terms of linearity, accuracy, precision, selectivity, LOQ and LOD according to the ICH guidelines.

A RP-HPLC method has been developed for the analysis of HYD. Compared to published HPLC methods, this method is simple, rapid and selective for HYD. The method uses a simple mobile phase, is precise, accurate and specific for HYD. Further investigations were performed to determine if the developed method was stability indicating.

CHAPTER 3

ANALYSIS OF HYDRALAZINE HYDROCHLORIDE TABLETS AND FORCED DEGRADATION STUDIES

3.1 INTRODUCTION

HPLC methods play a significant role in dissolution testing procedures as they provide a wide dynamic linear range, selectivity and sensitivity [221,222]. Reliable quality control in pharmaceutical analysis is based on the use of a validated analytical method [222]. Since dissolution data reflects drug stability and quality, the HPLC method should be validated as per ICH guidelines [222]. In this study, a validated HPLC method (§2.8) was applied to the analysis of HYD 50 mg commercial tablets purchased from a local pharmacy.

Stability testing is an imperative part of the process of drug product development [223]. The main purpose of stability testing is to provide documented data of how the quality of a drug substance or drug product varies with time under a variety of environmental conditions, *viz.* temperature, humidity and light [223].

Forced degradation is a process that involves degradation of drug substances at accelerated rates to generate degradation products that can be studied to determine the stability of a molecule [223–226]. It is a powerful tool used in pharmaceutical development in order to develop stability-indicating methods [223,227]. A stability-indicating HPLC method is required to assess the stability of optimised HYD sustained release microspheres under storage conditions.

3.2 EXPERIMENTAL

3.2.1 Aim

The main objective of these studies was to perform stability studies on HYD and to apply the developed and validated RP-HPLC method to analysis of commercial HYD tablets.

3.3.2 Materials

The materials used in these studies are summarised in §2.5.2. Stability studies were performed on the bulk HYD drug purchased from Skyrun (Taizhou, China).

3.3 APPLICATION OF THE ANALYTICAL METHOD

3.3.1 Specificity and selectivity

The specificity of a method is defined as the ability of an analytical procedure to accurately differentiate and quantitate an analyte of interest in the presence of other components that may be expected to be in a complex sample matrix [111,139,206,210]. The selectivity of an analytical method is the ability to distinguish an analyte of interest in the presence of any other extraneous components that may also be detectable like excipients [139,228].

To determine if the HPLC method (§2.6) was applicable to commercially available tablets, three commercially available medicines were purchased from a local pharmacy (Wallace's Pharmacy, Grahamstown, South Africa) and analysed. The commercially available HYD tablets used for these studies were Hyperphen[®]- 10, Sandoz-hydralazine[®]- 25 and Hyperphen[®]- 50 tablets containing 10, 25 and 50 mg HYD respectively, and drug content was analysed using the developed and optimised RP-HPLC method..

Twenty tablets were weighed and crushed in a mortar to form a fine powder. An aliquot of powder equivalent to the average weight of one tablet was weighed into a 100 mL A-grade volumetric flask. HYD is freely water soluble [38] and approximately 90 mL water was added to a volumetric flask and the contents were sonicated using a Branson[®] B12 Sonicator (Shelton, CN, USA) for 30 minutes. After sonication, the solution was allowed to cool to 22 °C and made up to volume. An aliquot of the solution was filtered through a 0.45 µm Millipore[®] Hydrophilic PVDF filter membrane (Millipore[®], MA USA) and then diluted (if necessary) to produce a solution of a final concentration of 100 µg/mL of HYD. PROP was added as an IS before spectrophotometrically analysing the samples.

The data from analysis of HYD tablets are summarised in Table 3.1. The average amount of HYD in commercial tablets was found to be within the range of 98.2–103.0% of the label claim. The percent recovery was calculated and the results were found to fall within USP specifications [39]. No interfering peaks were observed, thus the developed and optimised method (§2.7.6) was found to be selective for HYD in the presence of excipients. The absence of extra peaks on the chromatograms might mean that the excipients used in the tablets were not interfering with the analytes of interest or that the excipients do not absorb at 240 nm.

Table 3.1 Assay results for commercially available HYD tablets (n=5)

| Product name | Expected amount (mg) | Amount found (mg) \pm SD | %RSD | %Recovery |
|-------------------------------------|----------------------|----------------------------|------|-----------|
| Hyperphen [®] -10 | 10 | 9.95 \pm 0.005 | 0.16 | 99.5 |
| Sandoz hydralazine [®] -25 | 25 | 25.75 \pm 0.003 | 0.08 | 103.0 |
| Hyperphen [®] -50 | 50 | 49.11 \pm 0.002 | 0.06 | 98.2 |

To determine the specificity of the method, chromatograms were obtained from tablets and assessed for any interfering peaks. Results revealed that HYD and PROP eluted at 5.8 and 8.3 minutes respectively. Figure 3.1 shows a typical chromatogram obtained and there were no additional peaks observed. It can be concluded that there is no interference among HYD, PROP and excipients used in the commercially available tablets, therefore the method can be considered selective for the analysis of HYD in pharmaceutical dosage forms.

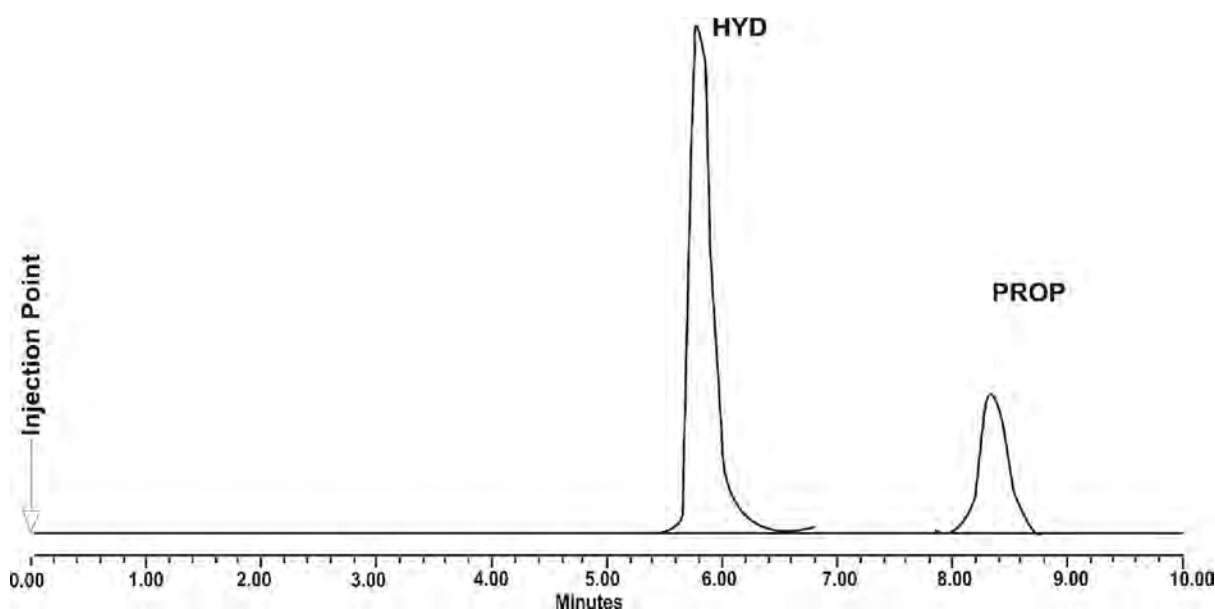


Figure 3.1 Typical chromatogram obtained from commercially available HYD tablets

3.3.2 *In vitro* release

The *in vitro* release of HYD was performed out on Hyperphen[®]-50 tablets using USP Apparatus 2. The study was conducted for a duration of 2 hours and the cumulative % HYD released were recorded as a function of time. Release studies were performed using a Hanson SR8 No 73-100-104 USP Apparatus 2 (Hanson Research, Chatsworth, CA, USA) coupled with an autosampler. The dissolution medium (900 mL, 0.1M Phosphate, pH 6.8, enzyme free) was continuously stirred at 100 rpm and temperature was maintained at 37 \pm 0.5 $^{\circ}$ C. 50 mg HYD tablets were dropped into the dissolution media and paddle rotation was set at 100 rpm.

Samples (5 mL) were withdrawn at 0, 5, 10, 15, 30, 45, 60, 75, 90, 105 and 120 minutes and filtered through 10 μ m filter hydrophilic HVP membranes. The volume withdrawn was replaced with an equivalent volume of fresh dissolution medium. The dissolution testing conditions are summarised in Table 3.2.

Table 3.2 Summary of dissolution test conditions

| | |
|---------------------------------|---|
| Parameter | USP Apparatus 2 (paddle) |
| Dissolution media | 0.1M Phosphate buffers at pH 6.8 |
| Volume | 900 mL |
| Temperature | 37 \pm 0.5 $^{\circ}$ C |
| Speed | 100 rpm |
| Sample volume | 5.0 mL |
| Sampling times (minutes) | 0, 5, 10, 15, 30, 45, 60, 75, 90, 105 and 120 |

The cumulative *in vitro* HYD released (Figure 3.2) showed approximately 30% release after 5 minutes, 80% release after 15 minutes and 90% after 75 minutes of dissolution. Visual inspections showed that the tablets completely disintegrated after 20 minutes of dissolution testing. No interfering peaks were observed from chromatograms obtained during dissolution.

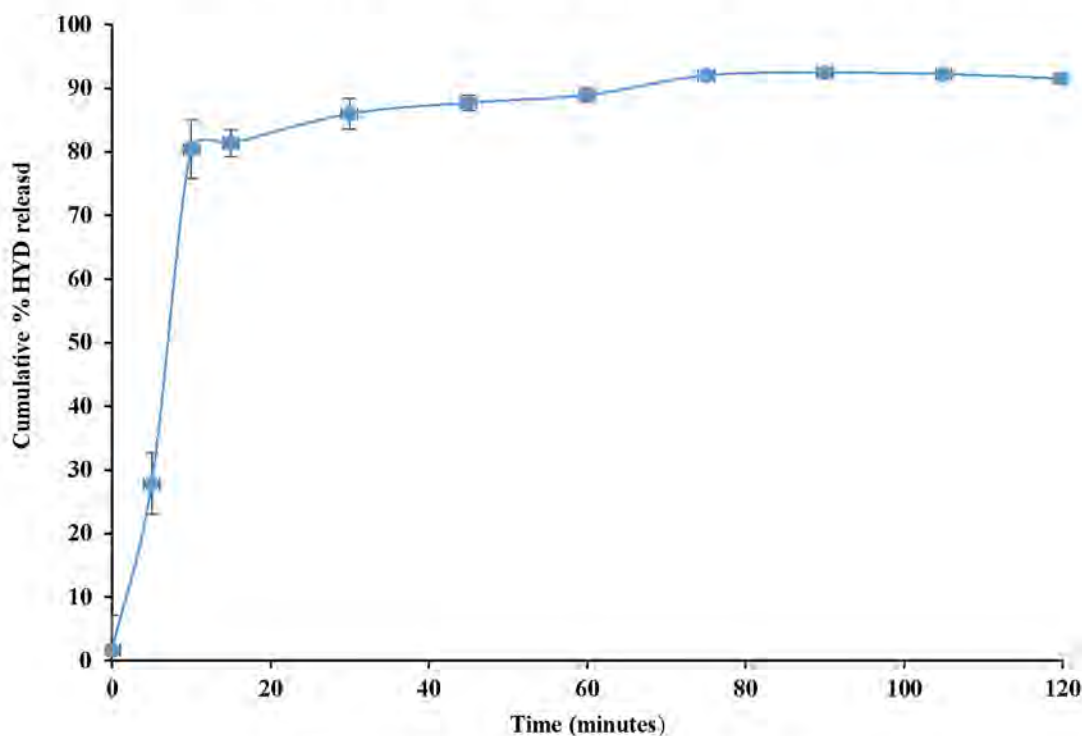


Figure 3.2 HYD release from Hyperphen[®] 50 mg tablets

3.4 STABILITY STUDIES

Stability testing of a drug substance should be performed using an accurate analytical method that quantitates the drug substance without interference from degradation products, process impurities and other potential impurities [111]. The ICH guidelines require conducting forced

degradation studies under a variety of conditions including, but not limited to, pH, temperature, light, oxidation, dry heat and acid or base hydrolysis to evaluate the ability of the method to separate the drug from degradation products [111,229].

The development of a suitable SIM provides a background for preformulation studies and provides an idea for developing suitable storage conditions [224]. A stability indicating method must resolve all significant degradation products from each other [180]. A SIM is an analytical procedure that is capable of discriminating between the major API from any degradation and/or degradation product(s) formed under defined conditions during the stability evaluation period [180,230].

Stability is a critical quality attribute of the API and the drug product. A stability profile needs to be established for a drug product to assure safety, efficacy and quality. Stress testing studies are conducted to challenge the specificity of stability-indicating and impurity-monitoring methods as part of the validation protocol. Another major goal is to investigate degradation products and pathways [230,231]. Various stability studies that can be done are summarised in Figure 3.3.

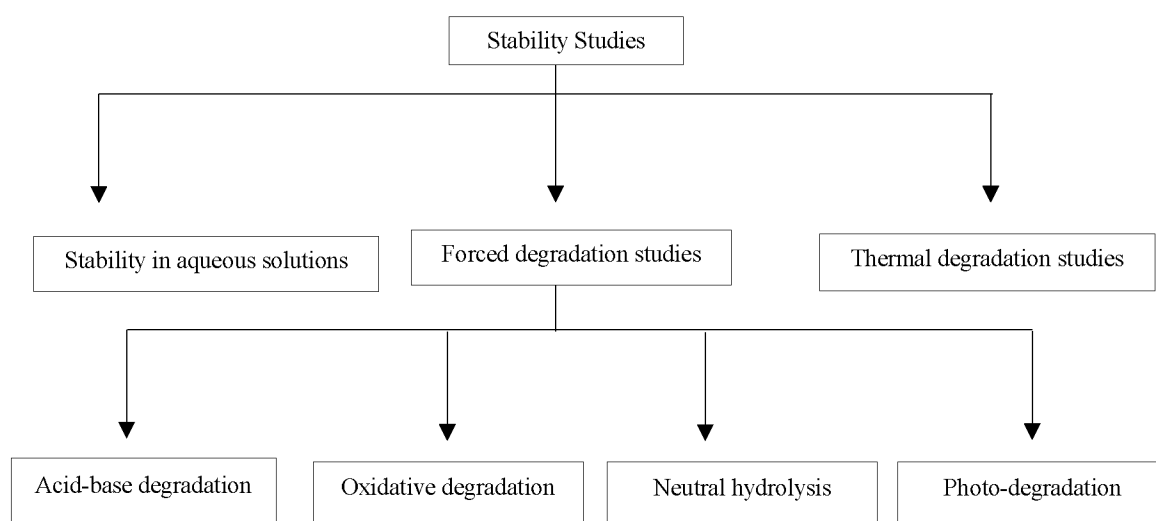


Figure 3.3 A schematic representation of the stability studies [231]

3.4.1 Stability in solution

The evaluation of stability of HYD in solutions was performed in stock solutions and in a mobile phase. These studies were mainly focused on evaluating changes (if any) in HYD concentration with time in different solutions. For accurate quantitation, HYD needs to show

stability in both stock solution and the mobile phase. Thus, it was necessary to perform stability studies of HYD in solutions.

3.4.1.1 Stability of HYD stock solutions

Approximately 10 mg HYD was accurately weighed and transferred into a 100 mL A-grade volumetric flask to which a mixture of ACN (50%) and water (50%) was added up to the mark to make 100 µg/mL HYD solution (§2.7.4.). The studies were performed at room temperature (22 °C) and in a refrigerator (4 °C). Samples from the refrigerator were allowed to equilibrate to room temperature before analysis. Samples were withdrawn after 24 hours and HYD concentration was determined spectrophotometrically using the developed and validated method. HYD concentration slightly decreased by approximately 1% after 7 days at 4 °C and 22 °C. No degradation peaks were observed, therefore HYD was found to be stable in the stock solution although fresh samples were to be prepared on a daily basis during analysis. This might be because the degradants do not absorb UV at 240 nm or they are retained in the column longer than the run time of 10 minutes. Table 3.3 shows the HYD percentage remaining in the stock solution for 7 days.

Table 3.3 Stability studies of HYD in stock solution (n=5)

| Time (days) | % Remaining \pm SD | |
|-------------|----------------------|-----------------|
| | 4 °C | 22 °C |
| 0 | 100.0 | 100.0 |
| 1 | 100.0 \pm 0.24 | 99.8 \pm 0.26 |
| 2 | 99.9 \pm 0.12 | 99.8 \pm 0.44 |
| 3 | 99.9 \pm 0.13 | 99.6 \pm 0.44 |
| 4 | 99.9 \pm 0.13 | 99.6 \pm 0.47 |
| 5 | 99.8 \pm 0.13 | 99.6 \pm 0.22 |
| 6 | 99.6 \pm 0.91 | 99.4 \pm 0.22 |
| 7 | 99.3 \pm 0.80 | 99.0 \pm 0.26 |

3.4.1.2 Stability of HYD in mobile phase

Approximately 10 mg HYD was accurately weighed and transferred into a 100 mL A-grade volumetric flask to which 100 mL of the mobile phase was added to make 100 µg/mL HYD solution. Since the chromatographic temperature was set at 25 °C, the stability of HYD in the mobile phase was performed at room temperature (22 °C) for one hour with samples withdrawn every 15 minutes to monitor changes in concentrations of HYD.

HYD was found to be stable in the mobile phase with approximately 0.1% loss after an hour as shown in Table 3.4. This concludes that the mobile phase does not have an impact on the quantitation of HYD as the run time was < 10 minutes.

Table 3.4 Stability studies of HYD in the mobile phase

| Time (minutes) | % Remaining \pm SD |
|----------------|----------------------|
| 0 | 100.0 |
| 15 | 100.0 \pm 0.16 |
| 30 | 100.0 \pm 0.10 |
| 45 | 100.0 \pm 0.14 |
| 60 | 99.9 \pm 0.31 |

3.4.2 Temperature studies

According to Arrhenius kinetics [232], increasing temperature increases the rate of any degradation process. Temperature is often used in conjunction with other stresses to increase reaction rates. Thermal or thermal/humidity stress testing is performed to force the degradation of a drug substance to its primary degradation products by exposure to thermal or thermal/humidity conditions over time [232].

3.4.2.1 Dry heat

The effect of temperature was investigated on HYD powder at 100 °C in the oven. Four 20 mg of HYD powder was weighed and transferred into four A-grade 100 mL volumetric flasks. The volumetric flasks were protected from light using aluminium foil and placed in an oven (Gallenkamp®, Loughborough, UK) set at 100 °C for 48 hours after which the samples were diluted with mobile phase and analysed using a validated HPLC method (§2.8). HYD sampling was done after 2, 8, 24 and 48 hours. HYD powder was found to be stable at this temperature as no degradation peaks were observed. A slight decrease in concentration was observed which might be due to loss of water of hydration as no degradation peaks were observed.

3.4.2.2 Effect of temperature on HYD solutions

To investigate if HYD degrades at elevated temperatures, six 100 µg/mL HYD samples were prepared in six different volumetric flasks. The samples were transferred to round bottom flasks and refluxed at temperatures of 50, 60, 70, 80, 90 and 100 °C using a Colora® Model NB-34980 Ultra-thermostat water bath (Lorch, Germany) for 4 hours. 1 mL aliquots were withdrawn from the round bottom flasks and transferred into amber vials prior to analysis with the validated HPLC method. HYD was found to be stable as no degradation peaks were observed and a summary

of the results is depicted in Table 3.5. The concentration of HYD remained constant after exposure to different temperature conditions for 4 hours.

Table 3.5 Summary of the effect of temperature on HYD (n=5)

| Temperature (°C) | Time (hours) | Observations | Comments |
|------------------|--------------|----------------------|--|
| 50 | 4 | No degradation peaks | HYD was found to be stable at this temperature |
| 60 | 4 | No degradation peaks | HYD was found to be stable at this temperature |
| 70 | 4 | No degradation peaks | HYD was found to be stable at this temperature |
| 80 | 4 | No degradation peaks | HYD was found to be stable at this temperature |
| 90 | 4 | No degradation peaks | HYD was found to be stable at this temperature |
| 100 | 4 | No degradation peaks | HYD was found to be stable at this temperature |

3.4.3 Forced degradation studies

Forced degradation is the process of subjecting drug compounds to extreme chemical and environmental conditions to determine product breakdown levels and preliminary degradation kinetics, and to identify degradant species [227]. As there is no formal regulatory guidance for forced degradation, it is recommended to use appropriate conditions to achieve 5-20% degradation [225,229,233–235].

3.4.3.1 Acid studies

The hydrolytic degradation of a new drug in acidic and alkaline conditions can be studied by refluxing a drug in 0.1N HCL or NaOH for 8 hours [236,237]. It is a chemical process that includes degradation of a chemical compound by reaction with water. Hydrolysis is one of the most common degradation chemical reactions over a wide range of pH [224,225,230,234,235]. Hydrolytic study under acidic conditions involves catalysation of ionisable functional groups present in a molecule by using HCL to generate acidic stress conditions for a sample [226,234] and testing is stopped when reasonable degradation is seen. When carrying out acid stress stability studies, a 0.1N HCL solution is used at an elevated temperature of 60 °C for 30 minutes [184].

3.4.3.1.1 Hydrochloric acid studies

Acidic degradation studies should be performed on a known concentration of the API in 0.1-1.0M solutions of either HCL or H₂SO₄ [184,226]. To evaluate the effect of HCL on the degradation of HYD, a 0.1N HCL solution was made by measuring 666 µL of 34% HCL into a 100 mL A-grade volumetric flask. HPLC grade water was added up to the 100 mL mark. Approximately 10 mg HYD was weighed and transferred into a round bottom flask, to which

100 mL of 0.1N HCL was added, making a final concentration of 100 µg/mL HYD solution. The water bath was set at 37 ± 0.5 °C and 100 ± 0.5 °C and monitored with a thermometer.

The effect of 0.1N HCL at 37 °C on HYD was evaluated at time intervals of 0, 2, 4, 6 and 8 hours and HYD concentration was slightly reduced by about 5% and no degradation peaks were observed on the chromatogram. The data obtained when HYD was subjected to acidic conditions of 0.1N HCL at 37 °C are summarised in Table 3.6.

Table 3.6 Degradation studies of 100 µg/mL HYD in 0.1N HCL at 37 °C

| Time (hours) | % Remaining \pm SD |
|--------------|----------------------|
| 0 | 100.0 |
| 2 | 99.3 ± 0.02 |
| 4 | 99.6 ± 0.04 |
| 6 | 99.0 ± 0.03 |
| 8 | 96.5 ± 0.05 |

No degradation peaks were observed from the chromatographic information obtained. This could be due to the fact that approximately 5% HYD had degraded; therefore the degradation products would be less than the lowest detectable amount or the degradation products do not absorb UV at 240 nm. Figure 3.4 depicts the chromatogram obtained from refluxing 100 µg/mL HYD in 0.1N HCL at 37 °C for 8 hours.

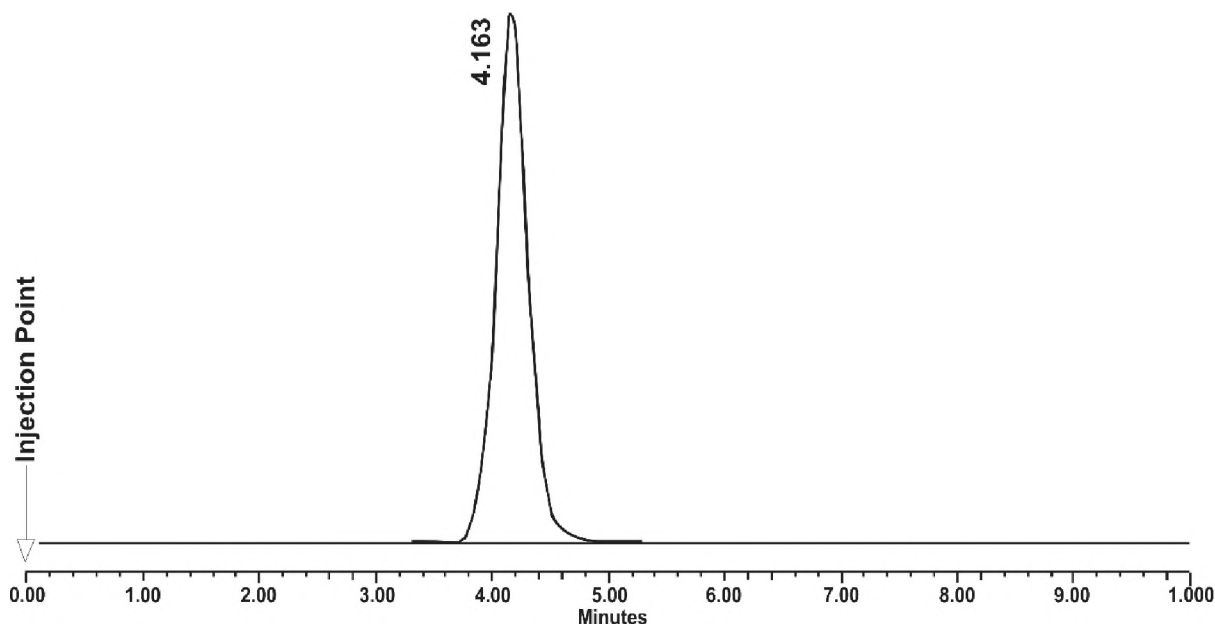


Figure 3.4 Typical chromatogram obtained after acidic stress studies of HYD in 0.1N HCL at 37 °C for 8 hours

When 0.1N HCL stability studies were performed at 37 °C for 8 hours, HYD was stable. Therefore, stability studies were further performed at an elevated temperature of 100 °C. To accelerate the degradation of HYD and evaluate the effect(s) of elevating temperature from 37 to 100 °C, a 100 µg/mL HYD solution in 0.1N HCL at 100 °C was performed under reflux.

Samples were withdrawn at 0, 2, 4, 6 and 8 hours and quantified using the developed and validated RP-HPLC method. These studies indicate that HYD slightly degraded in 0.1N HCL at 100 °C, that is, about 8% degraded after 8 hours. The small peak observed at 3.4 minutes could be due to a degradant of HYD. The rate of degradation of HYD in 0.1N HCL slightly increased when the temperature was elevated to 100 °C and these results correlate with previous reports [167,238]. The summarised degradation studies of 100 µg/mL HYD in 0.1N HCL at 100 °C are shown in Table 3.7.

Table 3.7 Degradation studies of 100 µg/mL HYD in 0.1N HCL at 100 °C

| Time (hours) | % Remaining \pm SD |
|--------------|----------------------|
| 0 | 100.0 |
| 2 | 98.8 \pm 0.82 |
| 4 | 98.2 \pm 0.24 |
| 6 | 92.2 \pm 0.56 |
| 8 | 92.1 \pm 0.40 |

Although the temperature was set at 100 ± 0.5 °C, HYD melts at 275 °C [37,38,56], therefore it would be stable at this elevated temperature. HYD is stable at acidic pH and degrades at pH values above 7 [239], hence the observed slow rate of degradation of HYD in HCL. No colour changes were observed when HCL was added to HYD. Figure 3.5 depicts the chromatogram obtained from refluxing 100 µg/mL HYD in 0.1N HCL at 100 °C for 8 hours.

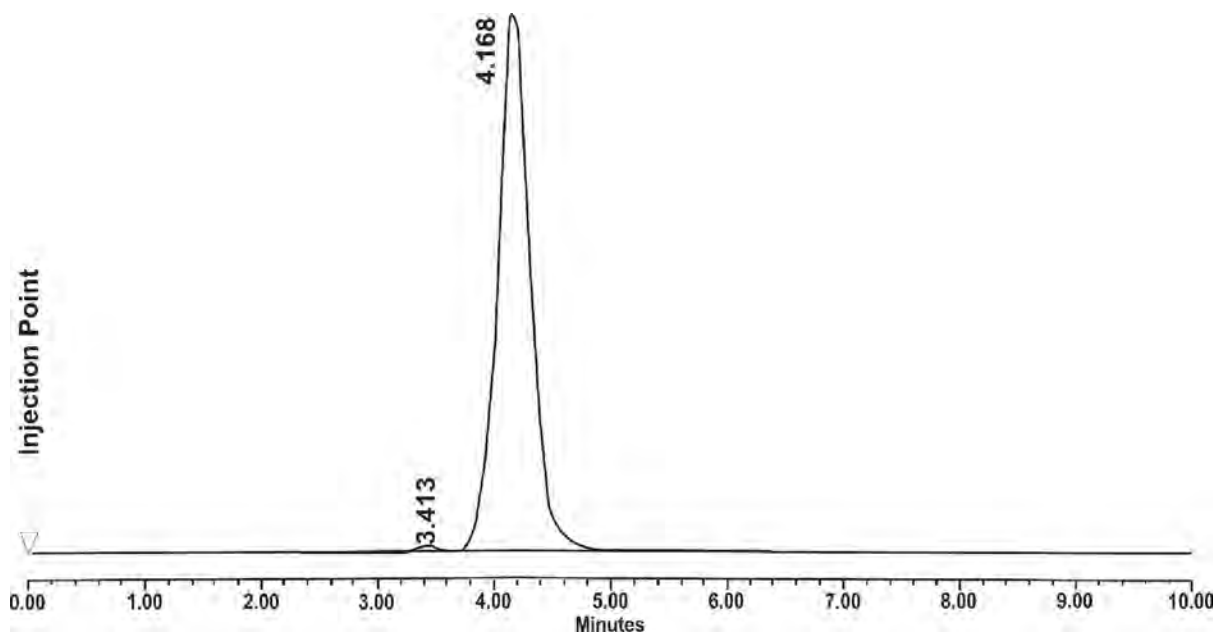


Figure 3.5 Typical chromatogram obtained after acidic stress studies of HYD in 0.1N HCL at 100 °C for 8 hours

3.4.3.1.2 Phosphoric acid studies

The degradation of HYD is catalysed by HPO_4^- ions in phosphate buffers [55]. Thus, to evaluate the stability of HYD in phosphoric acid (H_3PO_4), a 0.1M H_3PO_4 solution was made

by measuring and transferring 684 μL of 85% *ortho*-phosphoric acid into an A-grade volumetric flask and adding HPLC grade water up to the etched mark. 10 mg of HYD was weighed and transferred into a round bottom flask to which 100 mL of 0.1M H_3PO_4 was added to make a 100 $\mu\text{g/mL}$ HYD solution. The effect(s) of H_3PO_4 on HYD was performed under reflux and samples were withdrawn at 0, 2, 4, 6 and 8 hours and quantified spectrophotometrically using the HPLC method.

Stability studies of HYD in 0.1M H_3PO_4 were performed at $37 \pm 0.5^\circ\text{C}$ under reflux and samples were withdrawn at 0, 2, 4, 6 and 8 hours. HYD was stable over the time period as no degradation peaks were observed and the amount of HYD slightly decreased by approximately 3% and the chromatogram obtained is shown in Figure 3.6. No degradation peaks were observed. The summarised degradation studies of 100 $\mu\text{g/mL}$ HYD in 0.1M H_3PO_4 at 37°C are shown in Table 3.8.

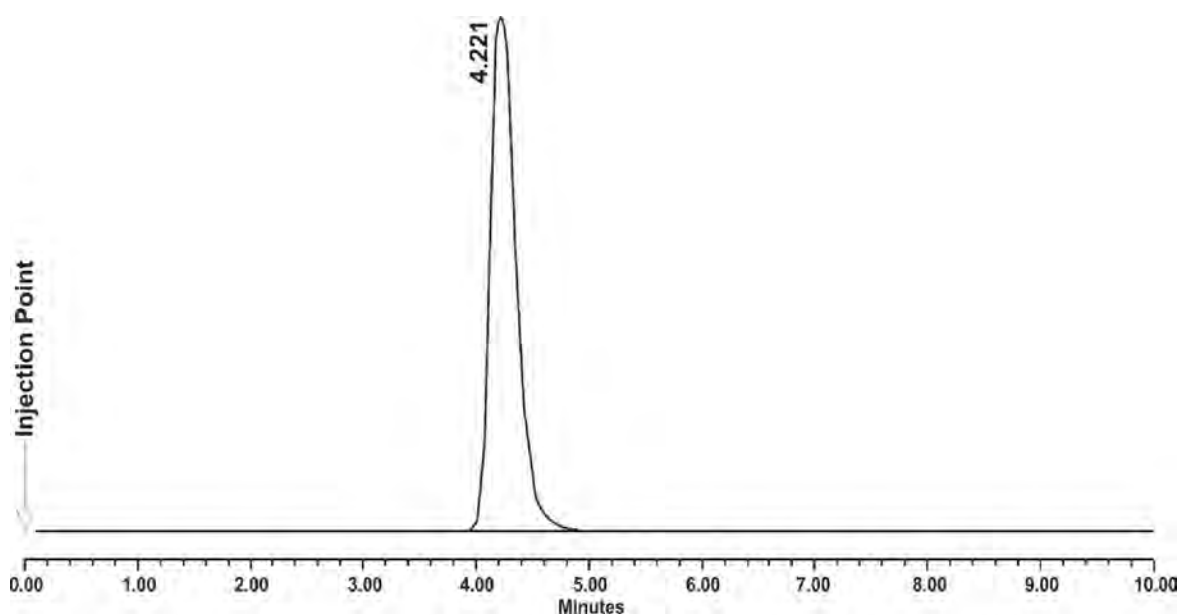


Figure 3.6 Typical chromatogram obtained after acidic stress studies of HYD in 0. H_3PO_4 at 37°C for 8 hours

Table 3.8 Degradation studies of 100 µg/mL HYD in 0.1M H₃PO₄ at 37 °C

| Time (hours) | % Remaining ± SD |
|--------------|------------------|
| 0 | 100.0 |
| 2 | 99.8 ± 0.53 |
| 4 | 99.2 ± 0.16 |
| 6 | 98.8 ± 0.59 |
| 8 | 98.6 ± 0.44 |

HYD was found to be stable in 0.1M H₃PO₄ at pH 3 at 100 °C, and this was most probably due to the fact that at pH 3.5, HYD has been reported to show maximum stability [55]. The chromatogram in Figure 3.7 shows only the HYD peak observed indicating that no degradation peak was observed within 10 minutes runtime. Table 3.9 supports the information obtained from the chromatogram with approximately 99% HYD remaining after 8 hours in 0.1M H₃PO₄ at 100 ± 0.5 °C. The rate of degradation of HYD in 0.1M H₃PO₄ was not affected by elevating the temperature to 100 °C. The chromatogram in Figure 3.7 supports the results obtained as there was no degradation peak observed on the chromatogram. The summarised degradation studies of 100 µg/mL HYD in 0.1M H₃PO₄ at 100 °C are shown in Table 3.9.

Table 3.9 Degradation studies of 100 µg/mL HYD in 0.1M H₃PO₄ at 100 °C

| Time (hours) | % Remaining ± SD |
|--------------|------------------|
| 0 | 100.0 |
| 2 | 100.2 ± 0.32 |
| 4 | 100.0 ± 0.30 |
| 6 | 99.5 ± 0.99 |
| 8 | 97.1 ± 0.94 |

The concentration decreased by approximately 3% after 8 hours in 0.1M H₃PO₄ at 100 °C and no degradation peaks were observed. The pH of 0.1M H₃PO₄ was found to be approximately 2.5 which is close to the pH of maximum stability of HYD. This could explain the stability of HYD in phosphate buffer at 37 and 100 °C. Figure 3.7 depicts the chromatogram obtained after refluxing 100 µg/mL HYD in 0.1M H₃PO₄ at 100 °C for 8 hours.

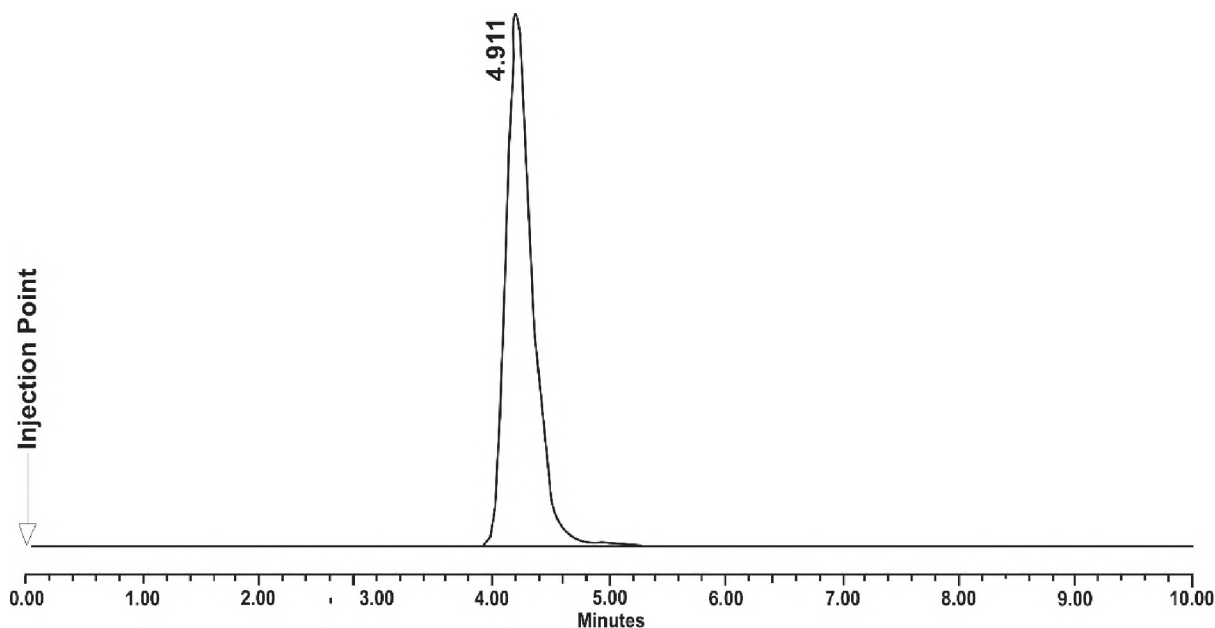


Figure 3.7 Typical chromatogram obtained after alkaline stress studies of HYD in 0.1M H_3PO_4 at 100 °C for 8 hours

3.4.3.2 Alkaline studies

Alkaline hydrolytic study under basic condition involves catalysation of ionisable functional groups present in a molecule using NaOH to generate basic stress conditions to the sample [226]. Alkaline studies should be performed on a known concentration of the API in 0.1-1.0M solutions of either NaOH or KOH [224,240]. NaOH has been reportedly used for alkaline stress stability studies [241–248] and therefore it was selected for alkaline degradation studies. The alkaline hydrolytic degradation of a new drug can be performed by refluxing the compound of interest in 0.1M NaOH for 8 hours [237].

To evaluate the effect of NaOH on the degradation of HYD, a 0.1M NaOH was prepared by measuring 0.4g NaOH (Merck Chemicals, Gauteng, South Africa) into a 100 mL volumetric flask. Water was added up to the mark and sonicated for 30 minutes. Approximately 10 mg HYD was weighed and transferred into round bottom flask to which 0.1M NaOH was added to make a 100 μ g/mL HYD. 1 mL aliquots were withdrawn at 0, 2, 4, 6 and 8 hours and analysed using the developed HPLC method. The resulting chromatogram is shown in Figure 3.8. HYD degrades in solutions with pH values > 7 to form phthalazine. The rate of degradation is dependent on the concentration of anion, pH and temperature, and at higher temperatures of 275 to 280 °C crystalline HYD degrades to form hydrazine [37,239]. A faint yellow solution was formed just after adding HYD into the NaOH which persisted for the duration of the study and the change of colour has been reported by Okeke *et al.* [239]. HYD degraded by approximately 90% and about 10% was quantified after 8 hours as shown in Table 3.10.

Table 3.10 Degradation studies of 100µg/mL HYD in 0.1M NaOH at 100 °C

| Time (hours) | % Remaining \pm SD |
|--------------|----------------------|
| 0 | 100.0 |
| 2 | 16.2 \pm 0.19 |
| 4 | 15.1 \pm 0.27 |
| 6 | 13.6 \pm 0.28 |
| 8 | 9.7 \pm 1.06 |

Degradation peaks were observed on the chromatogram, indicating that HYD is not stable under basic conditions. Although the HYD peak was well resolved at 4.5 minutes, four degradation peaks were observed at 2.0, 2.4, 3.4 and 3.6 minutes. The presence of extra chromatographic peaks suggests that HYD undergoes degradation in alkaline conditions and this is supported by the reduction of HYD concentration with time. Figure 3.8 depicts the chromatogram obtained after refluxing 100 µg/mL HYD in 0.1M NaOH at 100 °C for 8 hours.

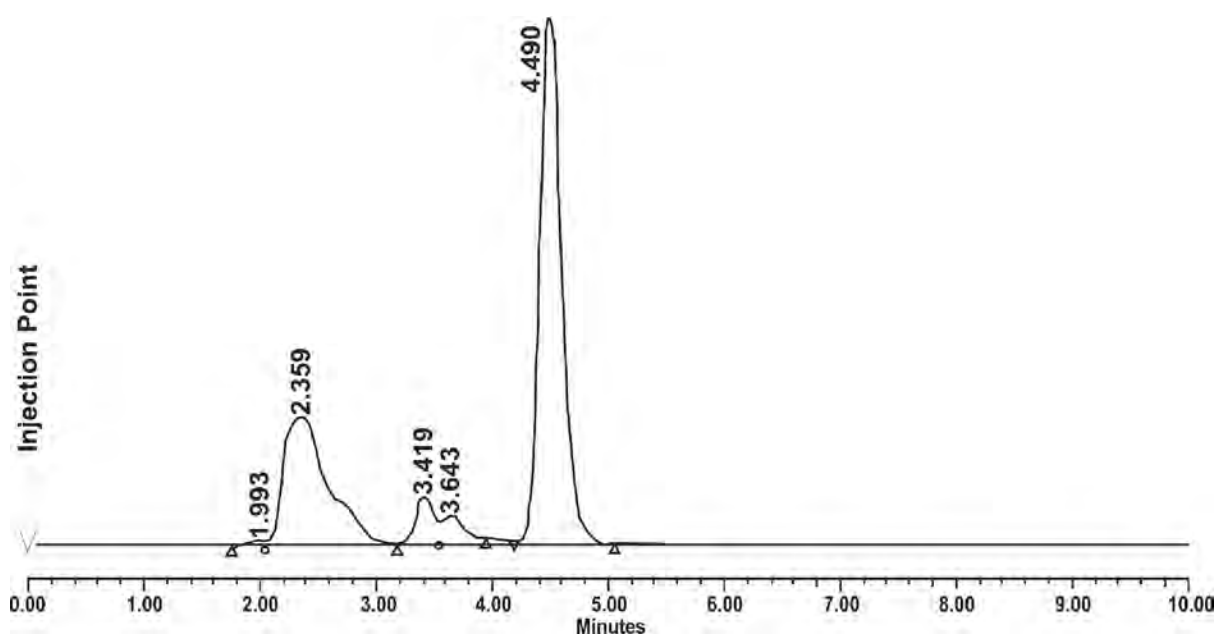


Figure 3.8 Typical chromatogram obtained after alkaline stress studies of HYD in 0.1M NaOH at 100 °C for 8 hours

3.4.3.3 Oxidative studies

Hydrogen peroxide (H₂O₂) is a very common oxidant to produce oxidative degradation products [225,226,249] due to its oxidative characteristics but other oxidising agents such as metal ions, oxygen, and radical initiators can also be used [224]. The oxidative degradation of a drug substance involves an electron transfer mechanism to form reactive anions, cations, amines, sulphides and phenols, and these are susceptible to electron transfer oxidation to form *N*-oxides, hydroxylamine, sulfones or sulfoxide [224]. Functional groups with labile hydrogen like benzylic carbon, allylic carbon and tertiary carbon are susceptible to oxidation to form hydroperoxides, hydroxide or ketone [224]. Oxidation can be performed under an oxygen

atmosphere or in the presence of peroxides. Free radical initiators and peroxides may be used to accelerate oxidation, therefore free radical and/or hydrogen peroxide conditions are strongly recommended at all stages of development [224,250].

For oxidative degradation with H_2O_2 , at least one of the storage conditions should be less than 30 °C as heating H_2O_2 solution increases the homolytic cleavage of the HO-OH bond to form the alkoxy radical [180,233]. The alkoxy radical is very reactive and may come to dominate the observed degradation pathway [180,233]. To avoid the cleavage of the HO-OH bond, oxidative stress degradation studies were performed in the dark at 22 °C.

To study the oxidative degradation of compounds, H_2O_2 in the concentration range of 3-30% v/v is used at temperatures not exceeding 40 °C [226,231,236]. Therefore, 3%, 15% and 30% v/v H_2O_2 solutions were used. The 3% and 15% v/v H_2O_2 solutions were prepared from the 30% H_2O_2 by serial dilutions whilst the 30% v/v H_2O_2 was used as provided. 10 mg of HYD was accurately weighed out and transferred to a 100 mL A-grade volumetric flask containing 100 mL of a 3% v/v H_2O_2 solution. Approximately 10 mg of HYD was accurately weighed out and transferred to a 100 mL A-grade volumetric flask containing 100 mL of a 15% v/v H_2O_2 solution. 10 mg of HYD was accurately weighed out and transferred to a 100 mL A-grade volumetric flask containing 100 mL of a 30% v/v H_2O_2 solution. The solutions were sonicated for 5 minutes. Oxidative studies were performed in the dark at 22 °C. Samples were withdrawn at 0, 2, 4, 6 and 8 hours and neutralised using sodium hydrogen sulphide (NaHS) before quantitatively analysing the concentration of HYD using the developed and validated RP-HPLC method.

HYD undergoes oxidative reactions to form hydrazones [251] and in this study, H_2O_2 was used as the oxidising agent. In 30% v/v H_2O_2 , HYD showed the fastest oxidative degradation. 15% v/v H_2O_2 showed moderate oxidative degradation and 3% v/v H_2O_2 showed the slowest oxidative degradation. HYD starts degrading immediately in contact with H_2O_2 . Approximately 70%, 46% and 17% HYD remained after stress studies in 3%, 15% and 30% v/v H_2O_2 respectively at 22 °C, in the dark, for 8 hours. Table 3.11 shows percentage remaining of HYD after every 2 hours in different concentrations of H_2O_2 .

Table 3.11 Degradation studies of 100 µg/mL HYD in 3%, 15% and 30% v/v H₂O₂ in the dark at 22 °C for 8 hours

| Time (hours) | 3% v/v H ₂ O ₂ | 15% v/v H ₂ O ₂ | 30% v/v H ₂ O ₂ |
|--------------|--------------------------------------|---------------------------------------|---------------------------------------|
| | % Remaining ± SD | % Remaining ± SD | % Remaining ± SD |
| 0 | 100.0 | 100.0 | 100.0 |
| 2 | 86.9 ± 1.71 | 75.4 ± 2.60 | 70.9 ± 1.90 |
| 4 | 77.9 ± 0.32 | 56.8 ± 0.31 | 62.8 ± 12.6 |
| 6 | 76.0 ± 0.32 | 53.8 ± 0.47 | 46.0 ± 1.23 |
| 8 | 69.1 ± 0.39 | 46.2 ± 1.96 | 17.1 ± 0.19 |

Chromatograms obtained from oxidative degradation studies of 100 µg/mL HYD in 3%, 15% and 30% v/v H₂O₂ are shown in Figure 3.9 to Figure 3.11. The peak at approximately 2.8 minutes was for the H₂O₂ and an additional degradation peak was observed in 30% v/v H₂O₂ at 2.2 minutes. No degradation peaks were observed when HYD was subjected to 3% and 15% v/v H₂O₂, but a decrease in concentration by approximately 30 and 50% respectively was observed after 8 hours. The absence of degradation peak might mean that the degradants do not absorb UV at 240 nm.

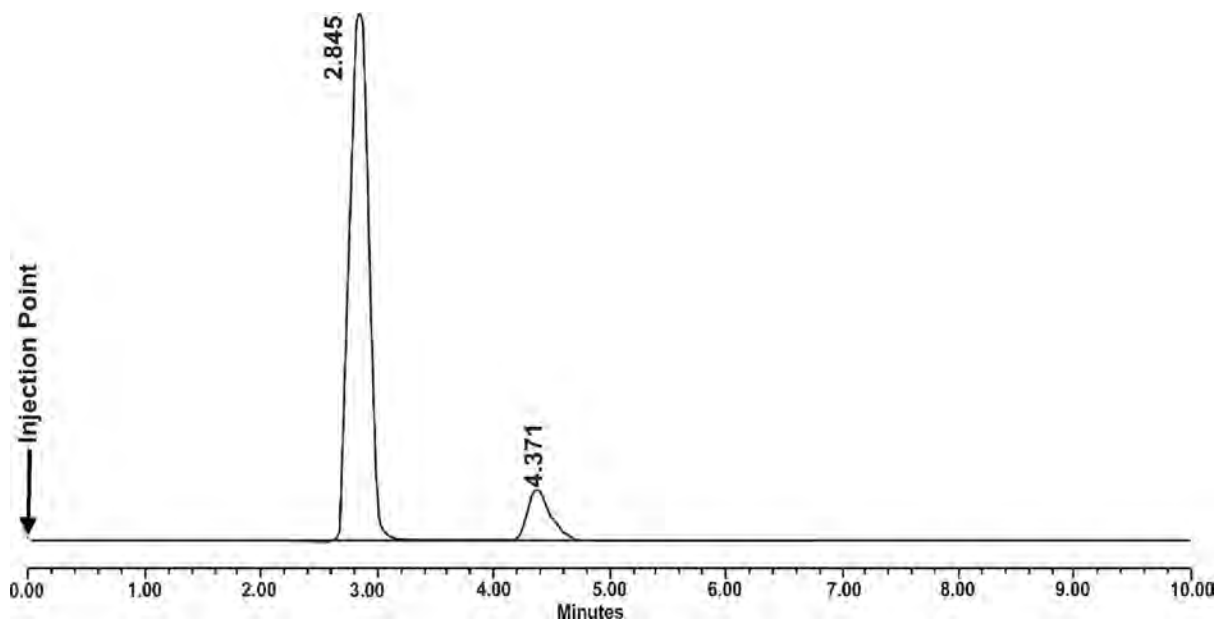


Figure 3.9 Typical chromatogram obtained from oxidative stress studies of HYD in 3% v/v H₂O₂ at 22 °C for 8 hours

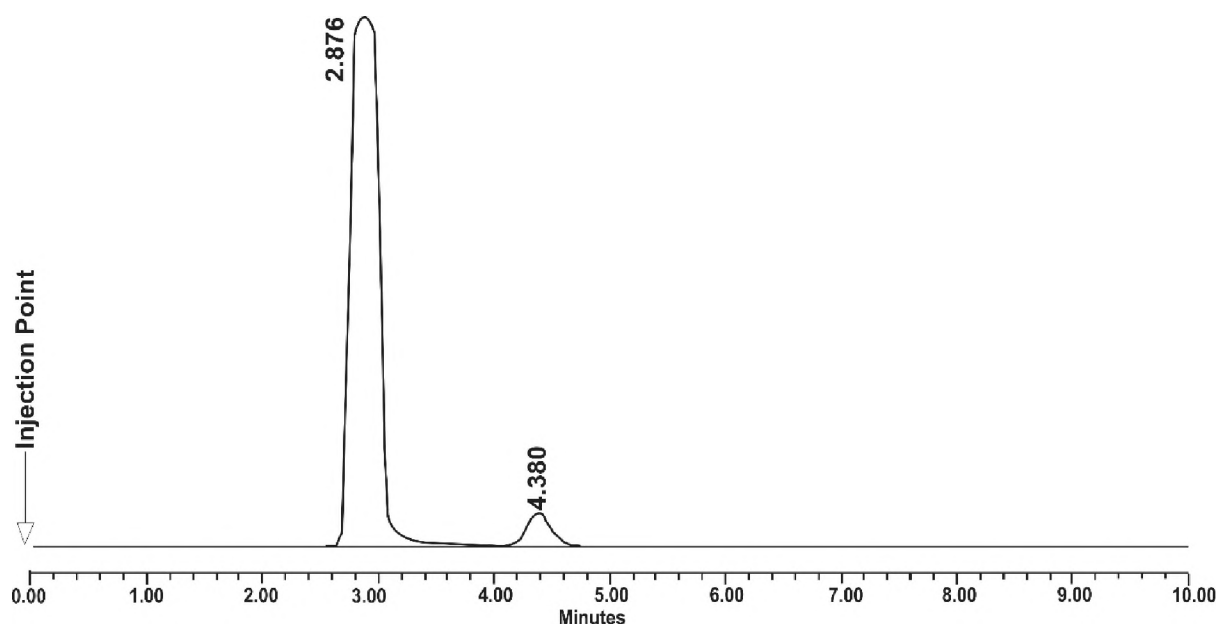


Figure 3.10 Typical chromatogram obtained from oxidative stress studies of HYD in 15% v/v H₂O₂ at 22 °C for 8 hours

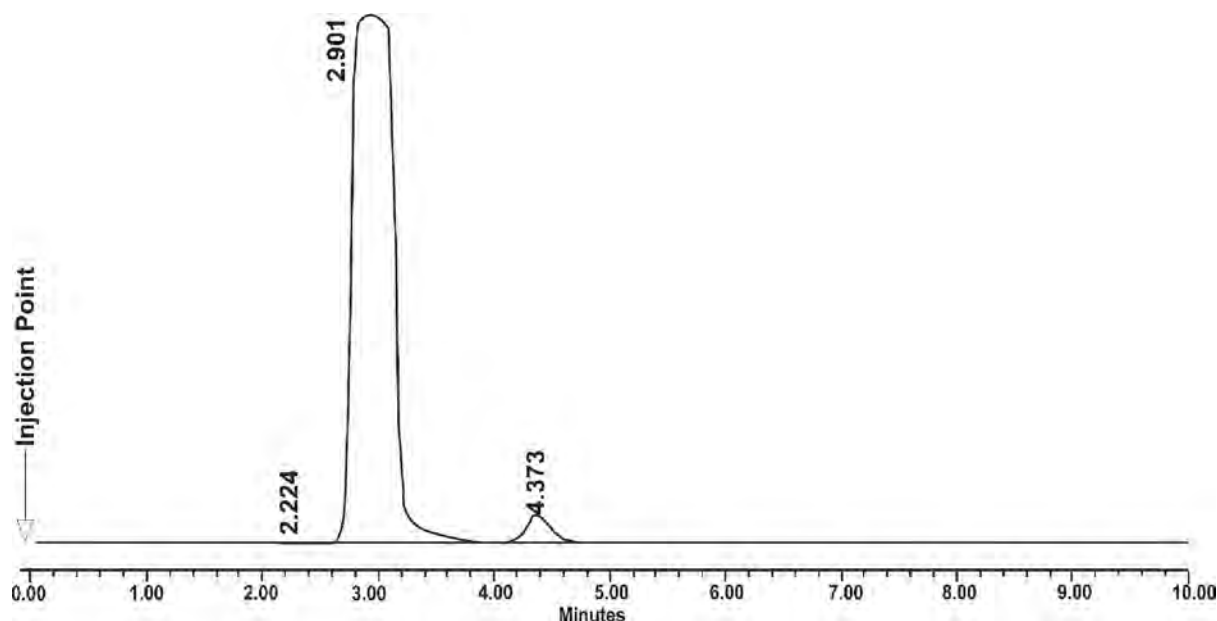


Figure 3.11 Typical chromatogram obtained from oxidative stress studies of HYD in 30% v/v H₂O₂ at 22 °C for 8 hours

3.4.3.4 Neutral hydrolysis

Hydrolysis is a solvolytic process in which drugs react with water to yield breakdown products of different chemical compositions and is the most common degradation reaction [225,226]. The effect of water at neutral pH was evaluated. Approximately 10 mg of HYD was accurately measured and transferred into a 100 mL A-grade volumetric flask to which water was added up to the mark. Neutral hydrolysis studies were performed at room temperature (22 °C) and elevated temperature (100 °C), under reflux, and sampling was done at 0, 2, 4, 6 and 8 hours. Table 3.12 shows the percentage remaining of HYD with time.

Table 3.12 Degradation studies of 100 µg/mL HYD in HPLC grade water at 22 and 100 °C for 8 hours

| Time (hours) | 22 °C | 100 °C |
|--------------|------------------|------------------|
| | % Remaining ± SD | % Remaining ± SD |
| 0 | 100.0 | 100.0 |
| 2 | 98.7 ± 0.72 | 75.3 ± 0.18 |
| 4 | 96.9 ± 0.46 | 65.3 ± 0.26 |
| 6 | 93.3 ± 0.75 | 64.4 ± 0.27 |
| 8 | 91.5 ± 0.23 | 63.9 ± 0.17 |

When stress studies of HYD were performed in HPLC grade water at 22 °C, no degradation peaks were observed after 8 hours. Figure 3.12 shows HYD peak at approximately 4.4 minutes.

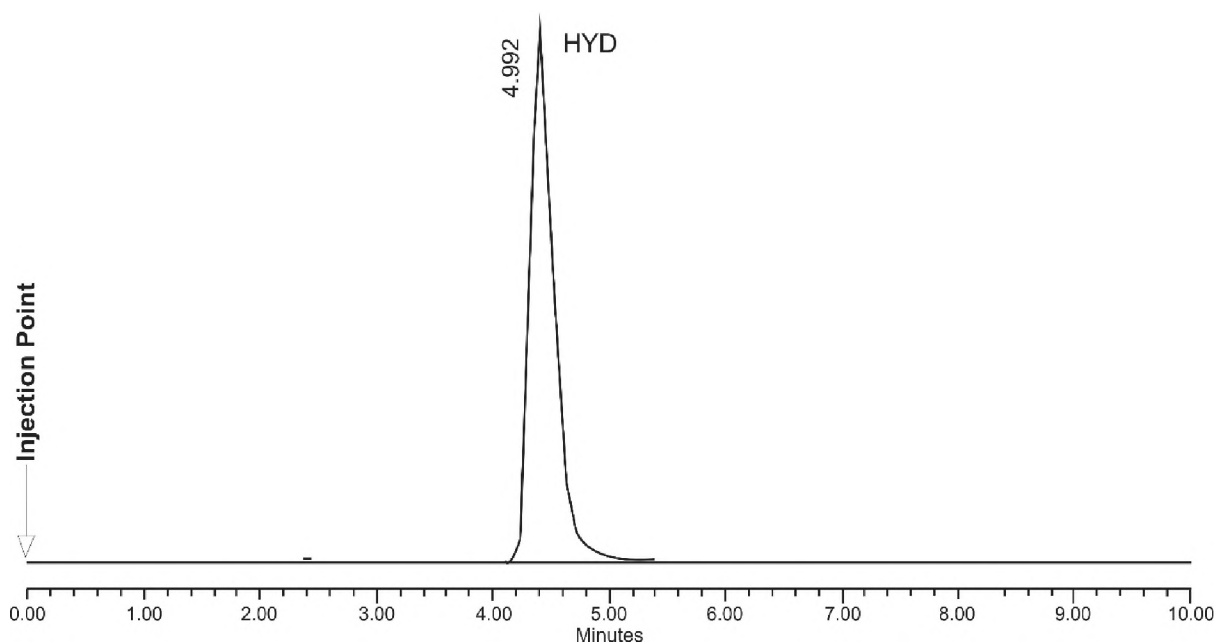


Figure 3.12 Typical chromatogram obtained from oxidative stress studies of HYD in HPLC grade water at 22 °C for 8 hours

When stress studies of HYD were performed in HPLC grade water at 100 °C for 8 hours, a degradation peak was observed at 3.4 minutes. Figure 3.13 shows the degradation chromatogram obtained from exposing HYD in water at 100 °C for 8 hours.

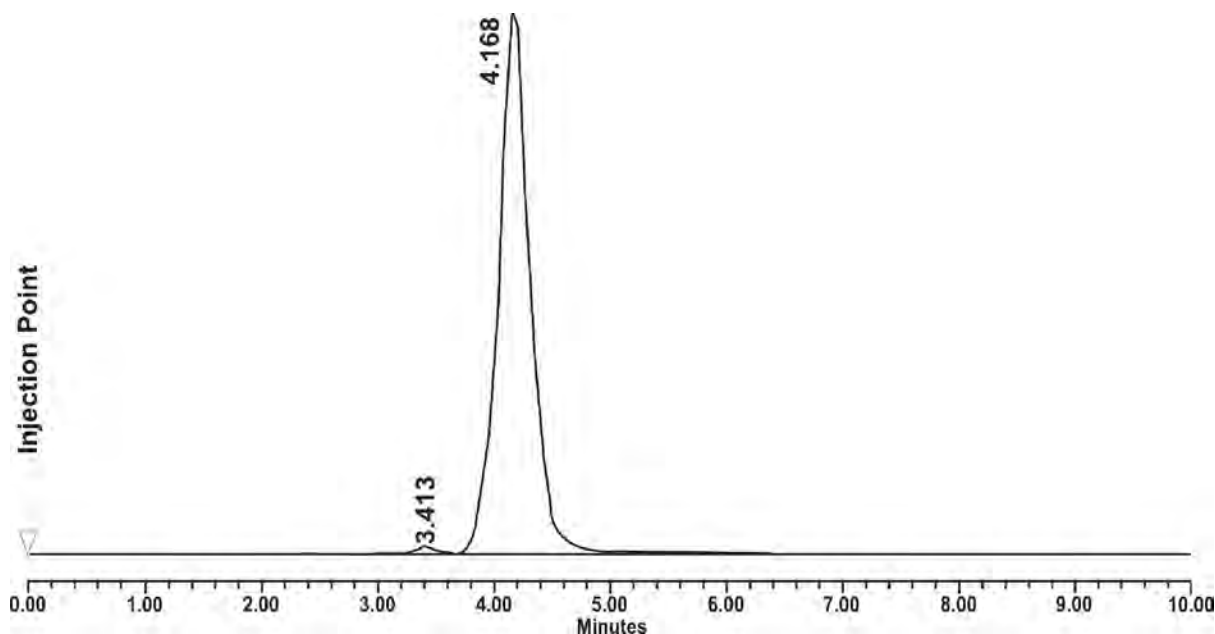


Figure 3.13 Typical chromatogram obtained from oxidative stress studies of HYD in HPLC grade water at 100 °C for 8 hours

3.4.3.5 Photostability studies

Photostability studies deal with the effect of light on the stability of pharmaceutical substances and/or products [252]. The rate and extent of photodegradation depends on the intensity of incident light and quantity of light absorbed by the drug molecule [184,234]. Photolytic degradation studies are performed by exposing the drug substance (in solid as well as in the solution form) or drug product to a combination of visible and UV light [226]. The most commonly accepted wavelength of light to cause photolytic degradation is in the range of 300-800 nm [226,230]. The photolytic degradation can occur through non-oxidative or oxidative reactions [226].

The investigation of the effect of light on an API is essential when studying stability since the information gained provides some insight and justification in respect of the storage conditions for that product. The ICH Q1B guideline [253] recommends the use of different sources of light in order to produce an output that is similar to the D65 or ID65 emission standards. The minimum light exposure should be 1.2 million lux hours with an energy of 200 Watts/ m² [237]. Forced degradation studies can be done on both, the solid state and aqueous solution or suspension forms of the API [227].

HYD powder and HYD solution were subjected to irradiation using an Atlas SUNTEST® CPS+ (Lisengericht, Germany) instrument for 24 hours. The lamp was set at 550 Watts/m² at an elevated temperature of 40 °C according to ICH specifications. Approximately 23.6% and 10%

of the HYD powder and solution degraded respectively but no degradation peaks were observed on all chromatograms generated (Figure 3.14).

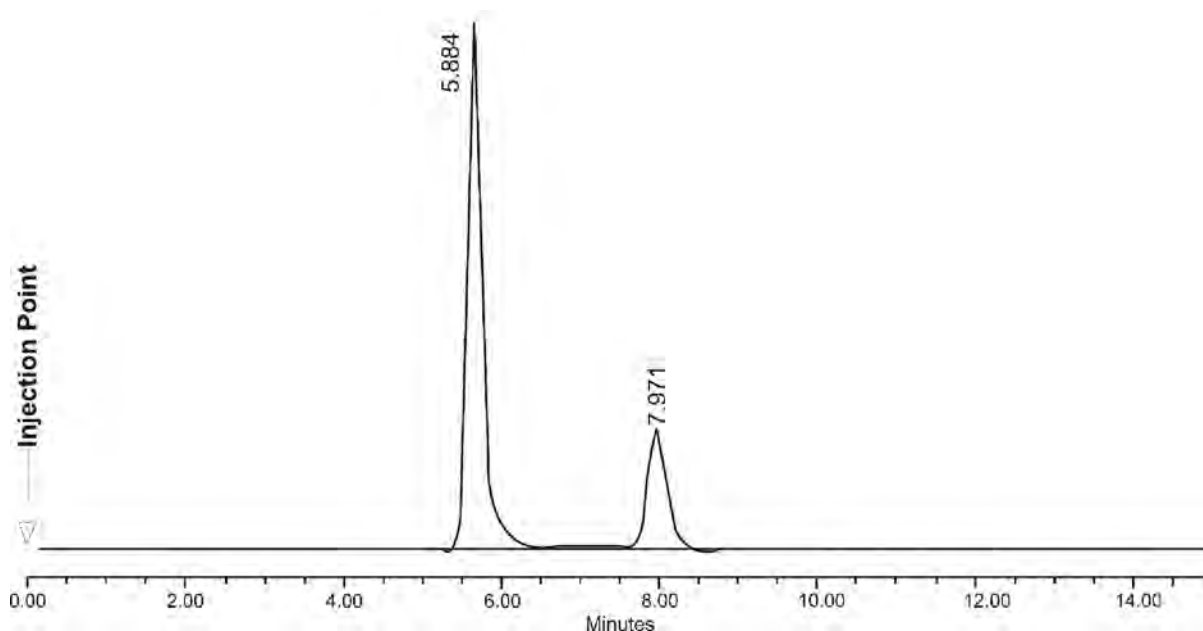


Figure 3.14 Typical chromatogram of 100 µg/mL HYD after exposure to 550 Watts/m² for 24 hours

3.5 CONCLUSIONS

The stability of HYD in solutions and effects of temperature on HYD in solution and solid state was performed. Accelerated degradation studies were performed in acidic, alkali, oxidative and photolytic conditions. The results reveal that HYD is susceptible to degradation in 0.1M NaOH (pH=13.0) and is oxidised in H₂O₂ solution to form additional chromatographic peaks. HYD was found to be stable in acidic media and increasing temperature had very slight effects on the rate of degradation.

The developed and validated method was successfully applied to the analysis of commercially available HYD tablets. The method was successfully used in the assessment of *in vitro* release and analysis of 50 mg HYD immediate release tablets with approximately 85% drug release within an hour of dissolution. No interfering peaks were observed indicating that the method was specific for quantitation of HYD as excipients used in Hyperphen[®]-50 did not affect the analysis of HYD. The absence of extra peaks on chromatograms might be due to excipients not absorbing UV at 240 nm or that the excipients were insoluble in water.

Forced degradation studies in HCL, H₃PO₄, NaOH, H₂O₂, H₂O and light indicated that degradants were resolved from HYD peak and that HYD could be qualitatively separated and

accurately quantified in the presence of degradants. The developed method was simple, linear, accurate, precise, sensitive, selective and stability indicating. The method was deemed appropriate for *in vitro* release analysis of HYD formulations.

CHAPTER 4

PREFORMULATION STUDIES

4.1 INTRODUCTION

Preformulation is the study of physicochemical properties of a drug component prior to formulation [207,254,255], and is used in optimising drug delivery [256,257]. Preformulation studies play a substantial role in the identification of anticipated formulation problems [103,255]. The successful formulation of a stable and effective dosage form depends on the careful selection of excipients that are added to facilitate administration, promote consistent release and bioavailability of a drug [255,258–260].

Preformulation studies are the first step in the rational development of dosage forms of a drug substance [261,262], hence identification and compatibility studies were performed on HYD. Fundamental preformulation studies include spectroscopy, solubility, melting point, stability and assay development [263,264]. Preformulation studies influence formulation components, manufacturing and packaging procedures [263,265,266].

The overall objective of preformulation studies is to generate useful information in developing stable, safe, bioavailable and reliable dosage forms which can be manufactured in bulk [263]. This information influences many of the subsequent events and approaches in formulation design and development [250,263,267]. Designing of preformulation studies is crucial as it relates to the relevance of results obtained to intended purpose [256].

4.2 SELECTION OF PHARMACEUTICAL EXCIPIENTS

4.2.1 Introduction

Pharmaceutical excipients are added in formulations to ensure the manufacture of a stable, convenient and acceptable formulation [263] and are selected on the basis of intended use, intended outcome and safety [268,269]. Excipient selection generally focuses on the appropriate characteristics of excipients such as functionality, material consistency and regulatory acceptance [269]. Excipients are known to facilitate administration and modulate drug release. Although considered pharmaceutically inert, physical and chemical interactions with active components are possible [270]. The formulator must consequently consider whether the supplier of the excipients is reliable or not. Cost, availability and accessibility

should also be considered when selecting excipients to include in a dosage form [271,272]. The choice of excipients for these studies was mainly dependent on design and desired release profile of HYD, availability, accessibility and safety.

4.2.2 Materials

All materials used in these studies are either generally regarded as safe (GRAS) and/or included in the Handbook of Pharmaceutical Excipients and appear in the FDA Indicative Ingredients Guide for general inclusion in oral formulations [273].

Table 4.1 shows all the compounds used during preformulation studies and appear on the GRAS list and/or are included in the FDA database for use as food additives in Europe. The physicochemical properties of HYD have been extensively studied in Chapter 1.

Table 4.1 Excipients used in preformulation studies

| Excipient | Commercial name | Abbreviation | Purpose | Supplier |
|------------------------------|------------------|--------------|---------|---------------|
| Hydralazine hydrochloride | - | HYD | API | Skyrun, China |
| Hydroxypropylmethylcellulose | Methocel® K100LV | HPMC | Binder | Colorcon |
| Methacrylic copolymer | Eudragit® RS PO | RS PO | Binder | Rohm Pharma |
| Microcrystalline cellulose | Avicel® 101 | MCC | Diluent | FMC |
| Acrylic acid polymer | Carbopol® 971P | CBP | Binder | Noveon |

4.2.2.1 Methacrylic acid copolymers

Methacrylic acid copolymer is a fully polymerised copolymer of methacrylic acid and acrylic or methacrylic ester [39,273,274]. Polymethacrylates are synthetic cationic and anionic polymers of dimethylaminoethyl methacrylates, methacrylic acid and methacrylic acid esters in varying proportions [39,273]. Several different types of methacrylic acid polymers are commercially available and may be obtained as dry powders, aqueous dispersions and organic solutions. Polymethacrylates are primarily used in oral capsule and tablet formulations as film-coating agents [273].

Three types of copolymers, namely Type A, Type B, and Type C are commercially available. Type C contains suitable surface-active agents. Ammonio methacrylate copolymers (Type A and Type B) consist of fully polymerised copolymers of acrylic and methacrylic acid esters with a low content of quaternary ammonium groups [273]. These copolymers vary in their methacrylic acid content and solution viscosity [268,269,273].

Eudragit® RS PO is a fine, white powder with a slight amine-like odour. Eudragit® RS (type B) contains 5% functional quaternary ammonium groups which give pH-independence permeability of the polymer. It has been used in the manufacture of microspheres as a release controlling agent [275–277]. It contains ethyl acrylate, methyl methacrylate and trimethylammonioethyl methacrylate chloride in a ratio of 1: 2: 0.2 respectively. It is a slightly water permeable and water insoluble compound, hence its ability to control the release of water soluble APIs. Eudragit® RS PO is soluble in acetone and alcohols [273], and therefore it was selected for Preformulation studies because acetone was used in the solvent evaporation technique.

4.2.2.2 Hydroxypropyl methylcellulose (HPMC)

Hydroxypropyl methylcellulose (HPMC) or Hypromellose is an odourless and tasteless, white or creamy-white fibrous or granular powder [273,274]. It is a non-ionic derivative, semi-synthetic polymer of cellulose ether and is stable over a pH range of 3.0-11 [278]. Its non-ionic nature minimises drug excipient interaction problems when used in acidic, basic or electrolytic systems and provides reproducible release profiles [278]. HPMC matrix systems are classified as swelling controlled systems which are unaffected by pH changes [278]. The drug release rate is controlled by the rate of penetration of media and erosion of the matrix [278]. HPMC is a mixture of alkyl hydroxyalkyl cellulose ether containing methoxyl and hydroxypropyl groups and the rate of drug release is affected by the nature of the substituents present in a polymer [278]. Compared to other swellable polymers used to control drug release, HPMC is the most widely used polymer due to its rapid hydration, good compression and gelling characteristics [278]. In addition, it has very low toxicity and is generally widely available for use [278]. Such advantages have triggered HPMC to be extensively used in cosmetics, pharmaceuticals and food industries [273,279].

HPMC has been used successfully in the manufacture of various pharmaceutical products [273]. Pharmaceutical functions of HPMC include its use as a bio-adhesive material, coating agent, controlled-release agent, dispersing agent, dissolution enhancer, emulsifying agent, emulsion stabilizer, extended-release agent, film-forming agent, foaming agent, granulation aid, modified-release agent, muco-adhesive, release-modifying agent, solubilizing agent, stabilizing agent, suspending agent, sustained-release agent, tablet binder, thickening agent and viscosity-increasing agent depending on the grade and amount used [273]. Methocel® K100LV has been used as a release rate controlling agent for many formulations [259,280–283].

There are a number of grades available that vary in viscosity and extent of substitution [273]. High-viscosity grades may be used to retard the release of drugs from a matrix at levels of 10–80% w/w in tablets and capsules. HPMC caramelises at temperatures ranging from 190 to 200°C, chars at 225–230 °C and is incompatible with some oxidising agents [273]. Methocel® K100M has a nominal viscosity of 100 000 mPa, K15M has 15 000 mPa and K100LV has 100 mPa [273] and these grades were selected for preformulation and formulation studies.

4.2.2.3 Microcrystalline cellulose (MCC)

Microcrystalline cellulose is a purified, partly depolymerised cellulose and commercially available in different particle sizes and moisture grades that have different properties and applications [273]. It occurs as a white or almost white, fine or granular powder. MCC is practically insoluble in water, in acetone and anhydrous ethanol [38].

MCC is used as a binder/diluent, lubricant and disintegrant, making it useful in tableting. It is hygroscopic and incompatible with strong oxidising agents [273]. MCC is not absorbed systemically following oral administration and thus has little toxic potential. Consumption of large quantities of cellulose may have a laxative effect, although this is unlikely to be a problem when cellulose is used as an excipient in pharmaceutical formulations [273]. MCC is listed as GRAS and also included in the FDA Inactive Ingredients Database [284]. Avicel® 101 was used for Preformulation and formulation studies.

4.2.2.4 Acrylic acid polymer

Carbomers are synthetic, high-molecular-weight acrylic acid polymers cross-linked with either allyl sucrose or allyl ethers of pentaerythritol [273]. They are formed from repeating units of acrylic acid [273]. Carbomers are white-coloured, ‘fluffy’, acidic, hygroscopic powder which contains between 52% and 68% of carboxylic acid (COOH) groups calculated on dry weight basis [273]. Carbomers have been used as bio-adhesive materials, controlled-release agents, emulsifying agents, emulsion stabilisers, rheology modifiers, stabilising agents, suspending agents and tablet binders [273]. Carbomer grades vary in aqueous viscosity, polymer type, and polymerization solvent. Carbopol® 971P has carboxylic acid content between 56% and 68% [273,274,285] and was used for preformulation studies.

4.3 API-EXCIPIENT COMPATIBILITY

Although considered pharmacologically inert, excipients can initiate, propagate or participate in chemical or physical interactions with drug compounds which may compromise the effectiveness of a medication [256]. Drug-excipient interaction(s) can either be beneficial or detrimental. Beneficial interactions are aimed to improve the solubility of poorly soluble drugs, increase dissolution rates, increase the rate of drug release, alter therapeutic activity, increase bioavailability and decrease unwanted side effects. Detrimental interactions can alter stability and bioavailability of drugs, thereby affecting their safety and/or efficacy [256].

The knowledge of drug excipient interaction is useful for formulation in order to select appropriate excipients [272]. Table 4.2 shows different techniques used to determine API-excipient interactions. Various methods can be used to determine API and excipient compatibility depending on, but not limited to, availability, accessibility, affordability and applicability of such methods. Thermal analysis can be used to investigate and predict any physicochemical interactions between components in a formulation. Therefore, it is useful in the selection of suitable chemically compatible excipients [103].

Table 4.2 Techniques used to determine API-excipient and excipient- excipient compatibility

[254,256,261,263,269,270,286–292]

| Technique | Measurement | Utility of Data |
|------------------|---|--|
| FT-IR | Absorption and transmission of different IR frequencies by a sample | Functional group(s) determination, compound identification and interactions |
| Microscopy | Magnified visualization of samples | Particle size, shape and morphology analysis |
| Chromatography | Interaction of sample with stationary and mobile phase | Purity testing and Chemical compatibility of API and excipients |
| XRD | Scattering of X-ray radiation by a sample | Characterisation of polymorphs |
| LC-MS/MS | Chromatographic separation and fragmentation of molecular species | Purity testing and characterisation of degradants |
| DSC | Enthalpy of transition by a substance as it is heated, cooled or maintained at a constant temperature | Physicochemical compatibility of API and excipients involving thermal changes |
| TGA | Change in weight of a substance as a function of temperature | Physicochemical compatibility of API and excipients involving thermal changes |
| MC | Heat absorbed or released by sample | Interactions between molecules and conformational changes |
| Thermomicroscopy | Photomicrography of a sample as a function of temperature | Morphological characteristics of drug and excipient separately and in mixtures using optical microscopy. Melting point and decomposition |
| RS | Inelastic scattering of laser radiation with loss of vibrational energy by a sample | Identification and interactions of API and excipients |
| IM | Measures power as a function of temperature/time | Characterising intermolecular interactions and recognising reactions |

FT-IR - Fourier Transform infrared spectroscopy

XRD - X-ray diffraction

DSC - Differential Scanning Calorimetry

TGA - Thermogravimetric Analysis

LC-MS Liquid Chromatography- Mass Spectroscopy

IM - Isothermal microcalorimetry

MC - Micro-calorimetry

RS - Raman spectroscopy

4.3.1 Types of Interaction

Interactions are classified into two broad groups, namely physical and chemical interactions [256,293,294]. They can be drug-excipient, drug-drug or excipient-excipient interactions although drug-excipient interactions occur more frequently than excipient-excipient interactions [268]. In addition, interactions can be direct or indirect. Changes in drug release are frequently a result of drug-excipient and excipient-excipient physicochemical interactions in the dosage form [272,295].

4.3.1.1 Physical interaction

Physical interactions are those which involve changes in the physical form of the formulation, including but not limited to colour changes, liquefaction, phase separation or immiscibility. Although difficult to detect, physical interactions are common and can result in organoleptic changes such as taste and odour [295]. Furthermore, physical interactions can affect the rate of dissolution, uniformity of dose or ease of administration which may affect bioavailability [256,268,295].

4.3.1.2 Chemical interaction

Chemical interactions involve chemical reaction(s) between drugs and excipients or drugs and impurities/residues present in the excipients to form different molecules [293]. They can be detrimental to the product as they produce degradation products. They can lead to degradation of the active ingredient, thereby reducing the amount available for therapeutic effect [256,293]. Common chemical reactions in pharmaceutical materials include but are not limited to oxidation, hydrolysis, dehydration, dissociation, isomerisation, elimination, cyclisation and photolysis [256,293,295]. Chemical interactions are indicated by the appearance of new peaks, gross broadening or elongation of an exo- or endothermic change [103,295]. They can involve direct reactions to form a covalent bond or indirect reactions due to catalysis or pH modification effects [295].

4.3.1.2.1 Direct reaction of drug and excipient

Direct reaction occur when API functional group(s) reacts with excipient functional group(s) resulting in bond formation(s) [295]. Nucleophilic reactions, esterification reactions and Maillard reactions between amide groups and carboxylic groups of reducing sugars are typical examples of direct reaction [261,295]. Maillard reaction was reported when fluoxetine hydrochloride was formulated with lactose [57,296].

4.3.1.2.2 Indirect reaction of the drug and excipient

Excipients can act as catalysts to increase degradation of drug molecules. Nucleophilic catalysis caused by excipients with polyhydroxyl functional groups leading to ester hydrolysis is a typical example of indirect catalysis reaction. Sucrose catalysed by the hydrolysis of

benzylpenicillin to benzylpenicillin acid is an example of the nucleophilic catalysis mechanism [295].

4.3.1.3 Therapeutic interaction (TI)

Therapeutic interactions (TI) are a type of *in vivo* compatibility. It involves changes in the therapeutic response of the formulation which is undesirable for the patient as well as the physician. TI can be subdivided into pharmacokinetic and pharmacodynamic interactions. Pharmacokinetic interactions include alteration of GIT absorption, altered metabolism, plasma protein binding and altered renal excretion [297–300].

4.3.2 Drug excipient compatibility

Drug excipient compatibility studies represent an important phase in the preformulation stage of the development and optimisation of all dosage forms [288]. The potential and actual physical and chemical interactions between drugs and excipients can affect the chemical, physical, bioavailability properties and stability of a dosage form [261,288], hence the importance of preformulation studies [301]. The compatibility screening studies involve the use of physical mixtures of a drug with one or more excipients. The proportion of excipients in the mixtures is usually kept high compared to that in the formulation to maximise the proportion of excipient/reacting species, thereby increasing the chance of incompatibility [301].

Until now, no universally accepted protocol is available for evaluating the compatibility of a drug with excipients. Frequently used analytical techniques for compatibility screening of API include, but are not limited to, differential scanning calorimetry, thermogravimetric analysis, differential thermal analysis, isothermal microcalorimetry, hot stage microscopy and other analytical methods, namely powder X-ray diffraction, Fourier transform infrared spectroscopy (FT-IR), scanning electron microscopy (SEM) and HPLC [301]. These techniques are important in the selection and screening of appropriate excipients to produce stable pharmaceutical dosage forms.

HYD contains reactive functional groups, therefore it is of utmost importance to determine the compatibility of HYD with all excipients used. FT-IR is a simple, rapid and non-destructive method to determine chemical changes of the API by determining functional groups. However, further Thin Layer Chromatography (TLC) studies need to be performed to determine if there

is no interaction [256]. The structure of the drug and of the excipient(s) gives a rough idea of possible interactions that might occur depending on present functional groups [103,256,291].

4.3.2.1 TGA

Thermogravimetric analysis (TGA) is a technique in which the changes in sample mass are determined as a function of temperature or time as the sample specimen is subjected to a controlled temperature programme in a controlled atmosphere [302]. TGA is used to characterise the decomposition, degradation and thermal stability of compounds under a variety of conditions [302]. Changes in sample mass might be due to adsorption of oxygen, thermal degradation, oxidation, or other heterogeneous reactions. Interpretation of TG data is often facilitated by comparison with data from other experimental techniques [302]. Thermal analysis plays a crucial role in compatibility screening studies and has been frequently employed for quick assessment of physicochemical incompatibility [301].

4.3.2.2 DSC

Differential scanning calorimetry (DSC) is a technique used to measure changes in heat required to maintain a sample and a reference at the same temperature as they are heated and cooled [288,301]. The DSC curves of pure components are compared to the curves obtained from 1:1 physical mixtures, based on an assumption that the thermal properties of the mixture are the sum of the individual components [301]. When the substance undergoes a thermal event, the difference in the heat flow to the sample and reference is monitored against time or temperature while the temperature is programmed in a specified atmosphere [271]. Incompatibility is indicated by a significant shift in the melting of the components or absence of a peak or appearance of a new exo/endothermic peak and/or variation in the corresponding enthalpies of reaction in the physical mixture [303]. However, slight changes in peak shape, height and width are expected due to possible differences in the mixture geometry [301]. DSC provides useful indications of the potential problems so that an excipient can be rejected at an initial stage of product development. Although DSC provides supreme and valuable thermal data, the conclusions based on DSC results alone may be misleading because interactions observed at elevated temperature may not be relevant under ambient conditions [301]. Therefore, DSC results must be interpreted in conjunction with complementary techniques such as isothermal microcalorimetry, FT-IR spectroscopy, SEM and X-ray diffraction [301].

4.3.2.3 FT-IR

FT-IR is based on the vibrations of the atoms of a compound due to nature and type of bonding present [304,305]. Interactions that result in dehydration, hydrate formation, polymorphic changes or transformation of crystalline to amorphous forms and vice versa during preformulation studies can easily be detected with FT-IR [301]. Drug-excipient interactions in the solid state can be shown using FT-IR by examination of wavelength shifts in the characteristic peak positions of either the drug or the excipient [256].

4.3.2.4 XRPD

X-ray powder diffraction (XRPD) is a technique that measures the intensity of x-rays scattered at different angles by a crystalline sample [306]. XRPD is used to study the atomic and molecular structure of crystalline substances such as drugs and excipients because crystalline material exhibits unique diffraction peaks. Diffractograms can be used to confirm the crystalline nature of a sample [254,302]. Therefore, this information is used to verify whether substances are crystalline or amorphous.

The lack of crystalline API peaks when a mixture is analysed could indicate that the material is amorphous or that the amount is too low to detect. XRPD analysis is helpful in the case of incompatibilities which occur during processes like compression and wet granulation [288].

This non-destructive analytical tool [306] is widely used for phase analysis, polymorph screening, crystallinity determination, crystallography and crystal structure determination, compatibility studies and stability studies. X-ray diffraction patterns of the mixture, prepared at room temperature, when compared with those of its individual components can show the appearance of new peaks and the disappearance of some of the peaks present in the individual components can be interpreted as a sign of incompatibility [256,291].

The X-ray diffractometric technique obtains information on substance structure at the atomic level. The analysis handles samples in the form of powders, solids and liquids. Powder diffraction is used for fingerprint purposes [254]. Nevertheless, absolute intensity may vary due to instrumental and experimental parameters [307].

4.4 METHODS

The physical and chemical interactions between drugs and excipients can affect the chemical nature, the stability and the bioavailability of drug products, and consequently, their therapeutic efficacy and safety [287]. Different methods are used for preformulation depending on the formulator and the intended dosage form. SEM, FT-IR, DSC, TGA and XRPD were selected for preformulation studies for HYD as they are relatively quick, accessible and can predict potential formulation problems.

4.4.1 SEM

The particle size and surface morphology for HYD and excipients were characterised using SEM (Tescan, VEGA LMU, Czech Republic). Samples were mounted onto a double-sided carbon stub, placed on a sample disc carrier (3mm height, 10mm diameter) and coated with gold particles under vacuum with a sputter coater (Balzers Union Ltd, Balzers, Lichtenstein) for 15 minutes at 20 kV.

4.4.2 Melting point determination

A Stuart SMP30 melting point apparatus (Stone, Staffordshire, UK) was used to determine the melting point of HYD. Three samples were placed into 100 mm glass capillary tubes. After a plateau of 260 °C (10 °C below the expected melting point of HYD) was reached, melting point samples were placed in the aluminium sample block inside the sample chamber. Ramping rate was set at 2.0 °C/min from plateau temperature and no changes occurred to the samples from 260 °C to 272 °C. The temperature at which the drug started decomposing was taken as the initial reading and the point at which the whole sample melted was recorded as the final reading. The exact melting point was confirmed using DSC studies of the pure drug. Generally, the presence of impurities and/or excipients in a compound will lower its melting point [308,309].

4.4.3 NMR

The Nuclear Magnetic Resonance (NMR) principle is based on radiation in the radiofrequency region of protons or carbon-13 atoms to excited state so that their spin switches from being aligned with to being aligned against an applied magnetic field [254,310]. The range of frequencies required to excite proton or carbon atoms is very characteristic of the chemical

structure of the molecule [310]. NMR spectroscopy has many applications in fields other than chemistry, including food science, medicine, pharmacy and biology [137,311]. It is an important technique for the solid-state characterization of materials, elucidation and confirmation of structure of materials [311–316]. The versatility and ability of NMR to distinctly differentiate nuclei in various intramolecular environments have placed it as the most reliable and dependable technique for identification tests of pure drugs [137]. The application of NMR to pharmaceutical topics has been fully published and demonstrated [137,311,313,317–319]. The main advantage of NMR is that it is non-invasive and non-destructive [311].

The NMR spectrum for HYD was generated using a Bruker 600 MHz NMR spectrometer (Rheinstetten, Germany). HYD was dissolved in DMSO and transferred into an ASTM Type 1 Class A borosilicate 178 mm thin walled NMR tube (Norell, Inc. Mays Landing, NJ) for the determination of the ^1H NMR and ^{13}C NMR. The tubes are specifically designed for high resolution NMR, are temperature resistant and are recommended for structural elucidation and confirmation of compounds [312]. Chemical shifts were reported in parts per million (ppm). All NMR spectra were determined at a frequency of 600 MHz using Bruker[®] Ultrashield spectrometer and in the standard sequence of 1H, 13C and DEPT-15 and all chemical shifts were recorded using Mnova[®] software (Mestrelab[®] Research, Santiago de Compostela, Spain).

4.4.4 DSC

DSC studies were performed using a PerkinElmer[®] DSC 6000 (Perkin Elmer[®] AG, Norwalk, Connecticut, USA). The DSC was connected to a computer via a TAC 6/ DX Thermal Analysis Instrument Controller. An inert atmosphere was maintained by passing nitrogen gas through the system at a rate of 20 mL/min to eliminate oxidative and pyrolytic effects. The heating rate of the DSC assembly was controlled at 10 °C/min over the temperature range of 30–445 °C. An empty aluminium pan was used as a reference. Each thermogram generated during the heating process was performed using 10 scans with a resolution of 4 per cm^{-1} . Pyris[®] Software was used to analyse DSC data generated. The appearance and/or disappearance of one or more peaks on the thermogram of HYD-excipient mixtures were considered an indication of interaction.

4.4.4.1 Sample preparation

Samples for DSC analysis of pure HYD, excipients and drug excipient mixtures (1:1) were prepared as summarised in Figure 4.1.

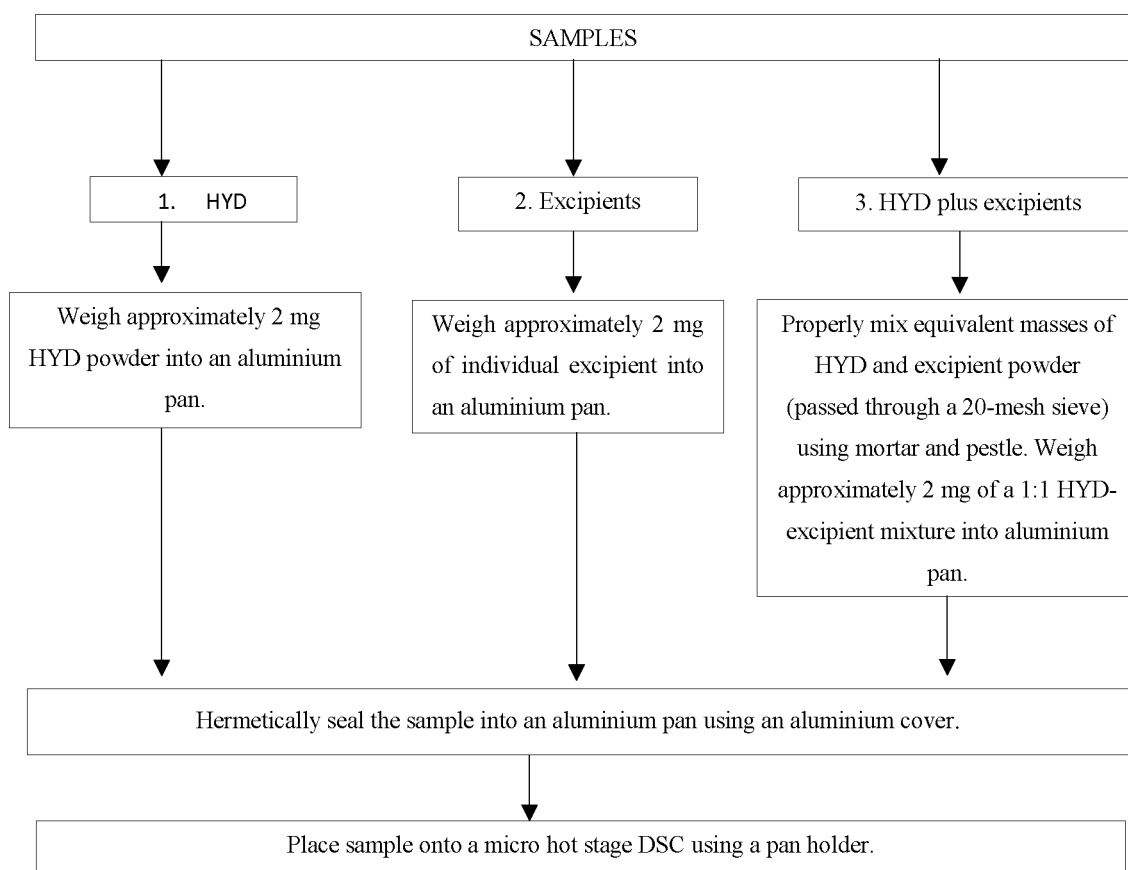


Figure 4.1 Summarises how the DSC for HYD, excipients and 1:1 Drug-excipient mixture sample were prepared

4.4.5 TGA

TGA experiments were conducted using a Model TGA 4000 Perkin Elmer Thermogravimetric Analyzer (Perkin Elmer®, Norwalk, Connecticut, USA) fitted with a platinum sample holder. The TGA was connected to a computer via a TAC 6/DX Thermal Analysis Instrument Controller. Approximately 4 mg of dry HYD and/or the binary mixtures (1:1) to be tested were weighed and placed into platinum crucibles. Measurements were performed in a nitrogen atmosphere (inert atmosphere) at a flow rate of 20 mL/min, a heating rate of 10 °C/min, and a temperature range of 30 to 600 °C. TGA measurements were performed only once. Pyris® Software was used to analyse TGA data generated.

4.4.6 FT-IR

A KBr disc method was used to generate the FT-IR spectrum of HYD, excipients and 1:1 mixtures of HYD and the excipients in the range 4000 to 650 cm^{-1} using a PerkinElmer® FT-IR spectrometer Spectrum 100 (Beaconsfield, England) apparatus. FT-IR for pure HYD and excipients was performed by placing approximately 3 mg of each sample on the KBr disc. Binary mixtures were made by weighing 5 mg of HYD and 5 mg of excipient. These were then mixed using a mortar and pestle. Approximately 3 mg of each mixture was placed on the KBr disc and spectrum data was collected over the IR range of 4000-650 cm^{-1} . Major functional groups from 4000 cm^{-1} to 1600 cm^{-1} present in HYD were analysed by superimposing the spectrums with that of pure HYD for potential drug-excipient interactions. This is because from 1300 cm^{-1} to 650 cm^{-1} is the fingerprint region specific for a compound, therefore it will never be the same for mixtures [137].

4.4.7 XRPD

X-ray diffraction studies were performed in order to obtain more information to support DSC and TGA results. XRPD patterns were recorded on a Bruker D8 Discover (Billerica, Massachusetts, USA) equipped with a proportional counter, using a $\text{Cu-K}\alpha$ radiation ($\lambda = 1.5405 \text{ \AA}$) nickel filter. The general voltage of the experiment was 30 kV and the general current 40 mA. Data were collected in the range from $2\theta = 10^\circ$ to 100° , scanning at $1.5^\circ \text{ min}^{-1}$ with a filter time-constant of 0.38s per step and a slit width of 6.0 mm. Samples were placed on a silicon wafer slide. The X-ray diffraction data were treated using the evaluation curve fitting (Eva) software. Baseline correction was performed on each diffraction pattern by subtracting a spline function fitted to the curved background.

4.5 RESULTS AND DISCUSSION

4.5.1 SEM

SEM allows characterization and analysis of surface morphology of materials and is useful especially when there are distinctive differences between the API and excipients. SEM does not give any information about the chemical structure/thermal behaviour of drug materials and requires sample preparation along with stage condition setup. The combination of SEM studies with other thermal and spectroscopic techniques offers some opportunities for the characterization of incompatibilities of materials [301,320].

The results indicate that there is variation in both particle size and particle morphology between the drug and excipients. Figures 4.2 to 4.6 show all obtained images when the samples were examined under the microscope. The SEM images obtained indicate clearly a variation in particle size and morphology; therefore, size reduction and sieving should be performed to facilitate proper powder mixing. HYD is acicular and cylindrical shaped whereas Eudragit® RS PO and Carbopol® 971P are angular shaped. Methocel® K100LV, K4M, K15M and K100M were found to be rod shaped. The SEM images obtained will also help after formulation to identify any changes that would have occurred (if any), and therefore SEM of all optimised formulations were performed. This is particularly helpful if a molecule can exist in different morphology.

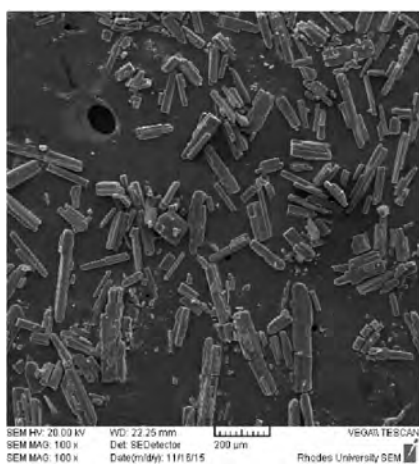


Figure 4.2 SEM image of HYD

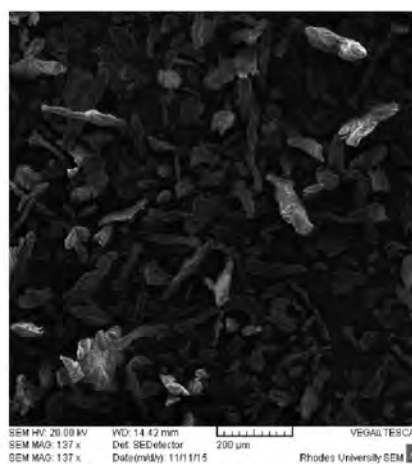


Figure 4.3 SEM image for Methocel® K100 LV

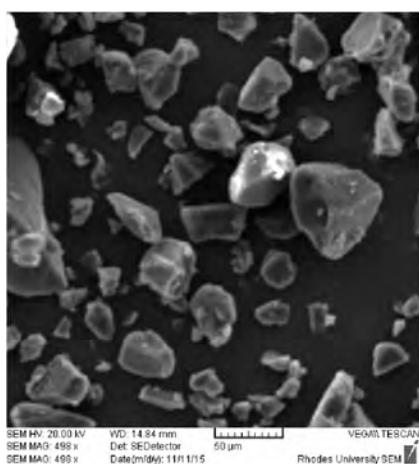


Figure 4.4 SEM image for Eudragit® RS PO

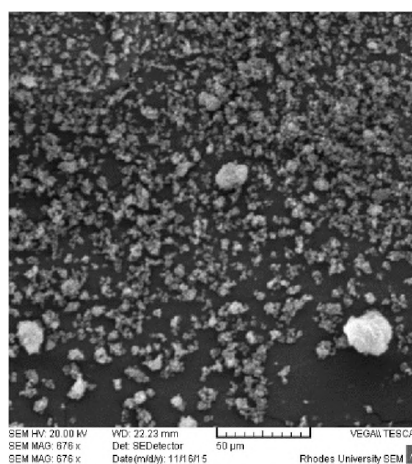


Figure 4.5 SEM image for Carbopol® 971P

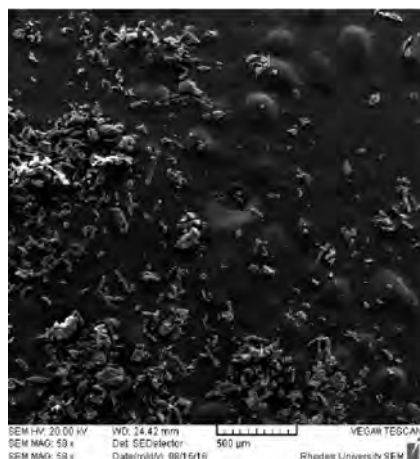


Figure 4.6 SEM image for Avicel® 101

4.5.2 Characterization of HYD

4.5.2.1 Melting point

The melting point was found to be in a range from 273 °C to 275 °C and correlates with previously reported melting points for HYD [37,38]. No changes were observed from the plateau temperature of 260 °C to 272 °C. HYD melted to a clear liquid before permanently crystallising to a yellow compound.

4.5.2.2 DSC

The DSC thermogram for HYD is shown in Figure 4.7 and shows a melting point of 279 °C. The DSC thermograms were interpreted on the basis of the direction of the peaks: positive peaks indicated an endothermic transition, whereas negative peaks are indicative of an exothermic transition. The thermogram shows a ΔH of -620 J/g indicating that decomposition occurs exothermically. HYD absorbs energy which then facilitates the decomposition of HYD. The decomposition of HYD starts at 275 °C and occurs over a wide range of temperature [37].

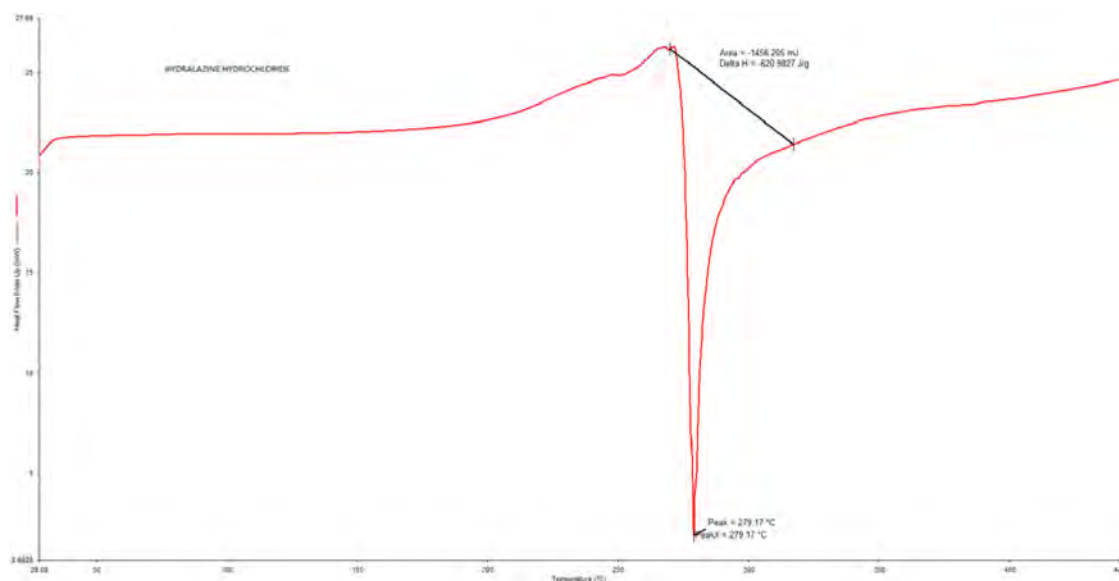


Figure 4.7 Typical DSC thermogram of HYD generated at a heating rate of 10 °C/min

4.5.2.3 TGA

The TGA thermogram for HYD is shown in Figure 4.8 and it shows that decomposition starts at around 250 °C. However, the majority of HYD decomposition occurs at 275 °C. At approximately 280 °C, about 70% of HYD had decomposed. The thermogram indicates that HYD decomposes in three stages and over a wide range of temperature (250 °C to 400 °C) [37]. This information correlates with the information obtained from DSC studies. These studies indicate that HYD is stable up to a temperature of 250 °C and suggest that it is unlikely for HYD to decompose under normal homogenising temperature, as temperature rarely exceed 100 °C.

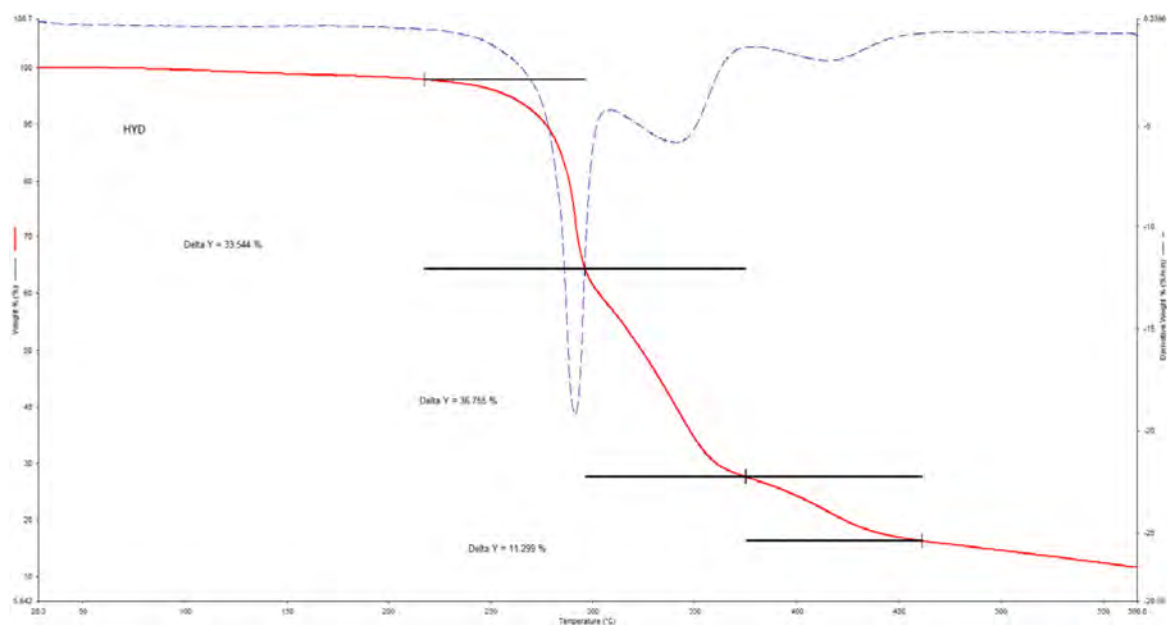


Figure 4.8 Typical TGA thermogram of HYD generated at a heating rate of 10 °C/min from 30 to 600 °C

4.5.2.4 FT-IR

FT-IR studies were carried out for pure HYD from 4000 cm^{-1} to 650 cm^{-1} at a resolution of 4 cm^{-1} . The FT-IR spectrum for HYD is shown in Figure 4.9. Resonance at 3429, 3027 and 1668 cm^{-1} were assigned to N-H functional groups, aromatic C-H and aromatic C=C stretching respectively. These resonances were labelled as characteristic functional groups of HYD for the entire FT-IR studies.

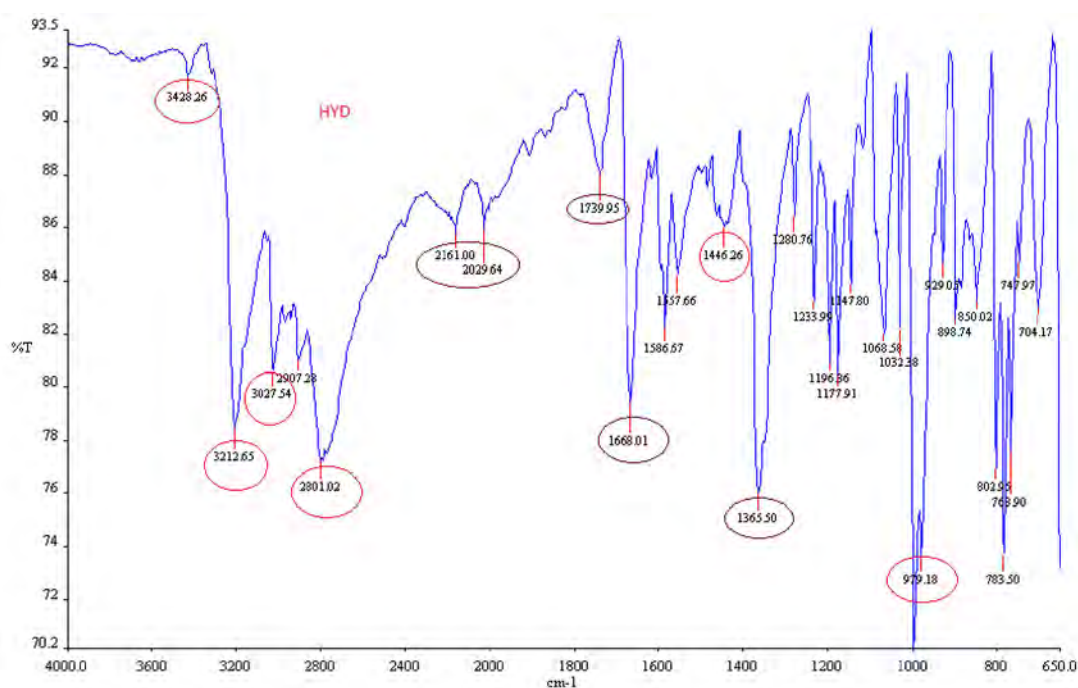


Figure 4.9 Typical FT-IR spectrum of HYD generated from 4000 cm^{-1} to 650 cm^{-1}

Table 4.3 shows the summarised functional groups obtained by observing the FT-IR spectra of HYD. These functional groups were monitored when doing FT-IR for the combination of HYD and excipients. The fingerprint region was not well studied as it would be different when HYD is mixed with excipients.

Table 4.3 Interpretation of FT-IR spectra for HYD [37]

| Frequency (cm ⁻¹) | Intensity | Assignment |
|-------------------------------|-------------------|---|
| 3429 | Weak (w) | N-H symmetric and asymmetric stretch (secondary amines) |
| 3210 | Strong (s), sharp | N-H stretch (primary amine) |
| 3027 | m-s | Ar C-H stretch |
| 1446-1670 | m-s (four bands) | Ring C=C stretch |
| 1668 | S | C=C stretch |
| 650-1500 | - | Fingerprint peaks (region) |

4.5.2.5 XRPD

X-ray was used to study the fingerprint characterisation of pure crystalline HYD using a Bruker D8 Discover (Billerica, Massachusetts, USA) equipped with a proportional counter, using Cu-K α radiation.

XRPD patterns of HYD are shown in Figure 4.10. HYD shows characteristic peaks at a diffraction angle of $2\theta = 11, 12, 20, 22, 25, 27, 28, 33$ and 39° . X-ray diffraction is used to study the atomic and molecular structure of crystalline substances such as drugs and excipients. X-rays diffraction patterns (diffractograms) can be used to confirm the crystalline nature of a sample. XRPD was successfully used in the determination of crystallinity of HYD.

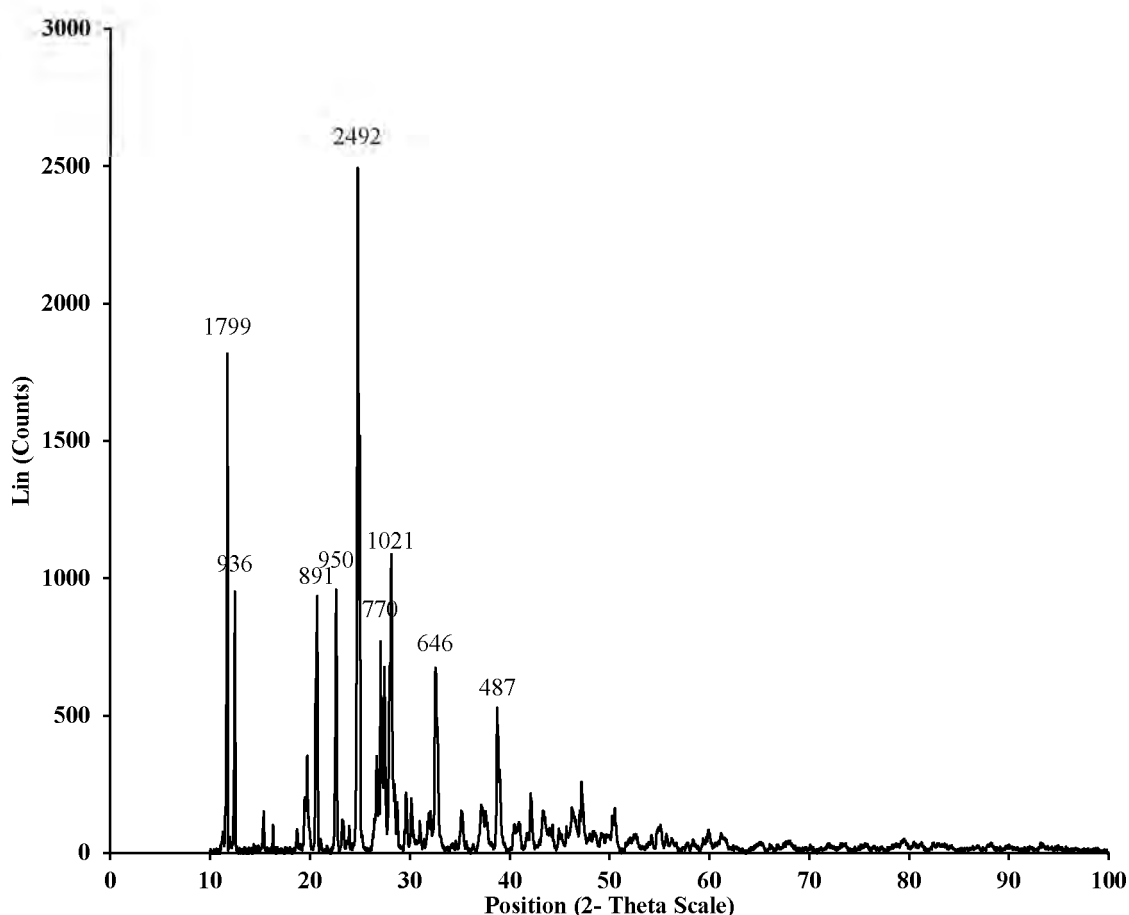


Figure 4.10 X-ray Diffraction patterns of crystalline HYD

4.5.2.6 NMR

NMR was used for the identification and characterisation of HYD and to identify whether impurities may have formed in the bulk API during transportation and storage. The presence of impurities may have an effect on the stability of the formulation. The reactive primary and secondary amines in HYD might undergo reactions. NMR characterisation is a non-selective approach, making it suitable for the analysis of mixtures.

Proton (^1H) NMR is the most commonly used form of NMR due to its sensitivity [310]. The ^1H NMR provides information about the intra- and inter-molecular resonances [254]. The proton is the most sensitive and most common nucleus detectable by NMR. The chemical shift is determined by the extent to which the proton is deshielded by the groups to which it is attached [310]. However, ^{13}C NMR has greater potential than ^1H NMR as it includes the direct observation of molecular backbones and the sensitivity of ^{13}C NMR to chemical shifts and small differences in the molecular environment [318]. The ^1H and ^{13}C chemical shift values were reported on the δ scale (ppm) relative to DMSO.

The ^1H NMR spectra of HYD are depicted in Figures 4.11 and the data are summarised in Table 4.4. The figures and tables provide information about the number of non-chemically equivalent nuclei or non-equivalent hydrogen present in the molecule and information about the atoms attached to those nuclei. The proton NMR of HYD revealed a sharp peak at 8.81 ppm that is due to a secondary amine and a doublet between 8.69 – 8.72 ppm that corresponds to the primary amine. The multiplet from 8.01 to 8.15 ppm corresponds to the 5-protons in the benzene rings. The singlet at 2.49 and 3.40 ppm corresponds to dimethyl sulfoxide (DMSO) and water respectively. The hydrogen NMR was enlarged from 7.9 to 8.9 ppm because that was the region of interest. The enlarged HNMR is also shown in Figure 4.11.

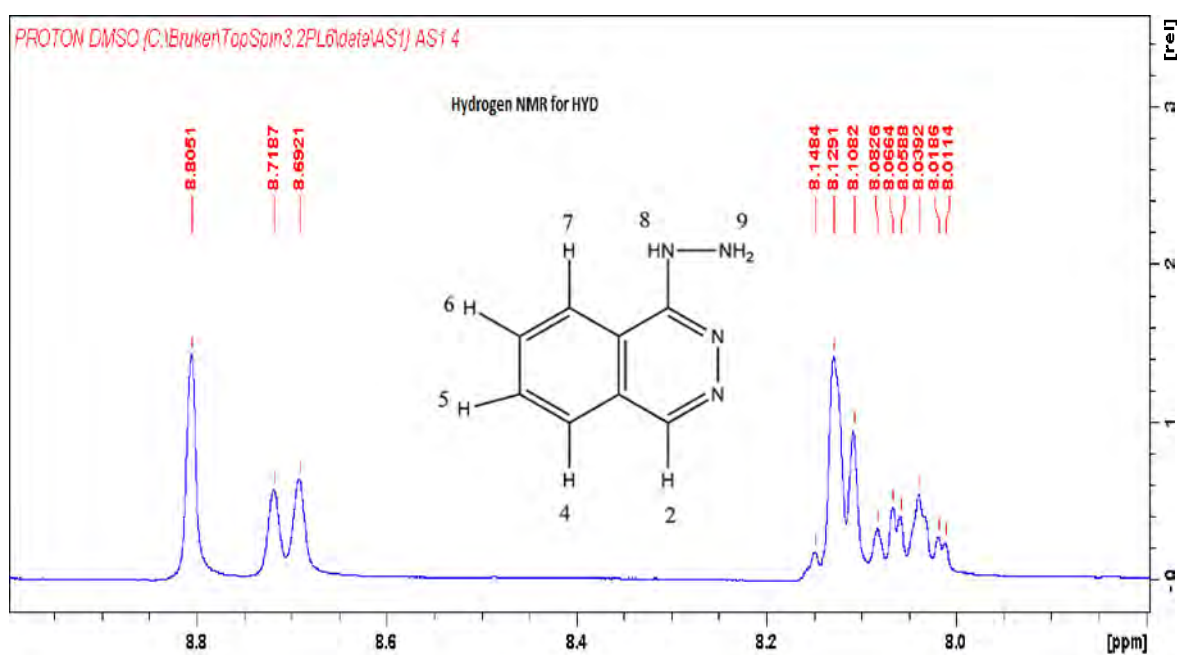
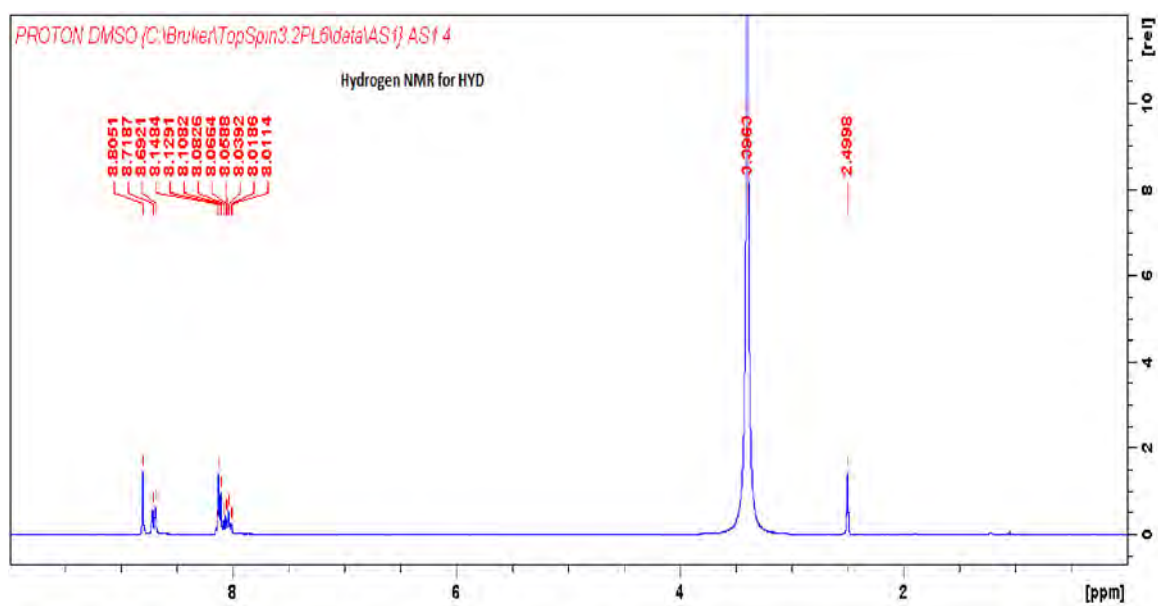


Figure 4.11 600 MHz ^1H NMR spectrum of HYD in DMSO

The named hydrogens in Figure 4.11 are summarised and characterised in Table 4.4. The ^1H NMR indicates that HYD was still in its pure form.

Table 4.4 Proton-NMR for HYD [54]

| Position | Node | Integration | Chemical Shift (ppm) | Multiplicity |
|----------|------------------|-------------|----------------------|--------------|
| 8 | N-H | 1H | 8.81 | S |
| 9 | N-H ₂ | 2H | 8.69-8.71 | D |
| 2 | C2-H | 2H | 8.01-8.15 | m |
| 4 | C4-H | 2H | 8.01-8.15 | m |
| 5 | C5-H | 2H | 8.01-8.15 | m |
| 6 | C6-H | 2H | 8.01-8.15 | m |
| 7 | C7-H | 2H | 8.01-8.15 | m |
| | | DMSO | 2.49-2.51 | s |
| | | Water | 3.40 | s |

s- singlet, d-doublet, m-multiplet

The ^{13}C NMR spectrum indicates the presence of 8 major signals. The signal at 151.45 ppm corresponds to the carbon in position 1. The signal at 143.56 ppm corresponds to the carbon on position 2 and 127.46 ppm corresponds to the carbon on position 4. The chemical shift at 128.54 ppm corresponds to carbon 4 whilst the signal at 135.73 ppm corresponds to carbon on position 5. The signal at 133.98 ppm corresponds to carbon 6 and the signal at 124.64 ppm corresponds to carbon on position 7. The chemical shift at 119.77 ppm corresponds to carbon on position 8 as described in Figure 4.12. The ^{13}C NMR of HYD provides enough evidence to confirm that the basic structure of HYD exists. The ^{13}C NMR spectra of HYD are depicted in Figure 4.12.

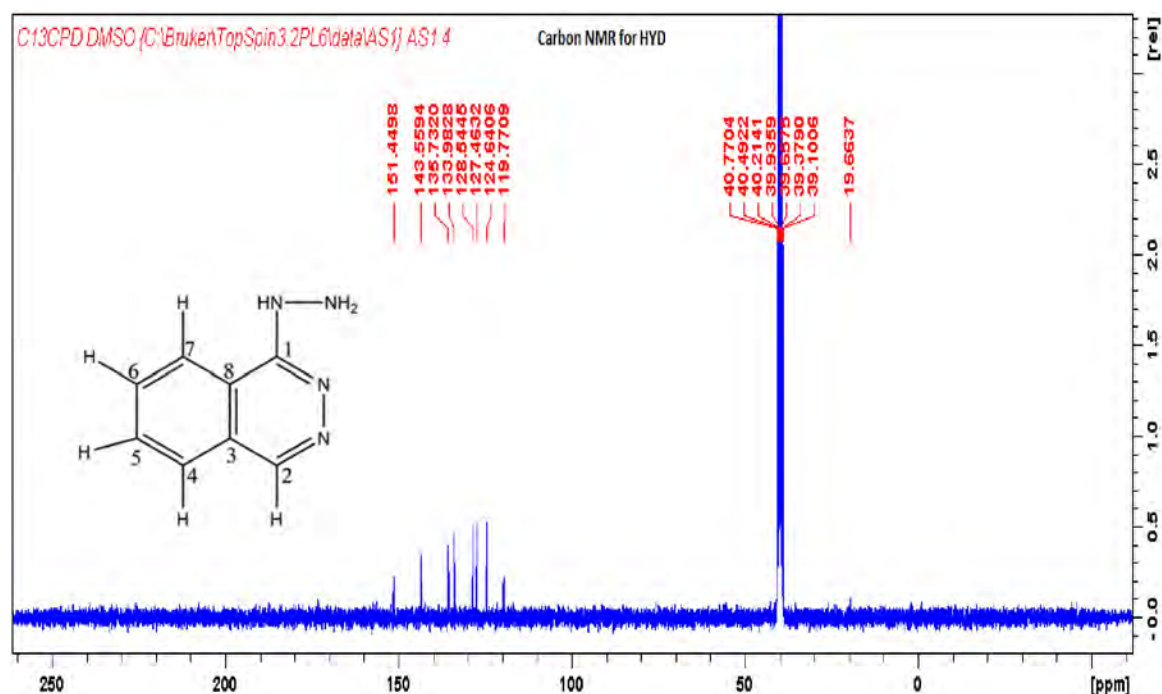


Figure 4.12 600 MHz ^{13}C NMR spectrum of HYD in DMSO

The summarised ^{13}C NMR of HYD are shown in Table 4.5. The ^{13}C NMR technique has been successfully employed in the characterisation of HYD.

Table 4.5 Carbon- NMR Data for HYD [54]

| Carbon position | Node | Chemical shift (ppm) |
|-----------------|------|----------------------|
| C1 | -C= | 151.45 |
| C2 | -C= | 143.56 |
| C3 | -C= | 127.46 |
| C4 | CH | 128.54 |
| C5 | CH | 135.73 |
| C6 | CH | 133.98 |
| C7 | CH | 124.64 |
| C8 | -C= | 119.77 |
| DMSO | - | 39.93 |

4.5.3 Compatibility studies using FT-IR, DSC and TGA

In the majority of cases, the melting endotherm of HYD was unaffected in all mixtures tested, with only slight changes observed in terms of peak broadening or shifting towards lower or higher temperatures. It has been reported that the quantity of material used, especially in API-excipient mixtures, can affect peak shape and enthalpy in such studies [258,271,303,321]. The minor changes in the melting endotherm of HYD may be due to the mixing of HYD and the excipient which lowers the purity of each component in the mixture and therefore does not necessarily indicate a potential incompatibility. To determine whether an incompatibility exists, additional techniques were used. Interactions in a sample are observed in DSC thermograms as changes in thermal events, such as the appearance of new peaks or a change in melting point of a material. The shapes of all TGA curves for HYD were similar or nearly identical to that observed for pure HYD except for that of the binary mixture of HYD and Carbopol® 971P.

4.5.3.1 DSC, TGA and FT-IR of HYD and Eudragit® RS PO

4.5.3.1.1 DSC

To evaluate the compatibility between HYD and Eudragit® RS PO, FT-IR, DSC and TGA, studies were performed on Eudragit® RS PO and a binary mixture of HYD and Eudragit® RS PO. Figure 4.13 depicts DSC results for Eudragit® RS PO, whilst Figure 4.14 depicts DSC results for the binary mixture of HYD and Eudragit® RS PO. Figure 4.13 indicates that Eudragit® RS PO undergoes thermal transition at around 394 °C, with a ΔH of 418 J/g. Therefore Eudragit® RS PO will not degrade during manufacturing and drying temperatures. The binary mixture of HYD and Eudragit® RS PO (1:1) ratio indicates a thermal transition at

274 °C for HYD. This reveals that the melting point for both compounds remains the same, thus no chemical changes occurred when the two compounds were mixed.

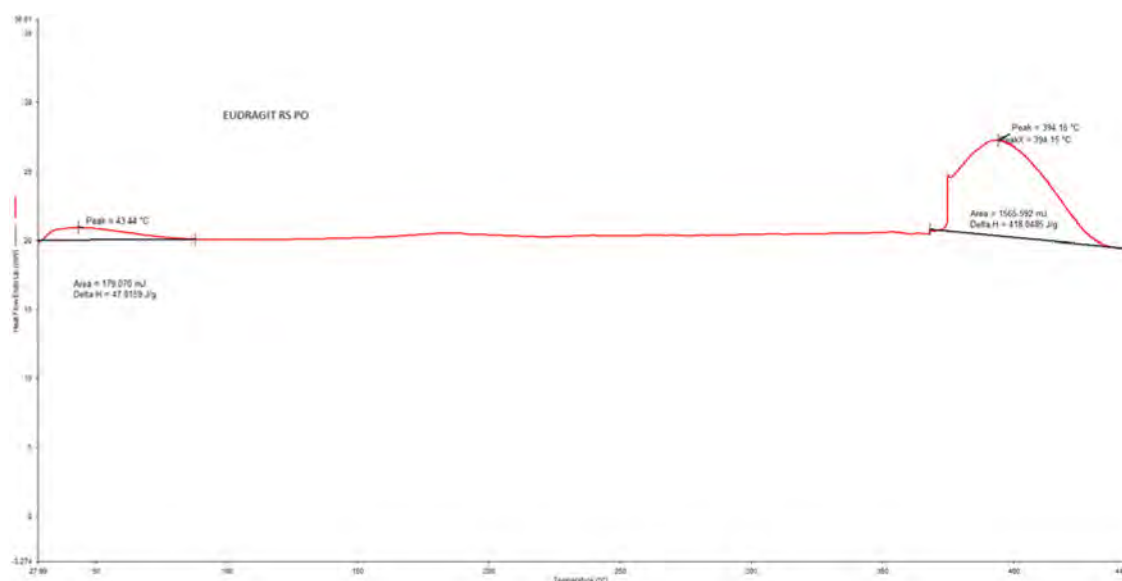


Figure 4.13 Typical DSC thermogram of Eudragit® RS PO generated at a heating rate of 10 °C/min

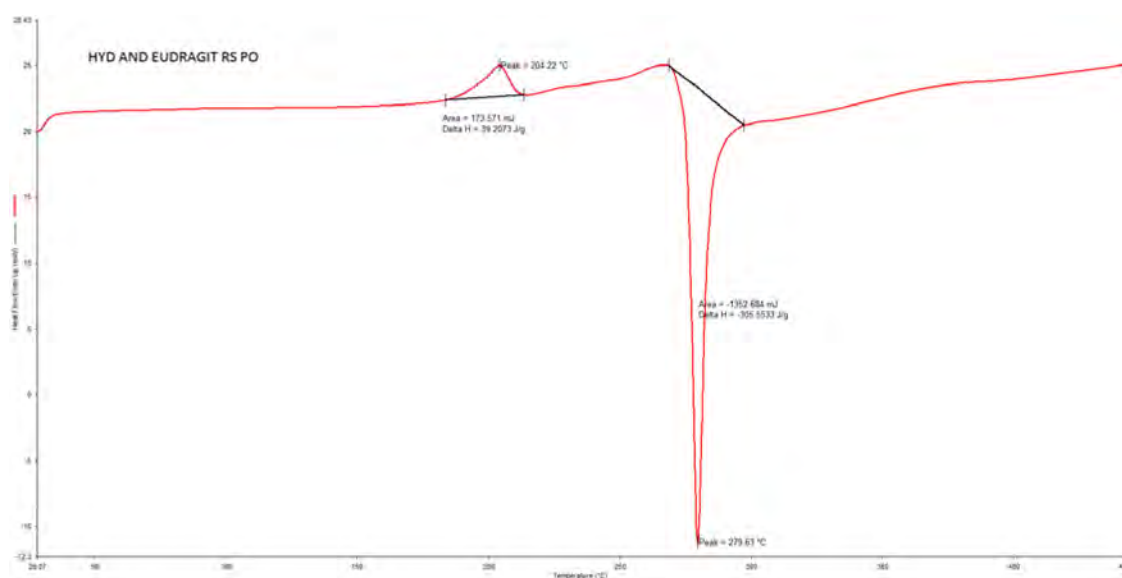


Figure 4.14 Typical DSC thermogram of a 1:1 binary mixture of HYD and Eudragit® RS PO generated at a heating rate of 10 °C/min

4.5.3.1.2 TGA

The TGA results obtained with a binary mixture of HYD and Eudragit® RS PO (1:1) are depicted in Figure 4.15. The TGA thermogram is similar to that of pure HYD indicating that the chemical composition of HYD was not affected by the addition of Eudragit® RS PO. The melting point of HYD was not affected by the addition of Eudragit® RS PO. The TGA results

indicate that the mixture is stable until 250 °C, meaning that both compounds should be stable under normal formulation and storage temperatures.

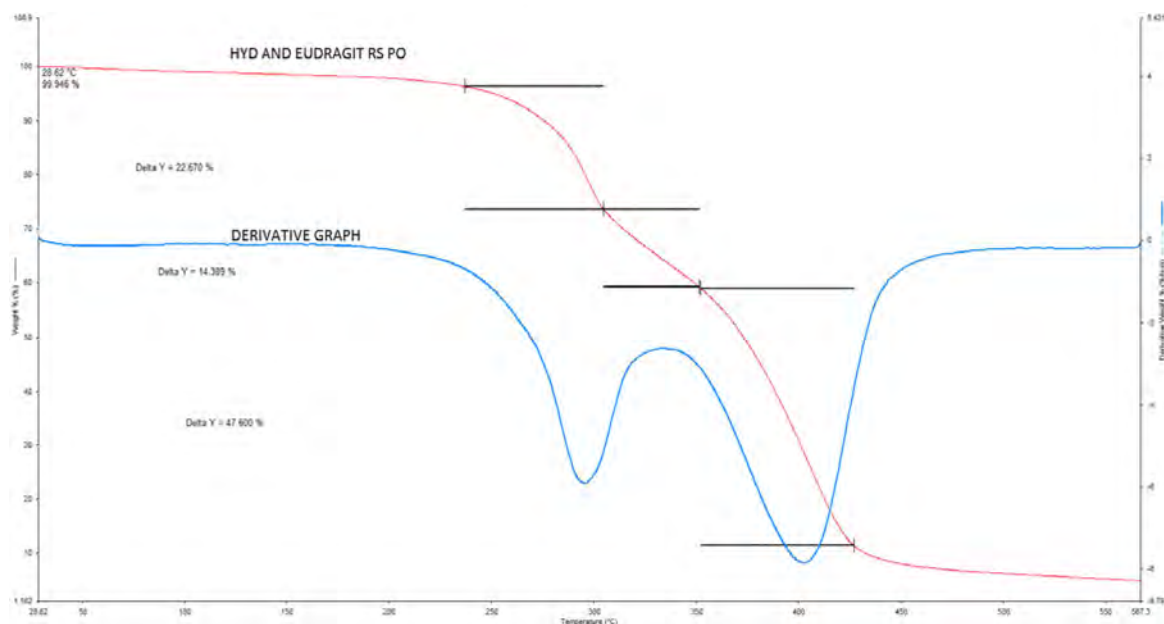


Figure 4.15 Typical TGA thermogram of a 1:1 binary mixture of HYD and Eudragit® RS PO generated at a heating rate of 10 °C/min from 30 to 600 °C

4.5.3.1.3 FT-IR

The primary peaks for HYD did not change in combination with Eudragit® RS, indicating that there were no vibrational energy changes and therefore a limited likelihood of an incompatibility between HYD and Eudragit® RS PO. FT-IR spectra for Eudragit® RS PO is shown in Figure 4.16 and the interpretation of the peaks are shown in Table 4.6. FT-IR spectra for Eudragit® RS PO indicates the presence of C=O, O=C-O-C and C-H stretches at 1723, 1143 and 2950 cm^{-1} respectively.

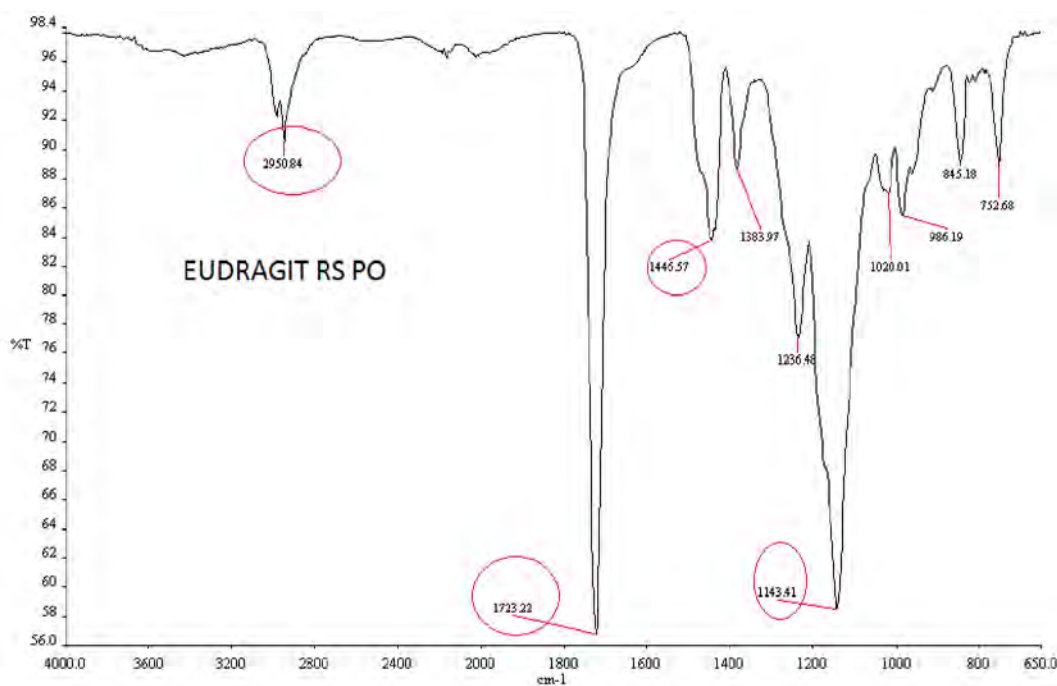


Figure 4.16 Typical FT-IR spectrum of Eudragit® RS PO generated from 4000 cm^{-1} to 650 cm^{-1}

Table 4.6 Interpretation of FT-IR results for Eudragit® RS PO

| Frequency (cm^{-1}) | Intensity | Assignment |
|--------------------------------|-----------|-------------------------|
| 2950 | s | C-H stretch |
| 1723 | s | C=O stretch |
| 1143 | s | O=C-O-C stretch (ester) |

Figure 4.17 shows FT-IR spectra for HYD and a binary mixture of HYD and Eudragit® RS PO. The characteristic peaks for both HYD and Eudragit® RS PO are still present, indicating that there was no interaction between the two compounds. FT-IR for HYD and the binary mixture of HYD and Eudragit® RS PO was interpreted in Table 4.7.

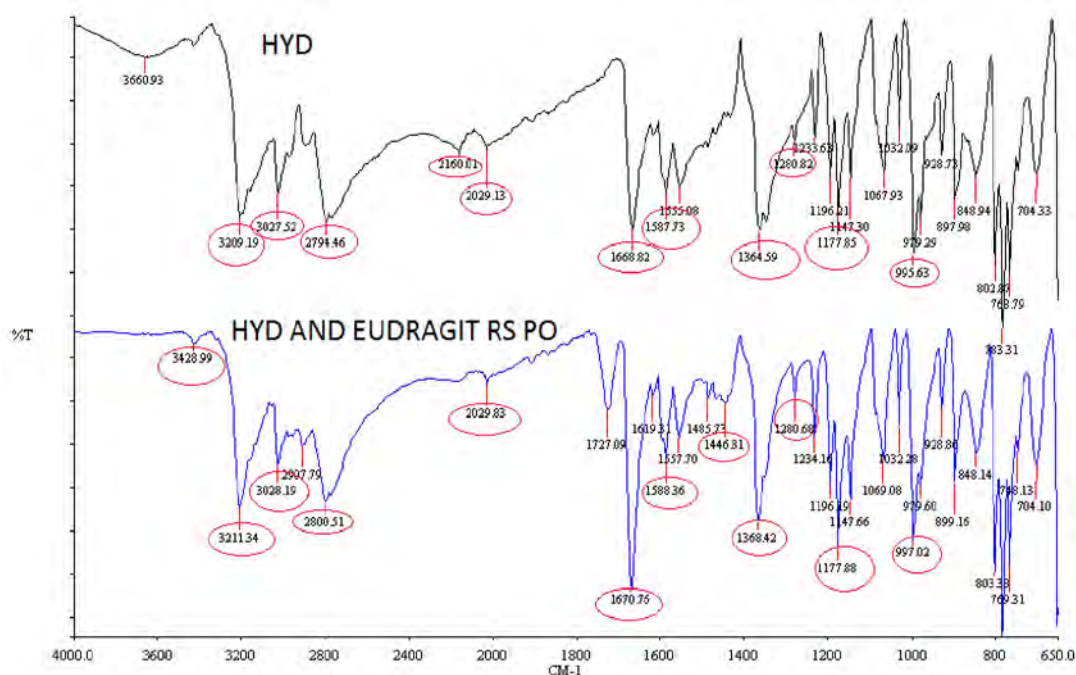


Figure 4.17 Typical FT-IR spectra of HYD and a 1:1 binary mixture of HYD and Eudragit® RS PO generated from 4000 cm^{-1} to 650 cm^{-1}

Table 4.7 Interpretation of FT-IR results of a 1:1 binary mixture of HYD and Eudragit® RS PO

| Frequency (cm^{-1}) | Intensity | Assignment |
|--------------------------------|-----------|-------------------------|
| 3428 | w | N-H stretch |
| 2950 | s | C-H stretch |
| 1723 | s | C=O stretch |
| 1147 | s | O=C-O-C stretch (ester) |
| 1446-1670 | s | C=C stretch |

FT-IR results for the binary mixture of HYD and Eudragit® RS PO indicate the presence of functional groups for HYD at 3428 and 1587 cm^{-1} for N-H stretch and C=C stretch respectively. It also indicates the presence of functional groups for Eudragit® RS PO at 1723 and 1147 cm^{-1} for C=O stretch and O=C-C-O-C stretch respectively. This indicates that there is no interaction between HYD and Eudragit® RS PO.

4.5.3.2 DSC, TGA and FT-IR of HYD and Methocel® K100LV

4.5.3.2.1 DSC

The DSC thermogram for Methocel® K100LV is shown in Figure 4.18. It shows that Methocel® K100LV melts at 365 °C, over a wide range of temperature, with a ΔH of 418 J/g. This is crucial for manufacturing as it indicates that Methocel® K100LV will not degrade during normal manufacturing and storage.

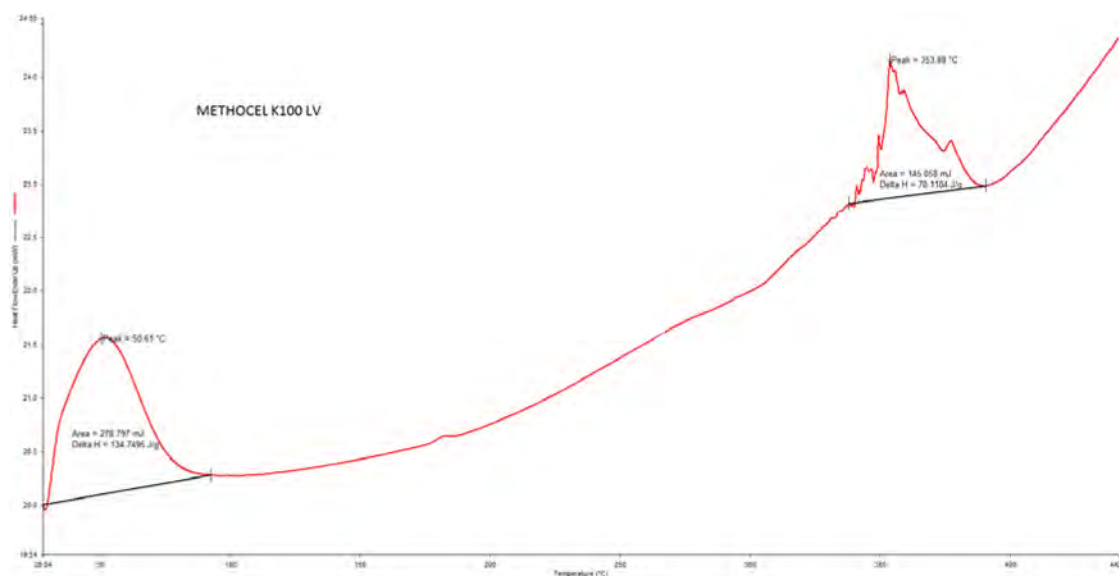


Figure 4.18 Typical DSC thermogram of Methocel® K100LV generated at a heating rate of 10 °C/min

The DSC thermogram for a binary mixture of HYD and Methocel® K100LV is shown in Figure 4.19. The exothermic peak for HYD is still present regardless of the intensity and ΔH reduction. The endothermic peaks for Methocel® K100LV are present indicating that Methocel® K100LV is compatible with HYD.

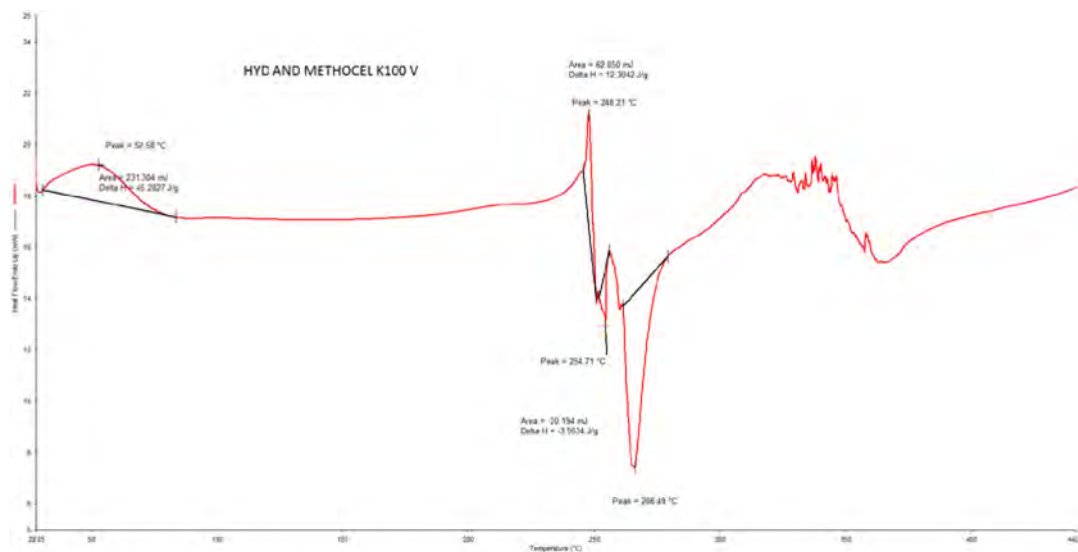


Figure 4.19 Typical DSC thermogram of a 1:1 binary mixture of HYD and Methocel® K100 LV generated at a heating rate of 10 °C/min

4.5.3.2.2 TGA

Further studies were performed using TGA. The TGA results for the binary mixture of HYD and Methocel® K100LV are shown in Figure 4.20. The results correlate with those found in

DSC and indicate that mass loss starts around 250 °C which is way above normal formulating and storage temperature. The derivative graph indicates that most decomposition happens in one sharp stage compared to that of pure HYD shown.

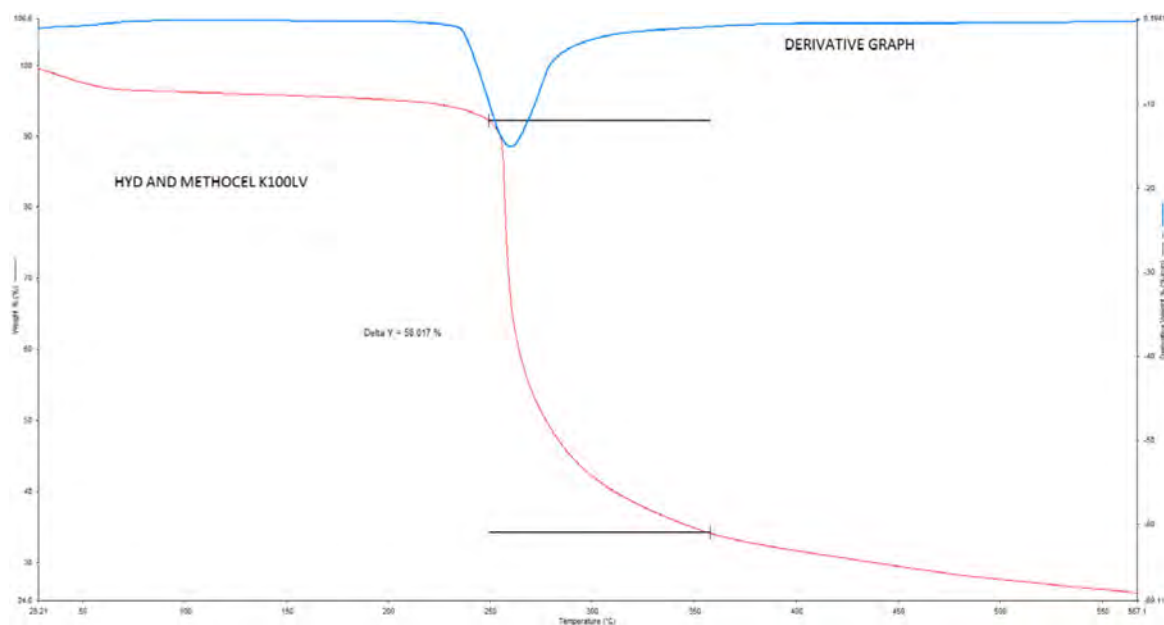


Figure 4.20 Typical TGA thermogram of a 1:1 binary mixture of HYD and Methocel® K100 LV generated at a heating rate of 10 °C/min from 30 to 600 °C

4.5.3.2.3 FT-IR

FT-IR spectra from 4000 cm^{-1} to 650 cm^{-1} for Methocel® K100LV is shown in Figure 4.21. It indicates function groups at 3210, 2801 and 1032 cm^{-1} for the OH (hydroxyl) group, C-H stretch and C-O stretches respectively. Interpretation of FT-IR for Methocel® K100LV are shown in Table 4.8.

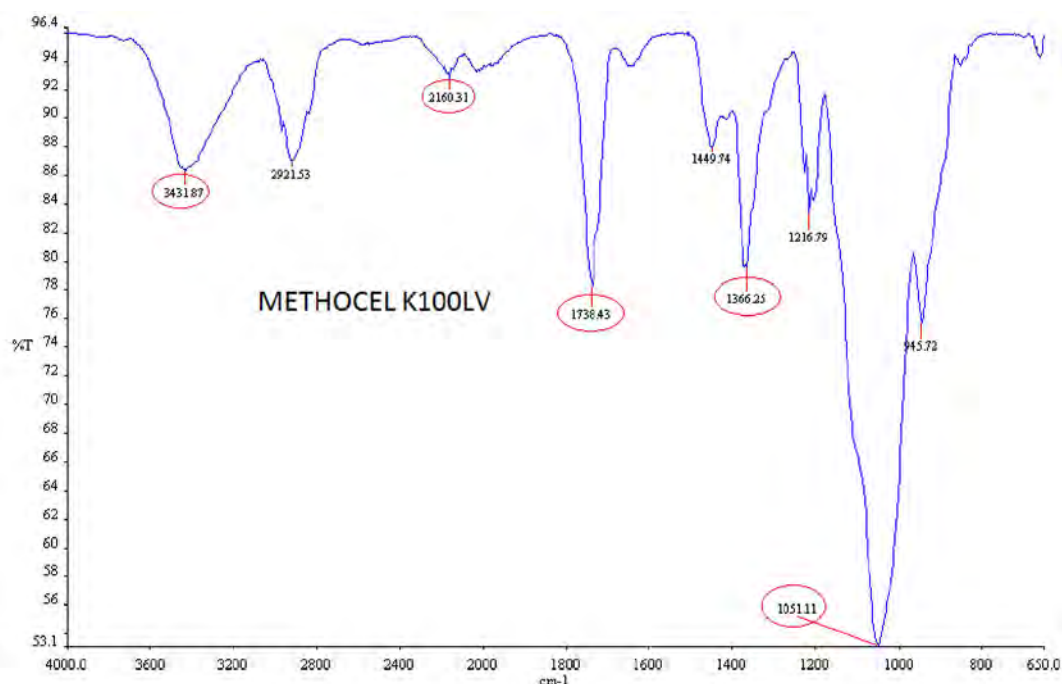


Figure 4.21 Typical FT-IR spectra of Methocel® K100LV generated from 4000 cm^{-1} to 650 cm^{-1}

Table 4.8 Interpretation of FT-IR spectra for Methocel® K100LV

| Frequency (cm^{-1}) | Intensity | Assignment |
|--------------------------------|-----------|-------------|
| 3210 | s | O-H stretch |
| 2801 | m | C-H stretch |
| 1032 | s | C-O stretch |

FT-IR spectra results for HYD and the binary mixture of HYD and Methocel® K100LV is shown in Figure 4.22 and interpreted in Table 4.9. FT-IR shows that the characteristic functional groups of HYD and Methocel® K100LV are still present in the binary mixture, therefore no interactions were observed.

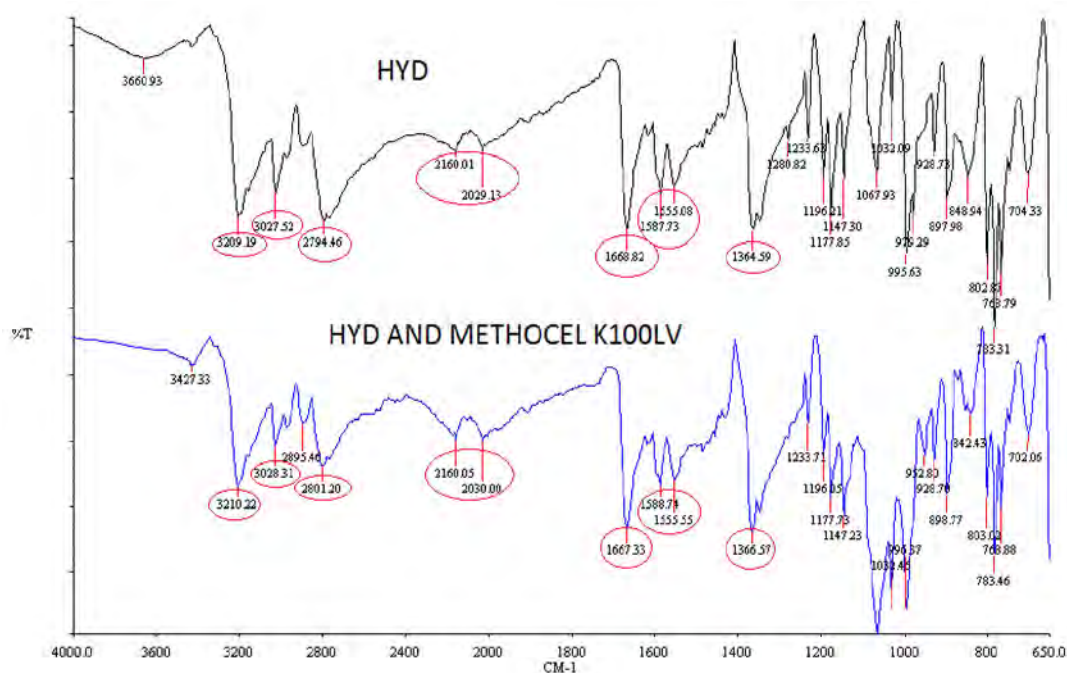


Figure 4.22 Typical FT-IR spectra of HYD and a 1:1 binary mixture of HYD and Methocel® K100LV generated from 4000 cm^{-1} to 650 cm^{-1}

Table 4.9 Interpretation of FT-IR spectra of binary mixture of HYD and Methocel® K100LV

| Frequency (cm^{-1}) | Intensity | Assignment |
|--------------------------------|-----------|------------------|
| 3427 | w | N-H stretch |
| 3210 | s | O-H stretch |
| 3027 | m | Ar C-H stretch |
| 2801 | m | C-H stretch |
| 1667 | s | C=C stretch |
| 1147-1588 | m | Ring C=C stretch |
| 1032 | s | C-O stretch |

FT-IR results indicate that the functional groups for HYD at 3428 and 1587 cm^{-1} for N-H stretch and C=C stretch respectively are still present. It also indicates that the functional and/or characteristic groups for Methocel® K100LV at 3210, 2801 and 1632 cm^{-1} are still present, indicating that HYD does not interact with Methocel® K100LV, hence Methocel® K100LV is regarded as compatible with HYD.

4.5.3.3 DSC, TGA and FT-IR of HYD and Avicel® 101

The use of a diluent is crucial in formulating. Diluents are regarded as inert but confirmation studies were to be performed if Avicel® 101 was compatible with HYD [322]. Diluents can affect drug release, therefore there was a need to carry out compatibility studies [323]. DSC, TGA and FT-IR were used for compatibility studies between HYD and Avicel® 101.

4.5.3.3.1 DSC

DSC thermogram in Figure 4.23 indicates that Avicel® 101 melts endothermically at approximately 350 °C, over a wide range of temperature with a ΔH of 469 J/g. Avicel® 101 is stable at normal compounding and storage temperatures.

The DSC for the binary mixture for HYD and Avicel® 101 is shown in Figure 4.24. The thermogram indicates the exothermic peak for HYD and the endothermic peak for Avicel® 101 present. This indicates that no chemical changes had occurred to either HYD or Avicel® 101 when they were mixed.

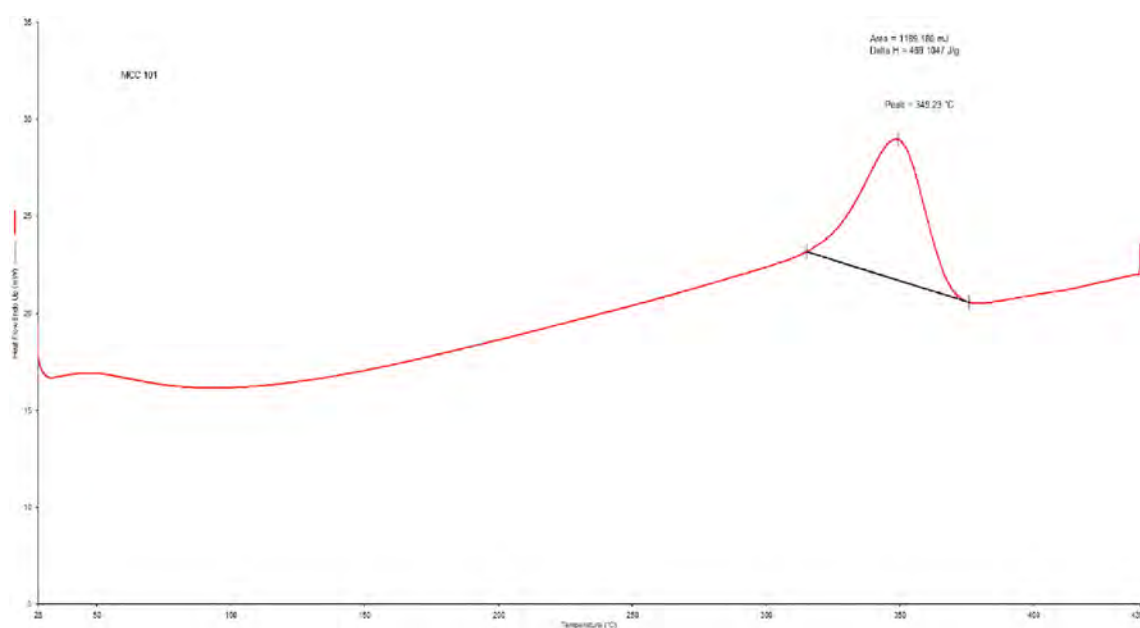


Figure 4.23 Typical DSC thermogram of Avicel® 101 generated at a heating rate of 10 °C/min

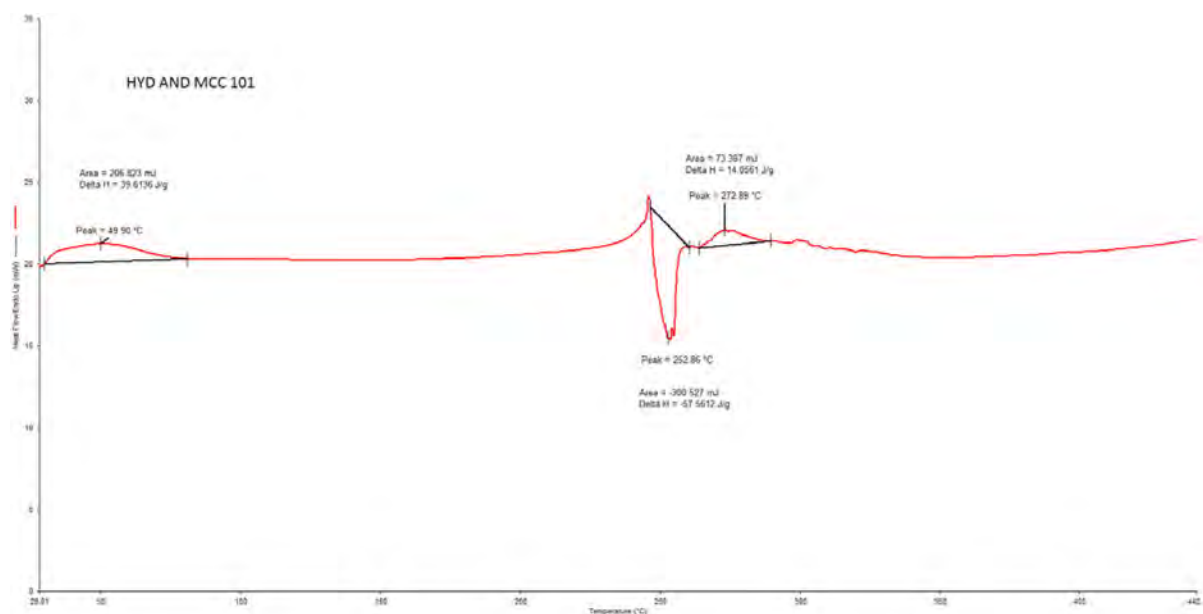


Figure 4.24 Typical DSC thermogram of a 1:1 binary mixture of HYD and Avicel® 101 generated at a heating rate of 10 °C/min

4.5.3.3.2 TGA

For further compatibility studies, TGA studies were performed to understand the weight changes that occur from a sample of a binary mixture of HYD and Avicel® 101. The TGA thermogram for the binary mixture of HYD and Avicel® 101 is shown in Figure 4.25. TGA thermogram indicates a 3 stage decomposition starts at approximately 250°C and ends at approximately 400°C. The initial drop in weight might be due to water loss from Avicel® 101. The derivative graph indicates that the most decomposition (about 60% mass loss) occurs in the first stage.

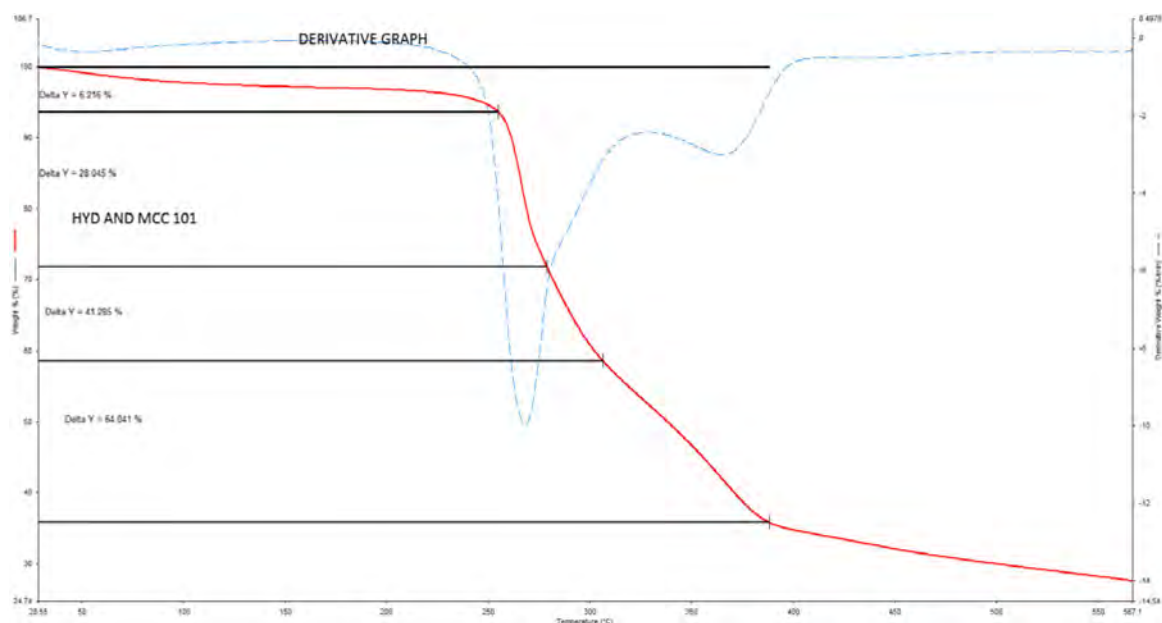


Figure 4.25 Typical TGA thermogram of a 1:1 binary mixture of HYD and Avicel® 101 generated at a heating rate of 10 °C/min from 30 to 600 °C

4.5.3.3 FT-IR

FT-IR spectra were generated for the binary mixture of HYD and Avicel® 101 to further evaluate any changes in functional and characteristic groups of both HYD and Avicel® 101. FT-IR spectra for Avicel® 101 is shown in Figure 4.26 and indicates major functional groups at 3333, 1053 and 1025 cm^{-1} for OH group, C-O group and C-O-C (ether) group respectively. Interpretation of the FT-IR spectra for Avicel® 101 is shown in Table 4.10.

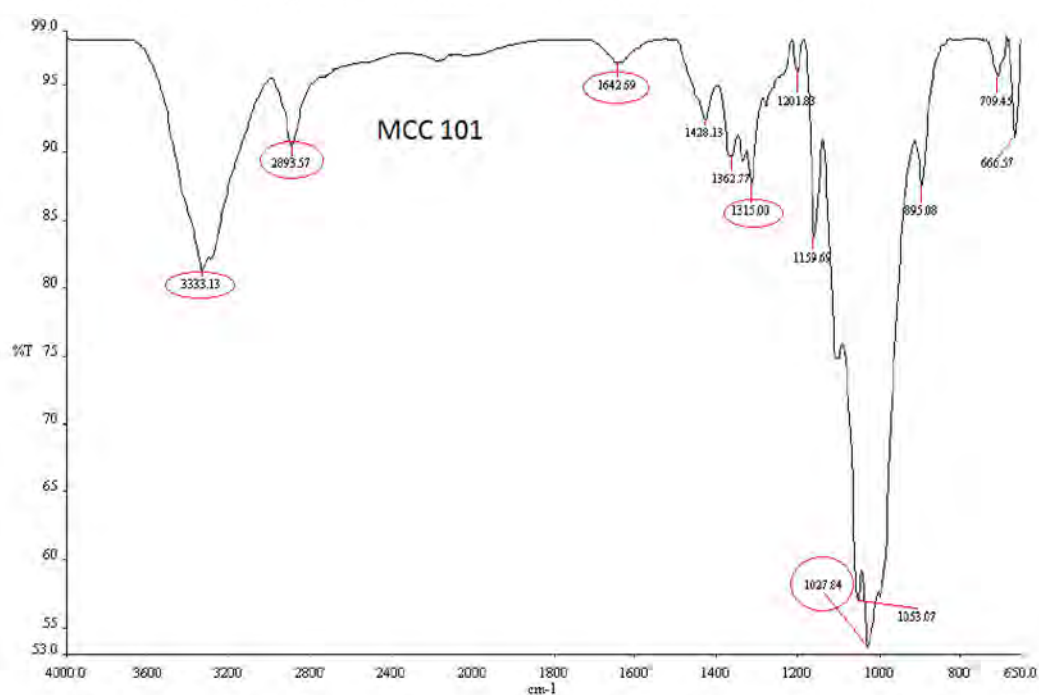


Figure 4.26 Typical FT-IR spectrum of Avicel® 101 generated from 4000 cm^{-1} to 650 cm^{-1}

Table 4.10 Interpretation of FT-IR spectra for Avicel® 101

| Frequency (cm ⁻¹) | Intensity | Assignment |
|-------------------------------|-----------|-------------------------------|
| 3333 | s, broad | O-H stretch |
| 1054 | s, broad | C-O-C stretch (ether linkage) |
| 1027 | s, broad | C-O stretch |

FT-IR spectra for HYD and the binary mixture of HYD and Avicel® 101 is shown in Figure 4.27 and interpreted in Table 4.11. Characteristics groups for both compounds were analysed. The binary mixture for HYD and Avicel® 101 shows functional groups at 3211, 1062 and 1031 cm⁻¹ for OH, C-O-C and C-O functional groups respectively for Avicel® 101. The spectra also show characteristic functional groups for HYD at 3027, 1739 and 1668 cm⁻¹ for aromatic C-H stretches, N-H bend, C=C stretch respectively. This shows that there is no interaction between HYD and Avicel® 101.

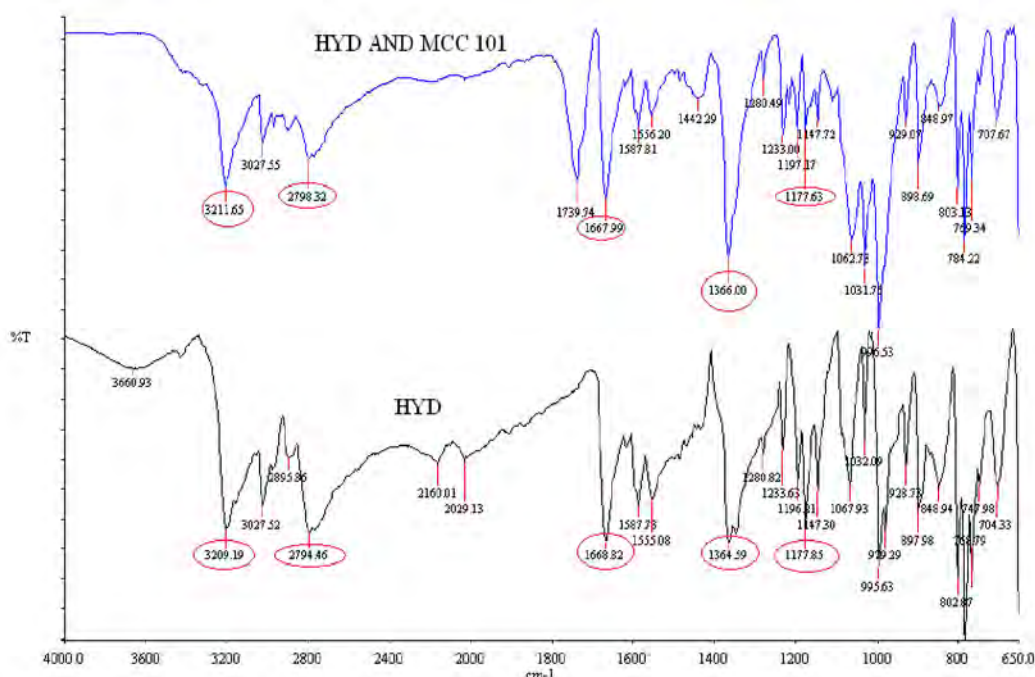


Figure 4.27 Typical FT-IR spectra of HYD and a 1:1 binary mixture of HYD and Avicel® 101 generated from 4000 cm⁻¹ to 650 cm⁻¹

Table 4.11 Interpretation of FT-IR results for the binary mixture of HYD and Avicel® 101

| Frequency (cm ⁻¹) | Intensity | Assignment |
|-------------------------------|-----------|---|
| 3333 | s, broad | O-H stretch (Avicel®) |
| 3027 | m | Ar C-H stretch (HYD) |
| 1739 | m | N-H bend (HYD) |
| 1668 | m | C=C stretch (HYD) |
| 1147-1587 | m-s | Ring C=C stretch (HYD) |
| 1054 | s, broad | C-O-C stretch (ether linkage) (Avicel®) |
| 1027 | s, broad | C-O stretch (Avicel®) |

4.5.3.4 DSC, TGA and FT-IR of HYD and Carbopol® 971P

4.5.3.4.1 DSC

A DSC thermogram for HYD and Carbopol® 971P is shown in Figure 4.28. The thermogram shows three distinctive endotherm peaks at 60 °C, 227 °C and an exotherm peak at 405 °C with ΔH of 157, 121 and -52 J/g respectively. Carbopol® 971P might have stability problems when manufacturing or storing at elevated temperatures.

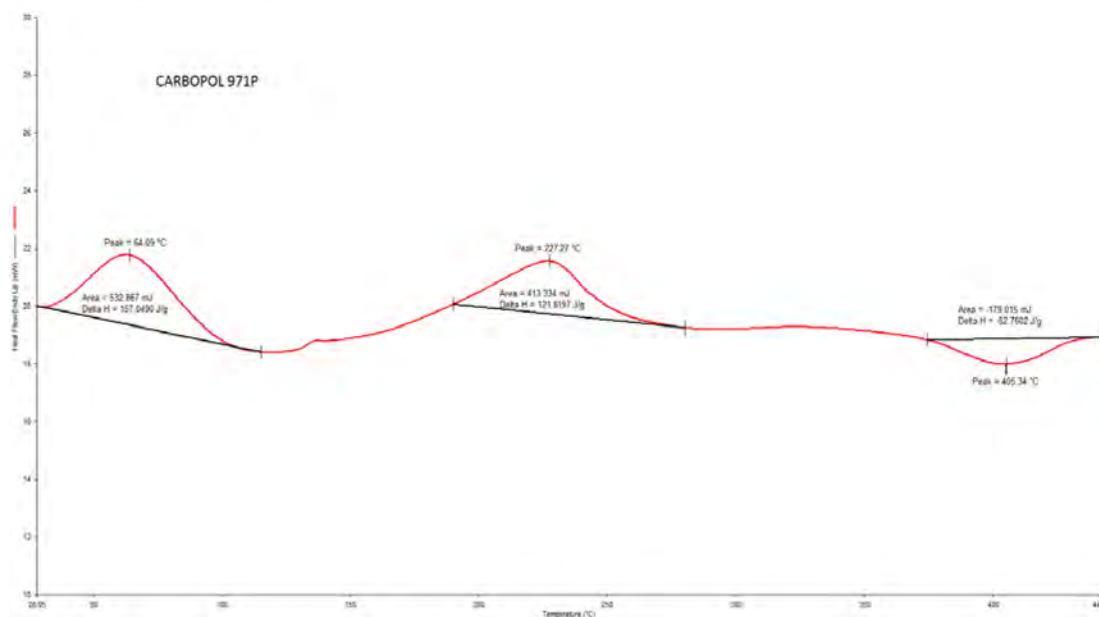


Figure 4.28 Typical DSC thermogram of Carbopol® 971P generated at a heating rate of 10 °C/min

A DSC thermogram for the binary mixture of HYD and Carbopol® 971P is shown in Figure 4.29. The disappearance of HYD exotherm peak can be clearly noted, indicating that there could be an interaction between HYD and Carbopol® 971P. The disappearance of the third Carbopol peak at 405 °C also indicates the probability of interaction between the two compounds. At 280 °C, TGA thermogram indicates an endotherm peak with ΔH of 69 J/g instead of an exothermic peak characteristic of HYD.

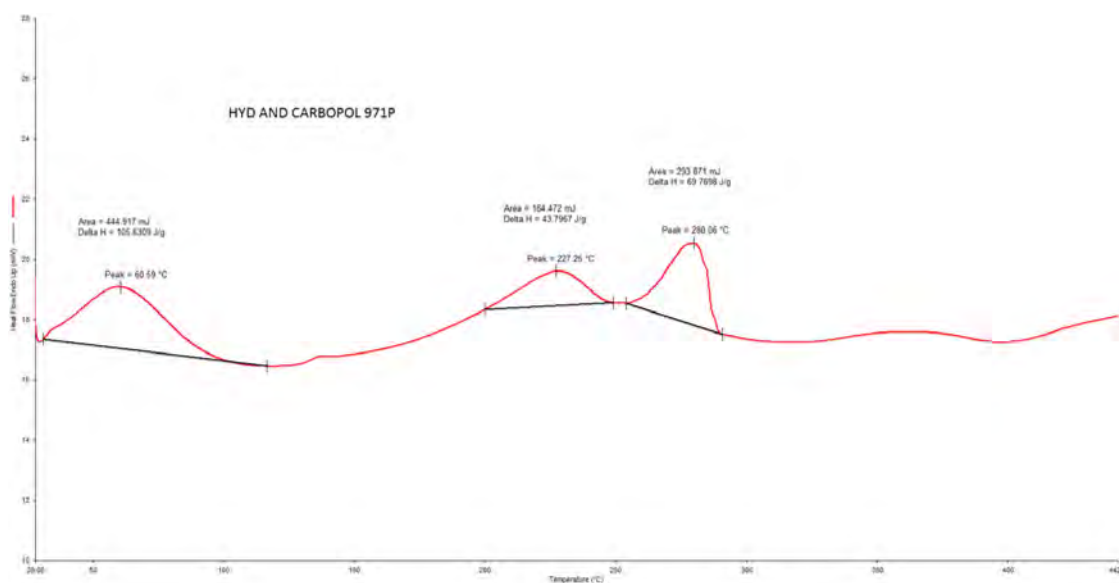


Figure 4.29 Typical DSC thermogram of a 1:1 binary mixture of HYD and Carbopol[®] 971P generated at a heating rate of 10 °C/min

4.5.3.4.2 TGA

A TGA thermogram for the binary mixture of HYD and Carbopol[®] 971P is depicted in Figure 4.30. The thermogram is different from that of pure HYD. A weight loss was observed at approximately 50 °C. Decomposition started at approximately 150 °C, with a major mass loss at 200 °C and a minor mass loss at 300 °C in two steps compared to the three step decomposition of HYD. The decomposition occurred earlier, most probably because the amide bond is not as strong as the amine and undergoes decomposition faster than the amine [324]. These results correlate with DSC results and FT-IR results, therefore Carbopol[®] 971P was not included as an excipient for formulation studies due to the possibility of interaction with HYD.

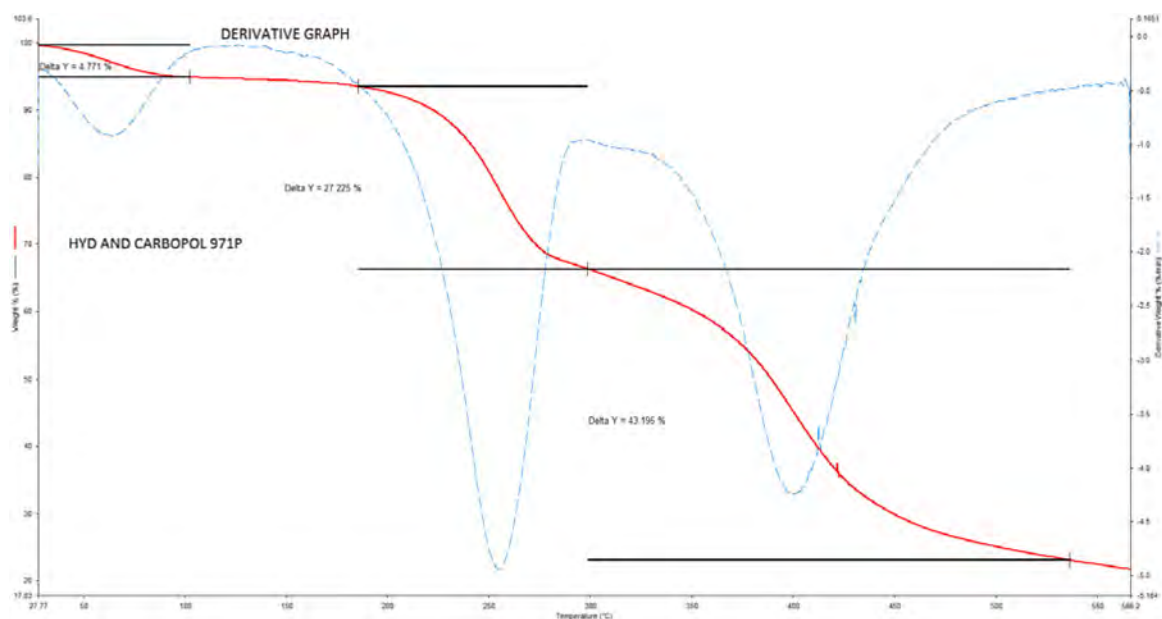


Figure 4.30 Typical TGA thermogram of a 1:1 binary mixture of HYD and Carbopol® 971P generated at a heating rate of 10 °C/min from 30 to 600 °C

4.5.3.4.3 FT-IR

The FT-IR spectra obtained for Carbopol® 971P is depicted in Figure 4.31 and interpreted in Table 4.12. The carboxylic acid functional group is indicated by the OH stretch and C=O stretch at 2936 and 1698 cm^{-1} respectively. These were the characteristic functional groups for Carbopol® 971P and were targeted during binary mixtures as the carboxylic acid is reactive.

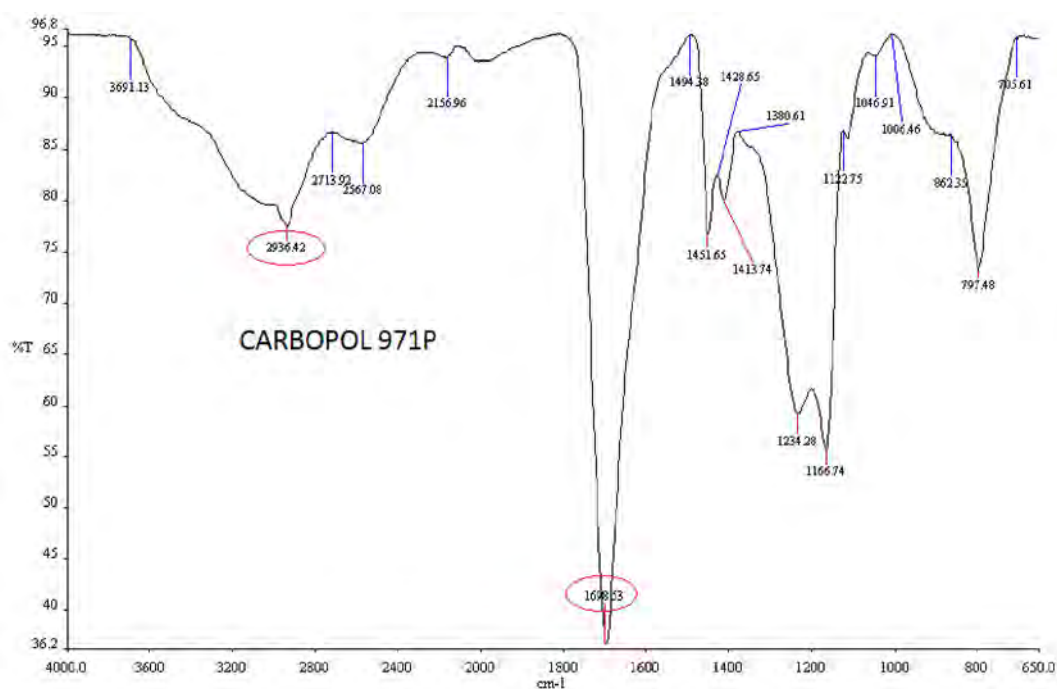


Figure 4.31 Typical FT-IR spectra of Carbopol® 971P generated from 4000 cm^{-1} to 650 cm^{-1}

Table 4.12 Interpretation of FT-IR spectra for Carbopol® 971P

| Frequency (cm ⁻¹) | Intensity | Assignment |
|-------------------------------|-----------|-------------|
| 2936 | s, broad | O-H stretch |
| 1147 | s, broad | C=O stretch |

The FT-IR spectrum for the binary mixture of HYD and Carbopol® 971P is shown in Figure 4.32 and interpreted in Table 4.13. FT-IR results indicate the disappearance of the OH functional group and the amine. This might be due to the formation of an amide bond between the secondary amine present in HYD and the carboxylic acid present in Carbopol® 971P. This indicates that there might be a potential interaction between the two compounds.

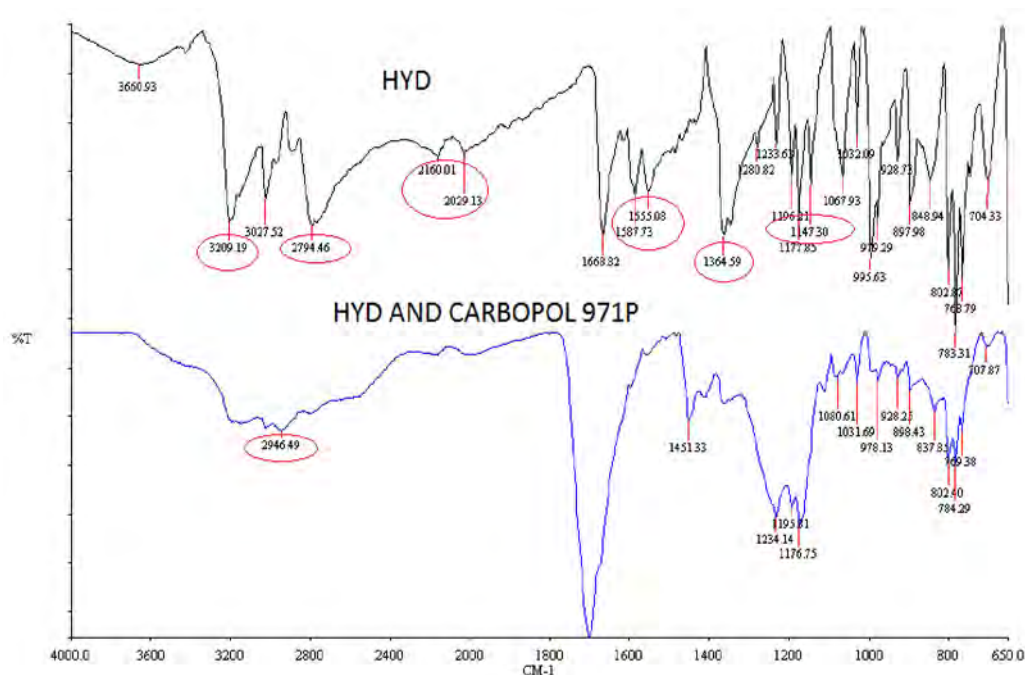


Figure 4.32 Typical FT-IR spectra of HYD and a 1:1 binary mixture of HYD and Carbopol® 971P generated from 4000 cm⁻¹ to 650 cm⁻¹

Table 4.13 Interpretation of FT-IR spectra for the binary mixture of HYD and Carbopol® 971P

| Frequency (cm ⁻¹) | Intensity | Assignment |
|-------------------------------|-----------|-------------|
| 2946 | w | N-H stretch |
| 1700 | s | C-H stretch |

4.5.3.5 Compatibility studies of a mixture of HYD, Eudragit®, Methocel® and Avicel®

To comprehensively carry out the preformulation studies and to evaluate any potential excipient-excipient interactions, HYD and all the excipients were mixed in a 1:1 ratio and FT-IR, DSC and TGA studies were performed. This was to understand how the excipients themselves interact with each other and/or how they mutually interact with the drug.

4.5.3.5.1 DSC

The DSC thermogram is shown in Figure 4.33 showing that the exothermic peak for the decomposition of HYD is still present. The peak is not as sharp compared to the one of the pure HYD as this could be due to the amount of HYD that would be present in the sample used as ΔH depends on the amount of HYD used. The purity of HYD and/or excipients is reduced by mixing, therefore the reduction of peak size and ΔH .

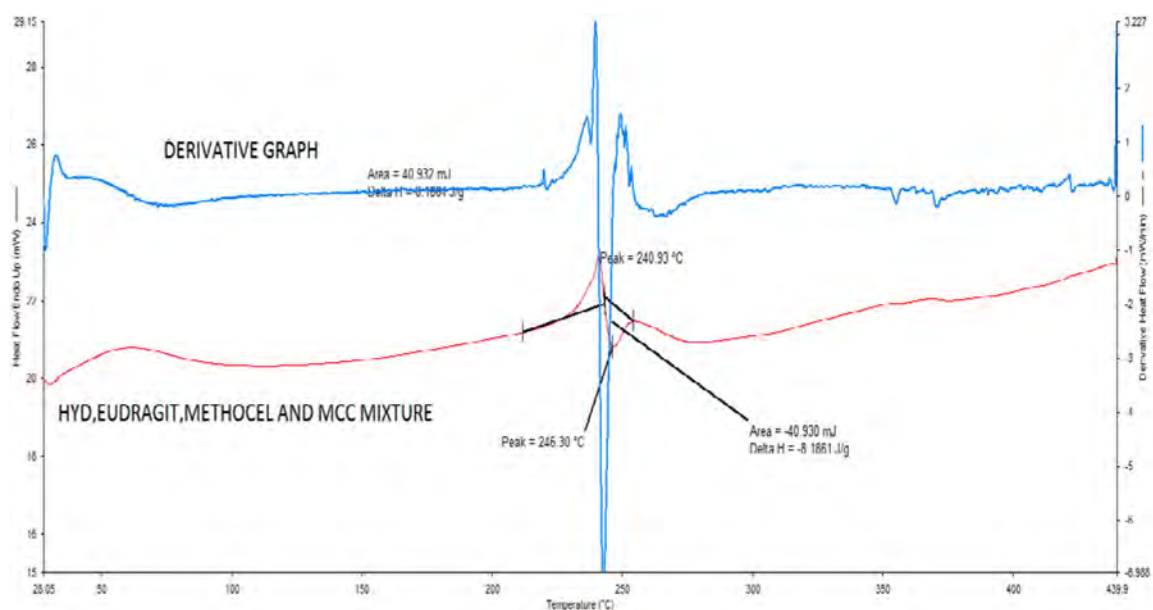


Figure 4.33 Typical DSC thermogram of a 1:1 mixture of HYD, Eudragit® RS PO, Methocel® K100LV and Avicel® 101 generated at a heating rate of 10 °C/min

4.5.3.5.2 TGA

The DSC thermogram was not sufficient to determine the changes occurring in the sample, therefore TGA studies were performed to determine the actual weight changes occurring over a wider range of temperature as shown in Figure 4.34. FT-IR confirmed the absence of incompatibility among HYD, Eudragit®, Methocel® and Avicel® used for formulation development and optimisation. The TGA thermogram obtained for the mixture of HYD, Eudragit®, Methocel® and Avicel® is shown in Figure 4.34. The thermogram shows that there are no major deviations from the TGA thermogram of pure HYD, indicating that there are no interactions between HYD and the excipients used in formulation development and optimisation.

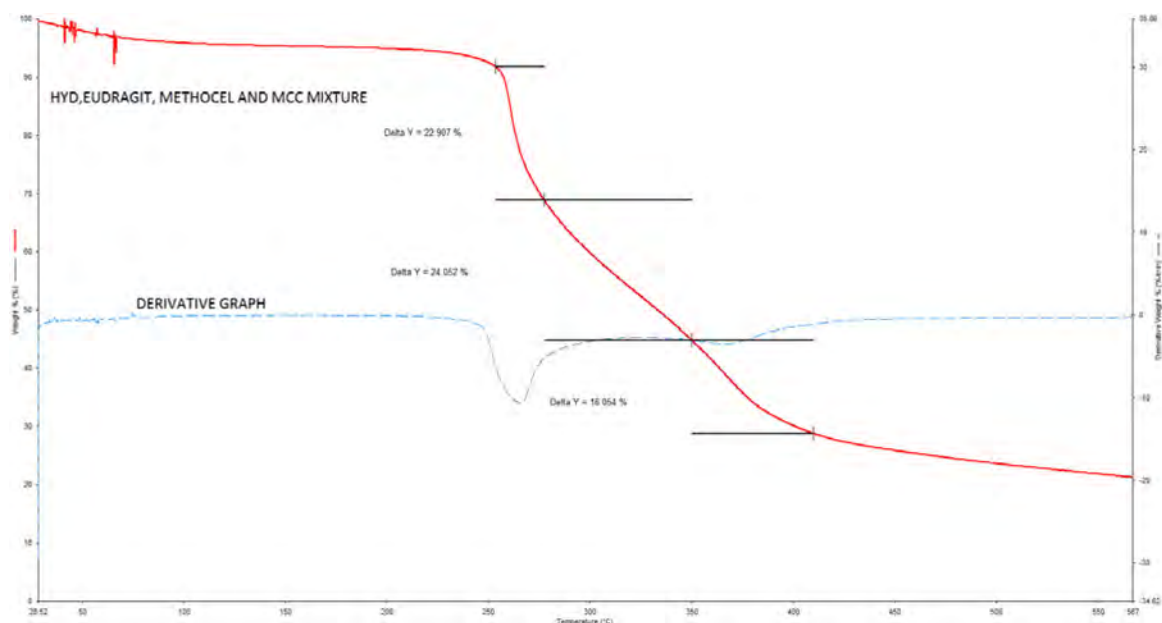


Figure 4.34 Typical TGA of a 1:1 mixture of HYD and all excipients used in formulation development and optimisation generated at a heating rate of 10 °C/min from 30 to 600 °C

4.5.3.5.3 FT-IR

The FT-IR spectra for HYD and mixture of HYD, Eudragit[®], Methocel[®] and Avicel[®] are shown in Figure 4.35. The characteristic bands observed at 3209, 3210 and 3027 cm^{-1} for N-H stretch (primary and secondary amine) and aromatic C-H stretch respectively are still present. The band at 1555 cm^{-1} was important as it represents the N-H bend of the primary amine. The presence of it indicates that there was no reaction that had occurred to the primary amine present in HYD. Most bands from pure HYD are still present in all mixtures, except for the fingerprint region as expected, confirming that there are no interactions between HYD and the excipients used.

A functional group at 3210 cm^{-1} was assigned for the OH group present in either Methocel[®] or Avicel[®]. A functional group at 1738 cm^{-1} was assigned for an ester functional group present in Eudragit[®] RS PO. Functional groups at 2800 and 1047 cm^{-1} were due to the C-H stretch and C-O stretch respectively for Methocel[®] K100LV. Functional groups at 3210 and 1053 cm^{-1} were due to OH and C-O-C functional groups of Avicel[®] 101. This indicates that no major changes occurred to functional groups present in HYD, Methocel[®] K100LV, Eudragit[®] RS PO and Avicel[®] 101.

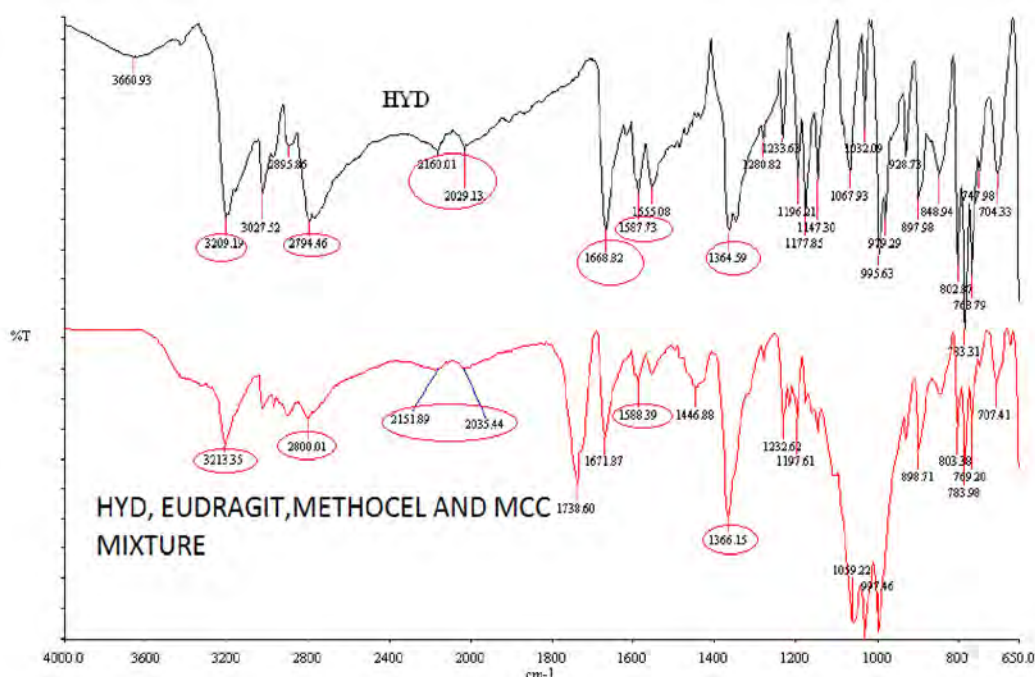


Figure 4.35 Typical FT-IR spectra of HYD and a 1:1 mixture of HYD and all excipients (Eudragit[®], Methocel[®] and Avicel[®]) used for formulation development and optimisation generated from 4000 cm^{-1} to 650 cm^{-1}

4.5.3.5.4 XRPD

XRPD can be used to confirm the crystalline nature of a sample. Therefore, this information is used to verify whether substances are crystalline or amorphous. XRPD in conjunction with other techniques can be quite informative [325].

XRPD is a direct measure of the crystal form of a material with atypical output being a plot of intensity vs the diffraction angle (2θ) [288]. A crystalline material exhibits a unique set of diffraction peaks and the lack of crystalline API peaks when a dosage form is analysed could indicate that the material is amorphous or that the loading is too low to detect using the parameters chosen [288]. XRPD analysis is of immense help in case of incompatibilities which occur during manufacturing processes that can lead to changes in crystallinity/amorphicity and polymorphic forms of API [288]. The non-destructive nature of XRPD makes it an ideal tool for systematic drug-excipient compatibility studies in preformulation [256,306,307].

HYD shows characteristic peaks at a diffraction angle of $2\theta = 11, 12, 20, 22, 25, 27, 28, 33$ and 39° . These peaks are present in the binary mixture of HYD, Eudragit[®] RS PO, Methocel[®] K100LV and Avicel[®] 101. XRPD of the binary mixture of HYD, Methocel[®], Eudragit[®] and Avicel[®] are shown in Figure 4.36. The majority of HYD characteristic peaks were observed in the binary mixture at $2\theta = 11, 12, 20, 22, 25, 27, 28, 33$ and 39° .

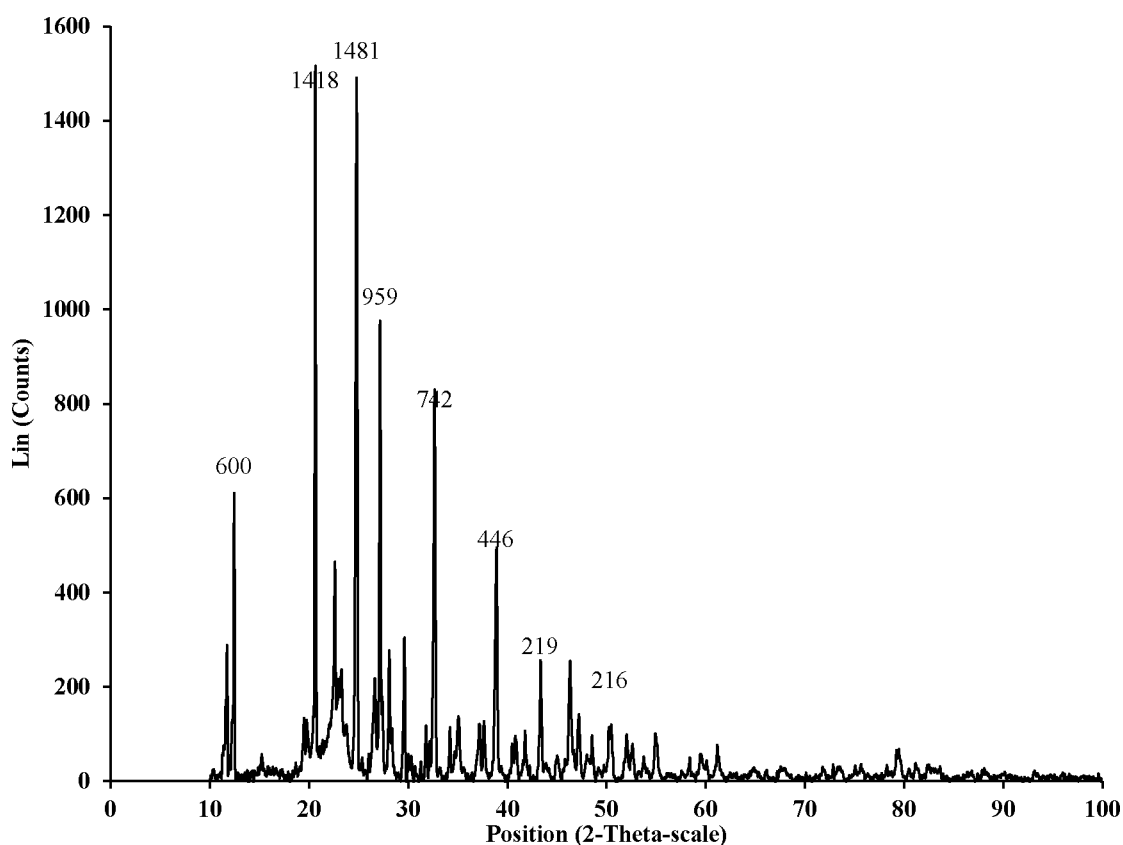


Figure 4.36 XRPD patterns of a 1:1 binary mixture of HYD, Eudragit®, Methocel® and Avicel® 101

The X-ray diffractogram of HYD and the binary mixture were superimposed as shown in Figure 4.37. Major characteristic peaks of HYD were observed in the binary mixture, indicating the absence of incompatibility between HYD and excipients used for formulation development and optimisation.

The superimposed diffractograms indicate that HYD is still present in its crystalline form, since all the characteristic peaks at $2\theta = 11, 12, 20, 22, 25, 27, 28, 33$ and 39° are still present, therefore indicating that HYD is compatible with these excipients.

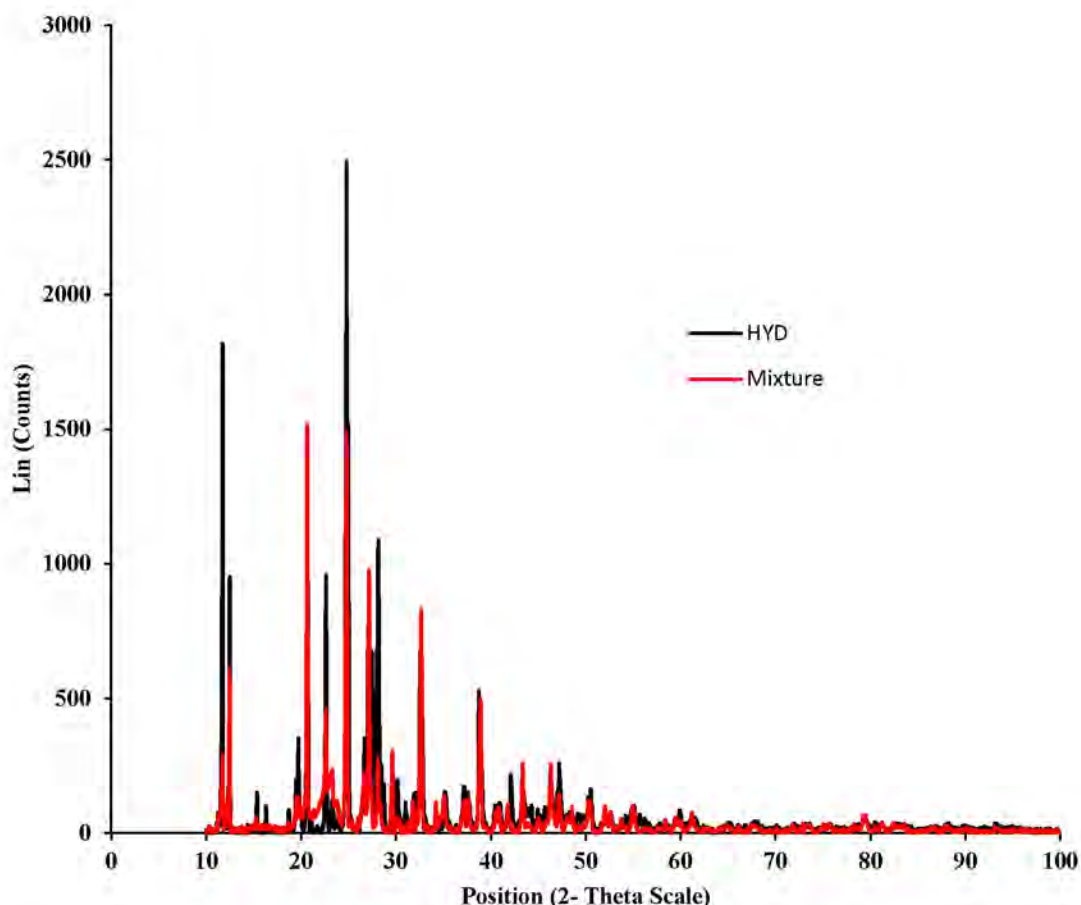


Figure 4.37 XRPD patterns of crystalline HYD (in black) and a 1: binary mixture of HYD, Eudragit®, Methocel® and Avicel® 101 (in red)

4.5.3.5.4 XRPD of a 1:1 mixture of HYD and Carbopol® 971P

HYD shows characteristic peaks at a diffraction angle of $2\theta = 11, 12, 20, 22, 25, 27, 28, 33$ and 39° . X-ray diffractogram of a binary mixture of HYD and Carbopol® 971P indicate peaks at a diffraction angle of $2\theta = 20, 22, 25$ and 27° . The intensity of these peaks has reduced due to the mixing of two compounds. The disappearance of some characteristic peaks might be due to incompatibility of HYD and Carbopol® 971P. The X-ray patterns of the binary mixture of HYD and Carbopol® 971P is shown in Figure 4.38.

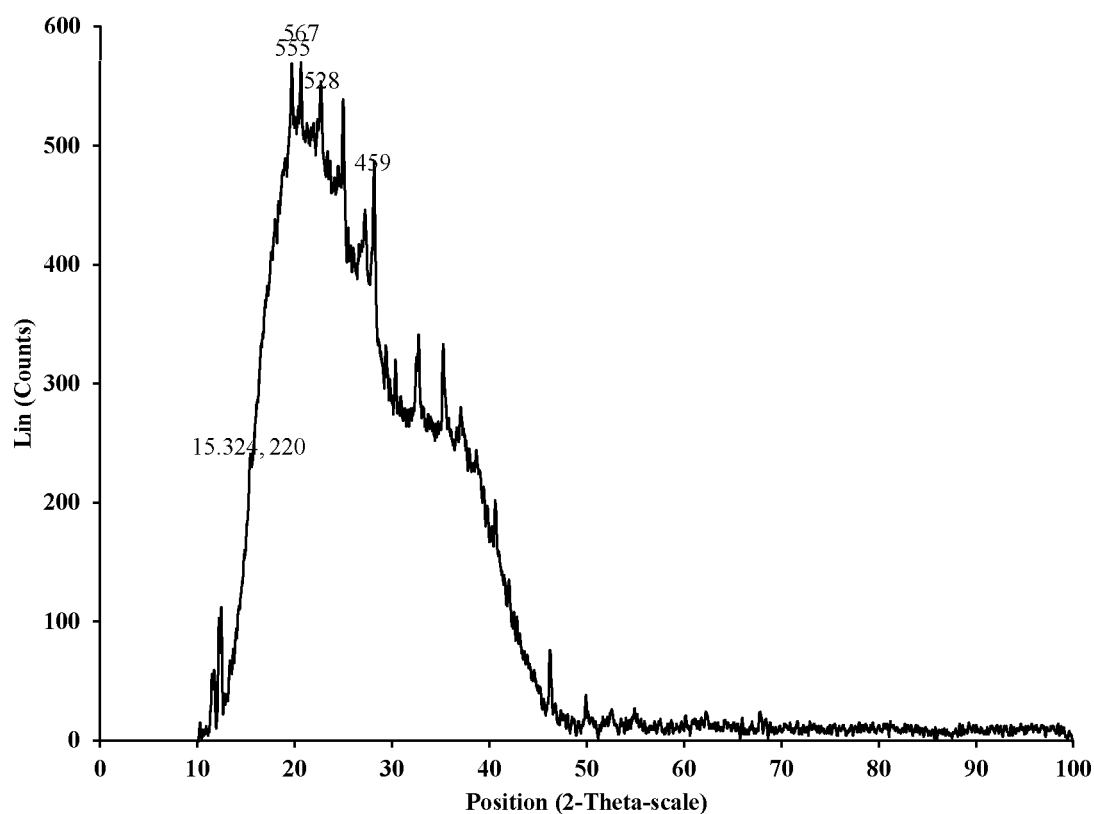


Figure 4.38 XRPD patterns of the binary mixture of HYD and Carbopol® 971P

The X-ray patterns of HYD and Carbopol® 971P were then superimposed with that of HYD. The patterns are different indicating possibilities of interactions. The presence of Carbopol might cause a reduction in the crystallinity nature of HYD, thus the efficacy of HYD might be affected by Carbomer polymers. The superimposed X-ray patterns are shown in Figure 4.39.

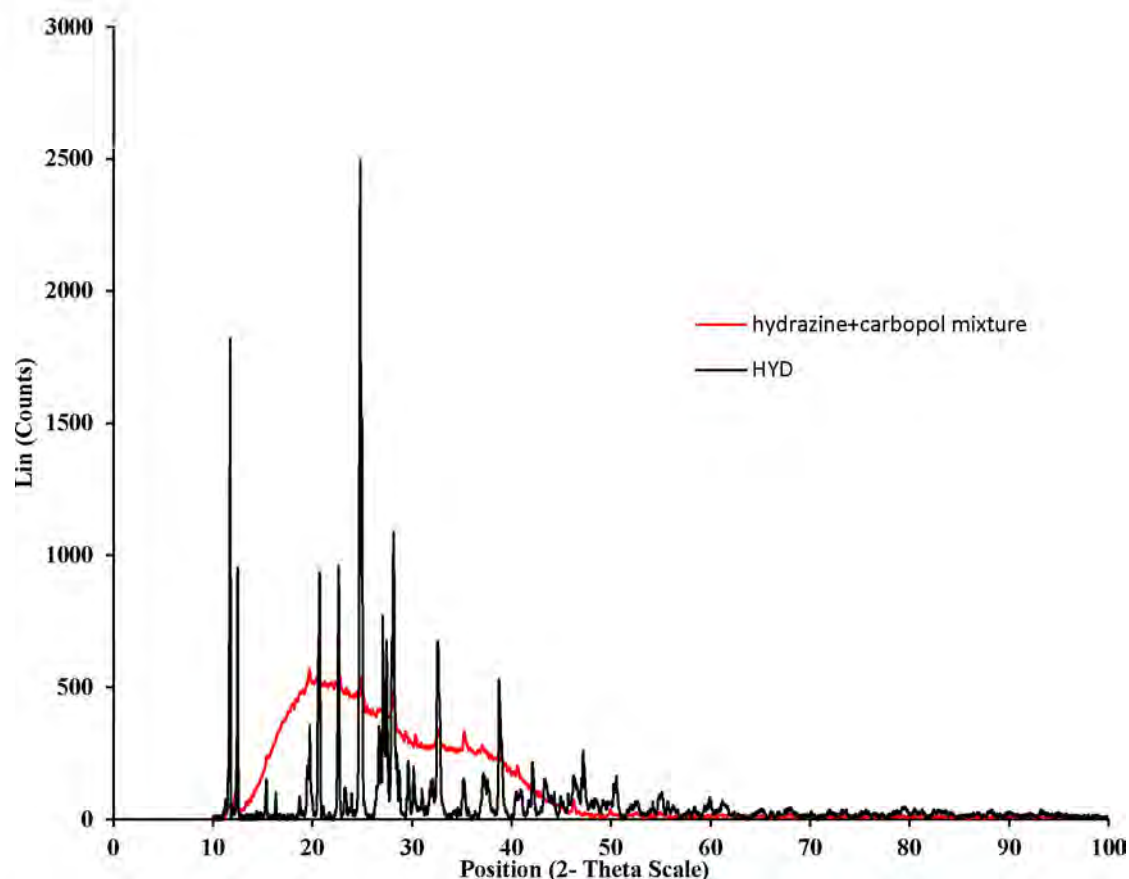


Figure 4.39 XRPD patterns of crystalline HYD (in black) and a 1:1 binary mixture of HYD and Carbopol® 971P (in red)

4.6. CONCLUSIONS

Preformulation studies play a significant part in anticipating formulation problems [103]. SEM images obtained indicate the difference between HYD and the excipients used in terms of shape, size and morphology. SEM indicates that HYD exists as acicular and cylindrical crystalline structure. Eudragit® RS PO exists as an angular crystalline shape. Although different in size, Methocel® K100LV and Avicel® 101 were found to exist as rod shaped particles. Proper powder mixing should be performed during formulation to avoid batch to batch variations.

The Stuart SMP30 apparatus has been successfully used to determine the melting point of HYD and it correlates with DSC thermogram. DSC thermogram revealed the decomposition of HYD exothermically at 275 °C over a wide range of temperature and HYD was found to be incompatible with Carbopol® 971P. The melting exotherm for HYD was present when most excipients, viz. Eudragit®, Methocel® and Avicel®, were mixed with HYD in a 1:1 ratio. The change in the value of ΔH value for HYD in combination with excipients may be due to the small amount of HYD in the sample mixtures. While DSC is a well-known technique for the

characterisation of pharmaceutical and polymeric materials, it has certain limitations in practical use. It is unable to provide insight into the changes to thermal events. Thus it is essential to combine DSC with other techniques to permit a greater understanding of any changes in the materials to be used [137]. DSC studies were coupled with TGA studies for conformational purposes. The results from TGA correlated with those obtained from DSC, therefore the use of this analytical technique provides an understanding of thermal changes in compounds.

The DSC thermogram indicated that there might be an interaction between HYD and Carbopol® 971P as the exotherm peak for HYD disappeared when HYD was mixed with Carbopol® 971P. This was confirmed by TGA and FT-IR results. The amine in HYD and carboxylic acid in Carbopol® 971P might have reacted to form an amide bond. The acrylic acid forms complexes with amine functional groups present in HYD [273]. Compatibility with HYD might vary between grades of Carbopols depending on the percentage of carboxylic acid present in different grades. Carbopols were not selected for formulation development because all Carbomer polymers are formed from repeating units of acrylic acid.

Thermal analysis is one of the most useful methods of analysis in collecting both physical and chemical information [254]. TGA can become an even stronger analytical technique when coupled with other thermal analysis techniques such as DSC and spectroscopic techniques such as FT-IR and mass spectrometry (MS) [326]. TGA was coupled with DSC as studies show that the use of both techniques is better than using one technique.

TGA results indicate that decomposition of HYD takes place in one major and two minor steps over a wide range of temperature (approximately 250 °C to approximately 450 °C). TGA studies indicate that the thermograms obtained from binary mixtures of HYD and excipients were similar to that of pure HYD. TGA thermogram indicates that all excipients selected for formulation development are stable during normal manufacturing and storage conditions, as weight loss started being prominent at 250 °C. Excipient-excipient interactions were eliminated when FT-IR, DSC and TGA studies were performed on a mixture of HYD, Methocel®, Eudragit® and Avicel® in a 1:1 ratio. TGA is a time consuming method and was performed for conformational purposes, therefore only studies for binary mixtures were performed. TGA thermogram concludes that no interactions occurred between HYD and excipients used for formulation development and optimisation studies. DSC and TGA results indicate that it is unlikely for HYD and excipients to decompose under normal homogenising temperature, as

temperature rarely exceeds 100 °C. Thus the homogenisation process should not affect the structure and crystallinity of these compounds as homogenisation processes are rarely performed at such elevated temperatures.

The results of structural clarification and potential incompatibilities were further confirmed using FT-IR studies. Infrared spectroscopy techniques are sensitive and can be used to identify possible and potential interactions between HYD and excipients [319]. FT-IR spectra for HYD indicate functional groups at 3429 cm⁻¹, 3210 cm⁻¹ and 1446 cm⁻¹ to 1670 cm⁻¹. These characteristic peaks were observed in all binary mixtures tested except with Carbopol® 971P, suggesting the possibility of chemical interactions between the HYD and Carbopol® 971P.

Comprehensive preformulation studies have been successfully performed using SEM, FT-IR, DSC and TGA techniques. These studies indicate that there is not sufficient evidence to indicate incompatibility among HYD, Eudragit® RS PO, Methocel® K100LV and Avicel® 101 used, thus all excipients studied were used for formulation development and optimisation except for Carbopol® 971P. These studies also gave an insight into temperature ranges that could be safely used during formulation, drying and storage. Based on the results from preliminary screening, all excipients can be selected for formulation development except Carbopol® 971P. From the well-constructed compatibility studies, Eudragit® RS PO, Methocel® K100LV and Avicel® 101 were finally selected as the excipients for formulation development and optimisation.

The results demonstrated the applicability of FT-IR, thermal analysis (DSC, TGA) and XRPD methods as fast screening analytical tools to check compatibility in the early stages of formulation studies. These studies provided sufficient and adequate knowledge for a formulator to proceed further with formulation studies. The information and knowledge gained from preformulation studies helped in selecting Eudragit® RS PO, Methocel® K100LV and Avicel® 101 for formulation development studies.

CHAPTER 5

DEVELOPMENT, MANUFACTURE AND ASSESSMENT OF SUSTAINED RELEASE HYDRALAZINE MICROSPHERES

5.1 INTRODUCTION

The goal of any drug delivery system is to provide a therapeutic amount of drug to the proper site in the body and then maintain the desired drug concentration [327]. Oral drug delivery is the most widely used route of administration among all the routes that have been explored for systemic delivery of drugs [32,102,103,328]. This route is the most natural, convenient and safe method of drug administration due to its ease of administration and patient acceptance [329–331]. Pharmaceutical products designed for oral delivery are mainly immediate release type or conventional drug delivery systems which are designed for immediate release of the drug for rapid absorption [31]. Controlled drug delivery technology represents one of the frontier areas of pharmaceutical science [332,333]. Controlled release (CR) systems aim to release drugs at a controllable rate over a prolonged period of time in order to maintain drug concentration at an effective level [334]. However, the relatively brief transit time of about 12 hours through the gastrointestinal tract (GIT) limits the duration of action that can be expected via the oral route [330].

Sustained release (SR) formulations can be designed to deliver an initial therapeutic dose of the drug (loading dose), followed by a slower and constant release of the drug [335]. SR systems are mostly designed to enhance drug therapy [336]. They have been devised to enable superior control of drug exposure over time, assist the drug in crossing physiological barriers, shield the drug from premature elimination, and target the drug to the desired site of action while minimising drug exposure elsewhere in the body [337,338]. SR formulations offer therapeutic advantages over conventional formulations including maintenance of optimal plasma concentration levels, increased duration of action of API and reduction of the occurrence of drug-related adverse effects [31,35]. The lower frequency of administration makes SR dosage forms a more convenient alternative to immediate release formulations, especially in patients with chronic conditions [31,35]. SR products provide an advantage over conventional dosage forms by optimising biopharmaceutics, pharmacokinetic and pharmacodynamics properties of drugs [31,34,336].

Despite the numerous advantages of SR formulations, there are some detriments associated with these technologies, viz. possible toxicity or non-biocompatibility of the employed polymeric carriers, the unpredicted and poor correlation between *in vitro* release and *in vivo* release, undesired degradation products, difficulty in dosage adjustment and poor systemic availability [35,334,339,340].

Microspheres offer various significant advantages as drug delivery systems. These include effective protection of the encapsulated API against degradation, the possibility of accurately controlling the drug release rate, easy administration and pre-programmed drug release profiles [330,332]. Microparticulate drug delivery systems are an interesting and promising option when developing SR system [31,332].

5.1.1 Microspheres

Microspheres constitute an important part of particulate drug delivery systems by virtue of their small size and efficient carrier capacity [341–344]. They are a type of drug delivery system in which particle size ranges from 1-1000 μm [345–347] in diameter, having a core of drug and entirely outer layers of polymers as coating material [329]. They are made of polymeric, waxy, or other protective materials that are biodegradable synthetic polymers and modified natural products. The natural polymers include gelatin and albumin whereas the synthetic polymers include polylactic acid and polyglycolic acid [344]. Microencapsulation is a process by which a drug substance is entrapped within discrete free-flowing polymeric particle microcapsule products [330,333,346,348,349]. They play a vital role in the development of controlled and/or sustained release drug delivery systems [344]. It has been reported that microspheres are a better choice of drug delivery system than many other types of drug delivery systems as they offer advantages of better patient compliance and detection of bimolecular interactions. Its applications are enormous as they are not only used for delivering drugs but also for targeting of specific sites [330].

Microencapsulation technology allows protection of the drug from the environment, stabilisation of sensitive drug substances, elimination of incompatibilities and/or taste masking. Henceforth, they play an important role in improving the bioavailability of drugs and minimising side effects [333]. Microspheres are essentially spherical in shape, whereas microparticles may be spherical or non-spherical in shape [345]. The types of microspheres commonly used in pharmaceutical science are briefly described in §5.1.1.1.

5.1.1.1 Types of microspheres

Microspheres are classified into different types, viz. bioadhesive, magnetic, floating and radioactive microspheres [350].

5.1.1.1.1 Bioadhesive microspheres

Bioadhesive microspheres adhere to the mucosal membranes such as buccal, ocular, rectal and nasal by means of interfacial forces [330,351–353]. Bioadhesive microspheres exhibit a prolonged residence time at the application site and absorption site, leading to the production of better therapeutic action [330,351]. Bioadhesive microspheres offer efficient absorption and enhanced bioavailability of drugs due to a high surface to volume ratio, prolonged contact with the mucous layer, controlled and/or sustained release of drugs from dosage forms and specific targeting of drugs to the absorption site [354–356].

5.1.1.1.2 Magnetic microspheres

The magnetic microsphere delivery system is important as it can be employed for targeted and localised drug therapy [357,358]. Magnetic carriers receive magnetic responses towards a magnetic field from incorporated materials of magnetic microspheres. Magnetic drug delivery has gained much momentum in chemotherapy and disease diagnosis. The different types are therapeutic magnetic microspheres and diagnostic microspheres [330,349,351]. Proteins and peptides can also be targeted through this system [351]. Magnetic microspheres find wide application in biomedical, bioengineering, and biological technology [358]. Magnetic microspheres vary widely in quality, sphericity, uniformity, particle size and particle size distribution, and as such an appropriate microsphere type needs to be chosen for a unique application [359]. A magnetically targeted drug delivery system involves binding a drug to a small biocompatible magnetically active component [350].

5.1.1.1.3 Floating microspheres

Floating microspheres are gastro-retentive floating drug delivery systems as they have less bulk density compared to that of the gastric fluid, thus their ability to remain buoyant in the stomach without being affected by gastric emptying rate and facilitate the release of API slowly at the desired rate [330,349,351,356,360,361]. They can prolong therapeutic effects, thereby reducing the frequency of dosing [330,349]. When microspheres come in contact with gastric

fluid, gel formers, polysaccharides, and polymers hydrate to form a colloidal gel barrier that controls the rate of fluid penetration into the device and consequent drug release [362]. As the exterior surface of the dosage form dissolves, the gel layer is maintained by the hydration of the adjacent hydrocolloid layer. The air trapped by the swollen polymer lowers density and confers buoyancy to the microspheres [355,356,362,363]. Floating microspheres provide an effective approach to the delivery of drugs that have poor bioavailability by maximising absorption [360,363]. Thus they are mostly useful and effective in the delivery of sparingly soluble and insoluble drugs [363].

5.1.1.1.4 Radioactive microspheres

Radioactive microspheres deliver high radiation doses to targeted areas without damaging the normal surrounding tissues [349,351,364]. Following administration, these microspheres get entrapped in the web of small blood vessels feeding a tumour and thus delivering the required concentration of radioactivity at the target site [364]. Another important advantage of radioactive microspheres is patient compliance since the radioactivity dose persists at a target site for at least four weeks [364].

5.1.1.1.5 Polymeric microspheres

Polymeric microspheres find application in a wide range of medical applications [365]. Polymeric microspheres can be used to deliver medication in a rate-controlled and targeted manner [366]. They can be classified as biodegradable polymeric microspheres and synthetic polymeric microspheres [330]. Biodegradable polymeric microspheres are biocompatible and/or bioadhesive in nature. Natural polymers such as starch are used because they are biodegradable, biocompatible, and also bioadhesive in nature. Biodegradable polymers prolong the residence time when in contact with the mucous membrane, therefore the rate and extent of drug release is controlled by the concentration of the polymer. The main drawback is, in clinical use, the drug loading efficiency of biodegradable microspheres is complex and it is difficult to control drug release. However, they provide a wide range of application in microsphere-based treatment [330,349,351]. Synthetic polymeric microspheres are widely used in clinical applications and have been reported to be safe and biocompatible [330,349,351].

5.1.2 Solvent evaporation

The solvent evaporation encapsulation technique has been widely used for the preparation of microspheres for SR of drugs [333,367–372]. It is the most commonly used technique to prepare microparticles or microcapsules [348,356]. Solvent evaporation involves the formation of an emulsion between a polymer solution and an immiscible continuous phase, whether aqueous or non-aqueous [329,351,373,374]. The processes are performed in a liquid manufacturing vehicle [375]. The microcapsule coating is dispersed in a volatile solvent which is immiscible with the liquid manufacturing vehicle phase. A core material to be microencapsulated is dissolved or dispersed in the coating polymer solution. With agitation, the core material mixture is dispersed in the liquid manufacturing vehicle phase to obtain the appropriate size microcapsule [376,377].

Solvent evaporation technique is based on the evaporation of the internal phase of an emulsion by agitation [354,373]. Generally, the polymeric coat material is dissolved in a volatile organic solvent. The drug core is then dissolved or dispersed in the above polymer solution to form a suspension, an emulsion or a solution. Then the organic phase is emulsified under agitation in a dispersing phase consisting of a non-solvent of the polymer, which is immiscible with the organic solvent, which contains an appropriate emulsifying agent. Once the emulsion is stabilised, agitation is maintained and the solvent evaporates, resulting in solid microspheres. The microspheres are recovered by filtration or centrifugation and are washed and dried [346]. The solvent evaporation technique offers several advantages [378] and is preferable to other preparation methods such as spray drying, sonication and homogenization because it requires only mild conditions such as ambient temperature and constant stirring [347,378]. Although the concept of the solvent evaporation technique is relatively simple, the physicochemical parameters governing this process are very complex. The solvent evaporation method has attracted the most attention because of its ease of use and scale-up and lower residual solvent potential compared to other processes [346].

Several innovative modifications of solvent evaporation techniques have been developed [346,379]. These include water-in-oil-in-water-in-oil (w/o/w/o), water-in-oil-in-oil (w/o/o), water-in-oil-in-oil-in-oil (w/o/o/o) and solid-in-oil-in-water (s/o/w), water-in-oil (w/o), thus widening the scope of the solvent evaporation technique [346].

5.2 MECHANISMS OF DRUG RELEASE FROM ORAL CONTROLLED RELEASE SYSTEMS

Oral CR formulations can be categorised based on their mechanism through which the API is released. Drug release mechanisms can be categorised broadly into chemical or physical mechanisms. The most published physical mechanisms of drug release from CR systems include diffusion, dissolution, erosion, ion exchange and osmotic controlled. Chemical mechanisms of drug release include chemical degradation and enzymatic degradation. These release mechanisms can occur alone or in synergism depending on the polymeric system employed in formulation development [380].

5.2.1 Physical mechanisms

5.2.1.1 Dissolution

In dissolution CR systems, drugs are coated with or encapsulated within slowly dissolving polymeric membranes (reservoir systems) or matrices (monolithic systems), respectively. In reservoir systems, drugs are protected inside polymeric membranes with low solubility. Drug release occurs upon dissolution of the polymeric membranes [334]. These systems are most commonly employed in the production of enteric coated dosage forms for either stomach protection or drug [381]. Dissolution controlled systems can be divided into reservoir and matrix systems. In the reservoir systems, the drug is coated with a matrix system and drug release is determined by the thickness and the dissolution rate of the polymeric membrane surrounding the drug [274]. In a matrix system, the drug is homogeneously distributed throughout the polymer and, as the polymer dissolves, drug molecules are released. In dissolution controlled systems, drug release is mainly affected by physicochemical properties of the drug and polymers used [274].

5.2.1.2 Diffusion

Diffusion controlled systems occur when a drug molecule diffuses from a region of higher concentration to a region of lower concentration through a polymeric membrane [35,274,382,383]. Diffusion controlled-release systems can be classified further as either reservoir or matrix devices [274,384,385]. In reservoir type of release mechanism, drug molecule diffusion within an aqueous solution is inhibited by the insoluble polymer matrix in which drug molecules must travel through tortuous pathways to exit the device [274]. Polymer

chains such as those in a cross-linked hydrogel form the diffusion barrier. Polymers used for diffusion controlled release can be fabricated as either the matrix in which the drug is uniformly distributed or as a rate-limiting membrane that protects the drug reservoir from the living environment [386]. Erosion products must be non-toxic and excretable or reabsorbable [35,337]. In diffusion controlled release systems, drugs are trapped in and released via diffusion through inert water-insoluble polymeric membranes (reservoir systems) or polymeric matrices (monolithic systems) [334].

5.2.1.2.1 Reservoir system

Reservoir-type devices refer to those having an inert coating material, which functions as a rate-controlling membrane [274,380]. The release rate remains relatively constant and is not affected by the concentration gradient, but most likely is related to the thickness and permeability of the polymeric membranes [380]. In this system, a water insoluble polymeric material encloses a core of drug. The drug will partition into the membrane and exchange with the fluid surrounding the particles. The active agent is released to the surrounding environment by diffusion process through the rate-limiting membrane. In the reservoir systems, the drug delivery rate remains fairly constant [31,328]. This system involves a membrane which controls the release of drugs from the matrix system. The drug will eventually diffuse through the membrane and its release is kept constant by the diffusion distance that the drug particles have to cover [278].

5.2.1.2.2 Matrix system

In the matrix devices, the drug or active agent is dispersed in a polymer matrix to form a homogeneous system known as a matrix system [387]. In matrix systems, drug release is more likely to be Fickian diffusion driven [388], which is associated with a concentration gradient, diffusion distance and the degree of swelling [380]. Diffusion occurs when the drug passes from the polymer matrix into the external environment. As the release continues, its rate normally decreases with this type of system, since the active agent has a progressively longer distance to travel and therefore requires a longer diffusion time to release [31]. Matrix system can be further divided into a hydrophobic or hydrophilic matrix system [389]. In hydrophobic matrix tablets, the release rate controlling components are water insoluble materials such as waxes, glycerides, fatty acids and polymers such as ethyl cellulose starch acetate or ammonio methacrylate copolymers (Eudragit®). Due to the insoluble nature of the matrix, the

formulation maintains its dimensions during drug release [385]. In hydrophilic matrices, the primary drug release rate controlling ingredients are polymers that swell on contact with the aqueous medium and form a gel layer on the surface of the system [390]. In the hydrophilic matrix, polymers such as cellulose ethers [hydroxypropylmethylcellulose (HPMC), hydroxypropyl cellulose (HPC), hydroxyethylcellulose (HEC)], xanthan gum, sodium alginate and poly(ethylene oxide) are commonly used in the production of compressed hydrophilic matrices, alone or in combination [385,391,392]. Drug release from hydrophilic matrix tablets is controlled by the formation of a hydrated viscous layer around the tablet which acts as a barrier to drug release by opposing penetration of water into the tablet and also the movement of dissolved solutes out of the matrix tablet [390].

5.2.1.3 Erosion

In erosion-controlled systems, the drug is dispersed uniformly throughout the hydrophilic polymer matrix. Once in contact with water, these systems swell [278,393] and drug dissolution occurs. The diffusion of the drug in the gel layer formed is slower than the polymer dissolution rate or erosion of the gel [385]. In the erodible hydrophilic matrix, the drug release can be controlled either by erosion in the case of poorly soluble drugs or by diffusion of the drug through the gel layer and erosion of the gel in the case of highly water soluble drugs. In addition, the strength of the gel layer influences drug release: using polymers of low viscosity grades leads to erosion-controlled release and zero-order kinetics [385,394]. Erosion, which may be surface erosion or bulk erosion, is the physical dissolution of the polymer as a result of its degradation. In surface erosion, water is confined to the surface of the matrix leading to chain scission of the surface matrix. In this case, the degradation rate is faster than the penetration of water into the polymer bulk and the drug will be released as the polymer matrix erodes [395]. The mechanism of erosion is shown in Figure 5.1.

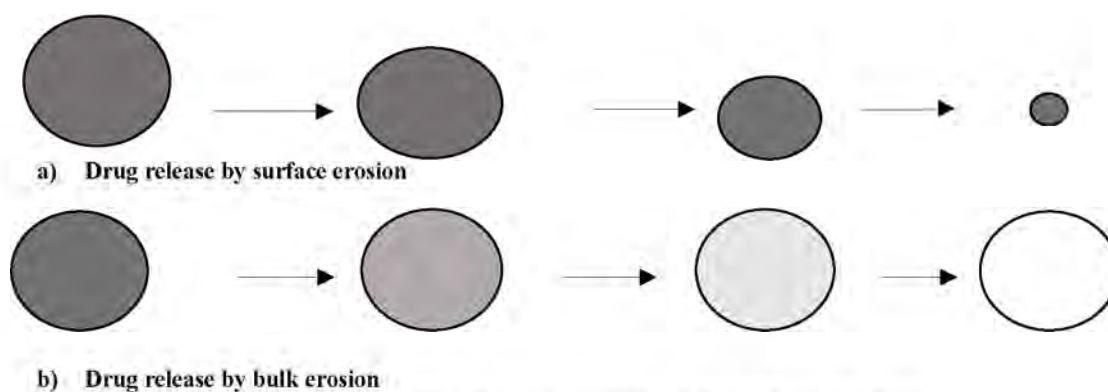


Figure 5.1 Drug release from microparticles (adapted from [395,396])

5.2.1.4 Osmotic

Osmosis can be defined as the spontaneous and natural movement of a solvent from a solution of lower solute concentration to a solution of higher solute concentration through an ideal semipermeable membrane [274,397]. The pressure applied to the higher concentration side to inhibit solvent flow is called the osmotic pressure [397]. Drug release is governed by solvent influx across a semipermeable membrane, which in turn carries the drug through a laser-drilled orifice [382]. The rate of drug release is dependent on the osmotic pressure of the formulation [382]. Osmotic systems operate on osmotic pressure and have been used in the development of zero-order drug release delivery systems [274,278,398]. Osmotic-based formulations contain a core tablet that is surrounded by a semipermeable membrane coating which has an orifice [398]. The core consists of a drug formulation that contains an osmotic agent and a water swellable polymer. The core tablet has two layers to it, one containing the active ingredient/drug known as the active layer and the second containing the osmotic agent which is also known as the push layer. The coating has one or more delivery ports through which a solution or suspension of the drug is released over time [398]. Water enters the tablet through the semipermeable membrane causing the drug to dissolve and suspend [278]. As the core absorbs water, it expands in volume and causes an increase in osmotic pressure [398]. The increase in osmotic pressure causes the dissolved/suspended drug to be pumped out of the one or more delivery orifices and release rate depends on the osmotic pressure of the release mechanism [274,278,399]. The rate at which the core absorbs water depends on the osmotic pressure generated by the core component and the permeability of the employed membrane coating [398]. The rate of drug delivery can be changed by altering the size of the delivery orifice and the thickness of the semipermeable membrane [278] and release drug at a rate that is independent of the pH and hydrodynamics of the external dissolution medium. The result is

a robust dosage form for which the *in vivo* rate of drug release is comparable to the *in vitro* rate, producing an excellent *in vitro/in vivo* correlation [397,398]. Basic osmotic systems are mostly useful in water soluble drugs but advanced push-pull osmotic delivery systems can deliver water insoluble drugs as well as water soluble drugs [274,400].

5.2.1.5 Ion-exchange

Ion exchange CR systems make use of water-insoluble ion-exchange resins polymeric materials containing abundant ionizable functional groups [274,334,401–403]. Ion-exchange resins (IER) are synthetic polymeric materials that contain basic or acidic groups that are able to interact with ionizable molecules to create insoluble complexes [401]. The drug is bound to the resin and released by exchanging with appropriately counter charged ions in contact with the ion exchange groups [404]. Drug release from ion-exchange resins depends on replacement of the drug molecule by other electrolytes, the area of dissolution, cross-linking density, ionic strength and coating of the drug-resin complex [274]. There are two types of ion-exchange CR systems based on the ionic properties of the resin. These are cationic resin for the release of anionic drugs and anionic resin for the release of cationic drugs [405].

5.2.1.6 Swelling

Swelling-controlled systems facilitate the diffusion of the API from and through an originally glassy polymer matrix [406] under countercurrent diffusion of water or biological fluid into the polymer matrix [407]. The polymer swells when in contact with water and transforms from a glassy to a rubbery state, forming a gel layer in which the dissolved drug can be transported due to increased mobility of the polymeric chains [385]. The gel layer prevents matrix disintegration and controls additional water penetration. Thus, water penetration, swelling, drug dissolution and diffusion and matrix erosion are the factors controlling the formation of the gel layer and consequently drug dissolution [408]. The drug release kinetics can be modified by the gel layer thickness and the rate at which it is formed. As the proportion of the polymer in the tablet increases, the gel formed reduces diffusion of the drug and delays the erosion of the matrix [385,408]. Swelling agents are three-dimensional networks of hydrophilic polymer chains that are chemically or physically cross-linked and can be divided into chemical and physical hydrogels [408,409].

5.2.2 Chemical mechanisms

For a chemical drug release mechanism to occur, the dosage form should consist of a bioerodible and/or biodegradable polymer matrix [410]. The release mechanism is degradation controlled and release is due to either surface and/or bulk erosion [340,410]. In bulk erosion, the material degrades homogeneously throughout the material [380,384] or deforms uniformly throughout the bulk of the material. As the deformation proceeds, the volume of the material remains constant while the mass of the material reduces, resulting in a decrease in the density of the degrading material. In the case of surface erosion, degradation is confined to the outer surface of the dosage form [380,384]. Drug release can be tailored in chemically controlled release systems by changing their chemical structure [334].

5.2.2.1 Chemical degradation

Chemically-controlled release is used to describe molecule release determined by reactions occurring within a delivery matrix [409]. Chemical release mechanisms are dosage forms that change their chemical nature when in contact with biological fluids. Biodegradable polymers are designed to change their structure due to hydrolysis of the polymeric chains, resulting in the collapse of the polymer matrix which facilitates drug release [340,380,409]. Chemically-controlled release can be further categorised according to the type of chemical reaction occurring during drug release [409]. Hydrolytic erosion can occur on the surface of the polymer like in polyorthoesters and polyanhydrides polymers or through bulk erosion [340,380,409]. Water is an important factor during hydrolysis, therefore water intrusion into the device is of significance for the study of degradation kinetics as well as release kinetics [380]. Polymer hydrolytic degradation may be defined as the scission of chemical bonds present in the polymer backbone by water [340] and may be catalysed by acids, bases, salts or enzymes [340,411]. The hydrophilic and hydrophobic nature of polymeric materials influences their degradation rate, and the susceptibility to hydrolysis follows this order [340].

5.2.2.2 Enzymatic degradation

Hydrolysis reactions may be catalysed by enzymes known as hydrolases, which include proteases, esterases, glycosidases, and phosphatases, among others [340]. This class of enzyme is responsible for the catalysis of several reactions in the human body. A suitable example is the hydrolytic enzymes present in the plasma and in the brush border membrane of the

intestines and lumen of the GIT. Hydrolytic enzymes are also present in the tubular epithelium of the kidneys, where they ensure the efficient hydrolysis of different substrates to facilitate absorption of nutrients and solutes [340]. Proteinase K, an endopeptidase enzyme responsible for the hydrolysis of peptides amides in keratin and other proteins, was found to accelerate the hydrolysis of poly (*L*-lactic acid) (PLLA) [340]. Another example is the lipase enzyme that hydrolyses ester bonds in polyesters in aqueous media. It was found that certain lipases enhanced the degradation of polycaprolactone (PCL) [340].

5.3 PROPOSED FORMULATION STUDIES

5.3.1 Background

Oral dosage forms are usually intended for systemic effects resulting from drug absorption through the various epithelia and mucosa of the GIT [103]. The most popular oral dosage forms are tablets, capsules, suspensions, solutions and emulsions [103]; consequently, the choice of technology used was the microencapsulation method. Conventional drug delivery systems are known to provide an immediate release of the drug, in which one cannot control the release of the drug and cannot maintain effective concentration at the target site for a longer time whereas controlled drug delivery systems offer prominent control of drug release [398].

The principle of the solvent evaporation method of microsphere manufacture is to dissolve the drug and carrier simultaneously in a common solvent, followed by the removal of the solvent by evaporation [412]. Identification of a common solvent for both drug and carrier can be problematic and complete solvent removal from the product can be a lengthy process. The solvent can be removed by various processes including vacuum drying, heating of the mixture, slow evaporation of the solvent at low temperature, rotary evaporators, spray drying and freeze drying [412].

5.3.2 Rationale for microspheres

Sustained release systems include any drug delivery system that achieves slow release of a drug over an extended period of time [33]. If a drug delivery system is successful in maintaining constant drug levels in the blood or target tissue, it is considered to be a controlled-release system [33]. The oral route of administration for sustained release systems has received greater attention because of more flexibility in dosage form design [33]. The development of microspheres by solvent evaporation method has been applied extensively in pharmaceutical

industries for various purposes such as controlled drug delivery, masking the taste and odour of drugs, and the protection of drug degradation [330,372,413–417]. Several methods such as mechanical agitation, homogenization, sonication, potentiometry and microfluidics can be utilised to disperse the oil phase into the continuous phase during the microspheres manufacturing process [418]. Microparticles have numerous medical applications such as oral, vaccine, intranasal and ocular delivery of drugs [395].

The BSC classifies Class II and III compounds as the most desirable compounds for CR so as to reduce the dosing frequency and side effects [343], and HYD is a BCS Class III compound (§1.2.2) due to its high water solubility and low gastrointestinal permeability [44]. HYD has a relatively short half-life and typical dosage regimens require administration of HYD two to four times a day. HYD is, therefore, a potential candidate for oral controlled delivery but the high water solubility of HYD presents formulation challenges. Therefore the objective of these studies was to develop, manufacture and evaluate sustained release microparticles of HYD.

5.4 MATERIALS

Excipients guarantee dosage form stability and bioavailability of the API. Excipients must present the characteristics required by their technological function but must meet safety requirements [268]. It is unacceptable to include an excipient in a pharmaceutical product that is not genuinely needed [419]. Excipients may be detrimental or beneficial to the stability of a formulation [419]. Detailed characterization(s) of these excipients is explained in Chapter 4.

5.4.1 HYD

HYD is the API of choice due to its short half-life and is normally administered two to four times daily [7]. Detailed physicochemical properties of HYD are fully described in Chapters 1 and 4.

5.4.2 Methocel® K100LV, K15M and K100M

Methocel® (Colorcon Ltd, Orpington, UK) is the propriety name for the methylcellulose derivative that is manufactured by Dow Chemical Company [273,274,382]. HPMC is a GRAS listed compound that is non-toxic and non-irritant, although ingestion of large quantities may lead to laxative effects [273,274,412].

Drug release from HPMC matrix systems is due to swelling when in contact with water and/or by erosion of the gel matrix layer [274]. Its applications include buccal delivery systems, gastro-retentive systems and colon delivery systems [274].

HPMC is a non-ionic derivative, semi-synthetic polymer of cellulose ether and is stable over pH range 3.0-11.0 [278]. It has been reported that matrices containing HPMC are not affected by pH [278]. HPMC matrix systems are classed as swelling controlled systems and are controlled by the rate of penetration of media and erosion of the matrix [278]. Compared to other swellable polymers used to control drug release, HPMC is said to have been the most widely used due to its rapid hydration, good compression and gelling characteristics [278].

5.4.3 Eudragit[®] RS PO and Eudragit[®] L 100

Eudragit[®] RS PO is a fine white powder with an amine-like odour that is comprised of 97% w/w of the dry polymer [273]. The dry powder polymers are stable at temperatures less than 30 °C. Above 30 °C, they form clumps which do not alter the quality of the product [273]. The Eudragit[®] polymers are listed in the FDA inactive ingredients' guide. The commonly used Eudragit[®] for the preparation of CR solid dispersions are Eudragit[®] L, RL, RS, RL PO and RS PO [273,412]. Eudragit[®] RS PO and L 100 were selected for formulation studies.

5.4.4 Avicel[®] (MCC)

MCC is manufactured by controlled hydrolysis of purified native cellulose, which dissolves the amorphous matrix but leaves the crystallites intact [102]. It has the chemical name cellulose and a CAS registry number of 9004-34-6 [273]. MCC is an odourless, tasteless crystalline white crystalline powder made up of porous particles that are primarily used as binder or diluent in oral tablet and capsule formulations [273]. MCC is a GRAS listed compound, regarded as non-toxic and non-irritant although large quantities may have a laxative effect [273]. It is a stable hygroscopic material and is not absorbed systemically after oral administration [273,420]. Avicel[®] was used as a diluent during formulation development and optimisation.

5.5 EXPERIMENTAL

5.5.1 Aim

The aim of these studies was to manufacture HYD loaded microsphere using the solvent evaporation technique.

5.5.1 Choice of method of manufacture

The design of microspheres includes selection of the most appropriate and suitable method of manufacture, considering the nature of the drug and polymers employed as well as the administration route [421]. Techniques based on solvent removal, such as solvent evaporation and solvent extraction, are frequently used to manufacture microspheres [421]. Thus solvent evaporation was selected as the method of microspheres manufacture due to its simplicity, popularity, accessibility and availability. The HYD loaded microspheres were prepared by the conventional emulsion solvent evaporation method which was adapted from the process described by Khamanga *et al.* [153] and modified specifically for HYD.

5.5.2 Screening for polymers

High viscosity grades of HPMC are suitable for delaying the drug release from the matrix [273,385]. The formulation variables which have the greatest impact on the release rate are matrix dimension and shape, amount of polymer and its molecular weight, drug load and drug solubility [385]. The release of a water soluble compound from an HPMC matrix involves the successive processes of penetration of a liquid into the matrix, hydration and swelling of the matrix, dissolution of the drug in the matrix and diffusion of the drug through the channels in the matrix [385].

Screening studies were performed for Methocel® K100LV, K15M, K100M, Eudragit® L 100 and RS PO. Carbopols were not included for formulation studies because preliminary preformulation studies indicated that there might be an interaction between carbopol® 971P and HYD, probably due to the formation of an amide bond between the amine and carboxylic acid functional groups present in HYD and carbopol® respectively. The screening was based on available polymers. The HPMC differ in viscosity and therefore differ in their extent to sustain release. Eudragit® RS PO on its own could not sustain release but its inclusion in the formula aided in the formation of microspheres. It was observed that Eudragit® L 100 did not aid in the formation of microspheres. The screening process was done based on SEM images and release profiles of each selected polymer.

It was observed that the use of less than 10 mL acetone was not appropriate as the solvent was not enough to dissolve the powder mass. It was also noted that for values above 16 mL, no microspheres would form as the concentration of the powder mass would be decreased by

increasing the amount of acetone, hence the choice of 12 mL acetone. For preliminary studies, the amount of acetone was kept constant. It is important to keep the beaker size and the beaker type the same as different beaker sizes were seen to affect the manufacture of microspheres. This is because the flow near the blades of the homogenizer will be different to the flow nearer to the beaker glass, therefore affecting the final product. Storing at room temperature was not best in evaporating all the acetone, therefore the use of a higher drying temperature for a prolonged time. Other factors which would affect the microspheres' formation were maintained constant. The constant formulation parameters are shown in Table 5.1.

Table 5.1 Summarised constant formulation parameters

| Formulation parameters | Value |
|--|---|
| Homogeniser | 4 blade butterfly |
| Spheronisation speed | 500 rpm |
| Spheronisation time | 7 hours |
| Amount of acetone | 12 mL |
| Amount of <i>n</i> -hexane | 10 mL |
| Beaker size | 400 mL |
| Amount of liquid paraffin (oil phase) | 120 mL |
| Amount of span 80 (emulsifier) (HLB 4.3) | 1.2 mL |
| Filter | 0.45 µm filter paper using Büchner funnel |
| Drying temperature | 25 °C |
| Drying time | 24 hours |

The amount of each formulation constituent was weighed according to amounts recorded in Table 5.2. This was mainly to investigate the effect of HPMC and Eudragit[®] polymer on HYD release and their impact in the manufacture of microspheres. It was observed that formulations containing HPMC polymers on their own did not manufacture microspheres, therefore the addition of Eudragit[®] polymer.

Table 5.2 Summarised formulation screening studies

| Constituents | F1 | F2 | F3 | F4 | F5 | F6 |
|------------------------------|------|------|------|------|------|------|
| HYD | 0.5g | 0.5g | 0.5g | 0.5g | 0.5g | 0.5g |
| Methocel [®] K100LV | - | - | 1g | - | - | 1g |
| Methocel [®] K15M | - | 1g | - | - | 1g | - |
| Methocel [®] K100M | 1g | - | - | 1g | - | - |
| Eudragit [®] RS PO | 1g | 1g | 1g | - | - | - |
| Eudragit [®] L 100 | - | - | - | 1g | 1g | 1g |

5.5.3 Preparation of microspheres

All formulation components were weighed individually using a Model PM top-loading balance (Mettler[®] Toledo, Zurich, Switzerland). The solvent evaporation method involves the emulsification of an organic solvent containing dissolved polymer and the dissolved or dispersed drug in an excess amount of continuous phase containing an emulsifier. The emulsion

is stirred using a homogenizer for several hours in order to allow the solvent to evaporate and facilitate the formation of microspheres [153,395].

HYD microspheres were prepared using Methocel[®] K100M, K15M, K100LV, Eudragit[®] RS PO and Eudragit[®] L 100 polymers. Approximately 0.5, 1.0 and 1.0g of HYD, Methocel[®] and Eudragit[®] respectively were accurately weighed and dissolved in 12 mL of acetone by stirring using a glass rod. The resultant milky white dispersion was poured into a vessel containing a mixture of 120 mL of liquid paraffin and 1.2 mL of span 80. The resulting emulsion was stirred for 2 hours using a homogenizer fitted with a four-blade “butterfly” propeller with a diameter of 50 mm (Virtis Company, USA). After stirring for 2 hours, 10 mL of *n*-hexane was added so as to harden the microspheres and stirring was continued for a further 5 hours to ensure complete evaporation of acetone. Following the removal of the acetone, the resultant microparticles were harvested by vacuum filtration using a Büchner funnel fitted with a 110mm Whatman filter paper. Light liquid paraffin was decanted, collected microspheres were washed 3 times with 50 mL aliquots of *n*-hexane, dried in an oven at 25 °C for 24 hours and stored at room temperature. The weight of each constituent was recorded on a batch production record and are included in Appendix II. A schematic representation of the manufacturing process is shown in Figure 5.2.

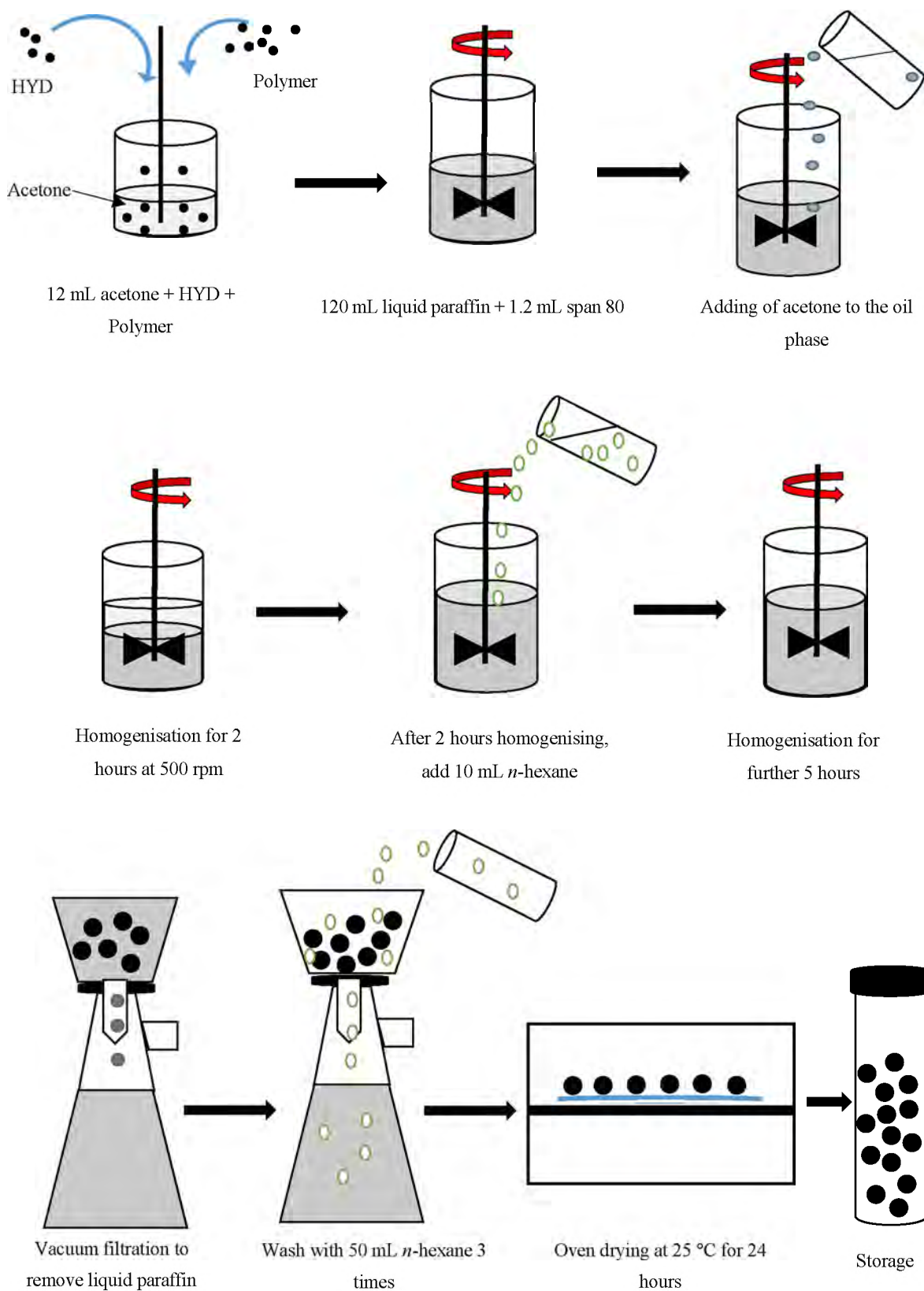


Figure 5.2 Schematic representation of solvent evaporation technique used in the manufacture of microspheres. Adapted from [153]

5.6 EVALUATION OF HYD MICROSPHERES

Manufactured HYD microspheres were evaluated using physical appearance, percentage yield, SEM, assay, encapsulation efficiency and cumulative *in vitro* HYD release.

5.6.1 Physical appearance

Batches were assessed on colour by physical examinations. Physical examination of manufactured products can be useful in assessing the purity of a compound and identifying contamination that occurred during the synthesis process [335,422]. Typical testing involves viewing the material against a white background under specified lighting and reporting the colour and form [423] and this method was used for evaluation of physical appearance.

5.6.2 SEM

The particle size and surface morphology for formulated microparticles were characterised using SEM (Tescan, VEGA LMU, Czech Republic). Samples were mounted onto a double-sided carbon stub, placed on a sample disc carrier (3mm height, 10mm diameter) and coated with gold particles under vacuum with a sputter coater (Balzers Union Ltd, Balzers, Lichtenstein).

5.6.3 Yield

Immediately after drying, the microspheres were weighed using a Model PM top-loading electronic balance (Mettler® Toledo, Zürich, Switzerland) and the amount found recorded before any other test was performed. The percentage yield was calculated using Equation 5.1. The final weight of microspheres was measured soon after drying, before any other characterization.

$$Yield(\%) = \frac{\text{amount of microspheres obtained (g)}}{\text{theoretical amount added (g)}} \times 100 \quad \text{Equation 5.1 [153]}$$

5.6.4 Assay

To estimate the amount of HYD in the final formulation, a mass of the bulk product equivalent to 100 mg was weighed and transferred to a 100 mL A-grade volumetric flask and made up to volume with water. The mixture was sonicated for 2 hours so as to ensure complete extraction and dissolution of HYD. After sonicating, 5 mL samples were withdrawn and filtered using

0.45 µm hydrophilic PVDF filter membranes. 1 mL was transferred into an amber-coloured vial to which 500 µL IS was added to all test solutions prior to HPLC analysis.

5.6.5 Encapsulation efficiency (EE)

To determine EE, 500 mg of microspheres was weighed which contained 100 mg HYD and washed with 10 mL of water to remove surface and free drug. The microspheres were then transferred to a 100 mL A-grade volumetric flask and made up to volume with water. The mixture was sonicated for 2 hours so as to ensure complete extraction and dissolution of HYD [352,424]. After sonicating, 5 mL samples were drawn and filtered using 0.45 µm hydrophilic PVDF filter membranes. 1 mL was measured and transferred into amber-coloured vials to which 500 µL IS was added. HYD content was determined spectrophotometrically using a developed and validated stability indicating HPLC method. EE was determined using Equation 5.2.

$$\text{Entrapment Efficiency (\%)} = \frac{\text{Weight of drug in microspheres}}{\text{Weight of drug fed initially}} \times 100 \text{ Equation 5.2 [425]}$$

5.6.6 *In vitro* release

All preliminary formulations were subjected to *in vitro* dissolution testing using 0.1M phosphate as the dissolution medium. The basket-membrane method was used so that release would be through a porous membrane. The study was conducted for a duration of 12 hours and the cumulative % HYD released was recorded as a function of time. Release studies were performed using a Hanson SR8 No 73-100-104 modified USP Apparatus 1 (Hanson Research, Chatsworth, CA, USA) coupled with an autosampler. A glass basket dialysis method (Figure 5.3) was used for dissolution studies as proposed by Abdel-mottaleb and Lamprecht [426]. The dissolution medium (900 mL, 0.1M Phosphate, pH 6.8, enzyme free) was continuously stirred at 100rpm and temperature was maintained at 37 +/- 0.5 °C.

The 0.1M phosphate buffer was prepared using potassium dibasic orthophosphate buffer and adding up to the volume with HPLC grade water. The pH was monitored using a Model GLP 21 Crison pH meter (Crison Instruments, Johannesburg, South Africa) adjusted to 6.8 using 0.1M NaOH. Approximately 900 mL of 0.1M phosphate buffer was measured and transferred to 1000 mL dissolution vessels.

The weight of microspheres containing approximately 80 mg HYD (n=3) was weighed and transferred into size 000 capsules prior to placing in a dialysis membrane that had been soaked overnight in dissolution medium to allow equilibration. The dialysis membrane was attached to the lower end of a glass tube of 22 mm internal diameter and 35 mm length replacing the original basket. The total surface area available for HYD release was 380 mm². Approximately 2 mL of dissolution media was added to the capsules to keep the membranes hydrated so that they did not break. The dialysis membrane, of MW cut off 12 000, was purchased from Sigma Aldrich® (St Louis, MI, USA) and was tied with a rubber band to prevent leakage when attached to the shaft of the dissolution apparatus. The tubes were then immersed in the dissolution vessel that contained 900 mL of dissolution media. The maximum HYD concentration was approximately 90 µg/mL which was within the linearity range of the calibration curve.

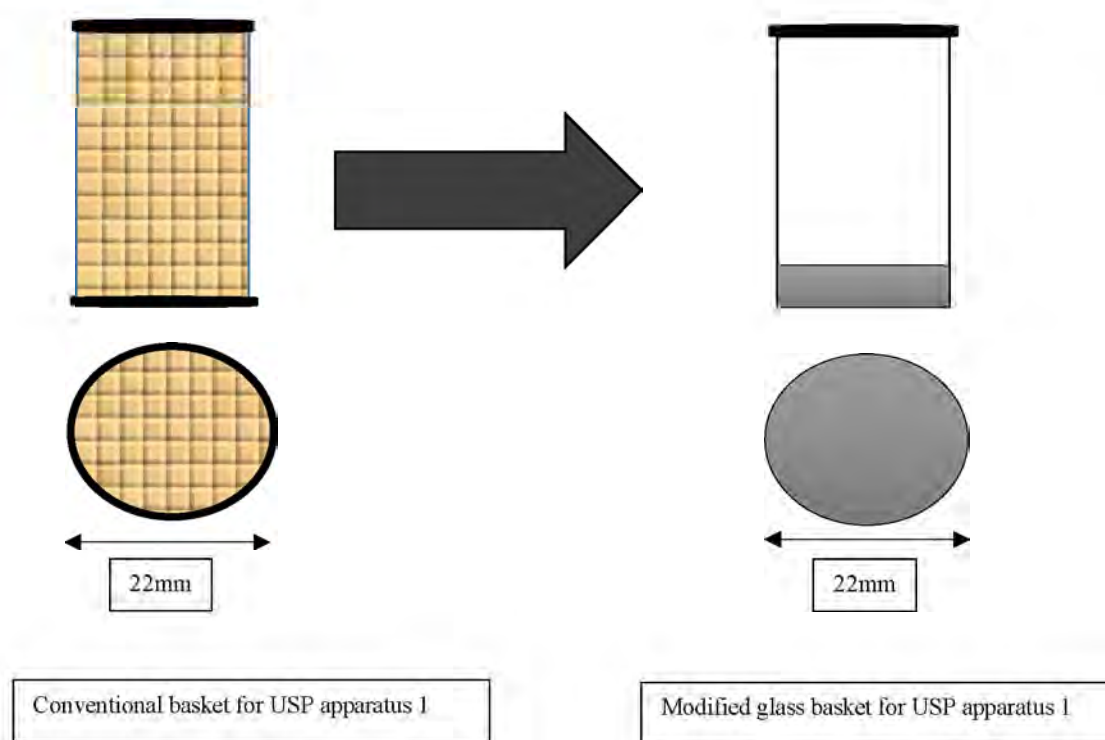


Figure 5.3 Design of the glass baskets (right) compared to conventional baskets (left) adapted from ([426])

Samples (5mL) were withdrawn at 5 minutes, 0.25, 0.5, 1, 2, 3, 4, 6, 8, 10 and 12 hours and filtered through 10 µm filter hydrophilic HVP membranes. The volume withdrawn was replaced with an equivalent volume of fresh dissolution medium. The dissolution testing conditions are summarised in Table 5.3.

Table 5.3 Summary of dissolution test conditions

| | |
|-------------------------------|--|
| Parameter | USP Apparatus 1 (Modified) |
| Dissolution media | 0.1M Phosphate buffers at pH 6.8 |
| Volume | 900 mL |
| Temperature | 37 ± 0.5 °C |
| Speed | 100 rpm |
| Sample volume | 5.0 mL |
| Sampling times (hours) | 0.0833, 0.25, 0.5, 1, 2, 3, 4, 6, 8, 10 and 12 |

5.7 RESULTS AND DISCUSSION

The effect of different polymers on the manufacture of microspheres was evaluated. For comparative purposes, all the other factors that could influence the formulations were kept constant. All polymers were used without further purification and are generally regarded as safe. Different grades of Methocel® and Eudragit® were evaluated and the best polymeric combination was selected for formulation optimisation studies. Each batch was formulated to contain 0.5g of HYD.

When the solution of solvent was poured into the continuous phase whilst stirring, finely dispersed droplets formed immediately and a milky emulsion was observed. Due to homogenisation, acetone was continuously mixed with the liquid paraffin, forming a milky suspension due to evaporation of acetone. With the diffusion of acetone out of the droplets into the continuous phase, the drug and the polymer remained within the droplets, which then was followed by solidification of the droplets to form microspheres. During formation of the droplets microparticles agglomerated to form an irregular mass and adhered to the propeller or the vessel wall. To avoid agglomeration and surface tension between the solutions, span 80 was added to the liquid paraffin during the manufacturing process. Span 80 increases the miscibility of the drug and polymer loaded acetone with liquid paraffin. The use of the emulgent results in a decrease in viscosity of the continuous phase that prevents conglutination of the emulsified droplets. In addition, the presence of span accelerates the solidification of droplets.

5.7.1 Physical appearance

The assurance of quality, safety and efficacy of the dosage forms on the market is controlled and/or monitored by regulatory authorities [427–429], such as the Medicines Control Council in South Africa [430]. HYD microspheres were obtained with different shapes, sizes and colours ranging from light brown to off-white depending on the type of polymers used. To

assess stability, the physical appearance was to be evaluated. The microspheres were off-white with varying shape and size depending on the type of polymers employed

5.7.2 SEM of preliminary formulations

Determination of microsphere morphology (shape and size) and morphological changes can be evaluated using optical, transmission and SEM [421]. In this study, SEM was selected for morphologic determination of formulated HYD microspheres because it provides vital information about the porosity and microstructure of the spheres [333]. The microspheres had particle size ranging from 100 μm to 1mm which was within the specified microsphere size range and the surface of the microspheres appeared to be rough. The size of microspheres was dependent on the type of polymers used. The basis of SEM was to determine the shape and size of formulation F1 to F6. The difference in shape and size observed using SEM might be mostly due to the polymers used because all the other factors that might affect microsphere size and shape were kept constant. Formulation F1 had rough clumped microspheres with HYD on the microsphere surface showing poor encapsulation of the drug. SEM results for formulation F2 showed spherically, clumped microspheres with better HYD encapsulation compared to F1. SEM results for formulation F3 showed spherical, discrete microspheres with some un-encapsulated HYD. Formulation F4 showed rod-like microparticles with polymer encapsulating the drug. Formulation F4 did not form microspheres but rather microparticles. Formulation F5 showed rough semi-spherical microparticles with the drug completely encapsulated. Formulation F6 showed a mixture of smooth microspheres and rough microparticles with least drug encapsulated. SEM images obtained for Formulation F1 to F6 are shown in Figure 5.4 to 5.9.



Figure 5.4 SEM image for F1

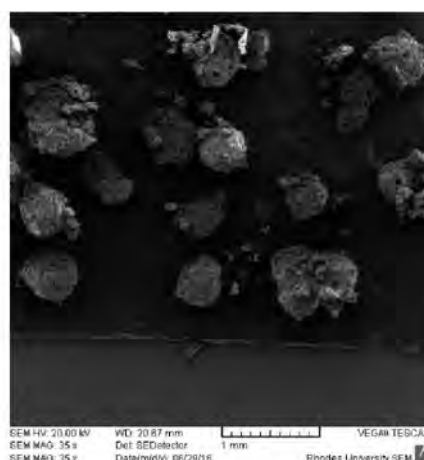


Figure 5.5 SEM image for F2



Figure 5.6 SEM image for F3

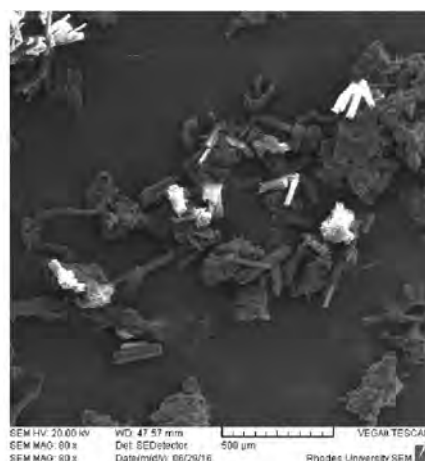


Figure 5.7 SEM image for F4

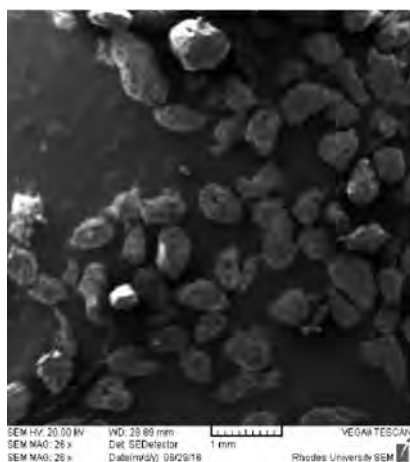


Figure 5.8 SEM image for F5

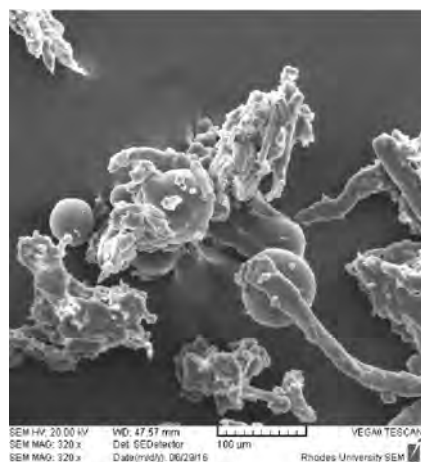


Figure 5.9 SEM image for F6

5.7.3 Yield

All formulations had a yield above 90%, with F6 having the lowest yield of 92% and F1 and F4 having the highest yield of 96%. All formulations showed high percentage yield perhaps due to the fact that small quantities of formulation constituents would be lost during mixing and filtering. The effect of changing Methocel® and Eudragit® polymers has shown minor effects on yield, perhaps due to the fact that the API and the polymers used are insoluble in liquid paraffin. The results for percentage yield are summarised in Table 5.4.

Table 5.4 Percentage Yield of F1 to F6

| Formulation | F1 | F2 | F3 | F4 | F5 | F6 |
|-------------|----|----|----|----|----|----|
| Yield (%) | 98 | 94 | 97 | 98 | 96 | 92 |

5.7.4 Assay

Assaying procedures are intended to measure the analyte present in a given sample [423]. The results obtained after assaying indicate that the microspheres had above 70% of HYD. The content of HYD for each formulation expressed as a percentage of the theoretical amount of HYD following assay are summarised in Table 5.5. The results obtained were evaluated with reference to the FDA compendial specifications range for the analysis of pharmaceutical products which specifies that drug content should be 95.0 to 105.0% [431]. However, HYD content should be 98.5 to 101.0% [38], therefore formulation F3 and F5 showed assay values within the specified FDA compendial range.

Table 5.5 Assay of F1 to F6 (n=3)

| Formulation | Assay (%) \pm SD |
|-------------|--------------------|
| F1 | 91.0 \pm 0.01 |
| F2 | 91.1 \pm 0.02 |
| F3 | 95.9 \pm 0.11 |
| F4 | 72.5 \pm 0.01 |
| F5 | 96.2 \pm 0.01 |
| F6 | 84.8 \pm 0.03 |

5.7.5 Encapsulation efficiency (EE)

A major problem related to the solvent evaporation technique is poor EE of water-soluble compounds [374,376], thus increasing EE is desirable [366]. Successful entrapment of drug within microcapsules is thus highly dependent on its solubility in the aqueous phase [374]. The EE for all formulations was high, ranging from 76 to 93%, perhaps due to the fact that HYD is insoluble in liquid paraffin, justifying the use of the o/o emulsion method for the manufacture of water soluble HYD. This is because, when the microspheres were washed, free drug and surface drug were removed. Formulations had varying EE because of different polymers used. High viscosity grade HPMC tends to hold the drug; therefore, the EE is lower due to HPMC retaining HYD in the formulation.

In all cases, the EE was lower than 95%, perhaps due to the fact that HPMC forms a matrix system, entrapping and retaining the drug and the presence of span 80 increased the miscibility of acetone with the light liquid paraffin which might increase partitioning of HYD into this phase. Theoretically, the use of high homogenising speeds would result in the production of smaller emulsion droplets [333], facilitating drug loss from the microparticles before they

harden and resulting in a low EE. The homogenising speed was thus kept constant for these studies.

It has been reported that high polymer concentration improves the EE mainly due to increased entanglement of polymeric chains [432]. Formulation F4 had the lowest EE compared to all the other formulations, perhaps due to the Methocel[®] K100M forming a thick gel around the drug and entrapping the drug. Consequently, only a small amount of the drug managed to dissolve into the aqueous media. Formulation F5 had the highest EE, perhaps due to HYD being encapsulated as depicted in Figure 5.8 and, since Methocel[®] K15M has a lower viscosity compared to Methocel[®] K100M, the gel formed would be less strong. Formulation F3 had the second highest EE, perhaps because of the low viscosity factor. The EE may be affected by the content of HYD and polymer in addition to the shape of the microparticle. Span 80 surfactant ensures that HYD is finely dispersed and embedded in the polymer matrix during microencapsulation. As HYD is hydrophilic, it is unlikely to have an affinity for the oil phase used although it might slightly partition into the oil phase. Therefore the EE would be affected mostly by the solubility of HYD in acetone and liquid paraffin and its interaction with the polymers used. The EE may also be affected by HYD and polymer content in addition to the shape of the microparticle. The EE for formulations F1 to F6 is summarised in Table 5.6.

Table 5.6 Encapsulation Efficiency (EE) of F1 to F6 (n=3)

| Formulation | EE (%) \pm SD |
|--------------------|-----------------------------------|
| F1 | 83 \pm 0.02 |
| F2 | 86 \pm 0.01 |
| F3 | 90 \pm 0.02 |
| F4 | 76 \pm 0.01 |
| F5 | 93 \pm 0.01 |
| F6 | 85 \pm 0.05 |

5.7.6 *In vitro* release

Dissolution is the process by which a solid enters in a solvent to form a solution [102]. Fundamentally, it is controlled by the affinity between the solid substance and the solvent. These studies aid in understanding the behaviour of these systems in terms of drug release and their efficacy [333]. The physical characteristics of the dosage form, the wettability of the dosage unit, the penetration ability of the dissolution medium, the swelling process and the disintegration of the dosage form are a few of the factors that may influence the dissolution characteristics [102]. It has long been recognised that the release of the active agent from a dosage form may be greatly influenced by the physicochemical properties of the drug, as well

as the dosage form. The availability of the drug is usually determined by the rate of release of the drug from the dosage form. The release of the drug from its dosage form is usually determined by the rate at which it dissolves in the surrounding medium [102].

All preliminary formulations were subjected to *in vitro* dissolution testing using 0.1M phosphate as the dissolution medium. The study was conducted for a duration of 12 hours and the cumulative % HYD released was recorded as a function of time. Pure HYD was used for dissolution testing prior to dissolution studies of dosage forms and the membrane was found to have no effect on the flux of HYD and water through the membrane.

5.7.6.1 Mechanism of HYD release

Since only Methocel[®] and Eudragit[®] polymers were used during these formulation studies and their amount remained constant, the mechanism of HYD release would be similar in all formulations. Alderman [433] suggested that different viscosity grades of HPMC can be used to modify the release rates of drugs [278]. The rationale was that higher viscosity grades have a higher gel viscosity, which would both slow drug diffusion in the gel layer and also render it more resistant to erosion [403]. When hydrophilic matrices are immersed in aqueous media, i.e. gastro-intestinal fluids, the polymer hydrates and swells resulting in an increase in size and gel formation. After some time the matrix dissolves or erodes allowing drug release. The drug is released by the process of diffusion through the gel layer at first and, after a while, through polymer erosion. Studies have shown that drug release from swellable hydrophilic matrices is dependent on the thickness of the hydrated layer that is formed during polymer hydration. The degree of swelling determines the rate of drug release. The thicker the gel layer, the slower the rate of drug release. Physiological factors of the GIT including pH, GIT transit time, GIT contents and intestinal motility can affect the release of drugs [278].

In relation to polymer solutions, viscosity is dependent upon the molecular weight of the polymer. Viscosity of polymer solutions is as a result of polymer chain hydration through hydrogen bonding of oxygen atoms in ether linkages, causing them to extend and form relatively open random coils [278]. The hydrated coils continue to hydrogen bond to additional water molecules causing entrapment within the coils. Thus, viscosity can, therefore, affect the extent of drug release from hydrophilic matrices [278]. Rahman *et al.* [281] evaluated the effect of viscosity grades of HPMC matrix systems as oral CR drug delivery systems using a non-steroidal anti-inflammatory drug [281] and the results demonstrated significant differences in

the drug release profile from different matrices. The drug release from the higher viscosity grade K100M was slower compared to the lower viscosity grade K100LV. The release rate was considerably dependent on the viscosity grade of HPMC as it showed a statistically significant increase in drug release with low viscosity HPMC [278,281].

HPMC is a hydrophilic polymer used in the preparation of oral CR dosage forms [434]. One of its important characteristics is its high swellability, which significantly affects incorporated drug release kinetics [434]. When in contact with water, HPMC expands leading to dramatic changes to the matrix system employed and the encapsulated drug diffuses out of the system. The rate of release depends on the chain length and degree of substitution of the HPMC type used [434]. The drug release rates are modulated by the rate of water transport and the thickness of the gel layer. Drug diffusion time and polymer chain relaxation time are two key parameters determining drug delivery from polymeric matrices [409].

HPMC substitution type can significantly modulate drug release and even the commercial source of an apparently similar grade of HPMC may cause differences in release [403]. HPMC particle size can have a considerable effect on matrix drug release [403]. Coarse particle size fractions of HPMC are thought to hydrate too slowly to allow SR and they can result in burst release. Coarse particle sizes of HPMC may also allow water penetration and disintegration to occur before the formation of the gel layer which protects the internal drug from dissolution. In contrast, smaller fractions of HPMC allow rapid hydration and uniform gel layer formation. In general, the higher the content of HPMC, the slower is the drug release rate [403].

Microspheres are heterogeneous systems, therefore the drug release from the polymer takes place through a diffusion process. The release of the drug is also determined by the extent of degradation of polymeric microsphere [333]. The influence of surfactant ratios, rate of solvent evaporation, solvent type and polymer concentration on the physicochemical characteristics, encapsulation efficiency and drug release from biodegradable microspheres have been reported [333,435]. These factors were kept constant in these studies so as to evaluate the influence of different polymer types on HYD release.

5.6.6.2 Formulation F1

Formulation F1 (n=3) showed sustained release of HYD, with approximately 60% HYD released in 6 hours and approximately 88% HYD released after 12 hours of commencing

dissolution testing. The rate of release of HYD was sustained because of Methocel® K100M and Eudragit® RS PO polymers. The high viscosity properties of Methocel® K100M might contribute to such low release after 12 hours. The total HYD released from F1 was incomplete, with approximately 88% released after 12 hours of dissolution testing. The thickness of the gel depends mostly on the polymers used and their viscosity grades. The cumulative release for F1 is shown in Figure 5.10.

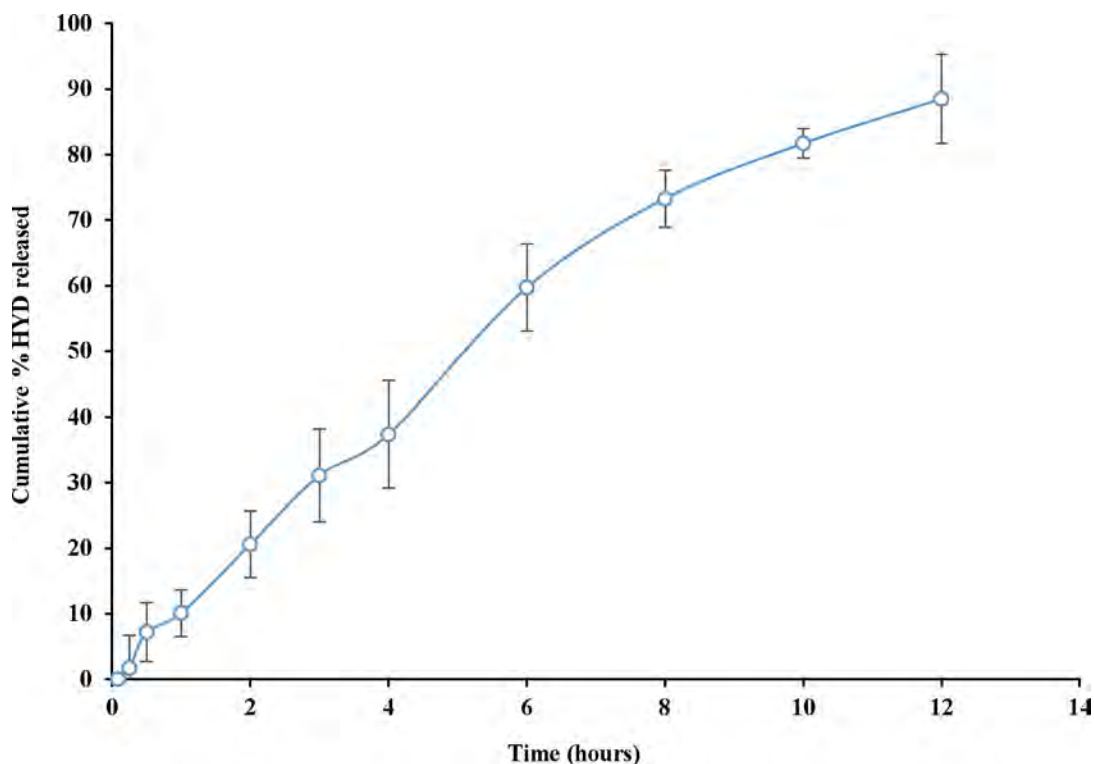


Figure 5.10 Cumulative % HYD released from formulation F1

5.6.6.3 Formulation F2

Formulation F2 (n=3) showed sustained release of HYD, with approximately 55% HYD released after 6 hours and approximately 92% HYD released after 12 hours. Since both F1 and F2 contained Eudragit® RS PO but different grades of HPMC, the HYD release rate of F2 was higher compared to F1, probably due to Methocel® K15M forming a less thick gel compared to that of Methocel® K100M. The cumulative release for F2 is shown in Figure 5.11.

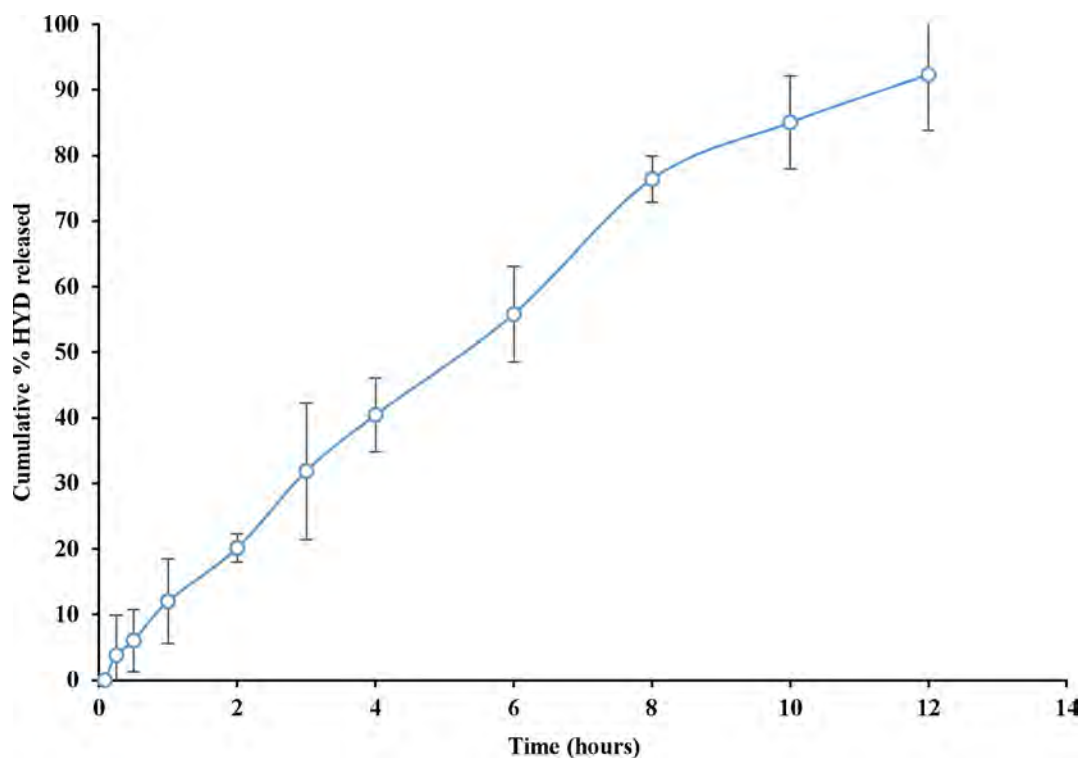


Figure 5.11 Cumulative % HYD released from formulation F2

5.6.6.4 Formulation F3

Formulation F3 (n=3) showed sustained release of HYD with approximately 61% HYD release after 6 hours and approximately 95% after 12 hours. Both formulation F2 and F3 contained Eudragit® RS PO but different grades of Methocel®, therefore the effect of K15M and K100LV was compared. Both formulations had approximately 55-60% released after 6 hours and approximately 92-95% after 12 hours indicating that the release of F2 and F3 was statistically similar. The cumulative release for F3 is shown in Figure 5.12.

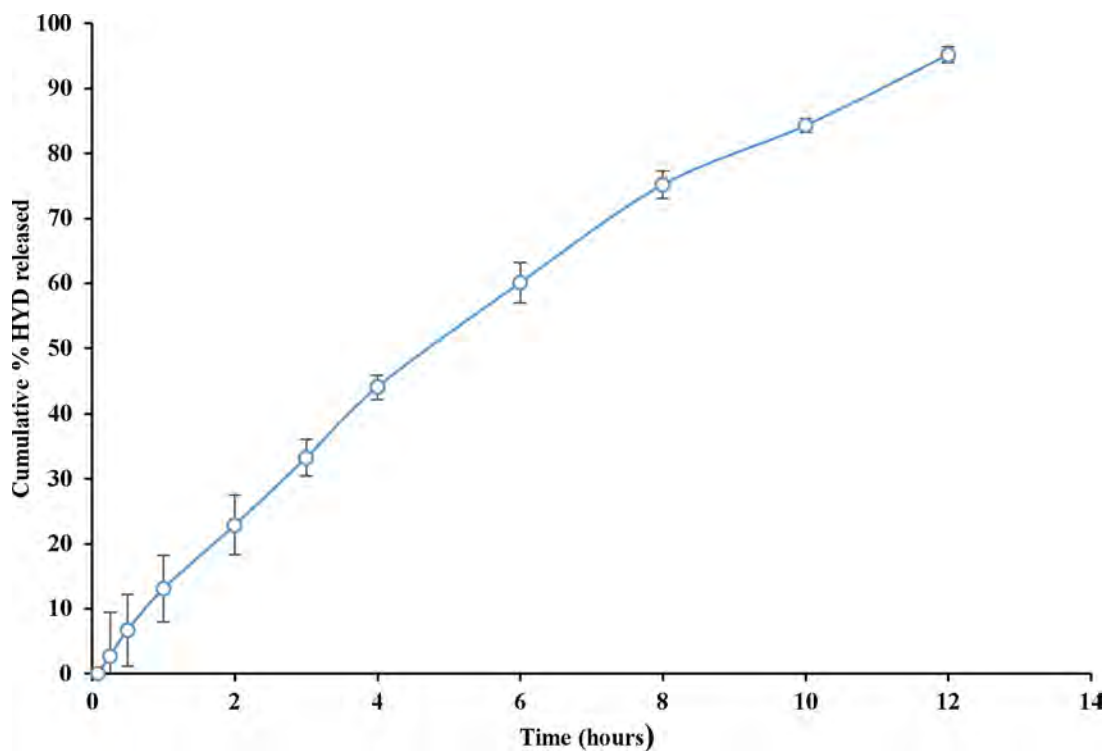


Figure 5.12 Cumulative % HYD released from formulation F3

5.6.6.5 Formulation F4

Formulation F4 (n=3) showed slow sustained release of HYD, with approximately 42% HYD released after 6 hours and approximately 70% after 12 hours. Formulation F1 and F4 contained the same Methocel® K100M but different Eudragit®, therefore the release of F1 and F4 was compared. Eudragit® L is water soluble and shows pH-dependent drug release whilst Eudragit® RS is a water insoluble, permeable polymer and shows pH-independent drug release [274,436–439]. Release profiles showed statistically similar release rates indicating that the type of Eudragit® used had no major effect on HYD release. The cumulative release for F4 is shown in Figure 5.13.

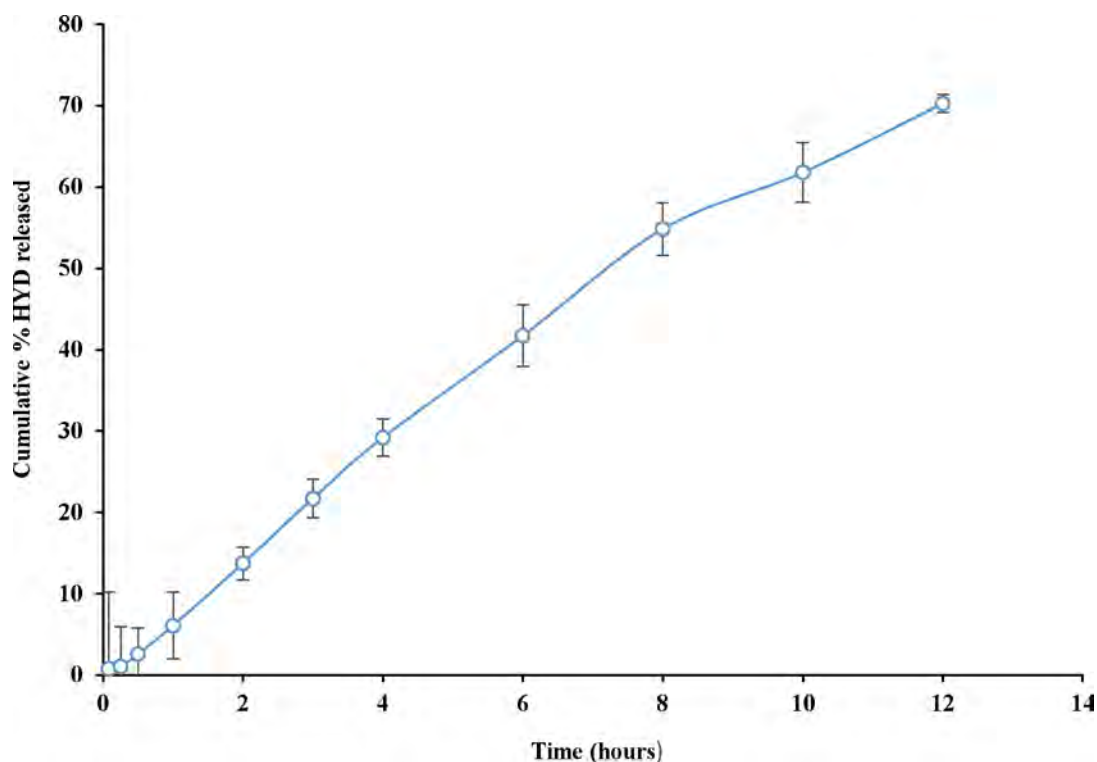


Figure 5.13 Cumulative % HYD released from formulation F4

5.6.6.6 Formulation F5

Formulation F5 (n=3) showed sustained release of HYD, with approximately 70% HYD released after 6 hours and approximately 96% after 12 hours. Formulation F5 and F2 had the same Methocel® K15M but different Eudragit®. The release of F2 and F5 were thus compared to assess the effect of Eudragit® polymers on HYD release. Eudragit® L 100 was selected as a water soluble polymer whilst Eudragit® RS PO was selected as a water insoluble, permeable polymer. The cumulative release for F5 is shown in Figure 5.14.

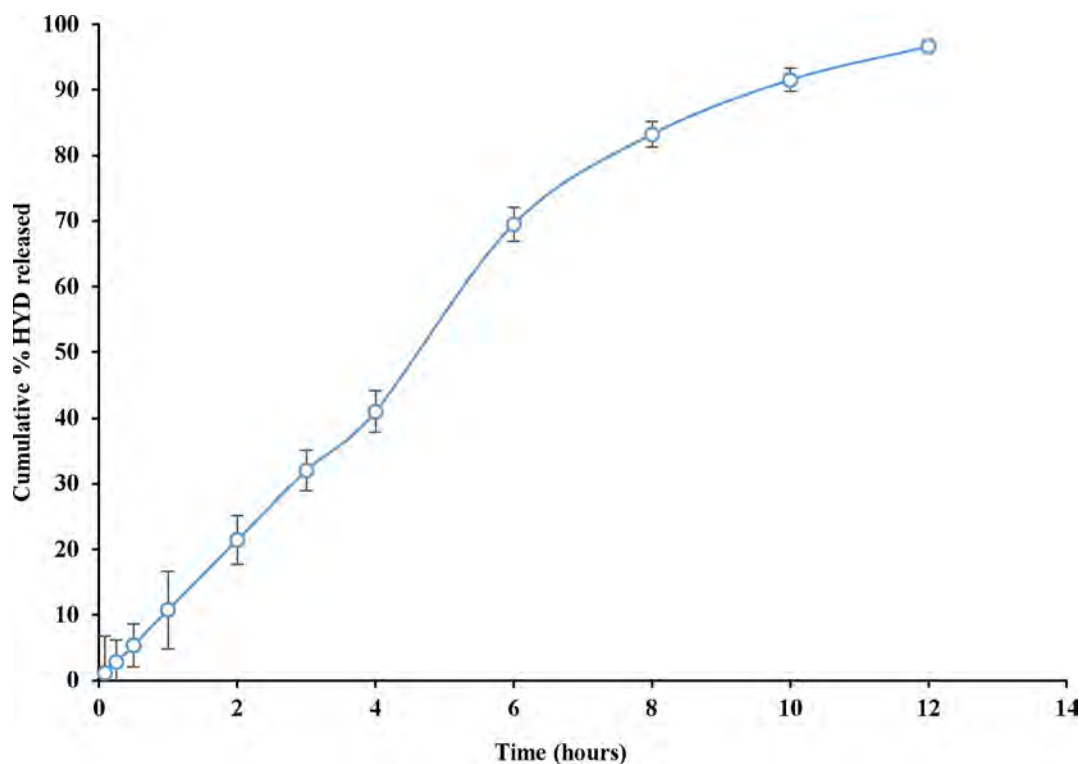


Figure 5.14 Cumulative % HYD released from formulation F5

5.6.6.7 Formulation F6

Formulation F6 (n=3) showed sustained release of HYD, with approximately 65% HYD released after 6 hours and approximately 88% after 12 hours. Formulation F3 and F6 contain the same Methocel[®] K100LV but different Eudragit[®] grades, so the release of F3 and F6 were compared to assess the effect of Eudragit[®] polymers on HYD release. The cumulative HYD release for F5 is shown in Figure 5.15.

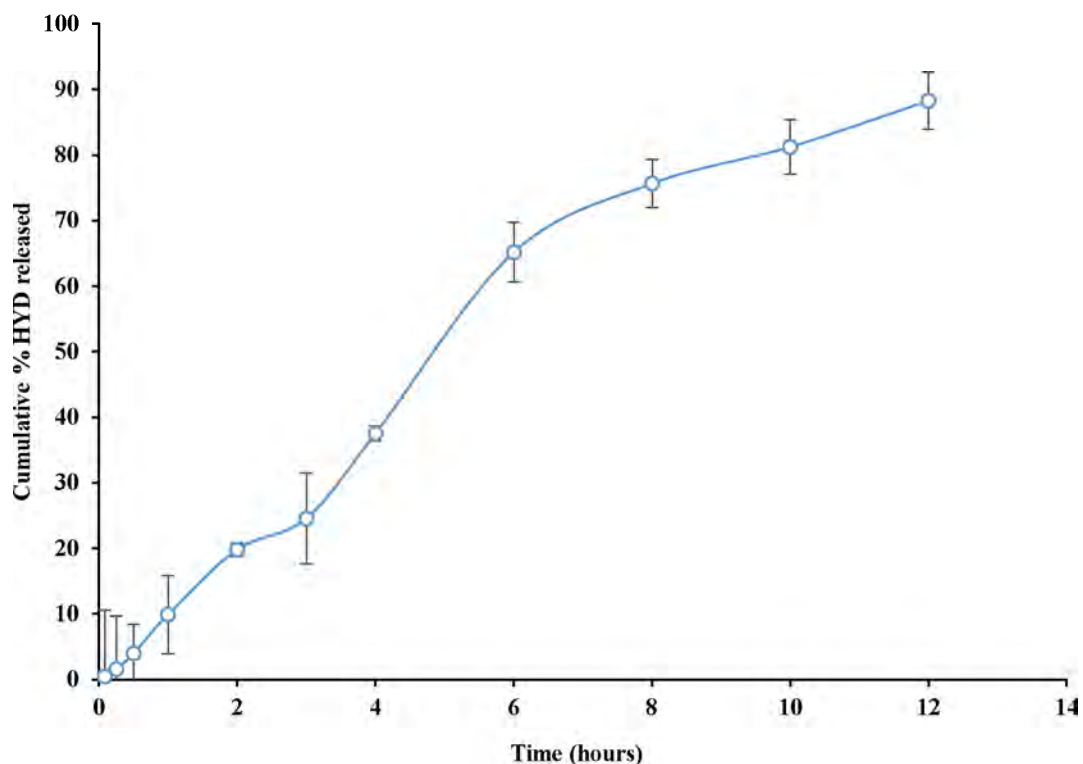


Figure 5.15 Cumulative % HYD released from formulation F6

In an attempt to comparatively evaluate the effect of polymers on release rates, dissolution profiles of formulation F1 to F6 were plotted on one graph. The graph shows that formulation F4 had the lowest cumulative release after 12 hours and that formulation F5 had the highest cumulative release after 12 hours. The dissolution profiles for formulation F1 to F6 are shown in Figure 5.16.

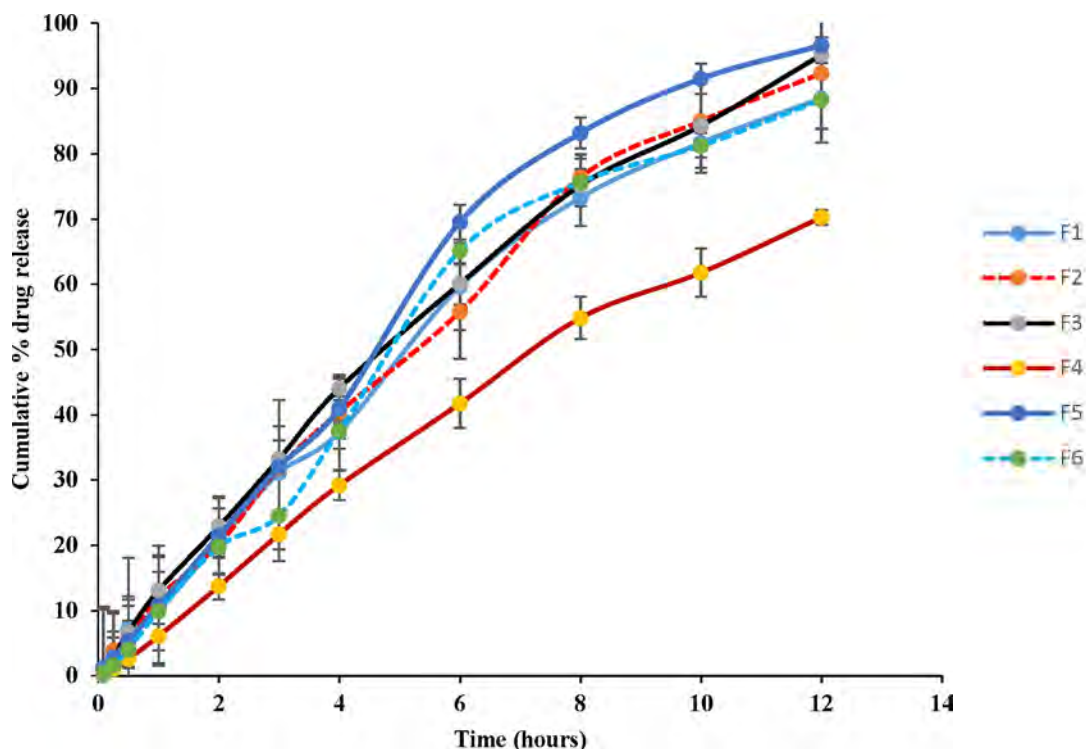


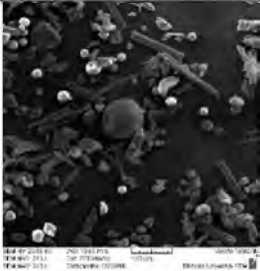
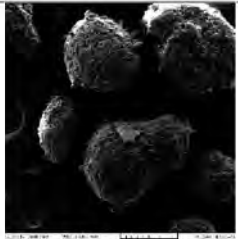

Figure 5.16 Cumulative % HYD released from formulations F1 to F6

The dissolution results were similar to previous reports on the effect of HPMC grades on release [281]. Formulations F1, F4 and F6 had incomplete HYD release, below the target of 90% after 12 hours and were not desirable as starting formulations for optimisation. Reports from previous work have reported that the type and level of polymers used mostly influence drug release [440–442]. Formulations manufactured using high grades of HPMC have been reported to produce thicker gel layers with more resistance to drug release and dissolution media penetration, showing slower drug release than those manufactured using lower viscosity grades of HPMC [443]. In an attempt to evaluate the effect of HPMC grades, formulations F1, F2 and F3 were compared using the same amount of the drug and polymers used. The release data from formulation F1 indicated that the use of high viscosity grade Methocel® K100M resulted in slow dissolution of HYD with incomplete drug release after 12 hours. Formulations F2, F3 and F5 showed the best HYD release, within the target of 90% after 12 hours. Formulation F3 was selected as the starting formulation for optimisation after evaluating EE, yield, assay and dissolution of both F2 and F3.

5.8 SCREENING FOR APPROPRIATE DILUENT

After obtaining the best polymers, a suitable diluent had to be found based on solubility in acetone and SEM. The shape and morphology of the microspheres were assessed and the diluent which produced smooth spherical microspheres was selected for further formulation optimisation studies. Diluents selected are indicated in Table 5.7.

Table 5.7 Diluent screening studies

| Diluent | Solubility in acetone | SEM, if applicable | comments |
|---------------------------|----------------------------------|--|--|
| Dibasic calcium phosphate | Practically insoluble in ether | | Not soluble in acetone. |
| Avicel® 101 | Practically insoluble in acetone |  | Presence of smooth and spherical microspheres obtained |
| Avicel® 102 | Practically insoluble in acetone |  | Rough and non-spherical microspheres obtained |
| Avicel® 103 | Practically insoluble in acetone |  | Rough non-spherical microspheres obtained |
| Lactose monohydrate | Practically insoluble in ether | — | Incompatible with HYD |
| Lactose anhydrous | Sparingly soluble in ether | — | Incompatible with HYD |

5.9 CONCLUSIONS

Hydrophilic matrix microspheres are among the most popular delivery systems for oral SR dosage forms through the GIT route [43,444]. This is largely because they offer precise modulation of drug release as a result of hydration of the constituent polymer(s), flexibility to obtain the desired drug release profiles, cost effectiveness, patient compliance and providing a constant, prolonged, and uniform therapeutic effect in blood levels [444].

To achieve the desired release rate, the relative rate of hydration of a polymer plays a critical role since the polymer selected must hydrate quickly enough to form a gel layer before the contents of the matrix tablet can dissolve. In addition, the higher the viscosity of the gel that is formed, the more resistant the gel is to dissolution and/or erosion [406,445]. The rate of polymer erosion is dependent on the viscosity of the HPMC grade being used in the formulation [392]. Tablets manufactured using high molecular weight and viscosity grade MC/HPMC show more resistance to polymer erosion than the low molecular weight and low viscosity grades [392].

All formulations were manufactured with an HPMC-based matrix and the effect of different viscosity grades of HPMC on performance was clearly investigated. On exposure to dissolution medium (0.1M Phosphate), HPMC hydrates, swells and forms a gel layer around the microspheres. The extent of swelling and release of HPMC differs with different viscosity. Different viscosity grades of HPMC polymer were used to evaluate their modulatory effect on drug release [102]. Formulations manufactured with high viscosity grades of HPMC exhibited lower cumulative percentage HYD release whilst formulations manufactured with low viscosity grades of HPMC exhibited higher cumulative percentage HYD release after 12 hours of dissolution testing.

Studies for appropriate diluent were investigated using SEM. From the above screening, it was observed that Avicel® 101 produced the most spherical and smooth microspheres, so it was selected for use during formulation optimisation studies.

Ideally, a successful microsphere system for drug delivery should be characterised by high yield, EE and drug loading capacity [446]. Formulation F3 showed the best microsphere size and shape as well as a higher EE (90%). A sustained release profile was observed with F3 with approximately 30% being released after 2 hours, 60% after 6 hours and 95% after 12 hours of

dissolution testing, therefore this formulation was selected for further formulation optimisation studies. For highly water soluble drugs like HYD, a stronger gel layer is required [102].

Eudragit® RS PO was selected over Eudragit® L 100 because of its low water permeability [447] and pH-independent drug release mechanism profiles, reducing the likelihood of HYD being released in bursts in acidic conditions [436]. Microspheres produced using Eudragit® RS PO were spherical and smooth compared to those produced using Eudragit® L 100. The combination of Eudragit® RS PO and Methocel® K100M have been reported to reduce water penetration and retard drug release [448] but Methocel® K100M was not selected for formulation optimisation as the release from formulation F1 showed less than 85% HYD being released after 12 hours. The formulation of sustained release formulations using Methocel® K100M, K15M, K4M and Eudragit® RS PO have been extensively studied [153,449–455]. The use of combinations of Methocel® K100LV and Eudragit® RS PO polymers for SR have not been extensively studied to date. Excipient type, solubility, permeability and concentration in the formulation have been reported to significantly affect drug release [102,456–458], therefore the effect of type of polymers was evaluated. The results showed that release of HYD from polymer microspheres can be sustained by manipulating the amount and type of polymers.

In summary, an o/o solvent evaporation technique was successfully used to manufacture HYD microspheres. Different formulation polymers were used to evaluate their effect on microsphere characterisation. The microspheres were characterised for their percentage yield, drug content, EE, particle size, surface morphology and drug release profile.

CHAPTER 6

FORMULATION OPTIMISATION, MATHEMATICAL MODELLING AND STABILITY TESTING OF HYDRALAZINE HYDROCHLORIDE MICROSPHERES

6.1 INTRODUCTION

Optimisation refers to improving the performance of a system, a process, or a product in order to obtain the maximum benefit from it and is performed using multivariate statistical techniques [156]. RSM is a collection of mathematical and statistical techniques based on the fit of a polynomial to the experimental data, which must describe the behaviour of a data set with the objective of making statistical provisions used in developing, improving and optimising processes [157,459–461]. RSM has been successfully applied to the development, modelling and optimisation of pharmaceutical products [151,462–467]. RSM trims down the number of experimental runs that are necessary to establish a mathematical trend in the experimental design region [463].

CCD is a response surface design which provides information on direct effects, pair-wise interactive effects and curvilinear variable effects and is widely used for formulation and process optimisation in the field of pharmaceuticals [151,154,463,468–470]. It also provides important applications in the design, development and formulation of new products, as well as in the improvement of existing product designs [459,460].

The objective of these studies was to use RSM to investigate the effects of formulation variables on the release of HYD from microspheres and to identify the combination of excipient levels required to produce predictable and optimal HYD release.

6.2 EXPERIMENTAL

A computer-aided optimisation technique using DoE was employed to investigate the effect of the amounts of various factors on the properties of HYD sustained release microspheres.

6.2.1 Aim

The main objective of these studies was to use RSM to optimise formulation and determine the drug release model which fits HYD release and formulation stability studies.

6.2.2 Materials

The materials used were described in §5.4.

6.2.3 Method

RSM in conjunction with CCD was used to optimise the formulation. Mathematical approaches and quadratic equations were used to evaluate the relationship between input and output variables. Formulations were manufactured on a laboratory scale and stored in sealed amber-coloured containers.

6.2.4 Experimental design

CCD was used to study the effects of formulation variables on EE, HYD content, yield and *in vitro* release of HYD and to optimise the microspheres. Methocel® K100LV, Eudragit® RS PO, homogenization speed, homogenization time and acetone amount were considered critical variables for the formulation optimisation. Thus the evaluation of the effect of one or combination of these critical variables was deemed necessary. Each factor was evaluated at five levels, viz. $-\alpha$, low (-1), centre (0), high (+1) and $+\alpha$. The upper and lower limits selected for the independent factors are shown in Table 6.1. Except for diluent amount which varies with the amount of polymers used, all the other formulation parameters were kept constant throughout the study. The EE (Y_1), cumulative release after 0.5 hours (Y_2), 2 hours (Y_3), 4 hours (Y_4), 6 hours (Y_5), 10 hours (Y_6), 12 hours (Y_7), yield (Y_8) and HYD content (Y_9) were selected as response variables to be studied.

Table 6.1 Translation of the coded levels used in CCD

| Independent factors | Levels of coded variables | | | | |
|--|---------------------------|----------------|------------|-----------------|------------|
| | - α | Low value (-1) | Centre (0) | High value (+1) | + α |
| Methocel [®] K100LV (X ₁) | 0.1g | 0.6g | 1g | 1.4g | 1.9g |
| Eudragit [®] RS PO (X ₂) | 0.1g | 0.6g | 1g | 1.4g | 1.9g |
| Homogenisation Speed (X ₃) | 124 rpm | 400 rpm | 600 rpm | 800 rpm | 1075 rpm |
| Homogenisation time (X ₄) | 4.6 hours | 6 hours | 7 hours | 8 hours | 9.4 hours |
| Acetone (X ₅) | 11.1 mL | 12,5 mL | 13.5 mL | 14.5 mL | 16.8 mL |

| Response Factors | Constraints |
|--|--------------------|
| EE (Y ₁) | Maximise (75-105%) |
| Cumulative release after 0.5 hours (Y ₂) | Minimise (0-15) |
| Cumulative release after 2 hours (Y ₃) | Minimise (0-20) |
| Cumulative release after 4 hours (Y ₄) | Minimise (10-30) |
| Cumulative release after 6 hours (Y ₅) | In range (40-65) |
| Cumulative release after 10 hours (Y ₆) | In range (60-80) |
| Cumulative release after 12 hours (Y ₇) | In range (85-105) |
| Yield (Y ₈) | Maximise (75-100) |
| Drug content (Y ₉) | Maximise (85-101) |

To avoid systemic error and bias, the generated CCD experimental runs were performed randomly using conditions listed in Table 6.2. ANOVA was used to analyse the data and to calculate the significance and relevance of the critical factors for each model.

Table 6.2 Actual experimental conditions for the CCD

| Formulation | STD | RUN | K100LV | RS PO | SPEED | TIME | ACETONE | Design Point Type |
|--------------------|------------|------------|---------------|--------------|--------------|-------------|----------------|--------------------------|
| CCD 001 | 29 | 1 | 0.6 | 0.6 | 800 | 8 | 14.5 | Factorial |
| CCD 002 | 42 | 2 | 1 | 1 | 600 | 7 | 16.8 | Factorial |
| CCD 003 | 50 | 3 | 1 | 1 | 600 | 7 | 13.5 | Centre |
| CCD 004 | 9 | 4 | 0.6 | 0.6 | 400 | 8 | 12.5 | Factorial |
| CCD 005 | 2 | 5 | 1.4 | 0.6 | 400 | 6 | 12.5 | Factorial |
| CCD 006 | 7 | 6 | 0.6 | 1.4 | 800 | 6 | 12.5 | Factorial |
| CCD 007 | 19 | 7 | 0.6 | 1.4 | 400 | 6 | 14.5 | Factorial |
| CCD 008 | 32 | 8 | 1.4 | 1.4 | 800 | 8 | 14.5 | Factorial |
| CCD 009 | 27 | 9 | 0.6 | 1.4 | 400 | 8 | 14.5 | Factorial |
| CCD 010 | 34 | 10 | 1.9 | 1 | 600 | 7 | 13.5 | Factorial |
| CCD 011 | 44 | 11 | 1 | 1 | 600 | 7 | 13.5 | Centre |
| CCD 012 | 17 | 12 | 0.6 | 0.6 | 400 | 6 | 14.5 | Factorial |
| CCD 013 | 39 | 13 | 1 | 1 | 600 | 4.6 | 13.5 | Factorial |
| CCD 014 | 3 | 14 | 0.6 | 1.4 | 400 | 6 | 12.5 | Factorial |
| CCD 015 | 5 | 15 | 0.6 | 0.6 | 800 | 6 | 12.5 | Factorial |
| CCD 016 | 47 | 16 | 1 | 1 | 600 | 7 | 13.5 | Centre |
| CCD 017 | 41 | 17 | 1 | 1 | 600 | 7 | 11.1 | Factorial |
| CCD 018 | 25 | 18 | 0.6 | 0.6 | 400 | 8 | 14.5 | Factorial |
| CCD 019 | 23 | 19 | 0.6 | 1.4 | 800 | 6 | 14.5 | Factorial |
| CCD 020 | 24 | 20 | 1.4 | 1.4 | 800 | 6 | 14.5 | Factorial |
| CCD 021 | 38 | 21 | 1 | 1 | 1075 | 7 | 13.5 | Factorial |
| CCD 022 | 49 | 22 | 1 | 1 | 600 | 7 | 13.5 | centre |
| CCD 023 | 40 | 23 | 1 | 1 | 600 | 9.4 | 13.5 | Factorial |
| CCD 024 | 46 | 24 | 1 | 1 | 600 | 7 | 13.5 | Centre |
| CCD 025 | 11 | 25 | 0.6 | 1.4 | 400 | 8 | 12.5 | Factorial |

Table 6.2 continued.....

| Formulation | STD | RUN | K100LV | RS PO | SPEED | TIME | ACETONE | Design Point Type |
|-------------|-----|-----|--------|-------|-------|------|---------|-------------------|
| CCD 026 | 35 | 26 | 1 | 0.1 | 600 | 7 | 13.5 | Factorial |
| CCD 027 | 48 | 27 | 1 | 1 | 600 | 7 | 13.5 | Centre |
| CCD 028 | 10 | 28 | 1.4 | 0.6 | 400 | 8 | 12.5 | Factorial |
| CCD 029 | 30 | 29 | 1.4 | 0.6 | 800 | 8 | 14.5 | Factorial |
| CCD 030 | 21 | 30 | 0.6 | 0.6 | 800 | 6 | 14.5 | Factorial |
| CCD 031 | 22 | 31 | 1.4 | 0.6 | 800 | 6 | 14.5 | Factorial |
| CCD 032 | 14 | 32 | 1.4 | 0.6 | 800 | 8 | 12.5 | Factorial |
| CCD 033 | 15 | 33 | 0.6 | 1.4 | 800 | 8 | 12.5 | Axial |
| CCD 034 | 26 | 34 | 1.4 | 0.6 | 400 | 8 | 14.5 | Axial |
| CCD 035 | 18 | 35 | 1.4 | 0.6 | 400 | 6 | 14.5 | Axial |
| CCD 036 | 12 | 36 | 1.4 | 1.4 | 400 | 8 | 12.5 | Axial |
| CCD 037 | 16 | 37 | 1.4 | 1.4 | 800 | 8 | 12.5 | Axial |
| CCD 038 | 8 | 38 | 1.4 | 1.4 | 800 | 6 | 12.5 | Axial |
| CCD 039 | 31 | 39 | 0.6 | 1.4 | 800 | 8 | 14.5 | Axial |
| CCD 040 | 4 | 40 | 1.4 | 1.4 | 400 | 6 | 12.5 | Axial |
| CCD 041 | 36 | 41 | 1 | 1.9 | 600 | 7 | 13.5 | Axial |
| CCD 042 | 45 | 42 | 1 | 1 | 600 | 7 | 13.5 | centre |
| CCD 043 | 13 | 43 | 0.6 | 0.6 | 800 | 8 | 12.5 | Factorial |
| CCD 044 | 28 | 44 | 1.4 | 1.4 | 400 | 8 | 14.5 | Factorial |
| CCD 045 | 37 | 45 | 1 | 1 | 124 | 7 | 13.5 | Axial |
| CCD 046 | 33 | 46 | 0.1 | 1 | 600 | 7 | 13.5 | Axial |
| CCD 047 | 20 | 47 | 1.4 | 1.4 | 400 | 6 | 14.5 | Axial |
| CCD 048 | 1 | 48 | 0.6 | 0.6 | 400 | 6 | 12.5 | Axial |
| CCD 049 | 6 | 49 | 1.4 | 0.6 | 800 | 6 | 12.5 | Axial |
| CCD 050 | 43 | 50 | 1 | 1 | 600 | 7 | 13.5 | Centre |

6.2.5 Manufacture of HYD microspheres

All batches were manufactured using the solvent evaporation method described in §5.5.3 and sufficient diluent, *viz.* Avicel® 101 was added to ensure that all batches had a total weight of 3.5g for comparative purposes.

6.2.6 Evaluation of HYD sustained release

All formulations were subjected to compendial and non-compendial testing previously described in §5.6. *In vitro* release studies on all CCD formulations were performed using modified USP Apparatus 1 and the method described in §5.6.6.

6.2.7 Stability testing

The manufactured optimised microspheres were subjected to short-term stability testing for 1 month. They were stored in amber-coloured polyethylene bottles and placed in a refrigerator maintained at 4 °C and Model KBF-240 Binder® climatic chambers (Binder GmbH® Ltd, München, Germany) maintained at 25°C/60% RH and 40°C/75% RH. The microspheres were assessed based on HYD content, EE and HYD release as well as visual inspection for changes in colour.

6.3 MATHEMATICAL MODELLING OF HYD RELEASE

Several drug release models of surface-eroding and bulk-eroding degradable systems have been reported in the literature [471–475]. In general, it is easier to model drug release from surface-eroding systems because the drug is released concurrently with the layer-by-layer erosion from the outermost surface of the matrix [471]. There are a number of kinetic models which describe the overall release of the drug from the dosage forms [476]. However, in these studies, zero-order, first-order, Higuchi, Hixson-Crowell and Korsmeyer-Peppas models are described.

6.3.1 Overview

Mathematical modelling of drug release data derived from sustained release delivery systems generates important information on mass transport mechanisms and the effects of device design parameters on the kinetics of API release from those systems [477]. The choice of an appropriate model is dependent on the API, excipients and composition of the delivery system. Mathematical modelling can be used to predict and/or design a dissolution profile based on an

understanding of the release kinetics of the API that are desired [478] and this approach was used for these studies [477,478]. HYD is highly soluble in aqueous media [37] and HYD release from a hydrophilic matrix would most likely be predominantly governed by a combination of diffusion, swelling and erosion of the polymeric matrix [478].

6.3.2 Zero-order model

Zero-order release kinetics refers to the process of constant drug release from a drug delivery device such as oral osmotic tablets, transdermal systems, matrix tablets with drugs of low solubility and other delivery systems [103,477,479,480]. Furthermore, the model describes drug dissolution from pharmaceutical dosage forms that do not disaggregate and release drugs slowly [476,478] and is desirable in order to minimise swings in drug concentration in the blood [337]. The model is applicable when the dosage releases the same amount of API per unit time [477,478,480]. In its simplest form, zero-order release can be represented by Equation 6.1 and can be achieved by surrounding a core tablet with a membrane that is permeable to both drug and water [337].

$$W_0 - W_t = kt \quad \text{Equation 6.1 [478]}$$

Where,

W_0 - Initial amount of drug in dosage form

W_t - Amount of drug in dosage form at time t

K - Proportionality constant/ zero-order release constant

t - Time

6.3.3 First-order model

First-order release mechanisms take place at a constant proportion of the drug concentration available at that time. This model has been used to describe absorption and/or elimination of some drugs [476,478,480].

The release of hydrophilic molecules from porous matrices usually follows a first-order release mechanism. The release of an API from these matrices is proportional to the amount of API remaining in the device and API release diminishes over time [478]. To investigate the release kinetic, experimental *in vitro* log cumulative percentage of drug remaining plotted versus time will result in a straight line [478,480]. The dissolution phenomenon of a solid particle in a liquid media implies a surface action, as can be seen by the Noyes–Whitney Equation 6.2.

$$\ln Q_t = \ln Q_0 + K_1 t \quad \text{Equation 6.2 [478]}$$

Where,

Q_t - Amount of drug released at time t

Q_0 - Initial amount of drug in the solution

K_1 - First-order release constant.

t - Time

6.3.4 Higuchi model

In 1961 and 1963, Higuchi developed several theoretical models to study the release of water soluble and low soluble drugs incorporated in semi-solid and/or solid matrixes [478,480]. The Higuchi model is one of the most successful theories at predicting drug release from a non-degradable monolithic system whereby drug particles are dispersed uniformly throughout the matrix [471]. A simplified Higuchi model can be expressed by Equation 6.3.

$$Q = \sqrt{D(2C - C_s)C_s t} \quad \text{Equation 6.3 [478]}$$

Where,

Q - Amount of drug released in time t per unit area

C - Drug initial concentration

C_s - Drug solubility in the matrix media

D - Diffusivity of the drug molecules (diffusion constant) in the matrix

t - Time

This model can be used to describe drug dissolution from several types of modified release dosage forms, transdermal systems and matrix tablets with water soluble drugs [476]. The experimental *in vitro* release of an API from a dosage form is said to follow the Higuchi model when a linear relationship is generated by plotting the cumulative % API released versus the square root of time [480].

6.3.5 Hixson-Crowell model

In 1931, Hixson and Crowell recognised that the particle regular area is proportional to the cubic root of its volume [476,478] and derived Equation 6.4 [478].

$$W_0^{\frac{1}{3}} - W_t^{\frac{1}{3}} = K_s t \quad \text{Equation 6.4 [478]}$$

Where,

W_0 - Initial amount of drug in the pharmaceutical dosage form

W_t - Remaining amount of drug in the pharmaceutical dosage form at time t

K_s (κ) - A constant incorporating the surface–volume relation.

t - Time

This model applies to pharmaceutical dosage forms such as tablets, where the dissolution of the API occurs in planes that are parallel to the surface of the tablet and dimensions of the tablet diminish proportionally over time [476,478]. The Hixson-Crowell Cube Root Law model describes API release from delivery systems in which there is a change over time of surface area and diameter of the dosage form [480].

6.3.6 Korsmeyer-Peppas model

Korsmeyer *et al.* [478] developed a simple, semi-empirical model, relating exponentially the drug release to the elapsed time (t) [478], as shown in Equation 6.5.

$$\frac{Q_t}{Q_\infty} = kt^n \quad \text{Equation 6.5 [477]}$$

Where,

Q_t - Absolute cumulative amount of drug released at time t

Q_∞ - Absolute cumulative amount of drug released at infinity time

k - Constant incorporating structural and geometric characteristic of the device

t - Time

n -Release exponent

The Korsmeyer-Peppas model is also called the power law [477]. If $n = 1$ then the release of API is best described by a zero-order kinetic process and is independent of time and this is an indication that API release is swelling controlled [477,478]. A value for $n = 0.5$ is an indication that API release is a diffusion controlled process. When n falls between 0.5 and 1.0, API release is considered to occur by anomalous (Non-Fickian) transport, where both diffusion and swelling transport mechanisms occur simultaneously [477,478]. Zero-order API release from thin polymeric films has also been described as Case-II transport in which the relaxation of macromolecules occurs on water uptake into a delivery system and this becomes the rate limiting step in API release [477]. The value of n varies according to the geometry of the delivery technology investigated and specific conditions have been derived for slabs, spheres and cylinders and are listed in Table 6.3.

Table 6.3 Interpretation of diffusional release mechanisms from polymeric films(adapted from [476–478])

| Release exponent (<i>n</i>) | | | Drug transport mechanism | Rate as a function of time |
|-------------------------------|-------------------|-------------------|--------------------------|----------------------------|
| Thin films | Cylinder | Sphere | | |
| 0.5 | 0.45 | 0.43 | Fickian diffusion | $t^{-0.5}$ |
| $0.5 < n < 1.0$ | $0.45 < n < 0.89$ | $0.43 < n < 0.85$ | Anomalous transport | t^{n-1} |
| 1.0 | 0.89 | 0.85 | Case II transport | Zero-order release |
| > 1.0 | > 0.89 | > 0.85 | Super case II transport | t^{n-1} |

6.3.7 Approaches for selecting the best-fit mathematical model

The first step in the model-dependent approach is to identify a mathematical model that accurately describes the dissolution profile [476,481]. Several approaches can be used to identify the mathematical model that best describes drug release [482]. One approach in determining the goodness of fit involves comparing the R^2 values obtained when the dissolution data are fitted to different mathematical models. The model that yields the highest R^2 value is regarded as the best fit model [478]. Besides the R^2 method, the correlation coefficient (R), the sum of squares of residues (SSR), the mean square error (MSE), the Akaike Information Criterion (AIC) and the F-ratio probability can also be used to test the applicability of the release models [478,481]. The model that described the release of HYD from microspheres was established by selecting the model that generated the highest R^2 value.

6.4 RESULTS AND DISCUSSION

6.4.1 Central composite design

Design Expert® (Version 7.01, Stat-Ease Inc., Minneapolis, MN, USA) statistical software was used to generate mathematical models that best described the relationship between independent and dependent variables. The individual effects of independent variables on responses were denoted by $X_1, X_2, X_3, \dots, X_n$, whereas the interactive effects were denoted by $X_1X_2, X_2X_3, \dots, X_nX_m$. The negative coefficient of the independent variable indicates an antagonistic effect on response and vice versa for the positive coefficient. The mathematical equations generated for all responses in terms of coded factors are shown in Equations 6.6a -6.6i.

$$Y_1 = 77.04 - 1.23X_1 + 7.63X_2 - 2.20X_3 - 2.52X_4 + 3.57X_5 - 3.95X_1X_2 + 4.42X_1X_3 + 2.84X_1X_4 + 0.60X_1X_5 + 2.44X_2X_3 + 2.23X_2X_4 + 3.12X_2X_5 - 0.95X_3X_4 - 1.96X_3X_5 - 0.097X_4X_5$$

Equation 6.6a

$$Y_2 = 1.96 - 0.45X_1 + 0.51X_2 - 0.028X_3 - 4.838E - 004X_4 + 0.11X_5$$

Equation 6.6b

$$Y_3 = 2.81 - 0.40X_1 + 0.36X_2 - 0.015X_3 - 0.043X_4 - 0.015X_5 + 0.15X_1X_2 + 0.092X_1X_3 + 0.028X_1X_4 - 0.066X_1X_5 - 0.23X_2X_3 - 0.023X_2X_4 + 0.025X_2X_5 + 0.20X_3X_4 + 0.19X_3X_5 + 0.15X_4X_5$$

Equation 6.6c

$$Y_4 = 5.77 - 0.51X_1 + 0.25X_2 + 0.13X_3 + 2.065E - 003X_4 + 0.051X_5$$

Equation 6.6d

$$Y_5 = 0.15 + 8.189E - 003X_1 - 3.063E - 003X_2 - 4.269E - 003X_3 - 2.280E - 003X_4 - 4.188E - 004X_5 - 6.195E - 003X_1X_2 - 3.137E - 003X_1X_3 + 4.288E - 003X_1X_4 + 6.338E - 003X_1X_5 + 6.995E - 003X_2X_3 - 4.126E - 003X_2X_4 - 6.625E - 003X_2X_5 - 2.722E - 003X_3X_4 - 2.687E - 003X_3X_5 - 2.741E - 003X_4X_5$$

Equation 6.6e

$$Y_6 = 57.44 - 3.38X_1 - 1.19X_2 + 2.51X_3 + 0.93X_4 - 0.34X_5 + 4.39X_1X_2 - 0.58X_1X_3 - 2.79X_1X_4 - 2.06X_1X_5 - 3.24X_2X_3 + 2.18X_2X_4 + 4.21X_2X_5 + 0.76X_3X_4 + 0.88X_3X_5 + 0.27X_4X_5 - 0.54X_1^2 + 0.78X_2^2 + 0.51X_3^2 - 2.78X_4^2 + 4.67X_5^2$$

Equation 6.6f

$$Y_7 = 63.52 - 4.75X_1 - 2.58X_2 + 3.23X_3 + 0.014X_4 - 0.23X_5 + 7.44X_1X_2 + 1.04X_1X_3 - 2.28X_1X_4 - 2.17X_1X_5 - 3.16X_2X_3 + 4.21X_2X_4 + 2.81X_2X_5 + 1.70X_3X_4 - 2.79X_3X_5 + 1.32X_4X_5 - 0.47X_1^2 + 0.48X_2^2 + 0.42X_3^2 - 2.92X_4^2 + 5.61X_5^2$$

Equation 6.6g

$$Y_8 = 94.93 + 1.41X_1 + 2.96X_2 - 0.84X_3 + 0.33X_4 + 0.22X_5 - 1.20X_1X_2 + 0.49X_1X_3 - 0.43X_1X_4 + 0.27X_1X_5 + 1.63X_2X_3 - 0.92X_2X_4 + 0.61X_2X_5 - 0.084X_3X_4 - 1.57X_3X_5 - 0.37X_4X_5 + 0.83X_1^2 - 1.75X_2^2 + 0.93X_3^2 + 0.37X_4^2 - 0.18X_5^2$$

Equation 6.6h

$$Y_9 = 74.59 - 1.57X_1 + 1.77X_2 + 0.091X_3 - 1.62X_4 + 1.31X_5 - 0.30X_1X_2 + 0.41X_1X_3 + 1.69X_1X_4 - 1.06X_1X_5 + 1.20X_2X_3 + 1.11X_2X_4 + 0.66X_2X_5 - 0.28X_3X_4 + 2.19X_3X_5 + 1.41X_4X_5 + 1.21X_1^2 - 0.88X_2^2 - 0.18X_3^2 + 0.82X_4^2 - 1.05X_5^2$$

Equation 6.6i

6.4.2 Model fitting

The models that fit the respective responses were assessed and are summarised in Table 6.4. The significant factors of each response were also summarised. Most of the responses were found to be affected by X_1 and X_2 . This is due to the polymeric excipients' impact on EE, drug release and yield. Y_8 was found to be affected by X_1 , X_2 , X_3 and X_5 . The concentration of the polymers significantly impacted on the yield whilst the homogenization speed impacted to a much less extent. It was observed that increasing homogenization speed resulted in the displacement of the microparticles from the emulsion due to the increase in kinetic energy of the particles and hence this affected the yield. Lower mixing speeds have been reported to be associated with lower mixing energy which would be insufficient for formation of microspheres [483].

Table 6.4 Summary of best fit models and significant factors

| Response | Fitting model | Significant factors |
|----------|---------------|---|
| Y_1 | 2FI | Methocel® K100LV (X_1), Eudragit® RS PO (X_2) and homogenization speed (X_3) |
| Y_2 | Linear | Methocel® K100LV (X_1) and Eudragit® RS PO (X_2) |
| Y_3 | 2FI | Methocel® K100LV (X_1) and Eudragit® RS PO (X_2) |
| Y_4 | Linear | Methocel® K100LV (X_1) |
| Y_5 | 2FI | Methocel® K100LV (X_1) |
| Y_6 | Quadratic | None |
| Y_7 | Quadratic | Methocel® K100LV (X_1) and Eudragit® RS PO (X_2) |
| Y_8 | Quadratic | Methocel® K100LV (X_1), Eudragit® RS PO (X_2), homogenization speed (X_3) and amount of acetone (X_5) |
| Y_9 | Quadratic | None |

6.4.2 Evaluation of the model for response Y_1 and Y_7

The mean least squares linear regression method was used to establish the mathematical model that best described the data for each response. All responses were evaluated using ANOVA, mean least square linear regression and fitness although, for simplicity reasons, only models for EE and HYD release after 12 hours are summarised. The other responses, models, and statistical analysis for response Y_2 - Y_6 , Y_8 and Y_9 are available on request. The experimental data were fitted to linear, 2FI and quadratic polynomials for all dependent variables. The best polynomials were suggested using the DoE software. A summary of the statistical parameters used for the selection criteria for response Y_1 and Y_7 are shown in Table 6.5.

Table 6.5 Summary of the model selection criteria for response Y_1 and Y_7

| Y ₁ | | | | | | | Y ₇ | | | | | | |
|------------------------------------|----------|----------------|-------------------------|--------------------------|---------------------|-----------|--------------------|----------|----------------|-------------------------|--------------------------|---------------------|-----------|
| Sequential model of sum of squares | | | | | | | | | | | | | |
| Source | SS | Df | MS | F-value | p-value Prob > F | Remarks | Source | SS | Df | MS | F-value | p-value Prob > F | Remarks |
| Mean vs Total | 2.967E+5 | 1 | 2.967E+5 | | | | Mean vs Total | 2.193E+5 | 1 | 2.193E+5 | | | Suggested |
| Linear vs Mean | 3623.41 | 5 | 724.68 | 6.62 | 0.0001 | | Linear vs Mean | 1718.12 | 5 | 343.62 | 1.11 | 0.3682 | |
| 2FI vs Linear | 2207.19 | 10 | 220.72 | 2.88 | 0.0103 | Suggested | 2FI vs Linear | 3658.14 | 10 | 365.81 | 1.25 | 0.2962 | |
| Quadratic vs 2FI | 182.50 | 5 | 36.50 | 0.44 | 0.8192 | | Quadratic vs 2FI | 2546.95 | 5 | 509.39 | 2.00 | 0.1089 | Suggested |
| Cubic vs Quadratic | 1146.92 | 15 | 76.46 | 0.84 | 0.6316 | Aliased | Cubic vs Quadratic | 4315.03 | 15 | 287.67 | 1.31 | 0.3116 | Aliased |
| Residual | 1276.96 | 14 | 91.21 | | | | Residual | 3084.20 | 14 | 220.30 | | | |
| Total | 3.052E+5 | 50 | 6103.59 | | | | Total | 2.347E+5 | 50 | 4693.13 | | | |
| Lack of fit tests | | | | | | | | | | | | | |
| Source | SS | df | MS | F-value | p-value Prob > F | Remarks | Source | SS | Df | MS | F-value | p-value Prob > F | Remarks |
| Linear | 4118.74 | 37 | 111.32 | 1.12 | 0.4771 | | Linear | 13363.49 | 37 | 361.18 | 10.50 | 0.0017 | |
| 2FI | 1911.56 | 27 | 70.80 | 0.71 | 0.7549 | Suggested | 2FI | 9705.35 | 27 | 359.46 | 10.45 | 0.0018 | |
| Quadratic | 1729.06 | 22 | 78.59 | 0.79 | 0.6869 | | Quadratic | 7158.40 | 22 | 325.38 | 9.46 | 0.0026 | Suggested |
| Cubic | 582.15 | 7 | 83.16 | 0.84 | 0.5893 | Aliased | Cubic | 2843.37 | 7 | 406.20 | 11.81 | 0.0021 | Aliased |
| Pure Error | 694.82 | 7 | 99.26 | | | | Pure Error | 240.84 | 7 | 34.41 | | | |
| Model summary statistics | | | | | | | | | | | | | |
| Source | SD | R ² | Adjusted R ² | Predicted R ² | PRESS | Remarks | Source | SD | R ² | Adjusted R ² | Predicted R ² | PRESS | Remarks |
| Linear | 10.46 | 0.4295 | 0.3646 | 0.2580 | 6260.59 | | Linear | 17.58 | 0.1121 | 0.0112 | -0.1971 | 18342.31 | |
| 2FI | 8.76 | 0.6911 | 0.5548 | 0.2994 | 5911.32 | Suggested | 2FI | 17.10 | 0.3509 | 0.0645 | -0.5032 | 23033.13 | |
| Quadratic | 9.14 | 0.7127 | 0.5146 | 0.1292 | 7346.86 | | Quadratic | 15.97 | 0.5171 | 0.1841 | -0.8363 | 28136.33 | Suggested |
| Cubic | 9.55 | 0.8486 | 0.4703 | -2.4250 | 28896.48 | Aliased | Cubic | 14.84 | 0.7987 | 0.2955 | -4.0837 | 77894.28 | Aliased |

SS-Sum of squares, MS-Mean square, df- degrees of freedom, SD- standard deviation

Analysis of the model for responses Y_1 and Y_7 were performed using the F -value and p -value. The p -values for Y_1 and Y_7 were found to be < 0.0001 and 0.1368 respectively. The selected model for Y_1 was significant and that of Y_7 not significant. However, some factors were found to be significant, viz. X_1X_2 and X_5^2 with p -values of 0.0134 and 0.0138 respectively, which were < 0.05 . Individual linear contribution of X_1 was significant for response Y_7 indicated by a p -value < 0.05 . The other individual linear contributions, cross-contributions and quadratic contributions of independent factors with p -values > 0.05 did not have significant effect(s) on response Y_7 . Table 6.6 summarises the ANOVA for Y_1 and Y_7 . The model for response Y_7 was also not significant because of the variations in R^2 , predicted R^2 and adjusted R^2 as shown in Table 6.6.

Independent factors including individual linear contributions of X_2 , X_3 and cross-contribution of X_1X_2 , X_1X_3 and X_2X_5 were found to have a significant effect on response Y_1 whereas other independent factors with p -values > 0.05 did not have a significant effect(s) on response Y_1 .

For response Y_1 , the predicted R^2 of 0.2994 is not as close to the adjusted R^2 of 0.5548 as one might normally expect. This may indicate a large block effect or a possible problem with the model and/or data. Things to consider are model reduction, response transformation and reduction of outliers. Adequate precision measures the signal to noise ratio. A ratio greater than 4 is desirable for adequate precision. A value of 11.604 indicates an adequate signal, therefore this model can be used to navigate the design space.

For response Y_7 , a negative predicted R^2 implies that the overall mean is a better predictor of the response than the current model. A value of 5.404 for adequate precision indicates an adequate signal, thus this model can be used to navigate the design space.

Table 6.6 ANOVA for the 2FI and Quadratic models for Y_1 and Y_7 respectively

| Y ₁ | | | | | | | Y ₇ | | | | | | |
|-------------------------------|----------------|----|-------------|----------|---------------------|-----------------|-------------------------------|----------------|----|-------------|----------|---------------------|-----------------|
| Source | Sum of squares | df | Mean square | F-value | p-value Prop > F | Remarks | Source | Sum of squares | df | Mean square | F-value | p-value Prop > F | Remarks |
| Model (2FI) | 5830.60 | 15 | 388.71 | 5.07 | < 0.0001 | Significant | Model (Quadratic) | 7923.21 | 20 | 396.16 | 1.55 | 0.1368 | not significant |
| X ₁ | 65.88 | 1 | 65.88 | 0.86 | 0.3604 | Not significant | X ₁ | 975.89 | 1 | 975.89 | 3.82 | 0.0402 | Significant |
| X ₂ | 2521.12 | 1 | 2521.12 | 32.89 | < 0.0001 | Significant | X ₂ | 288.09 | 1 | 288.09 | 1.13 | 0.2967 | Not significant |
| X ₃ | 210.18 | 1 | 210.18 | 2.74 | 0.1070 | Not significant | X ₃ | 451.81 | 1 | 451.81 | 1.77 | 0.1937 | Not significant |
| X ₄ | 274.31 | 1 | 274.31 | 3.58 | 0.0671 | Not significant | X ₄ | 8.033E-3 | 1 | 8.033E-3 | 3.148E-5 | 0.9956 | Not significant |
| X ₅ | 551.92 | 1 | 551.92 | 7.20 | 0.0112 | Significant | X ₅ | 2.32 | 1 | 2.32 | 9.078E-3 | 0.9247 | Not significant |
| X ₁ X ₂ | 500.07 | 1 | 500.07 | 6.52 | 0.0153 | Significant | X ₁ X ₂ | 1770.12 | 1 | 1770.12 | 6.94 | 0.0134 | significant |
| X ₁ X ₃ | 623.93 | 1 | 623.93 | 8.14 | 0.0073 | Significant | X ₁ X ₃ | 34.45 | 1 | 34.45 | 0.14 | 0.7160 | Not significant |
| X ₁ X ₄ | 258.21 | 1 | 258.21 | 3.37 | 0.0752 | Not significant | X ₁ X ₄ | 166.53 | 1 | 166.53 | 0.65 | 0.4257 | Not significant |
| X ₁ X ₅ | 11.40 | 1 | 11.40 | 0.15 | 0.7022 | Not significant | X ₁ X ₅ | 150.51 | 1 | 150.51 | 0.59 | 0.4487 | Not significant |
| X ₂ X ₃ | 190.61 | 1 | 190.61 | 2.49 | 0.1241 | Not significant | X ₂ X ₃ | 318.78 | 1 | 318.78 | 1.25 | 0.2728 | Not significant |
| X ₂ X ₄ | 158.87 | 1 | 158.87 | 2.07 | 0.1591 | Not significant | X ₂ X ₄ | 567.85 | 1 | 567.85 | 2.23 | 0.1465 | Not significant |
| X ₂ X ₅ | 311.88 | 1 | 311.88 | 4.07 | 0.0416 | Significant | X ₂ X ₅ | 253.12 | 1 | 253.12 | 0.99 | 0.3275 | Not significant |
| X ₃ X ₄ | 29.07 | 1 | 29.07 | 0.38 | 0.5421 | Not significant | X ₃ X ₄ | 92.48 | 1 | 92.48 | 0.36 | 0.5518 | Not significant |
| X ₃ X ₅ | 122.85 | 1 | 122.85 | 1.60 | 0.2141 | Not significant | X ₃ X ₅ | 248.64 | 1 | 248.64 | 0.97 | 0.3317 | Not significant |
| X ₄ X ₅ | 0.30 | 1 | 0.30 | 3.918E-3 | 0.9505 | Not significant | X ₄ X ₅ | 55.65 | 1 | 55.65 | 0.22 | 0.6440 | Not significant |
| | | | | | | | X ₁ ² | 12.10 | 1 | 12.10 | 0.047 | 0.8291 | Not significant |
| | | | | | | | X ₂ ² | 12.75 | 1 | 12.75 | 0.050 | 0.8246 | Not significant |
| | | | | | | | X ₃ ² | 9.67 | 1 | 9.67 | 0.038 | 0.8470 | Not significant |
| | | | | | | | X ₄ ² | 472.19 | 1 | 472.19 | 1.85 | 0.1842 | Not significant |
| | | | | | | | X ₅ ² | 1751.65 | 1 | 1751.65 | 6.87 | 0.0138 | Significant |
| Residual | 2606.38 | 34 | 76.66 | | | | Residual | 7399.24 | 29 | 255.15 | | | |
| Lack of Fit | 1911.56 | 27 | 70.80 | 0.71 | 0.7549 | not significant | Lack of Fit | 7158.40 | 22 | 325.38 | 9.46 | 0.0026 | Significant |
| Pure Error | 694.82 | 7 | 99.26 | | | | Pure Error | 240.84 | 7 | 34.41 | | | |
| Cor Total | 8436.98 | 49 | | | | | Cor Total | 15322.45 | 49 | | | | |

X₁- Methocel[®] K 100LV, X₂- Eudragit[®] RS PO, X₃- Homogenisation speed, X₄- homogenization time, X₅-amount of acetone. The missing values indicate that the parameters were not defined. Significant factors are highlighted in blue

6.4.3 Diagnostic plots

Model adequacy was tested using a normal probability plot of residuals, plot of studentized residuals versus predicted values and Box-Cox plot for power transformation.

6.4.3.1 Diagnostic plots for the model for response Y_1

The normal plot of residuals in Figure 6.1 reveals that the data pattern follows a straight line. This shows a direct correlation between input data and output results. The normal plot of residuals shows that the selected model can be used for the design space as the studentized residuals are within the normal percentage probability. The normal distribution of the data indicates the model adequacy for response Y_1 .

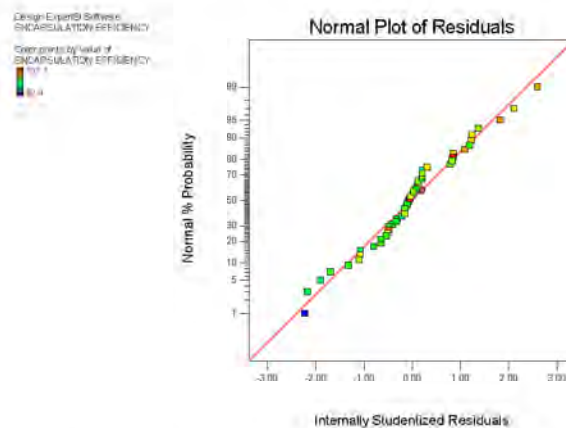


Figure 6.1 Normal plot of residuals for response Y_1

The plot of residuals versus those predicted for response Y_1 is shown in Figure 6.2. The residuals are approximately uniformly scattered above and below the y-axis and most points centralised on the y-axis line showing normal distribution, suggesting model adequacy.

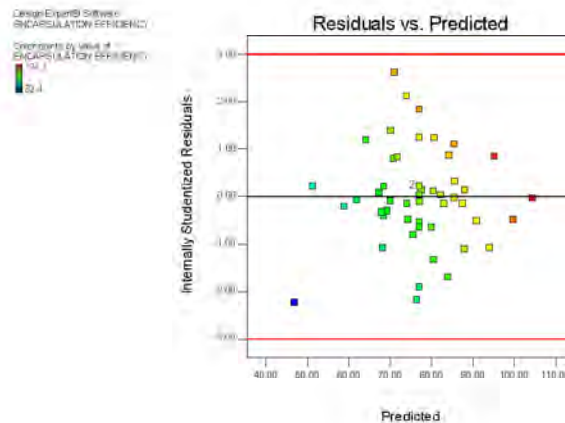


Figure 6.2 Plot of residuals vs. predicted for response Y_1

The Box-Cox plot for response Y_1 shown in Figure 6.3 has a lambda value of 1, indicating that transformation of raw data was not necessary. The diagnostic plots indicate that the model is applicable for the response selected and correlation can be determined between input variables and output variables.

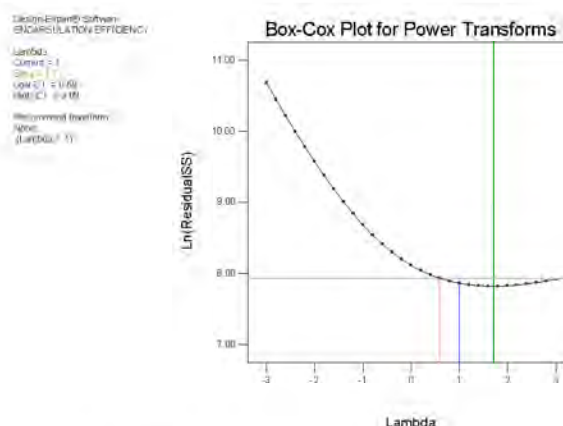


Figure 6.3 Box-Cox plot for response Y_1

6.4.3.2 Diagnostic plots for the model for response Y_7

The normal plot of residuals for response Y_7 in Figure 6.4 reveals that the data pattern follows a straight line. This shows a direct correlation between input data and results. The majority of the data is normally distributed and hence shows the adequacy of the model for response Y_7 .

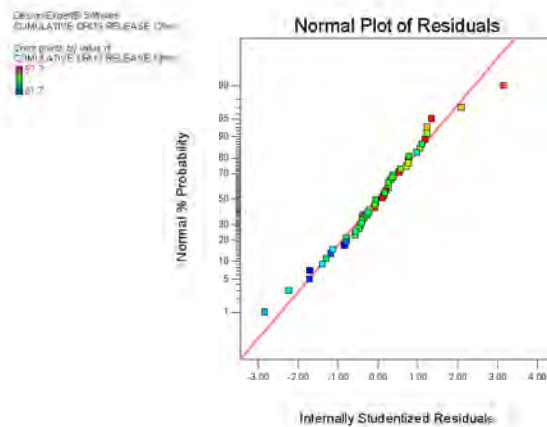


Figure 6.4 Normal plot of residuals for response Y_7

The residual versus predicted plot for response Y_7 (Figure 6.5) shows that most of the points are within the range except for one outlier point. Most of the points are scattered randomly within the range, showing that the model is adequate but without a clear pattern existing.

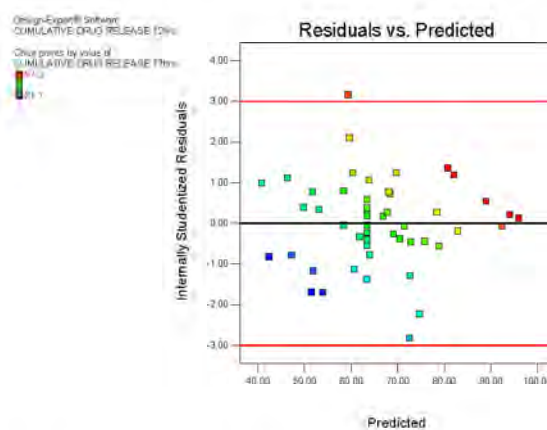


Figure 6.5 Plot of residuals vs. predicted for response Y_7

The Box-Cox plot for response Y_7 is shown in Figure 6.6. It shows that the current model has a lambda of 1. The lambda is also within the 95% CI, and therefore no transformation is necessary.

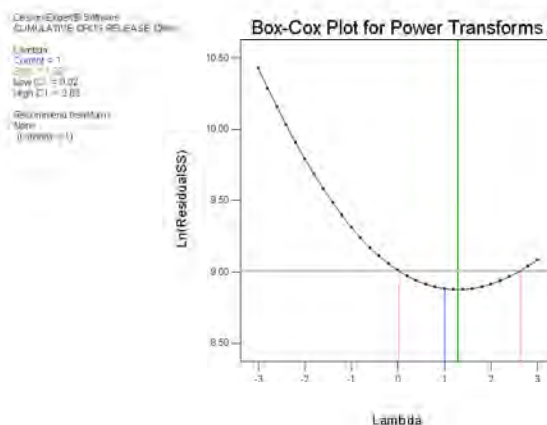


Figure 6.6 Box-Cox plot for response Y_7

6.4.4 Response surface plots

Two and three-dimensional response surface plots were used to study the interactive effects of input variables on the responses. For simplicity, only interactive effects of significant factors summarised in §6.4.2 and Table 6.4 are described.

6.4.4.1 Response surface plots for response Y_1

The contour and 3D RS plots evaluating the effect of Eudragit® RS PO and Methocel® K100LV are shown in Figures 6.7 and 7.8 respectively. Increasing the concentration of polymer led to an increase in EE due to the increased availability of the polymer for encapsulating HYD. A high polymer concentration leads to the formation of a thicker polymeric film around the drug molecules and encapsulation of more drug. These results are similar to previously reported studies where Methocel® and Eudragit® polymers were used in the formulation of ibuprofen, indomethacin and tramadol hydrochloride SR/CR dosage forms [333,344,374,417,445]. HYD, Eudragit® RS PO and Methocel® K100LV are all hydrophilic [37,443,484], therefore the use of an o/o emulsion facilitates the increase in EE due to the affinity of the hydrophilic drug for hydrophilic polymers. Also, the repulsive forces between the hydrophilic drug and the hydrophobic oil facilitate the encapsulation into the polymers.

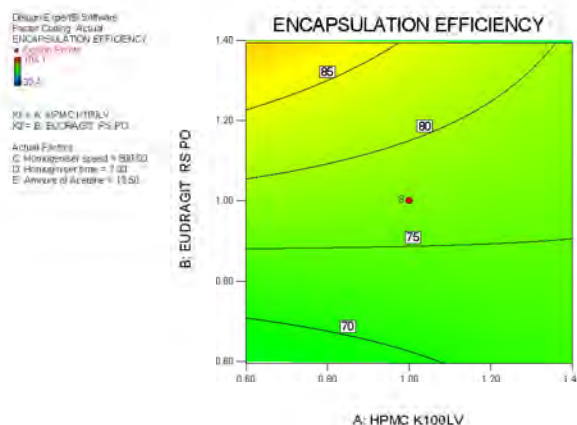


Figure 6.7 Contour plot depicting the effect of Eudragit® RS PO and Methocel® K100LV on EE

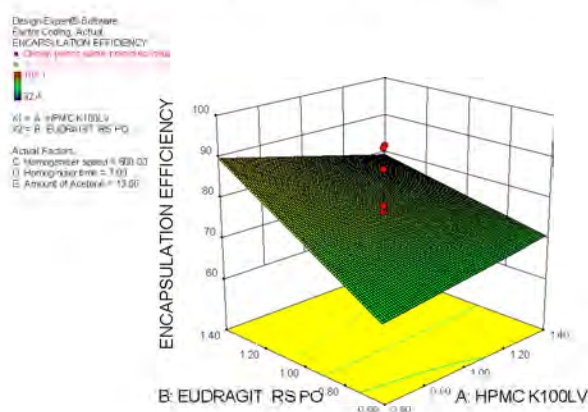


Figure 6.8 3D contour plot depicting the effect of Eudragit® RS PO and Methocel® K100LV on EE

The interactive effects of homogenisation speed and Methocel® K100LV were significant with a p -value less than 0.05. The contour and 3D plots that show the effect of homogenisation speed and Methocel® K100LV on EE are shown in Figures 6.9 and 7.10 respectively. The plots indicate that increasing homogenisation speed results in a decrease in EE. This is attributed to the increase in kinetic energy of the molecules at higher speed rendering it difficult for the encapsulation process to occur. Also, at higher speed, small microspheres would form which might result in less drug being encapsulated. The results are in agreement with previously published findings [153,376,485].

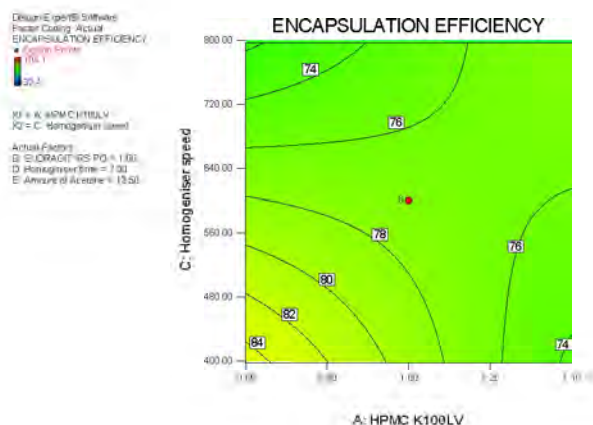


Figure 6.9 Contour plot depicting the effect of homogeniser speed and Methocel® K100LV on EE

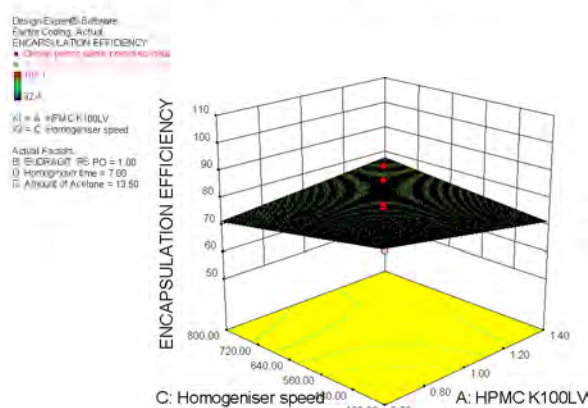


Figure 6.10 3D plot depicting the effect of homogeniser speed and Methocel® K100LV on EE

6.4.4.2 Response surface plots for response Y₇

The concentration of Eudragit® RS PO and Methocel® K100LV were the main significant factors for release with a p -value of 0.0134 (Table 6.4) which was < 0.05 . The two-dimensional contour plot for Y₇ in Figure 6.11 reveals that increasing the concentration of one or both polymers results in a decrease in HYD release. The decrease in % HYD released observed when the content of Methocel® K100LV was increased was as a result of an increase in the thickness and viscosity of the gel layer that forms around HYD molecules when hydration occurs, leading to an increase in the diffusional path length that manifests with slow HYD release. These observations are in agreement with previous studies reporting that increasing the content of HPMC in a matrix results in a decreased rate of API release [259,281,486]. The decrease in % HYD released observed when the content of Eudragit® RS PO was increased was as a result of the increase in the thickness of the polymeric matrix around the HYD which leads to reduced porosity and increased tortuosity, rendering it difficult for water to penetrate the polymers [366,487]. The decrease in porosity and increase in tortuosity of the drug's

diffusion path have inverse effects on drug release. Eudragit® RS PO is a water insoluble, permeable polymer and shows pH-independent drug release [274,436–439,484]. Both polymers have a synergistic effect on release, therefore increasing both polymers' concentration will result in profoundly retarded drug release. The corresponding 3D plot for Y₇ shown in Figure 6.12 reveals that HYD release at 12 hours was lowest when both polymeric excipients, viz. Eudragit® RS PO and Methocel® K100LV were at the maximum in the formulation. It also reveals that the highest HYD release was observed when both polymers were at their minimum. Research indicates the controlling of API release when using one or mixtures of the Eudragit® and Methocel® polymers [151,153].

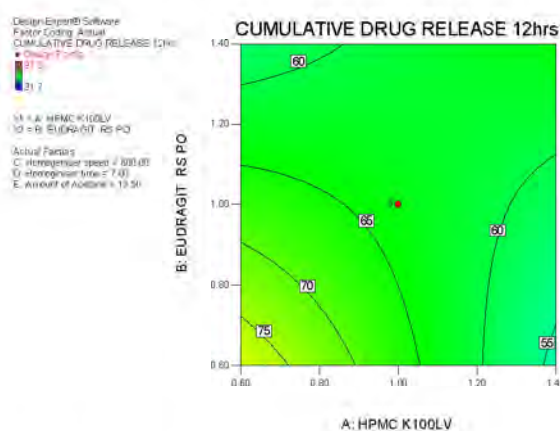


Figure 6.11 Contour plot depicting the effect of Eudragit® RS PO and Methocel® K100LV on release at 12 hours

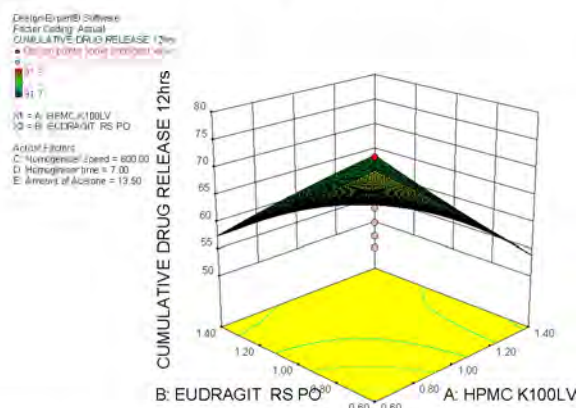


Figure 6.12 3D plot depicting the effect of Eudragit® RS PO and Methocel® K100LV on release at 12 hours

Visual inspection of dissolution testing revealed that the capsule shell dissolved within approximately 5 minutes after being placed in the dissolution medium. Under static conditions, the capsule shell was found to be intact after 30 minutes exposure to the dissolution medium. Photographs were taken (Figure 6.13) at different time intervals to observe the capsule shell dissolving and gel formation. Immediately after placing the capsule in water, it floats due to its

density being less than that of water. With increase in water uptake, the microspheres increase in density and start sinking because of hydration and swelling. The microspheres maintained the shape of the capsule for up to 12 hours.

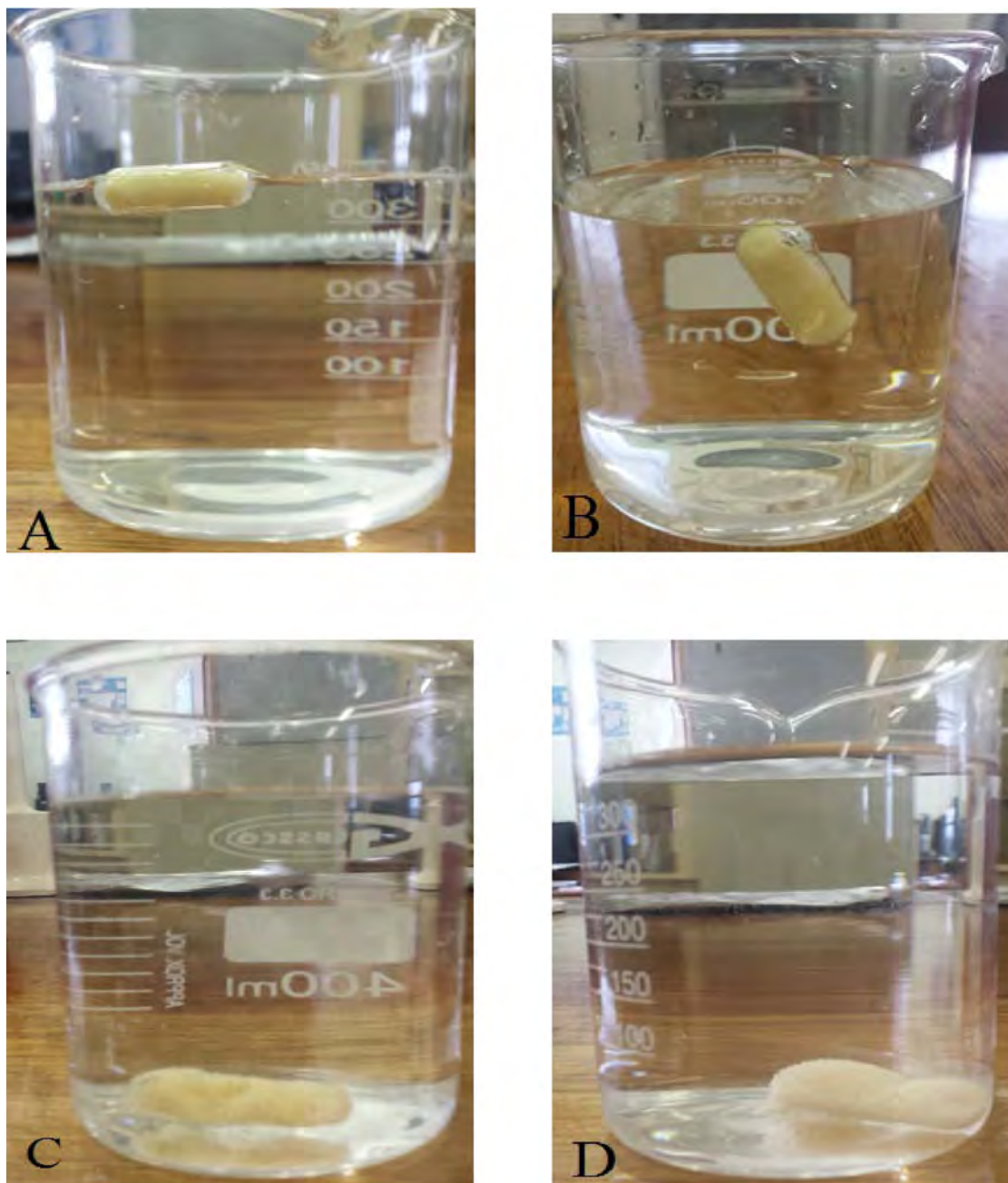


Figure 6.13 Photographs of sustained release HYD microspheres in capsules at (A) 4 minutes (B) 30 minutes (C) 6 hours and (D) 12 hours

6.4.5 Mathematical modelling

The release kinetics of HYD were investigated by fitting release data to several mathematical models. Mathematical modelling for the selected CCD runs were performed. An initial burst

was observed, followed by slower release up to the end of the dissolution test. The decrease in HYD release with time may be due to an increase in the thickness and stability of the gel layer that occurred with increased dissolution media entrance, resulting in a longer dissolution path length for drug release to occur.

No burst release was observed for formulations with high polymer(s) concentration(s). This could be due to the fact that the polymer was sufficient to encapsulate the drug, therefore controlling release and minimising surface drug. However, the release after 12 hours was not above 85% most probably due to the thickness of the gel, increased tortuosity and decreased porosity of the gel formed around the drug molecule which might have resulted in reduced HYD release.

The release for CCD runs were categorised into slow, moderate and fast. The fast releasing formulations had > 30% HYD release after 2 hours whereas the moderate have between 15 and 25% HYD release after 2 hours and the slow have < 15% HYD release after 2 hours. Eight of each category were selected for mathematical modelling. The HYD release kinetics experimental data were fitted to model dependent methods. The model with the highest R^2 values was deemed best fitting. No formulation showed zero-order release due to the curvature nature of the release profiles.

Faster releasing CCD runs had lower polymer concentration. The polymers could have not been sufficient to encapsulate the drug, hence the burst release of surface and unencapsulated drug that was seen. The mechanism of release was either anomalous or super case II indicating that release was controlled by either/or combination of diffusion, swelling and relaxation of the polymers [477,488,489]. The low concentrations of the polymer most probably caused the relaxation of the polymer with an increase in water entrance. These findings are in relation to published observations for water soluble drugs as well [484].

Moderate releasing CCD runs show that the release was mostly first-order. Dosage forms such as those containing water-soluble drugs in porous matrices release the drug in first-order mechanism, *viz.* drug release is proportional to the amount of drug remaining in its interior and the amount of drug released diminishes with time [476,478]. This could be due to the microspheres containing pores due to insufficient polymer concentration or uneven evaporation of solvents, leading to irregular patches at the surface of the microparticles.

Slow releasing CCD runs show that they are mainly controlled by the Higuchi model. This can be attributed to increased amount of polymers which might lead to an increase in tortuosity of the gel layer [102,490,491]. Water soluble polymers contribute to alteration in the porosity of the gel matrix around the drug molecules [102]. Gel growth occurs as water permeates in the matrix to hydrate the solid polymer particles immediately beneath the gel, which results in the thickness of the gel layer [102]. All these factors play a crucial role in controlling the release of HYD. Table 6.7 shows the summary of the R^2 for the zero-order, first-order, Higuchi, Korsmeyer-Peppas and Hixson-Crowell models used.

Table 6.7 Summary of mathematical model and release kinetic parameters for selected CCD runs

| Type | Batch | Model | | | | | | | | | | | |
|----------|---------|------------|--------|---------------|---------------|---------------|--------|----------------|----------|------------------|--------|---------------------|--------------------------|
| | | Zero-order | | First-order | | Higuchi | | Hixson-Crowell | | Korsmeyer-Peppas | | | |
| | | R^2 | k_0 | R^2 | k_1 | R^2 | k_H | R^2 | k_{HC} | R^2 | k | n | Drug transport mechanism |
| Fast | CCD 001 | 0.7633 | 8.4938 | 0.9689 | 0.283 | 0.9126 | 33.191 | 0.9010 | 0.2660 | 0.9277 | 15.885 | 0.9505 | Super case II transport |
| | CCD 002 | 0.9598 | 8.0736 | 0.9923 | 0.199 | 0.9758 | 29.880 | 0.9989 | 0.2199 | 0.9778 | 11.029 | 0.9327 | Super case II transport |
| | CCD 007 | 0.8460 | 6.1042 | 0.9521 | 0.120 | 0.9722 | 24.018 | 0.9250 | 0.1389 | 0.9397 | 19.351 | 0.6465 | Anomalous transport |
| | CCD 015 | 0.9763 | 7.1739 | 0.8965 | 0.168 | 0.9633 | 25.468 | 0.9467 | 0.1878 | 0.9774 | 12.503 | 0.8187 | Anomalous transport |
| | CCD 030 | 0.9018 | 8.7278 | 0.9965 | 0.277 | 0.9663 | 33.16 | 0.9870 | 0.2717 | 0.9320 | 10.195 | 1.0850 | Super case II transport |
| | CCD 039 | 0.9161 | 6.9160 | 0.8667 | 0.220 | 0.9920 | 26.416 | 0.9414 | 0.2096 | 0.9939 | 28.340 | 0.4752 | Anomalous transport |
| | CCD 041 | 0.9103 | 7.7154 | 0.9976 | 0.207 | 0.9867 | 29.496 | 0.9887 | 0.2174 | 0.9702 | 18.247 | 0.7357 | Anomalous transport |
| | CCD 043 | 0.9677 | 8.3007 | 0.9577 | 0.230 | 0.9781 | 30.631 | 0.9954 | 0.2409 | 0.9602 | 8.658 | 1.0939 | Super case II transport |
| CCD 046 | 0.8943 | 6.6061 | 0.9851 | 0.140 | 0.9864 | 25.465 | 0.9691 | 0.1597 | 0.9466 | 17.374 | 0.7080 | Anomalous transport | |
| Moderate | CCD 004 | 0.9645 | 8.2709 | 0.9831 | 0.218 | 0.9751 | 30.525 | 0.9970 | 0.2342 | 0.9489 | 8.768 | 1.0881 | Super case II transport |
| | CCD 005 | 0.9626 | 7.3403 | 0.9917 | 0.156 | 0.9820 | 27.213 | 0.9965 | 0.1826 | 0.9743 | 9.931 | 0.9621 | Super case II transport |
| | CCD 006 | 0.8496 | 4.8703 | 0.9194 | 0.077 | 0.9721 | 19.122 | 0.8992 | 0.0960 | 0.9566 | 15.087 | 0.6473 | Anomalous transport |
| | CCD 016 | 0.9535 | 6.4762 | 0.9943 | 0.113 | 0.9758 | 24.047 | 0.9839 | 0.1428 | 0.9739 | 7.428 | 1.0439 | Super case II transport |
| | CCD 017 | 0.9937 | 8.0264 | 0.8076 | 0.236 | 0.9113 | 28.212 | 0.9088 | 0.2405 | 0.9880 | 7.451 | 1.0343 | Super case II transport |
| | CCD 040 | 0.8015 | 3.6045 | 0.8625 | 0.051 | 0.9526 | 14.404 | 0.8514 | 0.0639 | 0.9341 | 14.655 | 0.5526 | Anomalous transport |
| | CCD 041 | 0.9103 | 7.7154 | 0.9976 | 0.207 | 0.9876 | 29.496 | 0.9886 | 0.2174 | 0.9702 | 18.247 | 0.7357 | Anomalous transport |
| | CCD 048 | 0.9448 | 6.1438 | 0.9947 | 0.107 | 0.9875 | 23.055 | 0.9833 | 0.1340 | 0.9300 | 8.843 | 0.9707 | Super case II transport |
| Slow | CCD 003 | 0.9364 | 5.6474 | 0.9762 | 0.088 | 0.9710 | 21.108 | 0.9613 | 0.1153 | 0.9704 | 12.017 | 1.0691 | Super case II transport |
| | CCD 008 | 0.9426 | 5.7244 | 0.9803 | 0.092 | 0.9744 | 21.362 | 0.9679 | 0.1189 | 0.9839 | 8.888 | 0.8915 | Super case II transport |
| | CCD 09 | 0.9067 | 5.2303 | 0.9594 | 0.086 | 0.9790 | 19.948 | 0.9485 | 0.1080 | 0.9374 | 11.874 | 0.7703 | Anomalous transport |
| | CCD 010 | 0.9866 | 4.5199 | 0.9974 | 0.063 | 0.9679 | 16.432 | 0.9959 | 0.0867 | 0.9769 | 4.903 | 1.0373 | Super case II transport |
| | CCD 011 | 0.9358 | 4.8017 | 0.9738 | 0.070 | 0.9808 | 18.044 | 0.9612 | 0.0932 | 0.9832 | 8.537 | 0.8380 | Anomalous transport |
| | CCD 013 | 0.9505 | 3.4047 | 0.9736 | 0.043 | 0.9819 | 12.701 | 0.9646 | 0.0603 | 0.9567 | 4.236 | 1.0232 | Super case II transport |
| | CCD 014 | 0.8201 | 3.0520 | 0.8611 | 0.039 | 0.9597 | 12.119 | 0.8476 | 0.0518 | 0.9333 | 9.863 | 0.6487 | Anomalous transport |
| | CCD 019 | 0.8102 | 2.5690 | 0.8410 | 0.032 | 0.9545 | 10.235 | 0.8284 | 0.0421 | 0.9343 | 8.451 | 0.6420 | Anomalous transport |

Highest R^2 are in bold

6.4.6 Formulation optimisation

The release of soluble drugs from matrices involves the sequential processes of infiltration of the medium into the matrix, hydration and swelling of the matrix, dissolution of the drug in the matrix, and then leaching of the solubilized drug through the interstitial channels [478,492]. Equation 6.7 shows a modified Higuchi equation, taking into account the surface area, tortuosity and porosity.

$$Q_t = S_q \left[\frac{DV_1}{\tau} (2A - V_1 C_s) C_s t \right]^{1/2} \quad \text{Equation 6.7 [492]}$$

Where,

Q_t - The amount of drug released after time t

D - The diffusion coefficient of the drug in the infiltrating medium

τ - The total tortuosity factor of the capillary system in tablet matrix

A - The total amount of drug present in the matrix

C_s - The solubility of the drug in the infiltrating medium

V_1 - The porosity of the matrix

S_q - The total surface area

The challenge is to minimise the burst effect encountered when the polymeric concentration is low and maximise the release when the polymeric concentration is high. Due to the hydrophilicity of HYD, the polymeric concentration should be high enough to reduce the burst effect. This, however, can lead to reduced amount being released after 12 hours as the polymeric gel thickness is increased.

A numerical optimisation approach using Design Expert[®] (Version 7.0.1, Stat-Ease Inc., Minneapolis, MN, USA) statistical software was used to identify formulations which would produce desired responses. The goals were to avoid burst release by minimising HYD release at 0.5 and 2 hours, maximise release of HYD at 12 hours and maximise EE. Table 6.8 shows the formulas for optimised formulations (OPT 1 and OPT 2). The optimal amount of acetone was 14.5 mL, the homogenisation speed was 400rpm and the homogenisation time was 7 hours. All the other factors (Table 5.1), viz. beaker size, amount of liquid paraffin, *n*-hexane, drying temperature and time and homogeniser were kept constant.

Table 6.8 Optimised formulations

| Ingredient | OPT 1 | OPT 2 |
|------------------|-------|-------|
| HYD | 0.50g | 0.5g |
| Methocel® K100LV | 0.56g | 0.61g |
| Eudragit® RS PO | 1.40g | 1.38g |
| Avicel® 101 | Sq. | Sq. |
| Total | 3.5g | 3.5g |

6.4.6.1 *In vitro* release from optimised formulations

The *in vitro* HYD release was performed using the dissolution method described in §5.6.6. The dissolution profiles for the optimised formulations (OPT 1 and OPT 2) are shown in Figures 6.14 and 6.15 respectively. Both release profiles show a burst release within 2 hours of commencing dissolution. This might be due to the surface drug being released before the formation of the gel and the high water solubility of HYD that provided the driving force for drug release. Both release profiles show post-dissolution time release and HYD being released in a sustained manner.

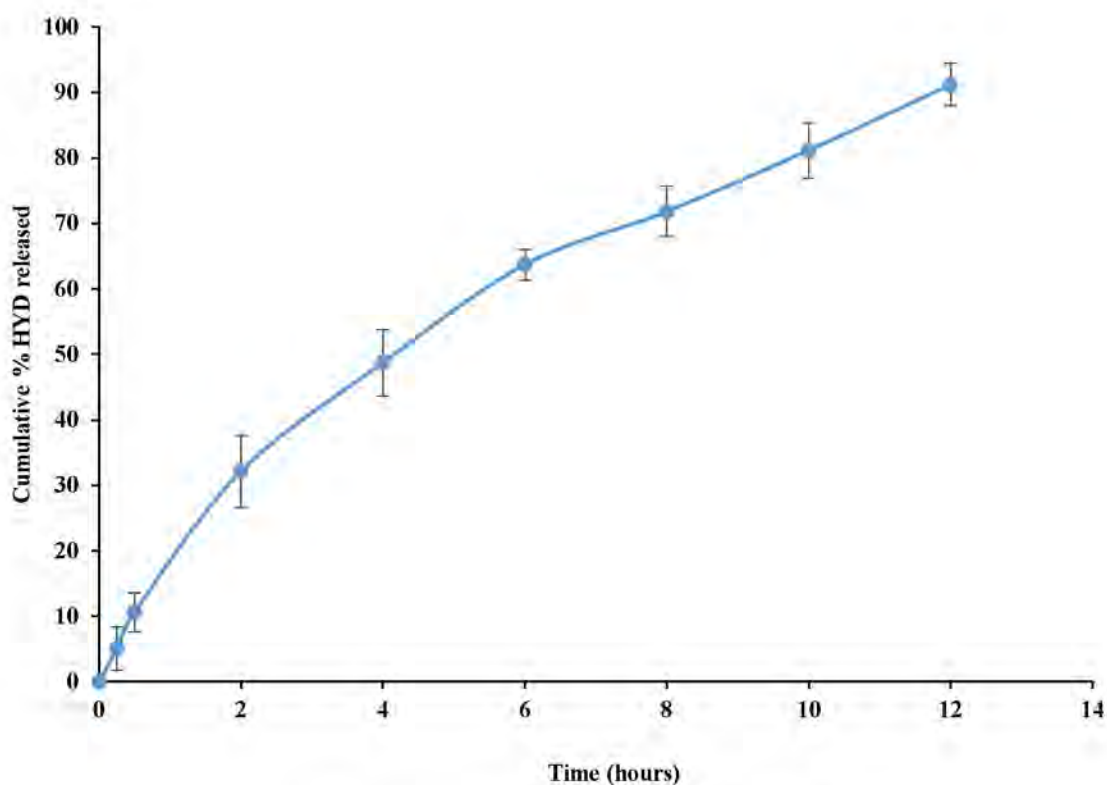


Figure 6.14 Cumulative % HYD released from OPT 1 (n=6)

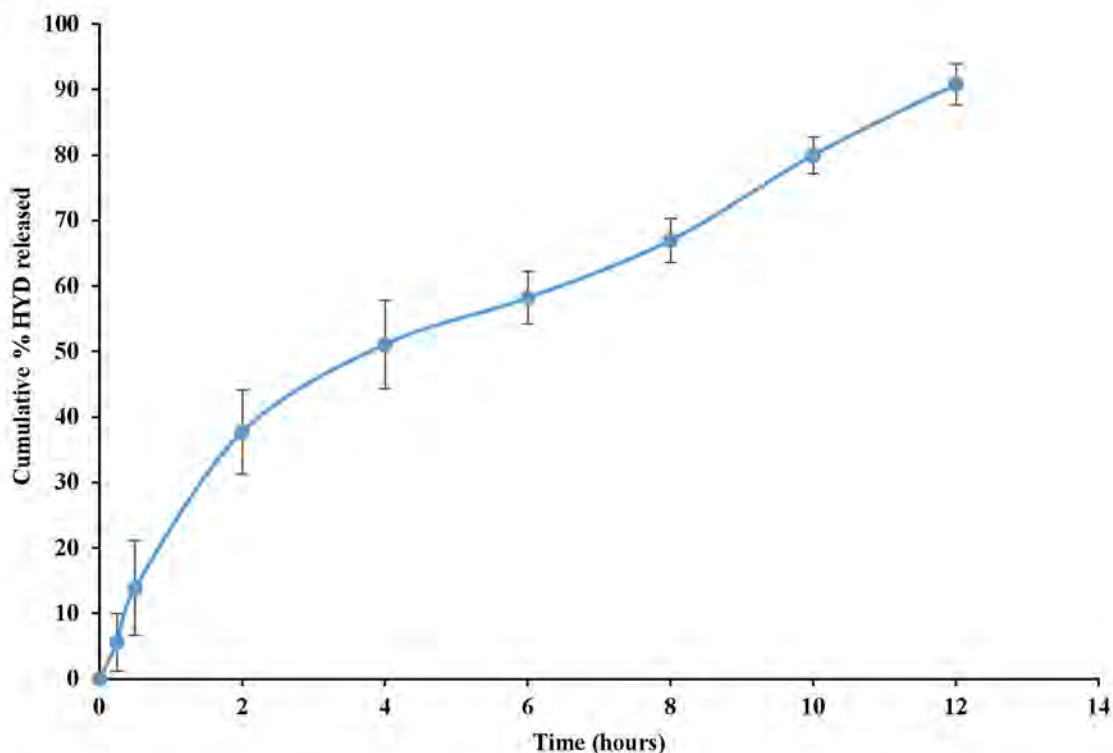


Figure 6.15 Cumulative % HYD released from OPT 2 (n=6)

The *in vitro* HYD release data were fitted to mathematical models in an attempt to establish the mechanism of HYD release from microspheres. The curvilinear nature of the cumulative percent HYD released versus time plots (Figure 6.14 and 6.15) suggests that HYD release from the microspheres does not follow zero-order kinetics. The R^2 values listed in Table 6.9 suggest that the data are best described using the Higuchi model as it yielded the highest R^2 values for both optimised formulations. These results correlate with other findings for water soluble APIs [466].

Table 6.9 Summary of mathematical model parameters for the optimised formulations

| Model | OPT 1 | | OPT 2 | |
|------------------|--------------------------|--------|--------------------------|--------|
| | K | R^2 | K | R^2 |
| Zero-order | 7.4842 | 0.9526 | 7.0846 | 0.9398 |
| First-order | 0.183 | 0.9774 | 0.1720 | 0.9527 |
| Higuchi | 27.56 | 0.9938 | 26.22 | 0.9904 |
| Hixson-Crowell | 0.202 | 0.9932 | 0.1904 | 0.9764 |
| Korsmeyer-Peppas | $k=10.160$ $n=0.9024$ | 0.9891 | $k=18.420$ $n=0.6653$ | 0.9704 |

Model with highest R^2 is in blue

6.4.6.2 EE and assay

The EE and assay for the optimised formulations, *viz.* OPT 1 and OPT 2, were determined using methods described in §5.6.5 and §5.6.4 respectively. Equation 5.2 was used to calculate

the EE of the optimised formulations. HYD content in OPT 1 and OPT 2 was found to be 99.83 and 99.89% whereas the EE was found to be 99.71 and 99.30% respectively. The optimised formulations have a high EE due to the polymers sufficiently encapsulating the drug. The homogenisation speed was ideal and the homogenisation time enough to allow for encapsulation. The use of an o/o emulsion led to high EE of hydrophilic API into hydrophilic polymers.

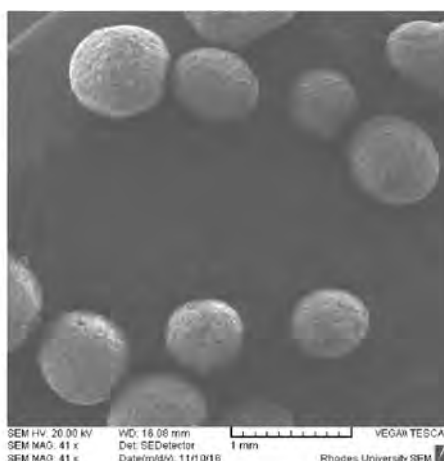
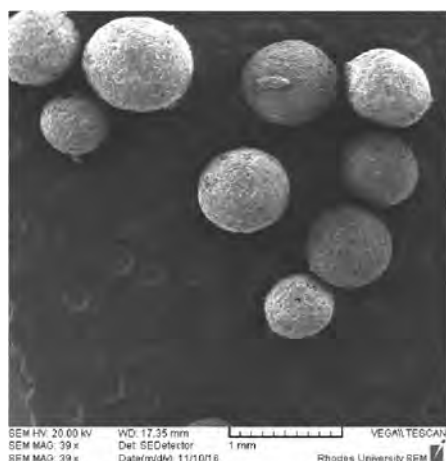
6.4.6.3 Yield

Immediately after drying and before any other test, the microspheres were weighed using a Model PM top-loading electronic balance (Mettler® Toledo, Zurich, Switzerland) and the amount found recorded. The percentage yield was calculated using Equation 5.1. The % yield of OPT 1 and OPT 2 was found to be 99.72 and 99.43% respectively. The high yield justifies the use of an o/o emulsion and the use of hydrophilic polymers.

6.4.6.4 Characterisation of optimised formulations

6.4.6.4.1 SEM

SEM studies were performed as described in §4.4.1. The surface morphology study by SEM indicated that the microspheres were spherical with a rough outer surface and drug present on the microsphere surfaces. These results are similar to those reported when Methocel® and Eudragit® RS PO polymers were used to evaluate the release of captopril, ibuprofen and gliclazide [369,493,494]. At higher magnification, the microspheres have small pores that are likely due to solvents evaporating through these pores. SEM for OPT 1 and OPT 2 are shown in Figure 6.16 and 6.17 respectively. The diameter of approximately 20 microspheres of each optimised formulation was measured using analysis Olympus software. The average diameters for OPT 1 and OPT 2 (Figure 6.18 and 6.19) were found to be $806 \pm 109\mu\text{m}$ and $717 \pm 83\mu\text{m}$ respectively. All the microspheres were within the size range of microspheres (1-1000 μm).



6.4.6.4.2 FT-IR

FT-IR was used to assess the crystalline nature of the optimised HYD formulations. Samples of the optimised formulation were mounted onto a KBr disc using an applied force of approximately 100N. The FT-IR spectrum was generated using an FT-IR Spectrum 100 spectrometer (Perkin-Elmer® Pty Ltd, Beaconsfield, England) in a scan range of between 4000 and 650 cm^{-1} at a resolution of 4 cm^{-1} . The spectrums obtained were superimposed on the one for the bulk drug. Characteristic peaks for HYD at 3211 cm^{-1} , 3027 and 1668 cm^{-1} were present in both optimised formulations. This indicates that HYD was still in its crystalline form, and was stable under the stated manufacturing conditions. There was no interaction between the drug and the excipients used. Also, the formulation process had no effect on characteristic and functional groups of HYD. Figures 6.20 and 6.21 show the FT-IR spectrums for OPT 1 and OPT 2 respectively.

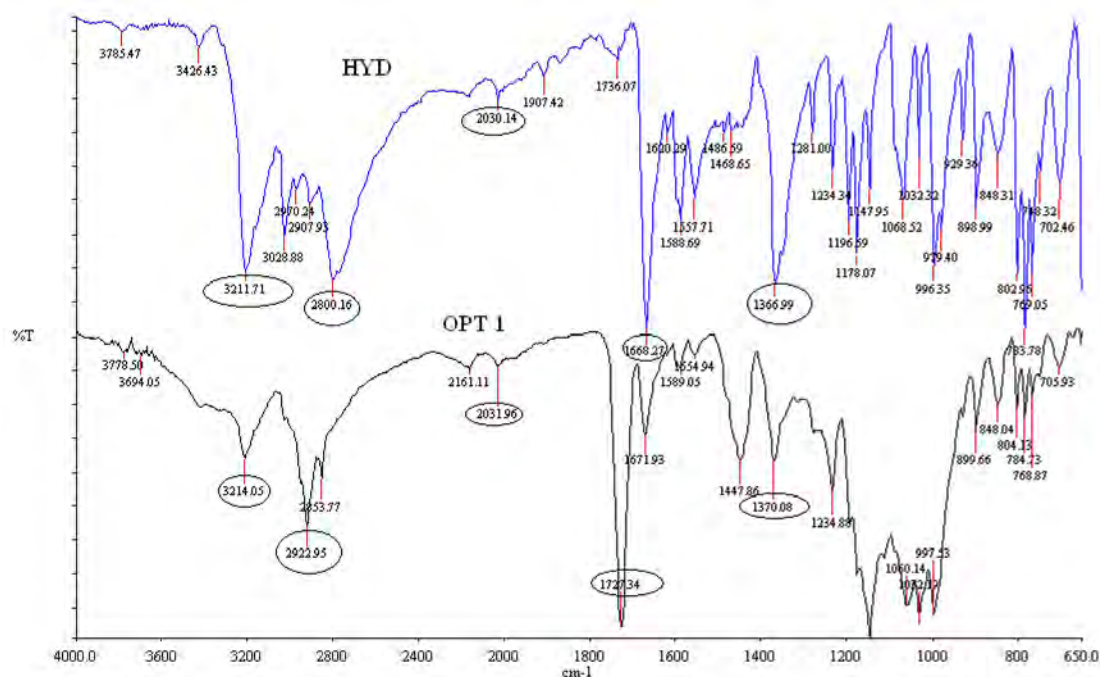


Figure 6.20 Typical FT-IR spectra of HYD and OPT 1 generated from 4000 cm^{-1} to 650 cm^{-1}

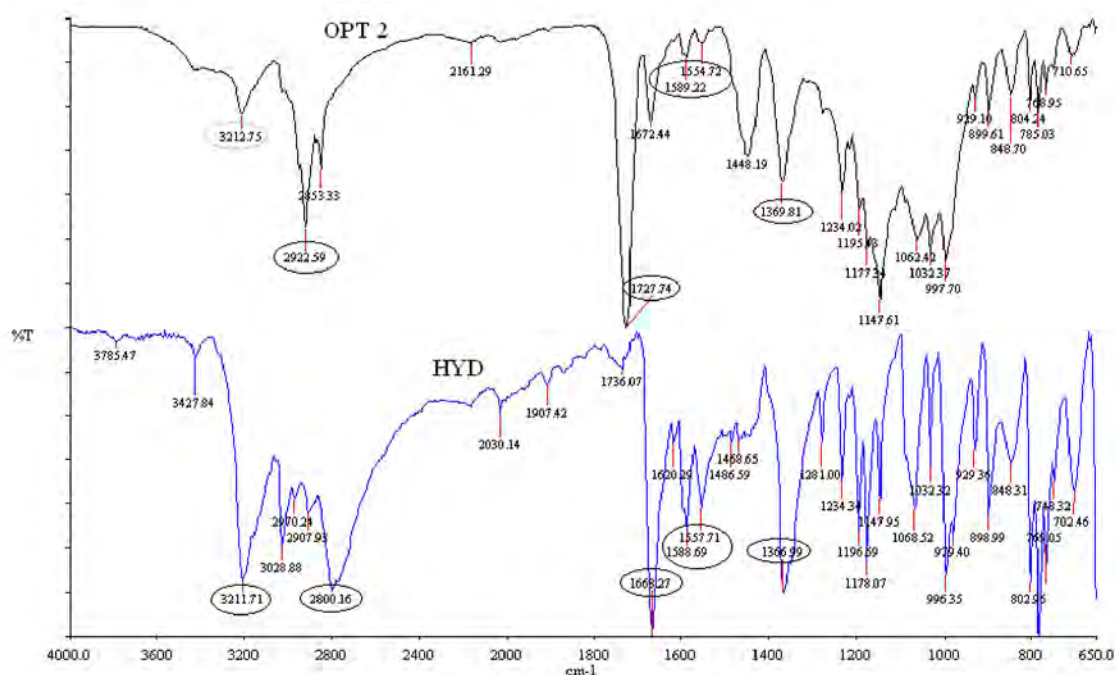


Figure 6.21 Typical FT-IR spectra of HYD and OPT 2 generated from 4000 cm^{-1} to 650 cm^{-1}

6.4.6.4.3 DSC

DSC was used to evaluate the polymorphism of optimised formulations using the method in §4.4.4. The OPT 1 thermogram shows exothermic and endothermic peaks at 246 and 291 $^{\circ}\text{C}$ with ΔH of -67 and 39 J/g respectively. The OPT 2 thermogram shows three exothermic peaks at 269, 276 and 312 $^{\circ}\text{C}$ with ΔH of -7, -55 and -133 J/g. HYD is still present in its crystalline

form regardless of a decrease in ΔH when compared to the pure HYD in Figure 4.7. The decrease in the melting point might be due to the presence of excipients. Figures 6.22 and 6.23 show the DSC for OPT 1 and OPT 2 respectively.

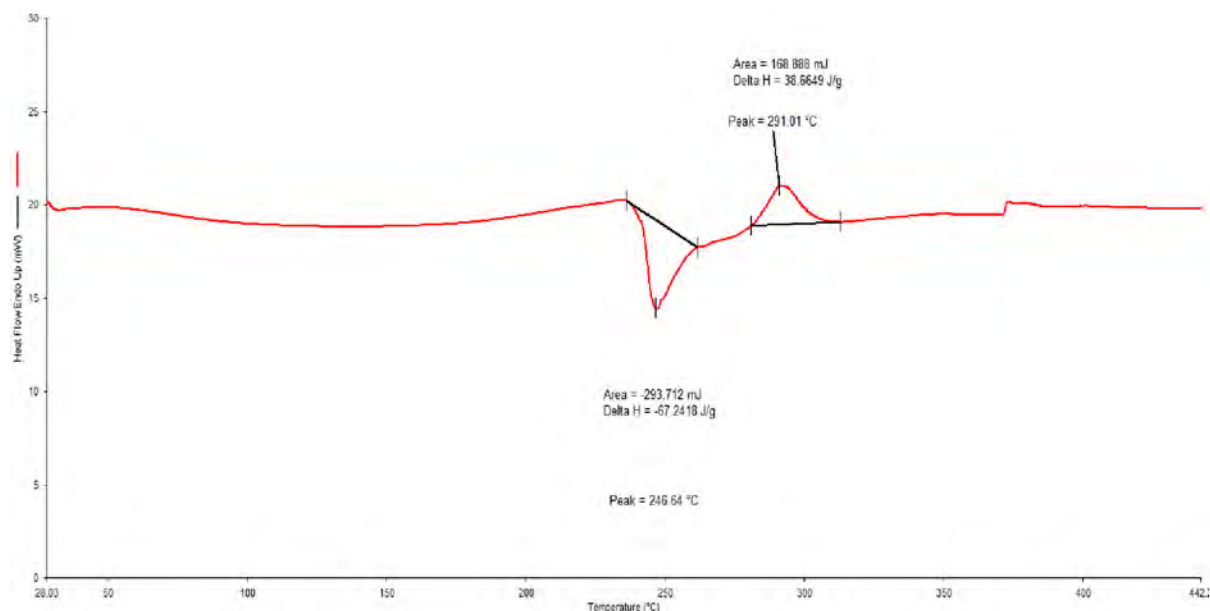


Figure 6.22 DSC thermogram of OPT 1 generated at a heating rate of 10 °C/min

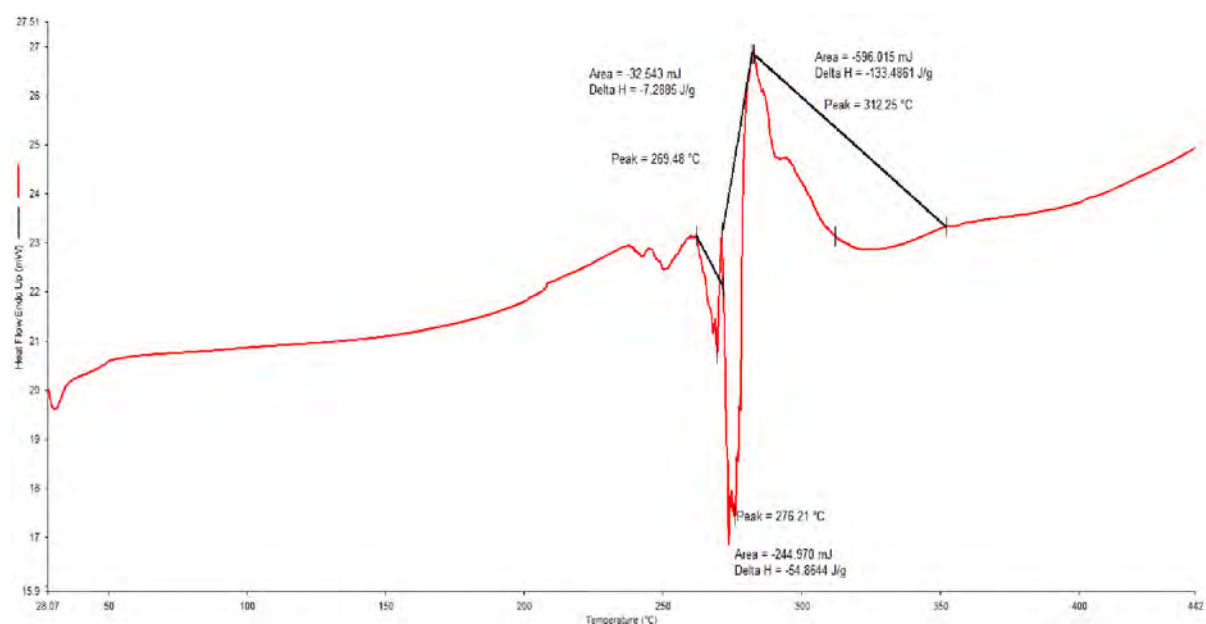


Figure 6.23 DSC thermogram of OPT 2 generated at a heating rate of 10 °C/min

6.4.6.4.4 XRPD

XRPD patterns of OPT 1 are shown in Figure 6.24. Characteristic peaks of HYD in the optimised formulations were observed at a diffraction angle of $2\theta = 12, 20, 24, 27, 28, 33$ and 35° . When compared to the original diffractogram of HYD (§4.5.2.5), the main characteristic

peaks of HYD do appear in the optimised formulations thus revealing that the homogenisation process and drying conditions did not affect the crystallinity nature of HYD.

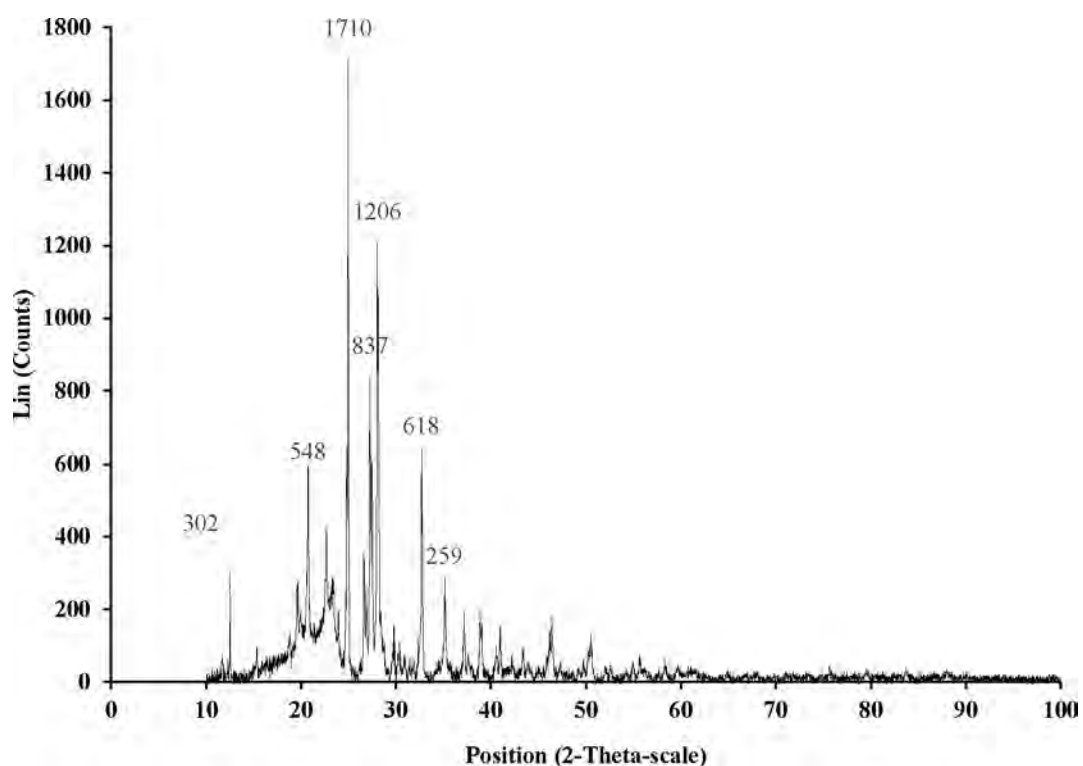


Figure 6.24 XRPD patterns of OPT 1

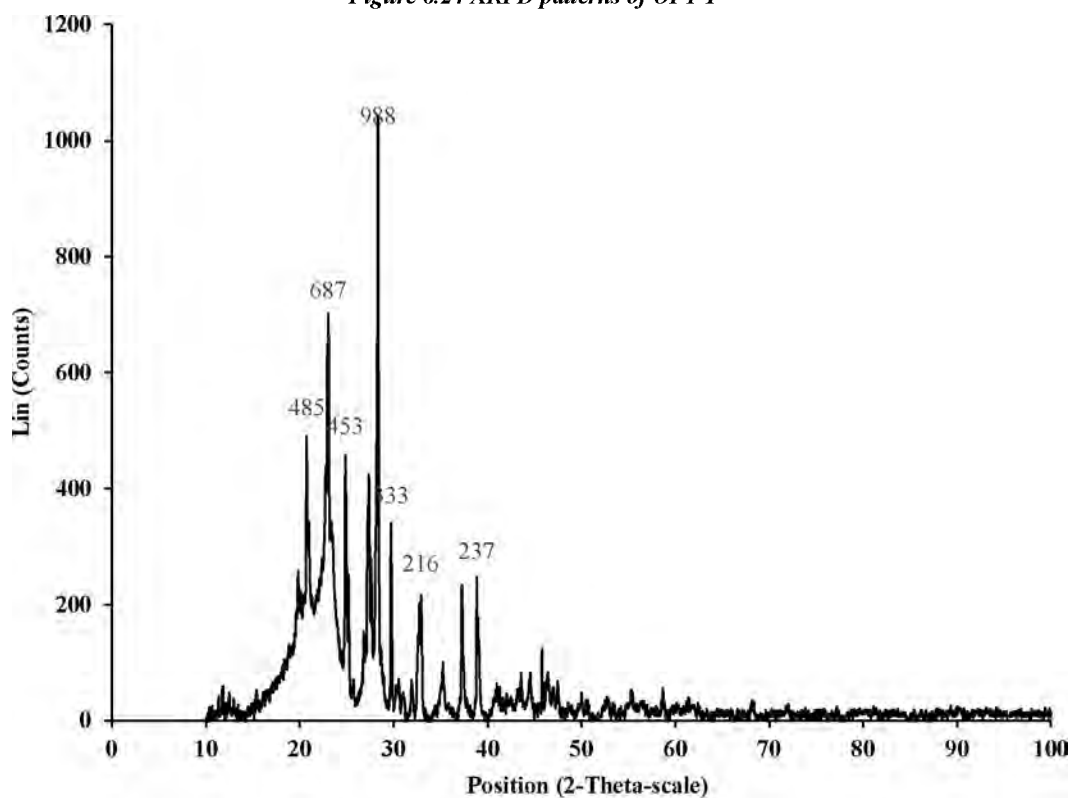


Figure 6.25 XRPD patterns of OPT 2

6.4.6.5 Comparison of OPT 1 and OPT 2 *in vitro* dissolution profiles

The similarity of *in vitro* dissolution profiles of a reference dosage form and a test dosage form can be evaluated using two model-independent parameters, viz. the difference factor (f_1) and the similarity factor (f_2) [102,477]. The model-independent mathematical approach was used for quantitative comparability of the dissolution profiles generated for OPT 1 and OPT 2. The f_1 is a measure of the percentage error between two dissolution profiles at each dissolution time point [477,478] and can be calculated using Equation 6.8. An f_1 value ≤ 15 indicates similarity between two dissolution profiles being compared [477].

$$f_1 = \frac{\sum_{t=1}^n |R_t - T_t|}{\sum_{t=1}^n R_t} \times 100 \quad \text{Equation 6.8 [477,495]}$$

Where,

f_1 - Difference factor

n - Sampling number

R_t - Percentage dissolved in the reference product at each time point

T_t - Percentage dissolved in the test product at each time point

The f_2 measures the similarity in the percent of dissolution between two dissolution profiles [477,478,496,497]. It is a logarithmic transformation of the sum-squared error of differences between the test and reference products [478]. f_2 values ≥ 50 indicate that two dissolution profiles are similar [495] and Equation 6.9 is used to calculate f_2 .

$$f_2 = 50 \times \log \left\{ \left[1 + \left(\frac{1}{n} \right) \sum_{t=1}^n w_j |R_t - T_t|^2 \right]^{-0.5} \times 100 \right\} \quad \text{Equation 6.9 [478]}$$

Where,

f_2 - Similarity factor

w_j - An optional weight factor

n - Sampling number

R_t - Percentage dissolved in the reference product at each time point

T_t - Percentage dissolved in the test product at each time point

In order for two dissolution profiles to be considered similar, the f_1 value should be close to 0 and f_2 value should be close to 100 [478]. For comparative purposes, OPT 1 was set as the reference and OPT 2 as the test. The f_1 and f_2 values listed in Table 6.10 reveal that the dissolution profiles obtained from OPT 1 and OPT 2 were similar. The f_1 value was found to be $\ll 15$ and the f_2 value $\gg 50$. The similarity might perhaps be due to the concentrations of the polymers being almost equal.

Table 6.10 Difference and similarity factors for dissolution profiles obtained from OPT 1 and OPT 2

| Profiles compared | f_1 | f_2 |
|--------------------|-------|-------|
| OPT 1 versus OPT 2 | 5.8 | 71.5 |

The results were confirmed with plotting the dissolution profiles for OPT 1 and 2 on one graph. Both release profiles indicate burst release within 2 hours and normalised sustained release afterwards. The graphs are similar and thus justify the results from the model independent similarity approach. Figure 6.24 shows the cumulative % HYD released of OPT 1 and 2.

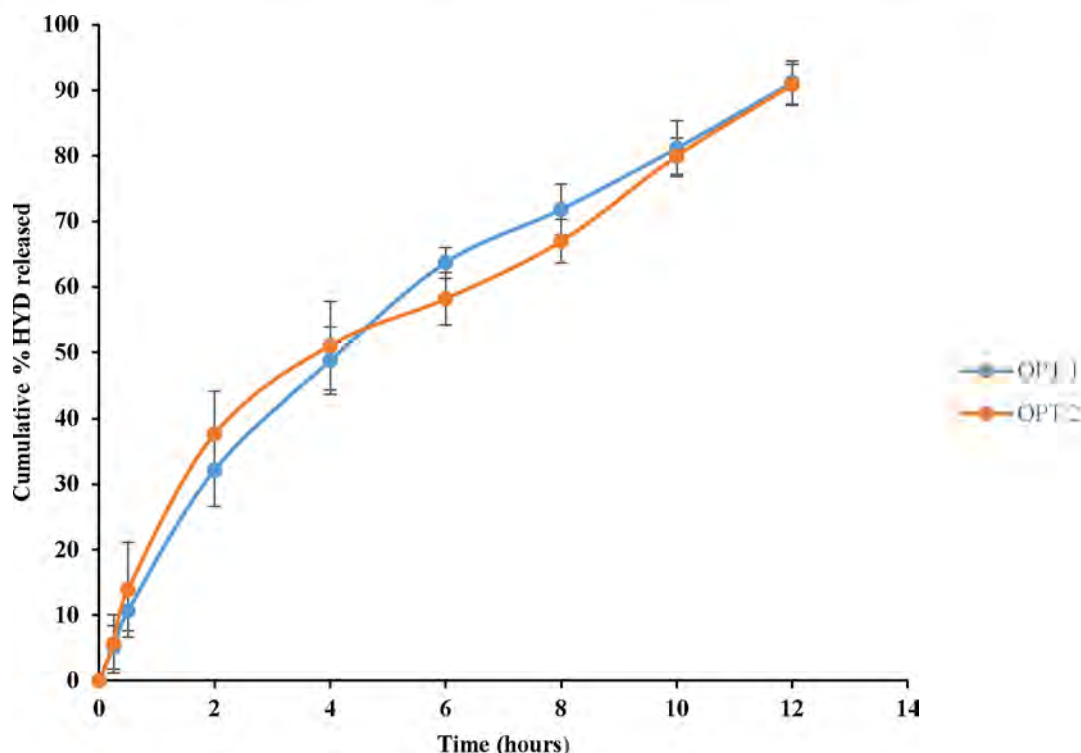


Figure 6.26 Comparative cumulative % HYD released from OPT 1 and OPT 2

6.4.7 Stability studies

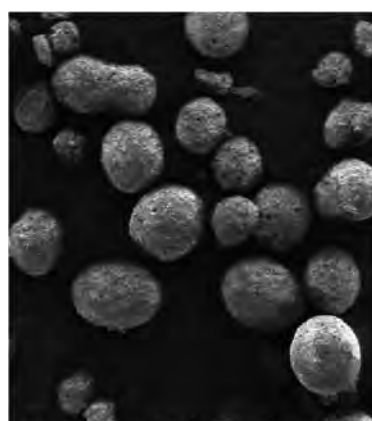
Stability of a pharmaceutical product may be defined as the capability of a particular formulation in a specific container/closure system to remain unchanged in its physical, chemical, microbiological and toxicological specifications [102]. Stability studies are routine procedures which ensure the maintenance of pharmaceutical product(s) safety, quality and efficacy throughout the shelf-life [498] and are, therefore, an important component of the product development process [499].

Stability testing evaluates the effect of environmental factors on the quality of the drug substance or a formulated product which is utilised for prediction of its shelf-life [498].

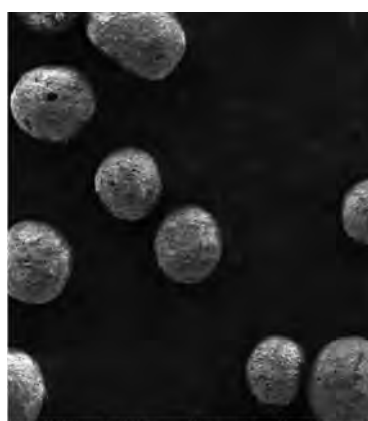
Moreover, the data generated during the stability testing is an important requirement for regulatory approval of any drug or formulation [500]. Stability studies (SS) evaluate the appearance and physical attributes, potency, and purity of a drug product throughout its stated shelf-life and are essential to determine the quality of a modified or repacked drug product [501]. Stability testing should be conducted on the dosage form packaged in the container closure system proposed to be used in the clinical trial [502]. The testing parameters will vary with different dosage forms [498].

Optimised formulations were stored for one month in the refrigerator at 4 °C and stability chambers at 25°C/60% RH and 40°C/75% RH and assessed every week. The physicochemical properties of the microspheres, viz. physical appearance, HYD content, EE and *in vitro* release were evaluated. SEM was performed after one month to evaluate any changes in shape and morphology of the microspheres after the stability testing period. The results from SEM indicated that no changes occurred to the shape or surface morphology of the microspheres (Figure 6.27). SEM results revealed that the microspheres remained intact for the duration of the stability studies.

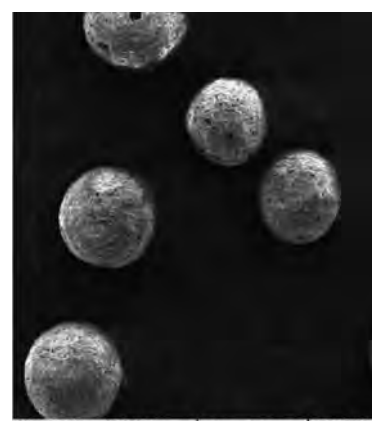
Stability results indicate that no significant changes occurred to HYD content throughout the duration of the study in different storage conditions. This was attributed to the stability of HYD in powder form. In addition, no significant changes occurred to the percentage HYD encapsulated throughout the duration of the stability study. Thus the polymers were stable at the stated storage conditions. Cumulative HYD release varied from approximately 50 to 66% and 86 to 93% after 6 hours and 12 hours respectively. It was observed that the release data of HYD did not change greatly. Minor changes occurred to EE and HYD content. This may be attributed to the spherical shape of the particles that remained intact (Figure 6.27). Table 6.11 to 6.13 summarise the results of the assay, EE and HYD release in different storage conditions and at different times.



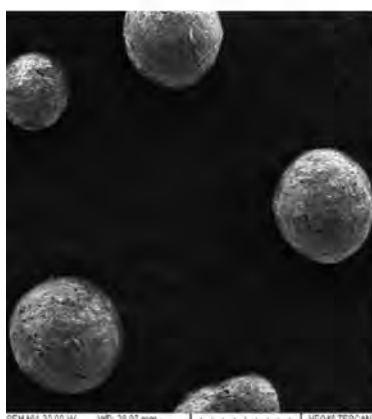
SEM image of OPT 1 after SS at 4 °C for 1 month



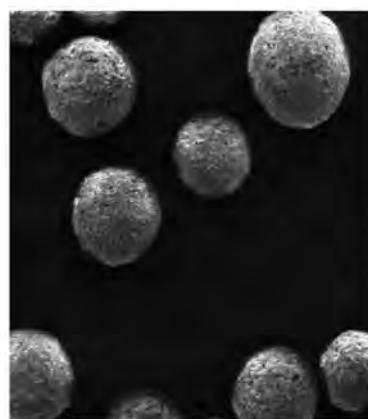
SEM image of OPT 1 after SS at 25°C/60% RH for 1 month



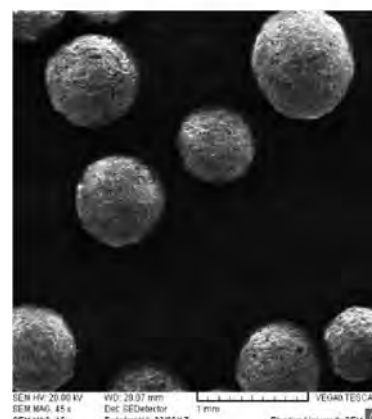
SEM image of OPT 1 after SS at 40°C/75% RH for 1 month



SEM image of OPT 2 after SS at 4 °C for 1 month



SEM image of OPT 2 after SS at 25°C/60% RH for 1 month



SEM image of OPT 2 after SS at 40°C/75% RH for 1 month

Figure 6.27 SEM images of optimised formulations after stability studies for 1 month

Table 6.11 Results of stability testing for the optimised formulations stored in the refrigerator at 4 °C

| Parameter | OPT 1 | | | | OPT 2 | | | |
|-----------------------|--------------|--------------|--------------|--------------|--------------|--------------|--------------|--------------|
| | Week 1 | Week 2 | Week 3 | Week 4 | Week 1 | Week 2 | Week 3 | Week 4 |
| Physical Appearance | No changes | No changes | No changes | No changes | No changes | No changes | No changes | No changes |
| HYD content (%) | 99.88 ± 0.38 | 99.82 ± 0.17 | 98.71 ± 0.11 | 98.18 ± 0.38 | 99.72 ± 1.48 | 98.82 ± 2.53 | 99.80 ± 0.16 | 97.17 ± 0.73 |
| EE (%) | 98.18 ± 2.99 | 98.72 ± 0.17 | 98.18 ± 0.03 | 99.27 ± 0.32 | 98.72 ± 1.32 | 99.20 ± 0.16 | 98.62 ± 0.14 | 98.94 ± 0.11 |
| % HYD released | | | | | | | | |
| 6 hours | 63.33 ± 1.03 | 51.80 ± 1.08 | 57.90 ± 0.27 | 66.18 ± 2.06 | 55.68 ± 1.08 | 49.23 ± 1.69 | 55.26 ± 2.46 | 56.07 ± 5.90 |
| 12 hours | 91.78 ± 4.16 | 91.64 ± 2.30 | 86.05 ± 2.94 | 91.31 ± 1.34 | 90.43 ± 4.88 | 92.01 ± 4.55 | 91.60 ± 6.46 | 89.09 ± 6.10 |

Table 6.12 Results of stability testing for the optimised formulations stored at 25°C/60% RH

| Parameter | OPT 1 | | | | OPT 2 | | | |
|-----------------------|--------------|--------------|--------------|--------------|--------------|--------------|--------------|--------------|
| | Week 1 | Week 2 | Week 3 | Week 4 | Week 1 | Week 2 | Week 3 | Week 4 |
| Physical Appearance | No changes | No changes | No changes | No changes | No changes | No changes | No changes | No changes |
| HYD content (%) | 99.97 ± 0.17 | 97.42 ± 1.22 | 99.48 ± 0.15 | 98.12 ± 1.10 | 99.01 ± 2.20 | 98.61 ± 1.59 | 98.33 ± 0.06 | 97.72 ± 1.14 |
| EE (%) | 99.81 ± 1.40 | 98.54 ± 0.33 | 99.16 ± 0.02 | 99.94 ± 2.25 | 98.49 ± 2.23 | 99.36 ± 0.35 | 98.96 ± 0.05 | 99.83 ± 0.55 |
| % HYD released | | | | | | | | |
| 6 hours | 54.94 ± 2.99 | 49.70 ± 4.46 | 48.62 ± 3.18 | 49.74 ± 3.54 | 50.77 ± 2.22 | 54.02 ± 0.36 | 51.05 ± 2.26 | 62.90 ± 1.74 |
| 12 hours | 90.29 ± 3.94 | 88.34 ± 5.30 | 87.91 ± 3.69 | 92.18 ± 3.92 | 89.98 ± 6.20 | 91.36 ± 0.54 | 89.39 ± 4.24 | 90.30 ± 0.39 |

Table 6.13 Results of stability testing for the optimised formulations stored at 40°C/75% RH

| Parameter | OPT 1 | | | | OPT 2 | | | |
|-----------------------|--------------|--------------|--------------|---|--------------|--------------|--------------|---|
| | Week 1 | Week 2 | Week 3 | Week 4 | Week 1 | Week 2 | Week 3 | Week 4 |
| Physical Appearance | No changes | No changes | No changes | Formulation changed colour to a pale yellowish colour | No changes | No changes | No changes | Formulation changed colour to a pale yellowish colour |
| HYD content (%) | 98.40 ± 0.75 | 96.74 ± 1.40 | 99.35 ± 0.07 | 99.82 ± 1.34 | 99.98 ± 1.29 | 98.83 ± 0.98 | 99.99 ± 0.17 | 99.60 ± 0.17 |
| EE (%) | 98.28 ± 0.27 | 99.50 ± 0.19 | 99.83 ± 0.10 | 95.55 ± 2.25 | 98.24 ± 0.28 | 99.16 ± 0.11 | 98.61 ± 0.06 | 99.55 ± 0.52 |
| % HYD released | | | | | | | | |
| 6 hours | 55.58 ± 4.22 | 55.33 ± 0.39 | 50.89 ± 1.23 | 52.91 ± 5.42 | 54.91 ± 0.23 | 53.42 ± 1.51 | 50.56 ± 3.18 | 59.83 ± 0.67 |
| 12 hours | 91.15 ± 3.70 | 89.63 ± 4.25 | 90.39 ± 4.10 | 91.03 ± 5.14 | 89.20 ± 4.69 | 90.13 ± 4.52 | 89.66 ± 2.68 | 88.36 ± 5.82 |

Furthermore, dissolution profiles obtained during the stability testing period were compared to the OPT 1 and OPT 2 profiles using the model independent approach (Equation 6.8 and 6.9). OPT 1 and OPT 2 were used as references whereas release profiles after 1, 2, 3 and 4 weeks were used as tests. Results indicate that the release profile for OPT 1 was similar over the duration of the stability period with f_1 and f_2 values ranging from 3.7 to 14.7 and 54.1 to 74.7 respectively. The release profiles for OPT 2 was also similar over the duration of the stability period with f_1 and f_2 values ranging from 4.7 to 14.6 and 53.9 to 76.3 respectively. Thus the release of HYD was not affected by the short-term storage conditions. Table 6.14 shows the summary of results from the model independent approach test.

Table 6.14 Model independent approach on comparison of the release of OPT 1 and OPT 2 under stability testing conditions

| Profiles compared | Stability testing conditions | | | | | | Comments |
|----------------------------------|------------------------------|-----------------------|-----------------------|-----------------------|-----------------------|-----------------------|----------|
| | 4 °C | | 25°C/ 60% RH | | 40°C/75% RH | | |
| | <i>f</i> ₁ | <i>f</i> ₂ | <i>f</i> ₁ | <i>f</i> ₂ | <i>f</i> ₁ | <i>f</i> ₂ | |
| OPT 1 versus OPT I after 1 week | 7.0 | 66.4 | 11.4 | 58.2 | 3.7 | 74.7 | Similar |
| OPT 1 versus OPT I after 2 weeks | 7.8 | 62.7 | 11.7 | 56.1 | 12.1 | 56.6 | Similar |
| OPT 1 versus OPT I after 3 weeks | 10.2 | 60.3 | 13.7 | 53.8 | 14.7 | 54.1 | Similar |
| OPT 1 versus OPT I after 4 weeks | 5.0 | 71.9 | 11.7 | 56.3 | 9.7 | 61.8 | Similar |
| OPT 2 versus OPT 2 after 1 week | 6.1 | 71.7 | 9.1 | 63.4 | 7.4 | 68.3 | Similar |
| OPT 2 versus OPT 2 after 2 weeks | 11.5 | 59.6 | 8.0 | 66.3 | 13.3 | 55.0 | Similar |
| OPT 2 versus OPT 2 after 3 weeks | 7.4 | 68.8 | 8.6 | 65.4 | 14.6 | 53.9 | Similar |
| OPT 2 versus OPT 2 after 4 weeks | 6.7 | 69.1 | 5.3 | 72.5 | 4.7 | 76.3 | Similar |

6.5 CONCLUSIONS

HYD loaded microspheres were manufactured using a solvent evaporation technique. The RSM approach was used to study the effects of selected formulation independent variables on dependent variables, *viz.* HYD release, EE, HYD content and yield. The approach was successfully employed and reduced the time and resources required for formulation development and optimisation. A three-factor CCD was used to determine the effects of Methocel® K100LV, Eudragit® RS PO, amount of acetone, homogenisation speed and time. ANOVA was successfully used to analyse the significance of models and independent variables. The results revealed that the Methocel® K100LV and Eudragit® RS PO content have a significant effect on HYD release and EE. The amount of acetone and homogenisation speed have a significant effect on EE and yield. Diagnostic plots, *viz.* normal probability plot of residuals, plot of studentized residuals versus predicted and Box-Cox plots were used to determine model adequacy for each response. Two-dimensional contour and three-dimensional response surface plots were used to visualise the impact of independent variables on dependent variables.

Formulation optimisation was done numerically using a statistical software. The optimised formulations were assessed for physical appearance, shape and surface morphology, *in vitro* HYD release, EE, HYD content and yield. HYD content met compendial specifications. Validation of results from the CCD experimental responses of the proposed optimal formulation was performed by comparing predicted and actual responses.

The release kinetics of HYD from formulations were established by fitting the *in vitro* HYD release data to mathematical models. The model that best described that data was established by selecting the model that produced the highest R^2 values.

Stability studies for the optimised formulations were performed in the refrigerator at 4 °C and stability chambers (Binder GmbH[®] Ltd, München, Germany) maintained at 25°C/60% RH and 40°C/75% RH. A stability-indicating HPLC method was used for assessing optimised formulations stability. After 4 weeks of storing at 40°C/75% RH, both optimised formulation had a slight colour change to faint yellow. No significant changes to HYD content, EE and release were observed. SEM results revealed that microspheres remained intact and no signs of brittleness were observed.

In conclusion, DoE using CCD was successfully applied to study the effect of formulation variables on several responses and the results obtained were used for optimisation studies. Further studies would include *in vivo* comparative release studies using a developed artificial digestive system.

CHAPTER 7

RESIDUAL SOLVENT DETERMINATION BY GAS CHROMATOGRAPHY

7.1 INTRODUCTION

Chromatography is an analytical technique which is based on the separation of molecules due to differences in their structure and/or composition [503,504]. Chromatography comprises moving a sample through the system to be separated into its various components over a stationary phase [505]. The molecules in the sample will have different interactions with the stationary support, leading to separation of similar molecules [503]. Chromatographic separations can be divided into several categories based on the mobile and stationary phases used, *viz.* TLC, gas chromatography (GC), paper chromatography and HPLC [503].

GC, a unique and versatile technique, is a physical separation technique in which components of a mixture are separated using a mobile phase of inert carrier gas and a solid or liquid stationary phase contained in a column [130,504,506–508]. The separation is based on the boiling point of the compound and interactions of the vaporised components in a mixture with the stationary phase as they are moved along by the mobile phase [503,509]. GC is one of the most widely used technique for analysing non-polar, semi-polar volatile and semi-volatile compounds. It is, thus, a very powerful tool for analysis of residual solvents [510]. It utilises gas as a mobile phase whilst the stationary phase can either be a solid or a non-volatile liquid and it is mainly applicable to volatile thermally stable compounds or compounds which can undergo derivatization reactions to thermally stable products [504,511].

Residual solvents, after manufacturing of microspheres by solvent evaporation, should be assessed using validated GC method(s) [102,435]. All chromatographic systems have a mobile phase that transports the analytes through the column and a stationary phase coated onto the column or on the resin beads in the column [435]. Acetone and *n*-hexane were used when the solvent evaporation method was applied to the manufacture of HYD microspheres. The development and validation of GC methods for these solvents were deemed necessary to quantify residual solvents in the formulated HYD microspheres.

7.2 INSTRUMENT OVERVIEW

7.2.1 Carrier gas

The carrier gas must be chemically inert and, therefore, should contribute minimally to the partitioning process. Commonly used gases include nitrogen, helium, argon and carbon dioxide, which are selected on the basis of inertness, dryness, type of detector, safety, cost, accessibility and availability [130,504,507]. The choice of carrier gas is often dependent upon the type of detector which is used [130,512]. The carrier gas system contains a molecular sieve to remove water and other impurities. The selection and linear velocity of the carrier gas will affect resolution and retention times. The optimal carrier gas linear velocity is characteristic for each gas [504].

7.2.2 Injector

Injectors are used to introduce the sample into the column [130,503,513]. Sample injection is of fundamental importance to the quality of the chromatographic analysis with GC. The most common injection method is where a microsyringe is used to inject a sample through a rubber septum into a flash vaporiser port at the head of the column [513].

The injector can be used in split or splitless mode and contains a heated chamber containing a glass liner into which the sample is injected through the septum. The sample vaporises to form a mixture of carrier gas, vaporised solvent and vaporised solutes [507].

7.2.3 Column (packed or capillary)

The column plays a crucial role in separating samples into their constituent components and is considered the heart of GC [503,514]. In GC, retention of analyte molecules occurs due to stronger interactions with the stationary phase than the mobile phase. The interactions can be categorised into three main types, *viz.* dispersive, dipole and hydrogen bonding. Columns vary in length and internal diameter and can either be packed or capillary [513].

7.2.3.1 Packed column

Packed columns are usually made from glass which is silanized to remove polar silanol (Si-OH) groups from its surface [310]. These columns have an internal diameter range from 2 to 5 mm. The columns are packed with particles of a solid support which are coated with liquid in the stationary phase. The most commonly used support is diatomaceous earth made mainly of

calcium silicate [310]. They are packed with a solid support coated with immobilised liquid stationary phase material. Most packed columns are 1.5 – 10 m in length and have an internal diameter of 2 – 4 mm [130,310,507,514].

7.2.3.2 Capillary columns

Capillary columns are made from fused silica, usually coated on the outside with polyamide to give the column flexibility [130]. Most capillary columns are 10 -120 m in length and have an internal diameter of 0.15 - 0.5 mm [130,507]. The wall of the column is coated with the liquid stationary phase. The most common coating type is organo-silicone polymers based [310]. Capillary columns are long hollow silica tubes with the inside wall of the column coated with immobilised liquid stationary phase material of various film thicknesses [310,513].

7.2.4 Column oven

The performance and response of the chromatograph columns and the detectors are very susceptible to changes in temperature [511]. Therefore, an oven is designed to insulate these components from the effects of ambient temperature changes and maintain a very stable temperature internally [503,507]. GC performance is directly correlated to the temperature stability of the columns and detector [511].

The oven heats rapidly to give excellent thermal control and heat is distributed throughout the oven using a fan [310]. The oven is cooled using a fan and vent arrangement usually at the rear of the oven [310]. A hanger or cage is usually included to support the GC column and to prevent it touching the oven walls as this can damage the column [310].

7.2.5 Detector

There are many detectors which can be used in GC [137]. Different detectors will give different types of selectivity [130]. A non-selective detector responds to all compounds except the carrier gas. A selective detector responds to a range of compounds with a common physical or chemical property and specific detectors respond to a single chemical compound [515]. Detectors can also be grouped into concentration dependent detectors and mass flow dependent detectors [515]. The signal from a concentration dependent detector is related to the concentration of solute in the detector and does not usually destroy the sample. Mass flow dependent detectors usually destroy the sample and the signal is related to the rate at which solute molecules enter the detector [515].

The detector responds to a physicochemical property of the analyte, amplifies this response and generates an electronic signal for the data system to produce a chromatogram [514]. Many different detector types exist and the choice is based mainly on the application, analyte, required sensitivity and whether quantitative or qualitative data is required [130]. The detector choices include Flame Ionization (FID), Electron Capture (ECD), Flame Photometric (FPD), Nitrogen Phosphorous (NPD), Thermal Conductivity (TCD) and Mass Spectrometer (MS) [130,137,514].

7.2.5.1 Flame ionisation (FID)

Since its introduction in 1958, FID has been the most frequently used detector in GC [509,515,516]. Combustion of an organic compound in a hydrogen/air flame results in a flame rich in electrons and ions [130,508]. When a carbon compound is eluted from the GC column into the hydrogen flame of the detector, a current will pass between electrodes placed near the flame which is held at a suitable potential giving a recordable signal [515,516]. Since the burning of pure hydrogen does not produce ions, the baseline signal of a FID system is near zero and is mostly caused by impurities in the hydrogen and the carrier gas [512].

7.2.6 Monitor

The monitor is usually computerised to ensure visual analyses of results obtained from the separation process. The data system can also be used to perform various quantitative and qualitative operations on the chromatogram. Figure 7.1 shows the schematic diagram of the major components of a gas chromatogram.

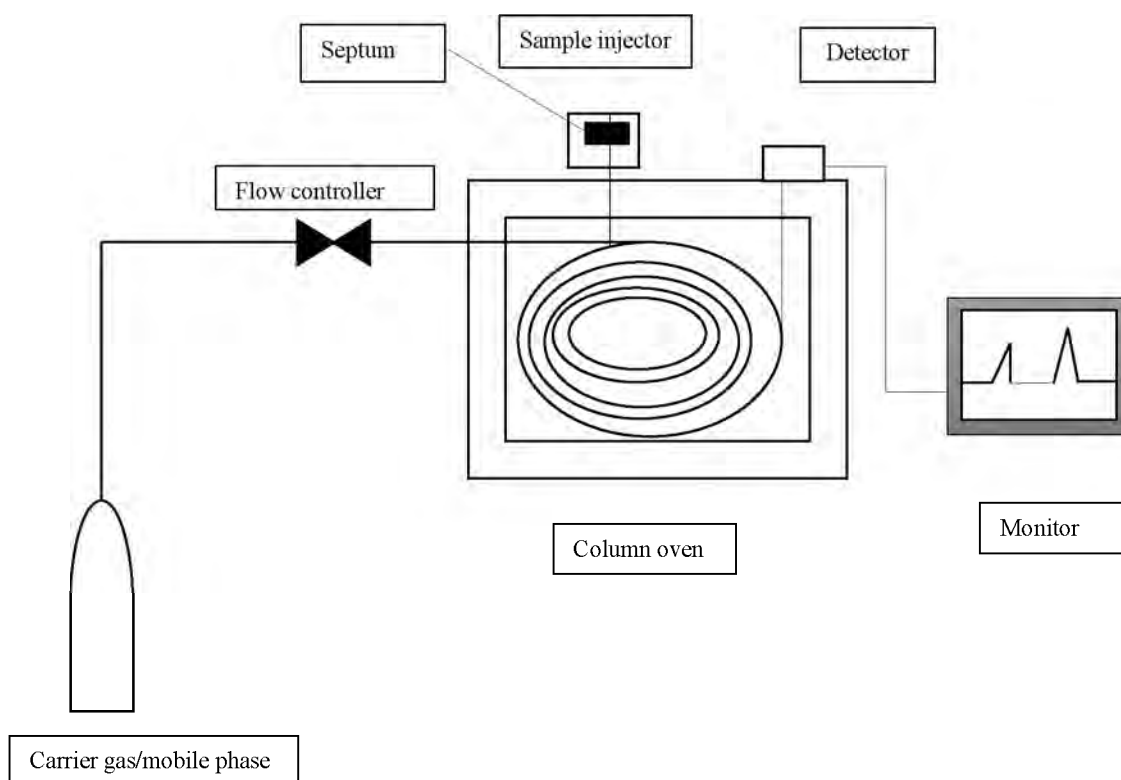


Figure 7.1 Schematic diagram of components of a typical GC (adapted from [130,310,513])

7.3 SOLVENT CLASSIFICATION

According to the British Pharmacopoeia (BP), Solvents are classified into four classes [38]. Class 1 solvents are known carcinogens and are strongly suspected of being harmful to humans and the environment. Class 2 solvents are non-genotoxic animal carcinogens and should be limited in pharmaceutical products because of their inherent toxicity. Class 3 solvents have low toxic potential to humans and should be used only where it would be impractical to remove them, and class 4 solvents are those for which no adequate toxicological data have been found [38,510,517]. Residual solvents are organic volatile chemicals that are used or produced in the manufacture of active substances or excipients, or in the preparation of medicinal products [38]. No therapeutic benefit are achieved from residual solvents, therefore all residual solvents should be removed to the extent possible to meet product specifications, good manufacturing practices, or other quality-based requirements [38]. Permitted daily exposure (PDE) is defined in the present guideline as a pharmaceutically acceptable intake of residual solvents [38]. Table 7.1 indicates the classification of compounds into three classes. Hexane and acetone are classified into class 2 and 3 with concentration limits of 290 and 5000 ppm respectively. They

were used during the manufacturing of microspheres by solvent evaporation technique. Acetone was used to dissolve the drug and polymers and *n*-hexane was used to harden and wash microspheres.

Table 7.1 Classification of residual solvents (adapted from [38])

| Class | Reasons | Examples | PDE | CL |
|-------|--|------------------------|-------------|---------|
| 1 | Solvents to be avoided. Known human carcinogens and strongly suspected human carcinogens and environmental hazards. | Benzene (carcinogenic) | 0.02 mg/day | 2 ppm |
| 2 | Solvents to be limited. Non-genotoxic animal carcinogens or possible causative agents of other irreversible toxicity such as neurotoxicity or teratogenicity | <i>n</i> -hexane | 2.9 mg/day | 290 ppm |
| 3 | Solvents with low toxic potential. Solvents with low toxic potential to man and no health-based exposure limit is needed | acetone | 50 mg/day | 5000ppm |

PDE- Permitted Daily Exposure, CL- Concentration limit

7.3.1 Analytical procedures

Validated GC technique is used to determine levels of residual solvents. If only Class 3 solvents are present, a non-specific method such as loss on drying may be used [38].

7.4 PUBLISHED GC ANALYTICAL METHODS FOR ACETONE AND HEXANE

Several methods have been reported for the determination of acetone and/or hexane in compounds [130,518–522]. A literature review of these methods was performed to give an insight into the type of columns, internal standards, detectors and mobile phases used. Most published methods used FID as the detector of choice, therefore FID was selected in this study. A summary of analytical methods that have been used for the determination of acetone and/or hexane are shown in Table 7.2.

Table 7.2 Summarised published GC methods for acetone and hexane

| CG | Column | FR (mL/min) | R _t (minutes) | Detector | LOD | IS | Ref |
|----------|---|-------------|---|----------|---------------------|--------------------------|-------|
| Nitrogen | Carbowax CG 745 [®] column (30 m x 0.53 mm) | 8 | Acetone= 1.2 <i>n</i> -propanol=2.9 | FID | 0.1 mg/L | <i>n</i> -propanol | [520] |
| Helium | CPWax 57 CB (WCOT Fused Silica), 25 m x 0.25 mm ID, DF = 0.2 µm. | 1.5 | Acetone=2.02 propanol=5.26 | FID | 0.75 mg/L | 1-propanol | [523] |
| Nitrogen | ZB-1 megabore column (30 m x 0.53 mm ID x 5 µm film thickness) | 2.5 | <i>n</i> -hexane= 6 Isooctane=10 | FID | | Isooctane | [524] |
| Helium | Rtx-1301, fused-silica, crossbound 6% cyanopropylphenyl-94% dimethyl polysiloxane (30 m x 0.53 mm, 3-µm film thickness, Restek, Bellefonte, PA) | 3.3 | Hexane= 7.9 Propanol=8.4 | FID | 14.5 ppm | <i>n</i> -propanol | [525] |
| Nitrogen | Carbopack C 80-100 mesh, 0.8% THEED (1 m x 3.17 mm ID). | 60 | Acetone=0.24 Oxitol=1.96 | FID | 0.023 nmol | Oxitol | [519] |
| Nitrogen | Carbowax 25 m x 0.3 mm ID x 0.4 µm film thickness | 55 | - | FID | 0.0055 mg/100 mL | - | [521] |
| Helium | DB-624 (100%dimethylpolysiloxane 30.0 m x 0.53 mm ID, 3.0 µm d.f. Capillary) | 2.8 | Acetone=6.0 Toluene= 15.4 | FID | 3.17 - 4.08 | toluene | [517] |
| Hydrogen | BAC1 15 m x 250 µ x 1.4 µm | 10 | Acetone= 0.98 <i>n</i> -hexane=1.03 <i>n</i> -propyl alcohol (IS)= 1.08 | FID | - | <i>n</i> -propyl alcohol | [526] |
| Helium | DB-5ms column (Agilent) capillary column of 30 m x 0.25 mm ID, 0.25 µm film thickness | 1 | - | MSD | - | diazinon | [527] |
| Helium | 30 m, 0.25 mm ID, 0.25 mm film HP-5MS fused-silica capillary column | 1 | Acetone= 9.2 Oxime=15.1 | MSD | 6.5nM | oxime | [518] |
| Nitrogen | 30 m x 0.32 mm, 1.8 µm GC column | 1 | <i>n</i> -hexane 8.6 | FID | - | - | [528] |

CG-carrier gas, FR-Flow rate, R_t- retention time, FID-flame ionisation detector, IS- internal standard, MSD-mass selective detector, ID- internal diameter

7.5 EXPERIMENTAL

7.5.1 Aim

The aim of these studies was to develop and validate GC methods for analysis of residual solvents in optimised laboratory scale formulations.

7.5.2 Materials and instrumentation

HPLC grade acetone and *n*-hexane were purchased from Merck[®] Laboratories (Merck[®], Wadeville, South Africa) and VWR[®] Chemicals respectively. Acetophenone was purchased from Saarchem[®] (Muldersdrift, South Africa). All other chemical reagents were of analytical grade and no further purification was performed.

The GC-FID system was performed on Agilent 7820A equipped with a flame ionisation detector (Agilent Technologies, California, USA). Data acquisitions were performed using an Agilent software (Agilent Technologies, California, USA). Helium was used as a mobile phase whilst hydrogen and air were used as auxiliary FID gases.

7.6 METHOD DEVELOPMENT

Method development is the process of proving that an analytical method is acceptable for intended use [504]. Several steps are considered for GC method development, *viz.* column selection, carrier gas selection, flow rate, temperature programming, injector temperature and detector temperature [504]. GC is a sensitive, accurate, reproducible, quantitative and versatile tool well adapted for the analysis of complex mixtures [504,529].

7.6.1 Column selection

Most columns in Table 7.2 were not available or accessible, therefore a trial and error method was used for column selection.

7.6.2 Internal standard selection

Different compounds were studied as potential internal standards (IS). Table 7.3 shows summarised results for different volatile compounds tested as potential IS. Tailing is usually associated with wrong columns [530] and it is usually expensive to keep trying new columns and different available compounds were therefore assessed as potential IS. The IS were chosen

on their similarities with either acetone or hexane. Heptane was chosen as the IS of choice as the peak was symmetrical and well resolved from acetone and *n*-hexane.

Table 7.3 Summarised compounds tested as potential IS

| COMPOUND | R _t | COMMENTS |
|---------------|----------------|---|
| Ethyl acetate | 1.8 | Too close to acetone and <i>n</i> -hexane |
| Pentane | 2.8 | Co-elution with <i>n</i> -hexane |
| Butane | 2.6 | Broad peak with tailing |
| Heptane | 4.6 | Well resolved from <i>n</i> -hexane and acetone but tailing |
| Ethanol | 5.5 | Well resolved from <i>n</i> -hexane and acetone and less tailing compared to that of heptane, therefore ethanol was selected to be the IS |

R_t-Retention time (minutes)

7.6.3 Solvent selection

Different solvents were tried based on their stability, effects on analyte peak shapes, boiling point and R_t. Most of the solvents had a R_t greater than those of the analytes of interest because of their higher boiling point. An appropriate solvent should be well resolved from compounds of interest and should not interfere with quantitation of the analyte. It should show stability by having less injection to injection variations.

Table 7.4 Different solvents tried on the ZB-Wax column

| Solvent | R _t | Comments |
|--------------|----------------|---|
| Butanol | 11.789 | Tailing of both <i>n</i> -hexane and ethanol |
| Cyclopentane | 4.4 | Tailing of acetone |
| Toluene | 9.8 | Tailing of acetone |
| Kerosene | 8.6-16.9 | Stability problems |
| Acetophenone | 12.88 | Fronting of ethanol which could be resolved by reducing the concentration of ethanol or increasing split ratio. |

R_t-Retention time (minutes)

7.6.4 System suitability testing

System suitability tests are an integral part of both gas and liquid chromatographic methods [39,504], and are used to verify that detection sensitivity, resolution and reproducibility of the chromatographic system are adequate for the analysis to be done [39]. Factors such as peak resolution, number of theoretical plates, peak tailing and capacity have been measured to determine the suitability of the used method [39,504].

7.6.4.1 Resolution

The degree of separation for an adjacent peak pair is described by the resolution and characterised by the distance between the signals relative to the signal width [513]. The

resolution, R_s , was calculated using Equation 2.4. A resolution of 1 is usually sufficient for qualitative analysis and resolution of ≥ 1.5 is desirable for quantitative analysis [116,509].

Table 7.5 summarises the resolution between all peaks of interest. The results are all above 1.5 showing that there is high resolution between the compounds of interest. R_s is dimensionless as both R_t and width are recorded in minutes. R_s should be > 5 [504] and all the resolution results were $\gg 5$, indicating that the peaks were well resolved.

Table 7.5 Summarised resolutions values between compounds of interest

| Compounds | Acetone and ethanol | Ethanol and acetophenone | <i>n</i> -Hexane and acetophenone |
|------------|---------------------|--------------------------|-----------------------------------|
| Resolution | ~50 | ~184 | ~642 |

7.6.4.2 Theoretical number of plates (N)

N is used to determine column efficiency [531]. It divides the continuous separation process in a number of discrete individual steps. Thus, the column consists of many consecutive segments, called theoretical plates, and for each plate an equilibrium between the solute in the stationary and mobile phase is assumed [513]. The height of a plate (H) and N are derived from the chromatogram using the R_t of a test solute and a measure for the peak width [513]. Equation 2.1 was used to calculate N .

The N values for acetone, *n*-hexane, ethanol and acetophenone were found to be approximately 60 570, 31 690, 22 597 and 201 490 plates respectively. N should be > 2000 [504] and all the N values are $\gg 2000$, therefore the system was deemed suitable for the analytes. The high values of N indicate that the method is suitable for the chromatographic analysis of these compounds.

7.6.4.3 Selectivity factor

The selectivity factor varies with temperature and stationary phase [532]. If two analytes co-elute at the same R_t on a column, they are not separated [513]. The separation factor, α , is the ratio of the adjusted R_t of two adjacent peaks. Equation 2.6 was used to calculate selectivity factor(s).

Table 7.6 shows the summarised selectivity factors between the compounds of interest. All the values are > 1 indicating that the methods were selective and the compounds well resolved.

Table 7.6 Summary of selectivity factor values

| Compounds | Selectivity factor |
|-----------------------------------|--------------------|
| Acetone and ethanol | ~1.8 |
| Ethanol and acetophenone | ~7.5 |
| <i>n</i> -Hexane and acetophenone | ~6.5 |

7.6.5 Optimised chromatographic conditions

Studies were performed to establish the best chromatographic conditions taking into account the various process parameters variables, viz. mobile and stationary phase, flow rate, temperature programming, injector temperature and detector temperature that could affect the separation technique. Different columns (§7.6.1), different temperature programs as well as different flow rates were tested and optimised. Literature review indicates that most GC methods are optimised using trial and error method [520,524] which is significantly different from HPLC method optimisation (§2.7).

7.6.5.1 Optimised chromatographic conditions for Acetone

The GC separation optimised chromatographic conditions were achieved using an Agilent GC 7820A (Agilent Technologies, California, USA) equipped with a FID, performed using ZB-Wax column with dimensions of 30 m length, 0.32 mm ID and 0.25 µm film thickness with an injection volume of 1 µL. The oven temperature was started at 30 °C and held for 8 minutes. Then it was raised to 170 °C at the rate of 20 °C/min and held at 170 °C for 2 minutes. Helium was used as a carrier gas with a constant flow rate of 1.6 mL/min with split mode 1:15. The injector temperature and the detector temperature were kept at 180 °C and 250 °C respectively. Data acquisition and processing were conducted using GC Agilent solution software (Agilent Technologies, California, USA). The optimised chromatographic conditions for acetone are summarised in Table 7.7.

7.6.5.2 Optimised chromatographic conditions for *n*-Hexane

The GC separation optimised chromatographic conditions were achieved using Agilent GC 7820A (Agilent Technologies) equipped with a FID, performed using DB 5 (-60 °C-425 °C) column with dimensions of 30 m length, 0.32 mm ID and 0.25 µm film thickness with an injection volume of 1 µL. All samples were introduced into the GC system manually using a 10 µL microsyringe. The oven temperature was started at 40 °C and held for 8 minutes. Then it was raised to 170 °C at the rate of 20 °C/min and held at 170 °C for 2 minutes. Helium was used as a carrier gas with a constant flow rate of 2.2 mL/min with split mode 1:15. The injector

temperature and the detector temperature were kept at 170 °C and 300 °C respectively. Data acquisition and processing were conducted using GC Agilent solution software. The optimised chromatographic conditions for both acetone and *n*-hexane are summarised in Table 7.7. Figure 7.2 and 7.3 show the typical chromatograms obtained when acetone and *n*-hexane were analysed using the optimised chromatographic conditions summarised in Table 7.7.

Table 7.7 Optimised chromatographic conditions for acetone and n-hexane

| Parameter | Acetone | n-hexane |
|-------------------------------------|--|---|
| Column | Zebtron® (ZB WAXplus 30 m x 0.32mm x 0.25µm) | DB 5 (30m x 0.32mm x 0.25µm) |
| Detector | FID | FID |
| Temperature set point (°C) | 30 | 40 |
| Injection temperature (°C) | 180 | 170 |
| Mode | Split | Split |
| Split ratio | 15:1 | 15:1 |
| Mobile phase (He) flow rate | 1.6 mL/min | 2.2 mL/min |
| Average velocity | 26.755 cm/sec | 35.216 cm/sec |
| Detector gas: | | |
| <i>H₂ flow</i> | <i>30 mL/min</i> | <i>30 mL/min</i> |
| <i>Air flow</i> | <i>400 mL/min</i> | <i>400 mL/min</i> |
| Detector temperature (°C) | 250 | 300 |
| Mobile phase | Helium | Helium |
| Make up (N ₂) flow rate | 5 mL/min | 5 mL/min |
| Injection volume | 1 µL | 1 µL |
| Injection mode | Manual | Manual |
| <i>R_t (minutes)</i> | <i>acetone 3.1</i> <i>ethanol 5.5</i> <i>acetophenone (Solvent) 15.5</i> | <i>n-hexane 2.0</i> <i>acetophenone (Solvent) 12.8</i> |

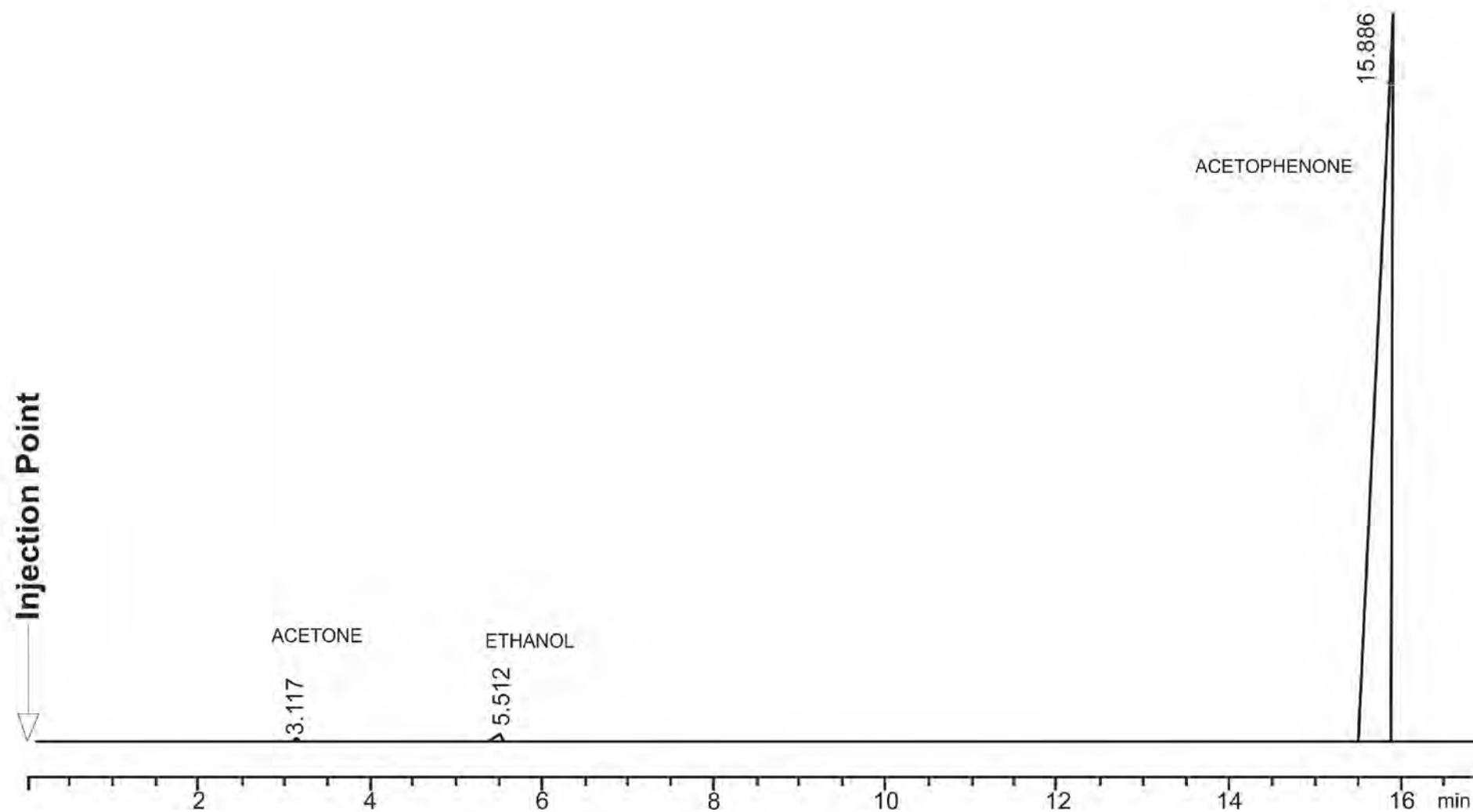


Figure 7.2 Typical chromatogram obtained of 1000 ppm acetone and 8 g/L ethanol in acetophenone solvent

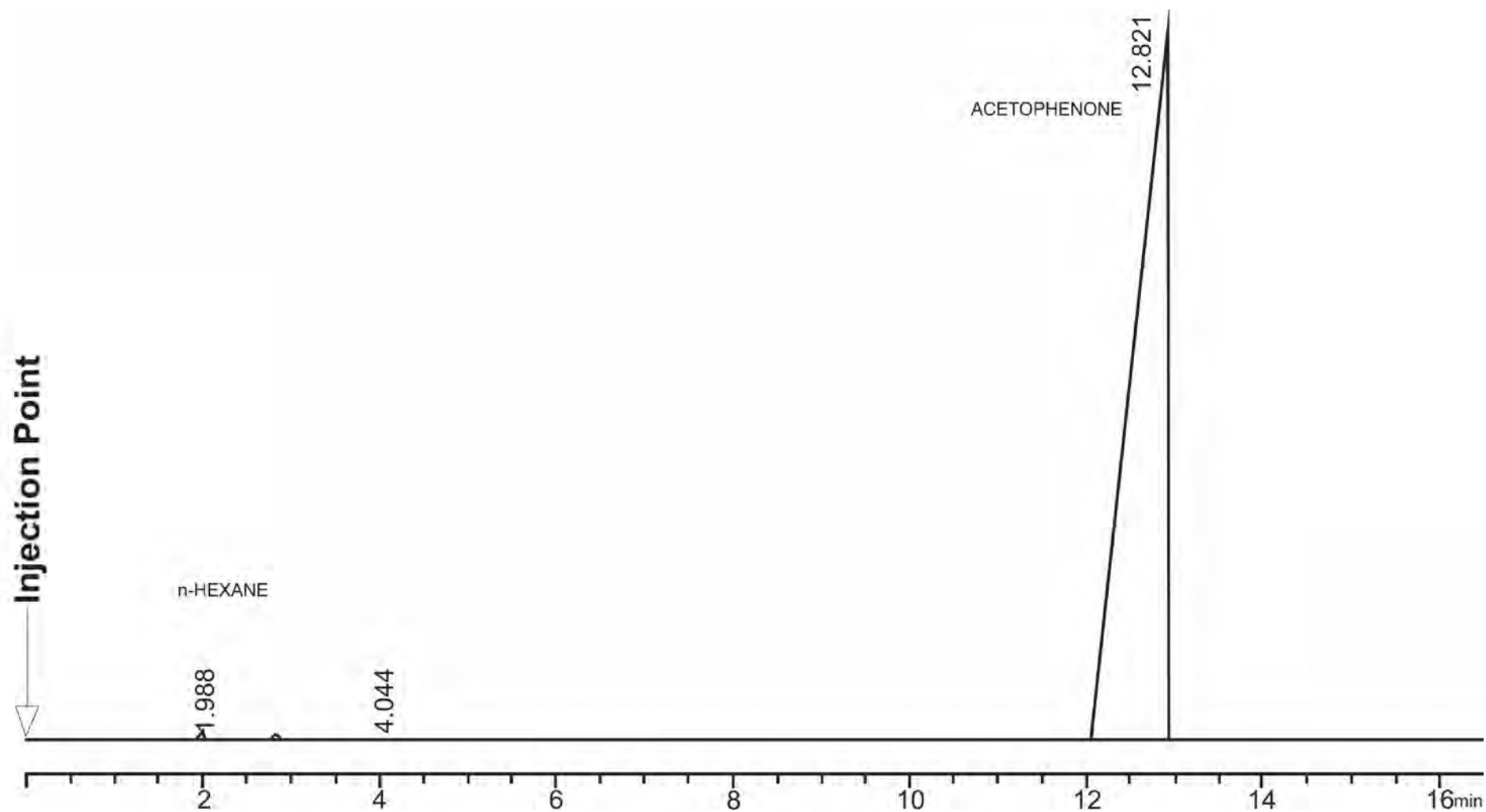


Figure 7.3 Typical chromatogram of 2000 ppm n-hexane in acetophenone solvent

7.7 METHOD VALIDATION

Method validation is the process of proving that an analytical method is acceptable for its intended use [512]. Method validation was performed according to ICH guidelines. The developed methods were validated with respect to linearity, range, precision, detection and quantitation limit. The method validation process was different to that of the HPLC (§2.8).

7.7.1 Linearity and range

The linearity of an analytical procedure is defined as its ability (within a given range) to obtain test results which are directly proportional to the concentration of analyte in the sample [504]. A linear relationship should be evaluated across the range of the analytical procedure [504]. The linearity standards should be prepared by dilution of a standard stock solution of the drug product components, using the proposed procedure and analysed using optimised chromatographic conditions, with a minimum of 3 injections per calibration point and a minimum of five concentrations [504,512]. The range of an analytical method is the interval between the upper and lower levels that have been demonstrated to be determined with precision, accuracy and linearity using the method [504]. A $R^2 > 0.999$ is generally considered acceptable. The y-intercept should be as close to zero as possible or less than a few percent of the response obtained from the targeted level [512].

The linearity for acetone was found in the range of 608 to 12171 ppm using ethanol as IS. Stock solutions of 40000 ppm acetone ($\rho = 0.791\text{ g/mL}$) in acetophenone were prepared by measuring 506 μL of HPLC grade acetone into a 10 mL A-grade volumetric flask. The weight of the pipetted acetone was recorded using Mettler® Model AG135 top-loading analytical balance (Mettler®, Zurich, Switzerland) and used to adjust the calibration curve concentrations. Acetophenone was added to the mark. Calibration curve concentrations were made by serial dilutions in 5 mL A-grade volumetric flasks to which IS was added. Approximately 63.4 μL absolute ethanol ($\rho = 0.789\text{ g/mL}$) was pipetted and added to 5 mL calibration curve solutions to make approximately 10 000 ppm IS concentration. Approximately 2 mL of calibration curve solutions were measured using 1000 μL pipette and transferred into vials. A 10 μL microsyringe was used to measure 1 μL . Manual injections were performed in ascending order of concentrations, viz. 608, 1825, 4260, 6085 and 12171 ppm.

The calibration curve was obtained by plotting PAR (§2.8.3) and the equation for the best-fit least squares regression line obtained was $y=0.0002x - 0.0383$ with a R^2 of 0.9962 as shown

in Figure 7.4. The y-intercept of 0.0383 was close to zero, which satisfies the specific criteria for linearity that specifies that the y-intercept should be < 2% of the response or near zero [211,212]. All the %RSD obtained for the calibration curve points were < 2%. Table 7.8 shows the summarised data for the calibration curve of acetone.

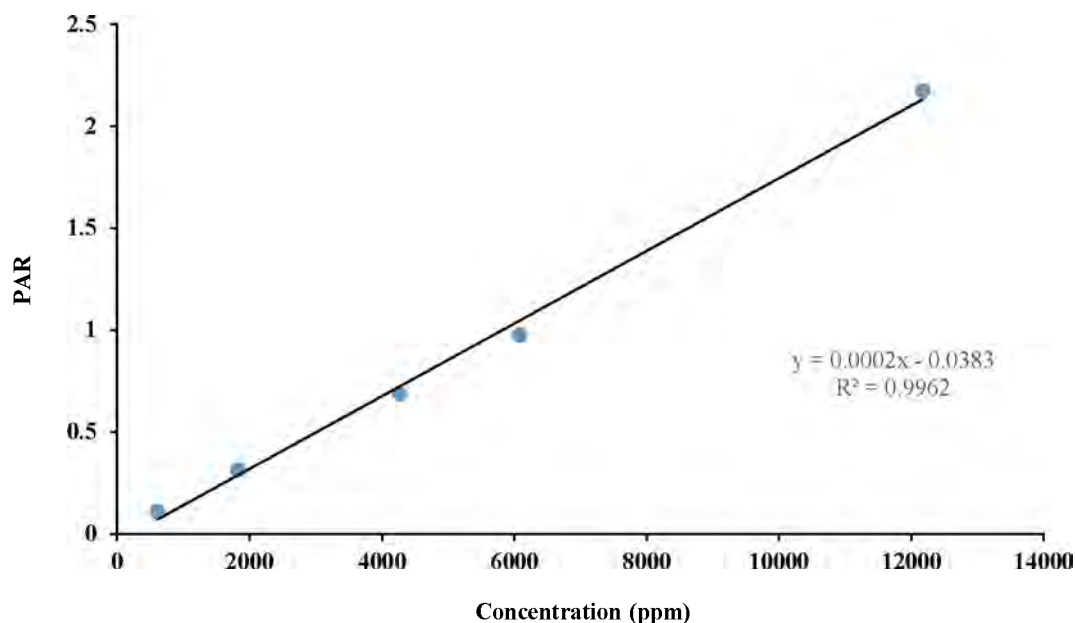


Figure 7.4 Typical calibration curve for acetone in the concentration range 608-12171 ppm

Table 7.8 Typical summarised calibration curve data for acetone over the concentration range 608-12171 ppm (n=3)

| Concentration (ppm) | Average PAR ± SD | %RSD |
|---------------------|------------------|------|
| 608 | 0.1080 ± 0.0004 | 0.33 |
| 1825 | 0.3126 ± 0.0036 | 1.17 |
| 4260 | 0.6873 ± 0.0016 | 0.23 |
| 6085 | 0.9747 ± 0.0051 | 0.53 |
| 12171 | 2.1727 ± 0.0324 | 1.49 |

The linearity for *n*-hexane was found in the range of 76 to 1530 ppm (Figure 7.5). Stock solutions of 4000 ppm *n*-hexane were made by pipetting 61.1 µL of HPLC grade *n*-hexane ($\rho = 0.6548\text{g/mL}$) into 10 mL A-grade volumetric flask and adding acetophenone to the mark. The weight of the pipetted *n*-hexane was recorded using Mettler® Model AG135 top-loading analytical balance (Mettler®, Zurich, Switzerland) and used to adjust the calibration curve concentrations. The serial dilution method was used to make the calibration curve concentrations. The calibration curve concentrations were prepared in 5 mL A-grade volumetric flasks. Approximately 2 mL of calibration curve solutions were measured using 1000 µL pipette and transferred into vials. A 10 µL microsyringe was used to measure 1 µL. Manual injections were performed in ascending order of concentrations, viz. 76.5, 229.5, 382.5, 535.5, 765.0 and 1530.0 ppm.

The calibration curve was obtained by plotting concentration against area and the equation for the best-fit least squares regression line obtained was $y = 1.2726x$ with a R^2 of 0.9889. The *n*-hexane calibration curve differ to that in §2.8.3 because no IS was added. The *y*-intercept was set at zero. As shown in Table 7.9, all the %RSD obtained for the calibration curve points were < 5%. The *n*-hexane area was found to directly vary with concentration.

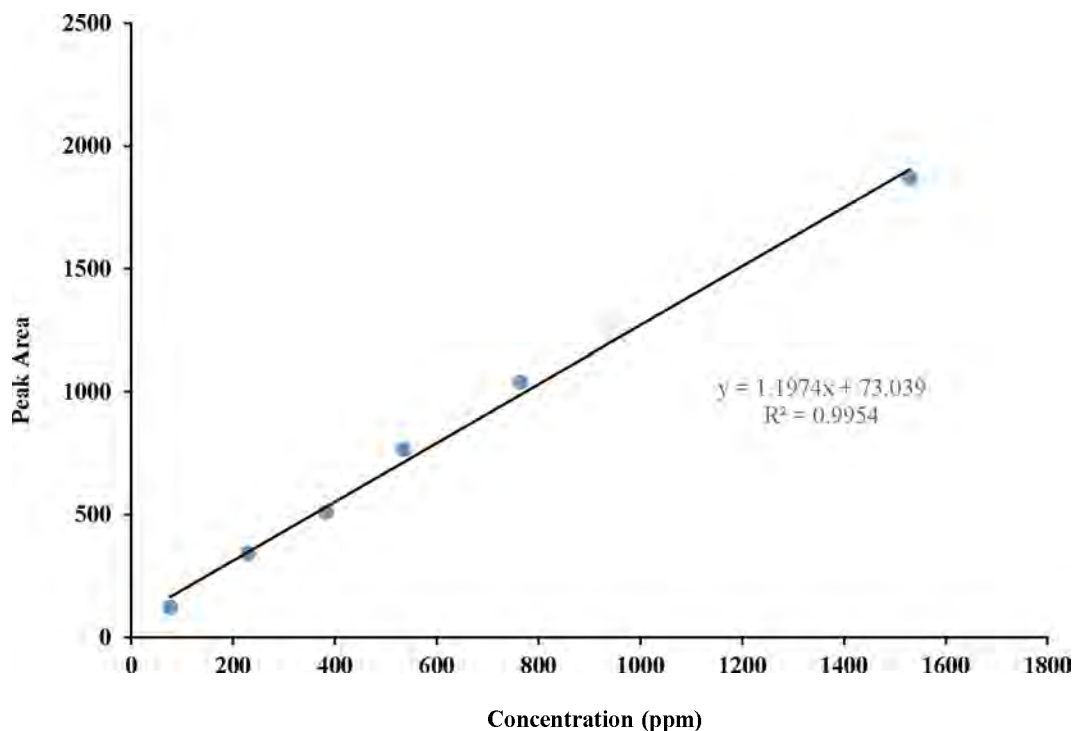


Figure 7.5 Typical calibration curve for *n*-hexane in the concentration range 76-1530 ppm

Table 7.9 Typical summarised calibration curve data for *n*-hexane over the concentration range 76-1530 ppm ($n=3$)

| Concentration (ppm) | Average area \pm SD | %RSD |
|---------------------|------------------------|------|
| 76.5 | 116.4779 \pm 1.0394 | 0.89 |
| 229.5 | 362.0948 \pm 8.8149 | 2.43 |
| 382.5 | 510.0242 \pm 15.8353 | 3.10 |
| 535.5 | 766.9128 \pm 34.1214 | 4.45 |
| 765.0 | 1040.643 \pm 19.5790 | 1.88 |
| 1530.0 | 1818.951 \pm 47.5473 | 2.61 |

7.7.2 Precision

Precision is the measure of agreement or closeness of analyte concentration to each other when the analyses are performed using identical conditions over a short period of time. The precision of the instrument is calculated by multiple injections of one sample solution [512].

7.7.2.1 Intraday precision

The intraday for acetone studies was performed using 4260 ppm, analysed seven times in one day and ethanol as IS. A % RSD of 0.51 was obtained which was < 5%. The average PAR of approximately 0.67 (Table 7.10) was obtained which was close to that obtained from calibration curve results of approximately 0.69, therefore the method was found to be precise for acetone.

Table 7.10 Intraday precision data for acetone

| Concentration (ppm) | Average PAR \pm SD | %RSD |
|---------------------|----------------------|------|
| 4260 | 0.6675 \pm 0.0034 | 0.51 |

The intraday for *n*-hexane studies were performed using 535.5 ppm, analysed seven times in one day as well, without an IS. A % RSD of approximately 4.7 was obtained which was < 5%. The average *n*-hexane area found was lower compared to the one found for the calibration curve showing stability problems with *n*-hexane. Table 7.11 shows the summarised intraday precision data for *n*-hexane.

Table 7.11 Intraday precision data for n-hexane

| Concentration (ppm) | Average area \pm SD | %RSD |
|---------------------|------------------------|------|
| 535.5 | 668.8043 \pm 31.1196 | 4.65 |

7.7.2.2 Inter-day precision

The inter-day precision studies for acetone were performed using 4260 ppm acetone fresh samples in two consecutive days. The % RSD was found to be < 2% and the average PAR was found to be 0.6675 and 0.6623 for the two consecutive days. The summarised data obtained for acetone inter-day precision studies are shown in Table 7.12.

Table 7.12 Inter-day precision data for acetone

| Day | Concentration (ppm) | Average PAR \pm SD | %RSD |
|-----|---------------------|----------------------|------|
| 1 | 4260 | 0.6675 \pm 0.0034 | 0.51 |
| 2 | 4260 | 0.6623 \pm 0.0063 | 0.95 |

The inter-day precision studies for *n*-hexane were performed using 535.5 ppm *n*-hexane fresh samples in two consecutive days. The % RSD was found to be < 5% and the average area was found to be 668 and 653 ppm for the two consecutive days. The summarised data obtained for acetone inter-day precision studies are shown in Table 7.13. The variations could be attributed to the lack of IS in the *n*-hexane GC studies.

Table 7.13 Inter-day precision data for *n*-hexane

| Day | Concentration (ppm) | Average area \pm SD | %RSD |
|-----|---------------------|------------------------|------|
| 1 | 535.5 | 668.8043 \pm 31.1196 | 4.65 |
| 2 | 535.5 | 653.6004 \pm 27.0099 | 4.13 |

7.7.2.3 Retention time (R_t) precision

The R_t is crucial in determining the validity of an analytical method. R_t for all GC studies were recorded and average R_t , standard deviation and %RSD calculated and summarised in Table 7.14. Average R_t of approximately 1.99, 3.13 and 5.51 minutes were found for *n*-hexane, acetone and ethanol respectively. The R_t of acetophenone under acetone and *n*-hexane conditions were found to be 15.90 and 12.87 minutes, respectively. The % RSD for R_t were all $< 2\%$ and thus indicate the reproducibility, validity and precision of the developed GC method.

Table 7.14 Summarised retention times for acetone, *n*-hexane, ethanol and acetophenone

| Compound | AVERAGE $R_t \pm$ SD | %RSD |
|--|----------------------|------|
| Acetone | 3.1275 \pm 0.013 | 0.42 |
| Hexane | 1.9917 \pm 0.021 | 1.03 |
| Ethanol | 5.5063 \pm 0.056 | 1.01 |
| Acetophenone as solvent for acetone | 15.896 \pm 0.019 | 0.12 |
| Acetophenone as solvent for <i>n</i> -hexane | 12.866 \pm 0.043 | 0.33 |

7.7.3 Dead volume

Dead volume is the time needed to transport the solute through the column and is the same for all solutes in a mixture [513]. The dead volume studies were performed to determine if the analytes of interest were retained. The dead volume can be determined based on the R_t of three consecutive *n*-alkanes or other members of a homologous series [513]. GC or HPLC grade *n*-pentane, *n*-heptane and *n*-hexane were analysed under acetone and *n*-hexane chromatographic conditions, except for the split ratio which was set at 1:300 instead of 1:15 and their average R_t recorded and applied in the calculation of dead volume. Equation 7.1 [513] was used to calculate dead volume time (t_M).

$$t_M = \frac{t_{n\text{-pentane}} \times t_{n\text{-heptane}} - t_{n\text{-hexane}}^2}{t_{n\text{-pentane}} + t_{n\text{-heptane}} - 2 \times t_{n\text{-hexane}}} \quad \text{Equation 7.1}$$

The dead volumes were found to be 1.70 and 1.85 minutes under *n*-hexane and acetone chromatographic conditions respectively (Table 7.15). The dead volume for both chromatographic conditions were different mainly due to the difference in mobile phase flow rate. These values were found to be less than the R_t of all analytes of interest.

Table 7.15 Dead volumes for acetone and *n*-hexane

| | |
|---|------|
| Dead volume under acetone chromatographic conditions | 1.85 |
| Dead volume under <i>n</i> -Hexane chromatographic conditions | 1.70 |

7.7.4 Detection limit

LOD is described in §2.8.2. Statistical method or experimental method can be used to determine the LOD [512]. The LOD for acetone and *n*-hexane were set at 912 and 153 ppm with % RSD of 1.1 and 4.4 respectively.

7.7.5 Quantitation limit

LOQ is described in §2.8.2. LOQ should be determined experimentally and should have a % RSD between 10-20%. The LOQ was set as a third of LOD, and therefore the LOQ for acetone and *n*-hexane were 304 and 51 ppm respectively.

7.8 APPLICATION OF GC TO SOLVENT EVAPORATION TECHNIQUES

7.8.1 Acetone extraction studies

Acetone residual analysis was done by extraction method. Approximately 1g of the HYD microspheres was accurately weighed, spiked with 2 mL of acetophenone and vortexed for 30 seconds using a Model G-560E Vortex-Genie2 mixer (Scientific Industries Inc., Bohemia, New York, USA), followed by centrifuging for 10 minutes using Model HN-SII Centrifuge (Damon IEC Division, Bedfordshire, England). The supernatant solution was collected into a 5 mL A-grade volumetric flask. The extraction process was performed three times. An IS was added to the 5 mL and acetophenone used to fill up to the 5 mL mark. Approximately 2 mL was transferred to a clean clear vial and analysis performed using the developed GC method.

7.8.2 *n*-Hexane extraction studies

Hexane residual analysis was done by extraction method. Approximately 1g of the HYD microspheres was accurately weighed, spiked with 2 mL of acetophenone and vortexed for 30 seconds using a Model G-560E Vortex-Genie2 mixer (Scientific Industries Inc., Bohemia, New York, USA), followed by centrifuging for 10 minutes using Model HN-SII Centrifuge (Damon IEC Division, Bedfordshire, England). The supernatant solution was collected into a 5 mL A-grade volumetric flask. Approximately 2 mL was transferred to a clean clear vial and analysis performed using the developed GC method.

7.8.3 Acetone extraction efficiency

The extraction efficiency of acetone was determined using 547 ppm acetone prepared using acetophenone. Approximately 1g of the HYD microspheres was accurately weighed, spiked with 2 mL of 547 ppm acetone in acetophenone. This solution was used to carry out extractions as described in §7.8.1

7.8.4 *n*-Hexane extraction efficiency

The extraction efficiency of *n*-hexane was determined using 535 ppm *n*-hexane prepared using acetophenone. Approximately 1g of the HYD microspheres was accurately weighed, spiked with 2 mL of 535 ppm *n*-hexane in acetophenone. This solution was used to carry out extractions as described in §7.8.2

7.8.5 Results and discussion

The results summarised in Table 7.16 show that the extracted amounts are 232 and 27 ppm for acetone and hexane respectively. This indicates that the drying process was sufficient enough to remove residual solvents. The acetone residual amount was found to be higher, most probably due to the formation of hydrogen bonds with excipients used or encapsulation of acetone into the microspheres. The *n*-hexane residual amount was very low because hexane is a nonpolar compound, and is more likely to form Van Der Waals forces with excipients which are weak bonds compared to hydrogen bonds. Although the boiling point of acetone and *n*-hexane are 56.1 and 68 °C respectively [533], the drying process at 30 °C for 24 hours was sufficient in evaporating these compounds from the formulations. Using solvent extraction method, the average amount of acetone and *n*-hexane found in 1g optimised formulation was approximately 232 and 27 ppm respectively (Table 7.16). The extraction efficiencies for acetone and *n*-hexane in 1g optimised formulation were found to be 5.7 and 1.0 respectively.

Table 7.16 Summarised extractions and limits of acetone and n-hexane

| Acetone | | <i>n</i> -Hexane | | COMMENTS |
|---------|----------|------------------|---------|--|
| Found | Limits | Found | Limits | |
| 232 ppm | 5000 ppm | 27 ppm | 290 ppm | The drying process was sufficient for the removal of acetone and hexane residuals. |

7.9 CONCLUSIONS

A GC method was developed, partially validated and successfully applied to the quantitation of residual solvents, *viz.* acetone and *n*-hexane in microspheres. The method was developed on a trial and error basis. To evaluate if the compounds were unretained or retained, dead volume studies were performed. System suitability testing studies were performed and the results indicate that resolution, *N* and selectivity met required acceptable ranges. Method validation was performed with respect to linearity, range, inter- and intra-day precision, *R*_t precision, LOQ and LOD. Linearity for acetone and *n*-hexane was determined in the range 608 to 12171 ppm and 76.5 to 1530.0 ppm respectively. The method was found to be precise with respect to inter and intra-day and *R*_t precision studies.

The residual amounts of acetone and hexane in 1g formulation were found to be 232 and 27 ppm respectively. These values were below the USP and BP concentration limits indicating that the drying process was sufficient enough to remove these solvents.

In conclusion, developed and validated GC methods have been successfully used in the determination and quantitation of residual solvents. Future studies include research in column selection that could be used to simultaneously detect both acetone and hexane using one column and one IS. The challenge is that *n*-hexane requires the use of columns with a thicker stationary phase. However, the difference in polarity between acetone and *n*-hexane makes it a challenge to maintain the stability of both compounds in one sample. Further studies could include stability studies of the developed method.

CHAPTER 8

CONCLUSIONS

Hypertension is an important medical and public health challenge. Besides being a major risk factor for CVD, it can also lead to kidney failure, blindness, rupture of blood vessels and cognitive impairment. Hypertension is universally underdiagnosed and/or inadequately treated in Sub-Saharan Africa. Regardless of the availability of effective and cost-effective treatment, target blood pressure levels are rarely achieved. The development of new compounds to combat hypertension is time consuming and expensive, and therefore the design and development of SR formulations that can optimise the delivery of existing compounds such as HYD may be an approach to improving the management of patients with hypertension and patients adherence.

HYD is used either alone or in combination for the management of chronic hypertension, chronic cardiac failure and hypertensive crises. HYD has a short plasma half-life and is normally administered two to four times daily. The short half-life of HYD and the need for multiple dosing makes the compound a potential candidate for inclusion in SR formulations.

An isocratic RP-HPLC method for the quantitation of HYD in formulations was developed and optimised using RSM in conjunction with a CCD approach. The optimised method was validated according to ICH guidelines. Design-Expert[®] software was used during method optimisation to generate thirty experiments that considered four key independent factors, *viz.* mobile phase composition, mobile phase pH, buffer molarity and flow rate whilst monitoring dependent factors responses, *viz.* R_t , resolution and peak tailing. The ACN content was varied between 20 and 60% v/v, buffer molarity between 20 and 50 mM, buffer pH between 3 and 5 and flow rate between 0.5 and 1 mL/min. Statistical analysis was used to evaluate the impact and significance of input variables to output variables. The ANOVA data generated revealed that ACN content, buffer molarity and pH had the most significant effects on R_t and the resolution of HYD and PROP. The optimised conditions were well predicted using numerical optimisation and Design-Expert[®] software since the predicted R^2 values were in close agreement with adjusted R^2 values. The optimised chromatographic conditions were: 65% v/v of ACN, 35% v/v of 5mM phosphate buffer adjusted to pH=3.0 mobile phase, at a flow rate of 0.8 mL/min and a column temperature of 25 °C. These yielded a R_t of 5.6 and 8.6 minutes for HYD and PROP respectively. The analytes of interest were well resolved with a resolution of 5.8. The peak tailing for HYD and PROP were found to be approximately 1.3 and 1.1 respectively. The optimised method was linear in the range 0.3-140.0 µg/mL with R^2 of 0.9998.

The LOQ was found to be 0.3 µg/mL and LOD was set at 0.1 µg/mL. The method was found to be precise with intra- and inter-day precision studies showing %RSD ranging from 0.03 to 1.58%. Accuracy was determined by applying the optimised method to the analysis of HYD samples of known purity at low, medium and high concentrations for three consecutive days. The method was found to be accurate as %Bias values were found to be in the range of -3.84 to 2.96%. Specificity studies were performed on commercial tablets, viz. Hyperphen[®] 10, 50 and Sandoz-Hydralazine[®] 25 mg. There were no interfering peaks, therefore the method is selective and specific for the analysis of HYD in pharmaceutical dosage forms. The method was successfully used in the assessment of *in vitro* release and analysis of 50 mg HYD immediate release tablets with approximately 85% drug release within the first hour of dissolution. No interfering peaks were observed indicating that the method was specific for quantitation of HYD as excipients used in Hyperphen[®]-50 did not affect the analysis of HYD.

Forced degradation studies were performed in acidic, alkali, oxidative and photolytic conditions. The results reveal that HYD is susceptible to degradation under alkaline conditions and is oxidised in H₂O₂ solutions. HYD was found to be stable in acidic media and increasing temperature had very slight effects on the rate of degradation. Forced degradation in HCL, H₃PO₄, NaOH, H₂O₂, HPLC water and light indicated that degradants were resolved from HYD peak and that HYD could be qualitatively separated and accurately quantified in the presence of degradation products.

A CCD approach was successfully used for the development of a simple, precise, accurate, rapid, selective and specific RP-HPLC analytical method for HYD and was successfully applied to the analysis of commercially available formulations and can be used for *in vitro* dissolution testing of HYD sustained release microspheres.

HYD was characterised using DSC, TGA, FT-IR, XRPD, SEM, ¹H NMR and ¹³C NMR. The ¹H NMR of HYD revealed a sharp peak at 8.81 ppm that was most likely due to a secondary amine and a doublet between 8.69 – 8.72 ppm that correspond to the primary amine. The multiplets from 8.01 to 8.15 ppm corresponds to 5-protons in the benzene rings. The ¹³C NMR spectrum showed the presence of 8 major signals for the 8 carbons present in HYD. The SEM images revealed that HYD exists as acicular and cylindrical particles. The XRPD patterns show characteristic peaks at a diffraction angle of 2θ = 11, 12, 20, 22, 25, 27, 28, 33 and 39° and that HYD was in its crystallinity form. The FT-IR spectra for HYD revealed resonances at 3429, 3027 and 1668 cm⁻¹ which were assigned to N-H functional group, aromatic C-H and aromatic

C=C stretching respectively. Stuart SMP30 melting point apparatus results indicated that the melting point of HYD was in the range 273 °C to 275 °C. The DSC thermogram for HYD revealed an exotherm peak at 275 °C as HYD melts with decomposition. The TGA thermogram indicates that HYD is stable up to 250 °C after which decomposition process starts in three stages and over a wide range of temperature. Most decomposition of the compound occurs at 275 °C, which is also the melting point of HYD. Complete HYD decomposition (> 90%) occurs at 450 °C, indicating that HYD decomposition occurs over a wide range of temperature. The results observed suggest that it is unlikely that HYD would decompose under normal homogenisation process and storage conditions during which temperatures rarely exceed 100 °C.

Preformulation studies have a significant part in anticipating formulation problems and were performed to determine the compatibility of HYD and excipients. HYD was found to be incompatible with Carbopol® 971P due to the disappearance of amine peak on FT-IR studies and the changes in DSC and TGA thermograms. The amine and carboxylic acid functional groups in HYD and Carbopol® 971P respectively might have reacted to form an amide bond. This incompatibility was confirmed using XRPD. HYD was found to be compatible with Eudragit® RS PO, Methocel® K100LV and Avicel® 101 as the characteristic peaks of HYD were still present in binary mixtures of these excipients and HYD. The DSC, TGA, XRPD and FT-IR studies provided a scientific basis for ensuring the purity, conformation and compatibility of HYD with excipients and therefore further formulation development of HYD microspheres was undertaken without any carbomer polymer.

The oral route of administration of drugs has been the most used and convenient route for drug delivery system. An o/o solvent evaporation technique procedure was used to manufacture HYD sustained release microspheres. The microspheres were characterised for their % yield, drug content, EE, particle size, surface morphology and drug release profile. Dissolution studies were performed using Hanson SR8 No 73-100-104 modified USP Apparatus 1 (Hanson Research, Chatsworth, CA, USA) in 0.1M phosphate buffer dissolution media. All formulations were manufactured with an HPMC-based matrix. The effect of different grades of Methocel® and Eudragit® on HYD release was investigated. Results revealed that formulations manufactured using high viscosity grade Methocel® K100M exhibited lower HYD release after 12 hours of dissolution testing than formulations containing lower viscosity grades of the polymer. Microspheres formed when using Eudragit® RS PO were smoother and

spherical compared to those manufactured using Eudragit® L 100. Consequently, Methocel® K100LV and Eudragit® RS PO were selected as the rate-controlling polymers in subsequent formulation studies. Avicel® 101 was selected as the diluent of choice as diluent screening studies revealed that Avicel® 101 produced smooth and spherical microspheres compared to Avicel® 102 and 103. Of the preliminary formulation studies performed, the formulation which had high EE, sustained release of the drug and maximum HYD release after 12 hours was selected for further formulation optimisation studies.

CCD was used to generate 50 experimental runs to evaluate the effect of independent variables, viz., amount of Methocel® K100LV and Eudragit® RS PO, homogenization speed and time and amount of acetone on the dependent variables. EE, HYD content, % yield and *in vitro* release of HYD. Design Expert® statistical software was used to generate mathematical models and the model that best described the relationship between independent and dependent variables identified. ANOVA was used to generate model equations. Significant factors had a p -value < 0.05 and non-significant factors had a p -value > 0.05 . The polymers were found to have significant effects on HYD release and EE. The polymers, homogenisation speed and the amount of acetone had significant effects on % yield. The normal probability plot of residuals, plot of studentized residuals versus predicted values and Box-Cox plot for power transformation were used for model adequacy testing. The typical release pattern observed for the optimised formulation exhibited an initial burst release during the first 2 hours of dissolution testing, attributed to either the high water solubility of HYD and/or the presence of surface drug on microspheres. The burst release was followed by a slower release rate of HYD. The *in vitro* HYD release data were fitted to mathematical models in an attempt to establish the mechanism of HYD release from microspheres. HYD release from optimised formulations was best described using the Higuchi model. Further studies should include comparison of HYD release profiles using alternative physiologically relevant buffers. The optimised formulations had high EE, HYD content and % yield, justifying the use of an o/o solvent evaporation technique. Both optimised formulations released approximately 90% after 12 hours of dissolution testing in 0.1M phosphate buffer. Dissolution profiles were compared using f_1 and f_2 method. FT-IR, DSC and XRPD were used to characterise HYD in the optimised formulation. The results revealed that HYD was not affected by the manufacturing and drying process as the characteristic peaks of HYD were present in FT-IR and XRPD studies and the exothermic peak of HYD was still present in the DSC thermogram. The optimised formulations were subjected to short-term stability testing for one month at 4 °C, 25°C/60% RH and

40°C/75% RH. The results revealed that there were no significant changes in appearance and physicochemical properties of the microspheres for one month. However, long-term stability studies would be required to determine the shelf-life of the microspheres.

GC methods for the identification and quantitation of residual solvents, *viz.* acetone and *n*-hexane were developed and optimised. Method validation was performed with respect to linearity and range, inter- and intra-day precision, R_t precision, LOQ and LOD. The drying process was deemed appropriate for the formulation studies because the residual amount of acetone and *n*-hexane in 1g HYD microspheres formulation were found to be 232 and 27 ppm respectively. These values were below the USP and BP concentration limits indicating that the drying process was sufficient enough to remove these solvents. These values were < than the PDE. These studies provide an insight on the applicability of GC headspace in quantifying residual solvents in formulations.

In conclusion, sustained release HYD microspheres have been developed, formulated and prepared using an o/o solvent evaporation technique and optimised using CCD approach in these studies. Residual solvents were also quantified. Residual solvent determination can be adapted to other studies that utilises the use of solvents in formulation studies. Future studies should include the development of a once daily dosing technology, which has the potential to address adherence issues experienced in SSA regions. Future studies beyond this work include scale up formulation studies, long-term formulation stability studies and application of this method to water soluble drugs. In addition Simulated gastric fluid (SGF) dissolution studies can be undertaken to facilitate the prediction of HYD release *in vivo*.

REFERENCES

1. U. Kintscher, The burden of hypertension, *EuroIntervention*, 9(3), 12–15 (2013).
2. J. Addo, L. Smeeth, and D. A. Leon, Hypertension in sub-Saharan Africa: a systematic review, *American Heart Association*, 50(6), 1012–1018 (2007).
3. Y. K. Seedat, Control of hypertension in South Africa: time for action, *South African Medical Journal*, 102(1), 25–26 (2012).
4. H. K. Chopra and N. C. Nanda, Textbook of Cardiology (A Clinical and Historical Perspective). London: jaypee brothers medical publishers, 2013.
5. A. Chockalingam, Impact of world hypertension day, *The Canadian Journal of Cardiology*, 23(7), 517–9 (2007).
6. J. Chen, Epidemiology of hypertension and chronic kidney disease in China, *Current Opinion in Nephrology and Hypertension*, 19(3), 278–82 (2010).
7. D. Rossiter and M. Blockman, South African Medicines Formulary, 12th ed. Cape Town: Health and Medical Publishing Group, 2016.
8. T. L. Lemke, D. A. Williams, R. F. Victoria, and W. S. Zito, Foye's Principles of Medicinal Chemistry, 6th ed. Philadelphia: Lippincott Williams and Wilkins, 2012.
9. R. T. Cole, A.P Kalogeropoulos, V. Vasiliki, M. Gheorghiade, A. Quyyumi, C. Yancy, J. Butler, Hydralazine and isosorbide dinitrate in heart failure: historical perspective, mechanisms, and future directions, *Circulation*, 123(21), 2414–2422 (2011).
10. B. K. Nanjwade, H. M. Bechra, V. K. Nanjwade, G. K. Derkar, and F. V. Manvi, Formulation and characterization of hydralazine hydrochloride biodegraded microspheres for intramuscular administration, *Journal of Bioanalysis and Biomedicine*, 3(1), 32–37 (2011).
11. B. G. Katzung, Basic and Clinical Pharmacology, 8th ed. New York: McGraw-Hill Companies, 2001.
12. V. Perkovic, R. Huxley, Y. Wu, D. Prabhakaran, and S. MacMahon, The burden of blood pressure-related disease: a neglected priority for global health, *American Heart Association*, 50(6), 991–997 (2007).
13. F. P. Cappuccio and M. A. Miller, Cardiovascular disease and hypertension in sub-Saharan Africa: burden, risk and interventions, *Internal and Emergency Medicine*, 11(3), 299–305 (2016).
14. P. M. Kearney, M. Whelton, K. Reynolds, P. Muntner, P. K. Whelton, and J. He, Global burden of hypertension: analysis of worldwide data, *The Lancet*, 365(1), 217–223 (2005).
15. Z. A. Anteneh, W. A. Yalew, and D. B. Abitew, Prevalence and correlation of hypertension among adult population in Bahir Dar city, northwest Ethiopia: a community based cross-sectional study, *International Journal of General Medicine*, 8(1), 175–85 (2015).
16. A. Chockalingam, N. R. Campbell, and J. G. Fodor, Worldwide epidemic of hypertension, *The Canadian Journal of Cardiology*, 22(7), 553–555 (2006).
17. World Health Organisation, The global burden of disease: 2004 update, World Health Organization, Geneva, Switzerland (2008).
18. D. T. Lackland and M. A. Weber, Global burden of cardiovascular disease and stroke: hypertension at the core, *Canadian Journal of Cardiology*, 31(5), 569–571 (2015).

19. M. J. Bloch, Worldwide prevalence of hypertension exceeds 1.3 billion, *Journal of the American Society of Hypertension*, 10(10), 753–754 (2016).
20. Y. K. Seedat, Recommendations for hypertension in sub-Saharan Africa, *Cardiovascular Journal of South Africa*, 15(4), 157–8 (2004).
21. G. Antonakoudis, L. Poulimenos, K. Kifnidis, C. Zouras, and H. Antonakoudis, Blood pressure control and cardiovascular risk reduction, *Hippokratia*, 11(3), 114–119 (2007).
22. P. E. Osamor and B. E. Owumi, Factors associated with treatment compliance in hypertension in southwest Nigeria, *Journal of Health, Population and Nutrition*, 29(6), 619–628 (2011).
23. S. Omoleke, S. Sambou, I. Abubakar, and A. L. Oyeyemi, Hypertension- the major cause of morbidity, hospitalisation and mortality among non-communicable diseases in the Gambia, *International Journal of Tropical Disease and Health*, 4(6), 661–671 (2014).
24. R. N. Peck, E. Green, J. Mtabaji, C. Majinge, L. R Smart, J. A Downs, D. W Fitzgerald, Hypertension-related diseases as a common cause of hospital mortality in Tanzania: a 3-year prospective study, *Journal of Hypertension*, 31(9), 1806–11 (2013).
25. S. Barron, K. Balanda, J. Hughes, and L. Fahy, National and subnational hypertension prevalence estimates for the Republic of Ireland: better outcome and risk factor data are needed to produce better prevalence estimates, *BMC Public Health*, 14(24), 1–10 (2014).
26. K. Steyn and A. Damasceno, Lifestyle and related risk factors for chronic diseases. The International Bank for Reconstruction and Development, 2006.
27. S. Bromfield and P. Muntner, High Blood Pressure: The leading global burden of disease risk factor and the need for worldwide prevention programs, *Current Hypertension Reports*, 15(3), 134–136 (2013).
28. R. Norman, T. Gaziano, R. Laubscher, K. Steyn, and D. Bradshaw, Estimating the burden of disease attributable to high blood pressure in South Africa in 2000, *South African medical journal*, 97(8), 692–698, 2007.
29. R. Harvey and P. C. Champe, Lippincott's Illustrated Reviews: Pharmacology, 4th ed. Philadelphia: Lippincott Williams and Wilkins, 2009.
30. J. T. Dipiro, R. L. Talbert, G. C. Yee, G. R. Matzke, B. G. Wells, and L. M. Posey, Pharmacotherapy A pathophysiologic Approach, 7th ed. New York: McGraw-Hill Companies, 2008.
31. S. Ummadi, B. Shravani, N. G. R. Rao, M. S. Reddy, and B. Sanjeev, Overview on controlled release dosage form, *International Journal of Pharma Sciences*, 3(4), 258–269 (2013).
32. G. Tiwari, S. Ruchi, B. Birendra, L. Bhati, L. S. Pandey, P. Pandey, S. K Bannerjee, Drug delivery systems: an updated review, *International Journal of Pharmaceutical Investigation*, 2(1), 2–11 (2012).
33. P. Mandhar and G. Joshi, Development of sustained release drug delivery system: a review, *Asian Pacific Journal of Health Sciences*, 2(1), 179–185 (2015).
34. P. Nidhi, C. Anamika, S. Twinkle, S. Mehul, J. Hitesh, and U. Umesh, Controlled drug delivery system: a review, *Indo American Journal of Pharmaceutical Sciences*, 3(3), 227–233 (2016).
35. P. R. Alli, P. B. Bargaje, and N. S. Mhaske, Sustained release drug delivery system: a modern formulation approach, *Asian Journal of Pharmaceutical Technology and Innovation*, 4(17), 108–118 (2016).
36. M. Kandler, G. Mah, A. Tejani, S. Stabler, and D. Salzwedel, Hydralazine for essential hypertension (Review), *The Cochrane Collaboration*, 1(11), 1–18 (2011).

37. Klaus Florey, *Analytical Profiles of Drug Substances* volume 8. New Jersey: Academic Press, 1979.
38. British Pharmacopoeia Commission Office, *British Pharmacopoeia*. The Stationery Office, 2012.
39. United States Pharmacopoeial Convection Inc., *United States Pharmacopoeia-National Formulary [USP-39/NF-33]*. 2016.
40. L. X. Yu *et al.*, Biopharmaceutics classification system: the scientific basis for biowaiver extensions, *Pharmaceutical Research*, 19(7), 921–925 (2002).
41. B. Vikaas and N. Arun, The biopharmaceutical classification system (BCS): present status and future prospectives, *International Research Journal of Pharmacy*, 3(9), 7–11 (2012).
42. M. P. Wagh and J. S. Patel, Biopharmaceutical classification system: scientific basis for biowaiver extensions, *International Journal of Pharmacy and Pharmaceutical Sciences*, 2(1), 12–19 (2010).
43. M. Säkkinen, Biopharmaceutical evaluation of microcrystalline chitosan as release-rate-controlling hydrophilic polymer in granules for gastro-retentive drug delivery, Citeseer, 2003.
44. World Health Organisation, Proposal to waive in vivo bioequivalence requirements for the WHO Model List of Essential Medicines immediate release , solid oral dosage forms (2005).
45. S. C. Sweetman, *Martindale: the complete drug reference*, 33th ed. London, 2002.
46. S. Imad, S. Nisar, and Z. T. Maqsood, A study of redox properties of hydralazine hydrochloride, an antihypertensive drug, *Journal of Saudi Chemical Society*, 14(3), 241–245 (2010).
47. C. C. Okeke, Stability of hydralazine hydrochloride in both flavored and nonflavored extemporaneous preparations, *International Journal of Pharmaceutical Compounding*, 7(4), 313–319 (2003).
48. World Health Organisation, *Accelerated Stability Studies of Widely Used Pharmaceutical Substances Under Simulated Tropical Conditions*, Geneva, Switzerland (2015).
49. S. Kumar, *Spectroscopy of Organic Compounds*, *Department of Chemistry*, 66, 1–36 (2006).
50. M. N. Dole, P. A. Patel, S. D. Sawant, and P. S. Shedpure, Advance applications of fourier transform infrared spectroscopy, *International Journal of Pharmaceutical Sciences Review and Research*, 7(2), 159–166 (2011).
51. K. R. Mahadik, B. S. Kuchekar, and K. R. Deshmukh, *Concise organic pharmaceutical chemistry : Pharmaceutical chemistry 11*. Nirali Prakashan, 2008.
52. D. Sriram and P. Yogeeswari, *Medicinal Chemistry*, 2nd ed. Pearson, 2010.
53. V. Šunjić and V. Petrović Peroković, *Organic chemistry from retrosynthesis to asymmetric synthesis*. Springer International Publishing, 2016.
54. N. G. Rathod and M. V Lokhande, Development and characterisation of process related impurity in hydralazine hydrochloride by some analytical technique, *Journal of Applicable Chemistry*, 3(5), 2011–2019 (2014).
55. S. Halasi and J. G. Nairn, Stability studies of hydralazine hydrochloride in aqueous solutions, *Journal of Parenteral Science and Technology*, 44(1), 30–4 (1989).
56. V. Das Gupta, K. R. Stewart, and C. Bethea, Stability of hydralazine hydrochloride in aqueous vehicles, *Journal of Clinical Pharmacy and Therapeutics*, 11(3), 215–223 (1986).
57. Y. Wu, J. Levons, A. S. Narang, K. Raghavan, and V. M. Rao, Reactive impurities in excipients: profiling, identification and mitigation of drug- excipient incompatibility, *AAPS PharmSciTech*, 12(4), 1248–1263

- (2011).
58. D. Chen, Hygroscopicity of pharmaceutical crystals, University of Minnesota, 2009.
 59. L. L. Brunton, K. . Parker, D. Blumenthal, and I. Buxton, Goodman and Gilman's Manual of Pharmacology and Therapeutics. New York, 2008.
 60. M. J. Ruiz-Magaña, R. Martínez-Aguilar, E. Lucendo, D. Campillo-Davo, K. Schulze-Osthoff, and C. Ruiz-Ruiz, The antihypertensive drug hydralazine activates the intrinsic pathway of apoptosis and causes DNA damage in leukemic T cells, *Oncotarget*, 7(16), 21875–21886 (2016).
 61. H. Lüllmann, K. Mohr, A. Ziegler, and D. Bieger, Color Atlas of Pharmacology, 2nd ed. Thieme, 2000.
 62. A. M. Gurney and M. Allam, Inhibition of calcium release from the sarcoplasmic reticulum of rabbit aorta by hydralazine, *British Journal of Pharmacology*, 114(1), 238–44 (1995).
 63. J.-L. Vincent, Understanding cardiac output, *Critical Care*, 12(4), 1–3 (2008).
 64. R. Pudil, R. Pelouch, R. Praus, M. Vašatová, and P. Hůlek, Heart failure in patients with liver cirrhosis, *Cor et Vasa*, 55(4), e391–e396 (2013).
 65. J. Feenstra, D. E. Grobbee, W. J. Remme, and B. H. C. Stricker, Drug-induced heart failure, *Journal of the American College of Cardiology*, 33(5), 1152–1162 (1999).
 66. K. Chatterjee, J. L. Rouleau, and B. M. Massie, Hydralazine in chronic CHF, *Acta Medica Scandinavica Supplementum*, 652(1), 99–113 (1981).
 67. H. S. Ribner, M. J. Zucker, C. Stasior, D. Talentowski, R. Stadnicki, and M. Lesch, Vasodilators as first-line therapy for congestive heart failure: a comparative hemodynamic study of hydralazine, digoxin, and their combination, *American Heart Journal*, 114(1), 91–6 (1987).
 68. K. Chatterjee, Hydralazine in heart failure, *Acta Medica Scandinavica Supplementum*, 8(4), 187–98 (1983).
 69. K. Chatterjee, T. A. Ports, B. H. Brundage, B. Massie, A. N. Holly, and W. W. Parmley, Oral hydralazine in chronic heart failure: sustained beneficial hemodynamic effects, *Annals of Internal Medicine*, 92(5), 600–4 (1980).
 70. J. T. Flynn and K. Tullus, Severe hypertension in children and adolescents: pathophysiology and treatment, *Pediatric Nephrology*, 24(6), 1101–1112 (2009).
 71. T. N. Webb, I. F. Shatat, and Y. Miyashita, Therapy of acute hypertension in hospitalized children and adolescents, *Current Hypertension Reports*, 16(4), 1–15 (2014).
 72. K. Watt, J. S. Li, D. K. Benjamin, and M. Cohen-Wolkowicz, Pediatric cardiovascular drug dosing in critically ill children and extracorporeal membrane oxygenation, *Journal of Cardiovascular Pharmacology*, 58(2), 126–32 (2011).
 73. L. L. Lilley, S. R. Collins, and J. S. Snyder, Pharmacology and the nursing process, 8th ed. London: Elsevier, 2014.
 74. B. G. Wells, J. T. Dipiro, T. L. Schwinghammer, and C. V Dipiro, Pharmacotherapy Handbook, 7th ed. London: McGraw-Hill Companies, 2009.
 75. L. Turner, Daily Drug Use, 9th ed. Cape Town: The Tincture Press, 2010.
 76. H. J. Walker and D. J. Geniton, Vasodilator therapy and the anesthetist: A review of nitroprusside, labetalol, hydralazine and nitroglycerin, *Journal of the American Association of Nurse Anesthetists*, 57(5), 435–444 (1989).

77. A. Nomura, H. Yasuda, K. Katoh, T. Akimoto, K. Miyazaki, and T. Arita, Hydralazine and furosemide kinetics, *Clinical Pharmacology and Therapeutics*, 32(3), 303–306 (1982).
78. L. M. White, S. F. Gardner, B. J. Gurley, M. A. Marx, P. L. Wang, and M. Estes, Pharmacokinetics and cardiovascular effects of ma-huang (*Ephedra sinica*) in normotensive adults, *Journal of Clinical Pharmacology*, 37(2), 116–22 (1997).
79. S. Lindeberg, B. Holm, P. Lundborg, C. G. Regardh, and B. Sandstrom, The effect of hydralazine on steady-state plasma concentrations of metoprolol in pregnant hypertensive women, *European Journal of Clinical Pharmacology*, 35(2), 131–135 (1988).
80. U. Elkayam and N. Gleicher, Cardiac problems in pregnancy: diagnosis and management of maternal and fetal disease. New York: Wiley-Liss, 1998.
81. T. M. Ludden, J. L. McNay, A. M. m. Shepherd, and M. S. Lin, Clinical pharmacokinetics of hydralazine, *Clinical Pharmacokinetics*, 7(3), 185–205 (1982).
82. N. R. Musso, C. Vergassola, A. Pende, and G. Lotti, Yohimbine effects on blood pressure and plasma catecholamines in human hypertension, *American Journal of Hypertension*, 8(6), 565–71 (1995).
83. E. Grossman, T. Rosenthal, E. Peleg, C. Holmes, and D. S. Goldstein, Oral yohimbine increases blood pressure and sympathetic nervous outflow in hypertensive patients, *Journal of Cardiovascular Pharmacology*, 22(1), 22–26 (1993).
84. P. A. Winstanley and E. Orme, The effects of food on drug bioavailability, *British Journal of Clinical Pharmacokinetics*, 28(1), 621–628 (1989).
85. R. K. Beck, Drug Reference for EMS Providers. London: Delmar, 2002.
86. A. Gonzalez-Fierro *et al.*, Pharmacokinetics of hydralazine, an antihypertensive and DNA-demethylating agent, using controlled-release formulations designed for use in dosing schedules based on the acetylator phenotype, *International Journal of Clinical Pharmacology and Therapeutics*, 49(8), 519–524 (2011).
87. J. T. Dipiro, W. J. Spruill, W. E. Wade, R. A. Blouin, and J. M. Pruemer, Concepts in clinical pharmacokinetics, 4th ed. Bethesda: American Society of Health-System Pharmacists, 2005.
88. R. Benigni and C. Bossa, Mechanisms of chemical carcinogenicity and mutagenicity: a review with implications for predictive toxicology, *Chemical Reviews*, 111(4), 2507–2536 (2011).
89. B. K. Sinha and R. P. Mason, Biotransformation of hydrazine derivatives in the mechanism of toxicity, *Journal of Drug Metabolism and Toxicology*, 5(2), 1–6 (2014).
90. M. Pretel, L. Marquès, and A. España, Drug-induced lupus erythematosus, *Actas Dermo-Sifiliográficas (English Edition)*, 105(1), 18–30 (2014).
91. R. Yung, S. Chang, N. Hemati, K. Johnson, and B. Richardson, Mechanisms of drug-induced lupus: comparison of procainamide and hydralazine with analogs in vitro and in vivo, *Arthritis and Rheumatism*, 40(8), 1436–1443 (1997).
92. D. Melton, C. D. Lewis, N. E. Price, and K. S. Gates, Covalent adduct formation between the antihypertensive drug hydralazine and abasic sites in double- and single-stranded DNA, *Chemical Research in Toxicology*, 27(12), 2113–2118 (2014).
93. J. R. Batchelor *et al.*, Hydralazine-induced lupus erythematosus: influence of HLA-DR and sex on susceptibility, *The Lancet*, 315(8178), 1107–1109 (1980).
94. L. A. Magee, C. Cham, E. J. Waterman, A. Ohlsson, and P. von Dadelszen, Hydralazine for treatment of severe hypertension in pregnancy: meta-analysis, *British Medical Journal*, 327(7421), 955–960 (2003).

95. J. P. Rocchiccioli, Hydralazine in heart failure: a study of the mechanism of action in human blood vessels, University of Glasgow, 2015.
96. A. T. Chemmanur and H. L. Bonkovsky, Hepatic porphyrias: diagnosis and management, *Clinics in Liver Disease*, 8, 807–838 (2004).
97. Q. T. Nguyen, S. R. Anderson, L. Sanders, and L. D. Nguyen, Managing hypertension in the elderly: a common chronic disease with increasing age, *American Health and Drug Benefits*, 5(3), 146–53 (2012).
98. S. W. Miller, Therapeutic drug monitoring in the geriatric patient, *Clinical Pharmacokinetics*, 45–71.
99. S. Itoh, A. Ichinoe, Y. Tsukada, and Y. Itoh, Hydralazine-induced hepatitis, *Hepato-gastroenterology*, 28(1), 13–6 (1981).
100. G. Enderlin, Discoloration of hydralazine injection, *American Journal of Hospital Pharmacy*, 41(4), 634 (1984).
101. C. Webster, Clinical Pharmacology. Wyoming: Teton NewMedia, 2001.
102. L. A. Felton, Remington Essentials of Pharmaceutics, 22nd ed. London: Pharmaceutical Press, 2012.
103. M. E. Aulton, Pharmaceutics The Science Of Dosage Form Design, 2nd ed. London: Churchill Livingstone, 2002.
104. A. J. Jounela, M. Pasanen, and M. J. Mattila, Acetylator phenotype and the antihypertensive response to hydralazine, *Acta Medica Scandinavica*, 197(4), 303–6 (1975).
105. J. M. Lesser, Z. H. C. D. And, and P. G. Dayton, Metabolism and disposition of hydralazine-³4C in man and dog, *The American Society for Pharmacology and Experimental Therapeutics*, 2(4), 351–360 (1974).
106. K. D. Haegele, H. B. Skrdlant, T. Talseth, J. L. McNay, A. M. Shepherd, and W. A. Clementi, Quantitative analysis of hydralazine pyruvic acid hydrazone, the major plasma metabolite of hydralazine, *Journal of Chromatography*, 187(1), 171–9 (1980).
107. F. Rafii, N. S. Fatemi, E. Danielson, C. M. Johansson, and M. Modanloo, Compliance to treatment in patients with chronic illness: A concept exploration, *Iranian Journal of Nursing and Midwifery Research*, 19(2), 159–67 (2014).
108. P. R. James and C. Nelson-Piercy, Management of hypertension before, during and after pregnancy, *British Cardiac Society*, 90(12), 1499–504 (2004).
109. F. A. Ghanem, A. Movahed, and C. A. Movahed, Use of antihypertensive drugs during pregnancy and lactation, *Cardiovascular Therapeutics*, 26(1), 38–49 (2008).
110. A. M. Sabir, M. Moloy, and B. P. S, HPLC method development and validation: a review, *International Research Journal of Pharmacy*, 4(4), 39–46 (2013).
111. H. V. Paithankar, HPLC method validation for pharmaceuticals: a review, *International Journal of Universal Pharmacy and Bio Sciences*, 2(4), 229–240 (2013).
112. B. Prathap, A. Dey, G. H. Srinivasa Rao, P. Johnson, and P. Arthanariswaran, A review- importance of RP-HPLC in analytical method development, *International Journal of Novel Trends in Pharmaceutical Sciences*, 3(1), 15–23 (2013).
113. W. J. Lough and I. W. Wainer, High performance liquid chromatography: fundamental principles and practice. London: Blackie Academic and Professional, 1996.
114. M. W. Dong, Modern HPLC for practicing scientists. New Jersey: Wiley-Interscience, 2006.

115. S. K. Bhardwaj, K. Dwivedi, and D. D. Agarwal, A review: HPLC method development and validation, *International Journal of Analytical and Bioanalytical Chemistry*, 5(4), 76–81 (2015).
116. J. A. Adamovics, *Chromatographic analysis of pharmaceuticals*. New York: M. Dekker, 1997.
117. J. A. Kent, *Handbook of Industrial Chemistry and Biotechnology*. New York: Springer Science and Business Media, 2012.
118. L. E. Pushpa and B. Sailaja, Bioanalytical method validation: an updated review, *Pharmaceutical Methods*, 1(1), 25 (2010).
119. T. Kupiec, Quality-control analytical methods: High-performance liquid chromatography, *International Journal of Pharmaceutical Compounding*, 8(1), 223–227 (2004).
120. M. Taleuzzaman, S. Ali, S. Gilani, S. Imam, and A. Hafeez, Ultra performance liquid chromatography: a review, *International Research Journal of Pharmacy*, 2(6), 1–5 (2015).
121. B. L. Peterson and B. S. Cummings, A review of chromatographic methods for the assessment of phospholipids in biological samples, *Biomedical Chromatography*, 20(3), 227–243 (2006).
122. S. H. Y. (Steven H.-Y. Wong and U. Timm, Therapeutic drug monitoring and toxicology by liquid chromatography, *Journal of Pharmaceutical Sciences*, 74(10), 1142–1143 (1985).
123. G. Guiochon, The limits of the separation power of unidimensional column liquid chromatography, *Journal of Chromatography A*, 1126, 6–49 (2006).
124. B. Buszewski and S. Noga, Hydrophilic interaction liquid chromatography (HILIC)- a powerful separation technique, *Analytical and Bioanalytical Chemistry*, 402(1), 231–47 (2012).
125. S. Studzińska and B. Buszewski, Effect of mobile phase pH on the retention of nucleotides on different stationary phases for high-performance liquid chromatography, *Analytical and Bioanalytical Chemistry*, 405(1), 1663–1672 (2013).
126. K. Ramni, K. Navneet, U. Ashutosh, O. . p Suri, and T. Arti, High Performance Liquid Chromatography detectors- a review, 2(5), 1–7 (2011).
127. S. Lindsay and J. Barnes, *High Performance Liquid Chromatography*, 2nd ed. New York: John Wiley and Sons, 1992.
128. B. V. Rao, G. N. Sowjanya, A. Ajitha, and V. U. M. Rao, A review on stability indicating HPLC method development, *World Journal of Pharmacy and Pharmaceutical Sciences*, 4(8), 405–423 (2015).
129. V. Kumar, R. Bharadwaj, G. Gupta, and S. Kumar, An overview on HPLC method development, optimization and validation process for drug analysis, *The Pharmaceutical and Chemical Journal*, 2(2), 30–40 (2015).
130. D. Harvey, *Modern Analytical Chemistry*, 1st ed. London, 2000.
131. K. D. Sanjay and H. D. . Kumar, Importance of RP-HPLC in analytical method development: a review, *International Journal of Pharmaceutical Sciences and Research*, 3(12), 4626–4633 (2012).
132. R. Malviya, B. V. O. . Pal, and P. K. Sharma, High performance liquid chromatography: a short review, *Journal of Global Pharma Technology*, 2(5), 22–26 (2010).
133. P. Chatrabhuji, C. Pandya, and M. Patel, *HPLC method for determination of APIs in pharmaceutical formulation*, 1st ed. North Carolina: Lulu Press, 2002.
134. S. Lakshmi, A review on chromatography with high performance liquid chromatography (HPLC) and its functions, *Journal of Pharmaceutical Analysis*, 4(1), 1–15 (2015).

135. V. Gupta, A. D. K. Jain, N. S. Gill, and K. Gupta, Development and validation of HPLC method- a review, *International Research Journal of Pharmaceutical and Applied Sciences*, 2(4), 17–25 (2012).
136. T. Sirard, Fundamentals of HPLC. Waters Corporation, 2012.
137. A. Kar, Pharmaceutical Drug Analysis, 2nd ed. New Delhi: New Age International Publishers, 2005.
138. M. . Charde, M. . Shinde, A. . Welankiwar, and K. Jitendra, Development of analytical and stability testing method for vitamin A palmitate formulation, *International Journal of Pharmaceutical Chemistry*, 5(4), 104–114 (2015).
139. S. L. Patwekar, R. Sakhare, and N. N. Nalbalwar, HPLC method development and validation- a general concept, *International Journal of Chemical and Pharmaceutical Sciences*, 6(1), 8–14 (2015).
140. S. Sood, Method development and validation using HPLC technique- a review, *Journal of Drug Discovery and Therapeutics*, 2(22), 18–24 (2014).
141. K. K. Chandrul and B. Srivastava, A process of method development: a chromatographic approach, *Journal of Chemical and Pharmaceutical Research*, 2(2), 519–545 (2010).
142. R. E. Schirmer, Modern methods of pharmaceutical analysis, 2nd ed. Boston: CRC Press, 1991.
143. K. V Kanth, N. Poorana Chandra Sainath, and S. T. Raja, Method development and validation- a review, *Journal of Advanced Pharmacy Education and Research*, 2(3), 146–176 (2012).
144. D. T. Manallack, The pK(a) distribution of drugs: application to drug discovery, *Perspectives in Medicinal Chemistry*, 1(1), 25–38 (2007).
145. P. G. Robinson, The effect of column length and column packing mesh size on the analysis of volatile fatty acids by gas chromatography using chromosorb 101, *Journal of Chromatography A*, 74(1), 13–19 (1972).
146. S. Hansen and S. Pedersen-Bjergaard, Bioanalysis of pharmaceuticals: sample preparation, separation techniques, and mass spectrometry. New York: Wiley and Sons, 2015.
147. I. D. Wilson and C. F. Poole, Handbook of methods and instrumentation in separation science volume 1. London: Elsevier, 2009.
148. M. Swartz, HPLC Detectors: a brief review, *Journal of Liquid Chromatography and related technologies*, 33, 1130–1150 (2010).
149. R. P. W. Scott, Liquid chromatography detectors. Library4science, 2003.
150. D. Bas and I. H. Boyaci, Modeling and optimization I: usability of response surface methodology, *Journal of Food Engineering*, 78, 836–845 (2007).
151. F. A. Chaibva and R. B. Walker, The use of response surface methodology for the formulation and optimization of salbutamol sulfate hydrophilic matrix sustained release tablets, *Pharmaceutical Development and Technology*, 17(5), 594–606 (2012).
152. L. D. King'ori and R. B. Walker, The use of response surface methodology to evaluate the impact of level 2 SUPAC – IR changes on the In vitro release of metronidazole and ranitidine from a fixed-dose combination tablet, *Dissolution Technologies*, 1(1), 28–36 (2012).
153. S. M. Khamanga, N. Parfitt, T. Nyamuzhiwa, H. Haidula, and R. B. Walker, The evaluation of Eudragit microcapsules manufactured by solvent evaporation using USP Apparatus 1, *Dissolution Technologies*, 1(1), 15–22 (2009).
154. S. M. Khamanga and R. B. Walker, The use of response surface methodology in the evaluation of captopril

- microparticles manufactured using an oil in oil solvent evaporation technique, *Journal of Microencapsulation*, 29(1), 39–53 (2012).
155. A. I. Khuri and S. Mukhopadhyay, Response surface methodology, *Advanced Reviews*, 2(1), 128–149 (2010).
 156. M. A. Bezerra, R. E. Santelli, E. P. Oliveira, L. S. Villar, and L. A. Escalaira, Response surface methodology (RSM) as a tool for optimization in analytical chemistry, *Talanta*, 76(1), 965–977 (2008).
 157. X. Zhang *et al.*, Response surface methodology used for statistical optimization of jeans- peptide production by *Bacillus subtilis*, *Electronic Journal of Biotechnology*, 13(4), 1–8 (2010).
 158. M. Dutka, M. Ditaranto, and T. Lovås, Application of a central composite design for the study of NO_x emission performance of a low NO_x burner, *Energies*, 8(1), 3606–3627 (2015).
 159. S. L. C. Ferreira *et al.*, Statistical designs and response surface techniques for the optimization of chromatographic systems, *Journal of Chromatography A*, 1158(1), 2–14 (2007).
 160. J. L. Anderson, A. Berthod, V. Pino, and A. M. Stalcup, *Analytical Separation Science*. New York: Wiley and Sons, 2015.
 161. A. I. Khuri, *Response surface methodology and related topics*. World Scientific Publishing Co, 2006.
 162. T. B. Solanki, P. A. Shah, and K. G. Patel, Central composite design for validation of HPTLC method for simultaneous estimation of olmesartan medoxomil, amlodipine besylate and hydrochlorothiazide in tablets, *Indian Journal of Pharmaceutical Sciences*, 76(3), 179–87 (2014).
 163. S. Hansen, S. Pedersen-Bjergaard, and K. Rasmussen, *Introduction to pharmaceutical chemical analysis*. West Sussex: John Wiley and Sons Inc, 2012.
 164. L. B. Lacagnin, H. D. Colby, and J. P. O'Donnell, Separation and quantitation of hydralazine metabolites by high-performance liquid chromatography, *Journal of Chromatography B*, 377, 319–327 (1986).
 165. B. Suhagia, S. P. Chauhan, and K. Shah, Analytical methodologies for the determination of hydralazine: a review, 3(2) (2014).
 166. J. K. Wong, T. H. Joyce III, D. H. Morrow, T. H. Joyce, and D. H. Morrow, Determination of hydralazine in human plasma by high-performance liquid chromatography with electrochemical detection, *Journal of Chromatography A*, 385, 261–266 (1987).
 167. K. S. Alexander, M. Pudipeddi, and G. A. Parker, Stability of hydralazine hydrochloride syrup compounded from tablets, *American Journal of Hospital Pharmacy*, 50(4), 683–6 (1993).
 168. D. P. Elder, D. Snodin, and A. Teasdale, Control and analysis of hydrazine, hydrazides and hydrazones—genotoxic impurities in active pharmaceutical ingredients (APIs) and drug products, *Journal of Pharmaceutical and Biomedical Analysis*, 54(5), 900–910 (2011).
 169. P. A. Reece, I. Cozamanis, and R. Zacest, Selective high-performance liquid chromatographic assays for hydralazine and its metabolites in plasma of man, *Journal of Chromatography*, 181(3–4), 427–40 (1980).
 170. T. M. Ludden, L. K. Ludden, K. E. Wade, and S. R. Allerheilgen, Determination of hydralazine in human whole blood, *Journal of Pharmaceutical Sciences*, 72(6), 693–5 (1983).
 171. J. Mañes, J. Mari, R. Garcia, and G. Font, Liquid chromatographic determination of hydralazine in human plasma with 2-hydroxy-1-naphthaldehyde pre-column derivatization, *Journal of Pharmaceutical and Biomedical Analysis*, 8(12), 795–798 (1990).
 172. V. Das Gupta, Quantitation of Hydralazine Hydrochloride in pharmaceutical dosage forms using High Performance Liquid Chromatography, *Journal of Liquid Chromatography*, 8(13), 2497–2509 (1985).

173. A. M. Di Pietra, P. Roveri, R. Gotti, and V. Cavrini, Spectrophotometric and chromatographic (HPLC) analysis of hydralazine, dihydralazine and hydrazine after derivatization with 2-nitrocinnamaldehyde, *Il Farmaco*, 48(11), 1555–1567.
174. T. Lessen, D. C. Zhao, and D.-C. (David) Zhao, Interactions between drug substances and excipients. 1. Fluorescence and HPLC studies of triazolophthalazine derivatives from hydralazine hydrochloride and starch, *Journal of Pharmaceutical Sciences*, 85(3), 326–329 (1996).
175. S. Halasi and J. G. Nairn, Quantitative determination of hydralazine hydrochloride and phthalazine in aqueous solutions by high performance liquid chromatography, *Journal Of Liquid Chromatography*, 12(12), 2397–2404 (1989).
176. E. M. Koves, Use of high-performance liquid chromatography-diode array detection in forensic toxicology, *Journal of Chromatography. A*, 692(1–2), 103–19 (1995).
177. W. J. Proveaux, J. P. O'Donnell, and J. K. Ma, Liquid chromatographic analysis of hydralazine and metabolites in plasma, *Journal of Chromatography*, 176(3), 480–484 (1979).
178. A. Kirthi, R. Shanmugam, S. M. Prathyusha, and J. Basha, A review on bioanalytical method development and validation by RP-HPLC, *Journal of Global Trends in Pharmaceutical Sciences*, 5(54), 2265–2271 (2014).
179. P. F. Vanbel and P. J. Schoenmakers, Selection of adequate optimization criteria in chromatographic separations, *Analytical and Bioanalytical Chemistry*, 394(5), 1283–9 (2009).
180. B. Prathap, G. H. S. Rao, G. Devdass, A. Dey, and N. Harikrishnan, A review on stability indicating HPLC method development, *International Journal of Innovative Pharmaceutical Research*, 3(3), 229–237 (2012).
181. M. Summers, K. J. Fountain, and O. R. Ds, Rapid Method Development through Proper Column Selection, *Waters*, 1–7 (2012).
182. A. J. Martin and R. L. Synge, A new form of chromatogram employing two liquid phases, *The Biochemical Journal*, 35(12), 1358–68 (1941).
183. J. Wang, J. D. MacNeil, and J. F. Kay, Chemical analysis of antibiotic residues in food. New Jersey: Wiley and Sons, 2012.
184. D. Saimalakondaiah *et al.*, Stability indicating HPLC method development and validation, *International Journal of Pharma Research and Review*, 3(10), 46–57 (2014).
185. P. Ravisankar, C. Naga Navya, D. Pravallika, and D. N. Sri, A review on step-by-step analytical method validation, *IOSR Journal Of Pharmacy*, 5(10), 2250–3013 (2015).
186. G. A. Shabir, Validation of high-performance liquid chromatography methods for pharmaceutical analysis: Understanding the differences and similarities between validation requirements of the US Food and Drug Administration, the US Pharmacopeia and the International Conf, *Journal of Chromatography A*, 987, 57–66 (2003).
187. J. A. Jönsson, Chromatographic theory and basic principles. Dekker, 1987.
188. S. Moldoveanu and V. David, Essentials in modern HPLC separations. London: Elsevier, 2013.
189. L. R. Snyder, J. J. Kirkland, and J. W. Dolan, Introduction to Modern Liquid Chromatography, 3rd ed. New Jersey: John Wiley and Sons, 2011.
190. B. Y. G. A. Shabir, Step-by-step analytical methods validation and protocol in the quality system, *Institute of Validation Technology*, 1(1), 4–14 (2005).

191. C. C. Chan, Y. C. Lee, X.-M. Zhang, and H. Lam, Analytical Method validation and Instrument Performance Verification. New Jersey: John Wiley and Sons Inc, 2004.
192. A. Bergeron, M. Furtado, and F. Garofolo, Importance of using highly pure internal standards for successful liquid chromatography/tandem mass spectrometric bioanalytical assays, *Rapid Communications in Mass Spectrometry*, 23(9), 1287–1297 (2009).
193. M. E. P. McNally, K. M. Usher, S. W. Hansen, J. S. Amoo, and A. P. Bernstein, Precision of internal standard and external standard methods in high performance liquid chromatography, 33(4), 40–46.
194. P. D. LaFleu, Accuracy in trace analysis: sampling, sample handling, analysis-volume 2. National Bureau of Standards Special Publication 442, 1976.
195. S. Sawant and N. Borkar, Method development of an simultaneous determination of common cough and cold ingredients by high performance liquid chromatography (HPLC) in multi component cough and cold oral drug products, *International Journal of Pharmaceutical, Chemical and Biological Sciences*, 4(4), 1029–1037 (2014).
196. A.-R. Alao and M. Konneh, A response surface methodology based approach to machining processes : modelling and quality of the models, *International Journal of Experimental Design and Process Optimisation*, 1(2), 240–261 (2009).
197. A. Fallon, R. F. G. Booth, and L. D. Bell, Applications of HPLC in biochemistry. New York: Elsevier, 1987.
198. D. Sýkora, E. Tesařová, and M. Popl, Interactions of basic compounds in reversed-phase high-performance liquid chromatography influence of sorbent character, mobile phase composition, and pH on retention of basic compounds, *Journal of Chromatography A*, 758(1), 37–51 (1997).
199. S. Babi, A. J. M. Horvat, and D. M. Pavlovi, Determination of pK a values of active pharmaceutical ingredients, *Trends in Analytical Chemistry*, 26(11), 1043–1061 (2007).
200. F. Gritti and G. Guiochon, Elution of propranolol as an ion-pair complex by buffer solutions on C18 - silica, *Analytical Chemistry*, 76(24), 7310–7322 (2004).
201. J. Dolan, A Guide to HPLC and LC-MC Buffer Selection, 2–19.
202. G. Shabir, A practical approach to validation of HPLC methods under current good manufacturing practices, *Journal of Validation Technology*, 1(1), 29–37 (2004).
203. C. M. Riley and T. W. Rosanske, Development and validation of analytical methods, 1st ed. Pergamon, 1996.
204. I. Singh, A. K. Rehni, R. Kalra, G. Joshi, and M. Kumar, Ion exchange resins: drug delivery and therapeutic applications, *Journal of Pharmaceutical Sciences*, 32(1), 91–100 (2007).
205. ICH Expert Working Group, ICH Harmonised Tripartite Guideline. Validation of Analytical Procedures: Test and Methodology (Q2(R1), 1–13 (2005).
206. K. Kalra, Method development and validation of analytical procedures, in *Quality Control of Herbal Medicines and Related Areas*, Rijeka, 2011, 3–16.
207. A. Satinder and S. Scypinski, Handbook of Modern Pharmaceutical Analysis, 2nd ed. Paris: Academic Press, 2001.
208. D. A. Armbruster and T. Pry, Limit of Blank, Limit of Detection and Limit of Quantitation, *The Clinical Biochemist Reviews*, 29(1), 49–52 (2008).
209. G. Geetha, K. N. G. Raju, B. V. Kumar, and M. G. Raja, Analytical method validation: an updated review,

210. L. Huber, *Validation of Analytical Methods*. New York: Informa Healthcare, 2007.
211. S. Chandran, R. S. P Singh, and A. Sajeev Chandran, Comparison of various international guidelines for analytical method validation, *Die Pharmazie- An International Journal of Pharmaceutical Sciences*, 62(1), 4–14 (2007).
212. O. Mcpolin, *Validation of analytical methods for pharmaceutical analysis*. Warrenpoint: Mourne Training services, 2009.
213. S. Kassey, R. P. Pulla, and K. V. Prakash, Development and validation of stability indicating RP-HPLC method for simultaneous estimation of isosorbide dinitrate and hydralazine HCL in combined pharmaceutical dosage form, *INDO American Journal of Pharmceutical Sciences*, 1(4), 219–229 (2014).
214. S. Daksh, A. Goyal, and C. k. Pandiya, Validation of analytical methods- strategies and significance, *International Journal of Research and Development in Pharmacy and Life Sciences*, 4(3), 1489–1497 (2015).
215. United Nations Office on Drugs and Crime, *Guidance for the Validation of Analytical Methodology and Calibration of Equipment used for Testing of Illicit Drugs in Seized Materials and Biological Specimens*, ST/NAR/41. 2009.
216. A. R. Shirode, A. P. Nath, and V. J. Kadam, Development and validation of RP-HPLC method for ziprasidone hydrochloride monohydrate, *International Journal of Pharmaceutical Sciences and Drug Research*, 8(2), 121–127 (2016).
217. M. E. Swartz and I. S. Krull, *Analytical method development and validation*. New York: M. Dekker, 1997.
218. J. Lindholm, *Development and validation of HPLC methods for analytical and preparative purposes*, Uppsala University, 2004.
219. M. Waksmundzka-Hajnos and J. Sherma, *High performance liquid chromatography in phytochemical analysis*. New York: CRC Press, 2011.
220. G. Lavanya, M. Sunil, M. M. Eswarudu, M. C. Eswaraiah, K. Harisudha, and B. N. Spandana, Analytical method validation: an updated review, *International Journal of Pharmaceutical Sciences and Research IJPSR*, 4(4), 1280–1286 (2013).
221. Y. Upadhyay, N. Sharma, G. S. Sarma, and R. K. Rawal, Application of RP–HPLC method in dissolution testing and statistical evaluation by NASSAM for simultaneous estimation of tertiary combined dosages forms, *Journal of Pharmaceutical Analysis*, 5(5), 307–315 (2015).
222. S. Ahuja and M. W. Dong, *Handbook of Pharmaceutical Analysis by HPLC*. London: Elsevier Academic Press, 2005.
223. N. Hasan *et al.*, Development, validation and application of RP-HPLC method: simultaneous determination of Antihistamine and preservatives with Paracetamol in liquid formulations and human serum, *The Open Medicinal Chemistry Journal*, 10(1), 33–43 (2016).
224. M. Blessy, R. D. Patel, P. N. Prajapati, and Y. K. Agrawal, Development of forced degradation and stability indicating studies of drugs- a review, *Journal of Pharmaceutical Analysis*, 4(3), 159–165 (2014).
225. T. Rawat and I. P. Pandey, Forced degradation studies for Drug Substances and Drug Products-Scientific and Regulatory Considerations, *Journal of Pharmaceutical Sciences and Research*, 7(5), 238–241 (2015).
226. K. K. Hotha, S. P. K. Reddy, K. V Raju, and L. K. Ravindranath, Forced degradation studies: practical approach- overview of regulatory guidance and literature for the drug products and drug substances, *International Research Journal of Pharmacy*, 4(5), 78–85 (2013).

227. N. G. Shinde, B. N. Bangar, S. M. Deshmukh, S. P. Sulake, and D. P. Sherekar, Pharmaceutical forced degradation studies with regulatory consideration, *Asian Journal of Research Pharmaceutical Sciences*, 3(4), 178–188 (2013).
228. M. Çelebier, T. Reçber, E. Koçak, and S. Altınöz, RP-HPLC method development and validation for estimation of rivaroxaban in pharmaceutical dosage forms, *Brazilian Journal of Pharmaceutical Sciences*, 49(2), 359–366 (2013).
229. P. Riddhiben, P. Piyushbhai, P. Natubhai, and S. B. M. Shah, Stability indicating HPLC method development- a review, *International Research Journal of Pharmacy*, 2(25), 79–87 (2011).
230. R. Shukla, R. Singh, S. Arfi, R. Tiwari, and G. Tiwari, Degradation and its forced effect: a trenchant tool for stability studies, *International Journal of Pharmacy and Life Sciences*, 7(4), 4987–4995 (2016).
231. T. P. Aneesh and A. Rajasekaran, Forced degradation studies- a tool for determination of stability in pharmaceutical dosage forms, *International Journal of Biological and Pharmaceutical Research*, 3(5), 699–702 (2012).
232. S. Shete, C. Dhale, and S. Joshi, Force degradation study to stability indicating method, *World Journal of Pharmacy and Pharmaceutical Science*, 3(8), 863–873 (2014).
233. G. Ngwa, Forced degradation as an integral part of HPLC stability- indicating method development, *Drug Delivery Technology*, 10(5), 1–4 (2010).
234. R. R. Parajuli, P. Dahal, P. Pokhrel, C. P. Acharya, and R. K. Binaya, Force degradation study and its importance in formulation development- a review, *Advanced Journal of Pharmacie and Life science Research*, 4(2), 43–53 (2016).
235. U. Deokate and A. M. Gorde, Forced degradation and stability testing: strategies and analytical perspectives, *International Journal of Pharmaceutical Sciences Review and Research*, 26(2), 242–250 (2014).
236. A. B. Roge, P. S. Tarte, M. M. Kumare, D. G. R. Shendarkar, and D. S. M. Vadvalkar, Forced degradation study: an important tool in drug development, 3(4) (2013).
237. M. Bakshi and S. Singh, Development of validated stability-indicating assay methods- critical review, *Journal of Pharmaceutical and Biomedical Analysis*, 28(6), 1011–1040 (2002).
238. Q. A. Xu and L. A. Trissel, Stability-indicating HPLC methods for drug analysis, 2nd ed. London: Pharmaceutical Press, 2003.
239. C. C. Okeke, T. Medwick, G. Nairn, K. Shaila, and L. T. Grady, Stability of hydralazine HCl in both flavored and nonflavored extemporaneous preparations, *International Journal of Pharmaceutical Compounding*, 7(4), 313–319 (2003).
240. M. F. Hossain, S. Bhadra, U. Kumar, and A. S. S. Rouf, The ICH guidance in practice: Stress degradation studies on aceclofenac and development of a validated stability-indicating reversed-phase HPLC assay in tablet dosage form, *Pharma Chemica*, 5(4), 131–146 (2013).
241. N. R. Doredla, B. Yengisetty, R. Bojjagani, and S. V. Madasu, Method development and validation of forced degradation studies of pioglitazone hydrochloride by using UV spectroscopy, *International Journal of PharmTech Research*, 4(4), 1750–1757.
242. K. Ruckmani, S. Z. Shaikh, P. Khalil, M. S. Muneera, and O. A. Thusleem, Determination of sodium hyaluronate in pharmaceutical formulations by HPLC–UV, *Journal of Pharmaceutical Analysis*, 3(5), 324–329 (2013).
243. B. Saini and G. Bansal, Degradation study on sulfasalazine and a validated HPLC-UV method for its stability testing, *Scientia Pharmaceutica*, 82(2), 295–306 (2014).

244. H. K. Trivedi and M. C. Patel, A stability indicating method for the determination of the antioxidant sodium bisulfite in pharmaceutical formulation by RP-HPLC technique, *Scientia Pharmaceutica*, 79(4), 909–20 (2011).
245. K. S. Rao, K. N. Kumar, and D. Joydeep, New stability indicating RP-HPLC method for the estimation of cefpirome sulphate in bulk and pharmaceutical dosage forms, *Scientia Pharmaceutica*, 79(4), 899–907 (2011).
246. M. Ajemni *et al.*, Stability-indicating assay for the determination of pentobarbital sodium in liquid formulations, *International Journal of Analytical Chemistry*, 1(1), 1–6 (2015).
247. Z. Xie, L. Wei, Q. Yang, M. Yang, H. Pan, and H. Liu, A stability-indicating HPLC method for simultaneous determination of creatine phosphate sodium and its related substances in pharmaceutical formulation, *Iranian Journal of Pharmaceutical Research*, 15(1), 119–130 (2016).
248. M. C. Damle and S. R. Salunke, Development and validation of stability-indicating HPLC method for determination of boceprevir, *International Research Journal of Pharmacy*, 7(8), 47–53 (2016).
249. R. Maheswaran, Scientific considerations of forced degradation studies in ANDA submissions, *Journal of Validation Technology*, 1(1), 92–96 (2012).
250. P. K. Desu, G. Vaishnavi, K. Divya, and U. Lakshmi, An overview on preformulation studies, *Indo American Journal of Pharmaceutical Sciences*, 2(10), 1399–1407 (2015).
251. G. Szász and Z. Budvári-Bárány, *Pharmaceutical chemistry of antihypertensive agents*. CRC Press, 1990.
252. A. Welankiwar, S. Saudagar, J. Kumar, and A. Barabde, Photostability testing of pharmaceutical products, *International Research Journal of Pharmacy*, 4(9), 11–15 (2013).
253. ICH Expert Working Group, ICH harmonised tripartite guideline. stability testing: photostability testing of new drug substances and products Q1B, 1–8 (1996).
254. K. N. Gohil, P. M. Patel, and N. M. Patel, Application of analytical techniques in preformulation study: a review, *International Journal of Pharmaceutical and Biological Archives*, 2(5), 1319–1326 (2011).
255. A. Tilak, R. Sharma, S. S. Gangwar, M. Verma, and A. K. Gupta, Significance of preformulation studies in designing, fabricating for pharmaceutical dosage forms, *Journal of Biomedical and Pharmaceutical Research*, 4(6), 35–45 (2015).
256. T. V. Sachin, M. N. Deodhar, and V. Prakya, Advances in analytical techniques used in predicting drug-excipient interactions, *International Journal Of Pharmacy and Technology*, 6(1), 6388–6417 (2014).
257. S. S. Bharate and R. A. Vishwakarma, Impact of preformulation on drug development, *Expert Opinion on Drug Delivery*, 10(9), 1239–1257 (2013).
258. A. B. Ahmed and L. Kanta Nath, Drug-excipients compatibility studies of nicorandil in controlled release floating tablet, *International Journal of Pharmacy and Pharmaceutical Sciences*, 6(2), 468–475 (2014).
259. D. T. Akhter, R. Uddin, N. H. Huda, and K. B. Sutradhar, Design and formulation of twice daily nifedipine sustained release tablet using methocel K15M CR and methocel K100LV CR, *International Journal of Pharmacy and Pharmaceutical Sciences*, 4(1), 121–124 (2012).
260. H. H. Tønnesen and J. Karlsen, Alginate in drug delivery systems, *Drug Development and Industrial Pharmacy*, 28(6), 621–630 (2002).
261. S. S. Bharate, S. B. Bharate, and A. N. Bajaj, Interactions and incompatibilities of pharmaceutical excipients with active pharmaceutical ingredients: a comprehensive review, *Journal of Excipients and Food Chemistry*, 1(3), 3–26 (2010).

262. Hår. Nyqvist, Preformulation studies of drug substances for solid dosage forms, *Drug Development and Industrial Pharmacy*, 12(7), 953–968 (1986).
263. G. Sahitya, B. Krishnamoorthy, and M. Muthukumaran, Importance of preformulation studies in designing formulations for sustained release dosage forms, *International Journal Of Pharmacy and Technology*, 4(4), 2311–2331 (2013).
264. P. M. S. Allaudin and J. Kunchithapatham, A review of preformulation studies of drugs, *International Journal of Pharmaceutical Research and Development*, 4(5), 64–74 (2012).
265. R. Gopinath and R. A. S. Naidu, Pharmaceutical preformulation studies – current review, *International Journal of Pharmaceutical and Biological Archives*, 2(5), 1391–1400 (2011).
266. M. Gibson, Pharmaceutical preformulation and formulation: A practical guide from candidate drug selection to commercial dosage form, 2nd ed. 199(6). 2005.
267. G. Chaurasia, A review on pharmaceutical preformulation studies in formulation and development of new drug molecules, *Intrnational Journal of Pharmaceutical Sciences and Research*, 7(6), 2313–2320 (2016).
268. G. Pifferi and P. Restani, The safety of pharmaceutical excipients, *Il Farmaco*, 58(1), 541–550 (2003).
269. S. P. Chaudhari, P. S. Pa, and P. S. Pradeep, Pharmaceutical excipients: a review, *International Journal of Advances in Pharmacy, Biology and Chemistry*, 1(1), 21–34 (2012).
270. M. Manikandan, K. Kannan, and R. Manavalan, Compatibility studies of camptothecin with various pharmaceutical excipients used in the development of nanoparticle formulation, *International Journal of Pharmacy and Pharmaceutical Sciences*, 5(4), 315–321 (2013).
271. R. Ceresole, Y. K. Han, M. A. Rosasco, L. R. Orelli, and A. Segall, Drug-excipient compatibility studies in binary mixtures of avobenzone, *Journal of Cosmetic Science*, 64(5), 317–328 (2013).
272. A. D. Ravi, S. Saxena, and D. Nagpal, A concise understanding of pharmaceutical excipients, *International Journal of Pharmacy and Pharmaceutical Research*, 3(3), 123–136 (2015).
273. M. E. Q. Raymond C Rowe, Paul J Sheskey, Handbook of Pharmaceutical Excipients, 6th ed. London: Pharmaceutical Press, 2009.
274. H. Wen and K. Park, Oral Controlled Release Formulation Design and Drug Delivery: Theory to Practice. New Jersey: John Wiley and Sons, 2010.
275. S. K. Sahoo, S. Dhal, P. Mohapatro, B. C. H. Behera, and B. B. Barik, Effect of processing temperature on eudragit RS PO microsphere characteristics in the solvent evaporation process, *Pharmazie*, 62(8), 638–9 (2007).
276. S. K. Sahoo, A. A. Mallick, B. Barik, and P. C. Senapati, Formulation and in vitro evaluation of eudragit® microspheres of stavudine, *Tropical Journal of Pharmaceutical Research*, 4(41), 369–375 (2005).
277. S. K. Sahoo *et al.*, Evaluation of controlled release theophylline microspheres prepared with cellulose acetate using solvent evaporation method, *Tropical Journal of Pharmaceutical Research*, 10(2), 195–201 (2011).
278. A. Nokhodchi, S. Raja, P. Patel, and K. Asare-addo, The role of oral controlled release matrix tablets in drug delivery systems, *BioImpacts*, 2(4), 175–187 (2012).
279. S. B. Tiwari and A. R. Rajabi-Siahboomi, Modulation of drug release from hydrophilic matrices, *Pharm Tech Europe*, 20(9), 24–32 (2008).
280. P. Gawali, A. Gupta, S. Kachare, and S. Kshirsagar, Formulation and evaluation of matrix-based sustained release tablets of quetiapine fumarate and the influence of excipients on drug release, *Journal of Chemical*

- and *Pharmaceutical Research*, 4(6), 3073–3081 (2012).
281. M. M. Rahman *et al.*, Evaluation of various grades of Hydroxypropylmethylcellulose matrix systems as oral sustained release drug delivery systems, *Journal of Pharmaceutical Sciences and Research*, 3(1), 930–938 (2011).
 282. A. Chaudhary, S. Pacharane, K. R. Jadhav, and V. . Kadam, Formulation and development of extended release tablet of lamotrigine, *International Journal of Pharma and Bio Sciences Research*, 2(1), 198–210 (2011).
 283. S. S. Khan, S. M. A. Islam, S. P. Hrita, and S. Reza, In-Vitro Study of low viscosity, and high viscosity direct compression and conventional grade hypromellose for modified release gliclazide tablets, *International Journal of Advances in Pharmaceutics*, 1(1), 9–15 (2012).
 284. C. for D. E. and Research, Drug Approvals and Databases- Inactive Ingredients Database Download.
 285. D. A. Miller, J. C. DiNunzio, W. Yang, J. W. McGinity, and R. O. Williams, Targeted intestinal delivery of supersaturated itraconazole for improved oral absorption, *Pharmaceutical Research*, 25(6), 1450–1459 (2008).
 286. J. Patil, S. Marapur, M. Kamalapur, and S. Shiralshetti, Pharmaceutical product development and preformulation studies : early approaches, present scenario and future prospects, *Research Journal of Pharmaceutical, Biological and Chemical Sciences*, 1(3), 782–789 (2010).
 287. D. Elena, B. Ede, L. Sorin, and C. Iuga, Compatibility studies between drugs and excipients in the preformulation phase of buccal mucoadhesive systems, *Farmacia*, 61(4), 703–712 (2013).
 288. P. Patel, K. Ahir, V. Patel, L. Manani, and C. Patel, Drug-excipient compatibility studies: first step for dosage form development, *The Pharma Innovation*, 4(5), 14–20 (2015).
 289. M. Chidambaram and K. Krishnasamy, Drug-drug/drug-excipient compatibility studies on Curcumin using non-thermal methods, *Advanced Pharmaceutical Bulletin*, 4(3), 309–312 (2014).
 290. V. V Prasanth, A. C. Moy, S. T. Mathew, and R. Mathapan, Microspheres- an overview, *International Journal of Research in Pharmaceutical and Biomedical Sciences*, 2(2), 332–338 (2011).
 291. S. K. Niazi, Handbook of Preformulation: chemical, biological, and botanical drugs. London: Informa Healthcare, 2007.
 292. R. Mwikali and S. Kavale, Factors affecting the selection of optimal suppliers in procurement management, *International Journal of Humanities and Social Science*, 2(14), 189–193 (2012).
 293. N. Fathima, T. Mamatha, H. K. Qureshi, N. Anitha, and J. Venkateswara Rao, Drug-excipient interaction and its importance in dosage form development, *Journal of Applied Pharmaceutical Science*, 1(6), 66–71 (2011).
 294. D. Zhou, Understanding physicochemical properties for pharmaceutical product development and manufacturing II: physical and chemical stability and excipient compatibility, *Journal of Validation Technology*, 1(1), 36–47 (2009).
 295. A. S. Narang and S. H. S. Boddu, Excipient applications in formulation design and drug delivery. 2015.
 296. D. D. Wirth *et al.*, Maillard reaction of lactose and fluoxetine hydrochloride, a secondary amine, *Journal of Pharmaceutical Sciences*, 87(1), 31–39 (1998).
 297. E. Spina, C. Hiemke, and J. de Leon, Assessing drug-drug interactions through therapeutic drug monitoring when administering oral second-generation antipsychotics, *Expert Opinion on Drug Metabolism and Toxicology*, 12(4), 407–422 (2016).

298. V. Kumar, B. Prasad, and S. Singh, Pharmaceutical issues in the development of a polypill for the treatment of cardiovascular diseases, *Drug Discovery Today: Therapeutic Strategies*, 5(1), 63–71 (2008).
299. K. Jackson, D. Young, and S. Pant, Drug-excipient interactions and their affect on absorption, *Pharmaceutical Science and Technology Today*, 3(10), 336–345 (2000).
300. G. Pifferi, P. Santoro, and M. Pedrani, Quality and functionality of excipients, *Il Farmaco*, 54(1), 1–14 (1999).
301. R. Chadha and S. Bhandari, Drug-excipient compatibility screening- role of thermoanalytical and spectroscopic techniques, *Journal of Pharmaceutical and Biomedical Analysis*, 87(1), 82–97 (2014).
302. T. Hatakeyama and F. . Quinn, Thermal Analysis : Fundamentals and Applications to Polymer Science, 2nd ed. New York: John Wiley and Sons Ltd., 1999.
303. P. Mura, A. Manderioli, G. Bramanti, S. Furlanetto, and S. Pinzauti, Utilization of differential scanning calorimetry as a screening technique to determine the compatibility of ketoprofen with excipients, *International Journal of Pharmaceutics*, 119(1), 71–79 (1995).
304. B. H. Stuart, Infrared Spectroscopy: Fundamentals and Applications, 8. Chichester: Wiley and Sons, 2004.
305. A. A. Bunaciu, H. Y. Aboul-Enein, and S. Fleschin, Recent applications of fourier transform infrared spectrophotometry in herbal medicine analysis, *Applied Spectroscopy Reviews*, 46(4), 251–260 (2011).
306. R. Das, E. M. Ali, and S. B. A. Hamid, Current applications of X-ray powder diffraction- a review, 38, 95–109 (2014).
307. A. Chauhan and P. Chauhan, Powder XRD technique and its applications in science and technology, *Journal of Analytical and Bioanalytical Techniques*, 5(5), 1–5 (2014).
308. D. M. Eike, J. F. Brennecke, and E. J. Maginn, Predicting melting points of quaternary ammonium ionic liquids, *Green Chemistry*, 5(1), 323–328 (2003).
309. E. Allen, The melting point of impure organic compounds, *Journal of Chemical Education*, 278–281 (1942).
310. D. G. Watson, Pharmaceutical Analysis A Textbook for Pharmacy Students and Pharmaceutical Chemists. Livingstone: Elsevier, 1999.
311. M. Malet-Martino and U. Holzgrabe, NMR techniques in biomedical and pharmaceutical analysis, *Journal of Pharmaceutical and Biomedical Analysis*, 55(1), 1–15 (2011).
312. E. E. Kwan and S. G. Huang, Structural elucidation with NMR spectroscopy: practical strategies for organic chemists, *European Journal of Organic Chemistry*, 16(1), 2671–2688 (2008).
313. P. D, N. Prthiban, K. D. Sathis, G. Somsubhra, D. Banji, and Saikiran, Solid state nuclear magnetic resonance spectroscopy- a review, *Asian Journal of Pharmaceutical and Clinical Research*, 4(4), 9–14 (2011).
314. U. Holzgrabe, B. W. K. Diehl, and I. Wawer, NMR spectroscopy in pharmacy, *Journal of Pharmaceutical and Biomedical Analysis*, 17, 557–616 (1998).
315. J. S. Bernstein, Applications of NMR to pharmaceutical technology, *Applied Spectroscopy Reviews*, 30(1–2), 119–137 (1995).
316. R. M. Maggio, N. L. Calvo, S. E. Vignaduzzo, and T. S. Kaufman, Pharmaceutical impurities and degradation products: uses and applications of NMR techniques, *Journal of Pharmaceutical and Biomedical Analysis*, 101(1), 102–22 (2014).

317. S. Singh and R. Roy, The application of absolute quantitative ^1H NMR spectroscopy in drug discovery and development, *Expert Opinion on Drug Discovery*, 11(7), 695–706 (2016).
318. L. A. Pieters and A. J. Vlietinck, Applications of quantitative ^1H - and ^{13}C -NMR spectroscopy in drug analysis, *Journal of Pharmaceutical and Biomedical Analysis*, 7(12), 1405–1417 (1989).
319. M. R. Siddiqui, Z. A. AlOthman, and N. Rahman, Analytical techniques in pharmaceutical analysis: a review, *Arabian Journal of Chemistry*, 1–13 (2013).
320. P. Rakesh, P. Charmi, and K. Rjesh, Quantitative analytical applications of FTIR spectroscopy in pharmaceutical and allied areas, *Journal of Advanced Pharmacy Education and Research*, 4(2), 145–157 (2014).
321. R. Gao, Y. Jin, Q.-Y. Yang, B.-W. Sun, and J. Lin, Study of stability and drug-excipient compatibility of estradiol and pharmaceutical excipients, *Journal of Thermal Analysis and Calorimetry*, 120(1), 839–845.
322. G. Kyuchoukov, A. Labbaci, J. Albet, and J. Molinier, Simultaneous influence of active and “inert” diluents on the extraction of lactic acid by means of Tri-n-octylamine (TOA) and Tri-iso-octylamine (TIOA), *Industrial and Engineering Chemistry Research*, 45(2), 503–510 (2006).
323. Y. E. Zhang and J. B. Schwartz, Effect of diluents on tablet integrity and controlled drug release, *Drug Development and Industrial Pharmacy*, 26(7), 761–5 (2000).
324. J. Deruiter, Amides and related functional groups, *Principles of Drug Action 1*, 1–16 (2005).
325. Z. E. Jassim and A. A. Hussein, Formulation and evaluation of clopidogrel tablet incorporating drug nanoparticles, *International Journal of Pharmacy and Pharmaceutical Sciences*, 6(1), 838–851 (2014).
326. W. Xu, S. Li, N. Whitely, and W.-P. Pan, Fundamentals of TGA and SDT, 1–7 (2005).
327. K. . Ramteke, V. . Jadhav, and S. N. Dhole, Microspheres: as carriers used for novel drug delivery system, *IOSR Journal of Pharmacy*, 2(4), 2250–3013 (2012).
328. S. Karna, S. Chaturvedi, V. Agrawal, and M. Alim, Formulation approaches for sustained release dosage forms: a review, *Asian Journal of Pharmaceutical and Clinical Research*, 8(5), 34–41 (2015).
329. H. Parmar, S. Bakliwal, N. Gujarathi, B. Rane, and S. Pawar, Different methods of formulation and evaluation of mucoadhesive microsphere, *International Journal of Applied Biology and Pharmaceutical Technology*, 1(3), 1157–1167 (2010).
330. S. Shaikh, G. J. Khan, S. Salman, F. Heena, S. Shaoor, and M. F. Shaikh, Microspheres as a multiparticulate drug delivery system: a review, *World Journal of Pharmacy and Pharmaceutical Sciences*, 5(1), 274–292 (2016).
331. Y. S. Tanwar, P. S. Naruka, and G. R. Ojha, Development and evaluation of floating microspheres of verapamil hydrochloride, *Brazilian Journal of Pharmaceutical Sciences*, 43(4), 529–534 (2007).
332. M. N. Singh, K. S. Y. Hemant, M. Ram, and H. G. Shivakumar, Microencapsulation: A promising technique for controlled drug delivery, *Research in Pharmaceutical Sciences*, 5(2), 65–77 (2010).
333. B. P. Kumar, I. S. Chandiran, B. Bhavya, and M. Sindhuri, Microparticulate drug delivery system: a review, *Indian Journal of Pharmaceutical Science and Research*, 1(1), 19–37 (2011).
334. C. T. Huynh and D. S. Lee, Controlled release, *Encyclopedia of Polymeric Nanomaterials*, 1(1), 1–12 (2014).
335. L. Shargel, S. Wu-Pong, and A. Yu, Applied Biopharmaceutics & Pharmacokinetics, 6e ed. New York: McGraw-Hill Medical, 2012.

336. M. Gupta and R. Brijesh, A review on: sustained release technology, *International Journal of Therapeutic Applications*, 8(1), 18–23 (2012).
337. J. Siepmann, R. A. Siegel, and M. J. Rathbon, Fundamentals and applications of controlled release drug delivery. New York: Springer Science and Business Media, 2012.
338. M. N. Shah, Review on sustained release matrix tablets: an approach to prolong the release of drug, *Journal of Pharmaceutical Science and Bioscientific Research*, 5(53) (2015).
339. C. Engineer, J. Parikh, and A. Raval, Review on hydrolytic degradation behavior of biodegradable polymers from controlled drug delivery system, *Trends in Biomaterials and Artificial Organs*, 25(2), 79–85 (2011).
340. H. S. Azevedo and R. L. Reis, Understanding Enzymatic Degradation of Biodegradable Polymers and Strategies to Control Their Degradation Rate, in *Biodegradable Systems in Tissue Engineering and Regenerative Medicine*, Boca Raton London: CRC Press, 2005, 177–202.
341. T. Sasidharan and S. C. Nair, Magnetic microsphere: a review, *Research Journal of Pharmacy and Technology*, 9(3), 281–290 (2016).
342. P. Tarun, S. Soni, B. Thakar, V. Pandya, and P. Bharadia, Magnetic microspheres as a targeted drug delivery system: a review, *International Journal for Pharmaceutical Research Scholars*, 1(2), 444–456 (2012).
343. P. Muntha, Microspheres- novel drug carriers, *Journal of Pharmacy and Pharmaceutical Sciences*, 3(3), 83–86 (2014).
344. G. Chinna, S. R. Shyam, K. V. M. Vimal, R. M. Sleeva, and K. M. Sai, Formulation and evaluation of indomethacin microspheres using natural and synthetic polymers as controlled release dosage forms, *International Journal of Drug Discovery*, 2(1), 8–16 (2010).
345. K. P. Meena, J. . Dangi, P. K. Samal, and K. P. Namdeo, Recent advances in microspheres manufacturing technology, *International Journal of Pharmacy and Technology*, 3(1), 854–893 (2011).
346. N. T. Hwisa, P. Katakam, B. R. Chandu, and S. K. Adiki, Solvent evaporation techniques as promising advancement in microencapsulation, *Vedic Research International Biolological Medicinal Chemistry*, 1(1), 8–22 (2013).
347. M. H. Abdallah *et al.*, Development and characterization of controlled release ketoprofen microspheres, *Journal of Applied Pharmaceutical Science*, 2(3), 60–67 (2012).
348. S. Kumari, M. Nagpal, G. Aggarwal, U. K. Jain, and S. Pankaj, Microparticles drug delivery system: a review, *World Journal of Pharmacy and Pharmaceutical Sciences*, 5(3), 543–566 (2016).
349. V. Deshmukh, S. Warad, R. Solunke, S. Walunj, S. Palve, and G. Jagdale, Microspheres: as new drug delivery system, *World Journal of Pharmacy and Pharmaceutical Sciences*, 2(6), 4504–4519 (2013).
350. G. Poovi, S. Padmapriya, and S. Lakshmi, Review on magnetic microsphere, *Global Journal of Pharmacology*, 9(4), 296–310 (2015).
351. N. Kadam and V. Suvarna, Microspheres: a brief review, *Asian Journal of Biomedical and Pharmaceutical Sciences*, 5(47), 13–19 (2015).
352. A. Garg and P. Upadhyay, Mucoadhesive microspheres: a short review, *Asian Journal of Pharmaceutical and Clinical Research*, 5(3), 24–27 (2012).
353. A. Pradesh and A. Pradesh, Microspheres as a promising mucoadhesive drug delivery system- review, *International Journal of Pharmaceutical Sciences Review and Research*, 23(2), 8–14 (2013).

354. M. Mohan, H. Sujitha, V. U. Maheshawara, M. A. Rao, and B. A. Kumar, A brief review on mucoadhesive microspheres, *International Journal of Research and Reviews in Pharmacy and Applied science*, 4(1), 975–986 (2014).
355. S. B. Gholap, S. K. Banarjee, D. D. Gaikwad, S. L. Jadhav, and R. M. Thorat, Hollow microsphere: a review, *International Journal of Pharmaceutical Sciences Review and Research*, 1(1), 74–79 (2010).
356. M. A. Gunjal and A. K. Gaikwad, A review on floating microspheres as gastroretentive drug delivery system, *American Journal of Pharmacy and Health Research*, 1(9), 1–21 (2013).
357. A. Chandna, D. Batra, S. Kakar, and R. Singh, A review on target drug delivery: magnetic microspheres, *Journal of Acute Disease*, 2(3), 189–195 (2013).
358. C. Pawan and P. Hemchand, Magnetic microsphere: as targeted drug delivery, *Journal of Pharmacy Research*, 2(5), 964–966 (2009).
359. S. Mukherjee and P. Bandyopadhyay, Magnetic microspheres: a latest approach in novel drug delivery system, *Journal of Pharmaceutical and Scientific Innovation*, 1(6), 39–43 (2012).
360. A. Hafeez, A. Maurya, J. Singh, A. Mittal, and L. Rana, An overview on floating microsphere: gastro retention floating drug delivery system (FDDS), *The Journal of Phytopharmacology*, 2(3), 1–12 (2013).
361. B. N. Singh and K. H. Kim, Floating drug delivery systems: an approach to oral controlled drug delivery via gastric retention, *Journal of Controlled Release*, 63(3), 235–259 (2000).
362. J. Y. Mukund, B. R. Kantilal, and R. N. Sudhakar, Floating microspheres: a review, *Brazilian Journal of Pharmaceutical Sciences*, 48(1), 17–30 (2012).
363. M. Gayathridevi, J. A. J. Nesalin, and T. T. Mani, Floating microsphere: a review, *International Journal of Research in Pharmacy and chemistry*, 6(3), 501–510 (2016).
364. V. R. Sinha, V. Goyel, and A. Trehan, Radioactive microspheres in therapeutics, *Pharmazie*, 59(6), 419–426 (2004).
365. K. Saralidze, L. H. Koole, and M. L. W. Knetsch, Polymeric microspheres for medical applications, *materials*, 3(1), 3537–3564 (2010).
366. S. Freiberg and X. X. Zhu, Polymer microspheres for controlled drug release, *International Journal of Pharmaceutics*, 282(2), 1–18 (2004).
367. M. Li, D. Poncelet, and O. Rouaud, Microencapsulation by solvent evaporation, *International Workshop on Bioencapsulation*, 1(1), 1–8 (2007).
368. M. Li, O. Rouaud, and D. Poncelet, Microencapsulation by solvent evaporation: State of the art for process engineering approaches, *International Journal of Pharmaceutics*, 363(1), 26–39 (2008).
369. N. Saha, I. Hasan, M. Nazmi, and S. M. Reza, Design and development of sustained release microspheres of ibuprofen by emulsification solvent evaporation method using polymeric blend, *Bangladesh Pharmaceutical Journal*, 16(1), 39–44 (2013).
370. X. Wei *et al.*, Biodegradable poly(ϵ -caprolactone)–poly(ethylene glycol) copolymers as drug delivery system, *International Journal of Pharmaceutics*, 381(1), 1–18 (2009).
371. J. L. Maia, M. H. A. Santana, and M. I. Re, The effect of some processing conditions on the characteristics of biodegradable microspheres obtained by an emulsion solvent evaporation process, *Brazilian Journal of Chemical Engineering*, 21(1), 1–12 (2004).
372. M. Ahmad, A. Madni, M. Usman, A. Munir, N. Akhtar, and H. M. S. Khan, Pharmaceutical microencapsulation technology for development of controlled release drug delivery systems,

373. A. Malik, N. Parvez, and P. K. Sharma, Novel methods of microsphere formulation, *World Applied Sciences Journal*, 32(5), 839–847 (2014).
374. T. Ansari, M. S. Hasnain, M. N. Hoda, and A. K. Nayak, Microencapsulation of pharmaceuticals by solvent evaporation technique: a review, *Elixir Pharmacy*, 47(1), 8821–8827 (2012).
375. P. Chaware, S. Sharma, A. Bhandari, and A. Garud, Bioadhesive microspheres: a review on preparation and in-vitro characterization, *World Journal of Pharmaceutical Research*, 4(2), 423–436 (2015).
376. S. Tiwari and P. Verma, Microencapsulation technique by solvent evaporation method (Study of effect of process variables), *International Journal Of Pharmacy and Life Sciences*, 2(8), 998–1005 (2011).
377. P. Singh, D. Prakasha, B. Ramesh, N. Singh, and T. T. Mani, Biodegradable polymeric microspheres as drug carriers: a review, *Indian Journal of Novel Drug Delivery*, 3(2), 70–82 (2011).
378. S. K. Basu and R. Adhiyaman, Preparation and characterization of nitrendipine- loaded eudragit RL 100 microspheres prepared by an emulsion-solvent evaporation method, *Tropical Journal of Pharmaceutical Research*, 7(3), 1033–1041 (2008).
379. A. Matsumoto, T. Kitazawa, J. Murata, Y. Horikiri, and H. Yamahara, A novel preparation method for PLGA microspheres using non-halogenated solvents, *Journal of Controlled Release*, 129(1), 223–227 (2008).
380. F. Yao and J. K. Weiyan, Drug release kinetics and transport mechanisms of non-degradable and degradable polymeric delivery systems, *Expert Opinion Drug Delivery*, 7(4), 429–444 (2010).
381. M. Kushal, M. Monali, M. Durgavati, P. Mittal, S. Umesh, and S. Pragna, Oral controlled release drug delivery system: an overview, *International Research Journal of Pharmacy*, 4(3), 70–76 (2013).
382. Donald L. Wise, *Handbook of Pharmaceutical Controlled Release Technology*. London: Marcel Dekker, 2000.
383. T. S. Keerthi, S. Vinupama, S. S. K. K. P. Singh, and S. K. Senthil, Biodecomposable polymeric microspheres: review, *International Bulletin of Drug Research*, 1(2), 81–99 (2010).
384. E. Holowka and S. K. Bhatia, *Drug Delivery: Materials Design and Clinical Perspective*, 197. New York: Spriger Science and Business Media, 2014.
385. R. Laitinen, *Physical modification of drug release controlling structures- hydrophobic matrices and fast dissolving particles*. Kuopio University Publications, 2009.
386. K. E. Uhrich, S. M. Cannizzaro, R. S. Langer, and K. M. Shakesheff, Polymeric systems for controlled drug release, *Chemical Reviews*, 99(11), 3181–3198 (1999).
387. D. Bhowmik, H. Gopinath, B. P. Kumar, S. Duraivel, and K. P. S. Kumar, Controlled release drug delivery systems, *The Pharma Innovation*, 1(10), 24–32 (2012).
388. B. A. Miller-chou and J. L. Koenig, A review of polymer dissolution, *Progress in Polymer Science*, 28(1), 1223–1270 (2003).
389. Y. Qiu and D. Zhou, Understanding design and development of modified release solid oral dosage forms, *Journal of Validation Technology*, 17(2), 23–32 (2011).
390. A. Akhgari, S. Rezaee, and A. Kuchak, Evaluation of the swelling, erosion and drug release from polysaccharide matrix tablets based on pectin and insulin, *Journal of Natural Pharmaceutical Products*, 6(1), 51–58 (2011).

391. H. Patel, D. R. Panchal, U. Patel, T. Brahmabhatt, and M. Suthar, Matrix type drug delivery system: a review, *Journal of Pharmaceutical Science and Bioscientific Research*, 1(3), 143–151 (2011).
392. M. U. Ghori and B. R. Conway, Hydrophilic matrices for oral control drug delivery, *American Journal of Pharmacological Sciences*, 3(5), 103–109 (2015).
393. R. Zarzycki, Z. Modrzejewska, and K. Nawrotek, Drug release from hydrogel matrices, *Ecological chemistry and engineerings*, 17(2), 117–136 (2010).
394. N. Kamaly, B. Yameen, J. Wu, and O. C. Farokhzad, Degradable controlled-release polymers and polymeric nanoparticles: mechanisms of controlling drug release, *Chemical Research in Toxicology*, 116(1), 2602–2663 (2016).
395. N. Sharma, S. Singh, P. Pawar, and S. Arora, Production techniques and versatile applications of microparticles as controlled drug delivery system, *International Journal of Innovative Drug Discovery*, 5(3), 93–101 (2012).
396. J. Siepmann and A. Gopferich, Mathematical modeling of bioerodible, polymeric drug delivery systems, *Advanced Drug Delivery Reviews*, 48(1), 229–247 (2001).
397. K. N. Patel and T. A. Mehta, A review on oral osmotically driven systems, *International Journal of Pharmacy and Pharmaceutical Sciences*, 5(3), 996–1004 (2013).
398. R. A. Keraliya *et al.*, Osmotic drug delivery system as a part of modified release dosage form, *ISRN Pharmaceutics*, 1(1), 1–9 (2012).
399. G. Vilar, J. Tulla-puche, and F. Albericio, Polymers and drug delivery systems, *Current Drug Delivery*, 9(4), 1–28 (2012).
400. N. Ahuja, V. Kumar, and P. Rathee, Osmotic-controlled release oral delivery system: an advanced oral delivery form, *The Pharma Innovation*, 1(7), 116–124 (2012).
401. D. P. Elder, Pharmaceutical applications of ion-exchange resins, *Journal of Chemical Education*, 82(4), 575–587 (2005).
402. T. Parashar, V. Singh, G. Singh, S. Tyagi, C. Patel, and A. Gupta, Novel oral sustained release technology: a concise review, *International Journal of Research and Development in Pharmacy and Life Sciences*, 2(2), 262–269 (2013).
403. P. Timmins, S. R. Pygall, and C. D. Melia, *Hydrophilic Matrix Tablets for Oral Controlled Release*. New York: Springer, 2014.
404. S. H. Jeong, N. H. Berhane, K. Haghighi, and K. Park, Drug release properties of polymer coated ion-exchange resin complexes : experimental and theoretical evaluation, *Journal of Pharmaceutical Sciences*, 96(3), 618–632 (2007).
405. M. V Srikanth, S. A. Sunil, N. S. Rao, M. U. Uhumwangho, and K. V. R. Murthy, Ion-exchange resins as controlled drug delivery carriers, *Journal of Scientific Research*, 2(3), 597–611 (2010).
406. S. M. Khamanga and R. B. Walker, Evaluation of rate of swelling and erosion of verapamil (VRP) sustained-release matrix tablets, *Drug Development and Industrial Pharmacy*, 32, 1139–1148 (2006).
407. T. J. Roseman and S. . Mansdorf, *Controlled Release Delivery Systems*. London: Marcel Dekker, 1983.
408. H. Omidian and K. Park, Swelling agents and devices in oral drug delivery, *Journal of Drug Delivery and Scientific Technology*, 18(2), 83–93 (2008).
409. C. Lin and A. T. Metters, Hydrogels in controlled release formulations: network design and mathematical modeling, *Advanced Drug Delivery Reviews*, 58(1), 1379–1408 (2006).

410. A. Gopferich, Mechanisms of polymer degradation and erosion, *Biomaterials*, 17(2), 103–114 (1996).
411. P. T. Wong and S. K. Choi, Mechanisms of drug release in nanotherapeutic delivery systems, *Chemical Reviews*, 115(9), 3388–3432 (2015).
412. T. K. Giri, K. Kumar, A. Alexander, H. Badwaik, and D. K. Tripathi, A novel and alternative approach to controlled release drug delivery system based on solid dispersion technique, *Bulletin of Facult of Pharmacy, Cairo University*, 1(1), 1–13 (2012).
413. A. Mahboubian, K. S. Hashemein, S. Moghadam, F. Atyabi, and R. Dinarvand, Preparation and in-vitro evaluation of controlled release PLGA microparticles containing triptoreline, *Iranian Journal of Pharmaceutical Research* (2010), 9(4), 369–378 (2010).
414. M. Mehta, S. Satija, P. Pandey, and M. Dahiya, Solvent evaporation technique: an innovative approach to increase gastric retention, *International Journal of Advanced Scientific Research*, 1(4), 60–67 (2016).
415. P. Phutane, S. Shidhaye, V. Lotlikar, A. Ghule, S. Sutar, and V. Kadam, In vitro evaluation of novel sustained release microspheres of glipizide prepared by the emulsion solvent diffusion-evaporation method, *J Young Pharrm*, 2(1), 35–41 (2010).
416. P. Trivedi, A. M. L. Verma, and N. Garud, Preparation and characterization of aceclofenac microspheres, *Asian Journal of Pharmaceutics*, 1(1), 110–115 (2008).
417. S. Kumari, A. Bhandari, and P. K. Sharma, Solvent evaporation as a imposing method for microencapsulation- a review, *Journal of Drug Discovery and Therapeutics*, 2(19), 13–20 (2014).
418. T. Fan, J. Feng, C. Ma, C. Yu, J. Li, and X. Wu, Preparation and characterization of porous microspheres and applications in controlled-release of abamectin in water and soil, *Journal of Porous Mater*, 21(1), 113–119 (2014).
419. M. I. Robertson, Regulatory issues with excipients, *International Journal of Pharmaceutics*, 187(1), 273–276 (1999).
420. S. Kamel, N. Ali, K. Jahangir, S. M. Shah, and A. A. El-Gendy, Pharmaceutical significance of cellulose: a review, *Express Polymer Letters*, 2(11), 758–778 (2008).
421. C. S. Gad, *Pharmaceutical manufacturing handbook: production and processes*. New Jersey: John Wiley and Sons, 2008.
422. J. Alligood *et al.*, *Physical Appearance Determination of a Drug Substance*.
423. S. K. Niazi, *Handbook of pharmaceutical manufacturing formulations: over-the-counter products*, 2nd ed. New York: Informa Healthcare, 2009.
424. R. C. Dhakar, S. D. Maurya, B. P. S. Sagar, S. Bhagat, S. K. Prajapati, and C. P. Jain, Variables influencing the drug entrapment efficiency of microspheres: a pharmaceutical review, *Der Pharmacia Lettre*, 2(5), 102–116 (2010).
425. S. Papadimitriou and D. N. Bikiaris, Novel self-assembled core-shell nanoparticles based on crystalline amorphous moieties of aliphatic copolyesters for efficient controlled drug release, *Journal of Controlled Release*, 138(1), 177–184 (2009).
426. M. M. A. Abdel-mottaleb and A. Lamprecht, Standardized in vitro drug release test for colloidal drug carriers using modified USP dissolution apparatus I, *Drug Development and Industrial Pharmacy*, 37(2), 178–184 (2011).
427. S. Handoo, V. Arora, D. Khera, P. K. Nandi, and S. K. Sahu, A comprehensive study on regulatory requirements for development and filing of generic drugs globally, *International Journal of Pharmaceutical Investigation*, 2(3), 99–105 (2012).

428. J. B. Calixto, Efficacy, safety, quality control, marketing and regulatory guidelines for herbal medicines (phytotherapeutic agents), *Brazilian Journal of Medical and Biological Research*, 33(2), 179–189 (2000).
429. world health organisation, Quality assurance for pharmaceuticals (2012).
430. R. Dessai, Medicines Control Council: General Information (2008).
431. Food and Drug Administration, Guidance for Industry Q1E Evaluation of Stability Data Guidance for Industry Q1E Evaluation of Stability Data, 1–17 (2004).
432. D. I. Rosca, F. Watari, and M. Uo, Microparticle formation and its mechanism in single and double emulsion solvent evaporation, *Journal of Controlled Release*, 99(1), 271–280 (2004).
433. D. Alderman, A review of cellulose ethers in hydrophilic matrices for oral controlled-release dosage forms, *International Journal of Pharmaceutical Technology production*, 5, 1–9 (1984).
434. J. Siepmann and N. A. Peppas, Modeling of drug release from delivery systems based on hydroxypropyl methylcellulose (HPMC), *Advanced Drug Delivery Reviews*, 48, 139–157 (2001).
435. P. B. O'Donnell and J. W. McGinity, Preparation of microspheres by the solvent evaporation technique, *Advanced Drug Delivery Reviews*, 28(1), 25–42 (1997).
436. M. Joshi, Role of eudragit in targeted drug delivery, *International Journal of Current Pharmaceutical Research*, 5(2), 58–62 (2013).
437. V. K. Nikam *et al.*, Eudragit a versatile polymer: a review, *Pharmacologyonline*, 1(1), 152–164 (2011).
438. D. S. Jones, Pharmaceutical applications of polymers for drug delivery. Rapra Technology Ltd, 2004.
439. S. Singh, Neelam, S. Arora, and Y. Singla, An overview of multifaceted significance of eudragit polymers in drug delivery systems, *Asian Journal of Pharmaceutical and Clinical Research*, 8(5), 1–6 (2015).
440. K. Saeio, Y. Pongpaibul, H. Viernstein, and S. Okonogi, Factors influencing drug dissolution characteristic from hydrophilic polymer matrix tablet, *Scientia Pharmaceutica*, 75(1), 147–163 (2007).
441. Z.-Z. Piao *et al.*, Comparison of release-controlling efficiency of polymeric coating materials using matrix-type casted films and diffusion-controlled coated tablet, *AAPS PharmSciTech*, 11(2), 630–6 (2010).
442. A. Körner, L. Piculell, F. Iselau, B. Wittgren, and A. Larsson, Influence of different polymer types on the overall release mechanism in hydrophilic matrix tablets, *Molecules*, 14, 2699–2716 (2009).
443. P. S. Hiremath and R. N. Saha, Controlled release hydrophilic matrix tablet formulations of isoniazid: design and in vitro studies, *AAPS PharmSciTech*, 9(4), 1171–8 (2008).
444. K. Krishnaraj, M. Joghi, N. Chandrasekar, M. Joghi, S. Muralidharan, and D. Manikandan, Development of sustained release antipsychotic tablets using novel polysaccharide isolated from *Delonix regia* seeds and its pharmacokinetic studies, *Saudi Pharmaceutical Journal*, 20(3), 239–248 (2012).
445. G. Subedi and R. Maharjan, Influence of different hydroxypropyl methylcellulose polymers in defining the micromeretic properties, erosion, drug entrapment and release from tramadol hydrochloride microspheres, *International Journal of Pharmacy and Pharmaceutical Research*, 5(1), 295–316 (2015).
446. T. Cerchiara *et al.*, Chitosan based micro- and nanoparticles for colon-targeted delivery of vancomycin prepared by alternative processing methods, *European Journal of Pharmaceutics and Biopharmaceutics*, 92, 112–119 (2015).
447. S. Singh Kadian and S. L. Harikumar, Eudragit and its pharmaceutical significance.

448. J. Siepmann, R. A. Siegel, and M. J. Rathbone, Fundamentals and applications of controlled release drug delivery. Springer, 2012.
449. S. S. Saha, M. Nazmi, N. Saha, and M. S. Reza, Preparation and evaluation of carbamazepine sustained release tablets, *Dhaka University Journal of Pharmaceutical Sciences*, 11(2), 173–180 (2013).
450. J. Patel and N. Shah, Formulation and evaluation of sustained release tablets containing atomoxetine hydrochloride, *Journal of Pharmaceutical Science and Bioscientific Research*, 4(3), 196–200 (2014).
451. P. Ige *et al.*, Design and development of sustained release swelling matrix tablets of glipizide for type 11 diabetes mellitus, *Farmacia*, 61(5), 883–901 (2013).
452. M. S. M. Patiwalla, S. Hethara, and M. R. Patel, Recent trends in sustained release oral drug delivery system: a promising approach, *International Journal of Pharmaceutical Research*, 4(3), 526–552 (2015).
453. K. P. R. Chowdary and G. S. Kalyani, Recent research on matrix tablets for controlled release- a review, *International Research Journal of Pharmaceutical and Applied Sciences*, 3(31), 142–148 (2013).
454. T. Ali *et al.*, Use of hydrophilic and hydrophobic polymers for the development of controlled release tizanidine matrix tablets, *Brazilian Journal of Pharmaceutical Sciences*, 50(4), 799–818 (2014).
455. C. S. Pravin, P. P. Sadashiv, and M. P. Ratnaparkhi, Formulation development and evaluation of sustained release matrix tablet of zidovudine, *American Journal of Advanced Drug Delivery*, 1(5), 691–705 (2013).
456. H. Thakkar and J. Desai, Influence of excipients on drug absorption via modulation of intestinal transporters activity, *Asian Journal of Pharmaceutics*, 9(2), 69–82 (2015).
457. A. Parr *et al.*, The effect of excipients on the permeability of BCS class III compounds and implications for biowaivers, *Pharmaceutical Research*, 33(1), 167–76 (2016).
458. P. Khadka *et al.*, Pharmaceutical particle technologies: an approach to improve drug solubility, dissolution and bioavailability, *Asian Journal of Pharmaceutical Sciences*, 9(6), 304–316 (2014).
459. S. Dan, N. Dan, and T. K. Pal, Application of response surface methodology (RSM) in statistical optimisation and pharmaceutical characterization of a matrix tablet formulation using metformin HCL as a model drug, *Innoriginal International Journal of Sciences*, 1(2), 1–6 (2014).
460. R. K. Ladani, M. J. Patel, P. P. Rakesh, and T. V Bhatt, Modern optimization techniques in field of pharmacy, *Research Journal of Pharmaceutical, Biological and Chemical Sciences*, 1(2), 148–157 (2010).
461. R. H. Myers, D. C. Montgomery, and C. M. Anderson-Cook, Response surface methodology: process and product optimization using designed experiments, 1st ed. New York: Wiley and Sons, 2015.
462. J. Malakar, A. K. Nayak, and S. Goswami, Use of response surface methodology in the formulation and optimization of bisoprolol fumarate matrix tablets for sustained drug release, *ISRN Pharmaceutics*, 1(1), 1–10 (2012).
463. G. Singh, R. S. Pai, and V. K. Devi, Response surface methodology and process optimization of sustained release pellets using taguchi orthogonal array design and central composite design, *Journal of advanced pharmaceutical technology and research*, 3(1), 30–40 (2012).
464. T. A. Wani, A. Ahmad, S. Zargar, N. Y. Khalil, and I. A. Darwish, Use of response surface methodology for development of new microwell-based spectrophotometric method for determination of atorvastatin calcium in tablets, *Chemistry Central Journal*, 6(134), 1–9 (2012).
465. U. Mandal, V. Gowda, A. Ghosh, S. Selvan, S. Solomon, and T. K. Pal, Formulation and optimization of sustained release matrix tablet of metformin HCl 500 mg using response surface methodology, *The Pharmaceutical Society of Japan*, 127(18), 1281–1290 (2007).

466. A. Bose, T. W. Wong, and N. Singh, Formulation development and optimization of sustained release matrix tablet of itopride HCl by response surface methodology and its evaluation of release kinetics, *Saudi Pharmaceutical Journal*, 21(1), 201–13 (2013).
467. A. R. Madgulkar, M. R. Bhalekar, V. . Kolhe, and Y. D. Kenjale, Formulation and optimization of sustained release tablets of venlafaxine resinates using response surface methodology, *Indian Journal of Pharmaceutical Sciences*, 71(4), 387–394 (2009).
468. S. Dhiman and S. Verma, Optimization of melt-in-mouth tablets of levocetirizine dihydrochloride using response surface methodology, *International Journal of Pharmacy and Pharmaceutical Sciences*, 4(1), 176–184 (2012).
469. A. Jirage, K. Shaikh, K. Vaishali, and P. Santosh, Optimization of ibuprofen carrying poly-(3-hydroxybutyrate) extended release tablet by central composite design, *Asian Journal of Biomedical and Pharmaceutical Sciences*, 6(59), 7–30 (2015).
470. G. Singh, R. S. Pai, and V. K. Devi, Optimization of pellets containing solid dispersion prepared by extrusion/spheronization using central composite design and desirability function, *Journal of Young Pharmacists*, 4(3), 146–156 (2012).
471. L. L. Lao, N. A. Peppas, F. Y. C. Boey, and S. S. Venkatraman, Modeling of drug release from bulk-degrading polymers, *International Journal of Pharmaceutics*, 418(1), 28–41 (2011).
472. S. N. Rothstein, W. J. Federspiel, and S. R. Little, A unified mathematical model for the prediction of controlled release from surface and bulk eroding polymer matrices, *Biomaterials*, 30(8), 1657–1664 (2009).
473. Y. Fu and W. J. Kao, Drug release kinetics and transport mechanisms of non-degradable and degradable polymeric delivery systems, *Expert Opinion on Drug Delivery*, 7(4), 429–444 (2010).
474. L. L. Lao, S. S. Venkatraman, and N. A. Peppas, Modeling of drug release from biodegradable polymer blends, *European Journal of Pharmaceutics and Biopharmaceutics*, 70(3), 796–803 (2008).
475. D. Y. Arifin, L. Y. Lee, and C.-H. Wang, Mathematical modeling and simulation of drug release from microspheres: implications to drug delivery systems, *Advanced Drug Delivery Reviews*, 58(12), 1274–1325 (2006).
476. S. Dash, P. N. Murthy, L. Nath, and P. Chowdhury, Kinetic modeling on drug release from controlled drug delivery systems, *Polish Pharmaceutical Society*, 67(3), 217–223 (2010).
477. A. Palmieri III, Dissolution theory, methodology and testing, 1st ed. Hockessin: Dissolution Technologies, Incorporated, 2007.
478. P. Costa and J. M. Sousa Lobo, Modeling and comparison of dissolution profiles, *European Journal of Pharmaceutical Sciences*, 13(1), 123–133 (2001).
479. G. Singhvi and M. Singh, Review: in-vitro drug release characterization models, *International Journal of Pharmaceutical Studies and Research*, 2(1), 77–84 (2011).
480. M. Jafari and B. Kaffashi, Mathematical kinetic modeling on isoniazid release from Dex-HEMA-PNIPAAm nanogels, *Nanomed Research Journal*, 1(2), 90–96 (2016).
481. M. R. Berry and M. D. Likar, Statistical assessment of dissolution and drug release profile similarity using a model-dependent approach, *Journal of Pharmaceutical and Biomedical Analysis*, 45(1), 194–200 (2007).
482. A. N. F. Versypt, D. W. Packa, and R. D. Braatz, Mathematical modeling of drug delivery from autocatalytically degradable PLGA microspheres—A review, *Journal of Controlled Release*, 165(1), 29–37 (2013).

483. N. Anarjan, H. Jafarizadeh-Malmiri, I. A. Nehdi, H. M. Sbihi, S. I. Al-Resayes, and C. P. Tan, Effects of homogenization process parameters on physicochemical properties of astaxanthin nanodispersions prepared using a solvent-diffusion technique, *International Journal of Nanomedicine*, 10(1), 1109–1118 (2015).
484. K. J. Wadher, R. B. Kakde, and M. J. Umekar, Formulation and evaluation of a sustained-release tablets of metformin hydrochloride using hydrophilic synthetic and hydrophobic natural polymers, *Indian Journal of Pharmaceutical Sciences*, 73(2), 208–15 (2011).
485. Y. A. Bhatt and D. A. Shah, Effect of processing variables in formulation and development of biodegradable microparticles, *International Journal of Pharmacy and Pharmaceutical Sciences*, 3(4), 234–239 (2011).
486. T. Phaechamud and W. Darunkaisorn, Drug release behavior of polymeric matrix filled in capsule, *Saudi Pharmaceutical Journal*, 24(1), 627–634 (2016).
487. H. Yasuda and J. T. Tsai, Pore size of microporous polymer membranes, *Journal of Applied Polymer Science*, 18(3), 805–819 (1974).
488. S. Sahoo, C. K. Chakraborti, and P. K. Behera, Development and evaluation of gastroretentive controlled release polymeric suspensions containing ciprofloxacin and carbopol polymers, *Journal of Chemical and Pharmaceutical Research*, 4(4), 2268–2284 (2012).
489. P. S. C. Bose, P. S. Reddy, V. Ravi, D. Sarita, and P. T. M. Kumar, Formulation and evaluation of sustained release floating tablets of diltiazem HCL using xanthan gum, *Research Journal of Pharmaceutical, Biological and Chemical Sciences*, 2(2), 319–328 (2011).
490. J. L. Ford, M. H. Rubinstein, and J. E. Hogan, Formulation of sustained release promethazine hydrochloride tablets using hydroxypropyl-methylcellulose matrices, *International Journal of Pharmaceutics*, 24(2), 327–338 (1985).
491. V. Patel and N. Patel, Statistical evaluation of influence of viscosity of polymer and types of filler on dipyrindamole release from floating matrix tablets, *Indian Journal of Pharmaceutical Sciences*, 69(1), 51–57 (2007).
492. K. Tahara, K. Yamamoto, and T. Nishihata, Overall mechanism behind matrix sustained release (SR) tablets prepared with hydroxypropyl methylcellulose 2910, *Journal of Controlled Release*, 35(1), 59–66 (1995).
493. S. M. Khamanga and R. B. Walker, In vitro dissolution kinetics of captopril from microspheres manufactured by solvent evaporation, *Dissolution Technologies*, 19(1), 42–51 (2012).
494. M. S. Rahman *et al.*, Preparation, characterization and in vitro-in vivo evaluation of glimepiride loaded polymeric microspheres, *International Journal of Pharmacy*, 4(4), 189–198 (2014).
495. D. Leblond, S. Altan, S. Novick, J. Peterson, Y. Shen, and H. Yang, In vitro dissolution curve comparisons: a critique of current practice, *Dissolution Technologies*, 23(1), 14–23 (2016).
496. T. G. Soni, J. U. Desai, C. D. Nagda, T. R. Gandhi, and N. P. Chotai, Mathematical evaluation of similarity factor using various weighing approaches on aceclofenac marketed formulations by model-independent method, *Pharmazie*, 63(1), 31–34 (2008).
497. M. C. Gohel, K. G. Sarvaiya, A. R. Shah, and B. K. Brahmabhatt, Mathematical approach for the assessment of similarity factor using a new scheme for calculating weight, *Indian journal of pharmaceutical sciences*, 71(2), 142–4 (2009).
498. P. Bhagyashree, G. Karishma, A. Sampada, P. Ankita, C. Pratibha, and V. Kailash, Recent trends in stability testing of pharmaceutical products: a review, *Research Journal of Pharmaceutical, Biological and Chemical Sciences*, 6(1), 1557–1569 (2015).

499. K. Huynh-Ba, Handbook of Stability Testing in Pharmaceutical Development. New York: Spriger Science and Business Media, 2009.
500. S. Bajaj, D. Singla, and N. Sakhuja, Stability testing of pharmaceutical products, *Journal of Applied Pharmaceutical Science*, 2(3), 129–138 (2012).
501. L. Shargel and I. Kanfer, Generic drug product development: solid oral dosage forms, 2nd ed. New York: CRC Press/Taylor and Francis Group, 2014.
502. K. Huynh-Ba, Handbook of stability testing in pharmaceutical development : regulations, methodologies, and best practices. New York: Springer, 2009.
503. T. Kupiec, Quality-control analytical methods: gas chromatography, *International Journal of Pharmaceutical Compounding*, 8(4), 305–309 (2004).
504. S. K. Bhardwaj, K. Dwivedi, and D. D. Agarwal, A review: GC method development and validation, *International Journal of Analytical and Bioanalytical Chemistry*, 6(1), 1–7 (2016).
505. H. Rotzsche, Stationary phases in gas chromatography. New York: Elsevier, 1991.
506. R. E. Clement and V. Y. Taguchi, Techniques for the gas chromatography-mass spectrometry identification of organic compounds in effluents. Queen's Printer for Ontario, 1991.
507. S. Z. Hussain and K. Maqbool, GC-MS: Principle, technique and its application in food science, *International Journal of Current Science*, 12(1), 116–126 (2014).
508. G. H. Jeffery, J. Bassett, J. Mendham, and R. C. Denney, Vogel's Textbook of quantitative chemical analysis, 5th ed. New York: John Wiley and Sons, 1989.
509. E. Heftmann, Chromatography: fundamentals and applications of chromatography and related differential migration methods, 6th ed. London: Elsevier, 2004.
510. K. Grodowska and A. Parczewski, Organic solvents in the pharmaceutical industry, *Acta Poloniae Pharmaceutica*, 67(1), 3–12 (2010).
511. Rosemount Analytical, Fundamentals of Gas Chromatography (2012).
512. R. L. Grob and E. F. Barry, Modern practice of Gas chromatography, 4th ed. New York: John Wiley and Sons Ltd., 2004.
513. K. Dettmer-Wilde and W. Engewald, Practical gas chromatography: a comprehensive reference. Springer-Verlag, 2014.
514. A. G. Piatanida and A. R. Barron, Principles of Gas Chromatography, 1–12 (2014).
515. V. V. Pillay, Modern Medical Toxicology., 4th ed. New Delhi: Jaypee Brothers Pvt. Ltd, 2013.
516. T. Holm, Aspects of the mechanism of the flame ionization detector, *Journal of Chromatography A*, 842(1), 221–227 (1999).
517. B. Sivasikiran, Y. N. Chowdary, V. Sreelakshmi, S. K. Shrivastava, and S. Pugazhendhy, Development and validation of a headspace gas chromatographic method for determination of residual solvents in bosentan monohydrate, *International Journal of PharmTech Research*, 6(2), 421–427 (2014).
518. C. Deng, N. Li, X. Wang, X. Zhang, and J. Zeng, Rapid determination of acetone in human blood by derivatization with pentafluorobenzyl hydroxylamine followed by headspace liquid-phase microextraction and gas chromatography / mass spectrometry, *Rapid Communications in Mass Spectrometry*, 19(1), 647–653 (2005).

519. J. Peinado, F. J. Lopez-Soriano, and J. . Argiles, Gas chromatographic method for the estimation of acetone and its metabolites in biological samples, *Journal of Chromatography*, 415, 372–376 (1987).
520. D. Palma de Oliveira, A simple and rapid method for urinary acetone analysis by headspace/gas chromatography, *Quimica Nova*, 30(5), 1362–1364 (2007).
521. H. K. Winterbach and P. J. Apps, A gas-chromatographic headspace method for the determination of acetone in bovine milk, blood and urine, *Journal of Veterinary Research*., 58(1), 75–79 (1991).
522. K. Kondo *et al.*, Sensitive determination of n-hexane and cyclohexane in human body fluids by capillary gas chromatography with cryogenic oven trapping, *Journal of AOAC International*, 84(1), 19–23 (2001).
523. H. Pontes *et al.*, GC determination of acetone, acetaldehyde, ethanol, and methanol in biological matrices and cell culture, *Journal of Chromatographic Science*, 47(4), 272–278 (2009).
524. P. C. F. de L. Gomes, É. D. D'Andrea, C. B. Mendes, and M. E. P. B. de Siqueira, Determination of Benzene, Toluene and n-hexane in urine and blood by headspace solid-phase microextraction/gas-chromatography for the biomonitoring of occupational exposure, *Journal of Brazil Society*, 21(1), 119–126 (2010).
525. Q. C. Li and K. A. Cohen, A capillary gas chromatographic procedure for the analysis of nine common residual solvents in water-insoluble bulk pharmaceuticals, *Journal of Chromatographic Science*, 36(1), 119–124 (1998).
526. T. D. Ruppel, Simultaneous and rapid separation of blood-alcohol compounds and commonly abused inhalants by headspace-gas chromatography (2006).
527. K. Maštovská and S. J. Lehotay, Evaluation of common organic solvents for gas chromatographic analysis and stability of multiclass pesticide residues, *Journal of Chromatography A*, 1040(1), 259–272 (2004).
528. J. Oostdijk, J. Kuipers, and G. Ramaprasad, Hexane for best separation of solvents and hexane isomers (2015).
529. R. Martino, M. Malet-Martino, V. Gilard, and S. Balayssac, Counterfeit drugs: analytical techniques for their identification, *Analytical and Bioanalytical Chemistry*, 398(1), 77–92 (2010).
530. E. C. Horning *et al.*, Quantitative analysis of fatty acids by gas-liquid chromatography, *journal of lipid research*, 5(1), 20–27 (1964).
531. B. Stuart, Gas chromatography. Royal Society of Chemistry, 2003.
532. K. Robards, P. R. Haddad, and P. E. Jackson, Principles and practice of modern chromatographic methods. Elsevier/Academic Press, 2004.
533. R. . Buntrock, The Merck Index: an encyclopedia of chemicals, drugs, and biologicals, 15th ed. New Jersey: Merck and Co., 2013.

APPENDIX I

BATCH MANUFACTURING RECORDS FOR F-001

Only one solvent evaporation record is included for this study. The records for the other batches, F-002 to F006, CCD-001 to CCD-050, OPT1 and OPT 2 are available on request.

BATCH PRODUCTION RECORD

Faculty of Pharmacy, Rhodes University, Grahamstown, 6140, South Africa.

Product Name: hydralazine

Batch number: F-001

Batch size: 2.5g

EQUIPMENT VERIFICATION

| Description | Type | Verified By | Confirmed By |
|-------------|-----------------------|-------------|--------------|
| Scale | Mettler Model PM 4600 | | |
| Homogeniser | Virtis | | |
| Vacuum pump | Aspirator A-2S | | |
| Oven | Memmert TV 50A | | |

MANUFACTURING APPROVALS

Batch record issued by: _____

Date: _____

Master record issued by: _____

Date: _____

BATCH MANUFACTURING RECORD

Faculty of Pharmacy, Rhodes University, Grahamstown, 6140, South Africa.

Product: Hydralazine
Batch ID Number: F-001
Batch Size: 2.5g

Date:
Start time:
End time:

Master formula and batch formula

| <i>Materials</i> | <i>Formula (%m/m or v/m)</i> | <i>Amount added (g)</i> | <i>Dispensed By</i> | <i>Checked By</i> |
|------------------|------------------------------|-------------------------|---------------------|-------------------|
| HYD | 20 | | | |
| Methocel® K100M | 40 | | | |
| Eudragit® RS PO | 40 | | | |
| Liquid paraffin | 120 mL | | | |
| Acetone | 12 mL | | | |
| <i>n</i> -hexane | 10 mL | | | |

Manufacturing Process

| Step | Procedure | Equipment | Time | Done By | Checked By |
|-------------|---|--|-------------|----------------|-------------------|
| 1 | Measure 120 mL liquid paraffin using measuring cylinder and transfer to a beaker | 400 mL beaker | | | |
| 2 | Measure 1.2 mL span 80 and add to the beaker containing liquid paraffin and homogenise at 1000 rpm for 5 minutes | 400 mL beaker | | | |
| 3 | Weigh all the materials, viz. HYD and polymers | Mettler analytical balance Model PM 4600 | | | |
| 4 | Measure 12 mL of acetone using 20 mL measuring cylinder and pour into beaker | 250 mL beaker | | | |
| 5 | Dissolve the weighed material in acetone | 250 mL beaker | | | |
| 6 | Mix the acetone dispersion with the contents in the 400 mL beaker | | | | |
| 7 | Homogenise at 500 rpm to prepare a homogenous oily phase | Three-blade Virtis Homogeniser | | | |
| 8 | After 2 hours, add 10 mL of <i>n</i> -hexane to harden the formed microcapsules and continue stirring for further 5 hours | 10 mL measuring cylinder | | | |
| 9 | Collect microspheres in a Buchner funnel, washed 2 -3 times with 50 mL <i>n</i> -hexane under vacuum | Eyela® Aspirator A-2S vacuum pump | | | |
| 10 | Dry microspheres at 25 °C for 24 hours and transfer to airtight amber-coloured containers | Oven | | | |

| | Prepared By | Verified By | Approved By |
|------------------|--------------------|--------------------|--------------------|
| Full name | | | |
| Signature | | | |
| Date | | | |

APPENDIX II

BATCH SUMMARY RECORDS

BATCH PRODUCTION RECORD

Faculty of Pharmacy, Rhodes University, Grahamstown, 6140, South Africa.

Formulator: Shakemore T Kangaasaru
Product: Hydralazine
Batch Number: F-001
Batch Size: 2.5g

Date: 15/06/2016
Temperature: 20 °C
Start time: 08H00
End time: 15H00

| Materials | Original formula (%w/w) | Working formula (g) | Amount added (g) |
|-----------------|-------------------------|---------------------|------------------|
| HYD | 20 | 0.5 | 0.49 |
| Methocel® K100M | 40 | 1 | 1.01 |
| Eudragit® RS PO | 40 | 1 | 1.00 |
| Total | 100 | 2.5 | 2.50 |

Manufacturing process

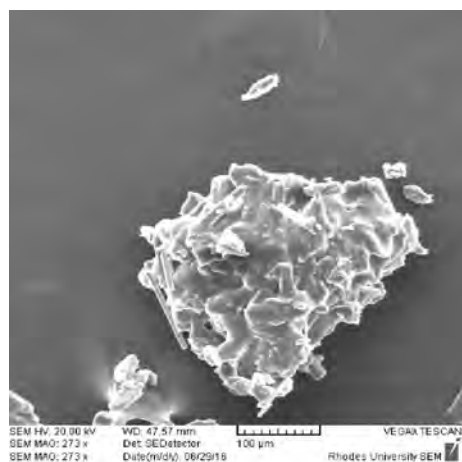
1. Dissolve 0.5 g HYD and the polymers (1g Eudragit® RS PO and 1g Methocel® K100M) in 12 mL acetone
2. Mix 120 mL liquid paraffin and 1.2 mL span 80 in a 400 mL beaker
3. Pour the milky solution containing the drug into the liquid paraffin and stir for 7 hours using a homogenizer at 500 rpm
4. After homogenising for 2 hours, add 10 mL *n*-hexane
5. Continue homogenising for the remaining 5 hours

Evaluation of HYD Microspheres

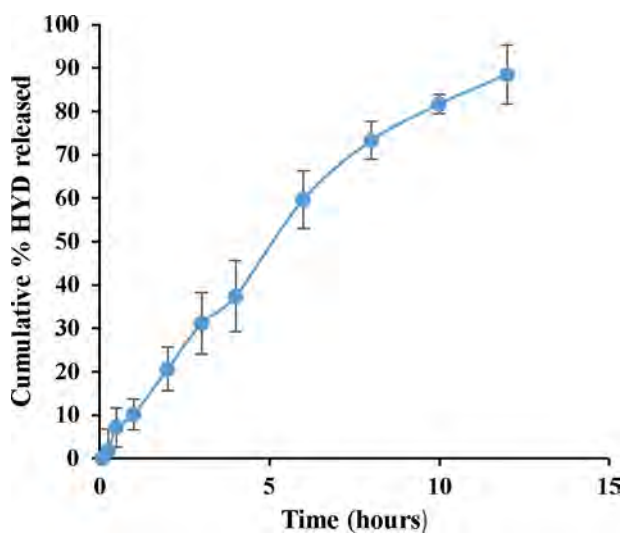
Characterisation of HYD microspheres:

1. Yield (%): 91
2. Encapsulation efficiency (%): 83
3. HYD content (%): 91

SEM image



In vitro dissolution profile



BATCH PRODUCTION RECORD

Faculty of Pharmacy, Rhodes University, Grahamstown, 6140, South Africa.

| | |
|---|---------------------------|
| Formulator: Shakemore T Kangausaru | Date: 16/06/2016 |
| Product: Hydralazine | Temperature: 19 °C |
| Batch Number: F-002 | Start time: 08H00 |
| Batch Size: 2.5g | End time: 15H00 |

| <i>Materials</i> | <i>Original formula (%w/w)</i> | <i>Working formula (g)</i> | <i>Amount added (g)</i> |
|------------------|--------------------------------|----------------------------|-------------------------|
| HYD | 20 | 0.5 | 0.49 |
| Methocel® K15M | 40 | 1 | 1.01 |
| Eudragit® RS PO | 40 | 1 | 1.00 |
| Total | 100 | 2.5 | 2.50 |

Manufacturing process

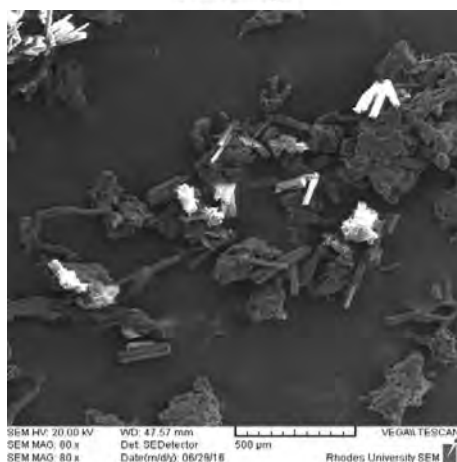
| | |
|----|--|
| 1. | Dissolve 0.5 g HYD and the polymers (1g Eudragit® RS PO and 1g Methocel® K15M) in 12 mL acetone |
| 2. | Mix 120 mL liquid paraffin and 1.2 mL span 80 in a 400 mL beaker |
| 3. | Pour the milky solution containing the drug into the liquid paraffin and stir for 7 hours using a homogenizer at 500 rpm |
| 4. | After homogenising for 2 hours, add 10 mL <i>n</i> -hexane |
| 5. | Continue homogenising for the remaining 5 hours |

Evaluation of HYD Microspheres

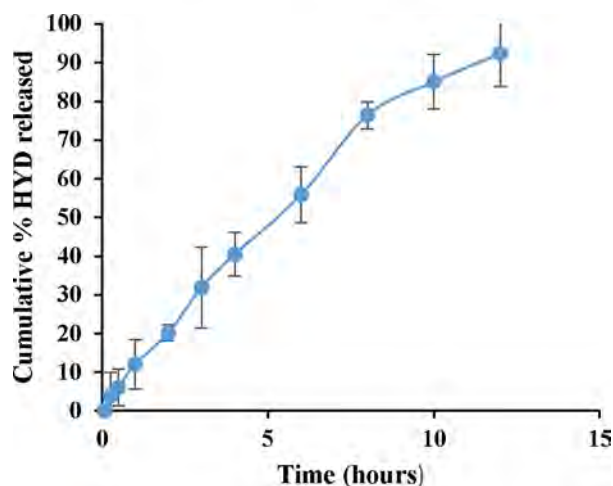
Characterisation of HYD microspheres:

1. Yield (%): 94
2. Encapsulation efficiency (%): 86
3. HYD content (%): 91

SEM image



In vitro dissolution profile



BATCH PRODUCTION RECORD

Faculty of Pharmacy, Rhodes University, Grahamstown, 6140, South Africa.

| | |
|---|---------------------------|
| Formulator: Shakemore T Kangausaru | Date: 17/06/2016 |
| Product: Hydralazine | Temperature: 19 °C |
| Batch Number: F-003 | Start time: 08H00 |
| Batch Size: 2.5g | End time: 15H00 |

| <i>Materials</i> | <i>Original formula (%m/m)</i> | <i>Working formula (g)</i> | <i>Amount added (g)</i> |
|-------------------|--------------------------------|----------------------------|-------------------------|
| HYD | 20 | 0.5 | 0.49 |
| Methocel® K100 LV | 40 | 1 | 1.01 |
| Eudragit® RS PO | 40 | 1 | 1.00 |
| Total | 100 | 2.5 | 2.50 |

Manufacturing process

| | |
|----|--|
| 1. | Dissolve 0.5g HYD and the polymers (1g Eudragit® RS PO and 1g Methocel® K100LV) in 12 mL acetone |
| 2. | Mix 120 mL liquid paraffin and 1.2 mL span 80 in a 400 mL beaker |
| 3. | Pour the milky solution containing the drug into the liquid paraffin and stir for 7 hours using a homogenizer at 500 rpm |
| 4. | After homogenising for 2 hours, add 10 mL <i>n</i> -hexane |
| 5. | Continue homogenising for the remaining 5 hours |

Evaluation of HYD Microspheres

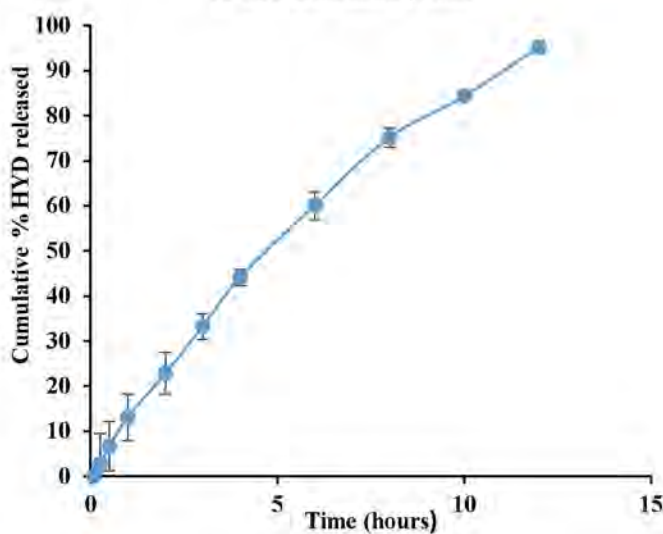
Characterisation of HYD microspheres:

1. Yield (%): 97
2. Encapsulation efficiency (%): 90
3. HYD content (%): 96

SEM image



***In vitro* dissolution profile**



BATCH PRODUCTION RECORD

Faculty of Pharmacy, Rhodes University, Grahamstown, 6140, South Africa.

| | |
|---|---------------------------|
| Formulator: Shakemore T Kangausaru | Date: 18/06/2016 |
| Product: Hydralazine | Temperature: 19 °C |
| Batch Number: F-004 | Start time: 08H00 |
| Batch Size: 2.5g | End time: 15H00 |

| <i>Materials</i> | <i>Original formula (%m/m)</i> | <i>Working formula (g)</i> | <i>Amount added (g)</i> |
|------------------|--------------------------------|----------------------------|-------------------------|
| HYD | 20 | 0.5 | 0.49 |
| Methocel® K100M | 40 | 1 | 1.01 |
| Eudragit® L 100 | 40 | 1 | 1.00 |
| Total | 100 | 2.5 | 2.50 |

Manufacturing process

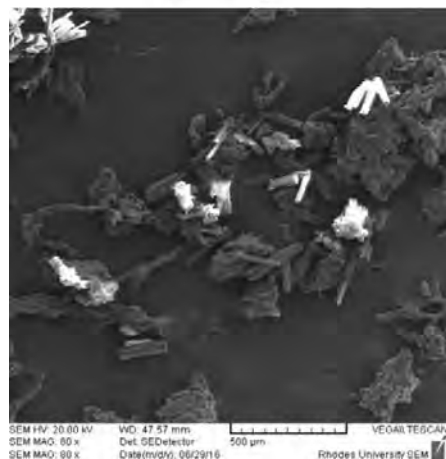
| | |
|----|--|
| 1. | Dissolve 0.5g HYD and the polymers (1g Eudragit® L 100 and 1g Methocel® K100M) in 12 mL acetone |
| 2. | Mix 120 mL liquid paraffin and 1.2 mL span 80 in a 400 mL beaker |
| 3. | Pour the milky solution containing the drug into the liquid paraffin and stir for 7 hours using a homogenizer at 500 rpm |
| 4. | Add 10 mL of <i>n</i> -hexane after 2 hours of stirring |
| 5. | Continue homogenising for the remaining 5 hours |

Evaluation of HYD Microspheres

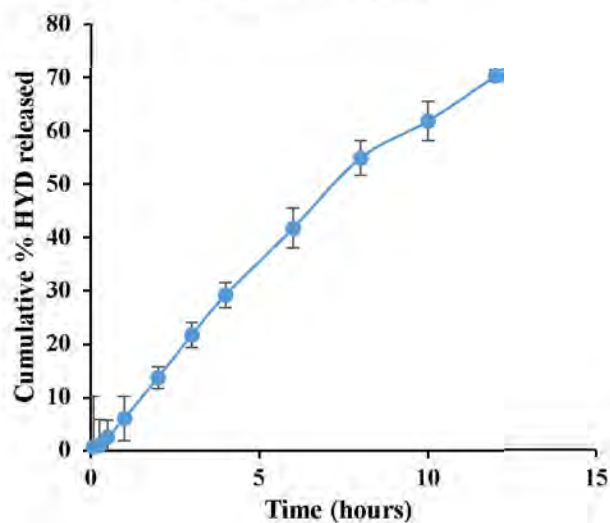
Characterisation of HYD microspheres:

1. Yield (%): 98
2. Encapsulation efficiency (%): 76
3. HYD content (%): 73

SEM image



In vitro dissolution profile



BATCH PRODUCTION RECORD

Faculty of Pharmacy, Rhodes University, Grahamstown, 6140, South Africa.

| | |
|---|---------------------------|
| Formulator: Shakemore T Kangausaru | Date: 19/06/2016 |
| Product: Hydralazine | Temperature: 19 °C |
| Batch Number: F-005 | Start time: 08H00 |
| Batch Size: 2.5g | End time: 15H00 |

| <i>Materials</i> | <i>Original formula (%w/w)</i> | <i>Working formula (g)</i> | <i>Amount added (g)</i> |
|------------------|--------------------------------|----------------------------|-------------------------|
| HYD | 20 | 0.5 | 0.49 |
| Methocel® K15M | 40 | 1 | 1.01 |
| Eudragit® L 100 | 40 | 1 | 1.00 |
| Total | 100 | 2.5 | 2.50 |

Manufacturing process

| | |
|----|--|
| 1. | Dissolve 0.5g HYD and the polymers (1g Eudragit® L 100 and 1g Methocel® K15M) in 12 mL acetone |
| 2. | Mix 120 mL liquid paraffin and 1.2 mL span 80 in a 400 mL beaker |
| 3. | Pour the milky solution containing the drug into the liquid paraffin and stir for 7 hours using a homogenizer at 500 rpm |
| 4. | After homogenising for 2 hours, add 10 mL <i>n</i> -hexane |
| 5. | Continue homogenising for the remaining 5 hours |

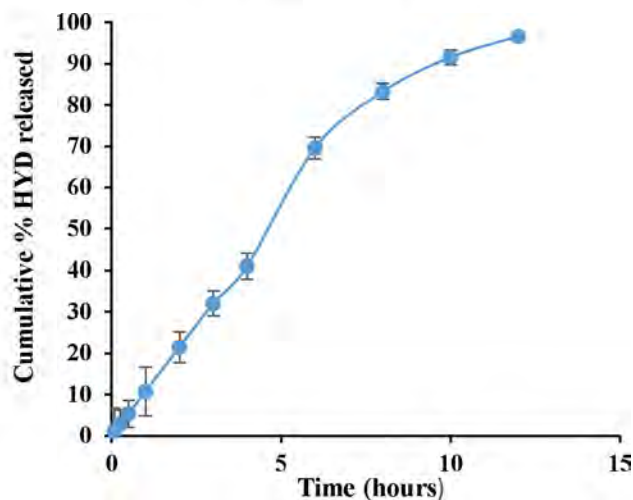
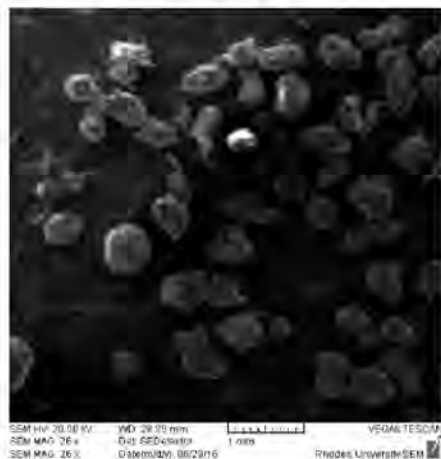
Evaluation of HYD Microspheres

Characterisation of HYD microspheres:

1. Yield (%): 96
2. Encapsulation efficiency (%): 93
3. HYD content (%): 96

In vitro dissolution profile

SEM image



BATCH PRODUCTION RECORD

Faculty of Pharmacy, Rhodes University, Grahamstown, 6140, South Africa.

Formulator: Shakemore T Kangausaru

Date: 20/06/2016

Product: Hydralazine

Temperature: 20 °C

Batch Number: F-006

Start time: 08H00

Batch Size: 2.5g

End time: 15H00

| Materials | Original formula (%m/m) | Working formula (g) | Amount added (g) |
|-------------------|-------------------------|---------------------|------------------|
| HYD | 20 | 0.5 | 0.49 |
| Methocel® K100 LV | 40 | 1 | 1.01 |
| Eudragit® L 100 | 40 | 1 | 1.00 |
| Total | 100 | 2.5 | 2.50 |

Manufacturing process

1. Dissolve 0.5g HYD and the polymers (1g Eudragit® L 100 and 1g Methocel® K100LV) in 12 mL acetone
2. Mix 120 mL liquid paraffin and 1.2 mL span 80 in a 400 mL beaker
3. Pour the milky solution containing the drug into the liquid paraffin and stir for 7 hours using a homogenizer at 500 rpm
4. After homogenising for 2 hours, add 10 mL *n*-hexane
5. Continue homogenising for the remaining 5 hours

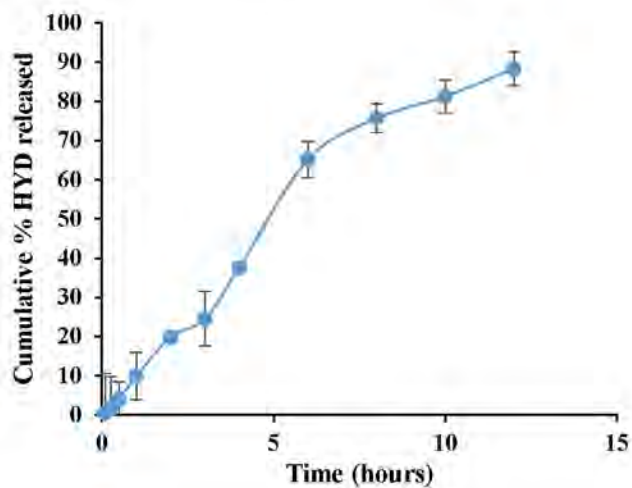
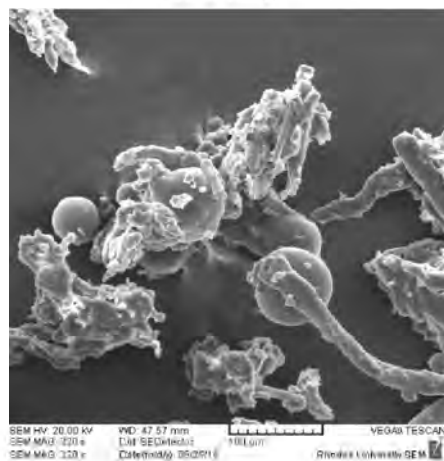
Evaluation of HYD Microspheres

Characterisation of HYD microspheres:

1. Yield (%): 92
2. Encapsulation efficiency (%): 85
3. HYD content (%): 85

In vitro dissolution profile

SEM image



BATCH PRODUCTION RECORD

Faculty of Pharmacy, Rhodes University, Grahamstown, 6140, South Africa.

| | |
|---|---------------------------|
| Formulator: Shakemore T Kangausaru | Date: 28/06/2016 |
| Product: Hydralazine | Temperature: 19 °C |
| Batch Number: CCD-HYD-001 | Start time: 14H00 |
| Batch Size: 3.5g | End time: 22H00 |

| <i>Materials</i> | <i>Original formula (%m/m)</i> | <i>Working formula (g)</i> | <i>Amount added (g)</i> |
|-------------------|--------------------------------|----------------------------|-------------------------|
| HYD | 14.3 | 0.5 | 0.51 |
| Methocel® K100 LV | 17.1 | 0.6 | 0.60 |
| Eudragit® RS PO | 17.1 | 0.6 | 0.62 |
| Avicel® 101 | Sq. | 1.8 | 1.81 |
| Total | 100 | 3.5 | 3.54 |

Manufacturing process

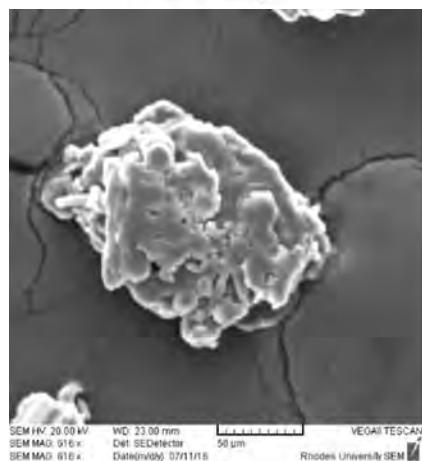
| |
|---|
| 1. Dissolve 0.5 g HYD, polymers (0.6g Eudragit® RS PO and 0.6g Methocel® K100LV) and 1.8g Avicel® 101 in 14.5 mL acetone |
| 2. Mix 120 mL liquid paraffin and 1.2 mL span 80 in a 400 mL beaker |
| 3. Pour the milky solution containing the drug into the liquid paraffin and stir for 8 hours using a homogenizer at 800 rpm |
| 4. After homogenising for 2 hours, add 10 mL <i>n</i> -hexane |
| 5. Continue homogenising for the remaining 6 hours |

Evaluation of HYD microspheres

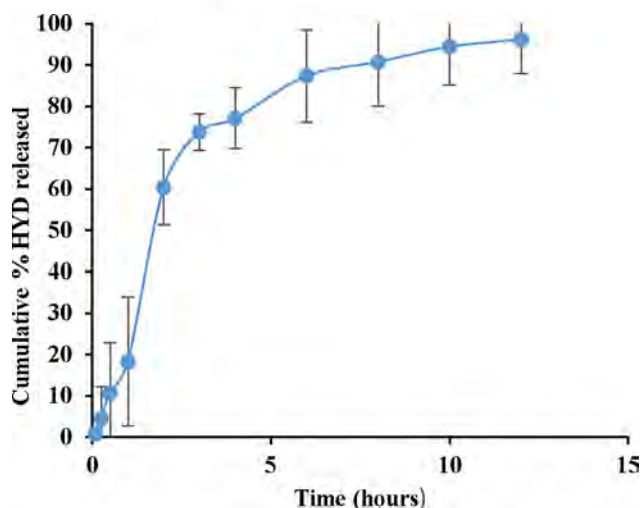
Characterisation of HYD microspheres:

1. Yield (%): 76.3
2. Encapsulation efficiency (%): 32.4
3. HYD content (%): 86.2

SEM image



In vitro dissolution profile



BATCH PRODUCTION RECORD

Faculty of Pharmacy, Rhodes University, Grahamstown, 6140, South Africa.

| | |
|---|---------------------------|
| Formulator: Shakemore T Kangausaru | Date: 29/06/2016 |
| Product: Hydralazine | Temperature: 20 °C |
| Batch Number: CCD-HYD-002 | Start time: 14H00 |
| Batch Size: 3.5g | End time: 21H00 |

| <i>Materials</i> | <i>Original formula (%m/m)</i> | <i>Working formula (g)</i> | <i>Amount added (g)</i> |
|-------------------|--------------------------------|----------------------------|-------------------------|
| HYD | 14.3 | 0.50 | 0.51 |
| Methocel® K100 LV | 28.6 | 1 | 1.01 |
| Eudragit® RS PO | 28.6 | 1 | 1.00 |
| Avicel® 101 | Sq. | 1 | 1.02 |
| Total | 100 | 3.5g | 3.54 |

Manufacturing process

| | |
|----|--|
| 1. | Dissolve 0.5 g HYD, polymers (1g Eudragit® RS PO and 1g Methocel® K100M) and 1g Avicel® 101 in 16mL of acetone |
| 2. | Mix 120 mL liquid paraffin and 1.2 mL span 80 in a 400 mL beaker |
| 3. | Pour the milky solution containing the drug into the liquid paraffin and stir for 7 hours using a homogenizer at 600 rpm |
| 4. | After homogenising for 2 hours, add 10 mL <i>n</i> -hexane |
| 5. | Continue homogenising for the remaining 5 hours |

Evaluation of HYD microspheres

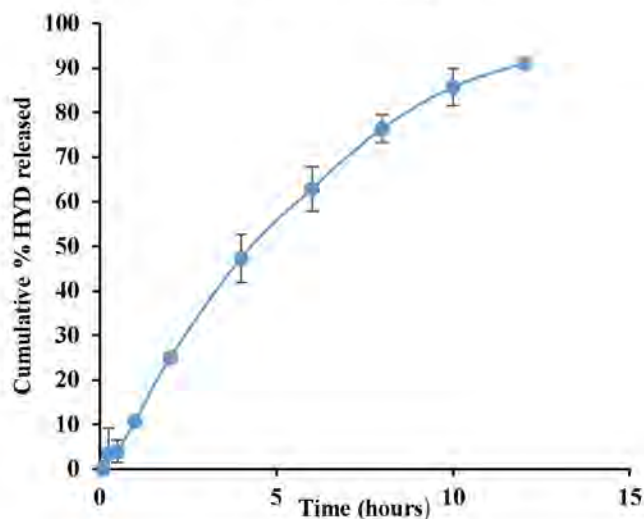
Characterisation of HYD microspheres:

1. Yield (%): 95.4
2. Encapsulation efficiency (%): 85.3
3. HYD content (%): 81.9

SEM image



In vitro dissolution profile



BATCH PRODUCTION RECORD

Faculty of Pharmacy, Rhodes University, Grahamstown, 6140, South Africa.

Formulator: Shakemore T Kangaasaru

Product: Hydralazine

Batch Number: CCD-HYD-003

Batch Size: 3.5g

Date: 30/06/2016

Temperature: 20 °C

Start time: 14H00

End time: 21H00

| Materials | Original formula (%m/m) | Working formula (g) | Amount added (g) |
|-------------------|-------------------------|---------------------|------------------|
| HYD | 14.3 | 0.50 | 0.50 |
| Methocel® K100 LV | 28.6 | 1 | 1.00 |
| Eudragit® RS PO | 28.6 | 1 | 1.00 |
| Avicel® 101 | Sq. | 1 | 1.02 |
| Total | 100 | 3.5g | 3.52 |

Manufacturing process

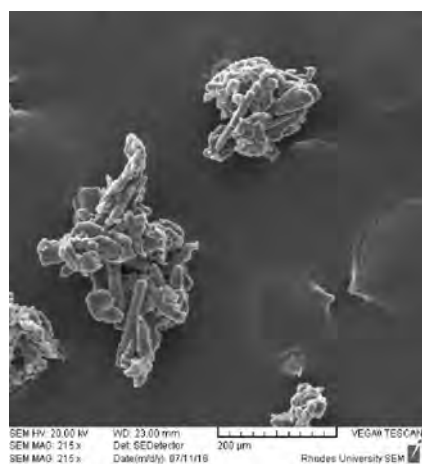
1. Dissolve 0.5 g HYD, polymers (1g Eudragit® RS PO and 1g Methocel® K100LV) and 1g Avicel® 101 in 13.5 mL acetone
2. Mix 120 mL liquid paraffin and 1.2 mL span 80 in a 400 mL beaker
3. Pour the milky solution containing the drug into the liquid paraffin and stir for 7 hours using a homogenizer at 600 rpm
4. After homogenising for 2 hours, add 10 mL *n*-hexane
5. Continue homogenising for the remaining 5 hours

Evaluation of HYD microspheres

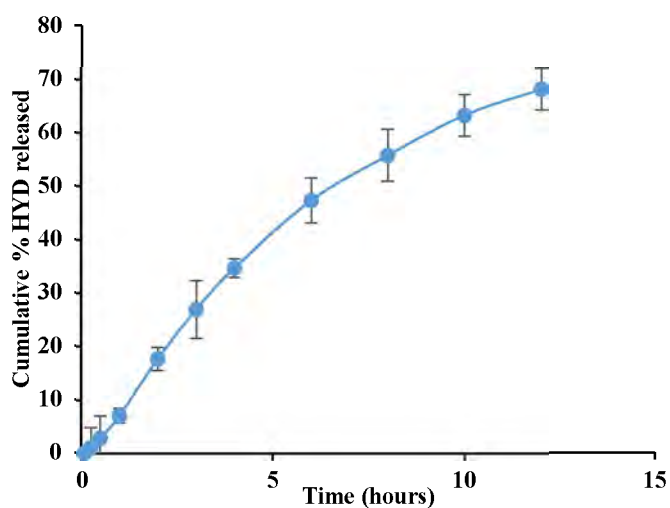
Characterisation of HYD microspheres:

1. Yield (%): 100.3
2. Encapsulation efficiency (%): 78.9
3. HYD content (%): 86.3

SEM image



In vitro dissolution profile



BATCH PRODUCTION RECORD

Faculty of Pharmacy, Rhodes University, Grahamstown, 6140, South Africa.

| | |
|---|---------------------------|
| Formulator: Shakemore T Kangausaru | Date: 30/06/2016 |
| Product: Hydralazine | Temperature: 20 °C |
| Batch Number: CCD-HYD-004 | Start time: 21H00 |
| Batch Size: 3.5g | End time: 05H00 |

| <i>Materials</i> | <i>Original formula (%m/m)</i> | <i>Working formula (g)</i> | <i>Amount added (g)</i> |
|-------------------|--------------------------------|----------------------------|-------------------------|
| HYD | 14.3 | 0.5 | 0.50 |
| Methocel® K100 LV | 17.1 | 0.6 | 0.60 |
| Eudragit® RS PO | 17.1 | 0.6 | 0.61 |
| Avicel®101 | Sq. | 1.8 | 1.81 |
| Total | 100 | 3.5g | 3.52 |

Manufacturing process

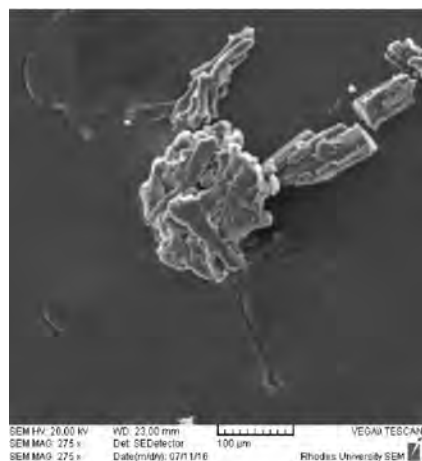
1. Dissolve 0.5 g HYD, polymers (0.6g Eudragit® RS PO and 0.6g Methocel® K100LV) and 1.8g Avicel® 101 in 12.5 mL acetone
2. Mix 120 mL liquid paraffin and 1.2 mL span 80 in a 400 mL beaker
3. Pour the milky solution containing the drug into the liquid paraffin and stir for 8 hours using a homogenizer at 400 rpm
4. After homogenising for 2 hours, add 10 mL *n*-hexane
5. Continue homogenising for the remaining 6 hours

Evaluation of HYD microspheres

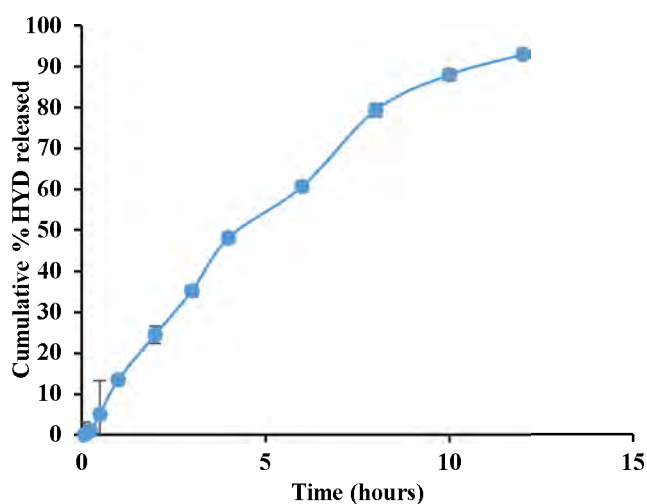
Characterisation of HYD microspheres:

1. Yield (%): 92.6
2. Encapsulation efficiency (%): 67.9
3. HYD content (%): 90.2

SEM image



***In vitro* dissolution profile**



BATCH PRODUCTION RECORD

Faculty of Pharmacy, Rhodes University, Grahamstown, 6140, South Africa.

| | |
|---|---------------------------|
| Formulator: Shakemore T Kangausaru | Date: 01/07/2016 |
| Product: Hydralazine | Temperature: 20 °C |
| Batch Number: CCD-HYD-005 | Start time: 07H00 |
| Batch Size: 3.5g | End time: 13H00 |

| <i>Materials</i> | <i>Original formula (%w/w)</i> | <i>Working formula (g)</i> | <i>Amount added (g)</i> |
|-------------------|--------------------------------|----------------------------|-------------------------|
| HYD | 14.3 | 0.5 | 0.50 |
| Methocel® K100 LV | 40 | 1.4 | 1.41 |
| Eudragit® RS PO | 17.1 | 0.6 | 0.60 |
| Avicel® 101 | Sq. | 1 | 1.00 |
| Total | 100 | 3.5g | 3.51 |

Manufacturing process

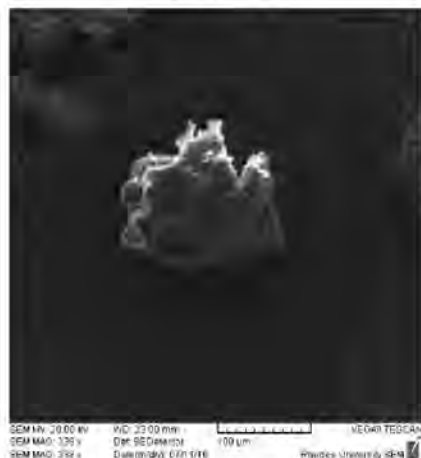
| |
|---|
| 1. Dissolve 0.5 g HYD, polymers (0.6g Eudragit® RS PO and 1.4g Methocel® K100LV) and 1g Avicel® 101 in 12.5 mL acetone |
| 2. Mix 120 mL liquid paraffin and 1.2 mL span 80 in a 400 mL beaker |
| 3. Pour the milky solution containing the drug into the liquid paraffin and stir for 6 hours using a homogenizer at 400 rpm |
| 4. After homogenising for 2 hours, add 10 mL <i>n</i> -hexane |
| 5. Continue homogenising for the remaining 4 hours |

Evaluation of HYD microspheres

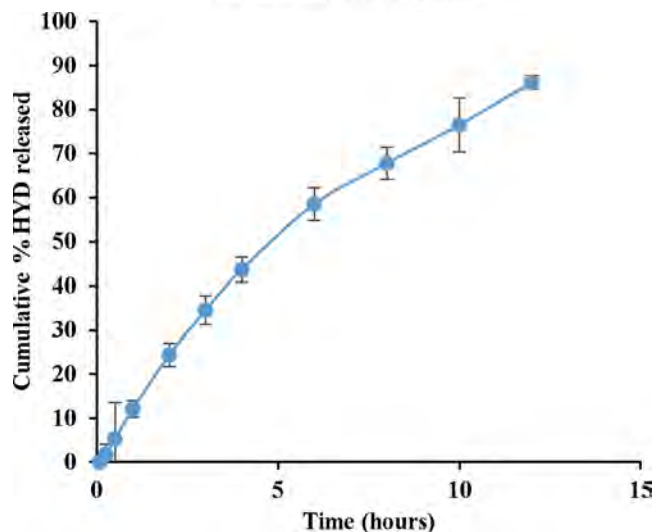
Characterisation of HYD microspheres:

1. Yield (%): 91.7
2. Encapsulation efficiency (%): 79.2
3. HYD content (%): 96.0

SEM image



In vitro dissolution profile



BATCH PRODUCTION RECORD

Faculty of Pharmacy, Rhodes University, Grahamstown, 6140, South Africa.

| | |
|---|---------------------------|
| Formulator: Shakemore T Kangausaru | Date: 01/07/2016 |
| Product: Hydralazine | Temperature: 21 °C |
| Batch Number: CCD-HYD-006 | Start time: 14H00 |
| Batch Size: 3.5g | End time: 20H00 |

| <i>Materials</i> | <i>Original formula (%m/m)</i> | <i>Working formula (g)</i> | <i>Amount added (g)</i> |
|------------------|--------------------------------|----------------------------|-------------------------|
| HYD | 14.3 | 0.5 | 0.51 |
| Methocel® K100LV | 17.1 | 0.6 | 0.60 |
| Eudragit® RS PO | 40 | 1.4 | 1.41 |
| Avicel® 101 | Sq. | 1.0 | 1.00 |
| Total | 100 | 3.5 | 3.52 |

Manufacturing process

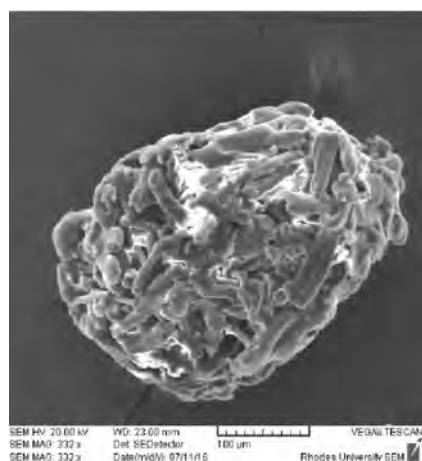
1. Dissolve 0.5 g HYD, polymers (1.4g Eudragit® RS PO and 0.6g Methocel® K100LV) and 1.5g Avicel® 101 in 12.5 mL acetone
2. Mix 120 mL liquid paraffin and 1.2 mL span 80 in a 400 mL beaker
3. Pour the milky solution containing the drug into the liquid paraffin and stir for 6 hours using a homogenizer at 800 rpm
4. After homogenising for 2 hours, add 10 mL *n*-hexane
5. Continue homogenising for the remaining 4 hours

Evaluation of HYD microspheres

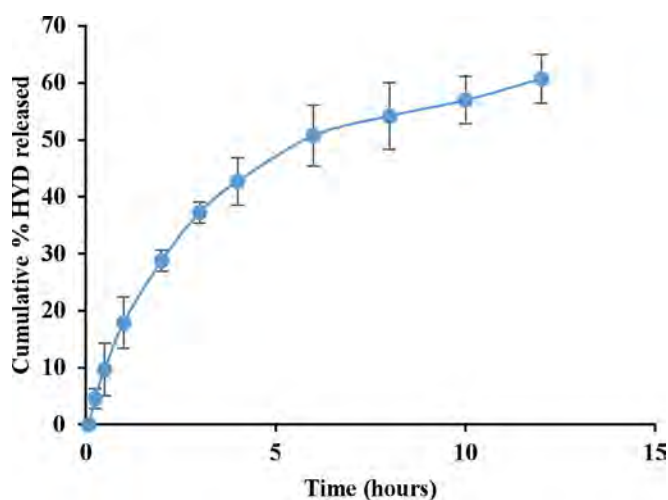
Characterisation of HYD microspheres:

1. Yield (%): 97.1
2. Encapsulation efficiency (%): 92.7
3. HYD content (%): 90.3

SEM image



In vitro dissolution profile



BATCH PRODUCTION RECORD

Faculty of Pharmacy, Rhodes University, Grahamstown, 6140, South Africa.

Formulator: Shakemore T Kangaasaru
Product: Hydralazine
Batch Number: CCD-HYD-007
Batch Size: 3.5g

Date: 30/06/2016
Temperature: 21 °C
Start time: 21H00
End time: 03H00

| Materials | Original formula (%m/m) | Working formula (g) | Amount added (g) |
|-------------------|-------------------------|---------------------|------------------|
| HYD | 14.3 | 0.5 | 0.51 |
| Methocel® K100 LV | 17.1 | 0.6 | 0.60 |
| Eudragit® RS PO | 40 | 1.4 | 1.41 |
| Avicel® 101 | Sq. | 1 | 1.00 |
| Total | 100 | 3.5 | 3.52 |

Manufacturing process

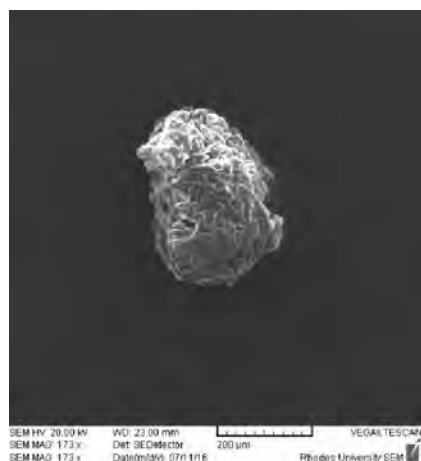
1. Dissolve 0.5 g HYD, polymers (1.4g Eudragit® RS PO and 0.6g Methocel® K100LV) and 1g Avicel® 101 in 14.5 mL acetone
2. Mix 120 mL liquid paraffin and 1.2 mL span 80 in a 400 mL beaker
3. Pour the milky solution containing the drug into the liquid paraffin and stir for 6 hours using a homogenizer at 400 rpm
4. After homogenising for 2 hours, add 10 mL *n*-hexane
5. Continue homogenising for the remaining 4 hours

Evaluation of HYD microspheres

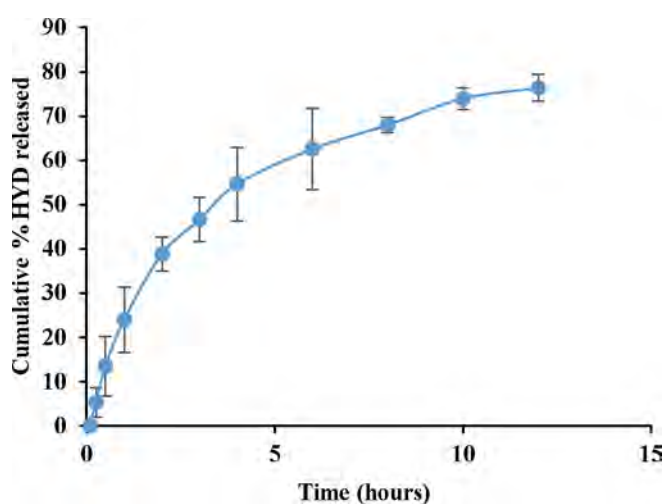
Characterisation of HYD microspheres:

1. Yield (%): 97.1
2. Encapsulation efficiency (%): 104.1
3. HYD content (%): 91.2

SEM image



***In vitro* dissolution profile**



BATCH PRODUCTION RECORD

Faculty of Pharmacy, Rhodes University, Grahamstown, 6140, South Africa.

| | |
|---|---------------------------|
| Formulator: Shakemore T Kangausaru | Date: 02/07/2016 |
| Product: Hydralazine | Temperature: 20 °C |
| Batch Number: CCD-HYD-008 | Start time: 13H00 |
| Batch Size: 3.5g | End time: 23H00 |

| <i>Materials</i> | <i>Original formula (%m/m)</i> | <i>Working formula (g)</i> | <i>Amount added (g)</i> |
|-------------------|--------------------------------|----------------------------|-------------------------|
| HYD | 14.3 | 0.5 | 0.51 |
| Methocel® K100 LV | 40 | 1.4 | 1.40 |
| Eudragit® RS PO | 40 | 1.4 | 1.41 |
| Avicel® 101 | Sq. | 0.2 | 0.21 |
| Total | 100 | 3.5 | 3.53 |

Manufacturing process

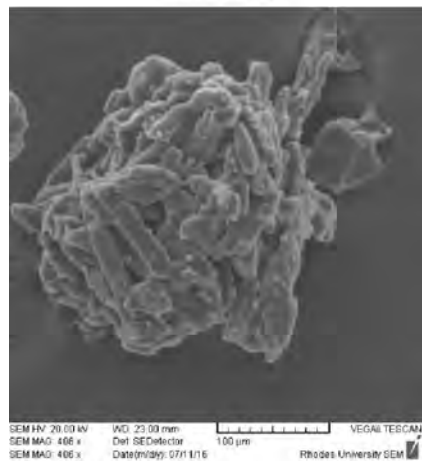
1. Dissolve 0.5 g HYD, polymers (1.4g Eudragit® RS PO and 1.4g Methocel® K100LV) and 0.2g Avicel® 101 in 14.5 mL acetone
2. Mix 120 mL liquid paraffin and 1.2 mL span 80 in a 400 mL beaker
3. Pour the milky solution containing the drug into the liquid paraffin and stir for 8 hours using a homogenizer at 800 rpm
4. After homogenising for 2 hours, add 10 mL *n*-hexane
5. Continue homogenising for the remaining 6 hours

Evaluation of HYD microspheres

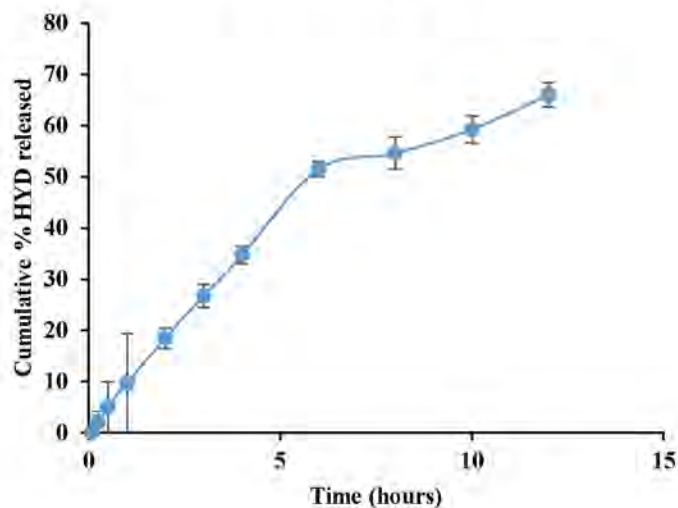
Characterisation of HYD microspheres:

1. Yield (%): 97.7
2. Encapsulation efficiency (%): 87.7
3. HYD content (%): 98.5

SEM image



In vitro dissolution profile



BATCH PRODUCTION RECORD

Faculty of Pharmacy, Rhodes University, Grahamstown, 6140, South Africa.

| | |
|---|---------------------------|
| Formulator: Shakemore T Kangausaru | Date: 03/07/2016 |
| Product: Hydralazine | Temperature: 20 °C |
| Batch Number: CCD-HYD-009 | Start time: 12H00 |
| Batch Size: 3.5g | End time: 20H00 |

| <i>Materials</i> | <i>Original formula (%m/m)</i> | <i>Working formula (g)</i> | <i>Amount added (g)</i> |
|-------------------|--------------------------------|----------------------------|-------------------------|
| HYD | 14.3 | 0.5 | 0.51 |
| Methocel® K100 LV | 17.1 | 0.6 | 0.60 |
| Eudragit® RS PO | 40 | 1.4 | 1.41 |
| Avicel®101 | Sq. | 1 | 1.00 |
| Total | 100 | 3.5 | 3.52 |

Manufacturing process

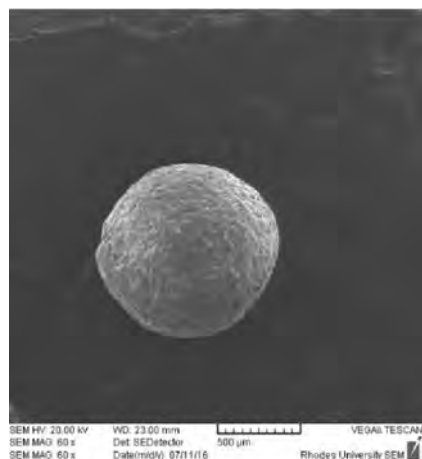
| | |
|----|--|
| 1. | Dissolve 0.5 g HYD, polymers (1.4g Eudragit® RS PO and 0.6g Methocel® K100LV) and 1g Avicel® 101 in 14.5 mL acetone |
| 2. | Mix 120 mL liquid paraffin and 1.2 mL span 80 in a 400 mL beaker |
| 3. | Pour the milky solution containing the drug into the liquid paraffin and stir for 8 hours using a homogenizer at 400 rpm |
| 4. | After homogenising for 2 hours, add 10 mL <i>n</i> -hexane |
| 5. | Continue homogenising for the remaining 6 hours |

Evaluation of HYD microspheres

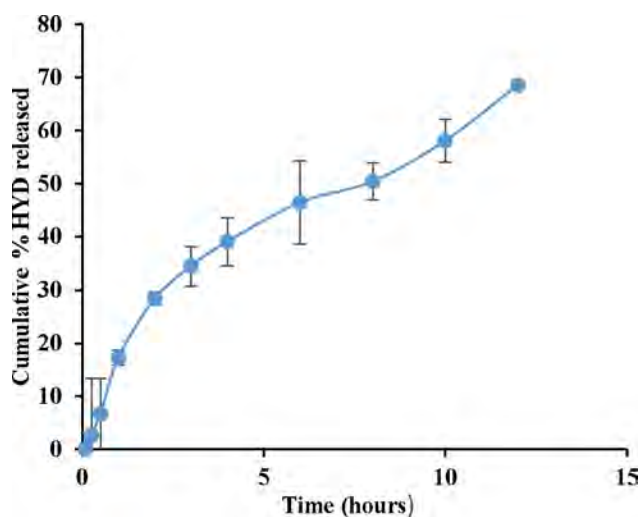
Characterisation of HYD microspheres:

1. Yield (%): 92.4
2. Encapsulation efficiency (%): 96.7
3. HYD content (%): 97.4

SEM image



In vitro dissolution profile



BATCH PRODUCTION RECORD

Faculty of Pharmacy, Rhodes University, Grahamstown, 6140, South Africa.

| | |
|---|---------------------------|
| Formulator: Shakemore T Kangausaru | Date: 04/07/2016 |
| Product: Hydralazine | Temperature: 20 °C |
| Batch Number: CCD-HYD-010 | Start time: 07H00 |
| Batch Size: 3.5g | End time: 14H00 |

| <i>Materials</i> | <i>Original formula (%m/m)</i> | <i>Working formula (g)</i> | <i>Amount added (g)</i> |
|-------------------|--------------------------------|----------------------------|-------------------------|
| HYD | 14.3 | 0.50 | 0.51 |
| Methocel® K100 LV | 55.7 | 1.95 | 1.95 |
| Eudragit® RS PO | 28.6 | 1.00 | 1.01 |
| Avicel® 101 | Sq. | 0.05 | 0.05 |
| Total | 100 | 3.5 | 3.52 |

Manufacturing process

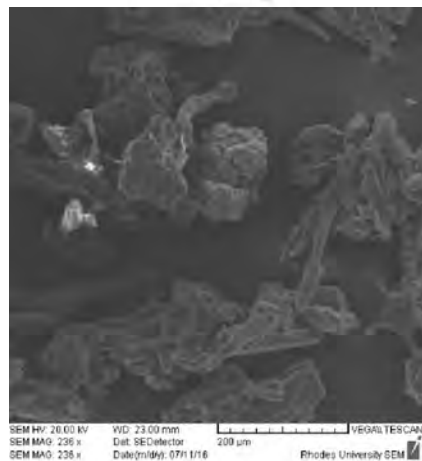
1. Dissolve 0.5 g HYD, polymers (1.95g Eudragit® RS PO and 1g Methocel® K100LV) and 0.05g Avicel®101 in 13.5 mL acetone
2. Mix 120 mL liquid paraffin and 1.2 mL span 80 in a 400 mL beaker
3. Pour the milky solution containing the drug into the liquid paraffin and stir for 7 hours using a homogenizer at 600 rpm
4. After homogenising for 2 hours, add 10 mL *n*-hexane
5. Continue homogenising for the remaining 5 hours

Evaluation of HYD microspheres

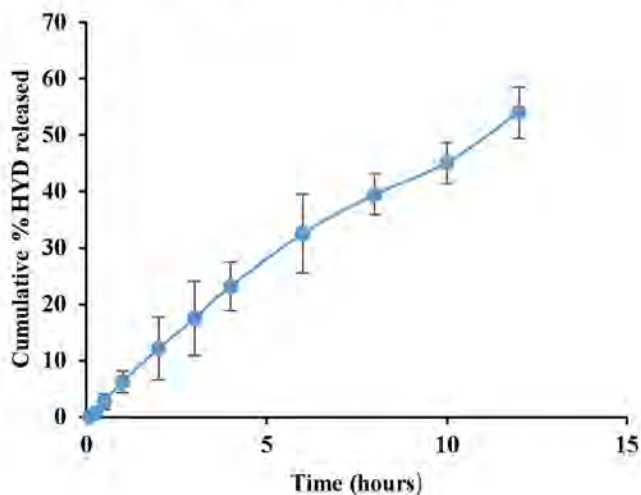
Characterisation of HYD microspheres:

1. Yield (%): 98.6
2. Encapsulation efficiency (%): 372.9
3. HYD content (%): 97.6

SEM image



In vitro dissolution profile



BATCH PRODUCTION RECORD

Faculty of Pharmacy, Rhodes University, Grahamstown, 6140, South Africa.

| | |
|---|---------------------------|
| Formulator: Shakemore T Kangausaru | Date: 04/07/2016 |
| Product: Hydralazine | Temperature: 20 °C |
| Batch Number: CCD-HYD-011 | Start time: 12H00 |
| Batch Size: 3.5g | End time: 20H00 |

| <i>Materials</i> | <i>Original formula (%m/m)</i> | <i>Working formula (g)</i> | <i>Amount added (g)</i> |
|-------------------|--------------------------------|----------------------------|-------------------------|
| HYD | 14.3 | 0.5 | 0.51 |
| Methocel® K100 LV | 28.6 | 1.0 | 1.01 |
| Eudragit® RS PO | 28.6 | 1.0 | 1.00 |
| Avicel® 101 | Sq. | 1.0 | 1.00 |
| Total | 100 | 3.5 | 3.52 |

Manufacturing process

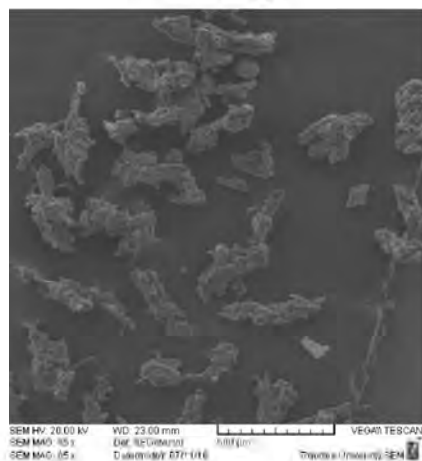
1. Dissolve 0.5 g HYD, polymers (1g Eudragit® RS PO and 1g Methocel® K100LV) and 1g Avicel® 101 in 13.5 mL acetone
2. Mix 120 mL liquid paraffin and 1.2 mL span 80 in a 400 mL beaker
3. Pour the milky solution containing the drug into the liquid paraffin and stir for 7 hours using a homogenizer at 600 rpm
4. After homogenising for 2 hours, add 10 mL *n*-hexane
5. Continue homogenising for the remaining 5 hours

Evaluation of HYD microspheres

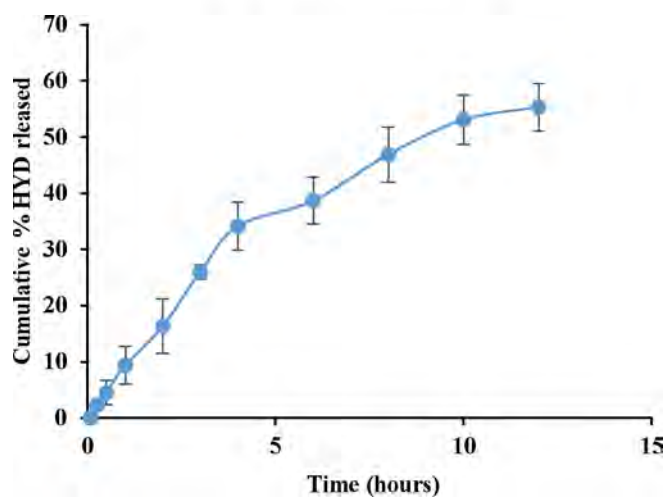
Characterisation of HYD microspheres:

1. Yield (%): 94.9
2. Encapsulation efficiency (%): 92.9
3. HYD content (%): 83.5

SEM image



***In vitro* dissolution profile**



BATCH PRODUCTION RECORD

Faculty of Pharmacy, Rhodes University, Grahamstown, 6140, South Africa.

| | |
|---|----------------------------|
| Formulator: Shakemore T Kangausaru | Date: 04/07/2016 |
| Product: Hydralazine | Temperature: 20 °C |
| Batch Number: CCD-HYD-012 | Start time: 21 H 00 |
| Batch Size: 3.5g | End time: 03 H 00 |

| <i>Materials</i> | <i>Original formula (%m/m)</i> | <i>Working formula (g)</i> | <i>Amount added (g)</i> |
|-------------------|--------------------------------|----------------------------|-------------------------|
| HYD | 14.3 | 0.5 | 0.50 |
| Methocel® K100 LV | 17.1 | 0.6 | 0.60 |
| Eudragit® RS PO | 17.1 | 0.6 | 0.60 |
| Avicel® 101 | Sq. | 1.8 | 1.80 |
| Total | 100 | 3.5 | 3.50 |

Manufacturing process

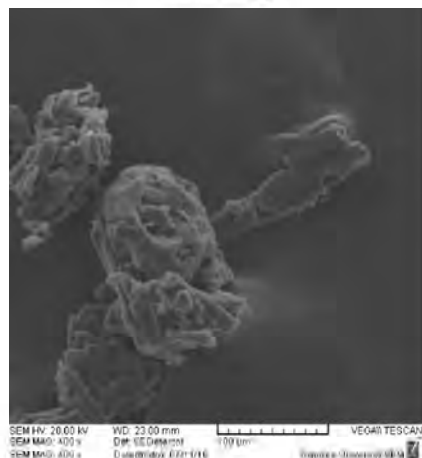
| |
|---|
| 1. Dissolve 0.5 g HYD, polymers (0.6g Eudragit® RS PO and 0.6g Methocel® K100LV) and 1.8g Avicel® 101 in 14.5 mL acetone |
| 2. Mix 120 mL liquid paraffin and 1.2 mL span 80 in a 400mL beaker |
| 3. Pour the milky solution containing the drug into the liquid paraffin and stir for 6 hours using a homogenizer at 400 rpm |
| 4. After homogenising for 2 hours, add 10 mL <i>n</i> -hexane |
| 5. Continue homogenising for the remaining 4 hours |

Evaluation of HYD microspheres

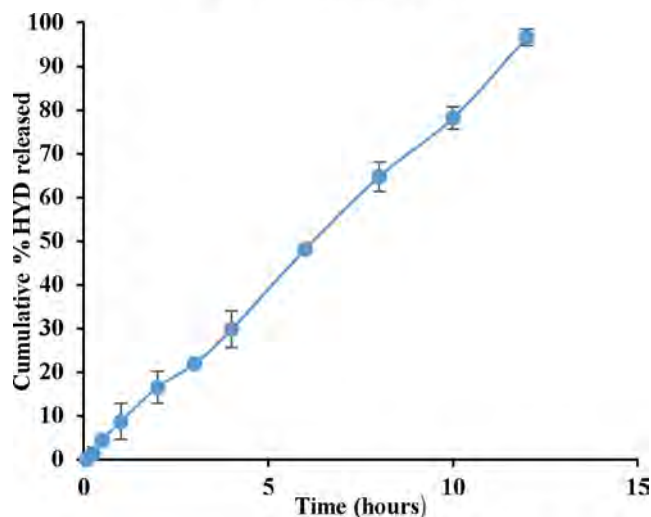
Characterisation of HYD microspheres:

1. Yield (%): 94.0
2. Encapsulation efficiency (%): 89.9
3. HYD content (%): 93.7

SEM image



***In vitro* dissolution profile**



BATCH PRODUCTION RECORD

Faculty of Pharmacy, Rhodes University, Grahamstown, 6140, South Africa.

| | |
|---|---------------------------|
| Formulator: Shakemore T Kangausaru | Date: 05/07/2016 |
| Product: Hydralazine | Temperature: 20 °C |
| Batch Number: CCD-HYD-013 | Start time: 06H30 |
| Batch Size: 3.5g | End time: 11H30 |

| <i>Materials</i> | <i>Original formula (%m/m)</i> | <i>Working formula (g)</i> | <i>Amount added (g)</i> |
|-------------------|--------------------------------|----------------------------|-------------------------|
| HYD | 14.3 | 0.5 | 0.50 |
| Methocel® K100 LV | 28.6 | 1.0 | 1.00 |
| Eudragit® RS PO | 28.6 | 1.0 | 1.00 |
| Avicel® 101 | Sq. | 1.0 | 1.00 |
| Total | 100 | 3.5 | 3.50 |

Manufacturing process

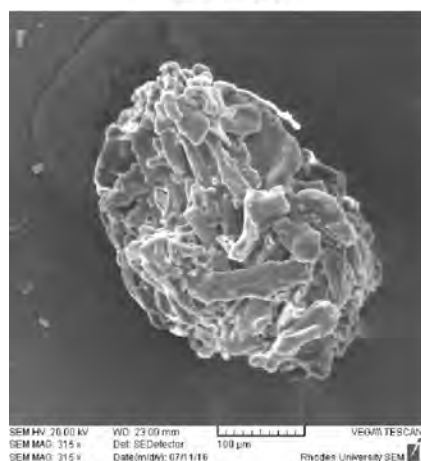
1. Dissolve 0.5 g of HYD, polymers (1g Eudragit® RS PO and 1g Methocel® K100LV) and 1g Avicel® 101 in 13.5 mL acetone
2. Mix 120 mL liquid paraffin and 1.2 mL span 80 in a 400 mL beaker
3. Pour the milky solution containing the drug into the liquid paraffin and stir for 5 hours using a homogenizer at 600rpm
4. After homogenising for 2 hours, add 10 mL *n*-hexane
5. Continue homogenising for the remaining 3 hours

Evaluation of HYD microspheres

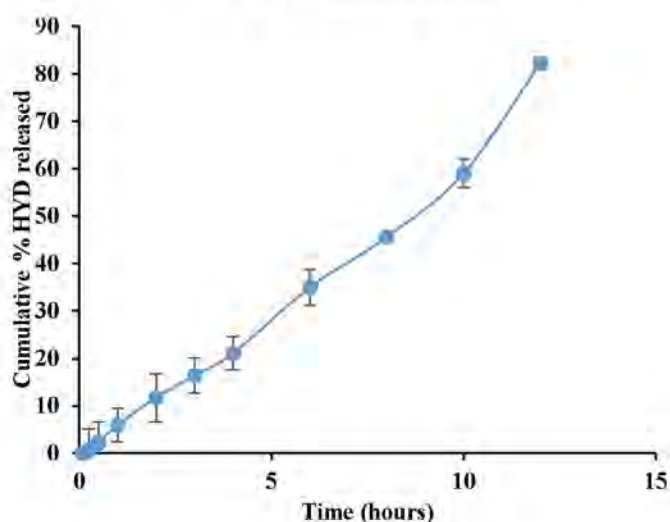
Characterisation of HYD microspheres:

1. Yield (%): 100
2. Encapsulation efficiency (%): 81.8
3. HYD content (%): 79.1

SEM image



In vitro dissolution profile



BATCH PRODUCTION RECORD

Faculty of Pharmacy, Rhodes University, Grahamstown, 6140, South Africa.

| | |
|---|---------------------------|
| Formulator: Shakemore T Kangaasaru | Date: 05/07/2016 |
| Product: Hydralazine | Temperature: 20 °C |
| Batch Number: CCD-HYD-014 | Start time: 14H30 |
| Batch Size: 3.5g | End time: 20H30 |

| <i>Materials</i> | <i>Original formula (%w/w)</i> | <i>Working formula (g)</i> | <i>Amount added (g)</i> |
|-------------------|--------------------------------|----------------------------|-------------------------|
| HYD | 14.3 | 0.5 | 0.50 |
| Methocel® K100 LV | 17.1 | 0.6 | 0.60 |
| Eudragit® RS PO | 40 | 1.4 | 1.41 |
| Avicel® 101 | Sq. | 1.0 | 1.00 |
| Total | 100 | 3.5 | 3.51 |

Manufacturing process

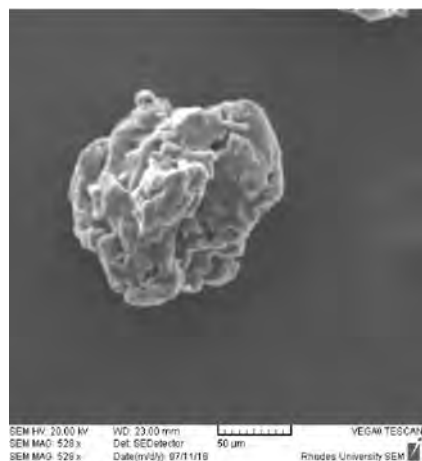
1. Dissolve 0.5 g HYD, polymers (1.4g Eudragit® RS PO and 0.6g Methocel® K100LV) and 1g Avicel® 101 in 12.5 mL acetone
2. Mix 120 mL liquid paraffin and 1.2 mL span 80 in a 400 mL beaker
3. Pour the milky solution containing the drug into the liquid paraffin and stir for 6 hours using a homogenizer at 400 rpm
4. After homogenising for 2 hours, add 10 mL *n*-hexane
5. Continue homogenising for the remaining 4 hours

Evaluation of HYD microspheres

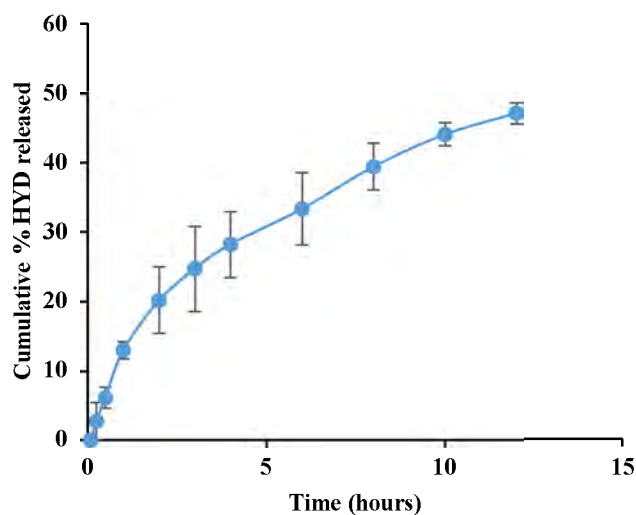
Characterisation of HYD microspheres:

1. Yield (%): 93.1
2. Encapsulation efficiency (%): 88.9
3. HYD content (%): 84.3

SEM image



***In vitro* dissolution profile**



BATCH PRODUCTION RECORD

Faculty of Pharmacy, Rhodes University, Grahamstown, 6140, South Africa.

| | |
|---|---------------------------|
| Formulator: Shakemore T Kangausaru | Date: 05/07/2016 |
| Product: Hydralazine | Temperature: 20 °C |
| Batch Number: CCD-HYD-015 | Start time: 21H00 |
| Batch Size: 3.5g | End time: 03H00 |

| <i>Materials</i> | <i>Original formula (%m/m)</i> | <i>Working formula (g)</i> | <i>Amount added (g)</i> |
|-------------------|--------------------------------|----------------------------|-------------------------|
| HYD | 14.3 | 0.5 | 0.50 |
| Methocel® K100 LV | 17.1 | 0.6 | 0.60 |
| Eudragit® RS PO | 17.1 | 0.6 | 0.60 |
| Avicel® 101 | Sq. | 1.8 | 1.82 |
| Total | 100 | 3.5 | 3.52 |

Manufacturing process

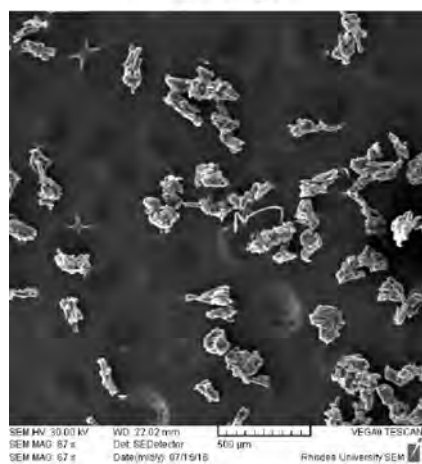
1. Dissolve 0.5 g HYD, polymers (0.6g Eudragit® RS PO and 0.6g Methocel® K100LV) and 1.8g Avicel® 101 in 12.5 mL acetone
2. Mix 120 mL liquid paraffin and 1.2 mL span 80 in a 400 mL beaker
3. Pour the milky solution containing the drug into the liquid paraffin and stir for 6 hours using a homogenizer at 800 rpm
4. After homogenising for 2 hours, add 10 mL *n*-hexane
5. Continue homogenising for the remaining 4 hours

Evaluation of HYD microspheres

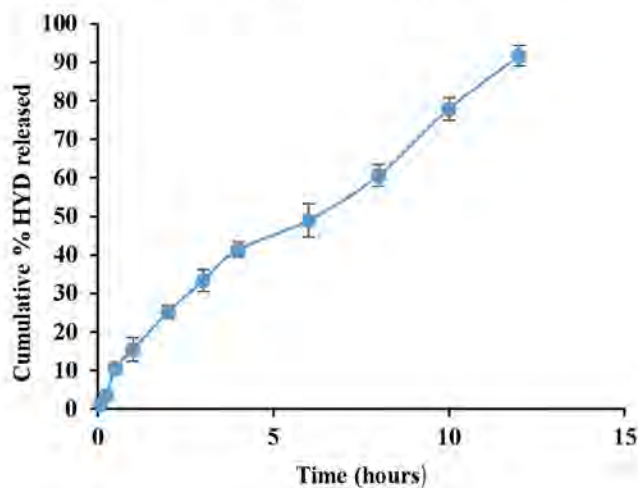
Characterisation of HYD microspheres:

1. Yield (%): 82.9
2. Encapsulation efficiency (%): 61.2
3. HYD content (%): 86.9

SEM image



In vitro dissolution profile



BATCH PRODUCTION RECORD

Faculty of Pharmacy, Rhodes University, Grahamstown, 6140, South Africa.

| | |
|---|---------------------------|
| Formulator: Shakemore T Kangausaru | Date: 06/07/2016 |
| Product: Hydralazine | Temperature: 20 °C |
| Batch Number: CCD-HYD-016 | Start time: 07H00 |
| Batch Size: 3.5g | End time: 14H00 |

| <i>Materials</i> | <i>Original formula (%m/m)</i> | <i>Working formula (g)</i> | <i>Amount added (g)</i> |
|-------------------|--------------------------------|----------------------------|-------------------------|
| HYD | 14.3 | 0.5 | 0.50 |
| Methocel® K100 LV | 28.6 | 1.0 | 1.00 |
| Eudragit® RS PO | 28.6 | 1.0 | 1.01 |
| Avicel® 101 | Sq. | 1.0 | 1.02 |
| Total | 100 | 3.5 | 3.53 |

Manufacturing process

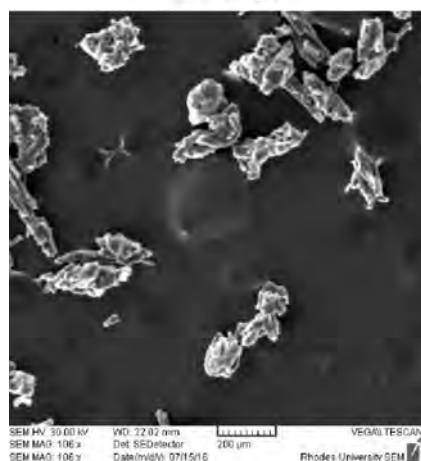
1. Dissolve 0.5 g of HYD, polymers (1g Eudragit® RS PO and 1g Methocel® K100LV) and 1g Avicel® 101 in 13.5 mL acetone
2. Mix 120 mL liquid paraffin and 1.2 mL span 80 in a 400 mL beaker
3. Pour the milky solution containing the drug into the liquid paraffin and stir for 7 hours using a homogenizer at 600 rpm
4. After homogenising for 2 hours, add 10 mL *n*-hexane
5. Continue homogenising for the remaining 5 hours

Evaluation of HYD microspheres

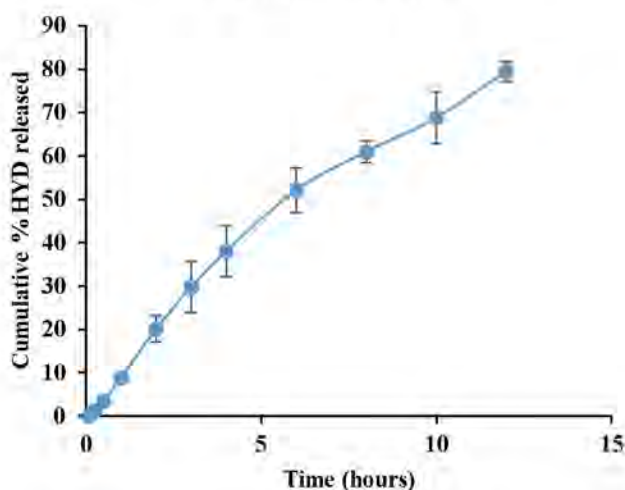
Characterisation of HYD microspheres:

1. Yield (%): 100.6
2. Encapsulation efficiency (%): 71.1
3. HYD content (%): 74.5

SEM image



In vitro dissolution profile



BATCH PRODUCTION RECORD

Faculty of Pharmacy, Rhodes University, Grahamstown, 6140, South Africa.

| | |
|---|---------------------------|
| Formulator: Shakemore T Kangausaru | Date: 06/07/2016 |
| Product: Hydralazine | Temperature: 20 °C |
| Batch Number: CCD-HYD-017 | Start time: 14H00 |
| Batch Size: 3.5g | End time: 21H00 |

| <i>Materials</i> | <i>Original formula (%w/w)</i> | <i>Working formula (g)</i> | <i>Amount added (g)</i> |
|-------------------|--------------------------------|----------------------------|-------------------------|
| HYD | 14.3 | 0.5 | 0.50 |
| Methocel® K100 LV | 28.6 | 1.0 | 1.00 |
| Eudragit® RS PO | 28.6 | 1.0 | 1.01 |
| Avicel® 101 | Sq. | 1.0 | 1.00 |
| Total | 100 | 3.5 | 3.51 |

Manufacturing process

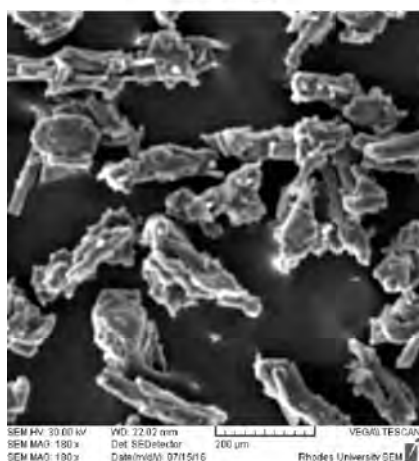
1. Dissolve 0.5 g HYD, polymers (1g Eudragit® RS PO and 1g Methocel® K100LV) and 1g Avicel® 101 in 11.1mL acetone
2. Mix 120 mL liquid paraffin and 1.2 mL span 80 in a 400 mL beaker
3. Pour the milky solution containing the drug into the liquid paraffin and stir for 7 hours using a homogenizer at 600 rpm
4. After homogenising for 2 hours, add 10 mL *n*-hexane
5. Continue homogenising for the remaining 5 hours

Evaluation of HYD microspheres

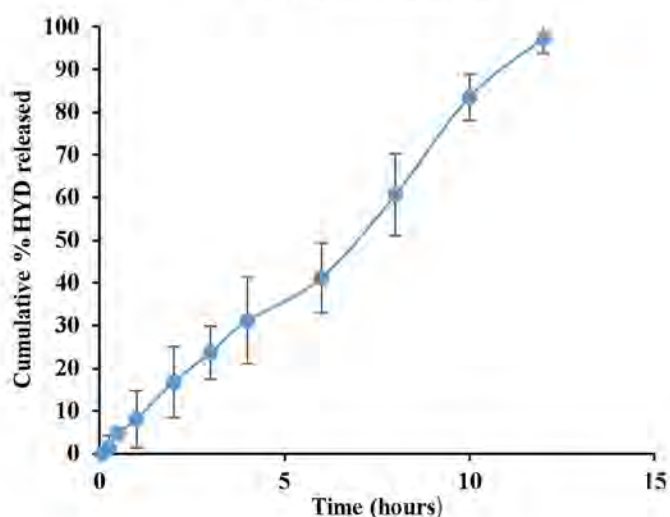
Characterisation of HYD microspheres:

1. Yield (%): 91.4
2. Encapsulation efficiency (%): 70.2
3. HYD content (%): 77.2

SEM image



In vitro dissolution profile



BATCH PRODUCTION RECORD

Faculty of Pharmacy, Rhodes University, Grahamstown, 6140, South Africa.

| | |
|---|---------------------------|
| Formulator: Shakemore T Kangaasaru | Date: 06/07/2016 |
| Product: Hydralazine | Temperature: 20 °C |
| Batch Number: CCD-HYD-018 | Start time: 21H00 |
| Batch Size: 3.5g | End time: 05H00 |

| <i>Materials</i> | <i>Original formula (%m/m)</i> | <i>Working formula (g)</i> | <i>Amount added (g)</i> |
|-------------------|--------------------------------|----------------------------|-------------------------|
| HYD | 14.3 | 0.5 | 0.50 |
| Methocel® K100 LV | 17.1 | 0.6 | 0.60 |
| Eudragit® RS PO | 17.1 | 0.6 | 0.60 |
| Avicel® 101 | Sq. | 1.8 | 1.81 |
| Total | 100 | 3.5 | 3.51 |

Manufacturing process

1. Dissolve 0.5 g HYD, polymers (0.6g Eudragit® RS PO and 0.6g Methocel® K100LV) and 1.8g Avicel® 101 in 14.5 mL acetone
2. Mix 120 mL liquid paraffin and 1.2 mL span 80 in a 400 mL beaker
3. Pour the milky solution containing the drug into the liquid paraffin and stir for 8 hours using a homogenizer at 400 rpm
4. After homogenising for 2 hours, add 10 mL *n*-hexane
5. Continue homogenising for the remaining 6 hours

Evaluation of HYD microspheres

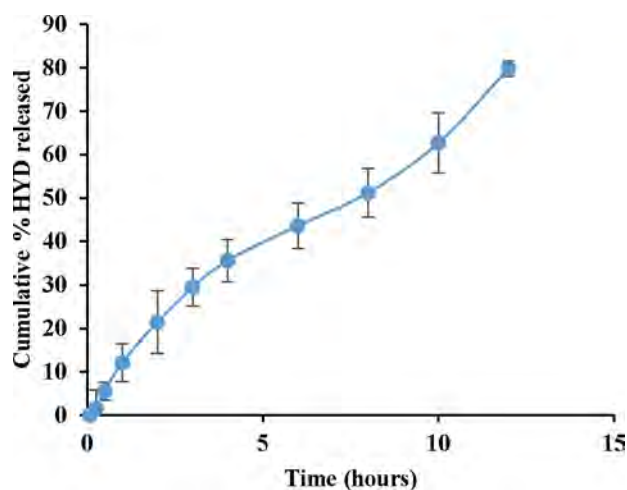
Characterisation of HYD microspheres:

1. Yield (%): 99.7
2. Encapsulation efficiency (%): 76.0
3. HYD content (%): 63.9

SEM image



In vitro dissolution profile



BATCH PRODUCTION RECORD

Faculty of Pharmacy, Rhodes University, Grahamstown, 6140, South Africa.

| | |
|---|---------------------------|
| Formulator: Shakemore T Kangausaru | Date: 07/07/2016 |
| Product: Hydralazine | Temperature: 20 °C |
| Batch Number: CCD-HYD-019 | Start time: 11H30 |
| Batch Size: 3.5g | End time: 17H30 |

| <i>Materials</i> | <i>Original formula (%m/m)</i> | <i>Working formula (g)</i> | <i>Amount added (g)</i> |
|-------------------|--------------------------------|----------------------------|-------------------------|
| HYD | 14.3 | 0.5 | 0.51 |
| Methocel® K100 LV | 17.1 | 0.6 | 0.60 |
| Eudragit® RS PO | 40 | 1.4 | 1.41 |
| Avicel® 101 | Sq. | 1.0 | 1.00 |
| Total | 100 | 3.5 | 3.52 |

Manufacturing process

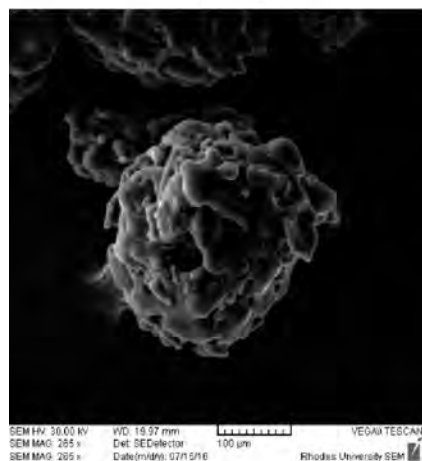
1. Dissolve 0.5 g HYD, polymers (1.4g Eudragit® RS PO and 0.62g Methocel® K100LV) and 1g Avicel® 101 in 14.5 mL acetone
2. Mix 120 mL liquid paraffin and 1.2 mL span 80 in a 400 mL beaker
3. Pour the milky solution containing the drug into the liquid paraffin and stir for 6 hours using a homogenizer at 800 rpm
4. After homogenising for 2 hours, add 10 mL *n*-hexane
5. Continue homogenising for the remaining 4 hours

Evaluation of HYD microspheres

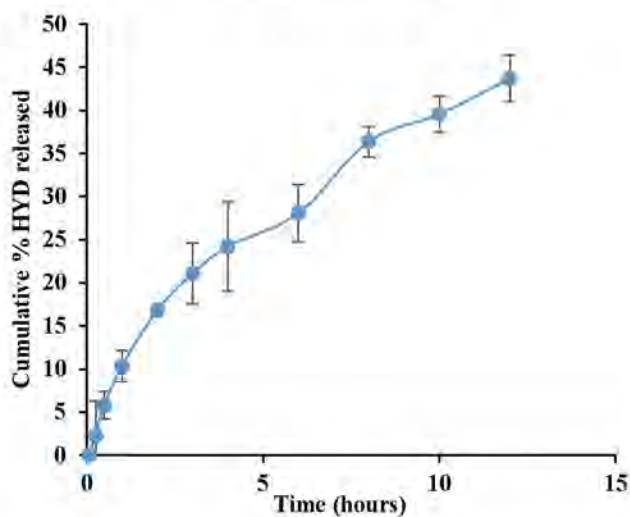
Characterisation of HYD microspheres:

1. Yield (%): 100
2. Encapsulation efficiency (%): 77.0
3. HYD content (%): 75.3

SEM image



In vitro dissolution profile



BATCH PRODUCTION RECORD

Faculty of Pharmacy, Rhodes University, Grahamstown, 6140, South Africa.

| | |
|---|---------------------------|
| Formulator: Shakemore T Kangausaru | Date: 07/07/2016 |
| Product: Hydralazine | Temperature: 20 °C |
| Batch Number: CCD-HYD-020 | Start time: 17H30 |
| Batch Size: 3.5g | End time: 23H30 |

| <i>Materials</i> | <i>Original formula (%m/m)</i> | <i>Working formula (g)</i> | <i>Amount added (g)</i> |
|-------------------|--------------------------------|----------------------------|-------------------------|
| HYD | 14.3 | 0.5 | 0.50 |
| Methocel® K100 LV | 40 | 1.4 | 1.40 |
| Eudragit® RS PO | 40 | 1.4 | 1.40 |
| Avicel® 101 | Sq. | 0.2 | 0.21 |
| Total | 100 | 3.5 | 3.51 |

Manufacturing process

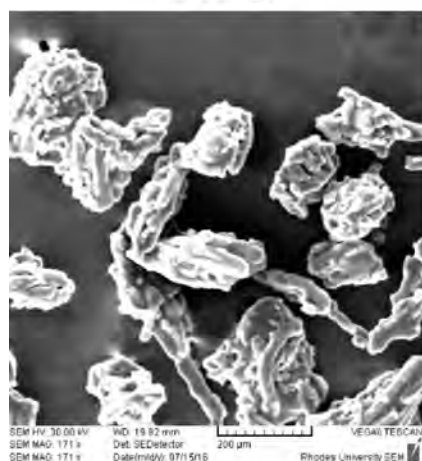
1. Dissolve 0.5 g HYD, polymers (1.4g Eudragit® RS PO and 1.4g Methocel® K100LV) and 0.2g Avicel® 101 in 14.5 mL acetone
2. Mix 120 mL liquid paraffin and 1.2 mL span 80 in a 400 mL beaker
3. Pour the milky solution containing the drug into the liquid paraffin and stir for 6hours using a homogenizer at 800 rpm
4. After homogenising for 2 hours, add 10 mL *n*-hexane
5. Continue homogenising for the remaining 4 hours

Evaluation of HYD microspheres

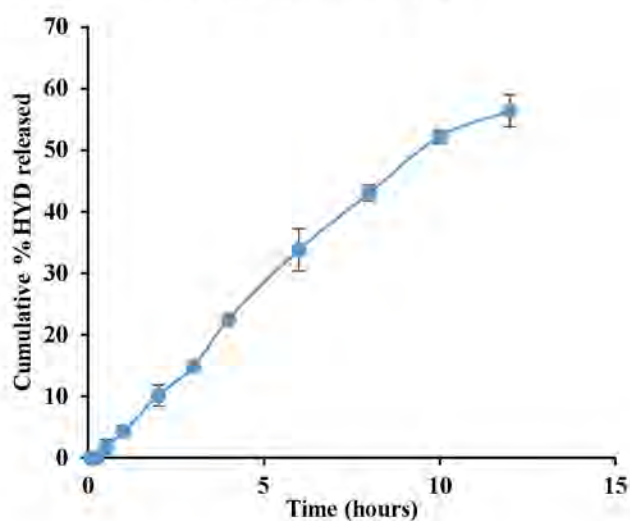
Characterisation of HYD microspheres:

1. Yield (%): 97.4
2. Encapsulation efficiency (%): 80.8
3. HYD content (%): 80.7

SEM image



In vitro dissolution profile



BATCH PRODUCTION RECORD

Faculty of Pharmacy, Rhodes University, Grahamstown, 6140, South Africa.

Formulator: Shakemore T Kangaasaru

Product: Hydralazine

Batch Number: CCD-HYD-021

Batch Size: 3.5g

Date: 07/07/2016

Temperature: 20 °C

Start time: 23H30

End time: 06H30

| Materials | Original formula (%m/m) | Working formula (g) | Amount added (g) |
|-------------------|-------------------------|---------------------|------------------|
| HYD | 14.3 | 0.5 | 0.50 |
| Methocel® K100 LV | 28.6 | 1.0 | 1.00 |
| Eudragit® RS PO | 28.6 | 1.0 | 1.00 |
| Avicel® 101 | Sq. | 1.0 | 1.01 |
| Total | 100 | 3.5 | 3.51 |

Manufacturing process

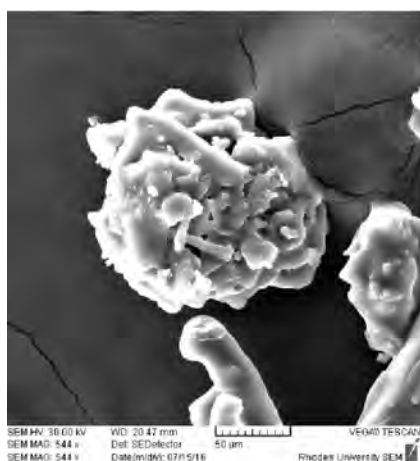
1. Dissolve 0.5 g HYD, polymers (1g Eudragit® RS PO and 1g Methocel® K100LV) and 1g Avicel® 101 in 13.5 mL acetone
2. Mix 120 mL liquid paraffin and 1.2 mL span 80 in a 400 mL beaker
3. Pour the milky solution containing the drug into the liquid paraffin and stir for 7 hours using a homogenizer at 1075 rpm
4. After homogenising for 2 hours, add 10 mL *n*-hexane
5. Continue homogenising for the remaining 5 hours

Evaluation of HYD microspheres

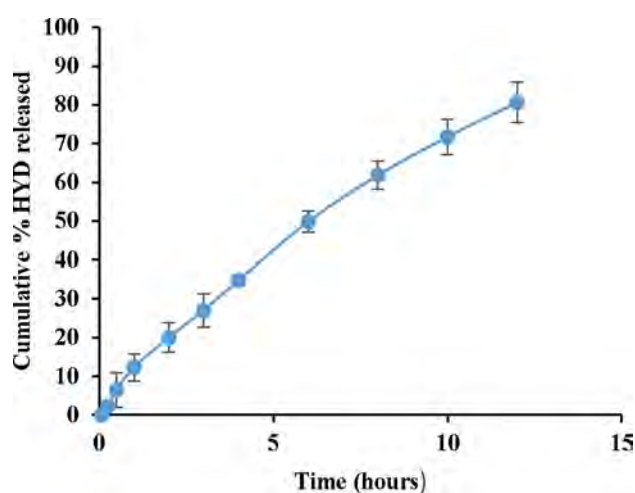
Characterisation of HYD microspheres:

1. Yield (%): 99.4
2. Encapsulation efficiency (%): 78.5
3. HYD content (%): 76.6

SEM image



In vitro dissolution profile



BATCH PRODUCTION RECORD

Faculty of Pharmacy, Rhodes University, Grahamstown, 6140, South Africa.

Formulator: Shakemore T Kangausaru

Date: 08/07/2016

Product: Hydralazine

Temperature: 20 °C

Batch Number: CCD-HYD-022

Start time: 08H00

Batch Size: 3.5g

End time: 15H00

| Materials | Original formula (%w/w) | Working formula (g) | Amount added (g) |
|-------------------|-------------------------|---------------------|------------------|
| HYD | 14.3 | 0.5 | 0.50 |
| Methocel® K100 LV | 28.6 | 1.0 | 1.00 |
| Eudragit® RS PO | 28.6 | 1.0 | 1.00 |
| Avicel® 101 | Sq. | 1.0 | 1.00 |
| Total | 100 | 3.5 | 3.50 |

Manufacturing process

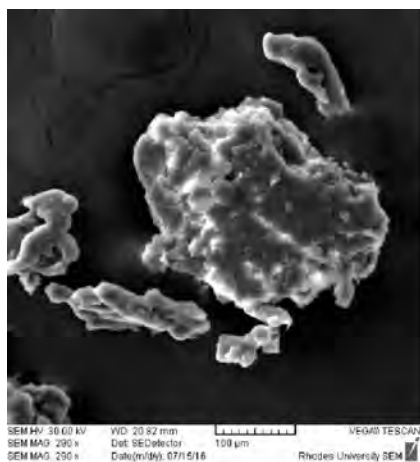
1. Dissolve 0.5 g HYD, polymers (1g Eudragit® RS PO and 1g Methocel® K100LV) and 1g Avicel® 101 in 13.5 mL acetone
2. Mix 120 mL liquid paraffin and 1.2 mL span 80 in a 400 mL beaker
3. Pour the milky solution containing the drug into the liquid paraffin and stir for 7 hours using a homogenizer at 600 rpm
4. After homogenising for 2 hours, add 10 mL *n*-hexane
5. Continue homogenising for the remaining 5 hours

Evaluation of HYD microspheres

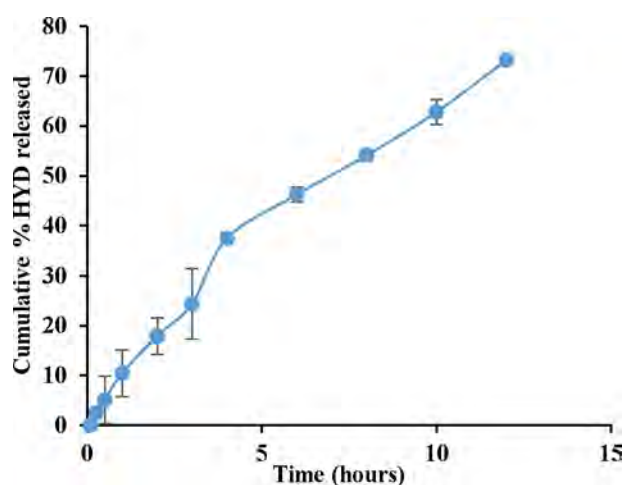
Characterisation of HYD microspheres:

1. Yield (%): 86.9
2. Encapsulation efficiency (%): 78.9
3. HYD content (%): 78.0

SEM image



In vitro dissolution profile



BATCH PRODUCTION RECORD

Faculty of Pharmacy, Rhodes University, Grahamstown, 6140, South Africa.

| | |
|---|---------------------------|
| Formulator: Shakemore T Kangausaru | Date: 08/07/2016 |
| Product: Hydralazine | Temperature: 20 °C |
| Batch Number: CCD-HYD-023 | Start time: 22H00 |
| Batch Size: 3.5g | End time: 07H30 |

| Materials | Original formula (%m/m) | Working formula (g) | Amount added (g) |
|-------------------|-------------------------|---------------------|------------------|
| HYD | 14.3 | 0.5 | 0.50 |
| Methocel® K100 LV | 28.6 | 1.0 | 1.00 |
| Eudragit® RS PO | 28.6 | 1.0 | 1.00 |
| Avicel® 101 | Sq. | 1.0 | 1.00 |
| Total | 100 | 3.5 | 3.50 |

Manufacturing process

1. Dissolve 0.5 g HYD, polymers (1g Eudragit® RS PO and 1g Methocel® K100LV) and 1g Avicel® 101 in 13.5 mL acetone
2. Mix 120 mL liquid paraffin and 1.2 mL span 80 in a 400 mL beaker
3. Pour the milky solution containing the drug into the liquid paraffin and stir for 9.5 hours using a homogenizer at 600 rpm
4. After homogenising for 2 hours, add 10 mL *n*-hexane
5. Continue homogenising for the remaining 7.5 hours

Evaluation of HYD microspheres

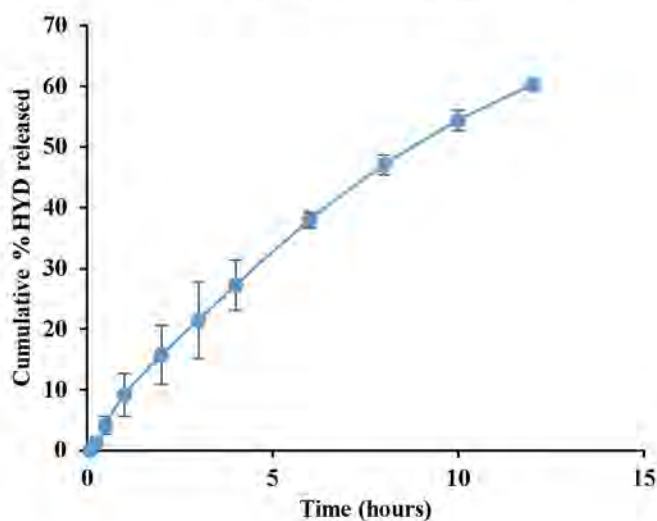
Characterisation of HYD microspheres:

1. Yield (%): 93.1
2. Encapsulation efficiency (%): 92.1
3. HYD content (%): 77.4

SEM image



In vitro dissolution profile



BATCH PRODUCTION RECORD

Faculty of Pharmacy, Rhodes University, Grahamstown, 6140, South Africa.

| | |
|--|---------------------------|
| Formulator: Shakemore T Kangaursu | Date: 08/07/2016 |
| Product: Hydralazine | Temperature: 20 °C |
| Batch Number: CCD-HYD-024 | Start time: 15H00 |
| Batch Size: 3.5g | End time: 22H00 |

| Materials | Original formula (%m/m) | Working formula (g) | Amount added (g) |
|-------------------|-------------------------|---------------------|------------------|
| HYD | 14.3 | 0.5 | 0.50 |
| Methocel® K100 LV | 28.6 | 1.0 | 1.00 |
| Eudragit® RS PO | 28.6 | 1.0 | 1.00 |
| Avicel® 101 | Sq. | 1.0 | 1.00 |
| Total | 100 | 3.5 | 3.50 |

Manufacturing process

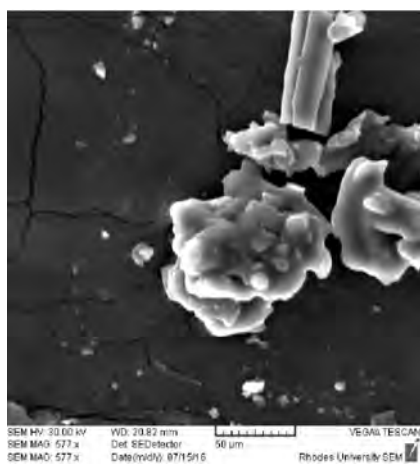
1. Dissolve 0.5 g HYD, polymers (1g Eudragit® RS PO and 1g Methocel® K100LV) and 1g Avicel® 101 in 13.5 mL acetone
2. Mix 120 mL liquid paraffin and 1.2 mL span 80 in a 400 mL beaker
3. Pour the milky solution containing the drug into the liquid paraffin and stir for 7 hours using a homogenizer at 600 rpm
4. After homogenising for 2 hours, add 10 mL *n*-hexane
5. Continue homogenising for the remaining 5 hours

Evaluation of HYD microspheres

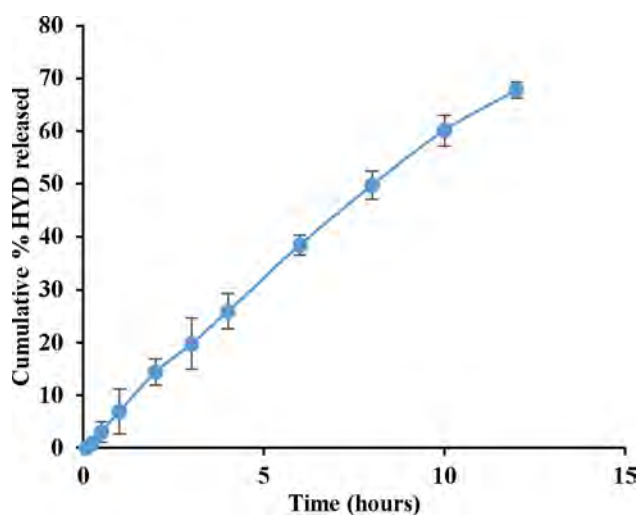
Characterisation of HYD microspheres:

1. Yield (%): 96.3
2. Encapsulation efficiency (%): 77.3
3. HYD content (%): 63.5

SEM image



In vitro dissolution profile



BATCH PRODUCTION RECORD

Faculty of Pharmacy, Rhodes University, Grahamstown, 6140, South Africa.

Formulator: Shakemore T Kangausaru

Date: 08/07/2016

Product: Hydralazine

Temperature: 20 °C

Batch Number: CCD-HYD-025

Start time: 08H00

Batch Size: 3.5g

End time: 16H00

| Materials | Original formula (%m/m) | Working formula (g) | Amount added (g) |
|-------------------|-------------------------|---------------------|------------------|
| HYD | 14.3 | 0.5 | 0.50 |
| Methocel® K100 LV | 17.1 | 0.6 | 0.61 |
| Eudragit® RS PO | 40 | 1.4 | 1.40 |
| Avicel® 101 | Sq. | 1.0 | 1.01 |
| Total | 100 | 3.5 | 3.52 |

Manufacturing process

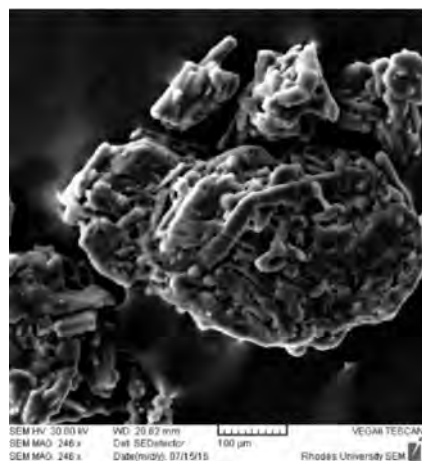
1. Dissolve 0.5 g HYD, polymers (1.4g Eudragit® RS PO and 0.6g Methocel® K100LV) and 1g Avicel® 101 in 12.5 mL acetone
2. Mix 120 mL liquid paraffin and 1.2 mL span 80 in a 400 mL beaker
3. Pour the milky solution containing the drug into the liquid paraffin and stir for 8 hours using a homogenizer at 400 rpm
4. After homogenising for 2 hours, add 10 mL *n*-hexane
5. Continue homogenising for the remaining 6 hours

Evaluation of HYD microspheres

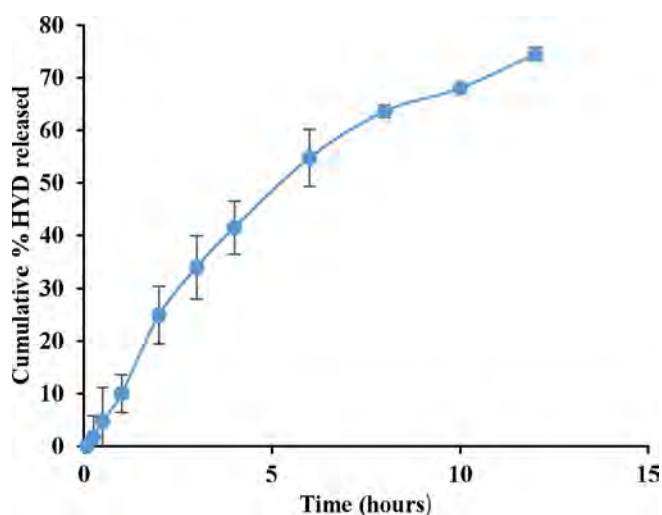
Characterisation of HYD microspheres:

1. Yield (%): 94.0
2. Encapsulation efficiency (%): 72.9
3. HYD content (%): 78.6

SEM image



In vitro dissolution profile



BATCH PRODUCTION RECORD

Faculty of Pharmacy, Rhodes University, Grahamstown, 6140, South Africa.

| | |
|---|---------------------------|
| Formulator: Shakemore T Kangausaru | Date: 09/07/2016 |
| Product: Hydralazine | Temperature: 19 °C |
| Batch Number: CCD-HYD-026 | Start time: 05H00 |
| Batch Size: 3.5g | End time: 22H00 |

| Materials | Original formula (%m/m) | Working formula (g) | Amount added (g) |
|------------------|-------------------------|---------------------|------------------|
| HYD | 14.3 | 0.5 | 0.50 |
| Methocel® K100LV | 28.6 | 1.0 | 1.01 |
| Eudragit® RS PO | 1.4 | 0.05 | 0.05 |
| Avicel® 101 | Sq. | 1.95 | 1.95 |
| Total | 100 | 3.5 | 3.51 |

Manufacturing process

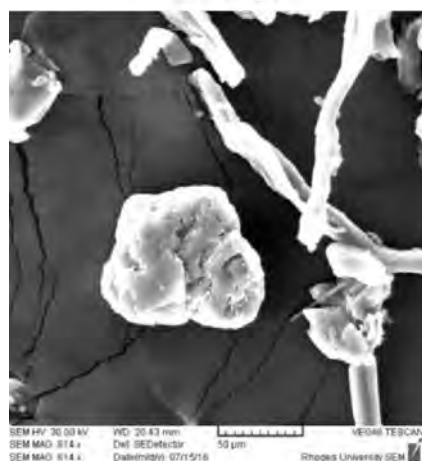
1. Dissolve 0.5 g HYD, polymers (1g Eudragit® RS PO and 0.05g Methocel® K100LV) and 1.95g Avicel® 101 in 13.5 mL acetone
2. Mix 120 mL liquid paraffin and 1.2 mL span 80 in a 400 mL beaker
3. Pour the milky solution containing the drug into the liquid paraffin and stir for 7 hours using a homogenizer at 600 rpm
4. After homogenising for 2 hours, add 10 mL *n*-hexane
5. Continue homogenising for the remaining 5 hours

Evaluation of HYD microspheres

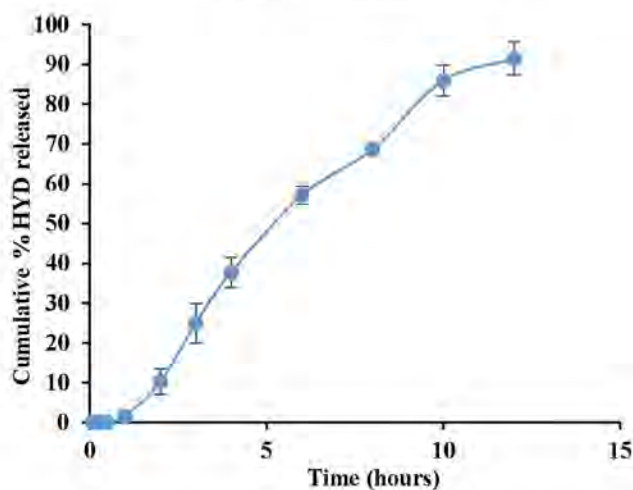
Characterisation of HYD microspheres:

1. Yield (%): 76
2. Encapsulation efficiency (%): 57.2
3. HYD content (%): 57.1

SEM image



In vitro dissolution profile



BATCH PRODUCTION RECORD

Faculty of Pharmacy, Rhodes University, Grahamstown, 6140, South Africa.

| | |
|---|---------------------------|
| Formulator: Shakemore T Kangausaru | Date: 09/07/2016 |
| Product: Hydralazine | Temperature: 19 °C |
| Batch Number: CCD-HYD-027 | Start time: 22H00 |
| Batch Size: 3.5g | End time: 05H00 |

| Materials | Original formula (%m/m) | Working formula (g) | Amount added (g) |
|-------------------|-------------------------|---------------------|------------------|
| HYD | 14.3 | 0.5 | 0.50 |
| Methocel® K100 LV | 28.6 | 1.0 | 1.00 |
| Eudragit® RS PO | 28.6 | 1.0 | 1.00 |
| Avicel® 101 | Sq. | 1.0 | 1.01 |
| Total | 100 | 3.5 | 3.51 |

Manufacturing process

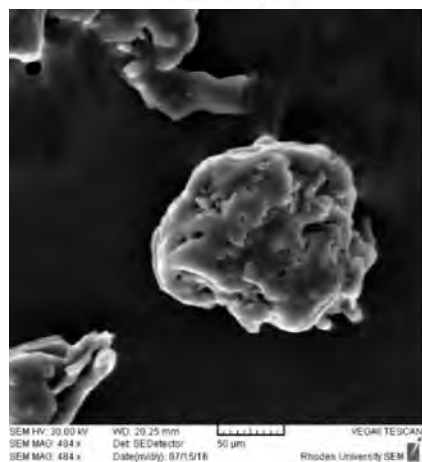
1. Dissolve 0.5 g HYD, polymers (1g Eudragit® RS PO and 1g Methocel® K100LV) and 1g Avicel® 101 in 13.5 mL acetone
2. Mix 120 mL liquid paraffin and 1.2 mL span 80 in a 400 mL beaker
3. Pour the milky solution containing the drug into the liquid paraffin and stir for 7 hours using a homogenizer at 600rpm
4. After homogenising for 2 hours, add 10 mL *n*-hexane
5. Continue homogenising for the remaining 5 hours

Evaluation of HYD microspheres

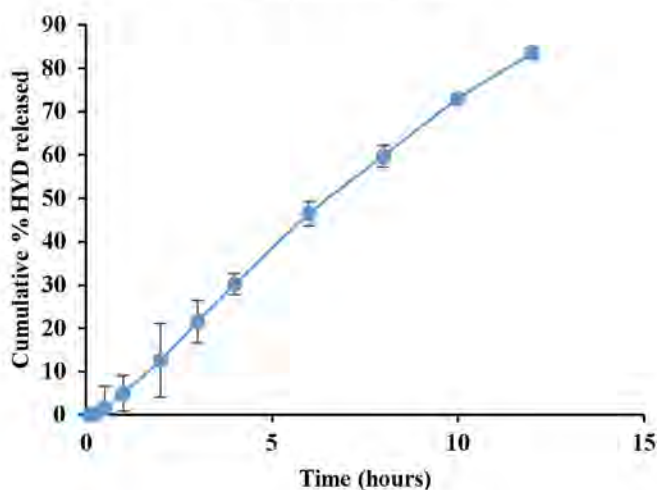
Characterisation of HYD microspheres:

1. Yield (%): 95.7
2. Encapsulation efficiency (%): 60.6
3. HYD content (%): 71.5

SEM image



In vitro dissolution profile



BATCH PRODUCTION RECORD

Faculty of Pharmacy, Rhodes University, Grahamstown, 6140, South Africa.

| | |
|---|---------------------------|
| Formulator: Shakemore T Kangausaru | Date: 10/07/2016 |
| Product: Hydralazine | Temperature: 19 °C |
| Batch Number: CCD-HYD-028 | Start time: 07H00 |
| Batch Size: 3.5g | End time: 15H00 |

| Materials | Original formula (%m/m) | Working formula (g) | Amount added (g) |
|-------------------|-------------------------|---------------------|------------------|
| HYD | 14.3 | 0.5 | 0.50 |
| Methocel® K100 LV | 40 | 1.4 | 1.41 |
| Eudragit® RS PO | 17.1 | 0.6 | 0.60 |
| Avicel® 101 | Sq. | 1.0 | 1.00 |
| Total | 100 | 3.5 | 3.51 |

Manufacturing process

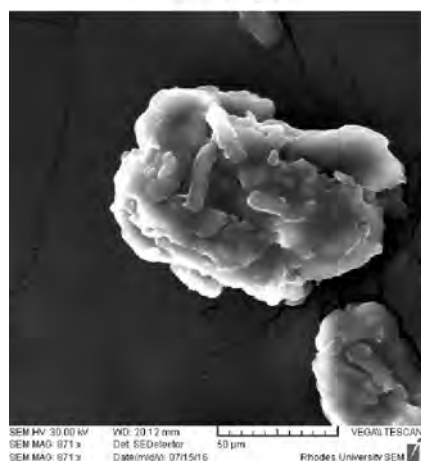
1. Dissolve 0.5 g HYD, polymers (0.6g Eudragit® RS PO and 1.4g Methocel® K100LV) and 1g Avicel® 101 in 12.5 mL acetone
2. Mix 120 mL liquid paraffin and 1.2 mL span 80 in a 400 mL beaker
3. Pour the milky solution containing the drug into the liquid paraffin and stir for 8 hours using a homogenizer at 400 rpm
4. After homogenising for 2 hours, add 10 mL *n*-hexane
5. Continue homogenising for the remaining 6 hours

Evaluation of HYD microspheres

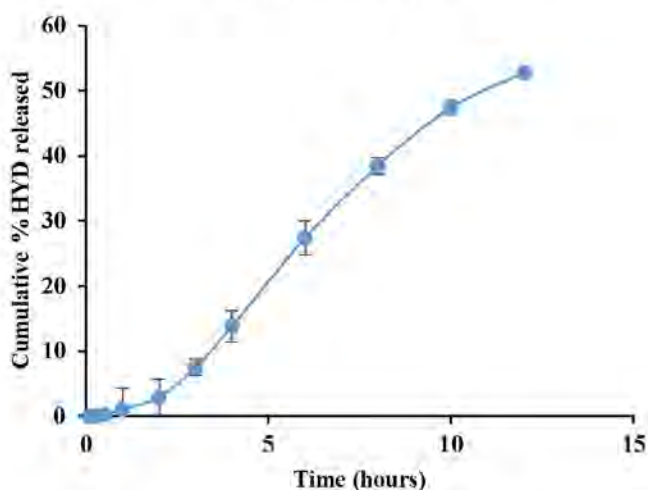
Characterisation of HYD microspheres:

1. Yield (%): 97.7
2. Encapsulation efficiency (%): 65.9
3. HYD content (%): 78.8

SEM image



In vitro dissolution profile



BATCH PRODUCTION RECORD

Faculty of Pharmacy, Rhodes University, Grahamstown, 6140, South Africa.

Formulator: Shakemore T Kangausaru

Product: Hydralazine

Batch Number: CCD-HYD-029

Batch Size: 3.5g

Date: 10/07/2016

Temperature: 19 °C

Start time: 15H00

End time: 23H00

| Materials | Original formula (%m/m) | Working formula (g) | Amount added (g) |
|------------------|-------------------------|---------------------|------------------|
| HYD | 14.3 | 0.5 | 0.50 |
| Methocel® K100LV | 40 | 1.4 | 1.40 |
| Eudragit® RS PO | 17.1 | 0.6 | 0.60 |
| Avicel® 101 | Sq. | 1.0 | 1.02 |
| Total | 100 | 3.5 | 3.52 |

Manufacturing process

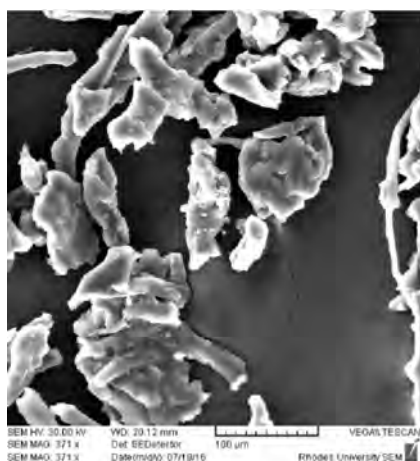
1. Dissolve 0.5 g HYD, polymers (0.6g Eudragit® RS PO and 1.4g Methocel® K100LV) and 1g Avicel® 101 in 14.5 mL acetone
2. Mix 120 mL liquid paraffin and 1.2 mL span 80 in a 400 mL beaker
3. Pour the milky solution containing the drug into the liquid paraffin and stir for 8 hours using a homogenizer at 800 rpm
4. After homogenising for 2 hours, add 10 mL *n*-hexane
5. Continue homogenising for the remaining 6 hours

Evaluation of HYD microspheres

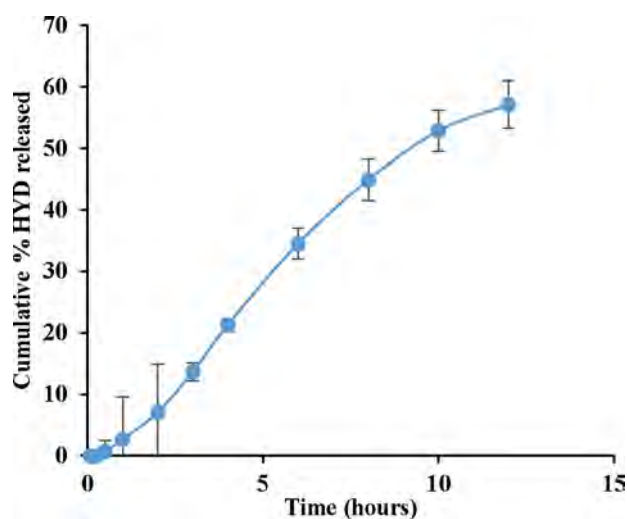
Characterisation of HYD microspheres:

1. Yield (%): 97.1
2. Encapsulation efficiency (%): 65.9
3. HYD content (%): 76.2

SEM image



In vitro dissolution profile



BATCH PRODUCTION RECORD

Faculty of Pharmacy, Rhodes University, Grahamstown, 6140, South Africa.

| | |
|---|---------------------------|
| Formulator: Shakemore T Kangausaru | Date: 10/07/2016 |
| Product: Hydralazine | Temperature: 19 °C |
| Batch Number: CCD-HYD-030 | Start time: 23H00 |
| Batch Size: 3.5g | End time: 05H00 |

| Materials | Original formula (%m/m) | Working formula (g) | Amount added (g) |
|------------------|-------------------------|---------------------|------------------|
| HYD | 14.3 | 0.5 | 0.50 |
| Methocel® K100LV | 17.1 | 0.6 | 1.40 |
| Eudragit® RS PO | 17.1 | 0.6 | 0.60 |
| Avicel® 101 | Sq. | 1.8 | 1.80 |
| Total | 100 | 3,5 | 3.50 |

Manufacturing process

1. Dissolve 0.5 g HYD, polymers (0.6g Eudragit® RS PO and 0.6g Methocel® K100LV) and 1.8g Avicel® 101 in 14.5 mL acetone
2. Mix 120 mL liquid paraffin and 1.2 mL span 80 in a 400 mL beaker
3. Pour the milky solution containing the drug into the liquid paraffin and stir for 6 hours using a homogenizer at 800 rpm
4. After homogenising for 2 hours, add 10 mL *n*-hexane
5. Continue homogenising for the remaining 4 hours

Evaluation of HYD microspheres

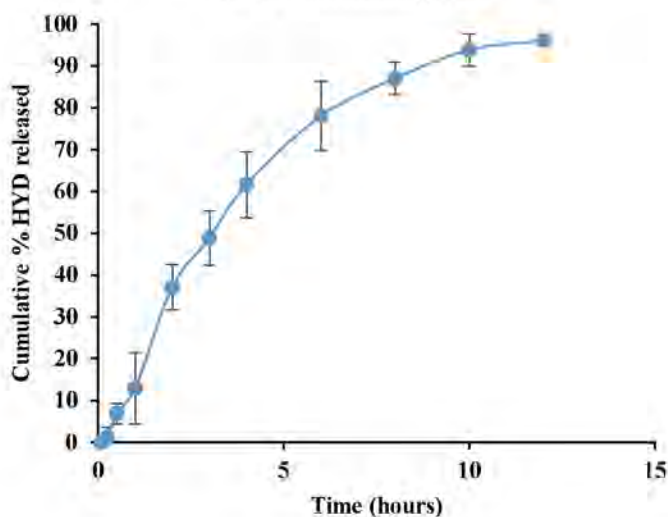
Characterisation of HYD microspheres:

1. Yield (%): 79.7
2. Encapsulation efficiency (%): 71.9
3. HYD content (%): 95.7

SEM image



In vitro dissolution profile



BATCH PRODUCTION RECORD

Faculty of Pharmacy, Rhodes University, Grahamstown, 6140, South Africa.

| | |
|---|---------------------------|
| Formulator: Shakemore T Kangausaru | Date: 11/07/2016 |
| Product: Hydralazine | Temperature: 19 °C |
| Batch Number: CCD-HYD-031 | Start time: 17H00 |
| Batch Size: 3.5g | End time: 23H00 |

| Materials | Original formula (%m/m) | Working formula (g) | Amount added (g) |
|------------------|-------------------------|---------------------|------------------|
| HYD | 14.3 | 0.5 | 0.50 |
| Methocel® K100LV | 40 | 1.4 | 1.40 |
| Eudragit® RS PO | 17.1 | 0.6 | 0.60 |
| Avicel® 101 | Sq. | 1.0 | 1.01 |
| Total | 100 | 3.5 | 3.51 |

Manufacturing process

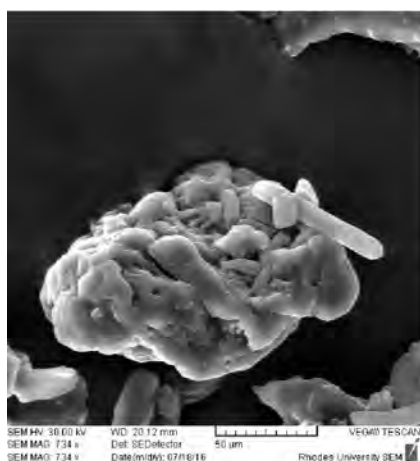
1. Dissolve 0.5 g HYD, polymers (0.6g Eudragit® RS PO and 1.4g Methocel® K100LV) and 1g Avicel® 101 in 14.5 mL acetone
2. Mix 120 mL liquid paraffin and 1.2 mL span 80 in a 400 mL beaker
3. Pour the milky solution containing the drug into the liquid paraffin and stir for 6 hours using a homogenizer at 800 rpm
4. After homogenising for 2 hours, add 10 mL *n*-hexane
5. Continue homogenising for the remaining 4 hours

Evaluation of HYD microspheres

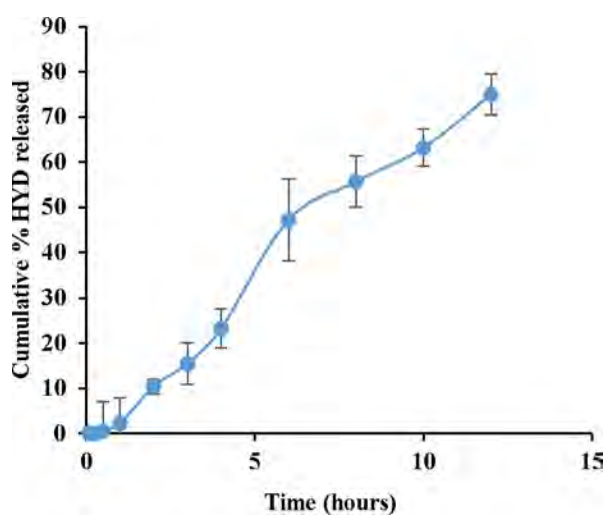
Characterisation of HYD microspheres:

1. Yield (%): 93.1
2. Encapsulation efficiency (%): 87.7
3. HYD content (%): 59.5

SEM image



In vitro dissolution profile



BATCH PRODUCTION RECORD

Faculty of Pharmacy, Rhodes University, Grahamstown, 6140, South Africa.

| | |
|---|---------------------------|
| Formulator: Shakemore T Kangaasaru | Date: 11/07/2016 |
| Product: Hydralazine | Temperature: 19 °C |
| Batch Number: CCD-HYD-032 | Start time: 23H00 |
| Batch Size: 3.5g | End time: 07H00 |

| Materials | Original formula (%m/m) | Working formula (g) | Amount added (g) |
|------------------|-------------------------|---------------------|------------------|
| HYD | 14.3 | 0.5 | 0.50 |
| Methocel® K100LV | 40 | 1.4 | 1.40 |
| Eudragit® RS PO | 17.1 | 0.6 | 0.60 |
| Avicel® 101 | Sq. | 1.0 | 1.00 |
| Total | 100 | 3.5 | 3.50 |

Manufacturing process

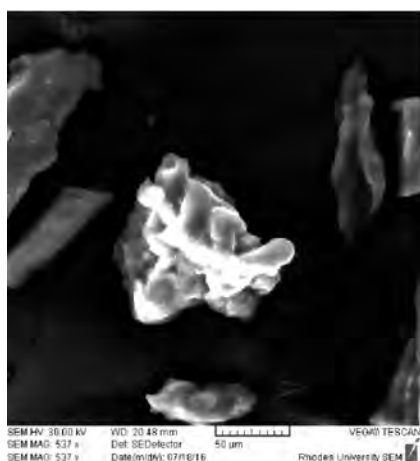
1. Dissolve 0.5 g HYD, polymers (0.60g Eudragit® RS PO and 1.4g Methocel® K100LV) and 1g Avicel® 101 in 12.5 mL acetone
2. Mix 120 mL liquid paraffin and 1.2 mL span 80 in a 400 mL beaker
3. Pour the milky solution containing the drug into the liquid paraffin and stir for 8 hours using a homogenizer at 800 rpm
4. After homogenising for 2 hours, add 10 mL *n*-hexane
5. Continue homogenising for the remaining 6 hours

Evaluation of HYD microspheres

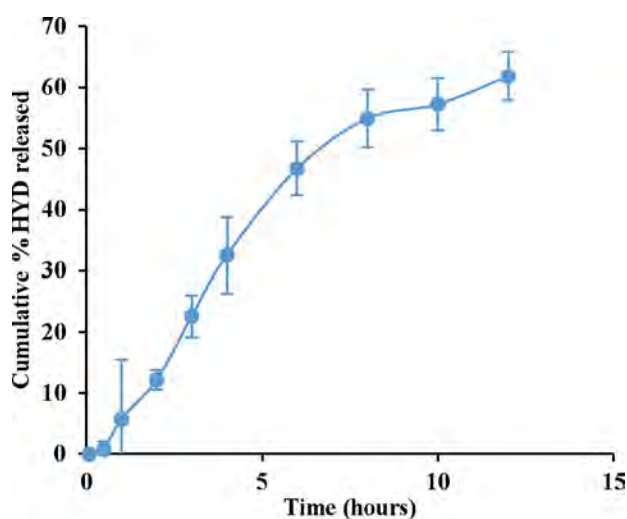
Characterisation of HYD microspheres:

1. Yield (%): 94.0
2. Encapsulation efficiency (%): 69.4
3. HYD content (%): 48.7

SEM image



In vitro dissolution profile



BATCH PRODUCTION RECORD

Faculty of Pharmacy, Rhodes University, Grahamstown, 6140, South Africa.

| | |
|---|---------------------------|
| Formulator: Shakemore T Kangausaru | Date: 12/07/2016 |
| Product: Hydralazine | Temperature: 19 °C |
| Batch Number: CCD-HYD-033 | Start time: 07H00 |
| Batch Size: 3.5g | End time: 15H00 |

| Materials | Original formula (%m/m) | Working formula (g) | Amount added (g) |
|------------------|-------------------------|---------------------|------------------|
| HYD | 14.3 | 0.5 | 0.50 |
| Methocel® K100LV | 17.1 | 0.6 | 0.60 |
| Eudragit® RS PO | 40 | 1.4 | 1.41 |
| Avicel® 101 | Sq. | 1.0 | 1.00 |
| Total | 100 | 3.5 | 3.51 |

Manufacturing process

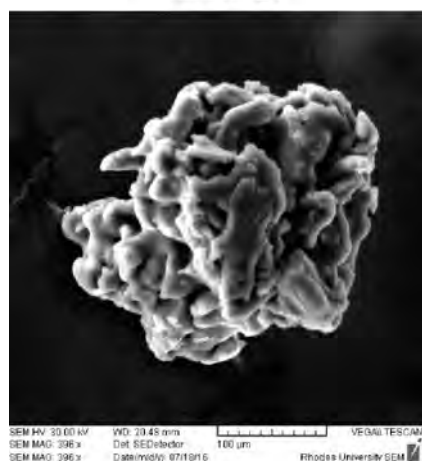
1. Dissolve 0.5 g HYD, polymers (1.4g Eudragit® RS PO and 0.6g Methocel® K100LV) and 1g Avicel® 101 in 12.5 mL acetone
2. Mix 120 mL liquid paraffin and 1.2 mL span 80 in a 400 mL beaker
3. Pour the milky solution containing the drug into the liquid paraffin and stir for 8 hours using a homogenizer at 800 rpm
4. After homogenising for 2 hours, add 10 mL *n*-hexane
5. Continue homogenising for the remaining 6 hours

Evaluation of HYD microspheres

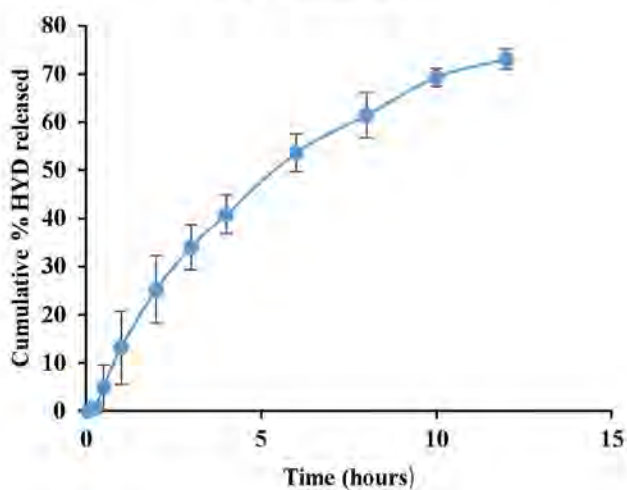
Characterisation of HYD microspheres:

1. Yield (%): 99.4
2. Encapsulation efficiency (%): 78.4
3. HYD content (%): 74.3

SEM image



In vitro dissolution profile



BATCH PRODUCTION RECORD

Faculty of Pharmacy, Rhodes University, Grahamstown, 6140, South Africa.

| | |
|---|---------------------------|
| Formulator: Shakemore T Kangausaru | Date: 12/07/2016 |
| Product: Hydralazine | Temperature: 19 °C |
| Batch Number: CCD-HYD-034 | Start time: 15H00 |
| Batch Size: 3.5g | End time: 23H00 |

| Materials | Original formula (%m/m) | Working formula (g) | Amount added (g) |
|------------------|-------------------------|---------------------|------------------|
| HYD | 14.3 | 0.5 | 0.50 |
| Methocel® K100LV | 40 | 1.4 | 1.41 |
| Eudragit® RS PO | 17.1 | 0.6 | 0.60 |
| Avicel® 101 | Sq. | 1.0 | 1.00 |
| Total | 100 | 3.5 | 3.51 |

Manufacturing process

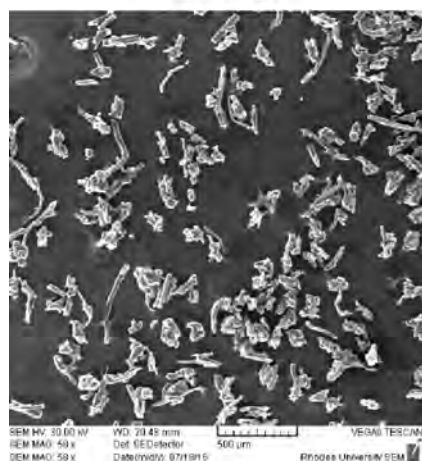
1. Dissolve 0.5 g HYD, polymers (0.6g Eudragit® RS PO and 1.4g Methocel® K100LV) and 1g Avicel® 101 in 14.5 mL acetone
2. Mix 120 mL liquid paraffin and 1.2 mL span 80 in a 400 mL beaker
3. Pour the milky solution containing the drug into the liquid paraffin and stir for 8 hours using a homogenizer at 400 rpm
4. After homogenising for 2 hours, add 10 mL *n*-hexane
5. Continue homogenising for the remaining 6 hours

Evaluation of HYD microspheres

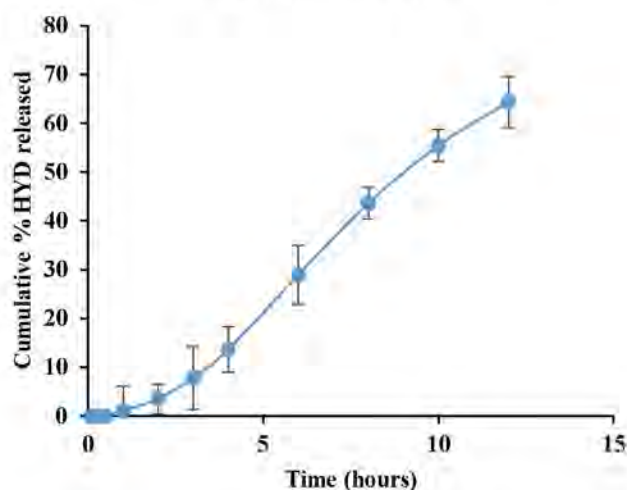
Characterisation of HYD microspheres:

1. Yield (%): 99.7
2. Encapsulation efficiency (%): 71.2
3. HYD content (%): 72.3

SEM image



In vitro dissolution profile



BATCH PRODUCTION RECORD

Faculty of Pharmacy, Rhodes University, Grahamstown, 6140, South Africa.

| | |
|---|---------------------------|
| Formulator: Shakemore T Kangausaru | Date: 12/07/2016 |
| Product: Hydralazine | Temperature: 19 °C |
| Batch Number: CCD-HYD-035 | Start time: 23H00 |
| Batch Size: 3.5g | End time: 06H00 |

| Materials | Original formula (%m/m) | Working formula (g) | Amount added (g) |
|------------------|-------------------------|---------------------|------------------|
| HYD | 14.3 | 0.5 | 0.50 |
| Methocel® K100LV | 40 | 1.4 | 1.40 |
| Eudragit® RS PO | 17.1 | 0.6 | 0.61 |
| Avicel® 101 | Sq. | 1.0 | 1.00 |
| Total | 100 | 3.5 | 3.51 |

Manufacturing process

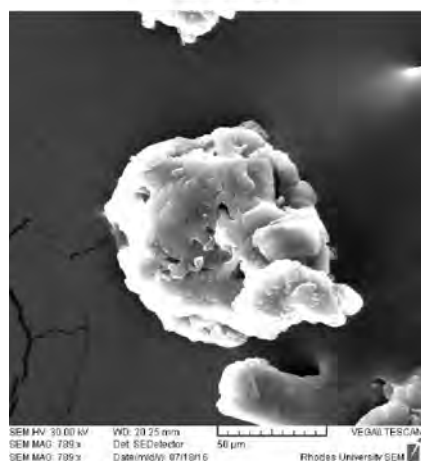
1. Dissolve 0.5 g HYD, polymers (0.6g Eudragit® RS PO and 1.4g Methocel® K100LV) and 1g Avicel® 101 in 14.5 mL acetone
2. Mix 120 mL liquid paraffin and 1.2 mL span 80 in a 400 mL beaker
3. Pour the milky solution containing the drug into the liquid paraffin and stir for 6 hours using a homogenizer at 400 rpm
4. After homogenising for 2 hours, add 10 mL *n*-hexane
5. Continue homogenising for the remaining 4 hours

Evaluation of HYD microspheres

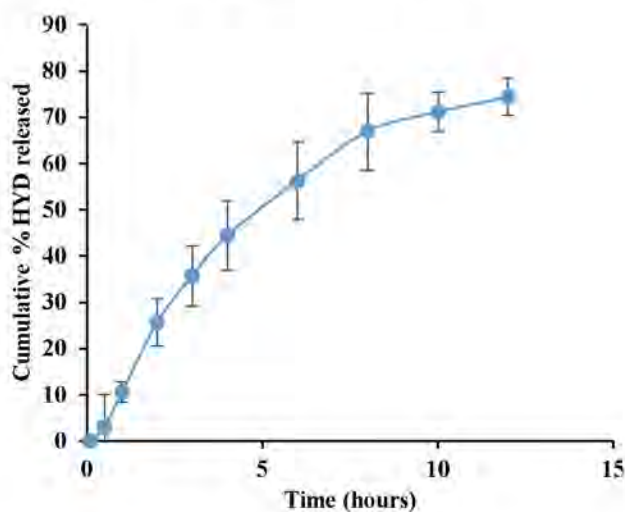
Characterisation of HYD microspheres:

1. Yield (%): 96.0
2. Encapsulation efficiency (%): 62.3
3. HYD content (%): 68.9

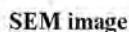
SEM image



In vitro dissolution profile



Faculty of Pharmacy, Rhodes University, Grahamstown, 6140, South Africa.



BATCH PRODUCTION RECORD

Faculty of Pharmacy, Rhodes University, Grahamstown, 6140, South Africa.

| | |
|---|---------------------------|
| Formulator: Shakemore T Kangaasaru | Date: 13/07/2016 |
| Product: Hydralazine | Temperature: 19 °C |
| Batch Number: CCD-HYD-037 | Start time: 22H00 |
| Batch Size: 3.5g | End time: 06H00 |

| Materials | Original formula (%m/m) | Working formula (g) | Amount added (g) |
|------------------|-------------------------|---------------------|------------------|
| HYD | 14.3 | 0.5 | 0.50 |
| Methocel® K100LV | 40 | 1.4 | 1.40 |
| Eudragit® RS PO | 40 | 1.4 | 1.40 |
| Avicel® 101 | Sq. | 0.2 | 0.21 |
| Total | 100 | 3.5 | 3.51 |

Manufacturing process

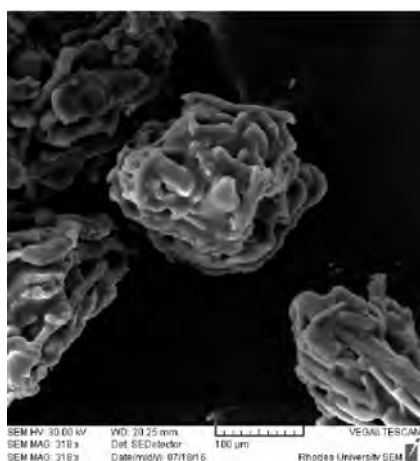
1. Dissolve 0.5 g HYD, polymers (1.4g Eudragit® RS PO and 1.4g Methocel® K100LV) and 0.2g Avicel® 101 in 12.5mL acetone
2. Mix 120 mL liquid paraffin and 1.2 mL span 80 in a 400 mL beaker
3. Pour the milky solution containing the drug into the liquid paraffin and stir for 8 hours using a homogenizer at 800 rpm
4. After homogenising for 2 hours, add 10 mL *n*-hexane
5. Continue homogenising for the remaining 6 hours

Evaluation of HYD microspheres

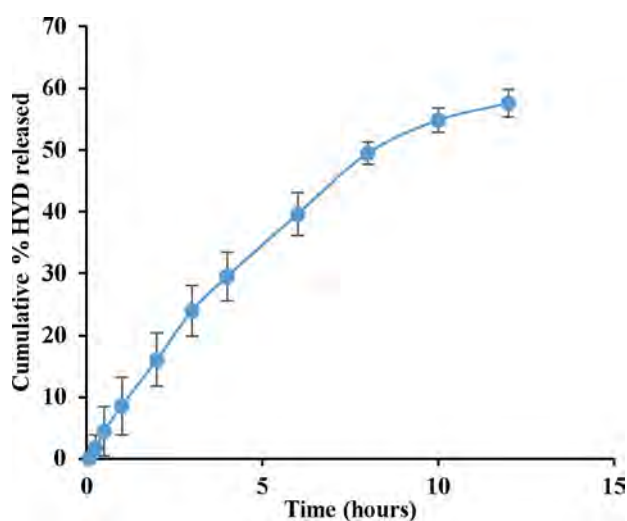
Characterisation of HYD microspheres:

1. Yield (%): 98.0
2. Encapsulation efficiency (%): 71.9
3. HYD content (%): 71.6

SEM image



In vitro dissolution profile



BATCH PRODUCTION RECORD

Faculty of Pharmacy, Rhodes University, Grahamstown, 6140, South Africa.

| | |
|---|---------------------------|
| Formulator: Shakemore T Kangaasaru | Date: 15/07/2016 |
| Product: Hydralazine | Temperature: 20 °C |
| Batch Number: CCD-HYD-038 | Start time: 07H00 |
| Batch Size: 3.5g | End time: 13H00 |

| Materials | Original formula (%m/m) | Working formula (g) | Amount added (g) |
|------------------|-------------------------|---------------------|------------------|
| HYD | 14.3 | 0.5 | 0.51 |
| Methocel® K100LV | 40 | 1.4 | 1.40 |
| Eudragit® RS PO | 40 | 1.4 | 1.40 |
| Avicel® 101 | Sq. | 0.2 | 0.21 |
| Total | 100 | 3.5 | 3.52 |

Manufacturing process

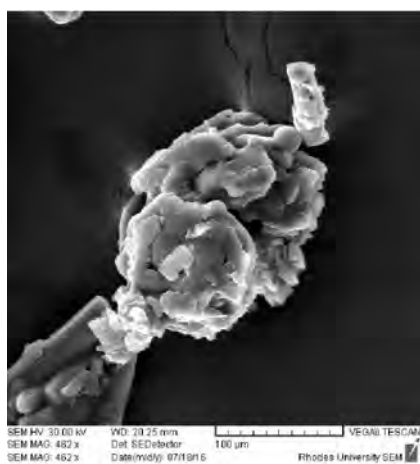
1. Dissolve 0.5 g HYD, polymers (0.60g Eudragit® RS PO and 0.62g Methocel® K100LV) and 1.81g Avicel® 101 in 12.5 mL acetone
2. Mix 120 mL liquid paraffin and 1.2 mL span 80 in a 400mL beaker
3. Pour the milky solution containing the drug into the liquid paraffin and stir for 8 hours using a homogenizer at 800 rpm
4. After homogenising for 2 hours, add 10 mL *n*-hexane
5. Continue homogenising for the remaining 6 hours

Evaluation of HYD microspheres

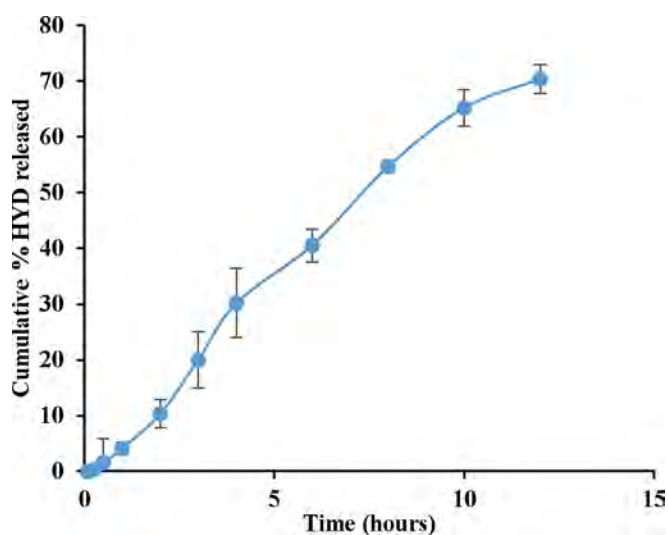
Characterisation of HYD microspheres:

1. Yield (%):
2. Encapsulation efficiency (%):
3. HYD content (%):

SEM image



In vitro dissolution profile



BATCH PRODUCTION RECORD

Faculty of Pharmacy, Rhodes University, Grahamstown, 6140, South Africa.

| | |
|---|---------------------------|
| Formulator: Shakemore T Kangaasaru | Date: 15/07/2016 |
| Product: Hydralazine | Temperature: 20 °C |
| Batch Number: CCD-HYD-039 | Start time: 13H30 |
| Batch Size: 3.5g | End time: 21H30 |

| Materials | Original formula (%m/m) | Working formula (g) | Amount added (g) |
|------------------|-------------------------|---------------------|------------------|
| HYD | 14.3 | 0.5 | 0.50 |
| Methocel® K100LV | 17.1 | 0.6 | 0.61 |
| Eudragit® RS PO | 40 | 1.4 | 1.40 |
| Avicel® 101 | Sq. | 1.0 | 1.00 |
| Total | 100 | 3.5 | 3.51 |

Manufacturing process

1. Dissolve 0.5 g HYD, polymers (1.4g Eudragit® RS PO and 0.6g Methocel® K100LV) and 1g Avicel® 101 in 14.5 mL acetone
2. Mix 120 mL liquid paraffin and 1.2 mL span 80 in a 400 mL beaker
3. Pour the milky solution containing the drug into the liquid paraffin and stir for 8 hours using a homogenizer at 800 rpm
4. After homogenising for 2 hours, add 10 mL *n*-hexane
5. Continue homogenising for the remaining 6 hours

Evaluation of HYD microspheres

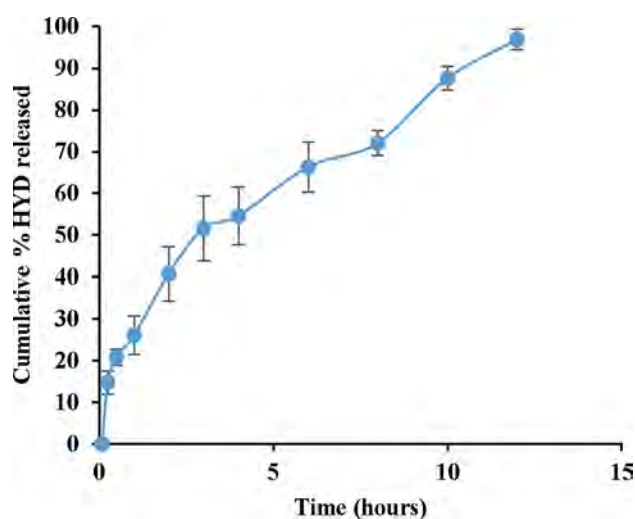
Characterisation of HYD microspheres:

1. Yield (%): 99.7
2. Encapsulation efficiency (%): 87.7
3. HYD content (%): 69.0

SEM image



In vitro dissolution profile



BATCH PRODUCTION RECORD

Faculty of Pharmacy, Rhodes University, Grahamstown, 6140, South Africa.

| | |
|---|---------------------------|
| Formulator: Shakemore T Kangausaru | Date: 16/07/2016 |
| Product: Hydralazine | Temperature: 20 °C |
| Batch Number: CCD-HYD-040 | Start time: 08H00 |
| Batch Size: 3.5g | End time: 14H00 |

| Materials | Original formula (%m/m) | Working formula (g) | Amount added (g) |
|------------------|-------------------------|---------------------|------------------|
| HYD | 14.3 | 0.5 | 0.51 |
| Methocel® K100LV | 40 | 1.4 | 1.40 |
| Eudragit® RS PO | 40 | 1.4 | 1.41 |
| Avicel® 101 | Sq. | 0.2 | 0.20 |
| Total | 100 | 3.5 | 3.52 |

Manufacturing process

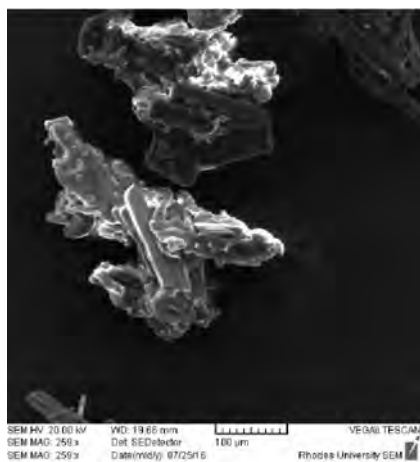
1. Dissolve 0.5 g HYD, polymers (1.4g Eudragit® RS PO and 1.4g Methocel® K100LV) and 0.2g Avicel® 101 in 12.5 mL acetone
2. Mix 120 mL liquid paraffin and 1.2 mL span 80 in a 400 mL beaker
3. Pour the milky solution containing the drug into the liquid paraffin and stir for 6 hours using a homogenizer at 400 rpm
4. After homogenising for 2 hours, add 10 mL *n*-hexane
5. Continue homogenising for the remaining 4 hours

Evaluation of HYD microspheres

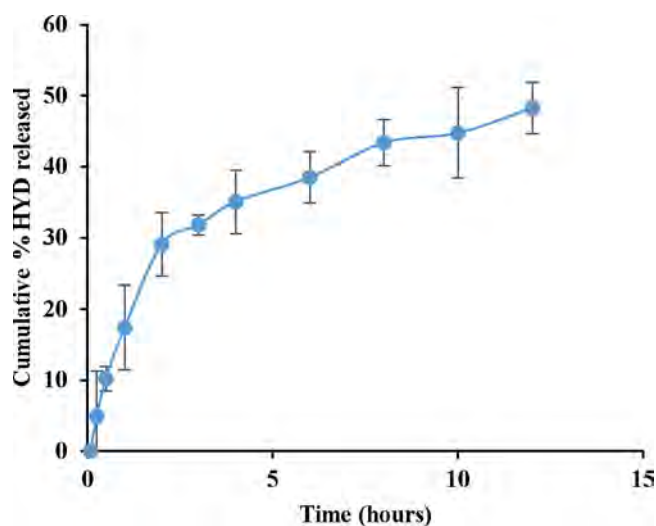
Characterisation of HYD microspheres:

1. Yield (%): 99.7
2. Encapsulation efficiency (%): 61.5
3. HYD content (%): 72.1

SEM image



***In vitro* dissolution profile**



BATCH PRODUCTION RECORD

Faculty of Pharmacy, Rhodes University, Grahamstown, 6140, South Africa.

Formulator: Shakemore T Kangaasaru

Date: 16/07/2016

Product: Hydralazine

Temperature: 20 °C

Batch Number: CCD-HYD-041

Start time: 14H00

Batch Size: 3.5g

End time: 22H00

| Materials | Original formula (%m/m) | Working formula (g) | Amount added (g) |
|------------------|-------------------------|---------------------|------------------|
| HYD | 14.3 | 0.50 | 0.51 |
| Methocel® K100LV | 40 | 1.00 | 1.00 |
| Eudragit® RS PO | 40 | 1.95 | 1.95 |
| Avicel® 101 | Sq. | 0.05 | 0.05 |
| Total | 100 | 3.5 | 3.51 |

Manufacturing process

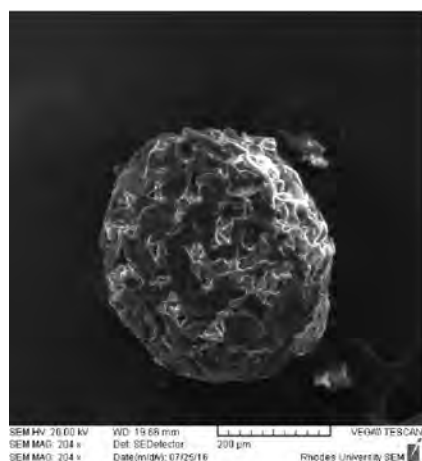
1. Dissolve 0.5 g HYD, polymers (1.95g Eudragit® RS PO and 1g Methocel® K100LV) and 0.05g Avicel® 101 in 13.5 mL acetone
2. Mix 120 mL liquid paraffin and 1.2 mL span 80 in a 400 mL beaker
3. Pour the milky solution containing the drug into the liquid paraffin and stir for 7 hours using a homogenizer at 600 rpm
4. After homogenising for 2 hours, add 10 mL *n*-hexane
5. Continue homogenising for the remaining 5 hours

Evaluation of HYD microspheres

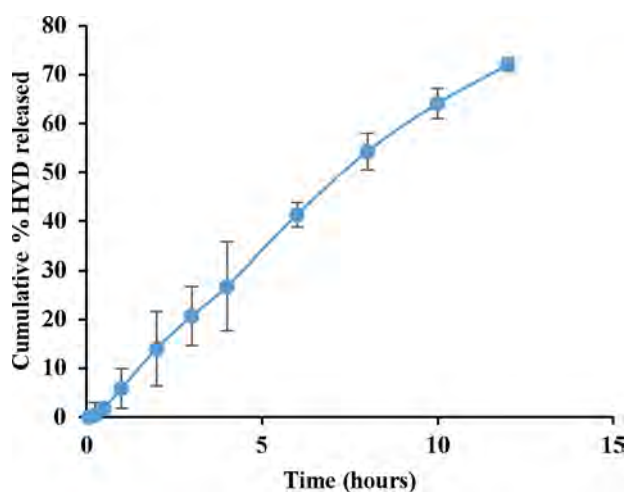
Characterisation of HYD microspheres:

1. Yield (%): 90.6
2. Encapsulation efficiency (%): 87.8
3. HYD content (%): 68.9

SEM image



In vitro dissolution profile



BATCH PRODUCTION RECORD

Faculty of Pharmacy, Rhodes University, Grahamstown, 6140, South Africa.

Formulator: Shakemore T Kangausaru

Product: Hydralazine

Batch Number: CCD-HYD-042

Batch Size: 3.5g

Date: 16/07/2016

Temperature: 20°C

Start time: 22H00

End time: 05H00

| Materials | Original formula (%m/m) | Working formula (g) | Amount added (g) |
|------------------|-------------------------|---------------------|------------------|
| HYD | 14.3 | 0.5 | 0.51 |
| Methocel® K100LV | 40 | 1.0 | 1.00 |
| Eudragit® RS PO | 40 | 1.0 | 1.00 |
| Avicel® 101 | Sq. | 1.0 | 1.01 |
| Total | 100 | 3.5 | 3.52 |

Manufacturing process

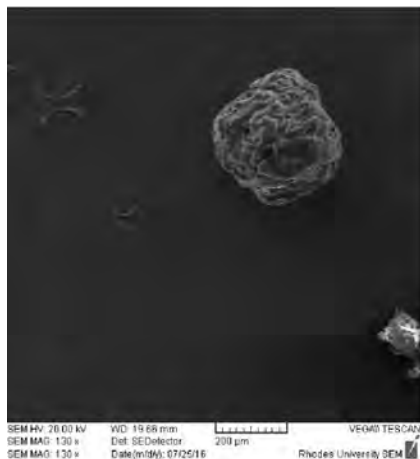
1. Dissolve 0.5 g HYD, polymers (1g Eudragit® RS PO and 1g Methocel® K100LV) and 1g Avicel® 101 in 13.5 mL acetone
2. Mix 120 mL liquid paraffin and 1.2 mL span 80 in a 400 mL beaker
3. Pour the milky solution containing the drug into the liquid paraffin and stir for 7 hours using a homogenizer at 600 rpm
4. After homogenising for 2 hours, add 10 mL *n*-hexane
5. Continue homogenising for the remaining 5 hours

Evaluation of HYD microspheres

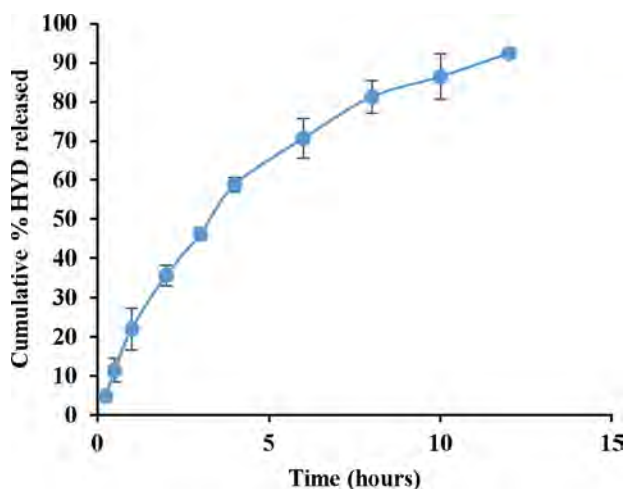
Characterisation of HYD microspheres:

1. Yield (%): 93.1
2. Encapsulation efficiency (%): 102.7
3. HYD content (%): 80.1

SEM image



In vitro dissolution profile



BATCH PRODUCTION RECORD

Faculty of Pharmacy, Rhodes University, Grahamstown, 6140, South Africa.

| | |
|---|--------------------------|
| Formulator: Shakemore T Kangausaru | Date: 16/07/2016 |
| Product: Hydralazine | Temperature: 20°C |
| Batch Number: CCD-HYD-043 | Start time: 08H00 |
| Batch Size: 3.5g | End time: 15H00 |

| Materials | Original formula (%m/m) | Working formula (g) | Amount added (g) |
|------------------|-------------------------|---------------------|------------------|
| HYD | 14.3 | 0.5 | 0.50 |
| Methocel® K100LV | 17.1 | 0.6 | 0.60 |
| Eudragit® RS PO | 17.1 | 0.6 | 0.60 |
| Avicel® 101 | Sq. | 1.8 | 1.81 |
| Total | 100 | 3.5 | 3.51 |

Manufacturing process

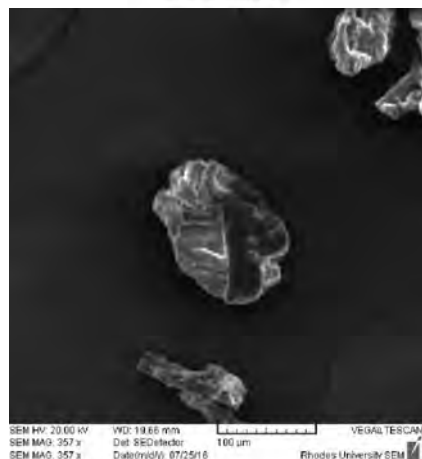
1. Dissolve 0.5 g HYD, polymers (0.6g Eudragit® RS PO and 0.6g Methocel® K100LV) and 1.8g Avicel® 101 in 12.5 mL acetone
2. Mix 120 mL liquid paraffin and 1.2 mL span 80 in a 400 mL beaker
3. Pour the milky solution containing the drug into the liquid paraffin and stir for 8 hours using a homogenizer at 800 rpm
4. After homogenising for 2 hours, add 10 mL *n*-hexane
5. Continue homogenising for the remaining 6 hours

Evaluation of HYD microspheres

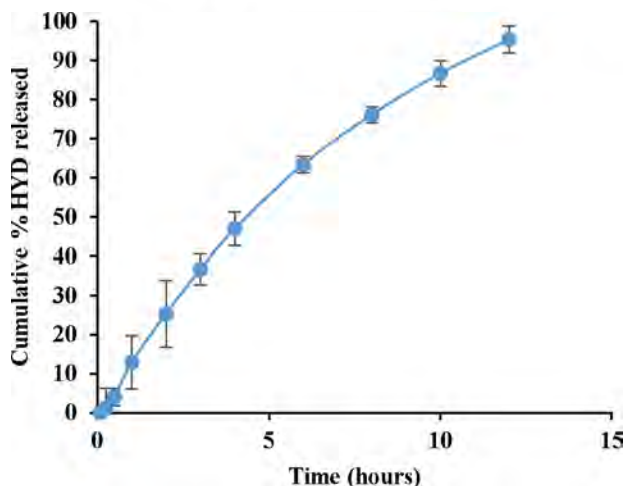
Characterisation of HYD microspheres:

1. Yield (%): 98.6
2. Encapsulation efficiency (%): 52.7
3. HYD content (%): 66.6

SEM image



In vitro dissolution profile



BATCH PRODUCTION RECORD

Faculty of Pharmacy, Rhodes University, Grahamstown, 6140, South Africa.

| | |
|---|---------------------------|
| Formulator: Shakemore T Kangausaru | Date: 16/07/2016 |
| Product: Hydralazine | Temperature: 20 °C |
| Batch Number: CCD-HYD-044 | Start time: 15H00 |
| Batch Size: 3.5g | End time: 23H00 |

| Materials | Original formula (%m/m) | Working formula (g) | Amount added (g) |
|------------------|-------------------------|---------------------|------------------|
| HYD | 14.3 | 0.5 | 0.50 |
| Methocel® K100LV | 40 | 1.4 | 1.40 |
| Eudragit® RS PO | 40 | 1.4 | 1.41 |
| Avicel® 101 | Sq. | 0.2 | 0.21 |
| Total | 100 | 3.5 | 3.52 |

Manufacturing process

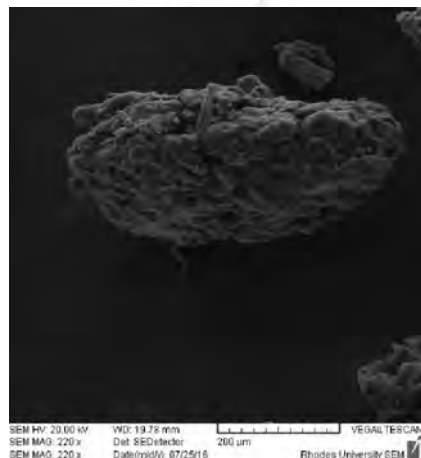
| |
|---|
| 1. Dissolve 0.5 g HYD, polymers (1.4g Eudragit® RS PO and 1.4g Methocel® K100LV) and 0.2g Avicel® 101 in 14.5 mL acetone |
| 2. Mix 120 mL liquid paraffin and 1.2 mL span 80 in a 400 mL beaker |
| 3. Pour the milky solution containing the drug into the liquid paraffin and stir for 8 hours using a homogenizer at 400 rpm |
| 4. After homogenising for 2 hours, add 10 mL <i>n</i> -hexane |
| 5. Continue homogenising for the remaining 6 hours |

Evaluation of HYD microspheres

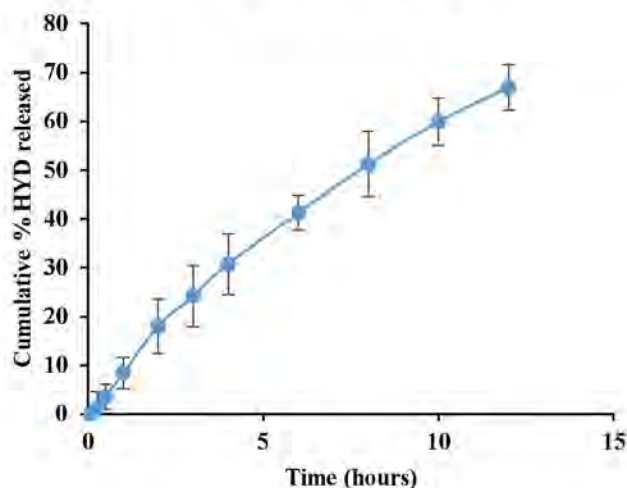
Characterisation of HYD microspheres:

1. Yield (%): 99.7
2. Encapsulation efficiency (%): 86.5
3. HYD content (%): 63.5

SEM image



In vitro dissolution profile



BATCH PRODUCTION RECORD

Faculty of Pharmacy, Rhodes University, Grahamstown, 6140, South Africa.

| | |
|---|---------------------------|
| Formulator: Shakemore T Kangausaru | Date: 17/07/2016 |
| Product: Hydralazine | Temperature: 19 °C |
| Batch Number: CCD-HYD-045 | Start time: 07H00 |
| Batch Size: 3.5g | End time: 14H00 |

| Materials | Original formula (%m/m) | Working formula (g) | Amount added (g) |
|------------------|-------------------------|---------------------|------------------|
| HYD | 14.3 | 0.5 | 0.50 |
| Methocel® K100LV | 28.6 | 1.0 | 1.00 |
| Eudragit® RS PO | 28.6 | 1.0 | 1.00 |
| Avicel® 101 | Sq. | 1.8 | 1.01 |
| Total | 100 | 3.5 | 3.51 |

Manufacturing process

1. Dissolve 0.5 g HYD, polymers (1g Eudragit® RS PO and 1g Methocel® K100LV) and 1g Avicel® 101 in 13.5 mL acetone
2. Mix 120 mL liquid paraffin and 1.2 mL span 80 in a 400 mL beaker
3. Pour the milky solution containing the drug into the liquid paraffin and stir for 7 hours using a homogenizer at 125 rpm
4. After homogenising for 2 hours, add 10 mL *n*-hexane
5. Continue homogenising for the remaining 5 hours

Evaluation of HYD microspheres

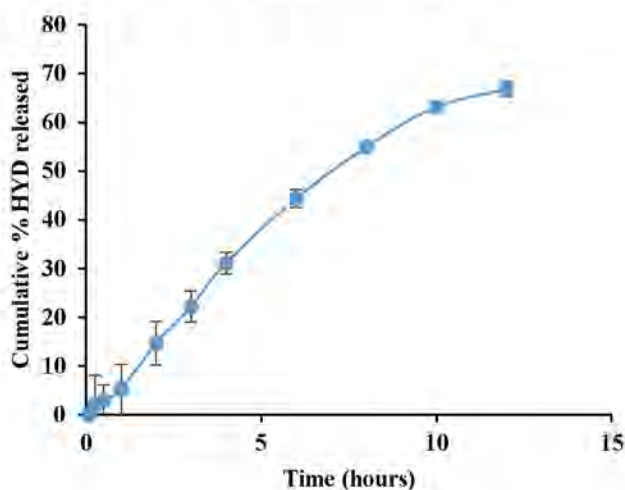
Characterisation of HYD microspheres:

1. Yield (%): 100.6
2. Encapsulation efficiency (%): 82.5
3. HYD content (%): 68.4

SEM image



In vitro dissolution profile



BATCH PRODUCTION RECORD

Faculty of Pharmacy, Rhodes University, Grahamstown, 6140, South Africa.

Formulator: Shakemore T Kangaasaru

Product: Hydralazine

Batch Number: CCD-HYD-046

Batch Size: 3.5g

Date: 17/07/2016

Temperature: 19 °C

Start time: 14H00

End time: 21H00

| Materials | Original formula (%m/m) | Working formula (g) | Amount added (g) |
|------------------|-------------------------|---------------------|------------------|
| HYD | 14.3 | 0.50 | 0.50 |
| Methocel® K100LV | 1.4 | 0.05 | 0.05 |
| Eudragit® RS PO | 28.6 | 1.00 | 1.00 |
| Avicel® 101 | Sq. | 1.95 | 1.95 |
| Total | 100 | 3.5 | 3.50 |

Manufacturing process

1. Dissolve 0.5 g HYD, polymers (1.00g Eudragit® RS PO and 0.05g Methocel® K100LV) and 1.95g Avicel® 101 in 13.5 mL acetone
2. Mix 120 mL liquid paraffin and 1.2 mL span 80 in a 400 mL beaker
3. Pour the milky solution containing the drug into the liquid paraffin and stir for 7 hours using a homogenizer at 600 rpm
4. After homogenising for 2 hours, add 10 mL *n*-hexane
5. Continue homogenising for the remaining 5 hours

Evaluation of HYD microspheres

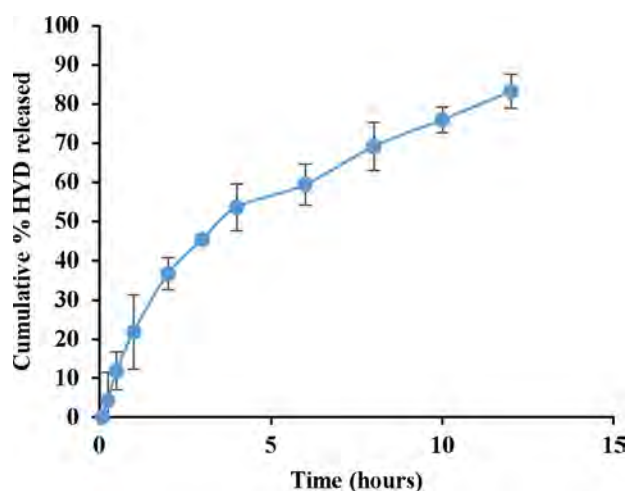
Characterisation of HYD microspheres:

1. Yield (%): 99.7
2. Encapsulation efficiency (%): 74.8
3. HYD content (%): 63.3

SEM image



In vitro dissolution profile



BATCH PRODUCTION RECORD

Faculty of Pharmacy, Rhodes University, Grahamstown, 6140, South Africa.

| | |
|---|---------------------------|
| Formulator: Shakemore T Kangausaru | Date: 18/07/2016 |
| Product: Hydralazine | Temperature: 19 °C |
| Batch Number: CCD-HYD-047 | Start time: 07H00 |
| Batch Size: 3.5g | End time: 13H00 |

| Materials | Original formula (%m/m) | Working formula (g) | Amount added (g) |
|------------------|-------------------------|---------------------|------------------|
| HYD | 14.3 | 0.5 | 0.50 |
| Methocel® K100LV | 40 | 1.4 | 1.40 |
| Eudragit® RS PO | 40 | 1.4 | 1.40 |
| Avicel® 101 | Sq. | 0.2 | 0.21 |
| Total | 100 | 3.5 | 3.51 |

Manufacturing process

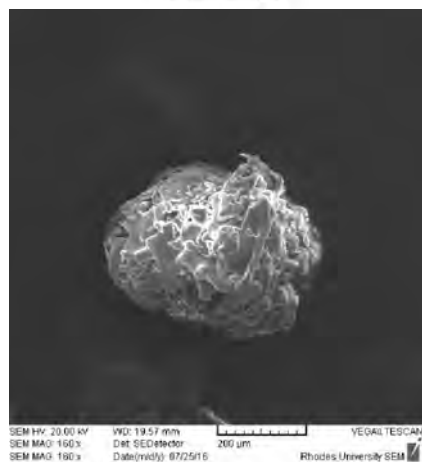
1. Dissolve 0.5 g HYD, polymers (1.4g Eudragit® RS PO and 1.4g Methocel® K100LV) and 0.2g Avicel® 101 in 14.5 mL acetone
2. Mix 120 mL liquid paraffin and 1.2 mL span 80 in a 400 mL beaker
3. Pour the milky solution containing the drug into the liquid paraffin and stir for 6 hours using a homogenizer at 400 rpm
4. After homogenising for 2 hours, add 10 mL *n*-hexane
5. Continue homogenising for the remaining 4 hours

Evaluation of HYD microspheres

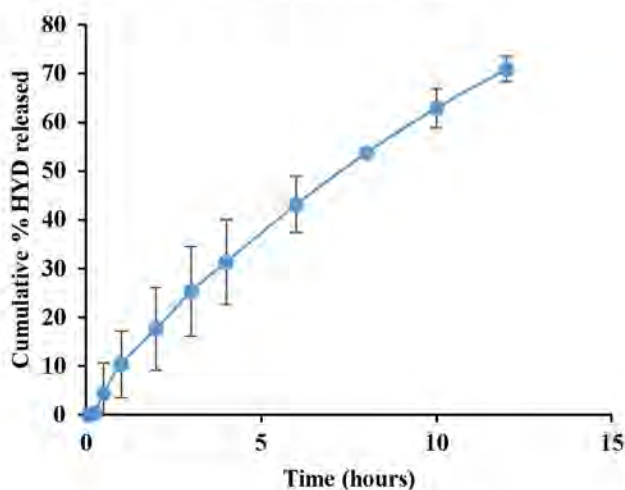
Characterisation of HYD microspheres:

1. Yield (%): 100.0
2. Encapsulation efficiency (%): 78.7
3. HYD content (%): 61.7

SEM image



In vitro dissolution profile



BATCH PRODUCTION RECORD

Faculty of Pharmacy, Rhodes University, Grahamstown, 6140, South Africa.

| | |
|---|---------------------------|
| Formulator: Shakemore T Kangausaru | Date: 23/07/2016 |
| Product: Hydralazine | Temperature: 19 °C |
| Batch Number: CCD-HYD-048 | Start time: 07H00 |
| Batch Size: 3.5g | End time: 13H00 |

| <i>Materials</i> | <i>Original formula (%m/m)</i> | <i>Working formula (g)</i> | <i>Amount added (g)</i> |
|------------------|--------------------------------|----------------------------|-------------------------|
| HYD | 14.3 | 0.5 | 0.50 |
| Methocel® K100LV | 17.1 | 0.6 | 0.60 |
| Eudragit® RS PO | 17.1 | 0.6 | 0.60 |
| Avicel® 101 | Sq. | 1.8 | 1.80 |
| Total | 100 | 3.5 | 3.50 |

Manufacturing process

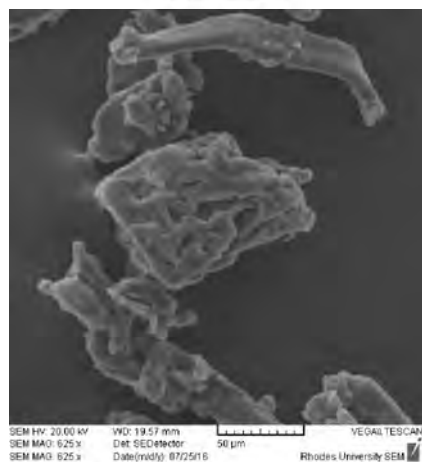
1. Dissolve 0.5 g HYD, polymers (0.6g Eudragit® RS PO and 0.6g Methocel® K100LV) and 1.8g Avicel® 101 in 12.5 mL acetone
2. Mix 120 mL liquid paraffin and 1.2 mL span 80 in a 400 mL beaker
3. Pour the milky solution containing the drug into the liquid paraffin and stir for 6 hours using a homogenizer at 400 rpm
4. After homogenising for 2 hours, add 10 mL *n*-hexane
5. Continue homogenising for the remaining 4 hours

Evaluation of HYD microspheres

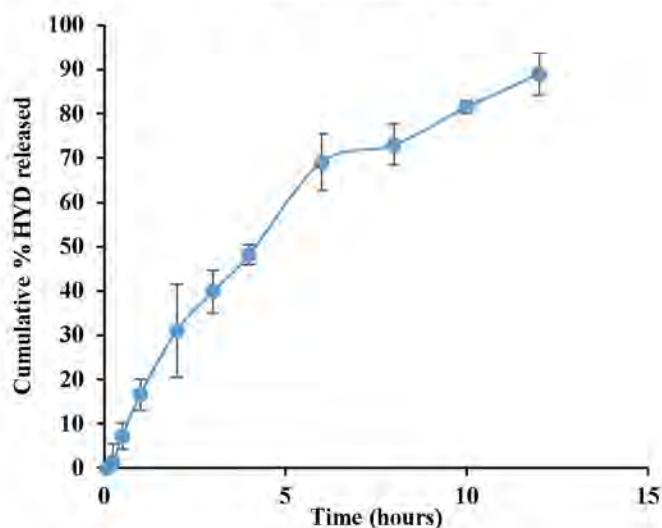
Characterisation of HYD microspheres:

1. Yield (%): 91.1
2. Encapsulation efficiency (%): 81.2
3. HYD content (%): 60.6

SEM image



***In vitro* dissolution profile**



BATCH PRODUCTION RECORD

Faculty of Pharmacy, Rhodes University, Grahamstown, 6140, South Africa.

| | |
|---|---------------------------|
| Formulator: Shakemore T Kangausaru | Date: 24/07/2016 |
| Product: Hydralazine | Temperature: 19 °C |
| Batch Number: CCD-HYD-049 | Start time: 13H00 |
| Batch Size: 3.5g | End time: 20H00 |

| Materials | Original formula (%m/m) | Working formula (g) | Amount added (g) |
|------------------|-------------------------|---------------------|------------------|
| HYD | 14.3 | 0.5 | 0.50 |
| Methocel® K100LV | 40 | 1.4 | 1.40 |
| Eudragit® RS PO | 17.1 | 0.6 | 0.60 |
| Avicel® 101 | Sq. | 1.0 | 1.01 |
| Total | 100 | 3.5 | 3.51 |

Manufacturing process

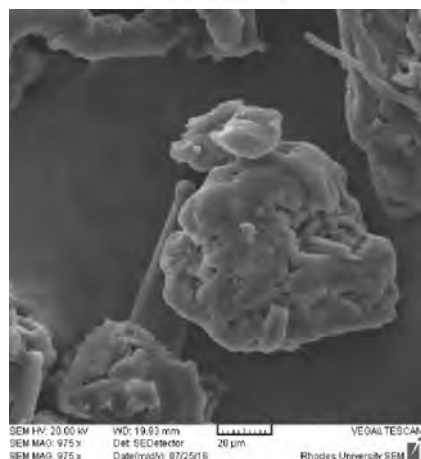
1. Dissolve 0.5 g HYD, polymers (0.6g Eudragit® RS PO and 1.4g Methocel® K100LV) and 1.81g Avicel® 101 in 12.5 mL acetone
2. Mix 120 mL liquid paraffin and 1.2 mL span 80 in a 400 mL beaker
3. Pour the milky solution containing the drug into the liquid paraffin and stir for 6 hours using a homogenizer at 800 rpm
4. After homogenising for 2 hours, add 10 mL *n*-hexane
5. Continue homogenising for the remaining 4 hours

Evaluation of HYD microspheres

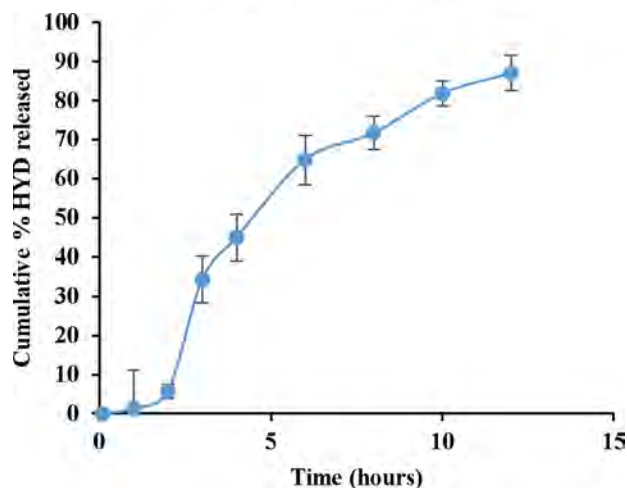
Characterisation of HYD microspheres:

1. Yield (%): 97
2. Encapsulation efficiency (%): 70.4
3. HYD content (%): 75.0

SEM image



In vitro dissolution profile



BATCH PRODUCTION RECORD

Faculty of Pharmacy, Rhodes University, Grahamstown, 6140, South Africa.

| | |
|---|---------------------------|
| Formulator: Shakemore T Kangausaru | Date: 24/07/2016 |
| Product: Hydralazine | Temperature: 19 °C |
| Batch Number: CCD-HYD-050 | Start time: 13H00 |
| Batch Size: 3.5g | End time: 20H00 |

| Materials | Original formula (%m/m) | Working formula (g) | Amount added (g) |
|------------------|-------------------------|---------------------|------------------|
| HYD | 14.3 | 0.5 | 0.50 |
| Methocel® K100LV | 17.1 | 1.0 | 1.00 |
| Eudragit® RS PO | 17.1 | 1.0 | 1.00 |
| Avicel® 101 | Sq. | 1.0 | 1.01 |
| Total | 100 | 3.5 | 3.51 |

Manufacturing process

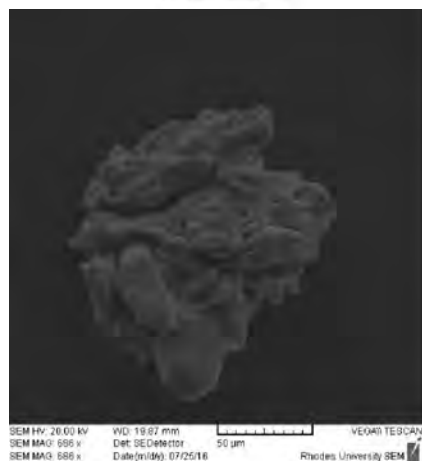
1. Dissolve 0.5 g HYD, polymers (1g Eudragit® RS PO and 1g Methocel® K100LV) and 1g Avicel® 101 in 13.5 mL acetone
2. Mix 120 mL liquid paraffin and 1.2 mL span 80 in a 400 mL beaker
3. Pour the milky solution containing the drug into the liquid paraffin and stir for 7 hours using a homogenizer at 600 rpm
4. After homogenising for 2 hours, add 10 mL *n*-hexane
5. Continue homogenising for the remaining 5 hours

Evaluation of HYD microspheres

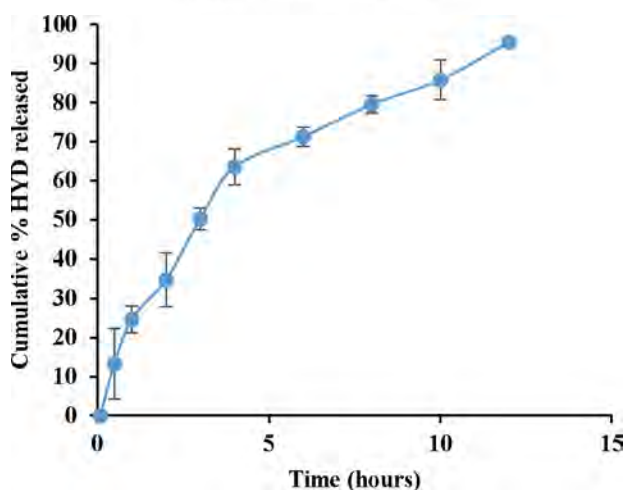
Characterisation of HYD microspheres:

1. Yield (%): 94.3
2. Encapsulation efficiency (%): 72.4
3. HYD content (%): 69/2

SEM image



***In vitro* dissolution profile**



BATCH PRODUCTION RECORD

Faculty of Pharmacy, Rhodes University, Grahamstown, 6140, South Africa.

Formulator: Shakemore Kangausaru

Date: 01/08/2016

Product: Hydralazine

Temperature: 19 °C

Batch Number: OPT-001

Start time: 07H00

Batch Size: 3.5g

End time: 14H00

| Materials | Original formula (%w/w) | Working formula (g) | Amount added (g) |
|------------------|-------------------------|---------------------|------------------|
| HYD | 14.3 | 0.5 | 0.50 |
| Methocel® K100LV | 16 | 0.56 | 0.57 |
| Eudragit® RS PO | 40 | 1.40 | 1.41 |
| Avicel® 101 | Sq. | 1.04 | 1.04 |
| Total | 100 | 3.5 | 3.51 |

Manufacturing process

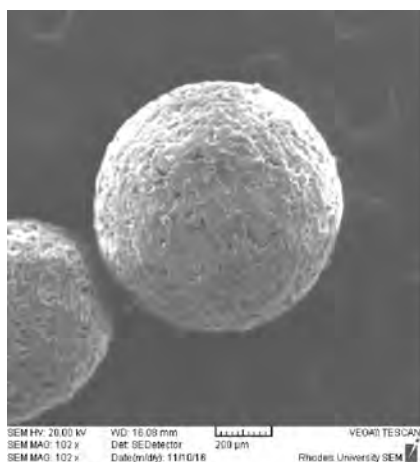
1. Dissolve 0.5 g HYD, polymers (1.4g Eudragit® RS PO and 0.56g Methocel® K100LV) and 1.04g Avicel® 101 in 14.5 mL acetone
2. Mix 120 mL liquid paraffin and 1.2mL span 80 in a 400 mL beaker
3. Pour the milky solution containing the drug into the liquid paraffin and stir for 7 hours using a homogenizer at 400 rpm
4. After homogenising for 2 hours, add 10 mL *n*-hexane
5. Continue homogenising for the remaining 5 hours

Evaluation of HYD microspheres

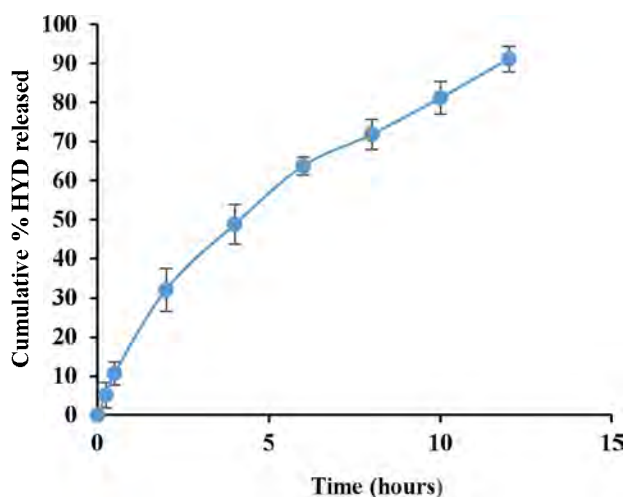
Characterisation of HYD microspheres:

1. Yield (%): 99.72
2. Encapsulation efficiency (%): 99.71
3. HYD content (%): 99.83

SEM image



In vitro dissolution profile



BATCH PRODUCTION RECORD

Faculty of Pharmacy, Rhodes University, Grahamstown, 6140, South Africa.

Formulator: Shakemore Kangaasaru
Product: Hydralazine
Batch Number: OPT-002
Batch Size: 3.5g

Date: 02/08/2016
Temperature: 19 °C
Start time: 07H00
End time: 14H00

| Materials | Original formula (%m/m) | Working formula (g) | Amount added (g) |
|------------------|-------------------------|---------------------|------------------|
| HYD | 14.3 | 0.50 | 0.50 |
| Methocel® K100LV | 17.4 | 0.61 | 0.61 |
| Eudragit® RS PO | 39.4 | 1.38 | 1.38 |
| Avicel® 101 | Sq. | 1.01 | 1.01 |
| Total | 100 | 3.5 | 3.50 |

Manufacturing process

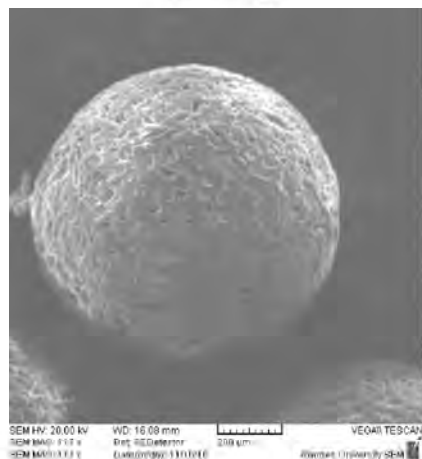
1. Dissolve 0.5 g HYD, polymers (1.38g Eudragit® RS PO and 0.61g Methocel® K100LV) and 1.01g Avicel® 101 in 14.5 mL acetone
2. Mix 120 mL liquid paraffin and 1.2 mL span 80 in a 400 mL beaker
3. Pour the milky solution containing the drug into the liquid paraffin and stir for 7 hours using a homogenizer at 400 rpm
4. After homogenising for 2 hours, add 10 mL *n*-hexane
5. Continue homogenising for the remaining 5 hours

Evaluation of HYD microspheres

Characterisation of HYD microspheres:

1. Yield (%): 99.43
2. Encapsulation efficiency (%): 99.30
3. HYD content (%): 99.89

SEM image



In vitro dissolution profile

